N73-16128

Contract No. NAS9-12705
DRL unnumbered
Line Item 4
DRD No. MA-129T
ASAO-PR20041-8

CR-128717

DEFINITION OF MULTIPATH/RFI EXPERIMENTS FOR ORBITAL TESTING WITH A SMALL APPLICATIONS TECHNOLOGY SATELLITE

by

J.N. Birch
R.H. French

DECEMBER 1, 1972

FINAL REPORT

Prepared for:

NATIONAL AERONAUTICS AND SPACE ADMINISTRATION
Manned Spacecraft Center
Houston, Texas 77058

THE Magnavox COMPANY
Advanced Systems Analysis Office
Silver Spring, Maryland 20910

Contract No. NAS9-12705
DRL unnumbered
Line Item 4
DRD No. MA-129T
ASAO-PR20041-8

DEFINITION OF MULTIPATH/RFI EXPERIMENTS FOR ORBITAL TESTING WITH A SMALL APPLICATIONS TECHNOLOGY SATELLITE

by

J. N. Birch
R. H. French

DECEMBER 1, 1972

FINAL REPORT

Prepared for
National Aeronautics and Space Administration
Manned Spacecraft Center
Houston, Texas 77058

Approved by: J. N. Birch
J. N. Birch, Director

THE MAGNAVOX COMPANY
Advanced Systems Analysis Office
8720 Georgia Avenue
Silver Spring, Maryland 20910

DISTRIBUTION

NASA Manned Spacecraft Center
R&T Space Station Procurement Section
Attn: Farris R. Tabor, Mail Code BC76
Houston, Texas 77058 (1)

NASA Manned Spacecraft Center
Technical Library Branch
Attn: Retha Shirkey, Mail Code JM6
Houston, Texas 77058 (4)

NASA Manned Spacecraft Center
Management Services Division
Attn: John T. Wheeler, Mail Code BM7
Houston, Texas 77058 (1)

NASA Manned Spacecraft Center
Communications Systems Analysis Branch
Attn: S. W. Novosad, Mail Code EE8 (94)

ABSTRACT

An investigation was made to define experiments for collection of RFI and multipath data for application to a synchronous relay satellite/low orbiting satellite configuration. A survey of analytical models of the multipath signal was conducted. Data has been gathered concerning the existing RFI and other noise sources in various bands at VHF and UHF.

Additionally, designs are presented for equipments to combat the effects of RFI and multipath: an adaptive delta mod voice system, a forward error control coder/decoder, a PN transmission system, and a wideband FM system. The performance of these systems was then evaluated.

Also, the report discusses techniques for measuring multipath and RFI. Finally, recommended data collection experiments are presented.

The report contains as an Appendix an extensive tabulation of theoretical predictions of the amount of signal reflected from a rough, spherical earth.

TABLE OF CONTENTS

TABLE OF CONTENTS (CONT.)

TABLE OF CONTENTS (CONT.)

TABLE OF CONTENTS (CONT.)

TABLE OF CONTENTS (CONT.)

TABLE OF CONTENTS (CONT.)

TABLE OF CONTENTS (CONT.)

LIST OF ILLUSTRATIONS

LIST OF ILLUSTRATIONS (CONT.)

LIST OF ILLUSTRATIONS (CONT.)

LIST OF ILLUSTRATIONS (CONT.)

LIST OF ILLUSTRATIONS (CONT.)

LIST OF ILLUSTRATIONS (CONT.)

LIST OF TABLES

LIST OF TABLES (CONT.)

LIST OF TABLES (CONT.)

LIST OF APPENDICES

ACKNOWLEDGMENT

The authors wish to acknowledge the significant technical contributions to this report by Mr. Malcom Lorang, of Magnavox Research Laboratories, and by Mr. Donald M. DeVito and Dr. David E. Cartier of The Magnavox Company Advanced Systems Analysis Office. The authors also extend their appreciation to Mssrs. Girard Shoushanian, Edward L. Benz, and Charles L. Morton II, all of The Advanced Systems Analysis Office, for their assistance in preparing the final copy of this report. Lastly, the authors also acknowledge the efforts of the secretaries, Colleen Hayes and Joan Gilbert, in typing this report.

The authors also acknowledge the technical direction provided by Mr. S. W. Novosad, of the Manned Spacecraft Center.

1. INTRODUCTION

This report represents a seven month effort undertaken by The Magnavox Company under contract NAS9-12705 to define possible multipath/RFI experiments for earth orbital relay satellite configurations using a small applications technology satellite (SATS). This study specifies hardware requirements for the recommended configurations and provides recommendations for additional areas of investigation.

Many of the proposed tracking and communication systems for the Space Shuttle have assumed the use of low directivity antennas on links operating in the VHF, UHF, and S-band frequencies. One possible communication link is proposed from a ground station to a synchronous TDRS (Tracking and Data Relay Satellite), and then to the low earth orbit manned vehicle. In this configuration it is well known that multipath and RFI effects are capable of degrading significantly the tracking and communications performance of certain systems. Considerable prior theoretical work has led to the development of various analytic techniques and mathematical models for prediction of the multipath and RFI environment and the degradation due to these effects. Signal processing techniques have been developed to combat the predicted degradation. However, the predictions from past studies vary widely according to the selection of the theoretical parameters used in the various mathematical models. The signal processing techniques heretofore proposed have not been tested in the actual multipath/RFI environment. Experimental data applicable to the TDRS configuration would be invaluable for determining the validity of the mathematical models and the associated signal processing techniques which have been proposed in the past. This study defines experiments for gathering such data.

The scope of this effort includes definition of experiments using the SATS both as the low orbiting platform in conjunction with a synchronous satellite and as the relay satellite in conjunction with aircraft or balloons. First, the existing mathematical models have been evaluated and the best theoretical parameter values to be used in these models have been determined.

Next, we present a discussion of Radio Frequency Interference (RFI). This discussion encompasses presentation of data on the RFI levels present in several bands of interest for the TDRS system, discussion of other noise sources ("trash noise"), a survey of current programs to collect RFI data, and a survey of existing and planned RFI collection equipments. In this last area, considerable detail is presented concerning a planned RFI measurements experiment for SATS.

As a part of this study, we have designed several hardware items which may have potential application to multipath and RFI tests. Specifically, we have designed an adaptive delta mod for voice which operates at 24.0 kb/s. We have also designed a K=5 rate 1/2 convolutional encoder/maximum-likelihood (Viterbi) decoder forward error control unit. The forward error control (FEC) unit will operate at a clock rate sufficient to accommodate the 24.0 kb/s stream. We have also designed a pseudonoise coder which will accommodate data rates of 2.0 kb/s, 6.0 kb/s, and 24.0 kb/s. The pseudonoise transmission system can also be operated in a clear mode. This clear mode is equivalent to a standard PSK modem. We have also provided a design in block diagram form for a wideband FM system based upon the work conducted for NASA by ADCOM, Inc. Detailed designs like those provided for

the pseudonoise transmitter/receiver are not provided for the wideband FM. The reason for this is based upon the conclusions arrived at through the analysis of the performance of the wideband FM system in the presence of RFI and multipath.

We then present an evaluation of the effects of multipath and RFI on clear-mode PSK, PN, and wideband FM systems. This analysis encompasses the effects of multipath and RFI both individually and in combination.

Next, we present a discussion of techniques for measuring multipath. We also present results of experiments, conducted by several organizations, to measure multipath using aircraft platforms.

We then survey other satellites and low altitude platforms for RFI and multipath measurements.

The report concludes with a section containing a summary of conclusions and recommendations. This section also presents tabulations of the costs which would be incurred by NASA in implementing the recommendations.

2. BACKGROUND

As a background to this report, this section discusses the current concepts behind Shuttle/TDRS Service and the existing concepts of the Small Applications Technology Satellite configuration.

2.1 MOST RECENT CONCEPTS BEHIND SHUTTLE/TDRS SERVICE

The primary objective of the Tracking and Data Relay Satellite System (TDRSS) is to insure that, as an integral part of NASA's tracking and data acquisition network, the estimated communications and tracking support required for the post-1975 earth-orbit space program will be satisfied. The mission model for that time period would include the following general classes of users:

a) scientific satellites
b) earth application satellites
c) earth-orbiting manned spacecraft

User needs would require increased coverage, high data rates, increased data processing capability, a minimum of on board data storage, and real time command and data acquisition capability.

It is essential that the service needs of the space program be satisfied in the most cost-effective manner, and that the service provided by the TDRSS be flexible enough to allow for changes in support requirements. Several preliminary studies [References 1, 2, 3, 4, 5, 6, 7, 8, 9, and 10] have been conducted concerning the TDRSS concept, and each has identified various technical problems and areas for trade-off. The most significant area of concern is that of providing communications links with satisfactory

information quality, insuring the operations capability of maintaining contact with the user spacecraft, and developing flexible tracking and data relay service.

2.1.1 TDRSS USER DEFINITION

The user spacecraft have needs and capabilities which cover a wide spectrum. To deal with such diverse needs the spacecraft have been categorized by NASA/GSFC according to data rate requirements into three generic types, namely:

	Forward Link Command Rate	Return Link Telemetry Rate
Low Data Rate (LDR) Users	100-1000 b/s	1-10 kb/s
Medium Data Rate (MDR) Users	100-1000 b/s	10-1000 kb/s
High Data Rate (HDR) Users	100-1000 b/s	>1 Mb/s

For each category range and range rate and the expected maximum number of simultaneous users has been prescribed.

2.1.2 POWER FLUX DENSITY AT THE EARTH'S SURFACE

The Interdepartment Radio Advisory Committee (IRAC) has put forth recommendations regarding the power flux density at the earth's surface from a signal emanating from an earth orbiting satellite. For the bands of interest to the TDRSS the most recent IRAC guidelines are:

Frequency Band	Flux Density in 4 kHz
VHF	-144 dBw/m^2 (recommended)
UHF	-150 dBw/m^2
S-band	-154 dBw/m^2

The carrier flux density at the earth's surface from an emitter with antenna gain G_T can be approximated by

$$\text{Flux density} = \frac{P_T \cdot G_T}{4\pi R^2}$$

where P_T = transmitter power in watts

G_T = antenna gain

R = distance from the emitter to earth in meters

To conform with the IRAC measurement, which is made in a 4 kHz bandwidth, and to take into account any spectrum spreading of the signal, the following relationship is used:

$$\text{Flux density (watts/m}^2\text{ 4 kHz)} = \frac{G_T \cdot P_T \cdot 4\times10^3 \text{ Hz}}{(4\pi R^2)\ BW}$$

With the TDRS at synchronous altitude the expression, when solved for spread bandwidth required to meet the flux density specification is,

$$\text{Spread bandwidth (BW)} = \frac{EIRP \cdot 4 \times 10^3}{4\pi R^2 \cdot [\text{Flux Density}]}$$

or in logarithmic notation

$$BW_{dB} \approx EIRP_{dB} + 36 - 162 - \text{Flux Density}_{dBm/m^2/4\ kHz}$$

The minimum spread bandwidth required to reduce the flux density to an acceptable level is presented in Table 2-1.

TABLE 2-1

BANDWIDTH SPREADING REQUIRED TO MEET IRAC SPECIFICATIONS

FREQUENCY BAND	EIRP	MINIMUM SPREAD BANDWIDTH
VHF	Not Applicable	Not Applicable
UHF	30 dBw	250 kHz
S-band	47 dBw	16 MHz

Current evaluation indicates that the 401 $\pm$ .5 MHz band is preferable for the LDR forward link and VHF is preferable for the LDR return link.

2.1.3 TDRSS TELECOMMUNICATION SUBSYSTEM DESIGN

The major constraints that impacted the TDRS telecommunication design are radio frequency interference (RFI), the multipath environment, and inclement weather at the ground station. The booster payload capability imposes weight, power, and volume limits on the spacecraft which correspondingly limit antenna size, system redundancy, etc. From the outset, the RFI and multipath presented the single most important technical problem area. The use of pseudonoise (PN) modulation and phased array antenna techniques offers a viable solution to these problems for the LDR users.

Telecommunication support required by the users is presented in Table 2-2. The table is divided into three basic categories: LDR user, MDR user, and manned user. The latter, in this case, is the Space Shuttle. In addition to those presented in the table, the ground station/TDRS link is required to operate at Ku-band, with a rain margin of +17.5 dB. Where there are multiple frequencies shown in the table, separated by a virgule (/), the option was given to the contractor to select one or more of these frequencies to support that channel's performance requirements optimally.

2.1.4 TELECOMMUNICATIONS RELAY PERFORMANCE

The integrated attributes of the TDRS design and the telecommunications system design provide a very flexible and high capacity communication, tracking and data acquisition support service. The design presented provides

TABLE 2-2

TDRS TELECOMMUNICATIONS SUPPORT

DESCRIPTION	LDR USER	MDR USER	MANNED USER (Shuttle)
No. of Users	Forward: 2 Return: 20	Minimum of 1	Minimum of 1
Frequency	Forward: VHF, UHF, S-Band Return: VHF	S-Band/X-Band/ K_u-Band	S-Band VHF Backup
Communications Requirement	Forward: 100-1000 b/s command Return: 1-10 kb/s data	Forward: 100-1000 b/s command Return: 10-1000 kb/s data	Forward: 2 kb/s command 1 or 2 voice at 24.0 kb/s Return: 76.8 kb/s data 1 or 2 voice at 24.0 kb/s
Constraints	• Linear Transponder in return link • High RFI • Flux Density (IRAC) VHF $\leq$ -144 dBw/m^2 UHF $\leq$ -150 dBw/m^2 S-Band $\leq$ -154 dBw/m^2 • EIRP = +30 dBw/channel • $G/T_s \leq$ -16 dB (at VHF) • BER = 10^{-5}	• Linear TDRS Transponder in return link • Variable Frequency • Flux Density (IRAC) S-Band $\leq$ -154 dBw/m^2 X-Band $\leq$ -150 dBw/m^2 K_u-Band $\leq$ -152 dBw/m^2 • BER = 10^{-5}	• User Antenna Gain=+3 dB • BER Voice: 10^{-3} Data: 10^{-4} • Flux Density (IRAC) VHF $\leq$ -144 dBw/m^2 S-Band $\leq$ -154 dBw/m^2 • User Transmit Power = 16 dBw

simultaneous support to 20 LDR users and 2 MDR users in the return link, 2 LDR users and 2 MDR users in the forward link, and simultaneous tracking of 20 LDR users through each TDRS. However, in the case of the LDR service even with a system that is optimized to combat interference, the service quality will be a function of the RFI levels, and in the case of the MDR service the quality will be a function of the characteristics of the user terminals.

2.1.4.1 LDR User Forward and Return Link Performance

The forward link signal for LDR service must contend with multipath, RFI, and ambient noise at the user spacecraft. The impact of these effects can be minimized by obtaining the maximum processing gain through a specific bandwidth allocation. The processing gain (PG) obtainable within the system RF bandwidth constraints is proportional to the ratio of the PN chip rate to the data rate. Forward link achievable data rates and rms range and range rate errors are shown in Figure 2-1.

The return link signal through the TDRS must be capable of simultaneously supporting a maximum of 20 LDR users. The choice of PN rates, sequence lengths, and user data rates are interdependent.

The return link performance curves shown in Figure 2-2 are based on 5-watt (37 dBm) user transmit power (P_T) levels. There are two distinct regions of the curves; (1) a lower region where RFI limits performance, and (2) an upper region where performance is limited by noise, multipath, and other user signals. The curves are conservative in that all potential losses have been considered.

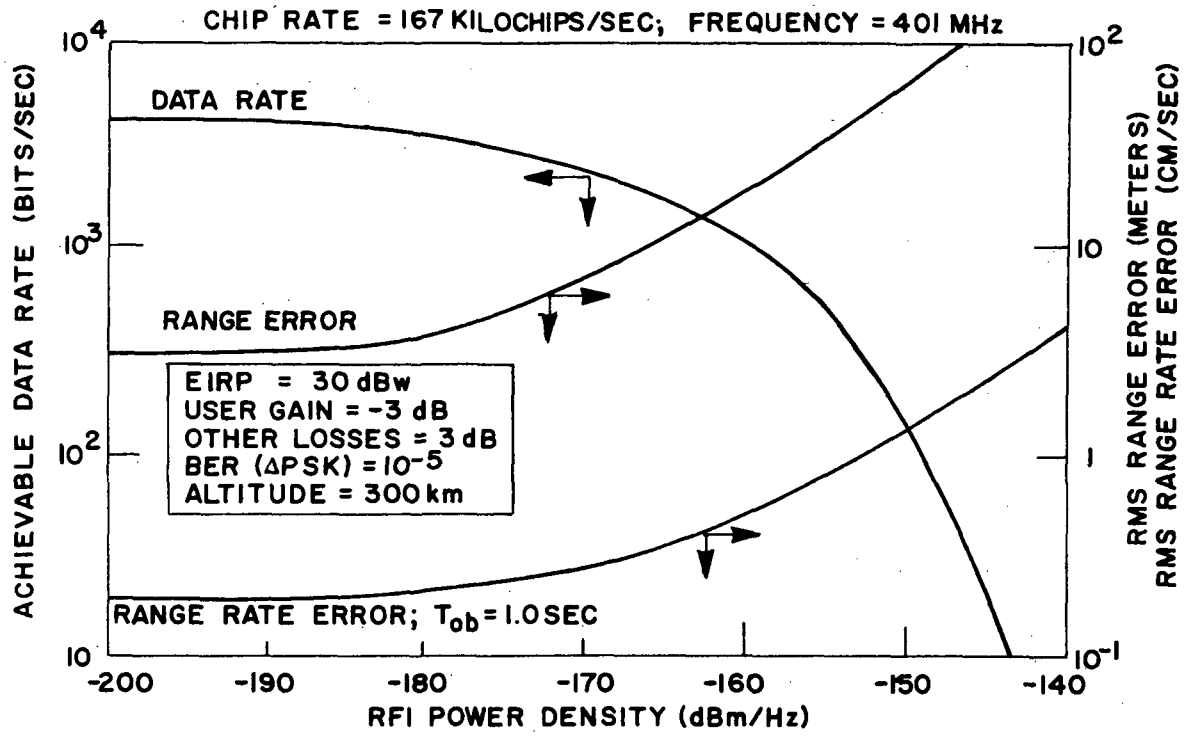

FIGURE 2-1 LDR FORWARD LINK PERFORMANCE: ACHIEVABLE DATA RATE, RANGE ERROR, AND RANGE RATE ERROR

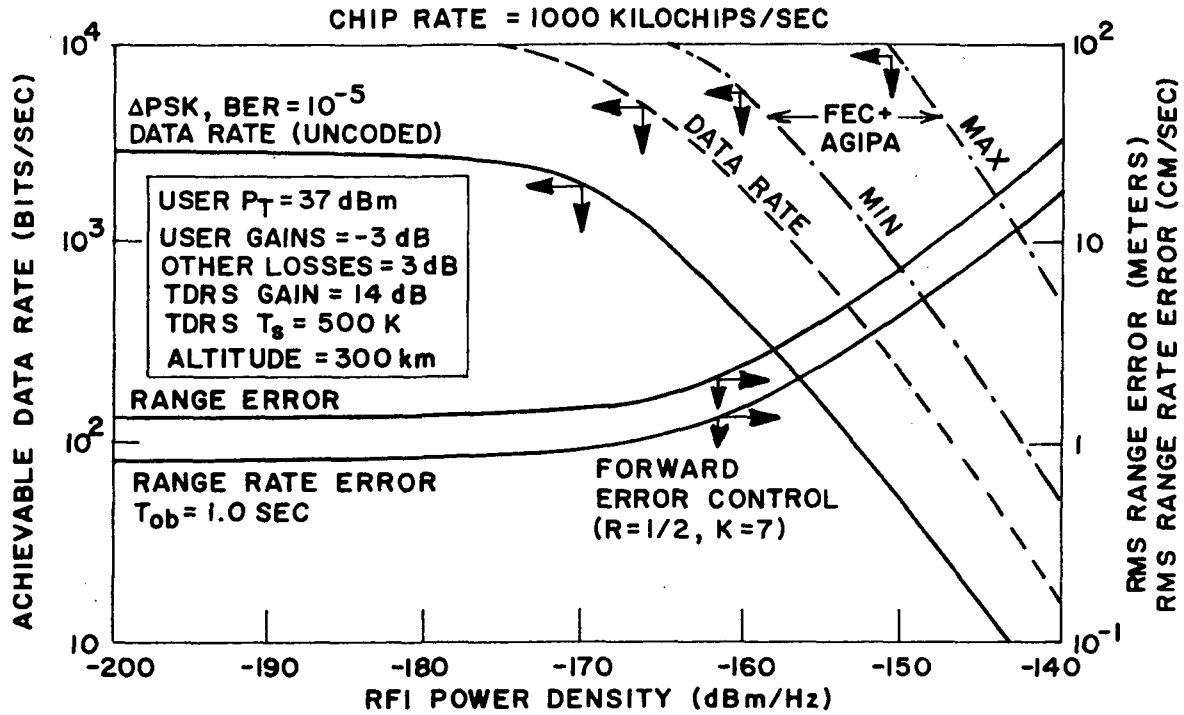

FIGURE 2-2 LDR RETURN LINK PERFORMANCE: ACHIEVABLE DATA RATE, RANGE ERROR, AND RANGE RATE ERROR

If forward error control (FEC) is applied to the return link, the achievable return link data rate is increased by a factor of four (6 dB) [Reference 2]. Moreover, application of the AGIPA (phased array antenna) processing enhances system performance in the presence of RFI by an additional 5 to 15 dB.

2.1.4.2 Detailed Manned User Performance

At this time the postulated manned user in the TDRSS during the first several years of operation is Space Shuttle. The specifications for the link support required for Shuttle are given in Table 2-3.

TABLE 2-3

SPACE SHUTTLE REQUIREMENTS AND CONSTRAINTS

- DATA RATE
  - Forward Link = 2 kb/s
  - Return Link = 76.8 kb/s
- VOICE
  - Forward Link = 24.0 kb/s (1 or 2 channels)
  - Return Link = 24.0 kb/s (1 or 2 channels)
- BIT ERROR RATE
  - Data = 10^{-4}
  - Voice = 10^{-3}
- SYSTEM MARGIN = +3 dB
- SHUTTLE ANTENNA GAIN = +3 dBi

The voice and data for Shuttle on both the forward and return link are multiplexed. The voice modulation is expected to be adaptive-delta-modulation. It has been shown that the required C/N_o to support a voice link with a BER = 10^{-3} and greater than 90% intelligibility is on the order of 49.8 dBHz. The data modulation is assumed to be ΔPSK, for which a

BER = 10^{-4} requires an E_b/N_o of approximately 8.7 dB, so that the required C/N_o is on the order of 41.7 dB-Hz assuming no margin.

2.1.4.3 Shuttle Forward Link Support

As stated, the forward link support for Shuttle consists of one 2 kb/s data link and a minimum of one, but preferably two, voice links multiplexed with the data. The available carrier-to-noise density into a 3 dBi Shuttle antenna is 58.45 dBHz. A typical power budget is presented in Table 2-4 for three modes of operation.

TABLE 2-4

SHUTTLE FORWARD LINK POWER BUDGET

ITEM	BUDGET
EIRP,(1) dBw	47.0
Losses:	
Space, dB	192.0
Polarization, dB	0.1
Pointing, dB	0.5
Shuttle Antenna Gain, dBi	3.0
Received Power, dBw	-142.6
System Noise Temperature,(2) dB	27.3
Boltzmann's Constant, dBw/°K-Hz	-228.6
Noise Density, dBw/Hz	-201.3
TDRS ΔCNR Degradation, dB	0.25
Available C/N_o, dBHz	58.45

(1) Increased EIRP for voice mode only
(2) Uncooled paramp (75°K). Assumed 3 dB line loss.

The carrier-to-noise densities required to support the links of interest (see Table 2-3) have been computed for a system margin of 3 dB, and are listed in Table 2-5. When the C/N_o requirements of Table 2-5 are compared to the C/N_o available (Table 2-4), an estimate of the total margin for the link can be made. These estimates of the total margin available are presented in Table 2-6.

TABLE 2-5

CARRIER-TO-NOISE DENSITY REQUIRED FOR SHUTTLE SUPPORT IN THE FORWARD LINK

LINK	MARGIN	REQUIRED C/N_o
Data (ΔPSK; BER=10^{-4})	3 dB	44.7 dBHz
Voice (Δ Mod; BER=10^{-3})	3 dB	52.8 dBHz
Data + 1 Voice	3 dB	53.44 dBHz
Data + 2 Voice	3 dB	56.16 dBHz

TABLE 2-6

ESTIMATES OF THE ADDITIONAL GAIN REQUIRED TO SUPPORT SPACE SHUTTLE IN THE FORWARD LINK

	DATA	DATA + 1 VOICE	DATA + 2 VOICE
C/N_o, Available	58.45	58.45	58.45
C/N_o, Required*	44.7	53.44	56.16
Total Margin	16.75	5.01	2.29

*Includes a 3 dB margin

Observation of the table indicates that no additional gain is required if the EIRP is 47 dBw. However, for an EIRP of 41 dBw (i.e. high power mode not used), a minimum additional forward link gain of approximately 2.99 dB is required. Link support with that minimum additional gain can be given to either a Data + 1 voice link, or a Data + 2 voice link. This improvement can be achieved through the use of forward error control (see Section 5.2). A rate one-half ($R=\frac{1}{2}$) convolutional code with constraint length of five (K=5), coupled to a Viterbi (maximum likelihood) decoder can provide the gain margin needed.

In addition, the TDRS has the capability to increase the output power over the S-band forward link by a factor of 6 dB. If a 25% duty factor is assumed for voice transmission then the system will provide EIRP of 47 dBw during voice transmission and 41 dBw at times when data only is transmitted. The additional 6 dB provides sufficient margin thereby offsetting the requirement for forward error control if a 25% duty factor is acceptable for Shuttle requirements.

2.1.4.4 Return Link Support

As indicated in Table 2-3, return link support requirements for Shuttle are a data rate 76.8 kbps ($BER=10^{-4}$) and one (acceptable) or two (preferrable) delta modulated voice links at 24.0 kb/s each ($BER=10^{-3}$). The carrier-to-noise density required for return link support of Shuttle is shown in Table 2-7. In the table a +3 dB system margin has been included. Table 2-8 provides an indication of the return link power budget, (i.e. the required transmit power) for Shuttle support. Table 2-8 shows that the additional power gain can be achieved with forward error control as described in the previous section.

TABLE 2-7

CARRIER-TO-NOISE DENSITY REQUIRED FOR SHUTTLE SUPPORT IN THE RETURN LINK

LINK	MARGIN	REQUIRED C/N_o INCLUDING MARGIN
Data: 76.8 kb/s (ΔPSK; BER=10^{-4})	3 dB	60.59 dBHz
Voice: 24.0 kb/s (Δ-Mod; BER=10^{-3})	3 dB	52.8 dBHz
Data + 1 Voice	3 dB	61.35 dBHz
Data + 2 Voice	3 dB	61.92 dBHz

TABLE 2-8

SHUTTLE RETURN LINK POWER BUDGET AT S-BAND

ITEM	DATA[1] (76.8 Kbps)	DATA + 1 VOICE[2]	DATA + 2 VOICE
C/N_o Required, dBHz	57.59	58.35[3]	58.92[4]
Path Loss,[5] dB	191.10	191.10	191.10
System Temperature,[5] dB	26.20	26.20	26.20
Boltzmann's Constant, $\frac{dBw}{°K\text{-}Hz}$	-228.60	-228.60	-228.60
Noise Density, dBw/Hz	-202.40	-202.40	-202.40
Pointing Loss, dB	0.10	0.10	0.10
Polarization Loss, dB	0.50	0.50	0.50
$G_{Shuttle}$, dBi	3.00	3.00	3.00
G_{TDRS}, dBi	30.90	30.90	30.90
ΔCNR Degradation, dB	0.50	0.50	0.50
System Margin	3.00	3.00	3.00
FEC Coding Gain,[6] dB	4.70	4.70	4.70
REQUIRED TRANSMIT POWER[7] dBw	*11.79*	*12.55*	*13.12*

(1) ΔPSK, BER = 10^{-4} (E_b/N_o = 8.7 dB)

(2) Voice is Delta-modulated at 24.0 kb/s; carrier modulation is ΔPSK (BER = 10^{-3}; C/N_o = 49.8 dBHz)

(3) Combined value of data (C/N_o = 57.59) and one voice (C/N_o = 49.8)

(4) Combined value of data (C/N_o = 57.59) and two voices (C/N_o = 52.8)

(5) Values selected at the point where their combined effect is maximum

(6) R=½, K=6 convolutional code with Viterbi decoder

(7) Transmit power into antenna

2.1.4.5 Combined Voice and Data Transmission

Simultaneously transmission of voice and data can be accomplished efficiently by several techniques: frequency, time, and phase multiplexing. Of the three phase multiplexing is the preferred technique. The phase multiplexing concept as applied to delta-modulated voice and straight binary data can be relayed in a concept referred to as quadraphase modulation (i.e. a quadrature carrier multiplexing). The system is fully digital with the exception of audio processing and filtering circuits and provides for transmission of a constant envelope signal.

2.2 SATS SPACECRAFT

A basic objective and outstanding characteristic of the SATS program is a standard spacecraft for flight testing applications experiments and concepts. The standard spacecraft concept has been proposed for many years. Whether for lack of advanced planning, or the necessity of designing for particular missions, or the desire for a fully integrated spacecraft and experiments, most spacecraft subsystems and structures were modified for each succeeding launch of a spacecraft series. Many of the modifications were desirable but not really mandatory. The objective of a standard SATS does not permit constant spacecraft subsystem and system redevelopment. Advanced subsystems would be considered experiments and would be flown such that the spacecraft could operate independently from them. After flight qualification, and, if required, modifications to the standard spacecraft could be performed on future models.

Mission and experiment requirements create most of the design problems on any spacecraft. These items can completely negate a standardized

spacecraft concept if they are not well defined or controlled. The standardized spacecraft will have to adapt to a variety of missions. The spacecraft will also have to use an experiment module separate from the basic spacecraft, with a controlled, specified interface. The capabilities of the SATS experimental package is presented in Table 2-9.

TABLE 2-9

SATS EXPERIMENTAL PACKAGE CAPABILITY

Power	30 watts orbital average, 28 volts ±2%
Weight	34 to 68 kg (75 to 150 lbs.)
Volume	283 Liters (10 cubic feet)
Telemetry	Variable formats and data rates
Command	Real Time and Stored
Data Storage	10^6 to 10^8 bits
Attitude Control System	Earth oriented ±.019 radian (±1°)
Thermal	Independence between spacecraft subsystems and the experiment

(From Reference 11)

2.2.1 EXPERIMENT REQUIREMENTS

It is recognized that a major problem in implementing a standardized spacecraft is the need to meet changing experiment requirements. In the past, most spacecraft systems have been designed to meet particular experiment requirements. The experiment and subsystems were then integrated within a common structure. Any change in experiment volume, weight, power, or data handling requirements from one launch to another required rearrangement, reintegration and general retest of the whole spacecraft. This always involved increased costs and time. The SATS design philosophy is to physically isolate the experiment and related hardware from the operational

subsystems (e.g. transmitter, controls, power supply, etc.). This concept has been used on the SAS and OV-1 and -3 satellites. The spacecraft would be integrated using major blocks of systems in modular form. These would include an experiment compartment or module, base module, solar array (paddles), and a propulsion module for the geosynchronous missions. The spacecraft design would develop an electrical, mechanical, and thermal interface specification for integrating all experiments. The volume limits are theoretically the vehicle envelope; however, the spacecraft would provide specific mounting platforms and covered volumes or the experiment could provide its own experiment module to mate with the standard base module interface. It should be noted that the experiment weight is defined as everything above the primary experiment module/base module interface, including the experiment module structure itself.

The electrical interface will consist of a standard set of electrical connections for power, command and data transfer between the experiment module and the subsystem module. Power will be made available to the experiment via the main bus. Any special voltage or regulation requirements will be met by the experimenter. Connections will be available for a fixed number of commands to, and housekeeping points from, the experiment module. The main data connections will consist of a fixed number of points, the sampling and formatting of which will be variable through the use of the programmable spacecraft data system. Any data storage or handling requirement in excess of that provided by the base module subsystems will be the responsibility of the experimenter.

2.2.2 DESIRED SPACECRAFT CHARACTERISTICS

The characteristics listed below were chosen to keep costs at a minimum and to realize quick reaction from experiment selection to data return.

a) To implement the design requirements and to maintain some packaging flexibility, the SATS spacecraft will adopt a random packaging concept. In many Explorer spacecraft the packaging goal has been efficiency of volume and weight for specific missions and experiments. This high density packaging is used for example on IMP's and SSS. The major disadvantage is that the spacecraft assembly, harness, balance, packaging, distribution, and integration is highly dependent on the exact dimension (height) of each and every electronic card. These cards are shaped and stacked such that a design change, poor volume estimate by designers or experimenters, electrical interference, or last minute modifications during the integration and test phase can cause extensive rearranging of the subsystems. This is expensive and time-consuming. Although the SATS base module is basically a fixed design, there is some flexibility with random packaging and excess volume. This will result in quick response to an unforeseen change.

b) The development costs and initial design will be reduced from previous spacecraft programs because available subsystems and hardware will be used with a minimal amount of modification. Use of subsystems presently being designed for other spacecraft programs will also be made wherever possible. On later spacecraft updating or improvement might be incorporated, this would only be done if mandatory.

c) Along the same line of reasoning, it is desirable to have as much commonality as possible among subsystems of each of the spacecraft types. This will be limited only by unique mission requirements.

d) The capability of adding a propulsion module is a required feature of the structural design. Auxiliary propulsion is required for synchronous orbit insertion (i.e. kick motor) and station keeping.

e) The fact that SATS is a test-bed spacecraft implies that a long lifetime is not required. Most experimenters indicate that lifetimes from a few hours or orbits to less than 6 months would be satisfactory to test feasibility or operation of an experiment. It is also desirable to have a short lifetime goal for other reasons. The orbital altitude can be set lower initially for better earth observation or geodetic measurements. Other mission parameters such as drift, inclination, and eccentricity are less critical. Redundancy can be reduced, but quality control and assurance will be maintained at a high level.

f) The spacecraft basic design would incorporate a large number of housekeeping channels to monitor the test and engineering performance of the experiments. Being a testbed spacecraft, a prime requirement is to determine the experiment status and examine its engineering and performance functions most critically. On most large spacecraft, because of the number of experiments and complex systems, the housekeeping channels are minimal for each experiment.

Table 2-10 presents a summary of the basic design parameters for the experimental satellite.

TABLE 2-10

SATS SPACECRAFT ANALYSIS

Power (orbital average) 28 volts ±2% regulation

Base Module	30 watts
Experiment	30 watts

Data Handling

1 to 40 kilobits/sec
Two switchable bit rates
Three Program Formats (2 fixed, 1 programmable)

Command

Real Time - 1024 bits/sec
Up to 128 delayed executions (half of these available to experiment)

Thermal

Isolation between experiment and base modules

Attitude Control

Three axis earth oriented
Stability ±.019 radian (±1°) pitch and roll; ±.038 radian (±2°) yaw
Maximum body control rate .0017 rad/sec (.01°/sec)
Determination ±.009 radian (±0.5°) pitch and roll, ±.038 radian (±2°) yaw

Communication

VHF for low data rate experiment and housekeeping data
S-band for wideband experiment data and tape recorder dump

Weight

Spacecraft at Launch:	up to 165 kg (364 lbs) Scout Configuration; approx. 685 kg (1500 lbs) Delta Configuration
Available for Experiment:	up to 68 kg (150 lbs) Scout Configuration approx. 91 kg (200 lbs) Delta Configuration

Volume Available for Experiment

Approximately 196 liters (7 ft^3)

Orbit

a) Scout Launch Vehicle: low altitude, typical inclinations of 0 (0°), .66 radian (38°), .87 radian (50°) or sun synchronous at various local times

b) Delta Launch Vehicle: geosynchronous orbit

3. CHANNEL DESCRIPTION

The channel between a low altitude aircraft or spacecraft and a synchronous relay satellite is illustrated in Figure 3-1.

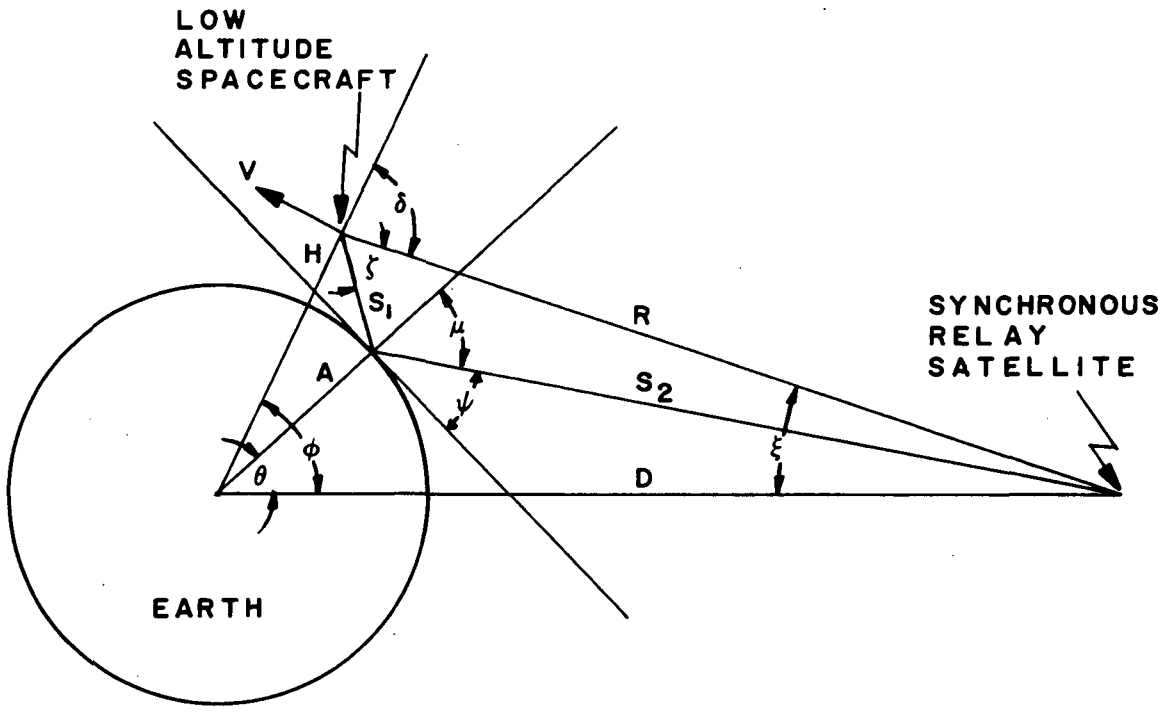

FIGURE 3-1 LOW ALTITUDE SATELLITE / SYNCHRONOUS RELAY SATELLITE GEOMETRY

Depending upon the antenna patterns associated with the low altitude platforms, the link between a synchronous relay satellite and the low altitude platform can be described by a number of statistical parameters.

Table 3-1 lists the deterministic parameters which characterize the link between a relay satellite and a lower altitude platform. Also shown in Table 3-1 are comments as to whether or not the parameter requires measurement. For example, in the case of differential time delay between the direct path and the indirect path no extensive measurement is required since the differential time delay is purely a matter of geometry and the

TABLE 3-1

COMPARISON OF THE RELATIVE MAGNITUDE OF THE PROPAGATION CHANNEL PARAMETERS FOR A SYNCHRONOUS RELAY SATELLITE/LOW ORBITING SATELLITE LINK

Description	VHF	S-band
Attenuation Effects:		
Free Space Attenuation		
Direct Path Loss	165-169 dB	189-192 dB
Indirect Path Loss	167-170 dB	191-193 dB
Ionospheric Absorption	<.1 dB	<.001 dB
Tropospheric Absorption	<.05 dB	<.3 dB
Losses due to Aurora	<1 dB	<.1 dB
Refraction:		
Ionospheric Refraction	$<10^{-3}$ radians	$<10^{-5}$ radians
Tropospheric Refraction	negligible	negligible
Signal Phase Delay:		
Ionospheric Effects	$= 10^{-8}$ sec	$= 10^{-8}$ sec
Tropospheric Effects	$= 10^{-6}$ sec	$= 10^{-8}$ sec
Birefringence	$< 10^{-9}$ sec	$< 10^{-9}$ sec
Multipath Time Delay	.2-30 msec	.2-30 msec
Polarization Rotation:		
Chromatic Aberration	<.035 radian/MHz	<.035 radian/MHz
Faraday Rotation*	= 3.49 radians	= .017 radian
Frequency Effects:		
Direct Path Doppler	0-4 kHz	0-57 kHz
Differential Doppler	0-2 kHz	0-34 kHz
Fading Bandwidth	0-2 kHz	0-40 kHz
Coherent Bandwidth	5-30 kHz	5-30 kHz

* For systems employing circularly polarized antennas, Faraday rotation effects are not encountered.

predicted value only need be confirmed by experiment. The same can be said for the differential doppler but with less conviction. Other theoretical parameter values are subject to the models which are employed, and for this reason require specific measurement.

3.1 GEOMETRIC PARAMETERS

Prior to defining the parameters which characterize the channel, the dynamic geometry of the synchronous relay satellite system must be analyzed to identify quantitatively each of the channel parameters. Each of the low altitude SATS spacecraft will present a unique time varying multipath geometry as illustrated in Figure 3-1. From the representation above of the synchronous relay satellite multipath geometry problem, the time varying relationships have been established. In Figure 3-1, R is the direct path between the synchronous relay satellite and low altitude SATS spacecraft. The reflected path consists of two components, S_2 from the synchronous relay satellite to earth and S_1 from the earth to the low altitude SATS spacecraft.

Assuming a smooth spherical earth and without considering the effects of the ionosphere and troposphere on such factors as polarization, attenuation, and path length, curves for several of the critical channel parameters have been plotted by Golden (Reference 12). These curves are representative of data that must be analyzed for the channel between the synchronous relay satellite and low altitude SATS spacecraft. The use of these curves will be apparent after the various parameters of the channel are defined.

By referring to Figure 3-1, functions can be found defining geometric parameters of the satellite configuration as a function of low altitude satellite location. The length of the direct path between a synchronous relay satellite and a low altitude SATS spacecraft is shown in Figure 3-2. Cutoff in the curves is due to obscuration of the user spacecraft by the earth. The angle where this occurs varies with altitude of the user. The differential path length, i.e., the difference in path length between the direct and reflected paths, is shown in Figure 3-3.

Figures 3-4, 3-5 and 3-6 show curves of the range rate of the direct and indirect paths ($S = S_1+S_2$ of Figure 3-1) as a function of low altitude SATS location for altitudes of 200 km, 1000 km, and 4000 km, respectively. Also shown on each of these curves is the difference in the range rates.

3.2 CHANNEL PARAMETERS

The parameters which characterize the channel between a synchronous relay satellite and low altitude SATS spacecraft are defined in this section.

Doppler shift of the transmitted signal over all paths is of importance because it is a factor in determining the total bandwidth required for a signal. Usually the direct path Doppler must be added to the known or expected instabilities in the carrier frequency of the transmission to determine the total required bandwidth.

3.2.1 DIRECT PATH DOPPLER

The direct path signal between a synchronous relay satellite and a low orbiting SATS can be considered to encounter a frequency shift, or Doppler shift, due to the relative velocity between the low altitude SATS

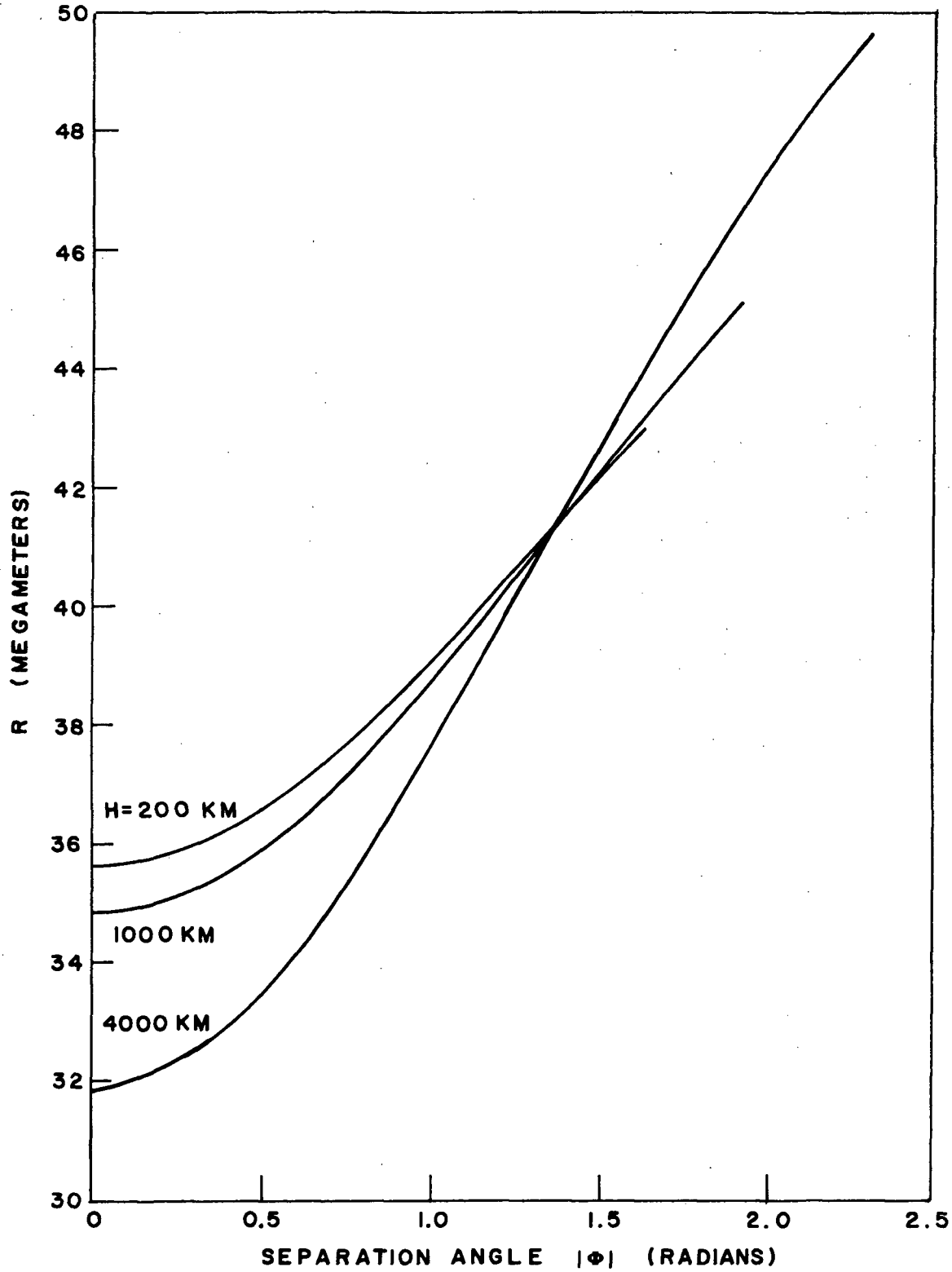

FIGURE 3-2 DIRECT PATH RANGE BETWEEN A LOW ALTITUDE SPACECRAFT AND A SYNCHRONOUS RELAY SATELLITE

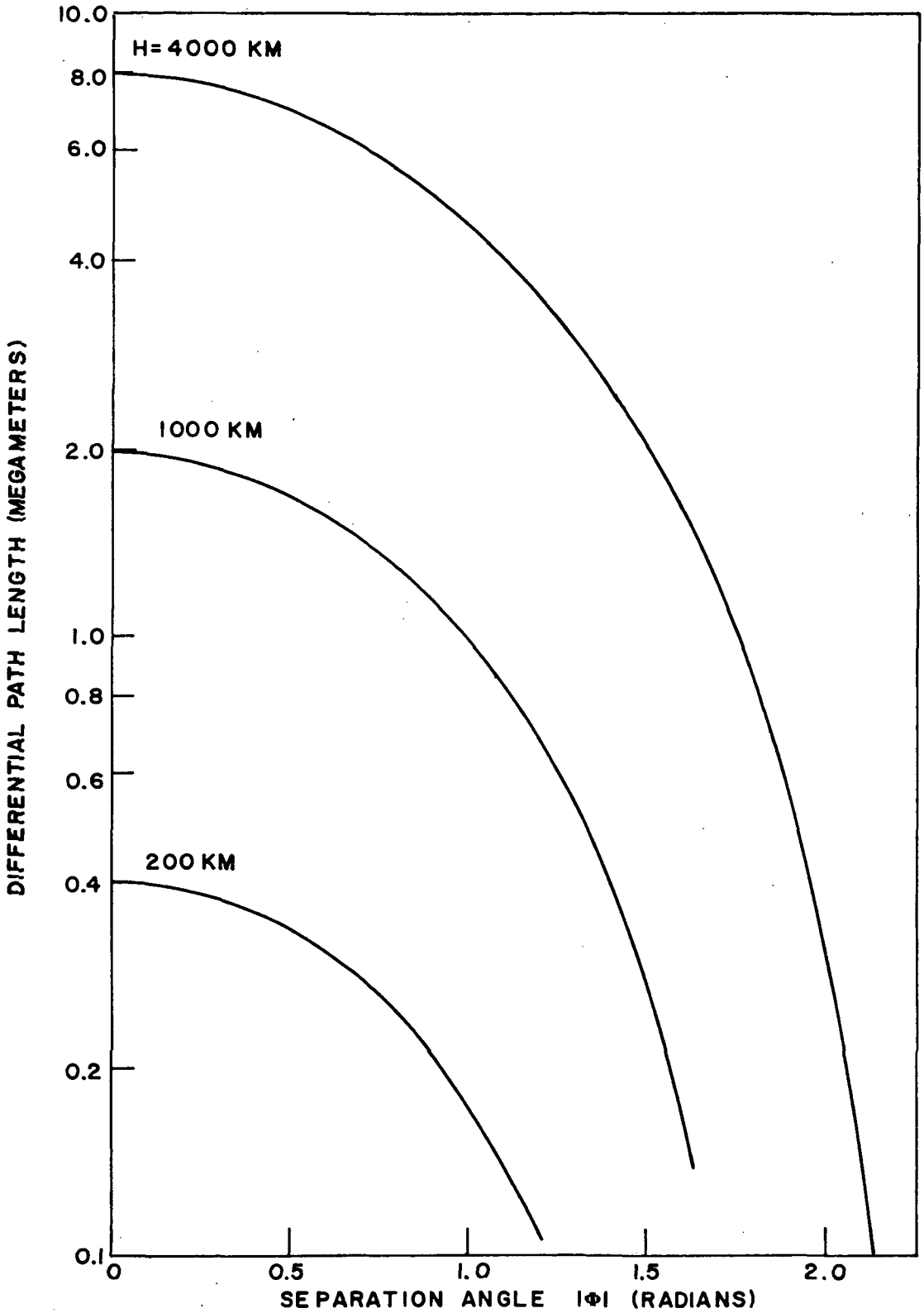

FIGURE 3-3 DIFFERENTIAL PATH LENGTH (Δ) BETWEEN A LOW ALTITUDE SPACECRAFT AND A SYNCHRONOUS RELAY SATELLITE

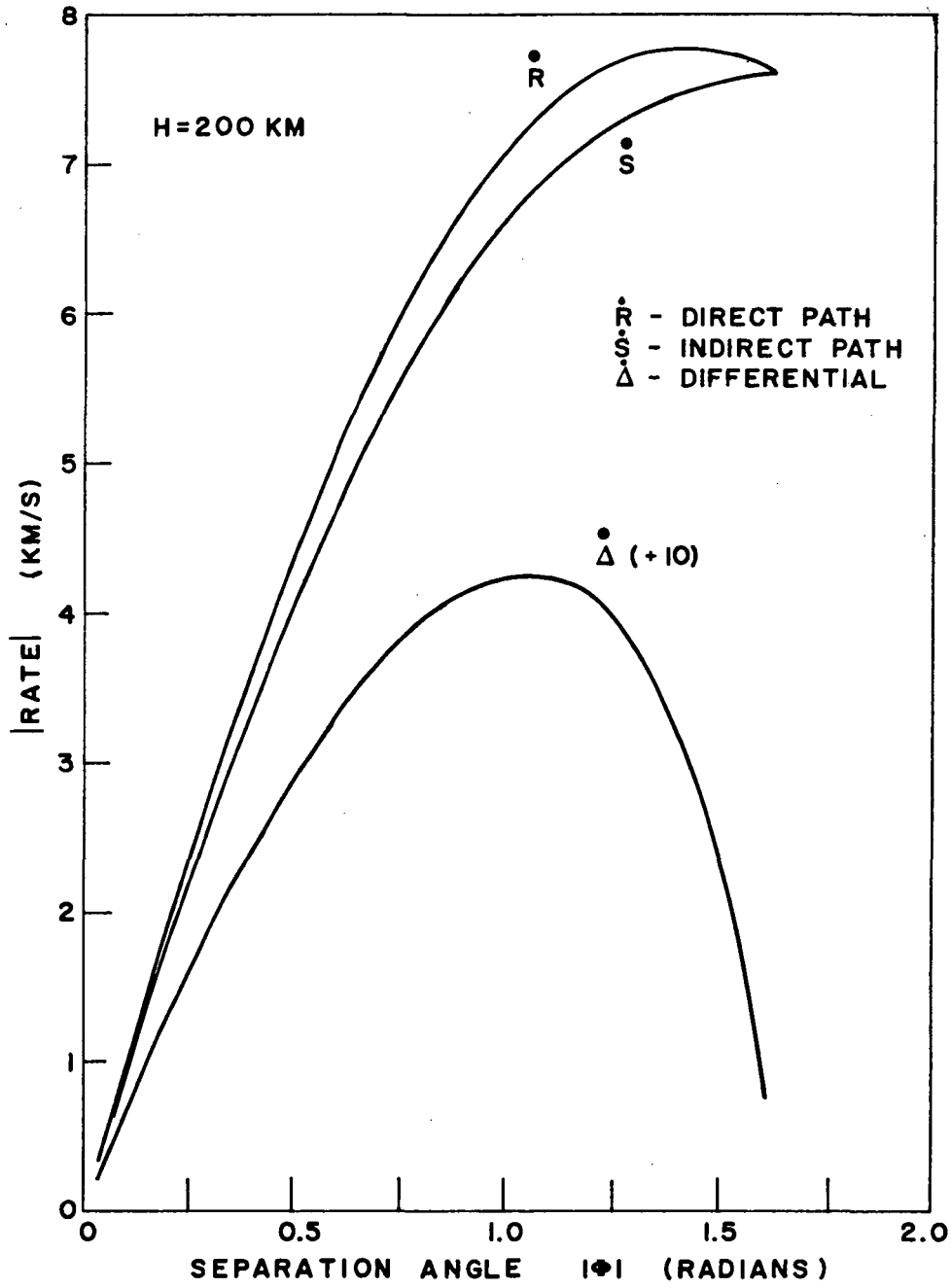

FIGURE 3-4 DIRECT PATH RANGE RATE, INDIRECT PATH RANGE RATE, AND DIFFERENTIAL RANGE RATE BETWEEN A LOW ALTITUDE (200 KM) SPACECRAFT IN A CIRCULAR ORBIT AND A SYNCHRONOUS RELAY SATELLITE

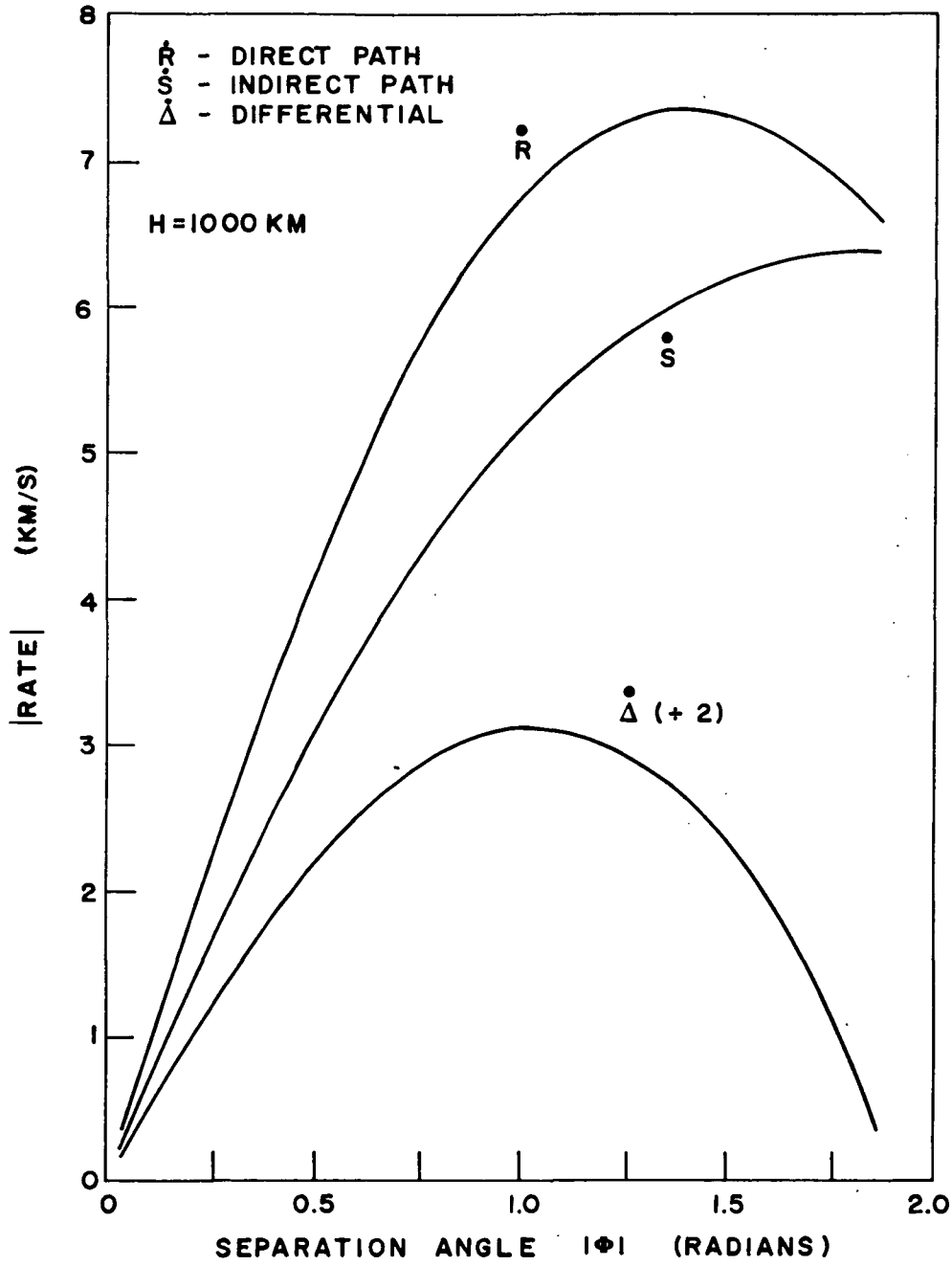

FIGURE 3-5 DIRECT PATH RANGE RATE, INDIRECT PATH RANGE RATE, AND DIFFERENTIAL RANGE RATE BETWEEN A LOW ALTITUDE (1000 KM) SPACECRAFT IN A CIRCULAR ORBIT AND A SYNCHRONOUS RELAY SATELLITE

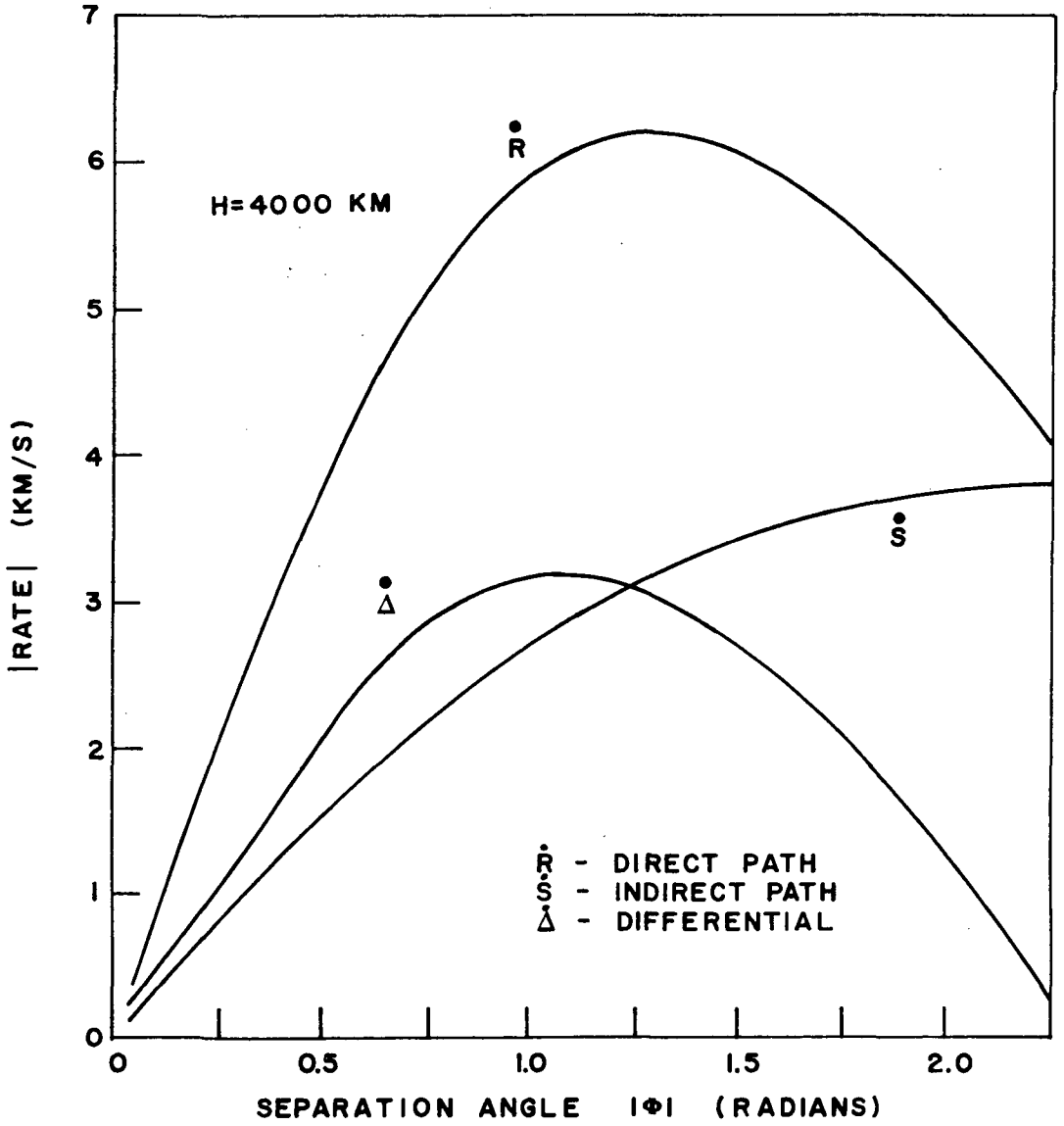

FIGURE 3-6 DIRECT PATH RANGE RATE, INDIRECT PATH RANGE RATE, AND DIFFERENTIAL RANGE RATE BETWEEN A LOW ALTITUDE (4000 KM) SPACECRAFT IN A CIRCULAR ORBIT AND A SYNCHRONOUS RELAY SATELLITE

and the synchronous relay satellite. This Doppler frequency is time-varying due to the changing geometry between the two spacecraft. The time rate of change of the Doppler shift is proportional to the time rate of change of the angle between the synchronous relay satellite and the low altitude SATS spacecraft.

The direct path Doppler frequency shift for three user satellite orbital altitudes is shown in Figure 3-7. These curves, for a 136 MHz carrier, show that the maximum Doppler shift is approximately 3800 Hz. Although curves are not shown for S-band, it can be calculated that for a 2.3 GHz carrier the maximum Doppler shift will be approximately 57 kHz. Thus the expected Doppler frequency range is 0 to approximately 57 kHz, depending on the height of the orbit.

3.2.2 INDIRECT PATH DOPPLER EFFECT

The indirect signal reflects off the earth at some random angle. This implies that there is some relative non-zero angle between the direct signal and the reflected signal at the earth's surface. Thus, a Doppler shifted signal is obtained from the multipath signal which is not equal to the Doppler signal from the direct path. This Doppler component due to specular reflection at the earth's surface is characterized in Figure 3.8. As we will show later, there is a diffuse component to the multipath signal due to irregularities in the surface of the earth. This diffuse component produces a Doppler spectrum or fading bandwidth which is also characterized in Figure 3-8. As shown in Figure 3-9, which is drawn for reasonable roughness factors and correlation lengths, the primary source of reflected

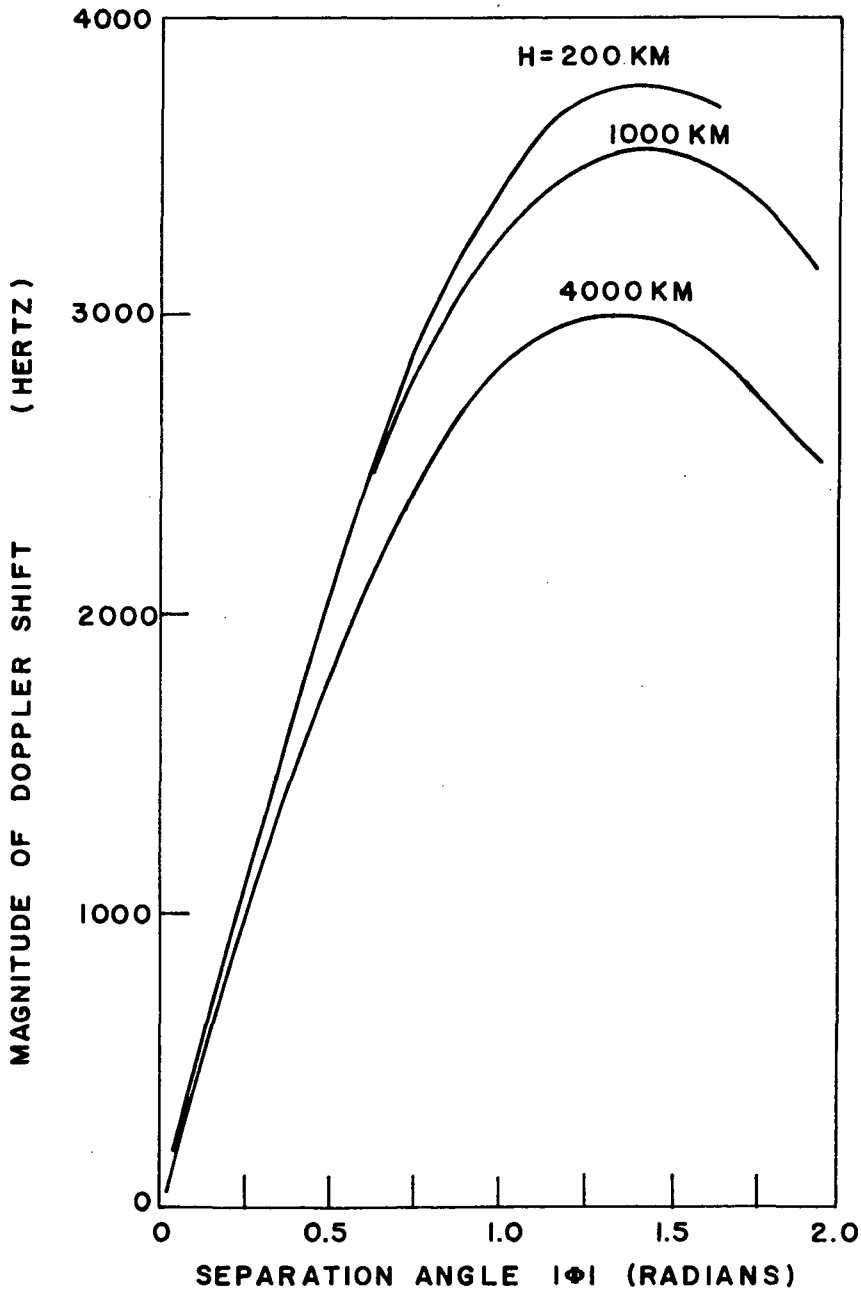

FIGURE 3-7 DOPPLER SHIFT OVER THE DIRECT PATH FOR 136 MHz CARRIER FREQUENCY

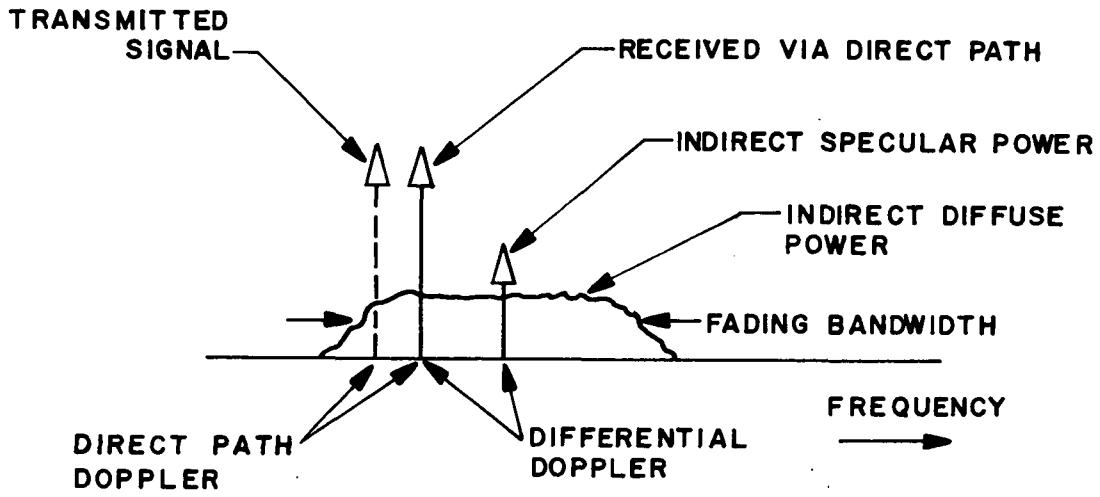

FIGURE 3-8 CHANNEL RESPONSE IN THE FREQUENCY DOMAIN

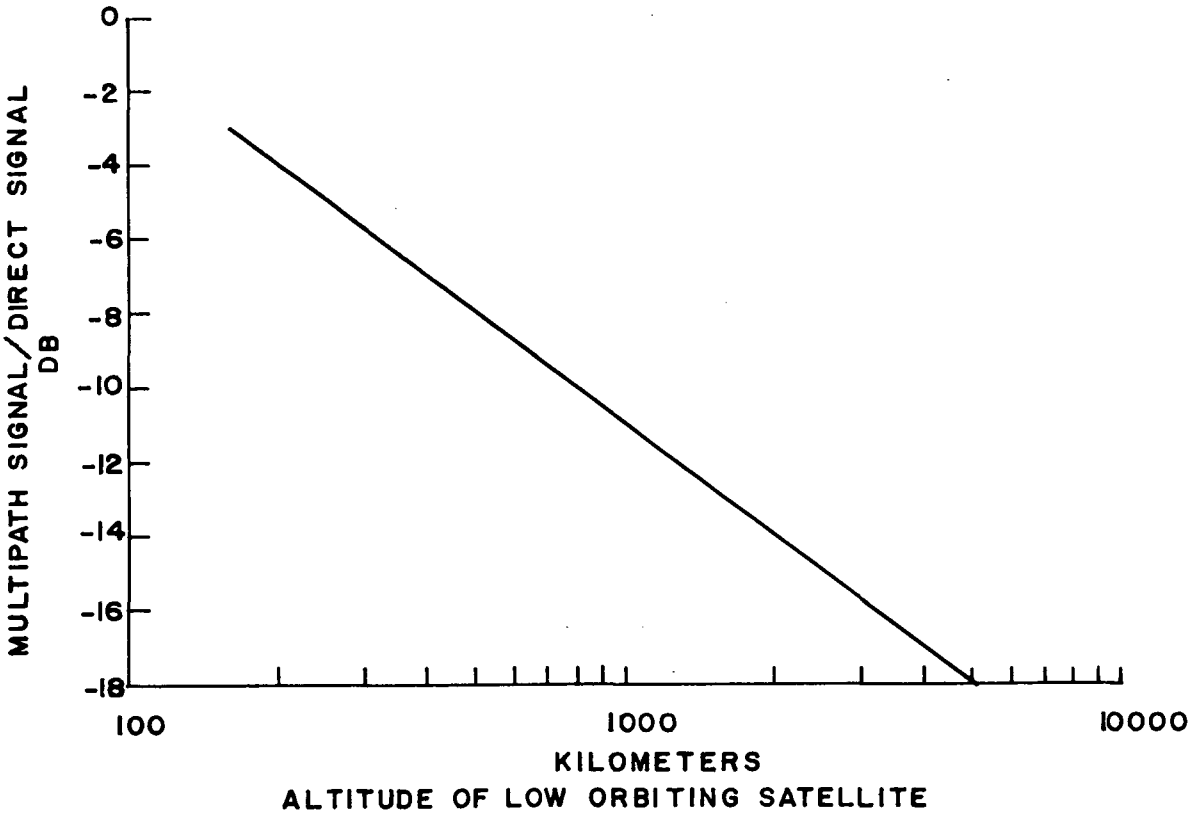

FIGURE 3-9 MULTIPATH/DIRECT SIGNAL RATIO AS A FUNCTION OF ORBITAL ALTITUDE

power is diffuse for grazing angles greater than 0.35 radians. Figure 3-10 shows the differential Doppler shift (i.e., difference between direct path Doppler and indirect path Doppler) as a function of the position of the low altitude satellite.

3.2.3 DIFFERENTIAL DELAY

This parameter is a measure of the difference in time delays between receiving the direct signal and the multipath signal. Figure 3-11 shows the total delay along the direct path as a function of low altitude SATS location. This is obtained by relating the direct path range (as shown in Figure 3-2) to the velocity of propagation (assumed to be the speed of light). Figure 3-12 shows the differential path length delays, or the difference in arrival time between the direct and indirect signals, as a function of SATS altitude. From Figure 3-12, this time delay can be seen to be approximately 0.2 milliseconds for a 200 km orbit at $\Phi = 1.57$ radians and 30 milliseconds for a 4000 km orbit at $\Phi = 0$.

3.2.4 COHERENT BANDWIDTH

Coherent bandwidth is another parameter which is important in the evaluation of any system exposed to multipath signals. The coherent bandwidth B_C can be defined in several ways, but two preferred methods are illustrated in Figure 3-13.

In Figure 3-13 we indicate that two transmitted carriers separated in frequency by Δf are received at the synchronous relay satellite from a low altitude spacecraft via the direct and the indirect paths. The value of Δf which is needed to produce a value of 1/2 for the normalized correlation coefficient between the two carriers received via the reflected path is defined as the coherent bandwidth B_C. This definition is <u>independent</u> of the signals

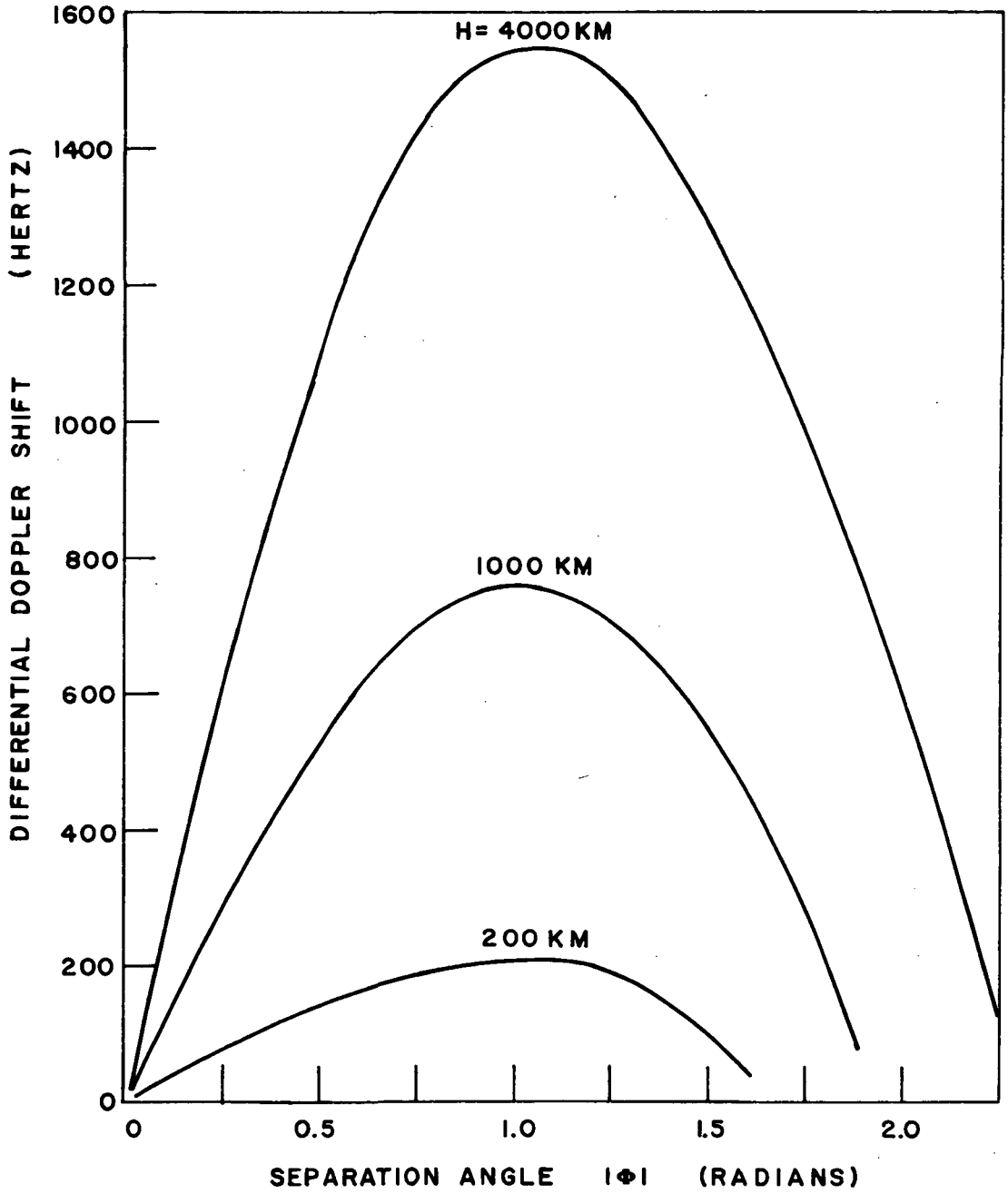

FIGURE 3-10 DIFFERENTIAL DOPPLER AS A FUNCTION OF LOW ALTITUDE SPACECRAFT POSITION

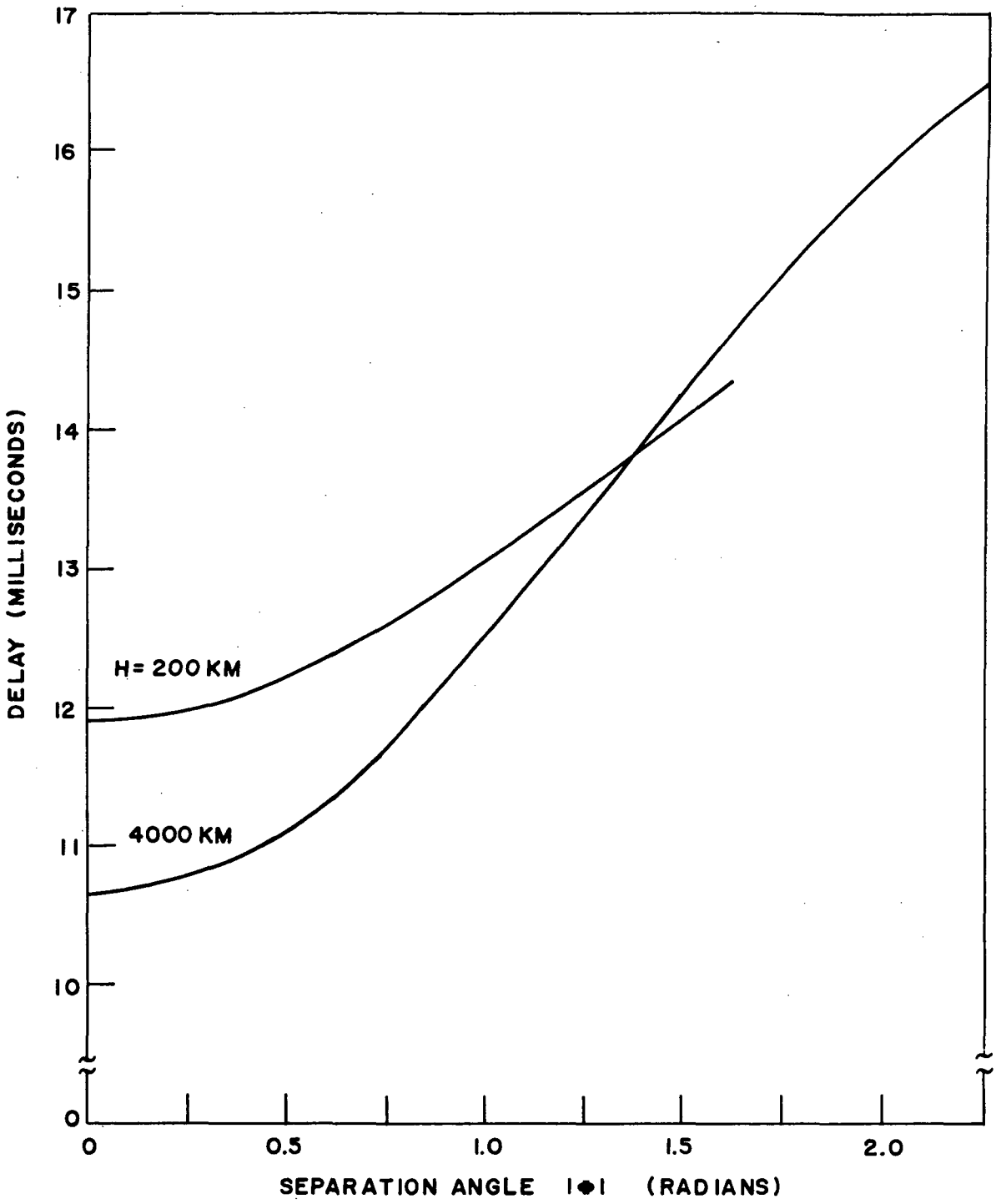

FIGURE 3-11 TOTAL DELAY ALONG DIRECT PATH AS A FUNCTION OF LOW ALTITUDE SPACECRAFT LOCATION

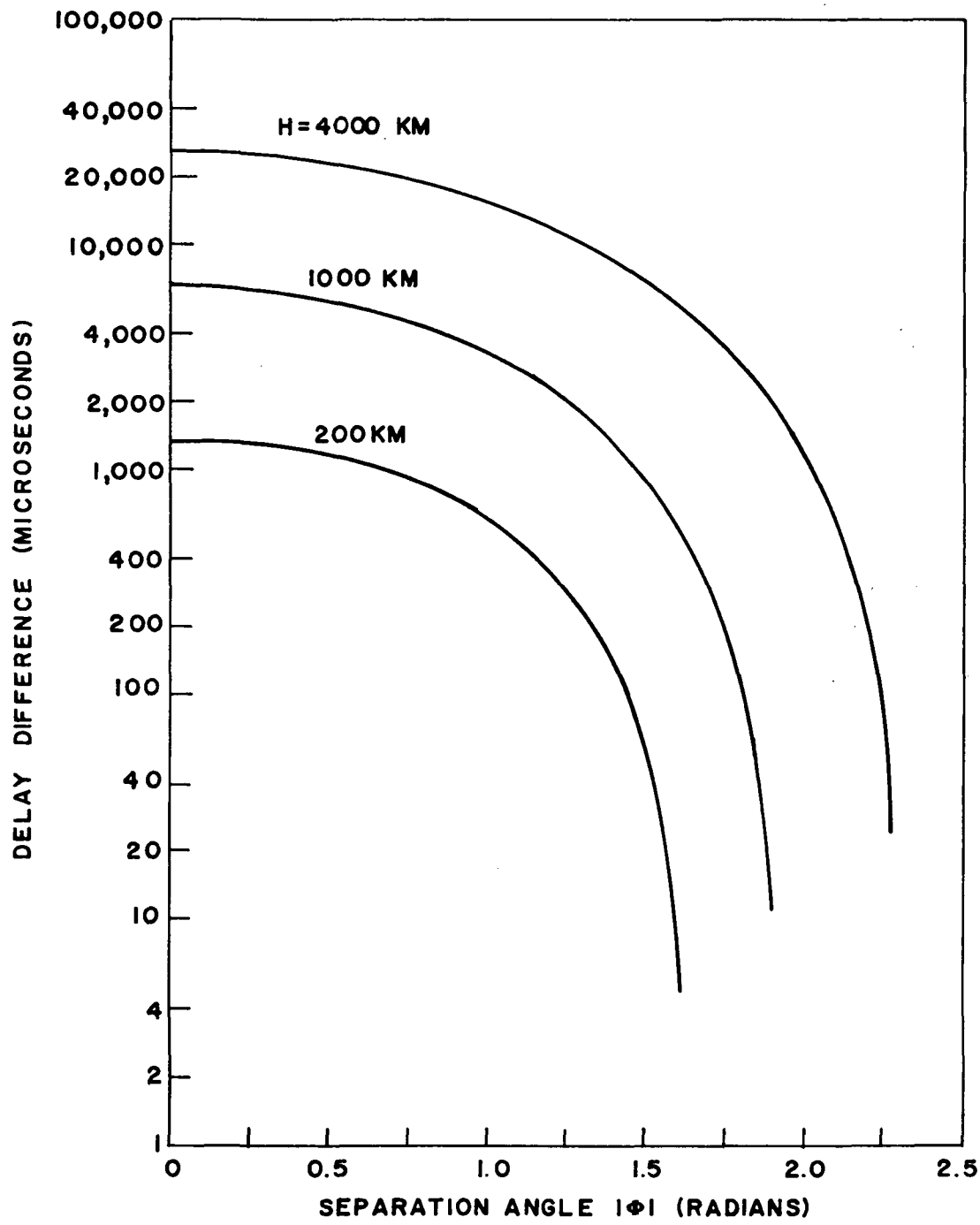

FIGURE 3-12 DIFFERENTIAL TIME DELAY AS A FUNCTION OF LOW ALTITUDE SPACECRAFT POSITION

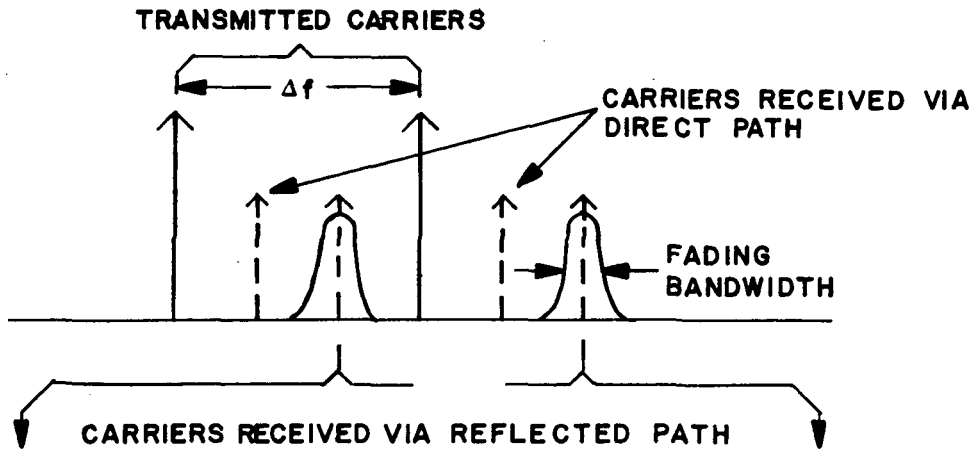

WHEN THE COMPLEX ENVELOPE CORRELATION FUNCTION BETWEEN THE TWO CARRIERS RECEIVED VIA THE REFLECTED PATH $\rho(\Delta f)$ IS EQUAL TO 0.5, THE VALUE OF Δf IS THE COHERENT BANDWIDTH.

a) FREQUENCY DEFINITION

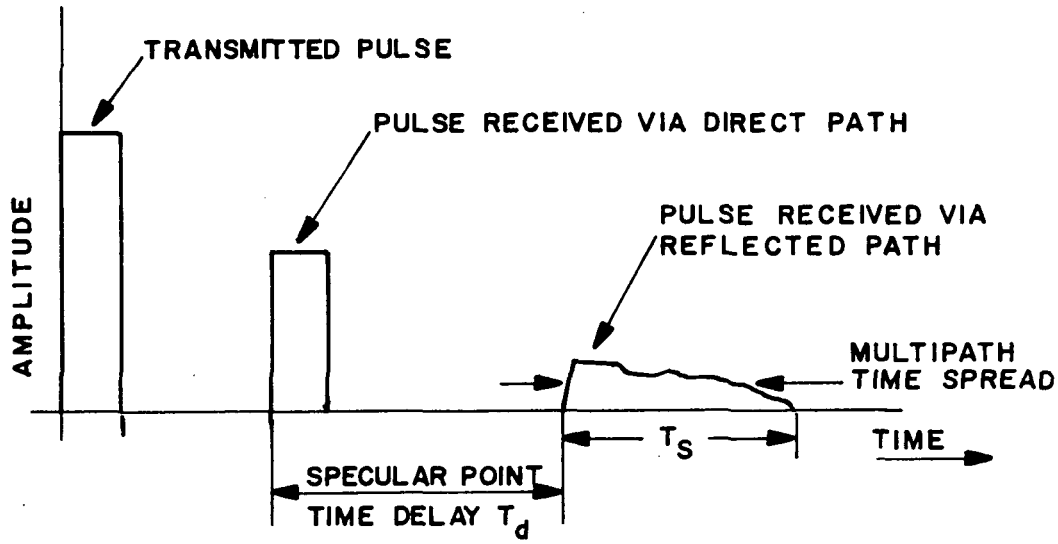

$$\text{AVERAGE MULTIPATH TIME SPREAD} = \frac{1}{\text{COHERENT B.W.}}$$

b) TIME DEFINITION

FIGURE 3-13 COHERENT BANDWIDTH

received via the direct path. Definition of coherent bandwidths based on the transmission of two CW signals separated in frequency is an accepted definition in the literature and is a measure of the coherent bandwidth of a fading channel. The inverse time spread is related to coherence bandwidth through some constant factor which is usually a statistical parameter such as the RMS spread in the time associated with the reflected signal. In the case of a synchronous relay satellite, B_C does not necessarily limit the data capacity of the transmission link.

As in Figure 3-13b, if a pulse is transmitted by a low altitude SATS it will be received after some time via the direct path at the synchronous relay satellite. At some time T_d later the multipath signal will arrive. The multipath signal will be varying with time and will be characterized by an average multipath time spread. The value of B_C is important from a system point of view in that various signaling techniques such as frequency diversity require that the carriers be spaced in excess of the coherent bandwidth in order to provide full diversity action or maximum system performance. Time spread in a reflected signal is also of importance when time hopping pulse transmission techniques are used as the basis for signaling schemes. Figure 3-14 represents the parameters previously described as a function of the grazing angle.

3.2.5 ATTENUATION EFFECTS

Figure 3-15 shows the regions of atmosphere. Due to density effects and diurnal effects the heights of these layers in the ionosphere shift, but are essentially as shown in the figure. The troposphere remains essentially at the 30 km height. Although low altitude satellites are located within the ionosphere, the multipath signal, and under some geometries

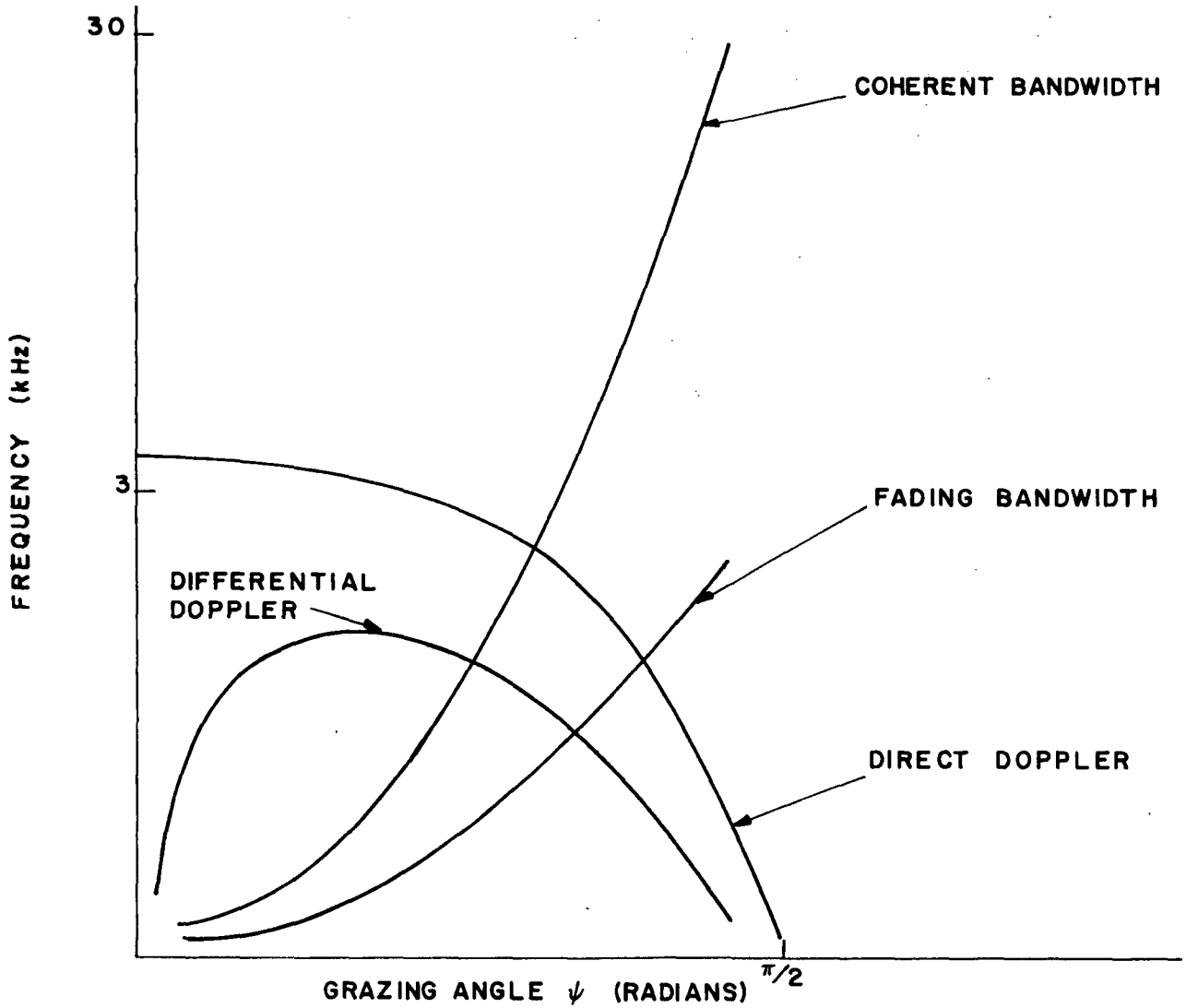

FIGURE 3-14 QUALITATIVE RELATIONSHIP OF FREQUENCY RANGE VS. GRAZING ANGLE FOR VARIOUS PARAMETERS

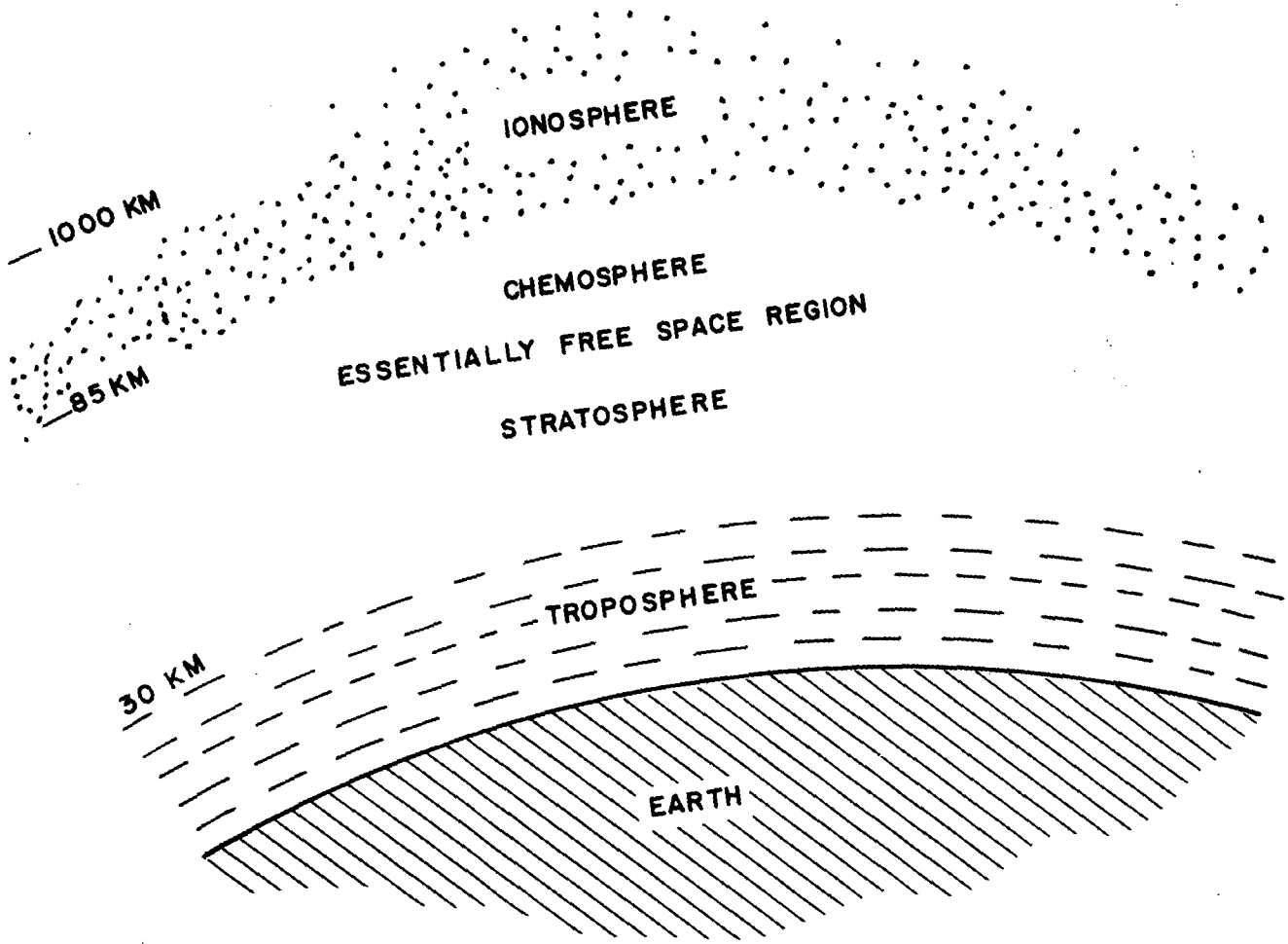

NOTE: ALTITUDES SHOWN ARE APPROXIMATE

FIGURE 3-15 THE REGIONS OF THE ATMOSPHERE

the direct signal (e.g. low grazing angle), will pass through the troposphere. For this reason, as well as for the sake of completeness, both tropospheric and ionospheric effects are discussed.

3.2.6 SPREADING OR SPATIAL LOSS

The energy in a transmitted signal decreases due to the spatial spreading of the wave as it travels through the space. This is not a function of absorption or scattering of the signal, but is strictly dependent on particle separation as it leaves a source. Since this loss is only a function of frequency and distance, it will be seen by the synchronous relay satellite and the low altitude satellite.

3.2.7 ATMOSPHERIC LOSSES

3.2.7.1 Ionospheric Absorption Losses

Ionospheric absorption loss can be attributed to the transfer of energy from the propagating electromagnetic wave to the motion of particles in the ionosphere. Many factors affect this loss or the electron density to be encountered. These can be described as follows:

1) carrier frequency
2) time of day - absorption is much higher in the daytime than at night
3) season of the year
4) sunspot activity
5) path length through the ionization regions
6) latitude-longitude effects

This effect will be seen, in part, by the direct signal from a low altitude satellite to or from the synchronous relay satellite. The reflected signal will see all of the ionosphere, and therefore is subject to this loss. It must be realized that any region seen by the reflected signal will be seen twice, once on its way to being reflected by the earth, and again after

reflection. When compared to free space path loss, this ionospheric loss is negligible.

3.2.7.2 Tropospheric Losses

Losses in the lower atmosphere are due almost entirely to molecular absorption by oxygen and uncondensed water vapor, and scattering by precipitation particles. Atmospheric models having loss characteristics similar to the actual troposphere have produced theoretical curves of the total molecular absorption for different propagation paths through the troposphere for signals traveling from the earth to outer-space. Precipitation scattering caused by rain, fog, snow, etc., can be considered single-particle scattering and this scattering becomes more of a factor as the size of the particles approach the wavelength of the signal. As can be seen in Figure 3-16, below 15 GHz the tropospheric absorption loss is essentially smooth and constant. Here, once again the tropospheric absorption will be seen to be negligible when compared to the spatial or free path loss.

3.2.7.3 Summary of Atmospheric Losses

At VHF and S-band, tropospheric and ionospheric losses are very small when compared to the free space path loss. Values for the free space loss will be found to be in the general ranges shown in Table 3-2.

TABLE 3-2

FREE SPACE PATH LOSS (ONE WAY)

FREQUENCY	ALTITUDE	LOSS
100-150 MHz	200 km	120 dB
2 GHz	200 km	145 dB
100-150 MHz	4,000 km	145 dB
2 GHz	4,000 km	170 dB
100-150 MHz	24,000 km	165 dB
2 GHz	24,000 km	190 dB

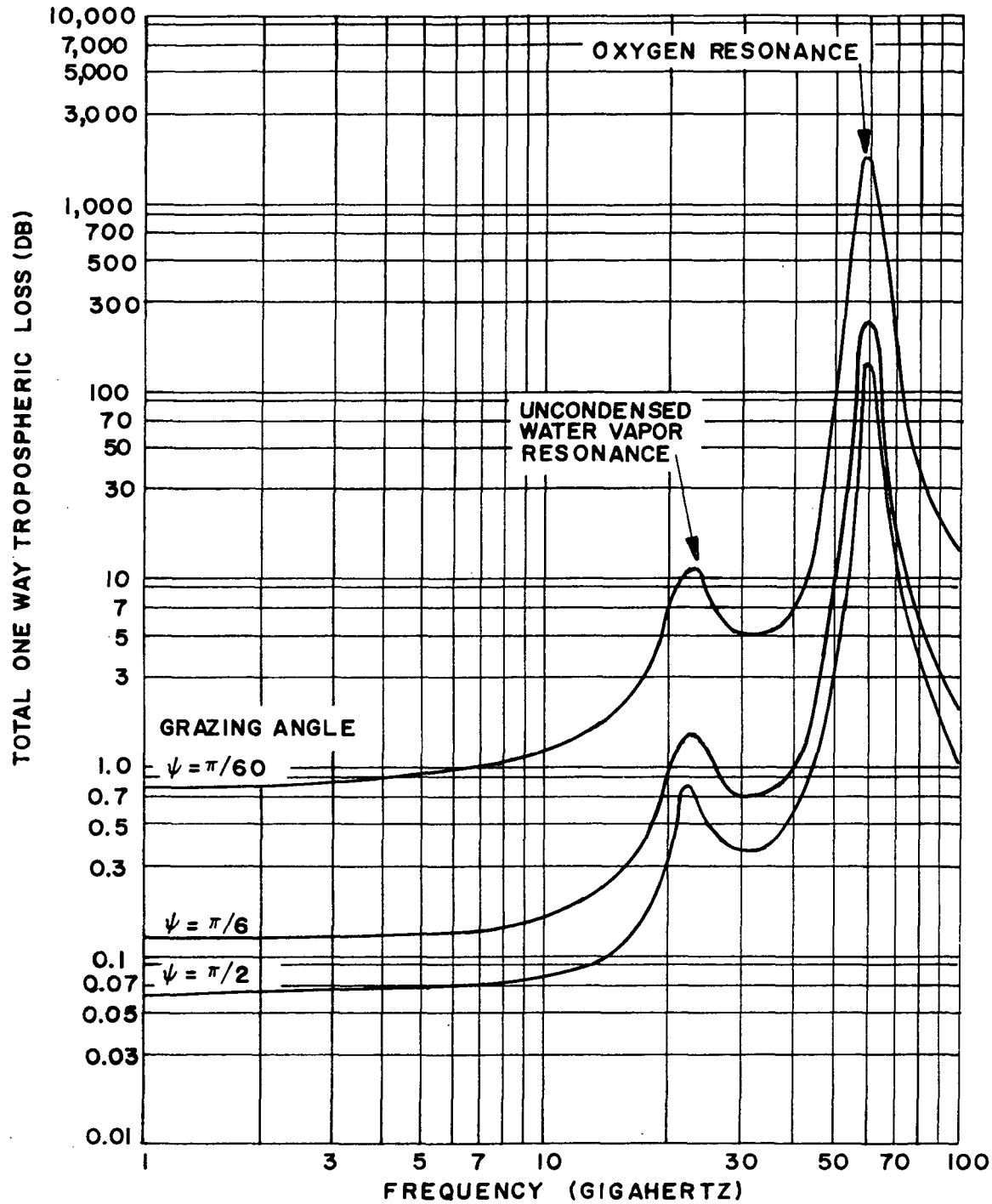

FIGURE 3-16 TROPOSPHERIC LOSS

3.2.8 GROUND LOSSES

The reflecting properties of the earth's surface are critical factors in determining the magnitude of the multipath signal and the nature of the signal (specular or diffuse). For a smooth plane of arbitrary conductivity and dielectric constant, the reflection coefficients are given by Fresnel's equations. Departures from a smooth earth can be taken into account by considering the divergence factor. This factor will be discussed in more detail in conjunction with the discussion of specific mathematical models.

The effect of a non-perfect reflecting surface is that some of the impinging energy is absorbed by the earth. The amount of absorption is dependent upon whether the polarization of the incident wave is horizontal or vertical. Phase shifts are encountered by the impinging signal. This further distorts the multipath signal. The ratio of the scattered power (multipath signal) to the direct power as a function of low altitude satellite aspect angle (angle δ in Figure 3-1) is discussed later in this report.

3.2.9 ATMOSPHERIC REFRACTION EFFECTS

The absorption losses due essentially to the transfer of energy from the signal to the media were described previously. There are other effects which take place that contribute not only to the losses in the system but to distortion or changing of the signal as it propagates through the media. These factors will now be discussed individually. It must be remembered that the indirect or multipath signal travels over a path consisting of free space, the troposphere, and the ionosphere. The multipath signal will see the ionosphere and troposphere twice. The direct signal will see no troposphere, but it will see some of the ionosphere, depending upon the orbital altitude.

As a signal passes through the atmosphere it is passing through a medium with continually changing properties, i.e., the temperature and moisture content are continually decreasing with height above the earth. The index of refraction is a function of the frequency, temperature, pressure, and moisture content in a medium and is found to decrease with height above the earth. This index, then, is a measure of the electron density in the ionosphere. Figure 3-17 indicates the variation of the index of refraction as a function of electron density in the ionosphere and frequency. Figure 3-18 shows the variation of the index of refraction in the troposphere. Figure 3-18 indicates that the tropospheric refractive index is a measure of the environment and is dependent on factors such as the relative humidity and is independent of frequency.

Snell's law shows that if the index of refraction of the new medium is lower than the original medium there is a bending of the signal away from the normal to the boundary surface. Similarly, there is a bending towards the normal if the signal is entering a medium of higher index of refraction. Since the normal atmosphere has a gradual change in its physical properties, the change in the wave direction is gradual. This refraction at a boundary (whether discrete or continuous) is accompanied by some reflection of the incident signal. This subject is treated in more detail by any standard text on electromagnetic waves (e.g., Reference 13). The result of this action is that as the reflected wave is passing through the atmosphere it is losing energy constantly changing direction and undergoing a phase shift.

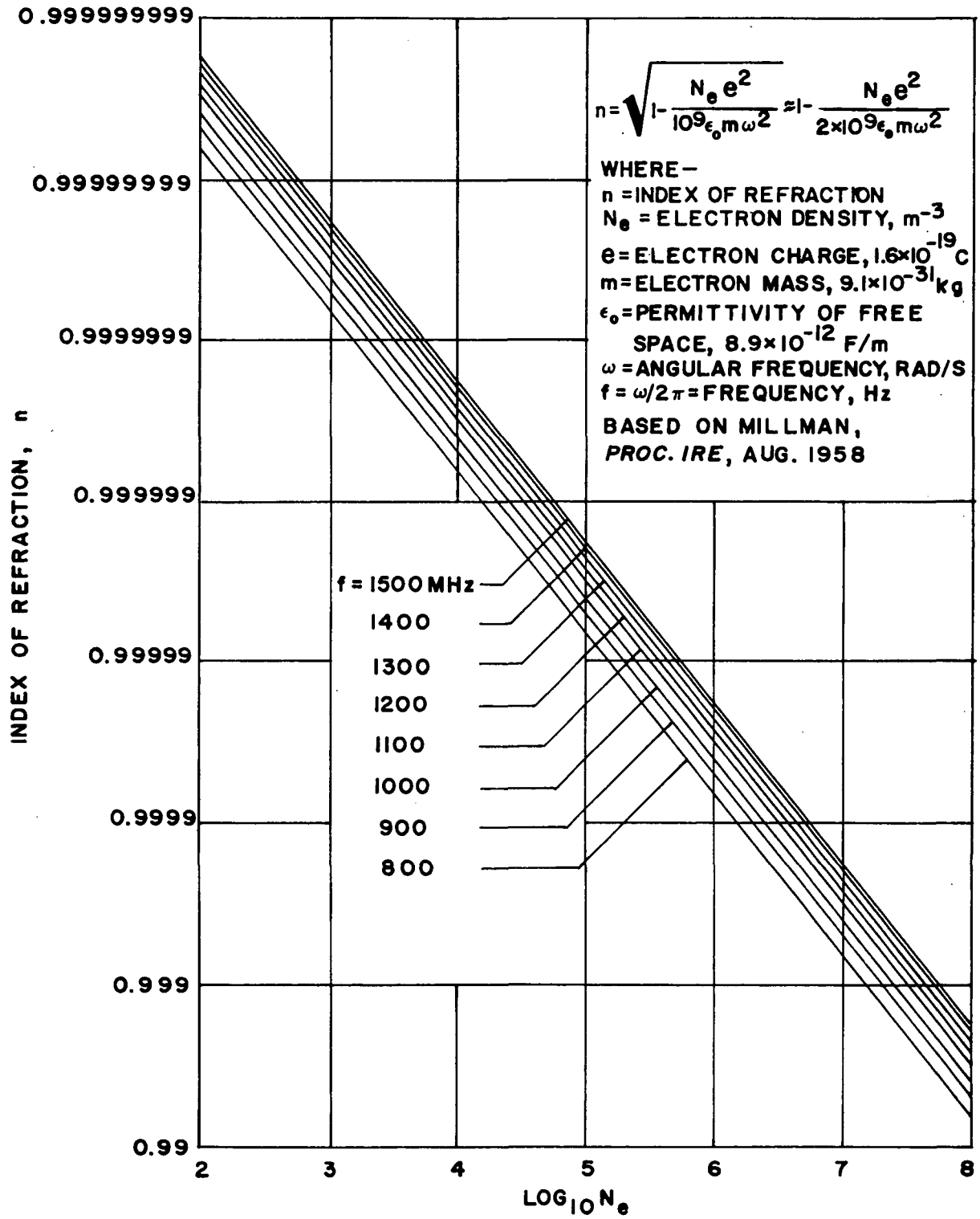

FIGURE 3-17 INDEX OF REFRACTION IN THE IONOSPHERE

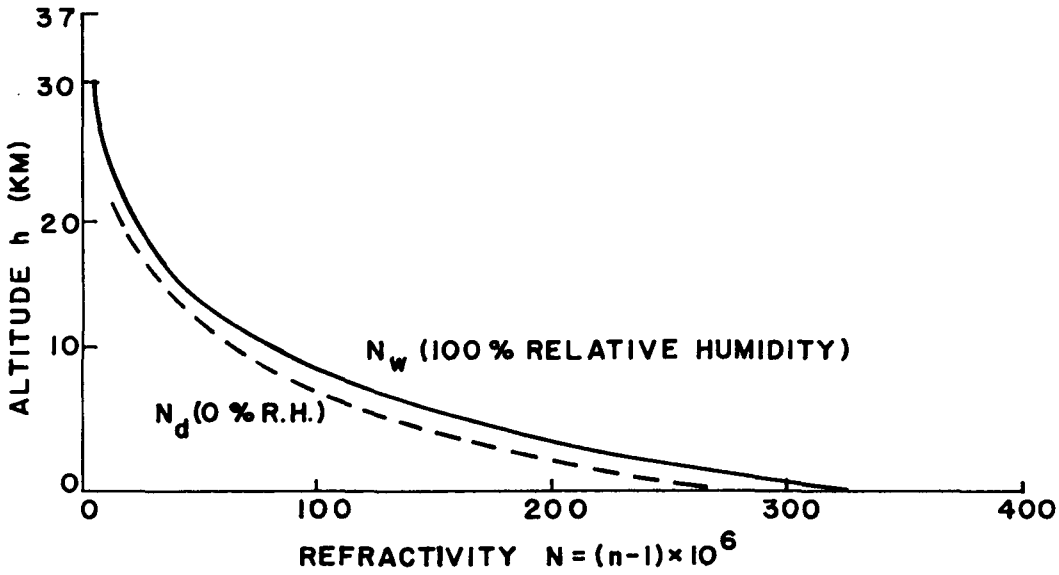

FIGURE 3-18 TROPOSPHERIC REFRACTIVITY

Errors in time of arrival of a signal result from refraction of the signal and the difference between the free space velocity of light and the actual velocity of light in the propagating medium. These time delays can be expressed as ranging errors. As a worst case, the direct signal can be considered as passing through the entire ionosphere prior to its free space path between the synchronous relay satellite and low altitude satellite. Worst-case ranging errors are summarized in Table 3-3.

3.2.10 POLARIZATION EFFECTS

3.2.10.1 Faraday Effect

An electromagnetic wave propagating in the ionosphere experiences a force due to the presence of the earth's permanent magnetic field. Thus,

TABLE 3-3

RANGE ERRORS

ERROR CONTRIBUTION	GRAZING ANGLE	
VHF (Mean Errors)	30°	90°
Troposphere - One Way	0.5 m	0.3 m
Two Way	1.0 m	0.6 m
Ionosphere - One Way	121.9 m	67.0 m
Two Way	243.8 m	134.0 m
TOTAL	244.8 m	134.6 m
S-Band (Mean Errors)		
Troposphere - One Way (Independent of Frequency)	0.5 m	0.3 m
Two Way	1.0 m	0.6 m
Ionosphere - One Way	negligible	
Two Way	0 m	0 m
TOTAL	1.0 m	0.6 m

waves traveling in the ionosphere are doubly refracted. Consequently the axis of polarization of linearly polarized waves is continuously rotated as the wave passes through the medium. One obvious problem to be encountered for a system using linearly polarized antennas is that this effect decouples the transmitter and receiver and manifests itself as as apparent power loss. Since the earth's magnetic field is not constant, this effect can not be circumvented by a simple misalignment of the transmitter and receiver polarization axes. The amount of rotation at VHF is dependent on the path length through the medium and the electron density in the medium. At S-band the effects of Faraday rotation are not significant.

3.2.10.2 Reflection

At a point of reflection there is a change in the sense of rotation or the sense of the polarization is shifted by π radians. The divergence factor will also determine the magnitude of the polarization vectors.

3.2.10.3 Discontinuities

Abrupt changes in the atmosphere cause abrupt changes in the absorption qualities of the environment, the velocity of the signal in the environment, and the refraction of the signal in the environment. The discussion below indicates not only causes of change in the electron density of the atmosphere but also discontinuities, or abrupt changes caused by simultaneous sudden decrease in moisture (moisture lapse) and sudden increases in temperature (temperature inversion) with increasing altitude.

When warm dry air flows from land out over cooler water, the evaporation of moisture from the water into the lower layer of air cools

the air, increases the moisture lapse rate, and produces a temperature inversion. This produces an abrupt change in the atmosphere.

Nocturnal cooling of the surface of the earth causes ducts to appear. These ducts may result from a cloudy sky which prevents much of the heat radiated from the earth from being dissipated smoothly into outer space; rapid temperature changes that appear from day to night over desert land; and solar activity.

If the atmosphere were quiet, it would be a reasonable task to define and model this environment. These discontinuities and sudden changes cause errors that must be accounted for in the model. Poularikas and Golden (Reference 14) described a manner of modeling this erratic ionosphere.

3.3 FADING

Another problem associated with the VHF/UHF frequencies is the existence of severe fading which occurs at the low (<0.26 radians) and high (>1.05 radians) latitudes. This fading is a function of the time of day.

Figure 3-19 shows data taken at the Quito, Ecuador STADAN site at 150 MHz and 400 MHz. The fading rate is quite slow but the fading depth can be 20 to 30 dB.

Since the Shuttle can be in low orbits, i.e. 160 km, ionospheric fading can be anticipated if the Shuttle/sun/earth orientation is conducive to fading. This factor must be considered in any system design, in addition to the multipath effects and RFI effects.

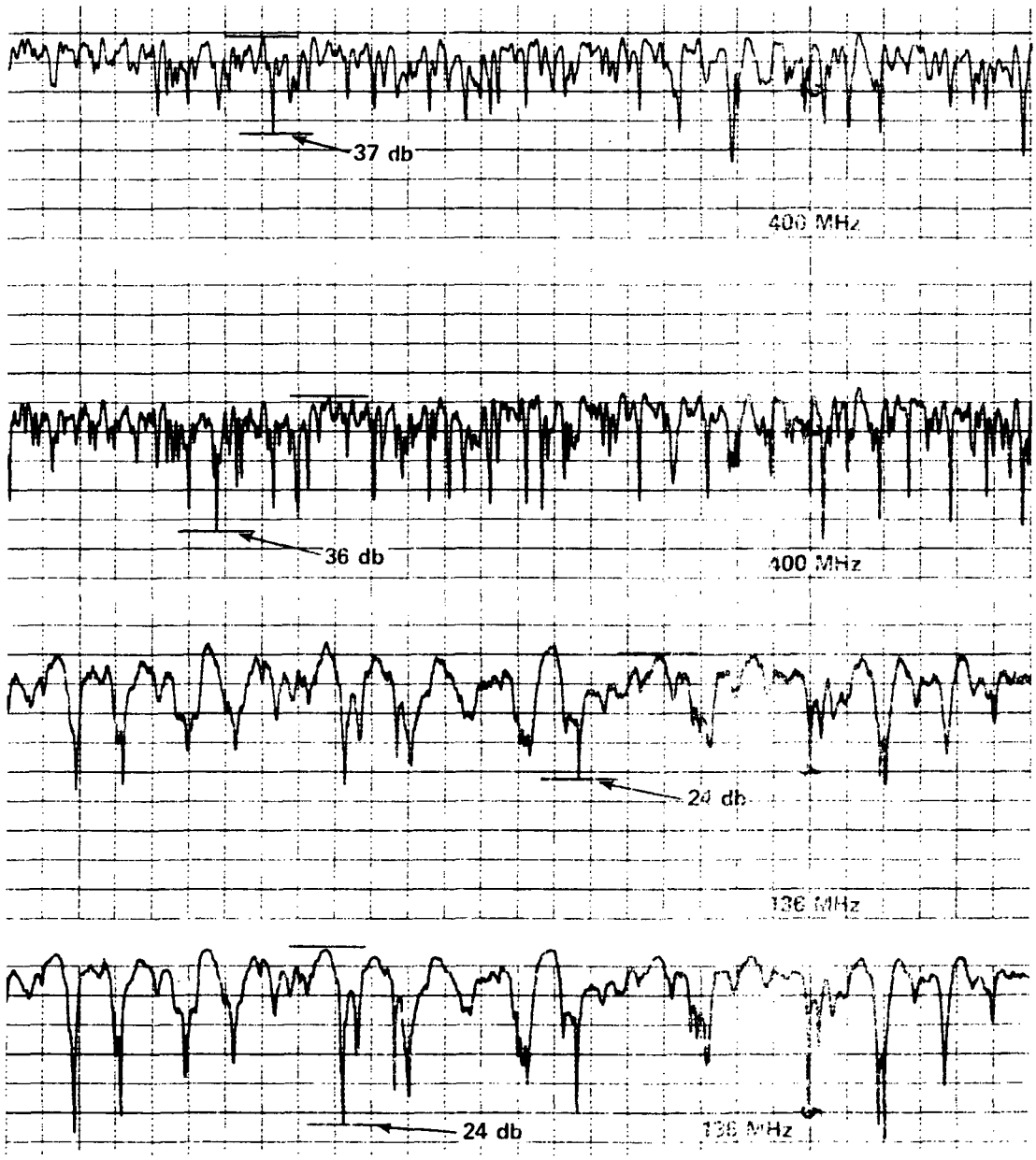

FIGURE 3-19 TELEMETRY SIGNAL POWER (AGC) FROM OAO-2 RECEIVED SIMULTANEOUSLY ON 136 MHz AND 400 MHz AT QUITO, ECUADOR. TRACES SHOW RIGHT AND LEFT HAND CIRCULAR POLARIZATION FOR EACH FREQUENCY

3.4 STATISTICAL CHANNEL PARAMETERS

Thus far our discussion has centered primarily upon those parameters which are deterministic in nature. However, on occasion we have alluded to parameters which must be described statistically. In particular, the nature of the reflections from the earth's surface must be treated by statistical models. This is not to say that the models will not also include some deterministic components; in fact, many models do include a deterministic divergence factor to account for the curvature of the earth.

Before entering into conclusions upon which of the existing mathematical models of the channel is best suited for the case at hand, we will summarize each of the candidate models. In preparation for this, we first present a summary of the reflection of a plane electromagnetic wave from the surface of the earth.

3.4.1 REFLECTION OF A PLANE WAVE FROM THE EARTH'S SURFACE

Reflection of a plane wave from the earth's surface may be modeled in terms of a plane wave impinging upon a plane dielectric from which it is reflected. The complete solution for the fields is obtained by matching the electric and magnetic fields at the interface between the two media, in this case the air and the earth. The solution may be expressed in terms of a reflection coefficient and a transmission coefficient which are in general complex quantities. This analysis may be found in any standard work on electromagnetic theory (e.g., Reference 13, pp. 75-77). As shown in Reference 15 the specular reflection coefficients may be written as:

$$\Gamma_v = R_{ov} e^{-i\phi_v} = \frac{\left(\frac{k_1}{k_0}\right)^2 \sin\psi - \sqrt{\left(\frac{k_1}{k_0}\right)^2 - \cos^2\psi}}{\left(\frac{k_1}{k_0}\right)^2 \sin\psi + \sqrt{\left(\frac{k_1}{k_0}\right)^2 - \cos^2\psi}} \tag{3-1}$$

$$\Gamma_h = R_{oh} e^{-i\phi_h} = \frac{\sin\psi - \sqrt{\left(\frac{k_1}{k_0}\right)^2 - \cos^2\psi}}{\sin\psi + \sqrt{\left(\frac{k_1}{k_0}\right)^2 - \cos^2\psi}} \tag{3-2}$$

where horizontal polarization is defined to mean that the electric vector is perpendicular to the plane of incidence, and vertical polarization is defined as the electric vector parallel to the plane of incidence.

The ratio $(k_1/k_0)^2$ is defined as the complex dielectric constant and is given by

$$\left(\frac{k_1}{k_0}\right)^2 = \frac{\varepsilon}{\varepsilon_0} - j\frac{\sigma}{\omega\varepsilon_0} = \varepsilon_1 - j\varepsilon_2 = \varepsilon_i \tag{3-3}$$

where the values of ε and μ for air are assumed to be essentially those for free space and the value of μ for the earth is also assumed to be essentially that of free space. In SI units the parameter $\varepsilon_2 = \sigma/\omega\varepsilon_0$ becomes $60\lambda\sigma$ where λ is expressed in units of meters and σ is expressed in units of ohm^{-1} meter^{-1}.

For wavelengths greater than roughly 20 centimeters, the properties of sea water are essentially independent of wave length (Reference 15). Both ε_1 and σ vary noticeably with temperature, ε decreasing and σ increasing as temperature increases. At 20 C, ε_1 is often taken equal to 80 or 81 but σ is subject to considerable variation due to local variations in the salinity of sea water. The values of σ and other electromagnetic parameters are shown in Table 3-4 (from Reference 15) for various types of earth surface. These values are only a guide rather than accurate sets of earth parameters.

TABLE 3-4

APPROXIMATE ELECTROMAGNETIC PROPERTIES
OF SOIL AND WATER

Medium	λ	σ mho/m	ε_1	ε_2	Q
Sea water.	3 m-20 cm	4.3	80	774	0.10
				52	1.5
20 - 25 C.	10 cm	6.5	69	39	1.8
28 C.	3.2 cm	16	65	30.7	2.1
Distilled water, 23 C.	3.2 cm	12	67	23	2.9
Fresh-water lakes. . .	1 m	10^{-3}-10^{-2}	80	0.06	1330
				0.60	133
Very dry sandy loam. .	9 cm	0.03	2	1.62	1.23
Very wet sandy loam. .	9 cm	0.6	24	32.4	0.74
Very dry ground. . . .	1 m	10^{-4}	4	0.006	670
Moist ground	1 m	10^{-2}	30	0.6	50
Arizona soil	3.2 cm	0.10	3.2	0.19	17
Austin, Tex., soil, very dry	3.2 cm	0.0074	2.8	0.014	200

(Adapted from Reference 15)

To account for the curvature of the earth a multiplicative factor D, termed the divergence factor, modifies the reflection coefficients defined above. As shown in Reference 15, the divergence factor is given by

$$D = \frac{a(S_1+S_2)\sqrt{\sin\mu\cos\mu}}{\sqrt{[(a+z_2)S_1\cos\tau_3+(a+z_1)S_2\cos\tau_1](a+z_1)(a+z_2)\sin\Phi}} \qquad (3\text{-}4)$$

where the geometrical parameters are defined in Figure 3-20.

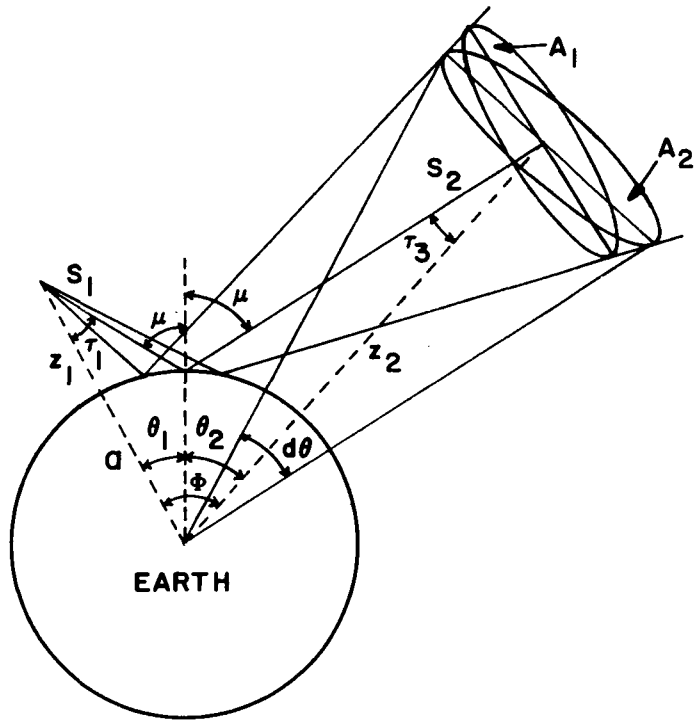

FIGURE 3-20 GEOMETRY FOR THE DIVERGENCE FACTOR D

Since the majority of the earth's surface is sea water, these values are used to approximate the electromagnetic properties of the earth for calculating reflection coefficients in the case of a low orbiting satellite and a synchronous relay satellite. In particular, we have assumed

that σ = 4.3 mhos/meter, ε_1 = 80, and ε_2 = 774 for the results which are presented in Appendix A.

3.4.2 THE MAGNAVOX MODEL

The Magnavox multipath model, as presented in Reference 2, is based primarily on the work of Duranni and Staras (Reference 3). In general the amount of reflected specular energy can be expressed as:

$$P_{specular} = g\langle p_s^2\rangle D^2 |R_o|^2 P_d \qquad (3\text{-}5)$$

where

$$\langle p_s^2\rangle = e^{-\left(\frac{4\pi\sigma}{\lambda}\sin\psi\right)^2}$$

ψ = grazing angle

g = a factor which is dependent on the antenna pattern of the low altitude satellite and controls the amount of power directed toward the surface

P_d = power received via the direct path

λ = wavelength

σ = rms height of the reflecting surface

D = average divergence factor associated with the spherical earth

$|R_o|^2$ = mean squared reflection coefficient

The amount of diffuse power is given by:

$$P_{diffuse} = gD^2 |R_o|^2 F(\psi,h) P_d \qquad (3\text{-}6)$$

where

h = user height above the earth

$F(\psi,h) \leq 1$

and the other quantities are as defined above.

The divergence factor D, as used in the Magnavox model, is defined graphically in Figure 3-21 as a function of grazing angle ψ with spacecraft altitude as a parameter.

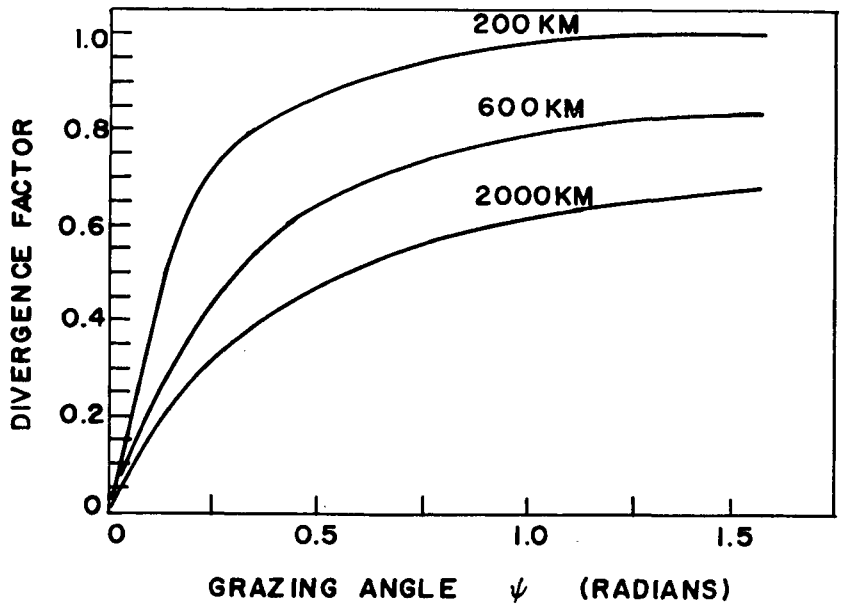

FIGURE 3-21 DIVERGENCE FACTOR VS. GRAZING ANGLE AND SPACECRAFT ALTITUDE

3.4.3 ADCOM MODEL

The ADCOM model (Reference 1) assumes that the reflected signal is composed of a specular component and a diffuse component. However, the approximations made by ADCOM yield a model of limited accuracy as compared to the actual physical situation. The effect of surface roughness is considered only when

$$\sigma \sin \psi > \lambda/8 \qquad (3\text{-}7)$$

where σ = RMS height of surface protrusions

ψ = grazing angle

λ = wavelength

On the basis of this equation ADCOM concludes that diffuse multipath will predominate at UHF and higher operating frequencies.

ADCOM approximates the overall effect of surface roughness as a reduction in the effective reflection coefficient to the range 0.1 to 0.3 and the introduction of a further fluctuation if the roughness is time varying, such as the disturbances due to wave motion at sea.

The ADCOM model, as with the other models to be discussed, uses the divergence factor D to account for the spherical shape of the earth. However, ADCOM severely limits the usefulness of their model by assuming D to be 1 for grazing angles greater than 0.035 radian. As can be seen from Figure 3-21 this assumption is hardly justified.

ADCOM does, however, take into account the extra extenuation due to the increased path lengths over the reflected path. This factor is given by

$$\Delta = \frac{R^2}{(R+\delta)^2} \approx 1 - \frac{2\delta}{R} \quad \text{for } \frac{\delta}{R} << 1 \qquad (3\text{-}8)$$

where R is the direct path length and δ is the path difference. However this difference may be small for many of the geometries under consideration.

ADCOM has also attempted to take into consideration atmospheric multipath due to variations in the ionosphere which may give rise to path splitting. They also consider the possibility of multipath from ducts formed in the troposphere.

Considering the limitation imposed by their assumptions concerning the divergence factor, even though the ADCOM model does include considerations

not taken into account by other models (e.g., atmospheric multipath), we reject their model as the best for a relay satellite configuration.

3.4.4 NOTRE DAME MODEL

The University of Notre Dame presents in Reference 9 two models for the channels between a low orbiting satellite and a synchronous relay satellite. These models assume FSK modulation and are written in terms of the total received signal for application to a problem of estimation theory.

In their first model the Notre Dame researchers consider the total received signal to be given by

$$r(t) = \begin{cases} s_1(t) + M\cos(\omega_1 t+\theta) + n(t) : H_1 \\ s_2(t) + M\cos(\omega_2 t+\theta) + n(t) : H_2 \end{cases} \tag{3-9}$$

where s_1 and s_2 are the signaling waveforms and n and θ are Gaussian variates. This model represents a strong direct path signal and a multipath signal which is diffuse only. The amplitude M of the fading component is considered to have the Rayleigh distribution

$$p(M) = \begin{cases} \frac{M}{\gamma_R^2} e^{-\frac{M^2}{2\gamma_R^2}}, & 0 \leq M < \infty \\ 0, & M < 0 \end{cases} \tag{3-10}$$

and a uniform phase distribution.

This model seems overly simplistic and does not explicitly contain reference to the parameters of the reflecting surface.

In their second model the Notre Dame researchers include more general spectra and fading components for both the direct and the reflected paths. Again they consider only non-coherent FSK modulations with no inter-symbol interference. In this case the received signal is modeled as

$$r(t) = \begin{cases} D\cos\omega_1 t + M_1\cos(\omega_1 t+\theta_1) + R\cos(\omega_1 t+\theta) + M_2\cos(\omega_1 t+\theta_2): H_1 \\ D\cos\omega_2 t + M_1\cos(\omega_2 t+\theta_1) + R\cos(\omega_2 t+\theta) + M_2\cos(\omega_2 t+\theta_2): H_2 \end{cases} \quad (3\text{-}11)$$

where M_1 and M_2 are independent Rayleigh variables with mean square values $2\gamma_D^2$ and $2\gamma_R^2$ and θ_1 and θ_2 are independent uniform random variables.

Again, the model seems overly simplistic in that no provisions are made for incorporating the physical parameters of the reflecting surface.

Since the Notre Dame models assume that the fading characteristics of the multipath channels are known and that, in some manner, we can determine the average reflected power as seen at the satellite, without actually specifying how this is to be determined, and since their models deal only with the effects of multipath on system performance rather than with multipath prediction, we choose to reject this model as the optimum model for the case at hand.

3.4.5 HUGHES AIRCRAFT COMPANY MODEL

The mathematical model for reflection of signals from the earth developed by Hughes Aircraft Company (Reference 4) requires assumptions concerning the roughness in order to arrive at analytical expressions which are useful for obtaining numerical results. Tractable equations can be obtained for smooth surfaces and for very rough surfaces. For intermediate roughness interpolation between the smooth surface approximation and the rough surface approximation may be used to obtain results. To provide a quantitative

criterion for surface roughness, consider the geometry of Figure 3-22 . The waves reflected from the two surface points will differ in phase by

$$\Delta\theta = \frac{4\pi h \cos \mu}{\lambda} \qquad (3\text{-}12)$$

where μ is the angle of incidence as shown in Figure 3-22, λ is the wavelength, and θ here represents signal phase. For a surface with randomly distributed surface variations, a smoothness factor may be defined by

$$q = \frac{4\pi\sigma \cos \mu}{\lambda} \qquad (3\text{-}13)$$

where σ is the standard deviation of the surface variation. Although there is no abrupt change between smooth surfaces and rough surfaces, the Rayleigh criterion is often used. This criterion is that

$$q < \frac{\pi}{2} \qquad (3\text{-}14)$$

If we may assume the surface variations are normally distributed, then for a flat perfectly reflecting surface the fraction of the incident power which is reflected coherently is given by

$$\rho = e^{-q^2} \qquad (3\text{-}15)$$

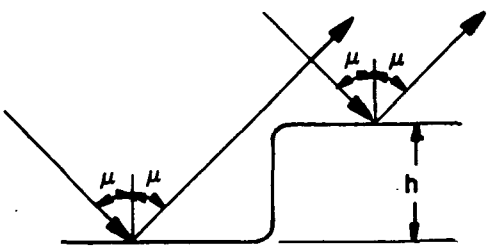

FIGURE 3-22 BASIC SURFACE VARIATION GEOMETRY

A more realistic smoothness criterion would be to require that at least 90% of the incident power is coherently reflected. This leads to a criterion for smoothness of $q < 0.324$. In a similar manner we might require that no more than 10% of the incident power be reflected coherently by a rough surface which leads to a criterion of $q > 1.52$ for a rough surface. The region between these, i.e., $0.324 < q < 1.52$, can be considered the transition region. It is in the transition region that both specular and diffuse scattering are present.

First we will consider the smooth earth model of Hughes Aircraft. The geometry is shown in Figure 3-23. Assuming scalar representation of the electromagnetic field, the received direct and reflected signals are given by

$$\frac{P_{direct}}{P_{radiated}} = \frac{G_1 G_2 \lambda^2}{16\pi^2 R^2} \tag{3-16}$$

$$\frac{P_{reflected}}{P_{radiated}} = \frac{G_3 G_4 \lambda^2}{16\pi^2 (S_1+S_2)^2} |R_0|^2 \tag{3-17}$$

where the parameters are defined as

G_1 = transmitting antenna gain in direction of direct path

G_2 = receiving antenna gain in direction of direct path

G_3 = transmitting antenna gain in direction of reflecting surface

G_4 = receiving antenna gain in direction of reflecting surface

R_0 = Fresnel reflection coefficient

and R, S_1, and S_2 are defined in Figure 3-23.

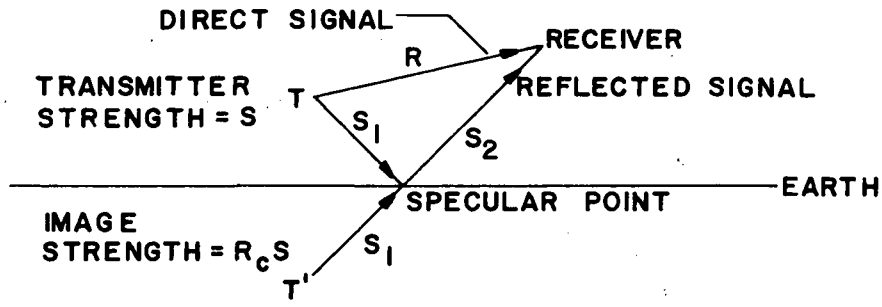

FIGURE 3-23 REFLECTION FROM A SMOOTH FLAT EARTH

Now considering that electromagnetic fields have a vector representation, the reflection of plane waves is dependent upon the polarization of the wave. In this context polarization refers to the orientation of the electric field vector. When considering reflection from a smooth surface, this direction is most conveniently referred to the transmission plane. That is, the plane containing the incoming propagation direction, the surface normal, and the reflection propagation direction. The polarization of an electromagnetic wave with respect to the reflecting surface and transmission plane is defined in Figure 3-24. The horizontally polarized plane wave's electric field is normal to a transmission plane while the vertically polarized

+ = Vertical (in-plane)
- = Horizontal

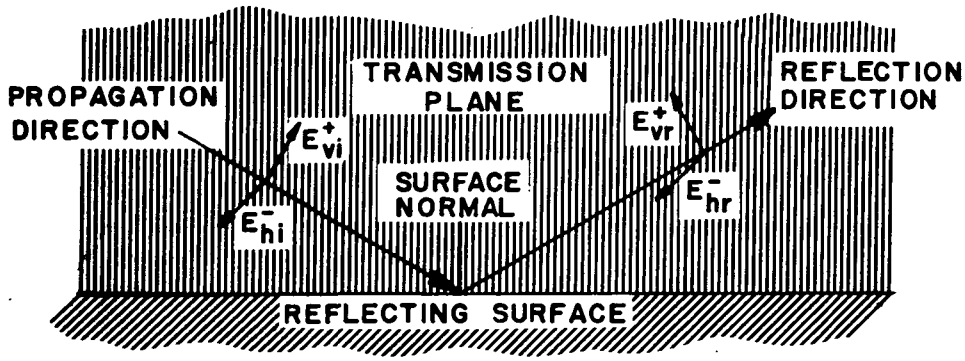

FIGURE 3-24 POLARIZATION VECTOR COMPONENTS DEFINED WITH RESPECT TO TRANSMISSION PLANE

component lies in the plane. By convention the component of the electric field which is parallel to the reflecting surface changes direction upon reflection. All other field components remain in their original direction. Using these conventions, a coherency factor, and the smoothness criterion discussed above, only the Fresnel reflection coefficients are needed to compute the received power.

The Hughes Aircraft model derives the following equations for the complex reflection coefficient:

$$\Gamma_v = \frac{\varepsilon' \cos \mu - \sqrt{\varepsilon' - \sin^2 \mu}}{\varepsilon' \cos \mu + \sqrt{\varepsilon' + \sin^2 \mu}} \qquad (3\text{-}18)$$

$$\Gamma_h = \frac{\cos \mu \mp \sqrt{\varepsilon' - \sin^2 \mu}}{\cos \mu + \sqrt{\varepsilon' + \sin^2 \mu}} \qquad (3\text{-}19)$$

where μ = angle of incidence

ε' = complex dielectric constant

This is equivalent to the definition presented earlier in this report.

To account for the curvature of the earth, a divergence factor multiplies the ratio of the direct path signal power to reflected signal power. This divergence factor, as used by Hughes Aircraft, is defined as

$$D = \frac{1}{1 + \xi(1+\cos^2\theta)/\cos\theta + \xi^2} \qquad (3\text{-}20)$$

where $\xi = \dfrac{2S_1S_2}{a(S_1+S_2)}$

a = earth radius

for the geometry of Figure 3-1. This divergence factor is plotted in Figure 3-25.

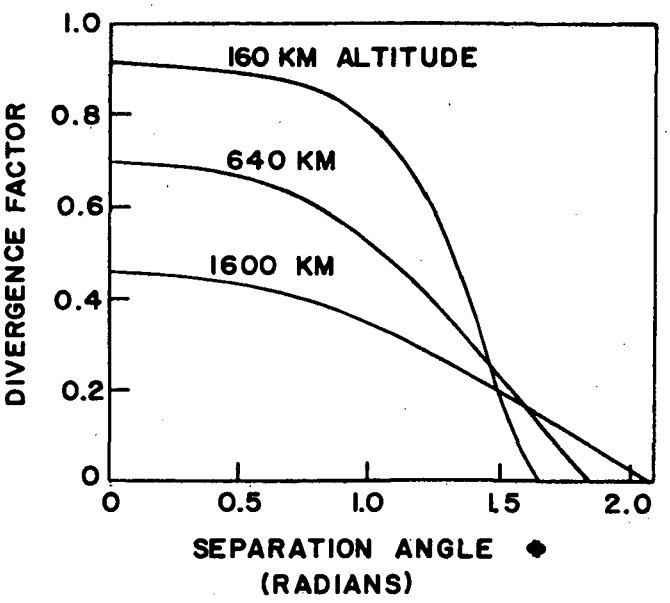

FIGURE 3-25 DIVERGENCE FACTOR FOR HUGHES AIRCRAFT COMPANY'S MODEL

Thus for a smooth earth the Hughes Aircraft model reduces to

$$\frac{P_{reflected}}{P_{direct}} = \left(\frac{G_3 G_4}{G_1 G_2}\right) \left[\frac{R^2}{(S_1+S_2)^2}\right] \rho D |R_0|^2 \qquad (3\text{-}21)$$

For a rough earth the model must be modified. In addition to assuming that the smoothness factor q is large, a second important assumption in the derivation of the reflected power formula is that the radii of curvature of the surface are large when compared to the wavelength of the signal. Although this condition may not always be satisfied, especially for land, it is a common condition for the sea and much of the land area. Since the sea is the best earth surface reflector, this condition is not overly restrictive.

Hughes Aircraft uses a probablistic approach to define the reflected power from a rough earth. To do this they consider the reflections from a small surface patch and integrate over the area of the earth visible to both satellites. In this manner they obtain for the reflected power

$$\frac{\langle P_{reflected} \rangle}{P_{direct}} = \frac{R^2}{4\pi G_1 G_2} \int_S \frac{G_3 G_4}{S_1^2 S_2^2} \, dC \qquad (3\text{-}22)$$

In equation 3-22, dC is an elemental area of the scattering surface, which is termed the scattering cross section.

To determine the scattering cross section Hughes Aircraft makes the assumption that the surface height variation about a zero mean value is Gaussian distributed with standard deviation σ and has an autocorrelation function given by

$$R(x) = e^{-x^2/T^2} \qquad (3\text{-}23)$$

where T represents the correlation distance. It is important to note that this autocorrelation function is such that the surface is considered isotropic. Based upon these statistics for the surface a very involved mathematical derivation given by Beckmann and Spizzichino (Reference 16) yields for the scattering cross section

$$dC = \frac{|R_0|^2}{\eta^2 \cos^4 \gamma} \, e^{-(\eta^{-2} \tan^2 \gamma)} \, dS \qquad (3\text{-}24)$$

where R_0 = the reflection coefficient (a function θ_s of Figure 3-26)

γ = the angle between V_B and the local vertical

dS = the area of the surface patch

η = roughness factor = $2\sigma/T$.

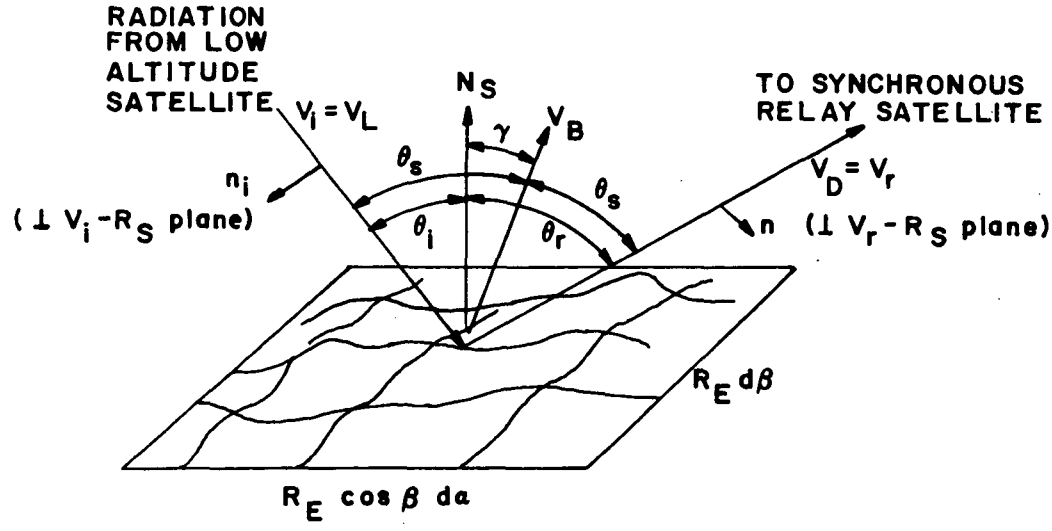

FIGURE 3-26 SCATTERING PATCH OF AREA $dS = R_E^2 \cos\beta\, d\alpha\, d\beta$

Hughes also accounts for shadowing of one portion of the surface by another portion. This effect is especially important at large incidence angles which correspond to large satellite separation angles and small grazing angles.

The shadowing function is derived based upon the conditional probability that the elemental surface area is not shadowed and is visible by the receiver, given that it is properly oriented to cause reflections towards the receiver. By using this probability in their derivations, not only are the surface characteristics included in the analysis, but also the fact that both satellites do not see the same surface area is included.

Several quantities must be defined. The angles θ_i and θ_r, as shown in Figure 3-26, may be calculated from

$$\cos\theta_i = \frac{-V_i \cdot N_s}{|V_i||R_s|} \qquad (3\text{-}25)$$

$$\cos\theta_r = \frac{V_r \cdot N_s}{|V_r||R_s|} . \qquad (3\text{-}26)$$

Now define

$$g_i = \frac{\cot \theta_i}{\eta} \tag{3-27}$$

$$g_r = \frac{\cot \theta_r}{\eta} \tag{3-28}$$

$$B_i = \frac{1}{2}\left[\frac{1}{g_i\sqrt{\pi}} \exp(-g_i^2) - \operatorname{erfc}(g_i)\right] \tag{3-29}$$

$$B_r = \frac{1}{2}\left[\frac{1}{g_r\sqrt{\pi}} \exp(-g_r^2) - \operatorname{erfc}(g_r)\right] \tag{3-30}$$

Two cases must now be considered. The first case is forward scatter, i.e. n_i and n_r form an angle less than $\pi/2$ radians. In this case the shadowing function as used in the Hughes model is given by

$$S = 1 - \frac{e^{-(B_i+B_r)}}{(B_i+B_r)} \tag{3-31}$$

The second case is back scatter, i.e. the angle between n_i and n_r is greater than $\pi/2$ radians. That is, if the point is visible from the low altitude satellite then it is visible from the synchronous relay satellite. In this case the shadowing function becomes

$$S = \frac{1-e^{-B_i}}{B_i} \tag{3-32}$$

Considering the shadowing function and a rough surface, the ratio of multipath power to direct path power in the Hughes model is given by

$$\frac{P_{reflected}}{P_{direct}} = \frac{R^2}{4\pi G_1 G_2} \int_S \frac{G_3 G_4 |R_0|^2 S(\theta)}{S_1 S_2 \eta^2 \cos^4\gamma} e^{-(\eta^{-2}\tan^2\gamma)} dS \tag{3-33}$$

This equation is representative of the rough earth model but the effects of antenna polarization have not been considered. Hughes also goes on with a

lengthy derivation to consider the effects of antenna polarization and derives complicated expressions for the multipath power in this case. This model is comprehensive in coverage of many factors which affect the reflected signal.

3.4.6 PAINTER'S MODEL

The model for multipath reflections from the earth developed by John Hoyt Painter of NASA Langley (see Reference 17) characterizes the channel between a low altitude satellite and a synchronous relay satellite by its impulse response. As the other models outlined in this report do, Painter considers deterministic specular reflection and nondeterministic diffuse reflection.

Painter's model uses the flat earth approximation shown in Figure 3-27. The assumed known quantities are the satellite altitudes and the distance along the surface of the earth between the two subsatellite points. Geometrical considerations are used to derive the length of the direct path, the length of the reflected path, the incident angle, the

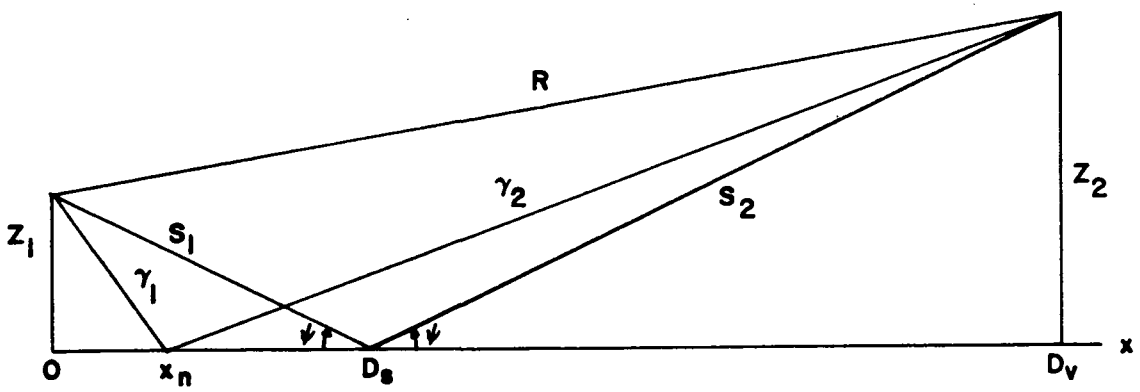

FIGURE 3-27 PAINTER'S FLAT EARTH MODEL

location of the specular point, and the path length difference. These quantities are given by

$$R = \sqrt{D_v^2 + (Z_2-Z_1)^2} \; ; \qquad S = \sqrt{D_v^2 + (Z_2+Z_1)^2} \qquad (3\text{-}33,\ 3\text{-}34)$$

$$\psi = \arctan\left(\frac{Z_1+Z_2}{D_v}\right) \; ; \qquad D_s = \left(\frac{Z_1}{Z_2+Z_1}\right) D_v \qquad (3\text{-}35,\ 3\text{-}36)$$

$$S = S_1+S_2 = \sqrt{R^2+4Z_1Z_2} \qquad (3\text{-}37)$$

The path length difference S-R is of particular importance and for small reflection angles may be approximated by

$$S-R \approx \frac{2Z_1Z_2}{R} \qquad (3\text{-}38)$$

The center and half-length of the first Fresnel zone for specular reflection are determined as

$$L_n = \frac{S}{2}\left\{\frac{\sqrt{nS\lambda[4Z_1Z_2+nS\lambda]}}{(Z_1+Z_2)^2+nS\lambda}\right\} \qquad (3\text{-}39)$$

$$x_n = \frac{D_v}{2}\left\{\frac{2Z_1(Z_1+Z_2)+nS\lambda}{(Z_1+Z_2)^2+nS\lambda}\right\} \qquad (3\text{-}40)$$

where n is the order, L_n is the half-length of the zone, and x_n is the center of the zone. The approximation was made in the derivation that S + n/4 = S.

Painter defines the complex reflection coefficient Γ, which is a function of frequency, reflection angle, soil conductivity, and relative dielectric constant, as

$$\Gamma = \frac{K \sin\psi - \sqrt{(\varepsilon-jx)-\cos^2\psi}}{K \sin\psi + \sqrt{(\varepsilon-jx)-\cos^2\psi}} \qquad (3\text{-}41)$$

where

$$x = 1.13 \times 10^{5} \left(\frac{\sigma}{\omega}\right)$$

$$K = \begin{cases} \varepsilon - jx \ ; \text{ vertical polarization} \\ 1 \quad ; \text{ horizontal polarization} \end{cases}$$

This is equivalent to the definition given previously in this report.

Now assume that the normalized received signal is given by

$$X(t) = \frac{1}{R}\{\exp[-j\beta R] + \frac{R}{S}\Gamma \exp[-j\beta S] + \frac{R}{S}[1-\Gamma]F \exp[-j\beta S]\}\exp[j\omega t] \quad (3\text{-}42)$$

where $\beta = \frac{\omega}{c}$ and F is a factor to account for the surface wave component. When the surface wave component is negligible (i.e., at VHF and higher frequencies) we find that the angle and amplitude disturbance of a sinusoidal signal due to specular multipath effects are given by

$$X(t) = \frac{1}{R}\exp[-j\beta R]\{1 + \frac{R}{S}\Gamma \exp[-j\beta(S-R)]\}\exp[j\omega t] \quad (3\text{-}43)$$

Writing the complex reflection coefficient in polar form we may then write the received signal as

$$X(t) = \frac{1}{R}\exp[-j\beta R]\{1+\rho \exp\{-j[\beta(S-R)-\phi_{\Gamma}]\}\}\exp[j\omega t]$$

$$\triangleq \frac{1}{R}\exp[-j\beta R]A\exp[-j\alpha]\exp[j\omega t] \quad (3\text{-}44)$$

where

$$\Gamma \triangleq |\Gamma|\exp[j\phi_{\Gamma}]$$

$$\rho \triangleq \frac{R}{S}|\Gamma|$$

$$A = \sqrt{1+\rho^2+2\rho\cos[\beta(S-R)-\phi_{\Gamma}]}$$

$$\alpha = \arctan \frac{\rho \sin[\beta(S-R)-\phi_{\Gamma}]}{1+\rho\cos[\beta(S-R)-\phi_{\Gamma}]} .$$

The physical received signal is given by the real part of the above equation, i.e.

$$x(t) = \mathrm{Re}\{X(t)\} = \frac{A}{R}\cos[\omega t - \beta R - \alpha] \tag{3-45}$$

Painter then goes on to develop a representation of the channel between the aircraft and the synchronous relay satellite in terms of the time varying impulse response of the channels. This impulse response may be separated into the sum of the responses for the direct path and the indirect path. Denoting the total impulse response as $h(t,q)$, where an input at time q produces a response at time t, we have

$$h(t,q) = h_d(t,q) + h_r(t,q) \tag{3-46}$$

where the subscript d denotes the direct path and the subscript r denotes the reflected path. After a rather lengthy derivation Painter finds that the impulse response of the reflected path is given approximately by

$$h_r(t) = \frac{|\Gamma|}{S(t)}\left\{(\cos\phi_\Gamma)\delta(t-\tau_r) - \frac{\sin\phi_\Gamma}{\pi(t-\tau_r)}\right\} \tag{3-47}$$

where the time dependence of the geometric quantity S is now explicitly indicated and $\delta(\cdot)$ is the Dirac delta function. It should be noted that this impulse response is noncausal; however for the frequency range of interest the causal time function may be approximated by the above noncausal approximation.

It is seen that the impulse response for the reflected path not only attenuates and delays the signal, but also distorts it. The distortion term is weighted by the sine of the argument of the reflection coefficient and is the Hilbert transform of the transmitted signal. The overall impulse

response for the time varying case may be written as:

$$h(t) = h_d(t)+h_r(t) = \frac{1}{R(t)}\delta[t - \frac{R(t)}{c} - q] + \frac{|\Gamma|}{S(t)}\left\{(\cos\ \phi_\Gamma)\delta\{[t - \frac{S(t)}{c}] - q\}\right.$$

$$\left. +(\sin\ \phi_\Gamma) \cdot \frac{1}{\pi\{[t - \frac{S(t)}{c}] - q\}}\right\} \qquad (3\text{-}48)$$

where the time varying nature of the geometrical parameters R and S is now shown explicitly.

The non-specular, i.e. diffuse, component of the reflected signal is modeled as a stochastic process, based upon the geometry shown in Figure 3-28. In this case the total signal received is the summation of the direct path signal and many reflected signals. It is evident that if the surface is reasonably well behaved with the radii of curvature large with respect to the wavelength λ, there are surface slopes at points other than the specular point which have the proper orientation to cause reflections between the low orbiting satellite and the synchronous relay satellite. The extent of the surface over which such reflection is possible is a function of the geometry and of the distribution of slopes over the surface.

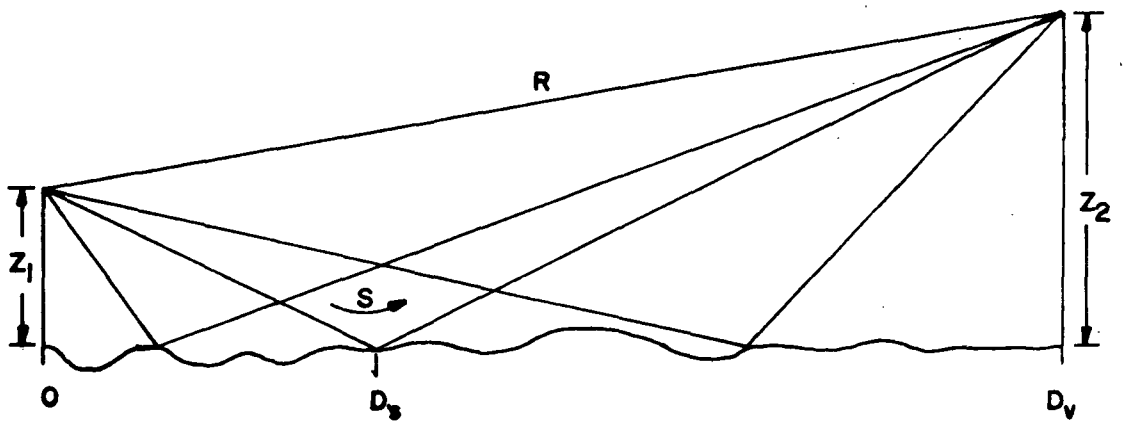

FIGURE 3-28 PAINTER'S MODEL FOR NON-SPECULAR REFLECTION

Consider a transmitted signal of the form $X(t) = m(t)e^{j\omega t}$. Then the signal received via the reflected path consists of contributions from those parts of the surface possessing the proper slope. Let the reflection from the i-th area be defined as

$$X_i(t) \triangleq \int_{-\infty}^{\infty} m(q)e^{j\omega q}h_i(t,q)dq \tag{3-49}$$

where $h_i(t,q)$ is the time varying impulse response for the i-th reflection. As in the case of specular reflection the individual reflections have the form

$$X_i(t) = \frac{|\Gamma_i|e^{j\phi_i}}{S_i} m(t - \frac{S_i}{c})e^{[j\omega(t - \frac{S_i}{c})]} \tag{3-50}$$

where S_i is the total reflection distance through the i-th reflection point. The reflection coefficient $|\Gamma|e^{j\phi_i}$ is less in magnitude than that for a plane earth since the curvature of the reflecting slope scatters the i-th wave in other than just the desired direction. The total reflected wave is given by a summation:

$$X_r(t) = \sum_i \frac{|\Gamma_i|e^{j\phi_i}}{S_i} m(t - \frac{S_i}{c})e^{-j\beta S_i}e^{j\omega t}. \tag{3-51}$$

Defining a differential distance

$$S-S_i = \frac{\nu_i}{\beta} \tag{3-52}$$

and a parameter

$$\chi_i = \frac{|\Gamma_i|}{|\Gamma|}\frac{S}{S_i} \tag{3-53}$$

and assuming the angle of the i-th reflection coefficient is equal to the angle of the plane earth reflection coefficient, Painter shows that

$$X_r(t) = \frac{\Gamma}{S} e^{-j\beta S} \sum_i m(t - \frac{S_i}{c})\chi_i e^{j\nu_i}e^{j\omega t}. \tag{3-54}$$

Painter now makes a crucial assumption. He assumes that the rate of variation of the modulation waveform is such that the waveform does not change appreciably during the time required for the wave to be reflected from the active reflecting area. This assumption is most restrictive at lower elevation angles. We now have

$$X_r(t) \approx \left[\frac{\Gamma}{S}\, m(t - \frac{S}{c}) e^{-j\beta S}\right]\left[\sum_i \chi_i e^{j\xi_i} e^{j\omega t}\right] \qquad (3\text{-}55)$$

This equation shows that under the appropriate restrictive assumption the reflected signal may be partitioned into a product of two functions one of which is dependent upon geometry, plane earth properties, and the modulation function; and the other of which is a weighted sum of unmodulated sinusoids which is the form treated comprehensively by Beckmann and Spizzichino (Reference 16).

To account for the statistical nature of the reflecting surface, Painter goes through a lengthy derivation to model the complex reflection coefficient $\rho(t)$. This complex Gaussian process is the scattering coefficient treated by Beckmann and Spizzichino and is equal to the complex ratio of actual reflected fields to that which would be reflected by a smooth perfectly conducting plane in the specular direction. The geometry of the situation is shown in Figure 3-29.

The random surface is denoted by $Z = \xi(x,y)$ and is oriented so as to have its mean value on the x-y plane. The solution for $\rho(t)$ is given by

$$\rho(t) = \frac{F_3}{A} \iint_A e^{i\vec{v}\cdot\vec{r}}\, dx\, dy \qquad (3\text{-}56)$$

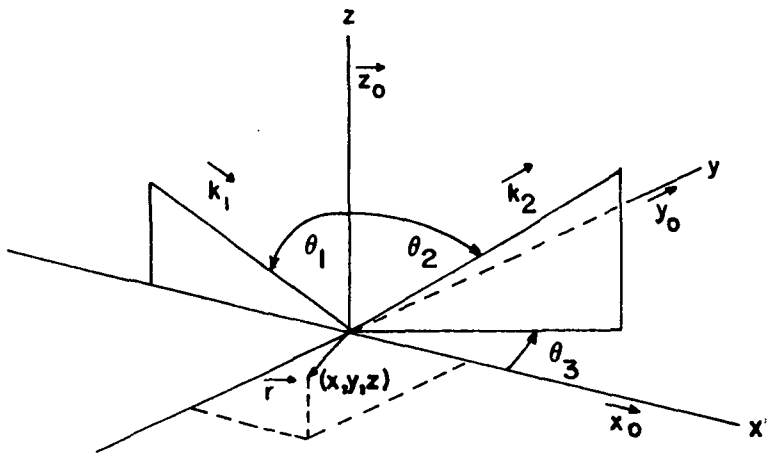

FIGURE 3-29 PHYSICAL OPTICS GEOMETRY FOR PAINTER'S MODEL OF ROUGH EARTH SCATTERING

where A is the area of the rough surface which is actually reflecting and $\vec{r}$ is the radial vector in x,y,z space. Painter also defines

$$\vec{v} = \vec{k}_1 - \vec{k}_2 \tag{3-57}$$

$$F_3 = \frac{1+\cos\theta_1 \cos\theta_2 - \sin\theta_1 \sin\theta_2 \cos\theta_3}{\cos\theta_1 (\cos\theta_1 + \cos\theta_2)} \tag{3-58}$$

$$\vec{v} = \beta[(\sin\theta_1 - \sin\theta_2 \cos\theta_3)\vec{x}_o - (\sin\theta_3 \sin\theta_3)\vec{y}_o - (\cos\theta_1 + \cos\theta_2)\vec{z}_o] \tag{3-59}$$

$$\vec{r} = x\vec{x}_o + y\vec{y}_o + \xi(x,y)\vec{z}_o \tag{3-60}$$

The general solution for $\rho(t)$ is quite involved geometrically.

Painter, drawing upon the work of Beckmann and Spizzichino (Reference 16), Staras (Reference 18), and Durrani and Staras (Reference 3), concludes that for the case of small surface roughness the reflection is concentrated in the specular direction and the active reflection area is not spread over a large part of the surface of the earth. Under these conditions the equation

defining $\rho(t)$ may be simplified considerably. Physically this is equivalent to saying that the roughness across the ray path from the aircraft to the synchronous relay satellite is no longer effective in the determination of the reflection coefficient. Thus for small surface roughness it is sufficient to assume a surface having roughness only in the x direction.

It is assumed by Painter that, over time intervals giving non-zero autocovariance for $\rho(t)$, the angle of incidence remains constant. It is also assumed that the reflecting surface is statistically stationary and that the active reflecting area is a window of length 2L. This assumption is not particularly realistic but little can be accomplished within a framework of a physical optics solution with other than this assumption. The length 2L is also assumed invariant over time intervals giving non-zero autocovariance.

Painter takes the surface as a stochastic process $\xi(x)$ having a second order Gaussian density $\rho_{\xi}(\xi_1,\xi_2;x_1,x_2)$. The reflection coefficient then simplifies to

$$\rho(t) = \frac{1}{2L}\int_{-L}^{L} e^{i\nu_z \xi(x)}\, dx \qquad (3\text{-}61)$$

where $\nu_z = 2\beta \cos\theta_1$

$$\beta = \frac{\omega}{c} = \frac{2\pi f}{c}$$

The window of length 2L is assumed to be moving in the direction of increasing x at a uniform rate $\dot{x} = v_s$. Thus time variation enters because the surface

is being translated with respect to the coordinate system. The autocovariance of $\rho(t)$ is given by

$$E\{[\rho(t_2)-\bar{\rho}(t_2)][\rho(t_1)-\bar{\rho}(t_1)]^*\} \triangleq C(t_2,t_1) \tag{3-62}$$

which is also the autocovariance of $z(t)$. The mean of $\rho(t)$ is obtained as

$$\bar{\rho}(t) = \frac{1}{2L}\int_{-L}^{L} E\{e^{i\nu_z\xi(x)}\}dx . \tag{3-63}$$

Painter then considers the autocorrelation function

$$R_{\rho\rho}(t_2,t_1) = E\{\rho(t_2)\rho^*(t_1)\} \tag{3-64}$$

Making the assumptions that the active reflection area window is of length 2L regardless of movement across the surface, the surface is weakly stationary, the surface autocorrelation is sufficiently narrow so that for all values of x' which are of interest the parameter

$$G(x) = e^{\nu_z^2 R_{\xi\xi}(x+x')} - 1 \tag{3-65}$$

is a marked maximum in the interval $[-2L,2L]$, a certain integral may be evaluated by steepest descent methods, and the function

$$\exp\left\{\frac{\nu_z^2 R''_{\xi\xi}(0)u^2}{2[1-\exp(-\nu_z^2\sigma_\xi^2)]}\right\} \tag{3-66}$$

is sufficiently narrow with respect to 2L that a certain integral may be approximated by integration between finite limits, Painter arrives at the conclusion that the autocovariance is given by

$$C(x') = \frac{\sqrt{2\pi}[1-\exp(-\nu_z^2\sigma_\xi^2)]^{3/2}[2L-|x'|]}{4L^2\nu_z\sigma_{\xi'}} \tag{3-67}$$

and the autocorrelation is given by

$$R_{\rho\rho}(x') = \exp\{-\nu_z^2\sigma_\xi^2\} + C(x') \qquad (3\text{-}68)$$

Painter uses these results in an extremely lengthy derivation to arrive at two stochastic processes which make up the defined complex diffuse reflection process. These two processes are low pass and non-stationary. They also are zero-mean by definition and are taken as uncorrelated; hence they are independent. At this point Painter uses a computer simulation to derive the diffuse signal.

Since Painter has chosen to emphasize the characterization of the channel by its impulse response, whereas we are interested primarily in a characterization of a channel in a manner such as to provide for ease of measurement experimentally of channel parameters, and since Painter's model is based upon a flat earth approximation, we choose to use another model as our selection of the best model for the configuration of a low orbiting satellite and a synchronous relay satellite. However, Painter's model is excellent for application to experiments using an aircraft or a balloon platform.

3.4.7 LINCOLN LABORATORIES MODEL

The Massachusetts Institute of Technology Lincoln Laboratories model described in Reference 19 is based upon the work of Beckmann and Spizzichino (Reference 16). However, the Lincoln Labs model does not present detailed definition of the divergence factor due to a spherical earth, nor do they define the diffuse component in terms of integrals and surface parameters. Rather, they rely on experimental measurement of the parameters.

The Lincoln Labs model defines the specular component of the multipath signal as

$$\frac{P_{specular}}{P_{direct}} = D^2|R_o|^2 e^{-\left[\frac{2\pi\sigma}{\lambda}\sin\psi\right]^2} \qquad (3\text{-}69)$$

where D = divergence factor

R_o = reflectivity

σ = surface roughness

λ = wavelength

which is essentially the same as the ESL model to be described next. However, they define the diffuse component as the difference between the total reflected power and the specular component, where the total reflected power is simply $D^2|R_o|^2$. Thus, the diffuse power, according to the Lincoln Labs model, is given by

$$\frac{P_{diffuse}}{P_{direct}} = D^2|R_o|^2\left[1-e^{-(\frac{2\pi\sigma}{\lambda}\sin\psi)^2}\right] \qquad (3\text{-}70)$$

Lincoln Labs notes that the ratio of the two components is quite dependent on the surface roughness, although the total reflected power is not.

The Lincoln Labs model, considering their less rigorous definition of the diffuse component, is less accurate than the ESL model (to be described next) for predicting the multipath environment encountered by a low orbiting satellite operating in conjunction with a synchronous relay satellite. However, for the case of an aircraft operating with a satellite relay, as may be the case in the experiments performed with a SATS, the Lincoln Labs model is felt to be adequate to define the multipath environment. Since it is

computationally considerably simpler than the ESL model, we believe that the Lincoln Labs model could be used for the situations of an aircraft and relay satellite.

3.4.8 THE ESL MULTIPATH MODEL

The ESL multipath model considers only the effect of reflection from the rough earth. Ionospheric effects are not included because their impact on the signals is minimal and detailed modeling would require knowledge of parameters (e.g., electron density in the ionosphere) which are not normally available and which vary significantly with time and location.

We summarize in this section the ESL rough earth scattering model as presented in References 6, 7, and 8. The model presented by ESL is a scalar model. This is considered adequate if the assumption is made that the receiver does not preserve polarization angle. The only polarization dependent term, which is the Fresnel coefficient, is evaluated for circular polarization.

The total power reflected from the earth surface is the sum of two components, one specular and one diffuse. The dominant component for satellite altitudes in the range 185 to 560 kilometers is the diffuse component; the specular component dominates over portions of the range 1850 to 5560 kilometers altitude. In all cases the reflected power is a decreasing function of satellite altitude.

The specular power reflected by the earth is a function of several factors including the RMS surface roughness, the wavelengths, the average value of the Fresnel coefficient, the shadowing of part of the reflecting area by surface peaks, and a divergence factor which models the curvature

of the earth. In particular, the specular component of the reflected signal is given by

$$\frac{P_{specular}}{P_{direct}} = \frac{e^{-(\frac{4\pi\sigma}{\lambda}\cos\mu_1)^2}}{(S_1+S_2)^2} D^2 \langle R_o \rangle^2 S(\mu_1)^2 \qquad (3\text{-}71)$$

where

$$D = \left[1 + \frac{2Z_1Z_2}{a(Z_1+Z_2)\cos\mu}\right]^{-\frac{1}{2}} \left[1 + \frac{2Z_1Z_2}{a(Z_1+Z_2)}\right]^{-\frac{1}{2}} = \text{divergence factor}$$

S_1 = distance of transmitter from specular point

S_2 = distance of receiver from specular point

$S(\mu_1) = \exp[-\frac{1}{4}\tan\mu_1 \operatorname{erfc}(k\cot\mu_1)]$

$k = \frac{T}{2\sigma}$

T = correlation length

σ = RMS roughness

$$\langle R_o \rangle = \frac{\sqrt{2}}{2}\sqrt{R_\perp^2+R_{11}^2} = \text{average Fresnel coefficient}$$

$$R_\perp = \frac{\left(K_{e_1}-K_{e_2}\sin^2\mu_1\right)^{\frac{1}{2}} - \sqrt{K_{e_2}}\cos\mu_1}{\left(K_{e_1}-K_{e_2}\sin^2\mu_1\right)^{\frac{1}{2}} + \sqrt{K_{e_2}}\cos\mu_1}$$

$$R_{11} = \frac{K_{e_1}\cos\mu_1 - \sqrt{K_{e_2}}\left(K_{e_1}-K_{e_2}\sin^2\mu_1\right)^{\frac{1}{2}}}{K_{e_1}\cos\mu_1 + \sqrt{K_{e_2}}\left(K_{e_1}-K_{e_2}\sin^2\mu_1\right)^{\frac{1}{2}}}$$

ε_0 = permeability of free space for the geometry

for the geometry shown in Figure 3-30.

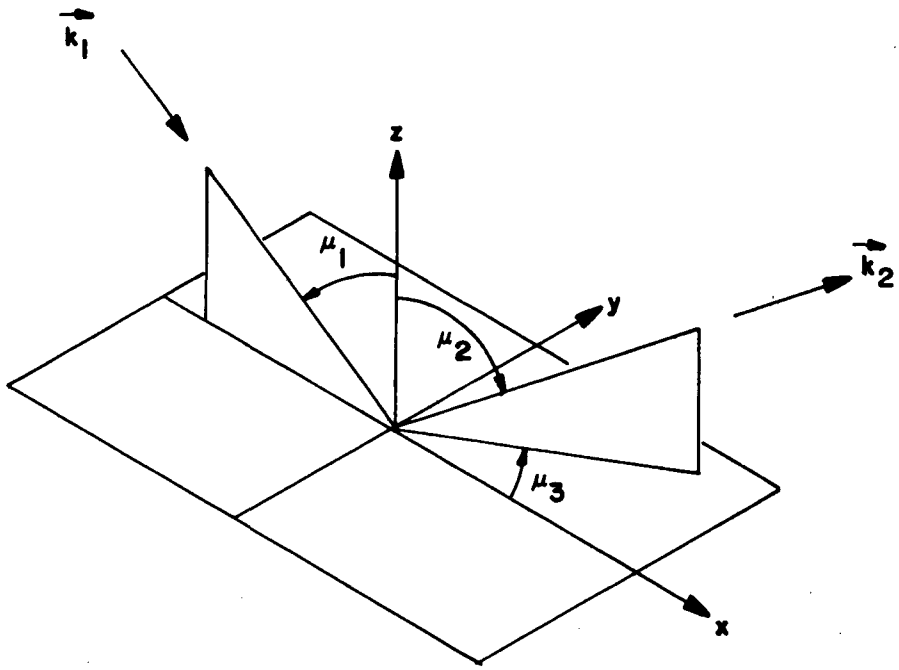

FIGURE 3-30 DEFINITION OF SCATTERING ANGLES

For small values of μ the general shape of the curve is determined by the exponential factor. The specular power decreases as the satellite altitude increases due to the effect of the divergence factor. The reflections from sea water, which has a larger dielectric constant than land, are approximately 2.5 dB greater than those from land. This is accounted for by the increase in value of the Fresnel coefficient as the dielectric constant increases. The surface roughness σ has a strong influence on the spectral power through the exponential factor. Large surface roughness produces a small specular reflection and small surface roughness produces large specular reflection. Even for incident angles μ below 1.2 radians a significant specular reflection can occur from relatively flat surfaces.

The correlation length T has a significant effect on the specular reflection only at high incident angles. This occurs because T appears only in the shadowing function which has a dominant effect only at the high incident angles. A large T corresponds to a flat terrain and hence less shadowing.

The expression for the diffuse component of the reflected signal is more complicated than the one for specular reflection. In the case of diffuse scattering, the reflected signal, after a lengthy derivation, is found to be given by:

$$\frac{P_{diffuse}}{P_{direct}} = \frac{2}{\pi}\langle |R_o|^2 \rangle \iint_S D^2 S(\mu_1) \left(\frac{\cos\mu F_3}{R_o}\right)^2 J \, ds \qquad (3\text{-}72)$$

where

$$J = \int_0^\infty J_o(V_{xy}\tau)\left(\chi_2(v_z,-v_z)-\chi(v_z)\chi^*(v_z)\right)\tau \, d\tau$$

R_o = Fresnel coefficient
D = Divergence factor
$S(\mu_1)$ = shadowing function
} same as for specular component

R_o = distance from the origin of the scattering surface to the receiver

$$V_{xy} = \sqrt{v_x^2+v_y^2}$$

$$\chi_2(v_z,-v_z)-\chi(v_z)\chi^*(v_z) = e^{-g(1-e^{-\tau^2/T^2})}-e^{-g}$$

$$g = \left[\frac{2\pi\sigma}{\lambda}(\cos\mu_1 + \cos\mu_2)\right]^2$$

λ = wavelength

σ = standard deviation of p.d.f. of surface irregularities

$$\vec{v} = (v_x, v_y, v_z) = \vec{k}_1 - \vec{k}_2$$

T = correlation length

$$F_3 = \frac{1+\cos \mu_1 \cos \mu_2 - \sin \mu_1 \sin \mu_2 \cos \mu_3}{\cos \mu_1 (\cos \mu_1 + \cos \mu_2)}$$

for the geometry of Figure 3-30.

We believe this model is the best choice for representing mathematically the communication link between a low altitude satellite and a synchronous relay satellite.

3.4.9 DESCRIPTION OF THE TIME-VARYING CHANNEL BETWEEN THE AIRCRAFT AND GEOSTATIONARY SATELLITE

In the previous sections we have described a multitude of mathematical models and have indicated our choice of a model, namely the ESL model, for the low altitude spacecraft/synchronous relay satellite configuration. In this section we summarize our choice for the aircraft/satellite link, as shown in Figure 3-31. This section is based upon the Lincoln Labs and Magnavox models previously discussed.

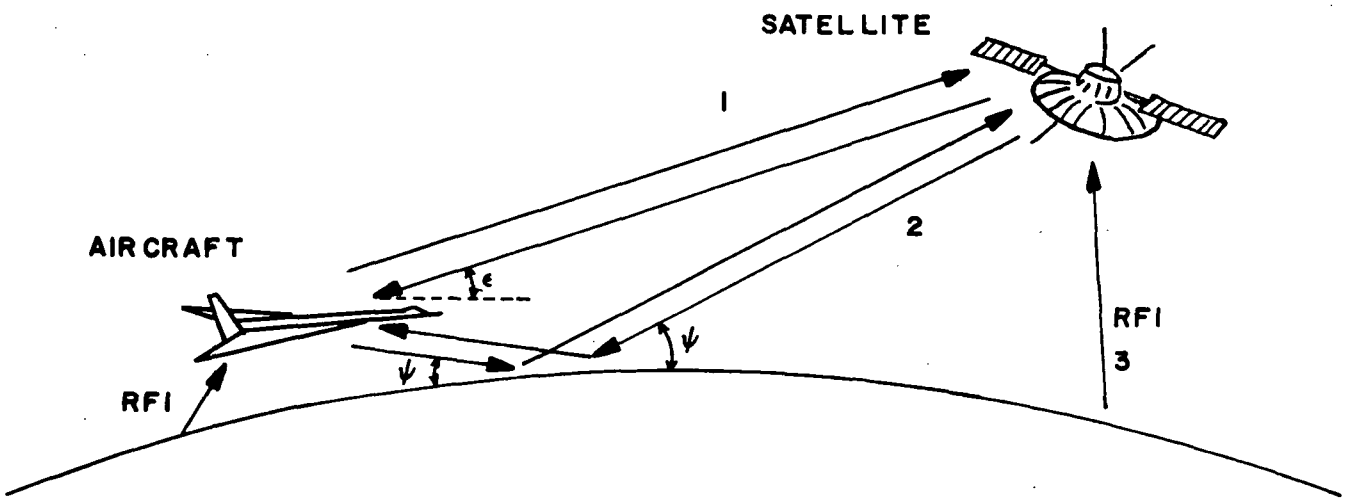

FIGURE 3-31 AIRCRAFT-TO-SATELLITE LINK CHARACTERISTICS

Several aircraft-to-satellite multipath tests have been conducted at VHF and UHF by various researchers. These include K. L. Jordan of Lincoln Laboratory, Collins Radio Company, and Alan Johnson of Wright-Patterson AFB. All researchers indicate that a combination of specular energy reflected from the earth's surface along with diffuse energy can be expected at VHF and UHF frequencies. Thus, the indirect signal or reflected signal can have two components, a specular component which is a replica of the transmitted signal and a diffuse component similar to random noise. In general, the amount of reflected specular energy is expressed by*

$$P_{specular} = g\langle\rho_s^2\rangle D^2 |R_o|^2 P_d \qquad (3\text{-}5)$$

where

$$\langle\rho_s^2\rangle = e^{-\left(\frac{4\pi\sigma}{\lambda}\sin\psi\right)^2}$$

ψ = grazing angle

g = a factor which is dependent on the aircraft antenna pattern and which controls the amount of power directed toward the surface

P_d = direct power

λ = wavelength

σ = rms height of the reflecting surface

D = average divergence factor associated with the spherical earth

$|R_o|^2$ = mean squared reflection coefficient

The amount of diffuse power is expressed by

$$P_{diffuse} = gD^2 |R_o|^2 P_d (1-\langle P_s\rangle^2) \qquad (3\text{-}6)$$

---

* These equations are identical to those presented in Section 3.4.2; they are repeated here for convenience of reference.

The divergence factor is shown in Figure 3-32 as a function of the grazing angle for various aircraft altitudes. We see that for low grazing angles the divergence factor serves to diminish the multipath or reflected signal. For VHF and UHF frequencies, the reflected signal should be primarily diffuse for $\psi > 0.35$ radians and normal surface conditions.

Scattering models of the earth's surface have been partially confirmed by measurement. These models usually rely upon a Gaussianly distributed height variation σ and some correlation distance T which, in this case, indicates the degree of correlation between one point on the earth and another. The reflected signal, consisting of specular and diffuse components, is illustrated in Figure 3-8 along with the signal that is received via the direct path. The signal received via the direct path will be offset from the true transmitted frequency by the direct path Doppler, and the indirect signal will be further offset by the differential Doppler associated with the indirect path relative to the direct path.

The diffuse energy associated with the indirect path will have some bandwidth referred to as the fading bandwidth, as illustrated in Figure 3-8. It can be shown that the fading bandwidth is related to the velocity of the aircraft, the RMS height variation of the surface σ, the correlation distance T along the surface of the ocean, and the grazing angle by:

$$B_F = \frac{\sqrt{2}v\sigma}{T\lambda} \sin \psi$$

where

v = aircraft velocity

λ = wavelength

ψ = grazing angle

T = correlation distance

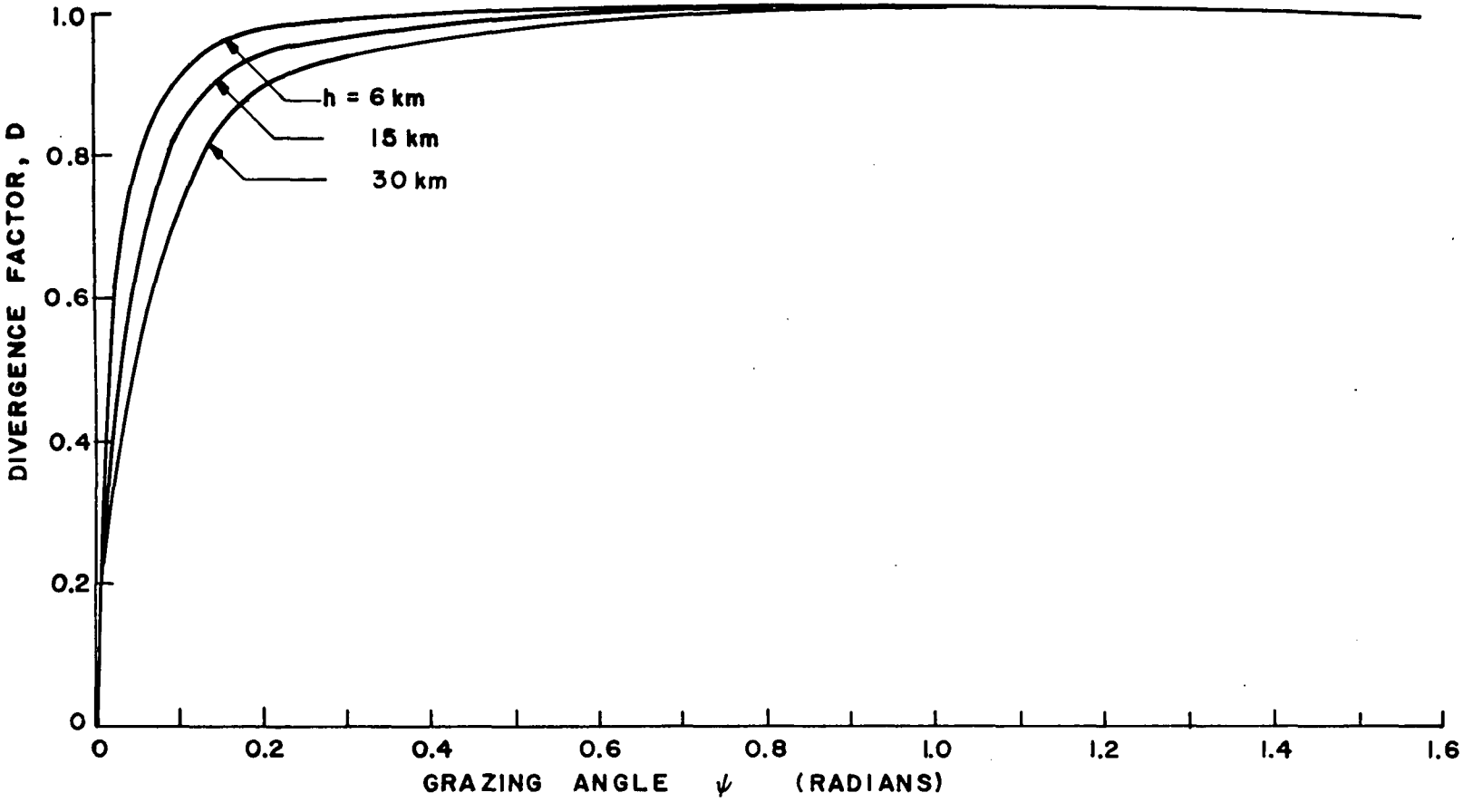

FIGURE 3-32 DIVERGENCE FACTOR VS. GRAZING ANGLE (AIRCRAFT-TO-SYNCHRONOUS SATELLITE LINK)

So far, we have established that the signal received at the satellite from the aircraft can be described by several parameters. First, there is the power associated with the direct path P_d, the total power associated with the indirect signal P_{ind}, the amount of power that is specular $(P_{specular})$ as opposed to diffuse $(P_{diffuse})$, the direct path Doppler, the indirect path differential Doppler, and the fading bandwidth associated with the diffuse component, and the coherent bandwidth.

If one isolates the indirect signal, one observes, in general, that the envelope will follow a Rician probability density, since this path consists of both a specular component and a diffuse component. If the reflected signal is completely diffuse, then we can expect the envelope of the reflected signal to have a Rayleigh envelope p.d.f. This has been observed by Lebow, et.al. (Reference 19) who used a pseudonoise signal between a satellite and an aircraft at 235 MHz to investigate the fading bandwidth. Thus, both diffuse and specular components can exist depending upon surface roughness and the correlation distance along the surface. Under most general cases, the reflected signal envelope will follow a Rician probability density when a constant envelope signal is transmitted.

When the direct signal is combined with the indirect signal at the spacecraft, the composite envelope of this complex signal (again assuming that constant envelope signals have been transmitted from the aircraft) will follow a generalized Rician density. The generalized Rician density for two constant envelope signals and a diffuse component is given by

$$P(R) = R \int_0^\infty r\, J_o(Rr)\, J_o(Ar)\, J_o(BR)\, e^{-\frac{r^2(N+P_{diff})}{2}}\, dr \qquad (3\text{-}73)$$

where

A = direct signal amplitude = $\sqrt{2P_{direct}}$

B = specular component amplitude = $\sqrt{2P_{specular}}$

N = noise

P_{diff} = diffuse power

It is easy to see from the above equation that the statistics associated with the composite signal received at the satellite from the spacecraft are quite complicated.

There will be an absolute delay between the direct signal and the signal reflected from the surface of the earth. The absolute differential delay between the direct and the indirect paths is τ_d. The value τ_d is a function of the aircraft altitude above the surface of the ocean, the grazing angle, and the altitude of the spacecraft (in this instance, it is assumed to be synchronous). The differential delay is given by $\tau_d \approx \frac{2h}{c} \sin \psi$ where the aircraft height is h and the grazing angle is ψ. The values of τ_d are shown graphically in Figure 3-33. The figure shows that the maximum value of τ_d exists when the aircraft is directly underneath the satellite. Figure 3-34 shows the direct path Doppler/Mach* and differential Doppler/Mach* vs. the grazing angle. Measured fading bandwidth data taken by Lincoln Labs is shown in Figure 3-35.

The coherent bandwidth of the path between the aircraft and satellite, which was defined in Figure 3-13, pertains only to the reflected signal. The coherent bandwidth B_c is inversely proportional to the time spread of the

---

* Mach 1 ≈ 330 m/s

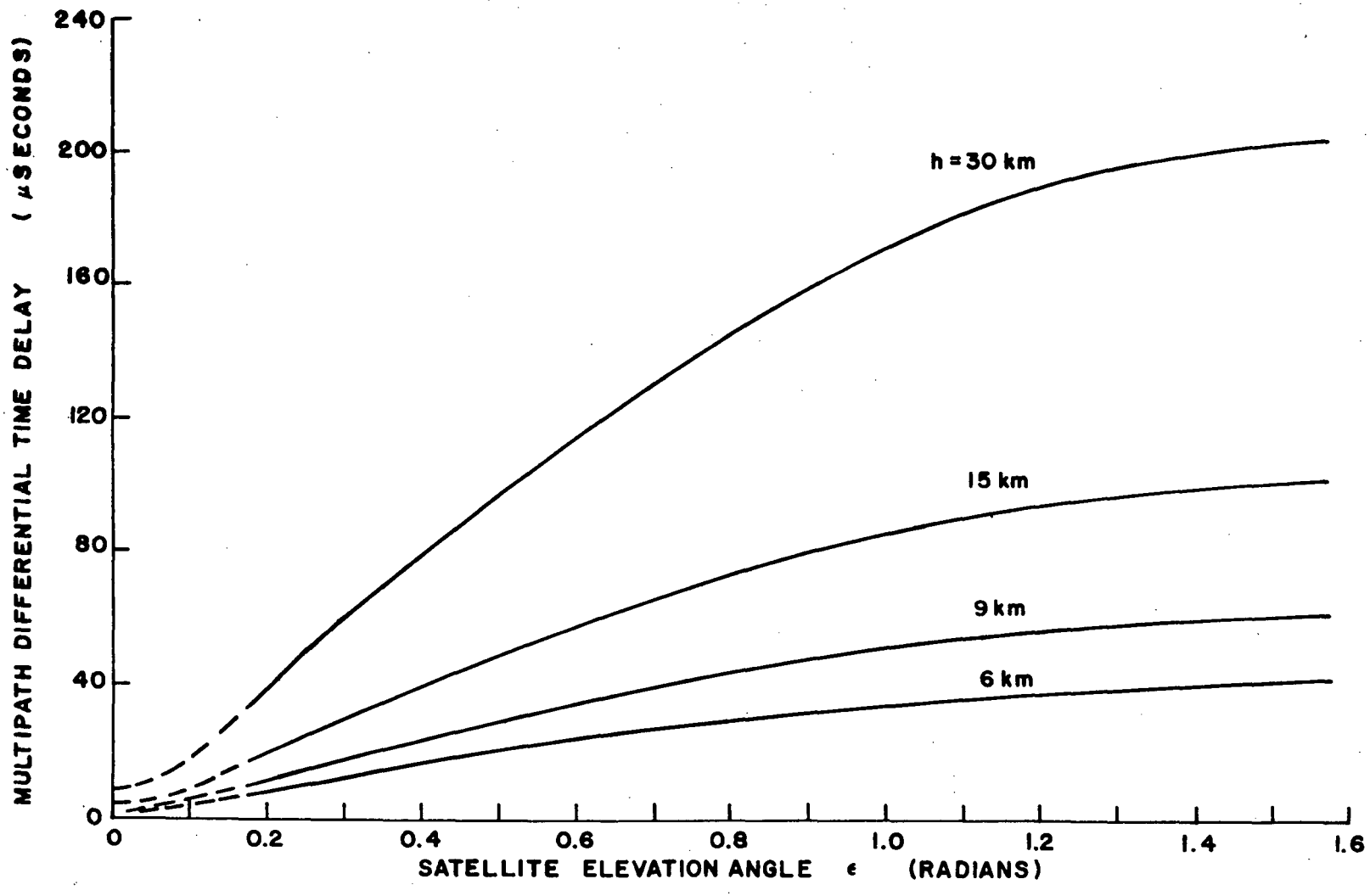

FIGURE 3-33 MULTIPATH DIFFERENTIAL TIME DELAY VS. SATELLITE ELEVATION ANGLE

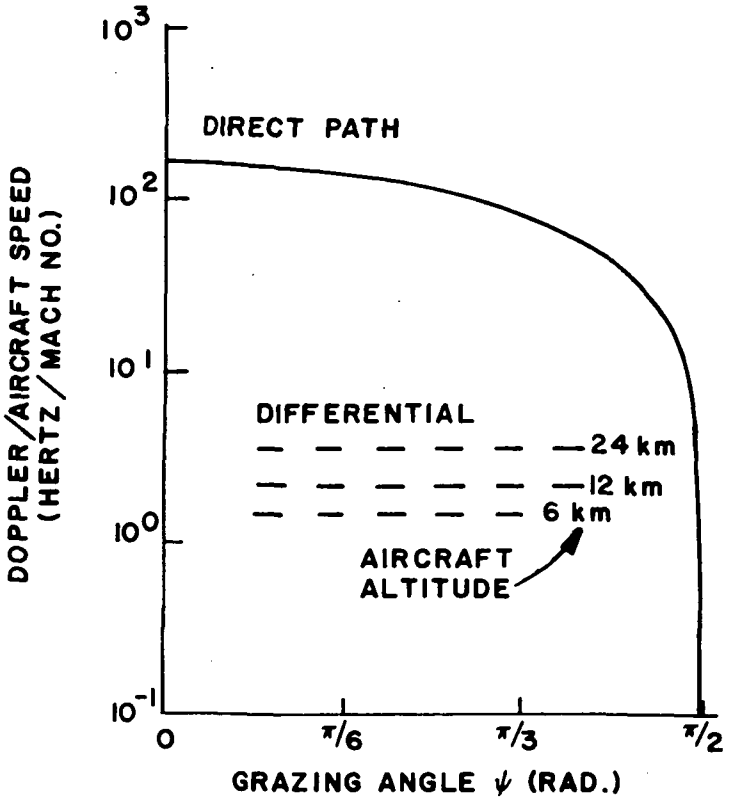

FIGURE 3-34 DIRECT PATH DOPPLER AND DIFFERENTIAL DOPPLER VS. GRAZING ANGLE AT VHF

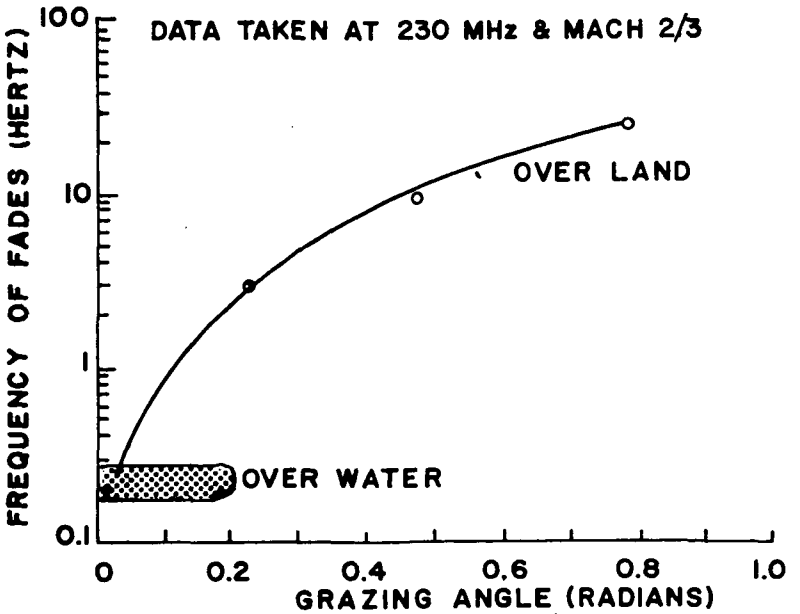

FIGURE 3-35 FADING BANDWIDTH VS. GRAZING ANGLE

reflected signal. The coherent bandwidth is given by

$$B_c = \frac{C \sin \psi}{h} \left(\frac{T}{\sigma}\right)^2 \qquad (3\text{-}74)$$

where

h = the height of the aircraft divided by the mean radius of the earth

C = speed of light

ψ = grazing angle

T = correlation distance

σ = surface roughness

Thus, the link between the aircraft and satellite can be summarized as a three-component path: a direct path, a specular indirect path, and a diffuse indirect path. In addition to the direct signal and the multipath signal there will be the ever-present additive noise at the input to the transponder at the satellite.

Table 3-5 summarizes the multipath parameters for an aircraft-to-synchronous satellite links at VHF.

3.5 RANGE OF PARAMETERS OF INTEREST

In the preceding sections we have presented the various multipath models which have been developed by various researchers. In this section we present a summary of the range of values of the various parameters of interest.

TABLE 3-5

MULTIPATH PARAMETERS FOR VHF AIRCRAFT/SYNCHRONOUS SATELLITE LINK

PARAMETER	EQUATION	MAGNITUDE AT VHF
$P_{specular}$	$g\|R_o\|^2 D^2 e^{-\left[\frac{4\pi\sigma}{\lambda}\sin\psi\right]^2}$	decreases rapidly for $\psi > 0.26$ radians
$P_{diffuse}$	$g\|R_o\|^2 D^2 \left[1-e^{-\left[\frac{4\pi\sigma}{\lambda}\sin\psi\right]^2}\right]$	referred to direct power at $\psi > 0.26$ radians
Direct Doppler	$f_o \frac{v}{C}\cos\psi$	0-160 Hz at Mach one**
Differential Doppler	$\frac{2vh}{R_e\lambda}\sin 2\psi$ *	2 Hz at 6.1 km
Coherent Bandwidth	$\frac{C \sin\psi}{h}(T/\sigma)^2$	dependent on σ/T values
Fading Bandwidth	$\frac{\sqrt{2}}{\lambda}\frac{\sigma}{T}\frac{v}{c}\sin\psi$	dependent on σ/T values
Differential Time Delay	$\frac{2h}{C}\sin\psi$	0-40 μsec at 6.1 km
Polarization of Reflected Signal	sense of reflection can reverse	horizontal predominates over vertical

* R_e is the equivalent earth radius.

** Mach one ≈ 330 m/s

As we have shown, the channel between the low orbiting satellite and a synchronous relay satellite may be characterized by these parameters:

- Ratio of multipath signal to direct path signal
- Polarization of signal
- Direct path Doppler shift
- Differential Doppler
- Fading bandwidth
- Coherent bandwidth
- Time delay between direct path signal and multipath signal

The anticipated values of these parameters are summarized in Tables 3-6 (for VHF) and 3-7 (for S-band). Since the experiments to be conducted may involve the use of aircraft as well as a SATS, values for aircraft are also included in the tables.

TABLE 3-6

CHANNEL PARAMETER BOUNDS FOR VHF PLATFORM

Channel Parameter	Range of values for VHF aircraft	Range of values for VHF low altitude SATS
Ratio of Direct to Reflected Signal	can be as low as 0 dB	can be as low as 0 dB
Polarizations of Received Direct and Reflected Signal	Lincoln Laboratory measurement indicate horizontal component dominates	
Specular vs Diffuse Multipath	Both specular and diffuse components exist. They can be of equal magnitude at low grazing angles.	
Direct Path Doppler	0 to $\pm$150 Hz at 300 m/s	0 to $\pm$4 kHz
Differential Doppler	0-1.5 Hz @ 6.1 km and 330 m/s	0 to $\pm$1500 Hz
Fading Bandwidth	0 to 5 Hz @ 330 m/s	0 to $\pm$2000 Hz
Coherent Bandwidth	0-500 kHz	0-30 kHz
Time Delay Between Direct and Multipath Signal	0 to 45 μs at 6.1 km	0-30 ms for 4000 km altitude

TABLE 3-7

CHANNEL PARAMETER BOUNDS FOR S-BAND PLATFORM

Channel Parameter	Range of values for S-Band aircraft	Range of values for S-Band low altitude SATS
Ratio of Direct to Reflected Signal	can be as low as 0 dB	can be as low as 3 dB
Polarizations of Received Direct and Reflected Signals	Polarization of reflected signal is reversed.	
Specular vs. Diffuse Multipath	Only diffuse components exist.	
Direct Path Doppler	0 to ±1.88 kHz at 300 m/s	0 to ±5 kHz
Differential Doppler	0 to 18.8 Hz at 6.1 km and 330 m/s	0 to ±18.8 kHz
Fading Bandwidth	0 to 62.5 Hz at 330 m/s	0 to ±25 kHz
Coherent Bandwidth	0 to 500 kHz	0 to 30 kHz
Time Delay Between Direct and Multipath Signals	0 to 45 μs at 6.1 km	0 to 30 ms for 4000 km altitude

4. RADIO FREQUENCY INTERFERENCE

In this section we discuss RFI as it applies to a low altitude spacecraft such as SATS and for SATS used as a relay satellite. Much work has been conducted on the Tracking and Data Relay Satellite program to determine or project the amount of RFI which will be seen by these two types of platforms. Most of the information presented in this section is based upon that work.

4.1 EXISTING RADIO FREQUENCY INTERFERENCE (RFI) LEVELS

Unintentional, upward directed RFI from emitters located on the earth and in view of both the Synchronous SATS and the low altitude SATS can be a source of interference which will be deleterious. In this section, RFI data is presented for the following links:

SYNCHRONOUS SATELLITE TO LOW ALTITUDE SATELLITE	LOW ATLTITUDE SATELLITE TO SYNCHRONOUS SATELLITE
Forward Link	Return Link
117.425-117.525 MHz	136-138 MHz
127.7-127.85 MHz	
148-155 MHz	
400.5-401.5 MHz	

Some of these bands contain relatively high powered constant envelope narrowband RFI sources. In order to evaluate the impact of RFI on the performance of the forward and return links, Magnavox has, with the assistance of Mr. John W. Bryan of NASA/Goddard Space Flight Center, evaluated pertinent information relative to RFI in the bands of interest. From computer tabulations provided by Bryan, an estimate of the worst case RFI distribution at the TDRS and user has been derived.

Moreover, ESL, Incorporated has recently concluded two related studies for NASA/GSFC (References 6 and 8) which explain the radio frequency interference problems relating to the synchronous SATS and the low altitude SATS. The RFI modeling by ESL consists of examination of data contained in the International Frequency List compiled by the International Frequency Registration Board of the International Telecommunication Union, the Jeppesen Air Manuals, CONUS emitter tabulations from the Electromagnetic Compatibility Analysis Center, and other sources. By a series of prediction programs ESL was able to provide an estimate of the power that would be received from each source of RFI at the SATS in synchronous orbit with an earth coverage antenna. Figures 4-1, 4-2, and 4-3 present a graphical indication of the RFI power density at a synchronous SATS located at positions of 11°W, 143°W, 112°E, respectively. These densities as presented here are distributed over the frequency band 117 to 155 MHz.

An assessment has also been made of the impact of RFI on the low altitude SATS. Assuming two user locations, 50°N 30°E and 38°N 88°W, the RFI density levels at the low altitude SATS are shown in Figures 4-4 and 4-5 respectively. In each case the low altitude SATS is equipped with an omni-directional antenna and is at an altitude of 1000 kilometers. As an indication of the coverage of this satellite, a satellite with an omnidirectional antenna at 1000 km centered at 38°N and 88°W will be in view of all of CONUS and parts of Mexico and Canada.

Through our own research; that of John Bryan of NASA; and that of ESL, Inc. we have concluded that of the bands of interest the 148-155 MHz band is the least usable as a command band. The number of emitters in the

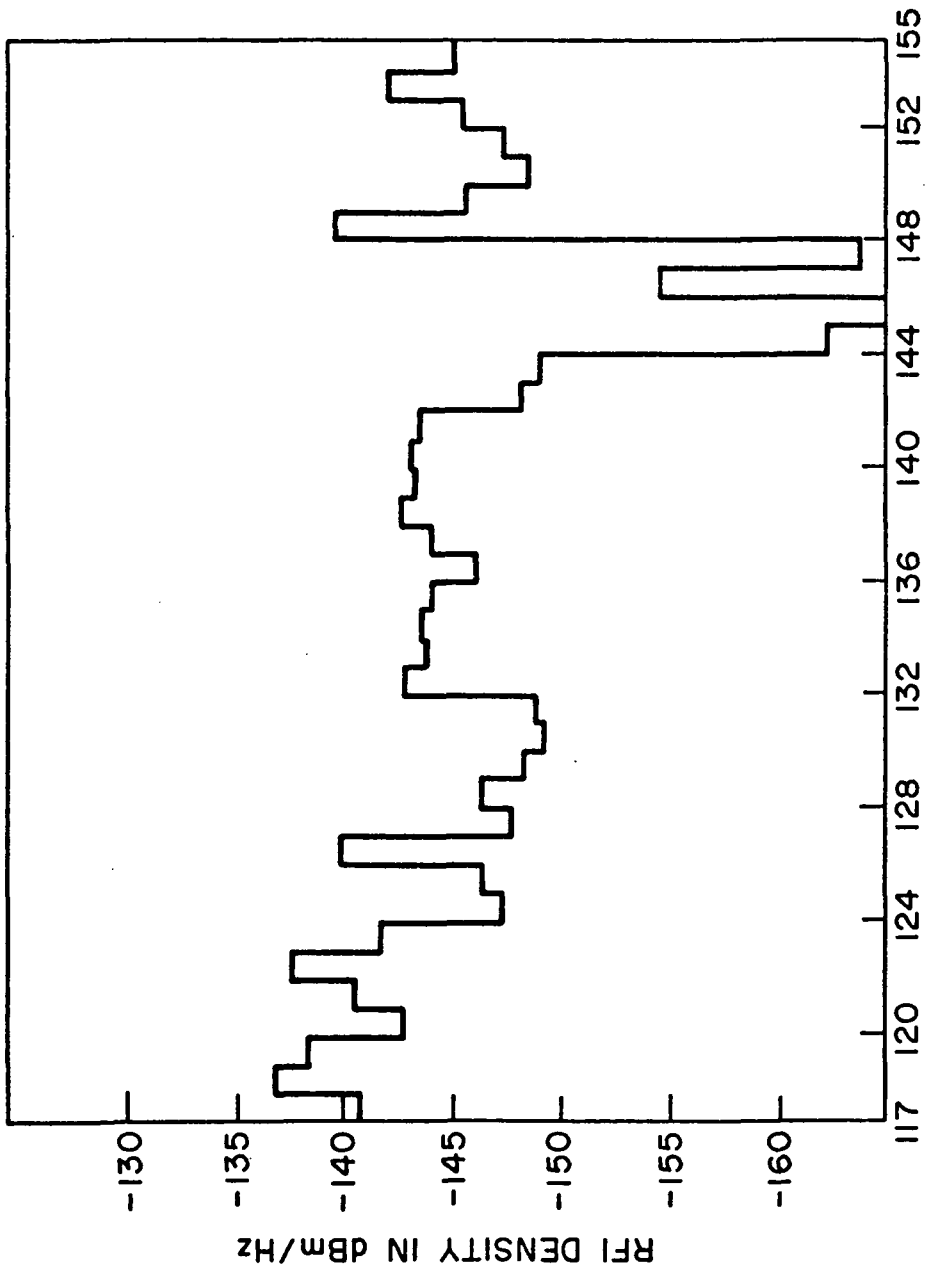

FIGURE 4-1 RFI POWER DENSITY FOR TDRS LOCATED AT 11° W

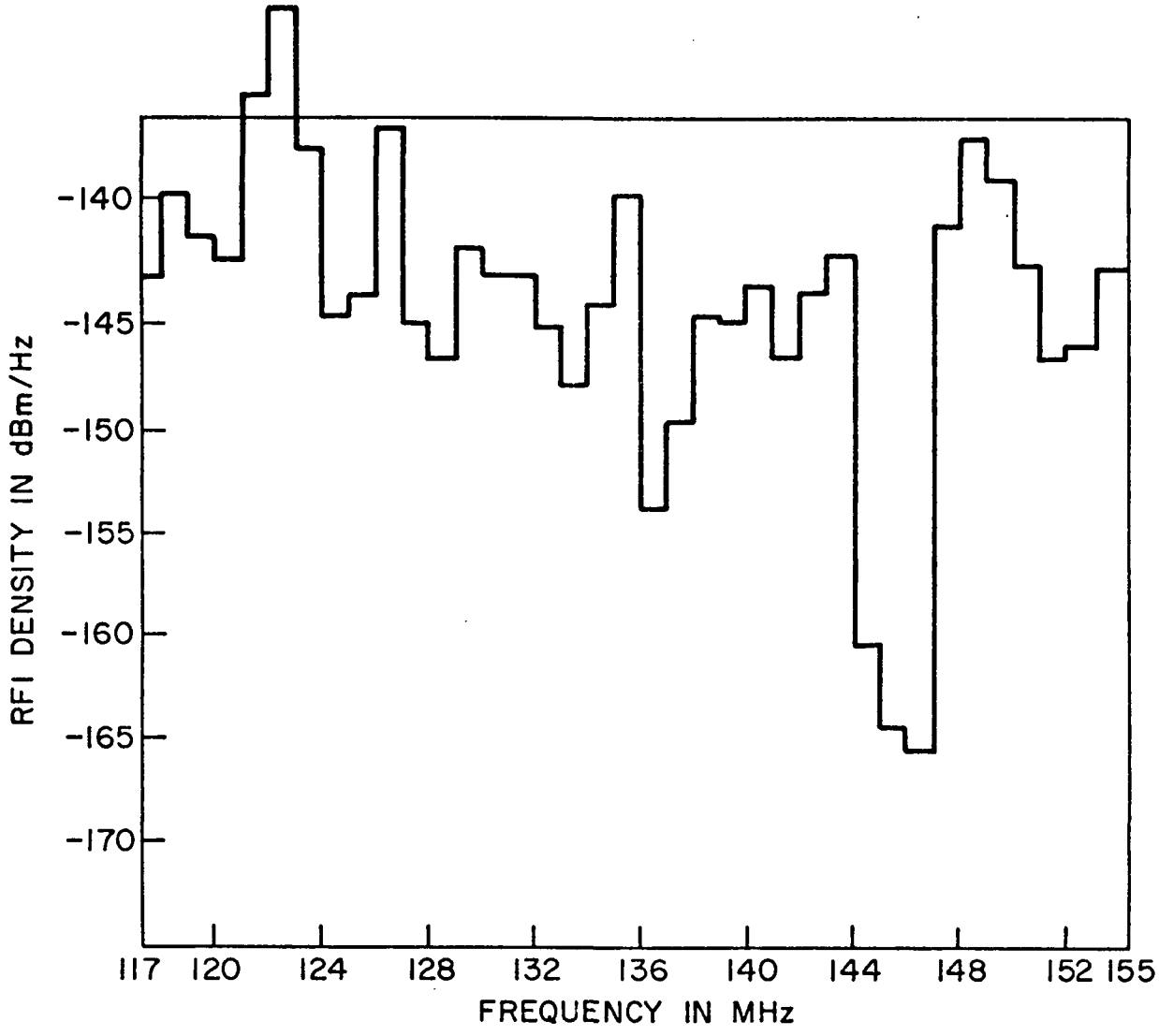

FIGURE 4-2 RFI POWER DENSITY FOR TDRS LOCATED AT 143° W

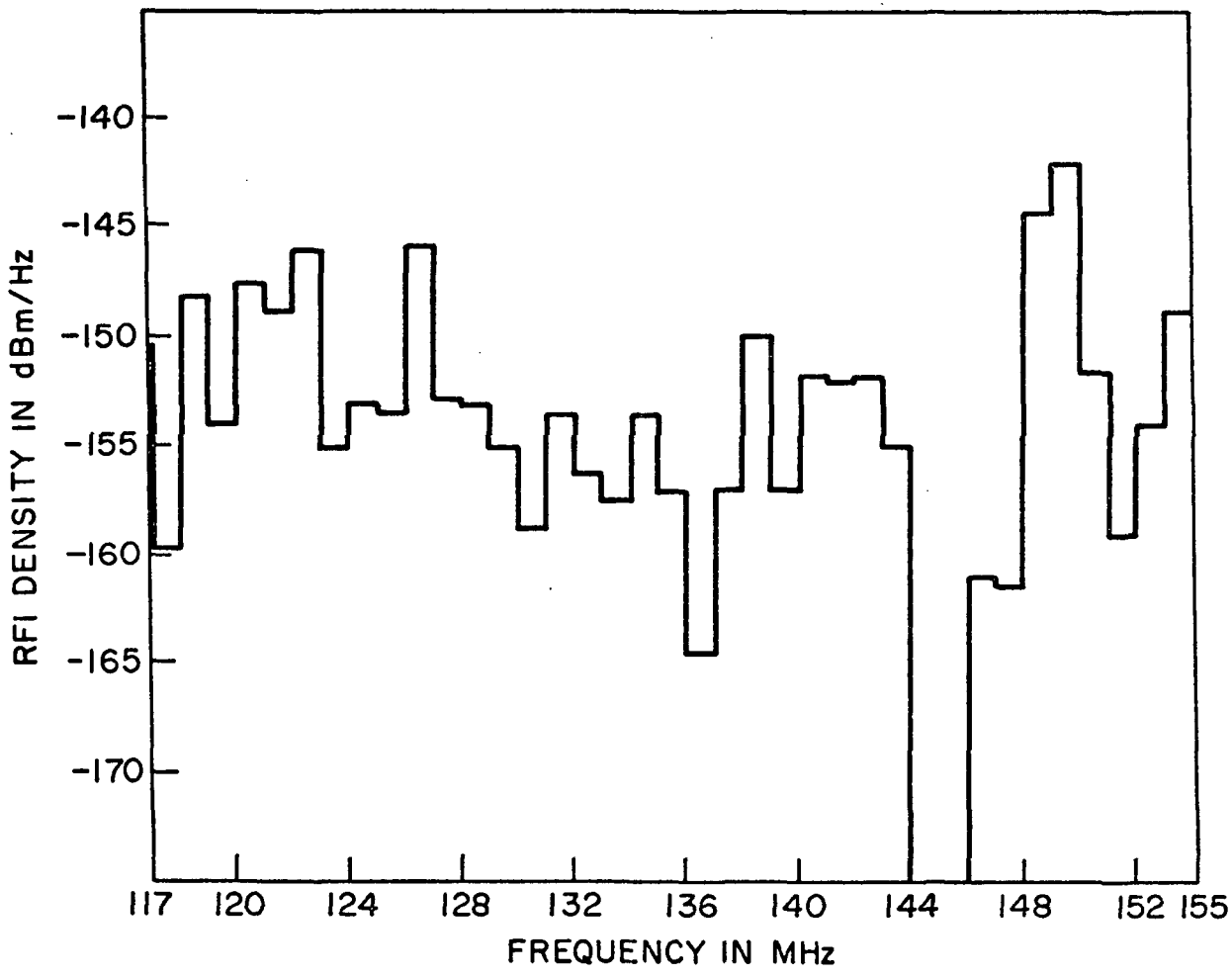

FIGURE 4-3 RFI POWER DENSITY FOR TDRS LOCATED AT 112° E

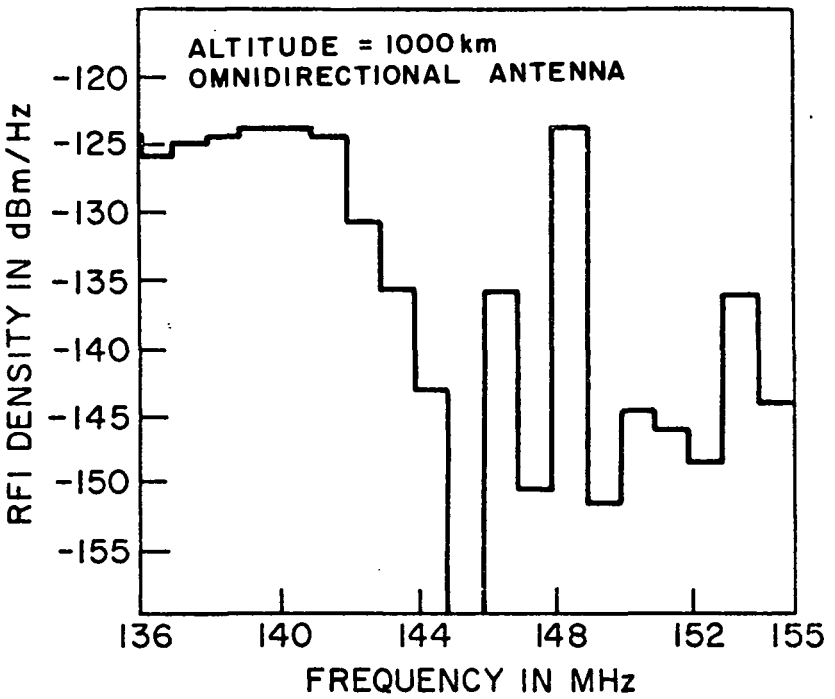

FIGURE 4-4 RFI POWER DENSITY AT USER SPACECRAFT LOCATED AT 50°N 30°E

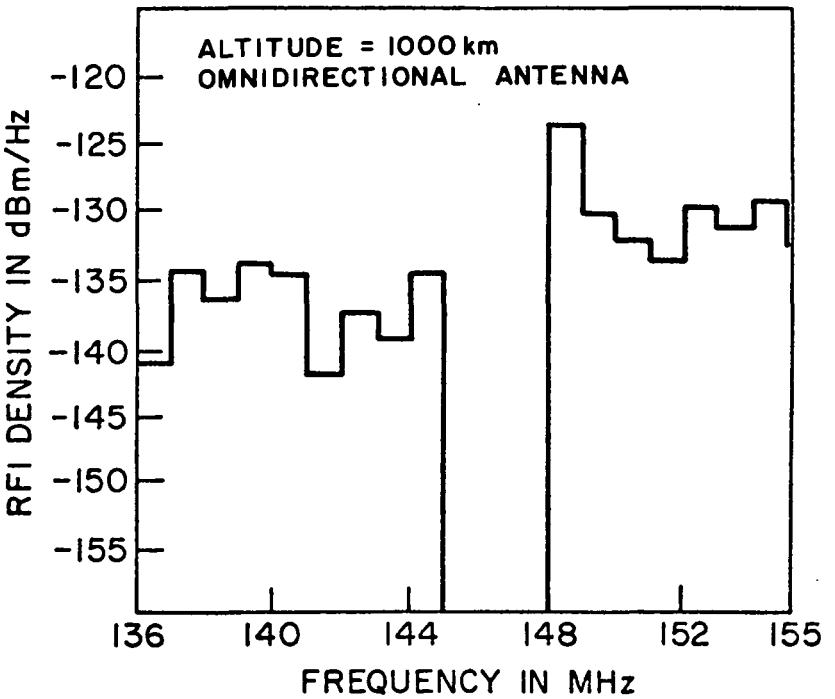

FIGURE 4-5 RFI POWER DENSITY AT USER SPACECRAFT LOCATED AT 38°N 85°W

127.70-127.85 MHz band has been estimated by Bryan as being:

- 28 communication emitters assigned to the band
- 122 communication emitters capable of being tuned in the band.

Bryan has conducted a frequency search in this band so that their effect on the low altitude SATS might be assessed.

The assumptions made regarding low altitude SATS for this assessment are the same as those mentioned previously, including the following:

- all ground based emitters are on and modulated
- all antenna patterns are uniform, omnidirectional, and zero dB gain
- ground based emitters are uncorrelated

The input RFI power at the low altitude SATS in a 10 kHz band centered around the carrier has been computed and is shown in Table 4-1.

TABLE 4-1

RFI SOURCES AT LOW ALTITUDE SATS IN THE 127.7-127.85 MHz BAND

Frequency	Average Power in 10 kHz Band	No. of Emitters
127.70 MHz	-83.4 dBm	6
127.75 MHz	-84.5 dBm	2
127.80 MHz	-81.0 dBm	14
127.85 MHz	-85.0 dBm	1

The number of emitters in the bands 136-138 MHz and 148-155 MHz and the received power at both the synchronous SATS and the low altitude SATS has been compiled by ESL. These data are presented in Tables 4-2 and 4-3 respectively.

TABLE 4-2

ESTIMATED RFI POWER AT THE SYNCHRONOUS SATS

SATS Location - (Synchronous Altitude)						
BAND (MHz)	11°W		143°W		112°E	
	Power (dBm)	Number of Emitters	Power (dBm)	Number of Emitters	Power (dBm)	Number of Emitters
136-137	-81.3	132	-87.8	56	-99.4	5
137-138	-79.4	235	-84.3	100	-91.8	10
148-149	-75.1	114	-70.8	789	-79.3	25
149-150	-81.0	70	-72.9	852	-76.9	58
154-155	-80.6	252	-79.9	216	-89.5	46

TABLE 4-3

ESTIMATED RFI POWER AT THE LOW ALTITUDE SATS

BAND (MHz)	SATS LOCATION (altitude - 1000 km)			
	38°N-88°W		50°N-30°E	
	Power (dBm)	Number of Emitters	Power (dBm)	Number of Emitters
136-137	-86.7	5	-71.0	130
137-138	-79.4	25	-70.0	178
148-149	-68.7	80	-69.0	15
149-150	-75.2	53	-97.0	2
154-155	-74.0	127	-89.6	6

The remaining band of interest is that in the range 400.5 MHz to 401.5 MHz. As of this time no attempt has been made to assess the effective RFI power at the low altitude SATS. We have, however, compiled from the International Frequency List (References 20 through 33) an estimate of the number of potential RFI sources in this band. This compilation is presented in Table 4-4 for the various ITU Regions.

TABLE 4-4

RFI SOURCES IN THE BAND 400.5-401.5 MHz

ITU REGION	EMITTER POWER ON THE GROUND (Watts)				
	0 - .9	1 - 9	10 - 99	100 - 999	≥1000
1	59	4	1	1	1
2	61	1	-	-	-
3	62	12	-	10	-

A preliminary evaluation of the RFI sources at S-band has been performed. Some results of that evaluation derived from the International Frequency List are shown in Table 4-5.

TABLE 4-5

RFI SOURCES AT S-BAND

ITU REGION	Emitter Power at Ground (Watts)				
	0-1	1-10	10-100	100-1000	>1000
1	15	78	40	14	16
2	2	72	15	1	1
3	--	15	24	--	--

4.2 TRASH NOISE

There is another important source of noise which should be considered and evaluated for its impact. Specifically, this interference is the sum total of the "trash" -- a more or less continuous background noise which originates in an urban environment and is due primarily to such things as ignition noise, switching transients, corona, etc. This continuous low level interference will interfere with the desired signals in the command band, and can have a deleterious effect on the antenna temperature at the user spacecraft.

Lincoln Laboratories associated with the Massachusetts Institute of Technology has carried out over the past several years the most comprehensive measurement and evaluation of this continuous background noise. They have concluded that those cities associated with the eastern seaboard can be modeled as an interference source with power uniformly distributed over an aperture which represents the city, and that in the UHF band (216-369 MHz) the power density/square meter/Hz will be in the range of 3×10^{-18} to 1×10^{-18} watts per square meter per Hz. These numbers are representative for moderately large cities such as Miami and Philadelphia.

A receiver on a low altitude spacecraft with gain pattern $G_r(\theta,\phi)$ relative to isotropic will receive a power dP_{tr} from a ρ distant differential source having a power density $C(\theta,\phi)$ watts/m^2-Hz, area dA, and gain pattern $G_t(\theta,\phi)$ given by:

$$dP_{tr} = B\left(\frac{\lambda}{4\pi\rho}\right)^2 G_r(\theta,\phi)\, G_t(\theta,\phi)\, C(\theta,\phi)dA^* \qquad (4\text{-}1)$$

where B = receiver bandwidth.

---

* $C(\theta,\phi)dA = dP_t$, the differential transmitted power (point source).

Using the geometry of Figure 4-6 the above equation becomes

$$dP_{tr} = \frac{\lambda^2}{16\pi^2} BG_r(\theta,\phi)\ G_t(\theta,\phi)\ C(\theta,\phi)\ \cot\theta\ d\theta d\phi$$

Integrating and dividing by Bk (k = Boltzman's constant) gives the general equation for the noise temperature at a receiving antenna due to a distributed noise source, such as the "trash" noise (ignition, generating plants, etc.) radiated by an urban area.

$$T_{tr} = \frac{\lambda^2}{16\pi^2 K} \int_0^{2\pi} \int_{-\pi/2}^{\pi/2} G_r(\theta,\phi)\ G_t(\theta,\phi)\ C(\theta,\phi)\ \cot\theta\ d\theta d\phi \qquad (4\text{-}2)$$

Assuming that a satellite at altitude h with an omnidirectional antenna is centered over a circular urban area of radius r, and that the effective transmitting pattern of the city is $G_t(\theta,\phi) = 1$, equation 4-2 becomes

$$T_{tr} = \frac{\lambda^2(2\pi)}{16\pi^2 K} \int_{\theta_1}^{\pi/2} C(\theta,\phi)\ \cot\theta\ d\theta \qquad (4\text{-}3)$$

where $\sin\theta_1 = \left[\frac{h}{(h^2+r^2)^{1/2}}\right] = \left[\frac{1}{1+(r/h)^2}\right]^{1/2}$.

The Lincoln Laboratory report (Reference 34) states that the power density was relatively constant at 10^{-17} watts/m^2-Hz over typical cities with the exception of New York which was 5-7 dB higher (see Figure 4-7). Since $C(\theta,\phi)$ is constant at C_o equation 4-3 reduces further to

$$T_{tr} = \frac{\lambda^2}{8\pi k} C_o\ \ln\left(\frac{\sin\pi/2}{\sin\theta_1}\right) = \frac{\lambda^2 C_o}{16\pi k}\ \ln[1+(r/h)^2] \qquad (4\text{-}4)$$

If $r \ll h$ then

$$T_{tr} \doteq \frac{\lambda^2 C_o}{16\pi K_o}\left(\frac{r}{h}\right)^2 \qquad (4\text{-}5)$$

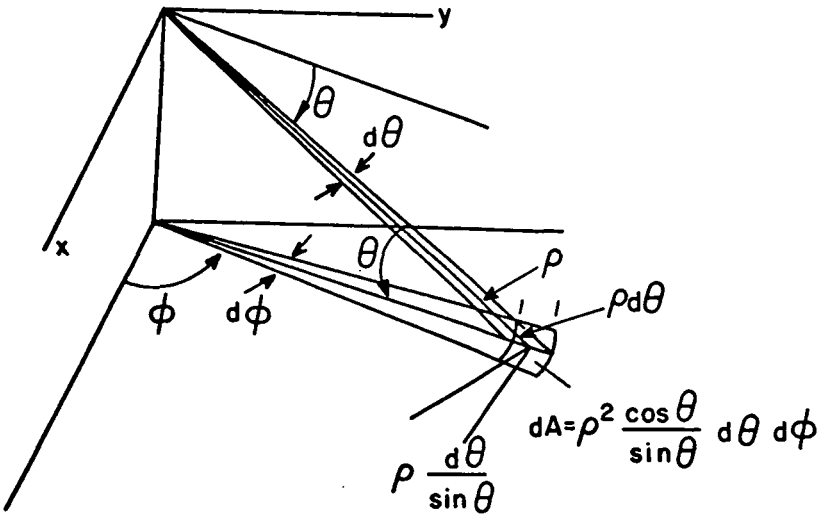

a) COORDINATE SYSTEM

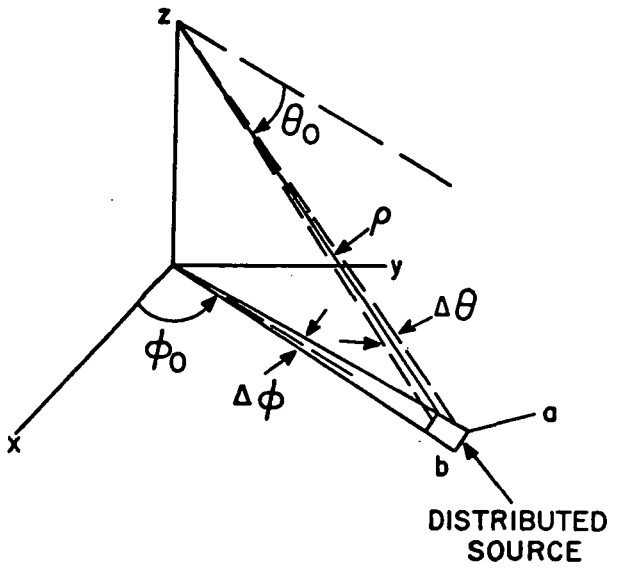

b) DISTRIBUTED SOURCE

FIGURE 4-6 GEOMETRY WHEN DISTRIBUTED SOURCE IS SMALL COMPARED TO RANGE

It is important also to realize that due to the large field of view of even low orbiting satellites,* the radius, r, used above can be large. This is the result of the appearance of many discrete point sources acting as one large area distributed source. Radius values can range from 200 km for the New York City area to 100 km for the Chicago area to negligible for water or desert areas. Estimates of trash noise temperature at a low altitude SATS are shown in Figure 4-8 for VHF and UHF.

4.3 CURRENT RFI DATA COLLECTION PROGRAMS

ESL, Inc., in Sunnyvale, California, under contract to NASA/GSFC, has compiled an extensive list of RFI emitters over the entire world. Based upon this compilation of both unclassified and classified emitters, ESL has projected the intensity of RFI as seen by a synchronous satellite over the VHF bands of interest. They have also projected the intensity of the RFI for a lower altitude spacecraft such as a user of the Tracking and Data Relay Satellite.

North American Rockwell, Seal Beach, California, has conducted RFI measurements along the West Coast of the United States using a Sabreliner which flies in an altitude of approximately 16.5 km (35,000 feet). A spectrum analyzer and a 14-track tape recorder, both on board the Sabreliner, are used to collect the RFI data. A total of eight bands, each 2 MHz wide, are scanned with a conventional spectrum analyzer and the output from this analyzer is recorded along with frequency sweep data, timing data, voice announcement, and band identification data. The analyzer is presently configured to accept VHF signals.

---

* The area of the U.S. is 9.37×10^6 km^2 or 1.8% of the earth's surface. The field of view of a 300 km orbiting satellite is 2.2%.

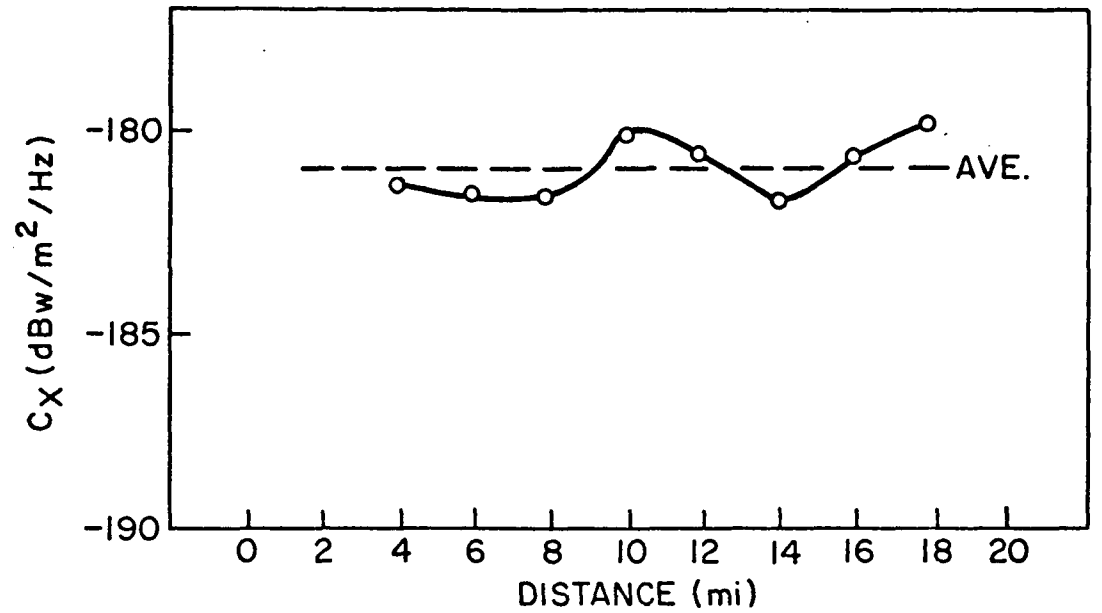

a) POWER DENSITY PROFILE

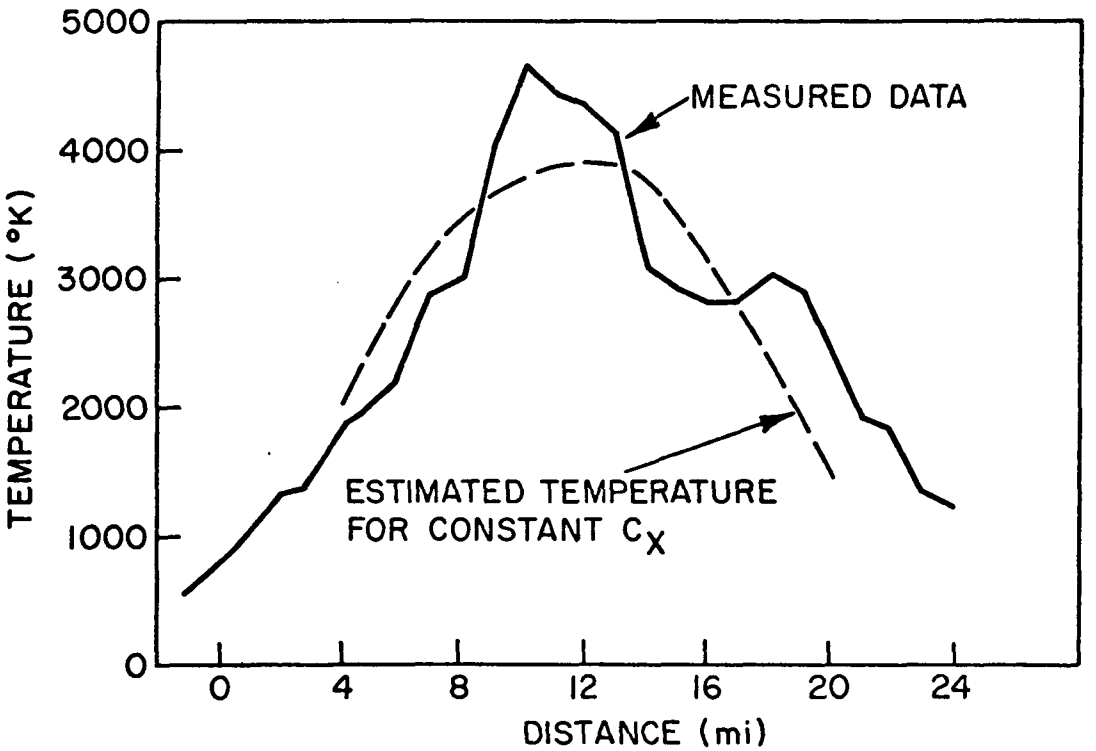

b) TEMPERATURE PROFILE

FIGURE 4-7 TRASH NOISE AT 305.5 MHz, MEASURED TRAVELING NORTH OVER MIAMI, FLORIDA AT 5.5 KILOMETERS ALTITUDE

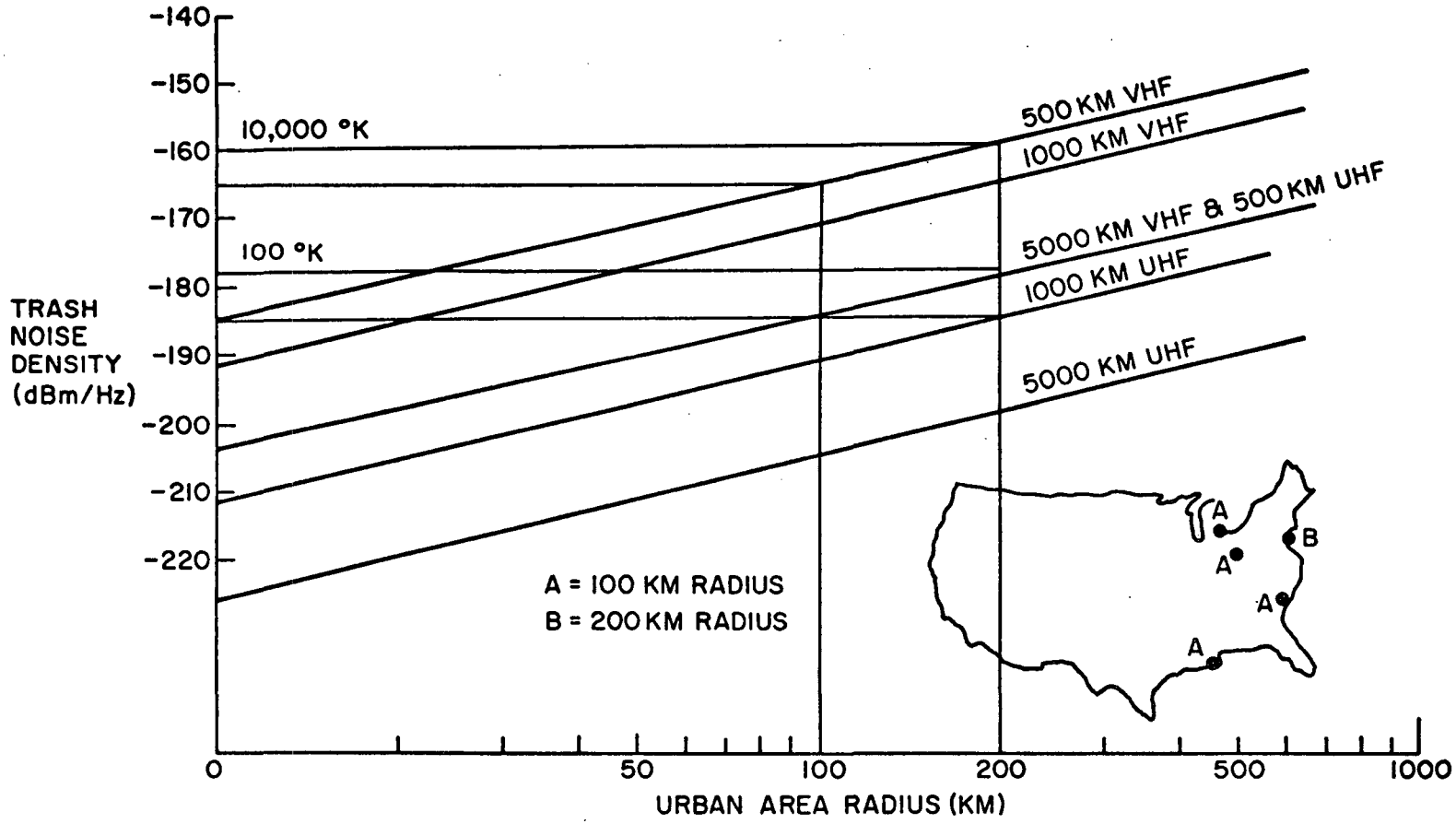

FIGURE 4-8 TRASH NOISE AT USER SPACECRAFT

After the data is recorded on board the aircraft, it is brought back for further processing. First, each of the tracks containing RFI data is digitized and properly formatted. Secondly, the processed digital tapes are compressed according to flight area and frequency. Thirdly, the output for the processed data is used in conjunction with a digital plotter to render RFI profiles. An A/D converter is used with an eleven-bit amplitude resolution at a sampling rate of 1 kHz per second to convert the analog RFI data from the spectrum analyzer into a usable digital representation. The analog to digital converter interfaces with an SDS-920 digital computer which controls the digitizing operation and formats the data into convenient blocks and proper record lengths of 1.77 cm ($\frac{1}{2}$ inch) digital tapes. The sampling rate of 1 kHz provides a sampling interval of 200 or 400 Hz for 10 or 5 second sweep time of a given 2 MHz band. With this sampling rate a single computer tape can handle two hours of analog data.

The program has the ability to plot the percentage of time that the signal exceeds a certain level, e.g.-90 dBm, in a given frequency bin 25 kHz wide. The program also has the ability to plot for a given power level, e.g. -65, -75, -85, -95 dBm, the percentage of time the level is exceeded. As many as eight 2 MHz bands are analyzed over the VHF spectrum. To do this a 2 MHz band is broken up into 81 frequency bins; two bins are 12.5 kHz wide, and 79 bins are 25 kHz wide. Both of these types of displays can be portrayed as a function of the time of day and locale.

To date extensive measurements have been made over the West Coast and the data is in the process of being reduced by North American Rockwell. The cost of these measurements and data reduction is on the

order of $40K. By flying over San Francisco, Los Angeles, and San Diego, a composite RFI picture of California can be created as shown in Figure 4-9 and Figure 4-10.

It is important to know that such data reduction facilities exist and can be operated at reasonable costs, that is, any 2 MHz bandwidth could be analyzed if properly interfaced with the North American RFI analyzer and reduced to provide meaningful RFI data, especially if it is collected from a higher altitude platform such as a low altitude SATS or a synchronous satellite.

Recently measurements at 136 MHz and 400 MHz have been conducted by NASA with support from Bendix. These tests were conducted using ground-based vans around the Baltimore, Maryland, area. The purpose of the RFI measurements was to determine the duty factors associated with signals on the air in these bands of interest and also to determine on a statistical basis what frequencies, of those assigned, were actually in operation. It has been determined by the Baltimore RFI measurements that the frequency band around 400 MHz is exceptionally clean. It must be pointed out, however, that a small sample of RFI may not be indicative of the RFI that is seen by a low altitude spacecraft at 400 MHz.

4.4 NASA RFI MEASUREMENT EQUIPMENT

4.4.1 GROUND-BASED RFI RECEIVER

NASA, under contract with Hughes, is developing a computer controlled RFI receiver which is to be used with the ATS-F satellite. Approval has been given for RFI measurements at C-band over ATS-F. RFI from the earth

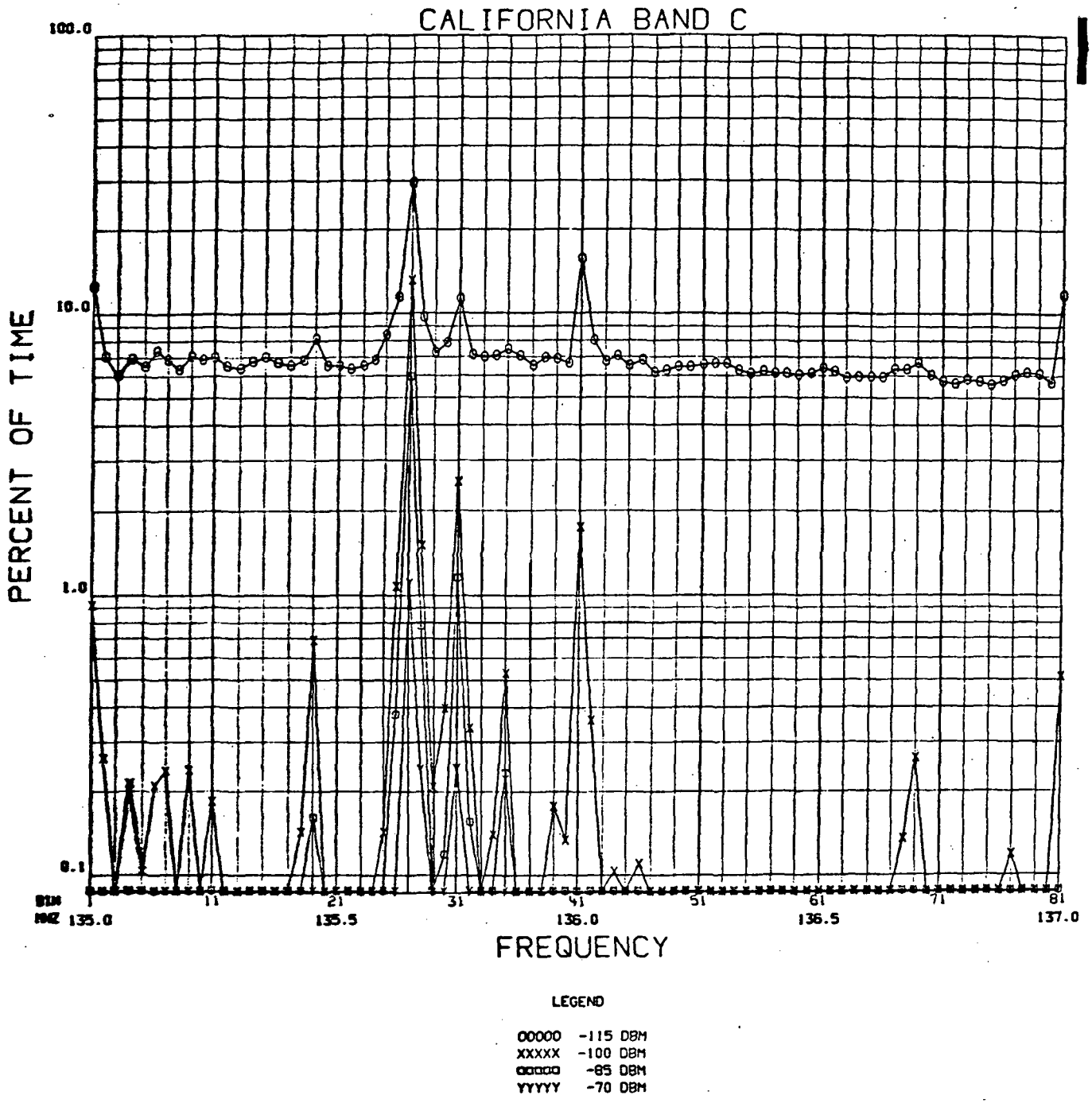

FIGURE 4-9 RFI DATA COLLECTED OVER CALIFORNIA (135 TO 137 MHz)

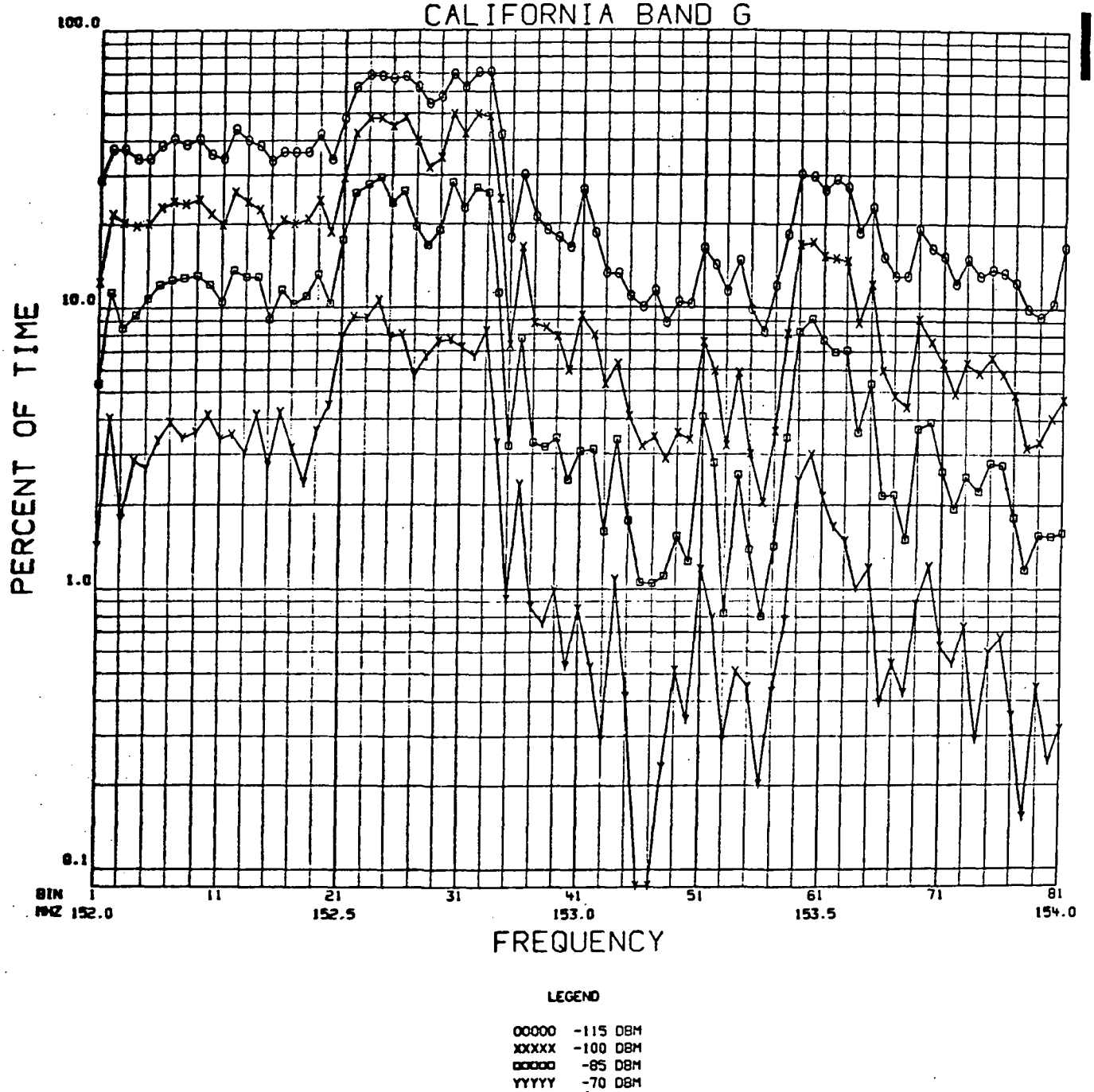

FIGURE 4-10 RFI DATA COLLECTED OVER CALIFORNIA (152 TO 154 MHz)

is received by the ATS-F satellite and relayed to the ground for analysis. The RFI receiver at the ground station is designed to operate at C-band with the first IF at 2250 MHz. The sensitivity, as measured in a 10 MHz bandwidth at this S-band frequency, is -80 dBm which corresponds to a carrier-to-noise ratio of +10 dB. The local oscillator in the receiver is computer controlled and is designed to step in frequency in increments of 10 kHz, 100 kHz, or 1 MHz. The ultimate frequency resolution of the RFI analyzer is 10 kHz. The frequency stability is approximately 1 kHz and the dynamic range is in excess of 40 dB. The scanned spectrum can be displayed and is A/D converted to an accuracy of 0.5 dB. Spectrum samples are taken at a rate of 20,000 per second. Measurements include the mean value of the signal, peak value, and total power. These measurements are digitized and stored in memory along with the frequency calibration data associated with the analyzer. The equipment and overall system is calibrated by transmitting a known signal level to the satellite and this calibration signal is relayed to the ground station.

While current plans call for C-band RFI measurements only, it is understood that there is a distinct possibility that RFI measurements will be extended to VHF and perhaps UHF if required. Some modifications to the existing C-band equipment will be necessary to make measurements at VHF, but these modifications are not considered major.

4.4.2 SATELLITE-BASED RFI RECEIVER

NASA is currently developing, under contract with AIL, a space-qualified RFI receiver designed to survey three frequency bands. These are:

- Band A - 108 to 174 MHz
- Band B - 440 to 478 MHz
- Band C - 1535 to 1665 MHz

The receiver is being designed to provide a predetection output multiplexed with frequency and signal strength information which can be telemetered to STDN stations at S-band.

The RFI receiver is being designed with the ITOS-class satellite in mind. However, experiments using SATS have been recommended and are discussed in Section 4.5.

The RFI receiver will be digitally controlled from the ground by means of a 28 bit serial command which can be transmitted to the satellite at a rate of 10 bps. The function of the commands, besides turn-on and turn-off, will be to instruct the RFI receiver to search Band A, B, or C. The tuning range will be designated by a start frequency (f_1) and a stop frequency (f_2). The ground station will also be able to select the tuning increments within the band (f_2)-(f_1); for example 25 kHz, 50 kHz, 100 kHz or 200 kHz.

The rate at which the RFI receiver will be able to change from one frequency to another is given in Table 4-6.

TABLE 4-6

SATELLITE RFI RECEIVER FREQUENCY STEPPING RATES
400 steps per second
200 steps per second
100 steps per second
50 steps per second
25 steps per second
5 steps per second
1 step per second
2 steps per minute
1 step per minute
1 step per 10 minutes
1 step per 110 minutes

Settling time will be equal to or less than .5 ms and the translation frequency accuracy will not exceed 5 parts in 10^6 over a 10 hour period or 5 parts in 10^5 over a one year period.

All filters will have a shape factor of at least two to one. The noise figure in Band A and B will be 5 dB and no greater than 7.7 dB in Band C.

The receiver will have the capability of storing a minimum of 16 commands. These commands will select frequency band, start and stop frequencies, frequency step size, stepping rate, predetection converter bandwidth, AM detector bandwidth, gain control (both manual and automatic), MGC and AGC time constant, AM and AM/FM select switch, telemetry rate, etc.

The RFI receiver will be equipped with both AM and FM detectors. The AM detector sensitivity in Band A for a 25 kHz predetection bandwidth will be -115 dBm. The same is true for Band B. In Band C the sensitivity will be -112.3 dBm in a predetection bandwidth of 25 kHz. For the FM detector to achieve 15 dB of quieting with 25 kHz predetection filter, the above sensitivities also hold.

In the predetection mode signals are transmitted to the ground station with predetection bandwidths of 25 to 200 kHz after translation in the satellite to a center frequency of 500 kHz. This composite signal is then used to frequency modulate an S-band carrier for the spacecraft to ground station link. In addition to detected RFI energy and predetection RFI energy, the receiver is configured to transmit to the ground telemetry data at 6400 or 3200 b/s. This telemetry will convey status of the receiver

in terms of tuned frequency, power supply voltage, temperature, stepping rate, stepping size, detector output selected, AGC, etc. The telemetry data will phase-shift modulate a subcarrier at approximately 19.2 kHz.

The receiver described above has not been delivered to NASA (delivery is expected by March 1973). However, the receiver concept has been accepted and extended in a recommended SATS RFI experiment which is described below.

4.5 SATS RADIO FREQUENCY INTERFERENCE MEASUREMENTS (RFI)

This section presents an outline of proposed experiments for measuring RFI with a SATS. The material contained in this section is extracted, in large part, from Reference 11.

4.5.1 BACKGROUND INFORMATION

The objective of the RFI measurement experiment is to determine the characteristics of earth-based signal sources that can interfere with ground-to-satellite and satellite-to-satellite communications. RFI measurements will be made on a global basis to determine the geographical distribution of RFI as a function of frequency and time to guide the selection of optimum frequencies for future orbital missions.

Such RFI measurements are vital to the present development and design of Tracking and Data Relay Satellite (TDRS), Air Traffic Control (ATC), data collection systems on Sychronous Meteorological Satellite (SMS) and Earth Resources Technology Satellite (ERTS), and domestic communications systems.

The RFI experiment will utilize a single receiver with multiple front ends and programmed tuning to cover selected RF bands. Data storage

will be provided by the SATS tape recorder to provide coverage in those locations which are out of range of direct ground station support. The band from 108-174 MHz will be monitored to cover the frequencies used by the TDRS for low data rate telemetry and commands required for spacecraft monitoring and control. The 240 to 478 MHz band will be monitored to cover the data collection frequencies used in platform-to-spacecraft data links for earth resources and meteorology programs. The 1535 to 1665 MHz band will be monitored to cover the L-band frequencies recently allocated by the World Administrative Radio Conference (WARC) for oceanic and domestic air traffic control via satellite relay. The receiver will also cover the frequency bands 12.5 GHz to 12.75 GHz and 14.0 GHz to 14.5 GHz. These bands were allocated by the 1971 WARC for earth-to-space communications and will be shared with domestic communications ground links.

Figure 4-11 illustrates the antenna configuration for the proposed SATS RFI experiment. The weight budget for the SATS is shown in Table 4-7.

TABLE 4-7

SATS RFI MISSION WEIGHT ESTIMATE	
Elliptical Weight Penalty	5.5 kg (12 lbs)
Experiment Units	12.8 (50 lbs)
Experiment Module Structure	4.6 (10 lbs)
Total Experiment Module Weight	32.9 kg (72 lbs)
Base Module	96.5 (213.5 lbs)
Launch Vehicle Adaptor	14.6 (32.0 lbs)
Total Mission Weight	144 kg (317.5 lbs)

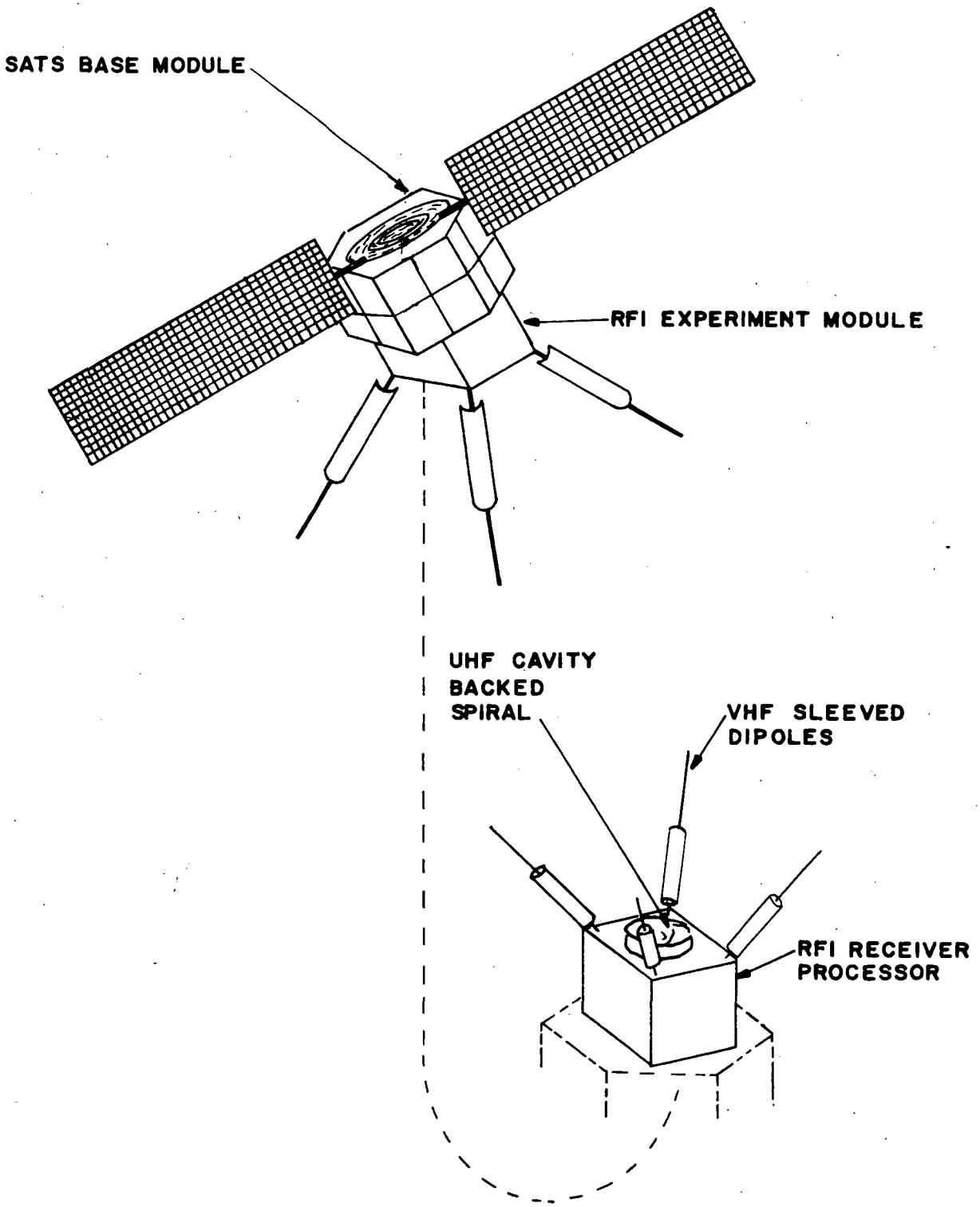

FIGURE 4-11 SATS RFI EXPERIMENT MODULE CONFIGURATION

4.5.2 DATA HANDLING

The RFI experiment data will be sampled by the telemetry encoder at approximately 6400 b/s, formatted with spacecraft housekeeping and timing then recorded by the spacecraft tape recorder. Once per orbit the tape recorder will be played back to a ground station. A commandable mode is also available to provide real time data.

During experiment data collection it is intended to shut off the telemetry beacon in order to gather RFI data in the VHF band.

4.5.3 COMMUNICATIONS

The SATS communications subsystems were chosen from existing designs and primarily from the SAS-D Program. This design, as shown in Figure 4-12, provides the maximum possible flexibility to meet various experiment data rate requirements. The communications links utilize VHF for tracking and low data rate experiment transmissions as well as command reception. A commandable S-band transmitter is used during the tape recorder playback and wideband real time experiment data modes. Data storage is consistent with the practical limits of existing tape recorders (8×10^7 bits) and a command memory will provide for experiment operation over remote sites.

4.5.3.1 Telemetry Encoder System

The telemetry encoder system performs the function of gathering science and engineering or housekeeping data from all systems in the spacecraft and formatting these data into a PCM serial bit stream suitable for transmission to the tracking stations. The system provides all timing and control signals necessary to accomplish this task.

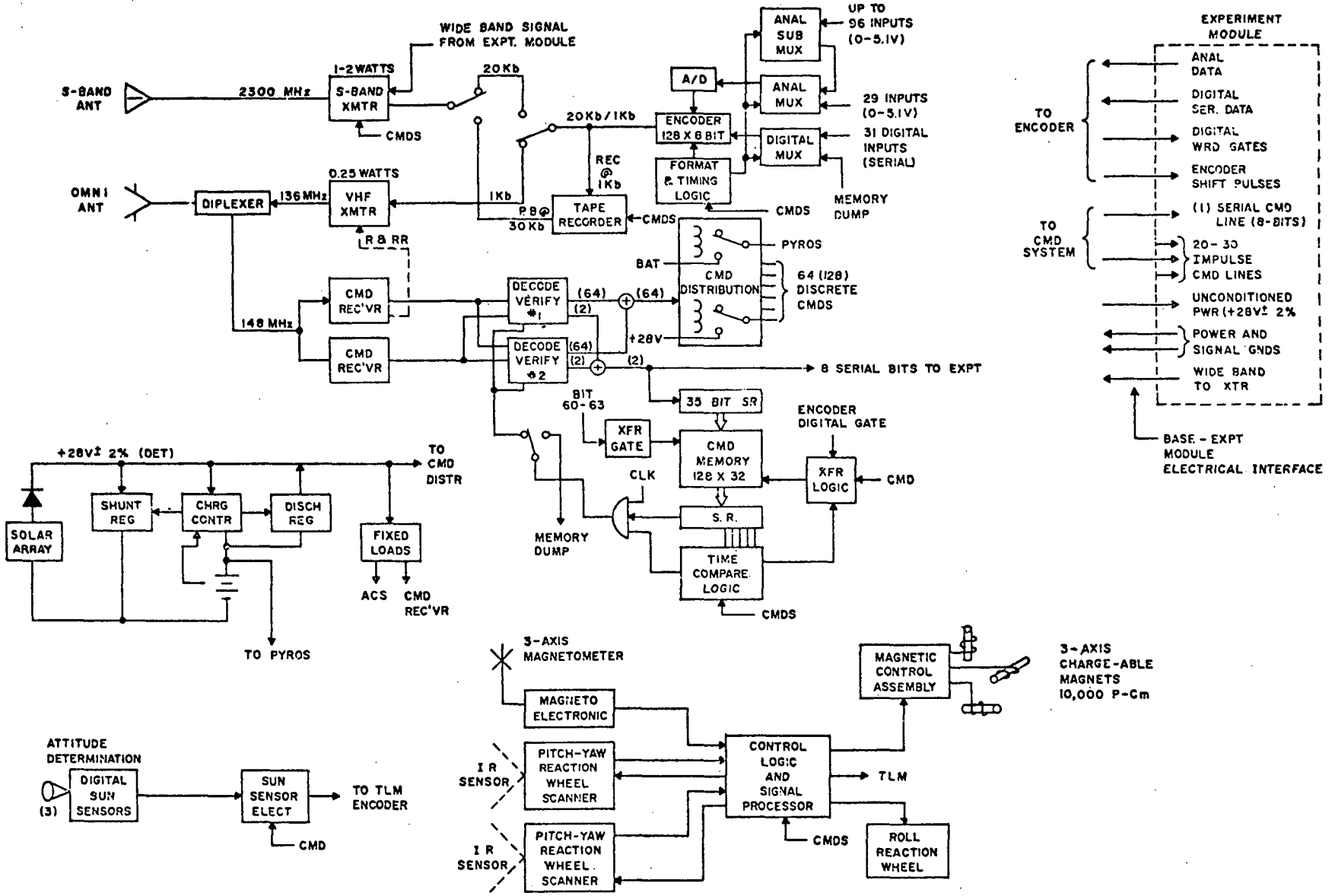

FIGURE 4-12 SATS LOW ORBIT BASE MODULE ELECTRICAL SYSTEM

The encoder's multiplex unit generates a 128 by 8 bit word frame having both fixed and variable word positions for main frame and subframe data. The fixed word positions include a frame synchronization pattern, submultiplex position, spacecraft time, etc. The word time at which any gate is sampled is selected by one of three 128 by 7-bit format memories. Two of these are read-only fixed format memories, and the third is a variable format memory that is loaded by ground command. The format memories are selectable by command and would include (1) engineering only, (2) engineering plus experiment and (3) experiment formats. The experiment only format would probably include a minimum amount of sub-multiplexed engineering data for attitude determination and spacecraft health status. Exact frame formats are selected after a mission is defined.

Timing and data rate is selectable by ground command. Different bit rates may be selected in binary steps from 1 Kbps to 40 Kbps by hand wiring the appropriate taps of the countdown circuits. The output logic then generates a PCM split phase signal for transmitter modulation.

The system is designed to permit inclusion of a convolutional encoder, if one should be required on some future mission. Also, it is designed to be fully compatible with an on-board computer such as will be used on the SAS-D spacecraft.

The timing generator should countdown from a crystal which will be a binary multiple of one second such as 524,288 Hz or 1,048,576 Hz. Forty-four stages of countdown would give more than six months turnover time.

The experimenter and/or the transmitted time would not require all available binary outputs but the selection of the desired outputs could be controlled. Tentative proposals would be RF transmittal of 24 bits of spacecraft clock to give one second resolution and one year of operation before turnover. Eight to sixteen lines of parallel timing information could be furnished the experimenter. This would permit moderately complex timing functions. If more complex functions are desired the experimenter could reconstruct the clock from this information and generate his own logic functions.

4.5.3.2 SATS Command Systems

The SATS command system (Figure 4-13) will be capable of providing 128 impulse commands and up to 64 individual 12-bit serial digital data commands. These commands may be either real time or stored for delayed execution. The decoders will operate in a time shared mode for command execution of either the real time or stored commands.

The command system will conform to the GSFC PCM/FSK Command Data System Standard.

The command format (Figure 4-14) is fixed, consisting of 64 bits for either real time or stored commands. A bit rate of 1024 bits per second is planned. The command execution rate will be approximately 64 milliseconds. An additional increment of time will be required for the initial uplink synchronization.

The RF command link will use seven parity bits to determine the existence of errors in the detected data bits received.

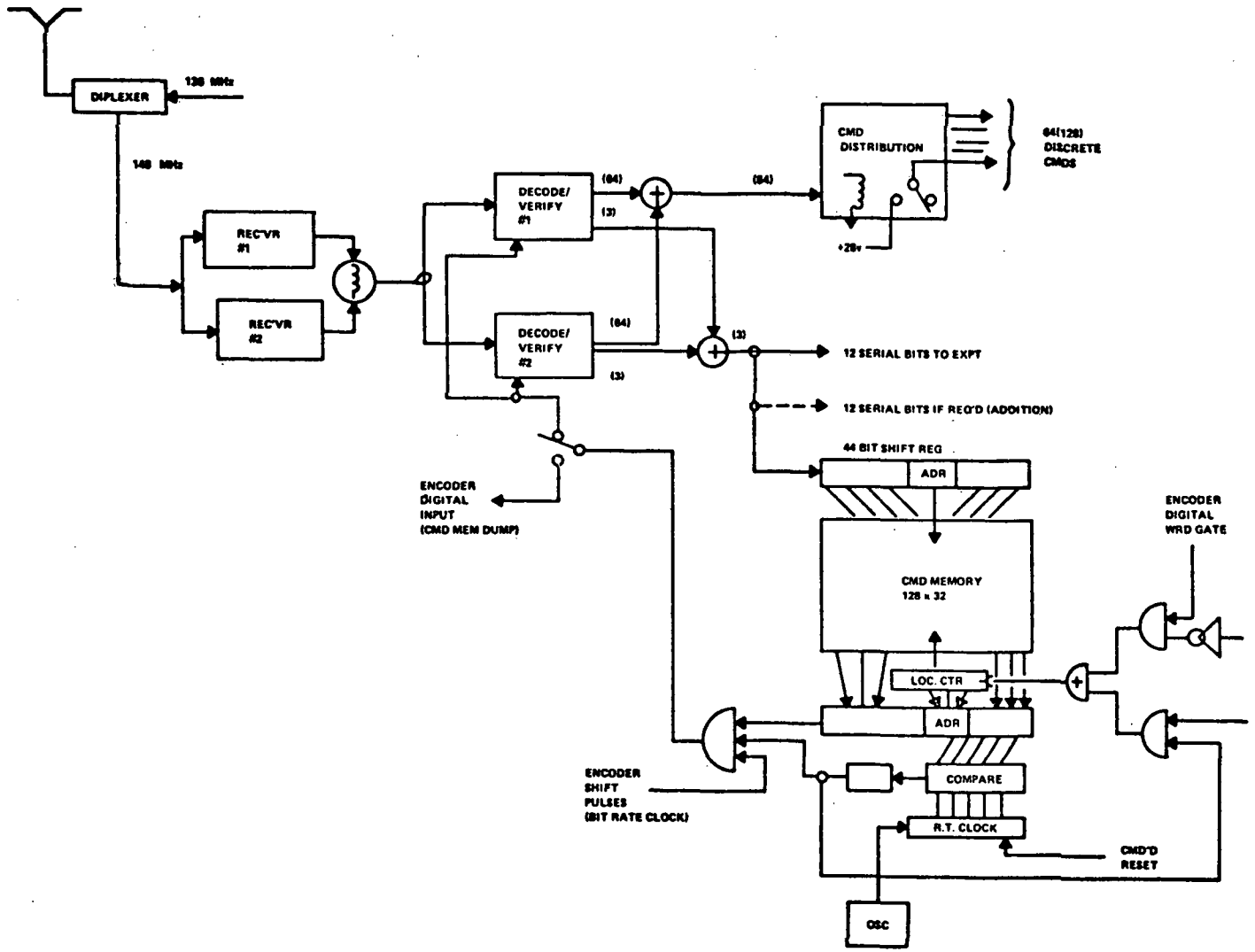

FIGURE 4-13 SATS COMMAND SYSTEM

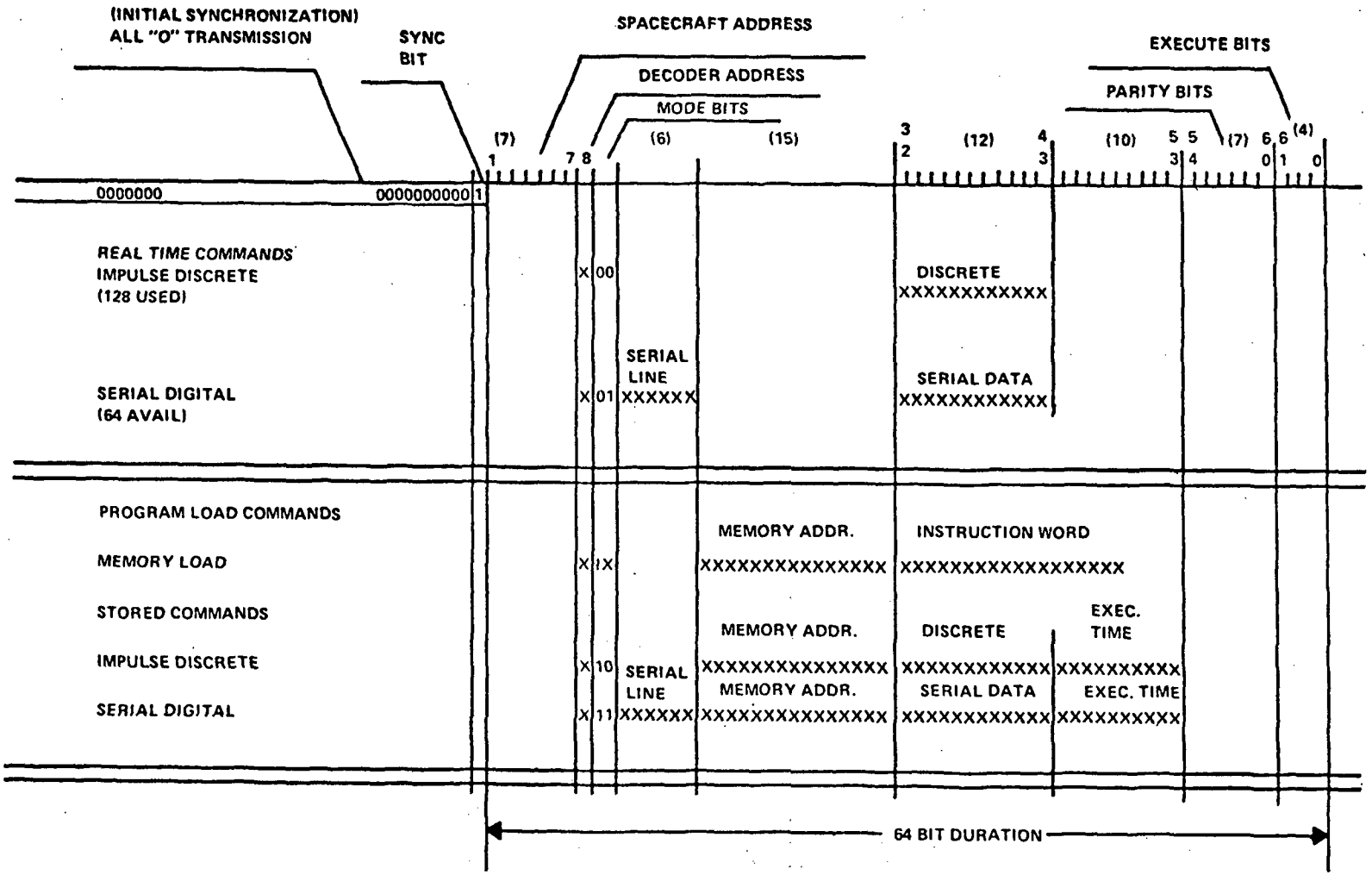

FIGURE 4-14 SATS COMMAND FORMATS

Forty-four data bits are available to the Command Storage processor. Nineteen of these bits are required by the command system to execute the desired command from storage. The remaining twenty-five bits are available for storing and timing the delayed command.

The time share capability of the decoder execution logic will eliminate conflicts between the real time and delayed commands. Command execution will alternate between real time and delayed commands, should both become available simultaneously. This mode effectively doubles the on-board command execution rate.

4.5.3.3 Command Memory and Time Compare Logic

The Command Memory and Time Compare Logic, shown in Figure 4-13, provides on-board storage and delayed execution of 128 spacecraft commands. This function is performed by providing storage for 4096 bits of command data (128 commands x 32 bits per command) and then executing these commands at specified time intervals. As shown in the command format in Figure 4-14, the time interval is represented by 10 bits which can accommodate 256 minutes of operation with the smallest interval being 15 seconds. For normal operation, execution of stored command sequences may be initiated by a time compare with spacecraft clock or a command from ground. In case of an anomaly on-board a command sequence may be initiated by a "trouble flag" which would act as a real time interrupt having priority over normal operation. This command sequence would place the spacecraft into a "safe" (probably minimum power) operating mode.

4.5.3.4 SATS Tape Recorder

The SATS tape recorder will be a small reel-to-reel recorder being developed by the GSFC. The tape transport and the recorder electronics will be housed in separate containers.

The total storage capability of the tape recorder design is 8×10^7 bits. Using this limitation and a 120 minute recording time, playback time results in a maximum input bit rate of 11,000 bits per second. The playback of data in a 5 minute period will require a maximum rate of 264,000 bits per second. These parameters represent the design limit for the recorder and do not reflect the spacecraft requirements. Two possible spacecraft design parameters are shown in Table 4-8.

TABLE 4-8

POSSIBLE DESIGNS FOR SATS TAPE RECORDER

Design Parameters	Option 1	Option 2
No. Tracks	4	1
Total Storage	4.6×10^7 bits	7.2×10^6 bits
Length of Tape	122m (400 ft.)	122m (400 ft.)
Packing Density	945 bits/cm (2400 bpi)/track	590 bits/cm (1500 bpi)
Tape Speed -		
Record	1.7 cm/s (0.67 ips)	1.7 cm/s (0.67 ips)
Playback	40.6 cm/s (16 ips)	40.6 cm/s (16 ips)
Ratio	24:1	24:1
Power - Playback	6 watts	4.5 watts
- Record	4 watts	2.5 watts
Size	15.2 × 17.4 × 12.7 cm. (6 × 6 7/8 × 5 in.)	15.2 × 17.4 × 12.1 cm (6 × 6 7/8 × 4 3/4 in.)
Weight	3.6 kg (8 lbs)	3.6 kg (8 lbs)
Input Bit Rate	6,400 b/s	1,000 b/s
Output Bit Rate	153,600 b/s	24,000 b/s
Record Time	120 min.	120 min.
Playback Time	5 min.	5 min.

4.5.3.5 S-Band Transmitter

An S-band transmitter will be provided for transmission of experiment data to the ground. In order to provide flexibility to the experimenter, a power output of 2 watts has been selected. This power output will provide a PCM capability of several megabits/second (limited by data handling and modulator capability), or a wide-band analog capability with bandwidth determined by the experimenter's required signal-to-noise ratio. Modulating frequencies from 1 kHz to 2 MHz can be accommodated. The transmitter efficiency will be 20%.

4.5.3.6 VHF Transmitter

The VHF (136 MHz) transmitter will provide 250 milliwatts of phase modulated RF for transmission of spacecraft housekeeping parameters and, possibly, low bit rate experiment data. This transmitter will be similar to one flown on RAE and will have an efficiency of about 30%. It will be crystal controlled, with a frequency stability of .002% and will have a phase modulation capability of ± 1 radian.

4.5.3.7 VHF Command Receiver

Redundant 148 MHz PCM command receivers will be utilized. The receiver is a standard design that has been used on many Goddard spacecraft. It is a double-conversion, superheterodyne type with crystal control of frequency, and characterized by small size and weight and low power drain (80 milliwatts). Construction is on standard printed circuits.

4.5.3.8 Summary of SATS RFI Experiment

A summary of pertinent SATS RFI experiment data is given in Table 4-9.

TABLE 4-9

SATS RFI EXPERIMENT CHARACTERISTICS

Launch Vehicle:	Scout-D		
Altitude Control:	Three axis stabilized (earth oriented)		
	Stability ±0.017 radian (±1°) pitch and roll ±0.034 radian (±2°) yaw		
Orbital Parameters:	Perigee	Apogee	Inclination
	560 km	650 km	1.048 radian (60°)
Data Handling:	1 to 40 kb/s Two switchable bit rates Three program formats (2 fixed, 1 programmable)		
Data:	Video (real time) 10^{-3} kHz to 750 kHz Real time - 6.4×10^{3} b/s Total bit storage per orbit - 3.5×10^{7} bits		
Command:	Real time 1024 b/s Up to 128 delayed executions ($\frac{1}{2}$ available to the experiment)		
Communications:	VHF - for low data rate experiments and housekeeping data S-band - for wideband experiment data and tape recorder data		

4.5.4 NETWORK SUPPORT

Network and spacecraft planning is based on the assumption of compatibility with existing network facilities. It is also assumed that no unique project equipment will be required.

4.5.4.1 Range Support

Range support for metric data and/or monitoring of flight event parameters (launch to spacecraft separation) will be within the normal depth of launch support.

4.5.4.2 Telemetry

The GSFC Network will support the SATS spacecraft VHF telemetry and S-band telemetry downlinks with the existing facilities listed in Table 4-10.

Specific Network support will be fully defined when all support requirements are known. However, the SATS telemetry system will utilize NASA data standards and be fully compatible with all network stations.

TABLE 4-10

GSFC NETWORK FACILITIES

BDA	S-band, 9.14 m (30-foot) antenna VHF, 136 MHz
CAPE	S-band, 9.14 m (30-foot) antenna SATAN
ROS	S-band, 25.9 m (85-foot) antenna SATAN
CYI	S-band, 9.14 m (30-foot) antenna VHF, 136 MHz
ACN	S-band, 9.14 m (30-foot) antenna VHF, 136 MHz
HAW	S-band, 9.14 m (30-foot) antenna SATAN
GDS/MOJ	S-band, 9.14 m (30-foot), 12.2 m (40-foot), or 25.9 m (85-foot), antenna SATAN
HSK/ORO	S-band, 25.9 m (85-foot), antenna SATAN
MAD	S-band, 25.9 m (85-foot), antenna
ALA	S-band, 25.9 m (85-foot), antenna SATAN
QTO	SATAN
JOB	S-band, 12.2 m (40-foot) antenna SATAN

4.5.4.3 Command

Since the spacecraft will fly a VHF command system, Network command support can be provided by all STDN stations except Honeysuckle Creek, Australia, which will be covered by Orrorral, Australia.

The Network will be equipped with the Spacecraft Command Encoder (SCE) system for the SATS launch with which the SATS command system will be compatible.

4.5.4.4 Tracking

Network tracking will be provided by the GRARR, minitrack and USB stations as required by orbital accuracy requirements.

If SATS is placed in a 1.048 radian (60°) inclined circular orbit at 500 km, to make RFI measurements the contact time with the ground station network must be known. Furthermore, suppose that SATS is used to represent Shuttle in this orbital configuration. Then the station contact times summarized in Table 4-11 are representative of the support that can be afforded SATS for either RFI or multipath measurements.

4.6 SKYLAB AS A LOW ALTITUDE PLATFORM FOR RFI MEASUREMENTS

Skylab I will be launched 30 April 1973 and the first manned mission is anticipated to begin 1 May 1973 for approximately 28 days. The first manned mission is referred to as Skylab II. Subsequent manned missions, Skylab III and IV will be conducted in July for 56 days, and again in October for 56 days. After the manned missions have been completed the Skylab satellite will be used primarily for solar observatory experiments.

An interesting possibility is to use the Skylab as a means of measuring RFI from the earth. At the beginning of Skylab IV, an RFI receiver similar to that described in Section 4.4.2 , could be placed on board and interfaced with the telemetry links and the command links associated with Skylab. The RFI receiver would have to be virtually self-contained and simple interfaces would have to be provided. Prime power could probably be provided from the Skylab power source. Table 4-12 shows the external communication capabilities of the Skylab satellite. We would anticipate using the S-band transmitter in the FM mode, with a 2 MHz base bandwidth, to transmit the RFI data to the ground for analysis and data reduction.

TABLE 4-11

SHUTTLE 1 TRACKING COVERAGE SUMMARY, 500 km CIRCULAR ORBIT, 55° INC. TEL.

10/ 1/70 0 H 29.7 M TO 10/15/70 0 H 0.0 M

STA	STA CONTACT TOTAL (HRS.)	NO. CON-TACTS	AVG. COV. PER CONTACT (MINS.)	TOTAL COVERAGE W/O STA
MIL3	8.23	60	8.23	99.34
EDA3	10.46	73	8.60	95.00
CYI3	8.53	62	8.25	96.16
ACN3	7.31	52	8.44	92.97
GWM3	7.59	53	8.59	92.59
HAW3	8.22	59	8.36	91.97
MAD8	13.05	95	8.24	91.64
GDS8	10.33	76	8.16	90.48
ORRE	6.71	56	7.19	93.45
OTO4	4.56	40	6.85	95.94
JOB4	8.67	64	8.12	94.30
SAN4	10.81	77	8.43	89.49
TAN4	6.42	52	7.41	96.50
ROSE	6.31	55	6.88	99.64
ALA4	4.48	44	6.11	95.62

TOTAL COVERAGE
102H 21M 56.00S

TOTAL CONTACT
121H 40M 58.00S

NO. OF REVS. 199

COVERAGE PER DAY
7H 19M 21.36S

NO. OF GAPS GE 100.00 3

COVERAGE GAPS GE 100.00

DATE M	D	Y	TIME H	M	SPAN (MINS)	REV
10	4	70	21	48.5	135.0	57
10	9	70	21	39.2	123.6	128
10	10	70	21	18.6	135.0	142

TABLE 4-12

SKYLAB EXTERNAL COMMUNICATIONS

Frequency, MHz	Power	Modulation	Bit Rate	TRANS RCV	Antenna Type	Antenna Location	Use
230.4	2w	FM/PCM	--	T	Whip		Launch TLM
230.4	10w	FM/PCM	51.2 kb/s	T		Extended	Orbital TLM
235.0	10w	FM/PCM	112.64 or 126.72 depending on source selected	T	Discone	from Airlock	Voice, TLM Down data
246.3	10w	FM/PCM		T			
450.0	n.a.	FM	200 b/s 20 characters per second	R	Whip	AM	Ground-command teleprinter
296.8	7.6w	AM 3.95 kHz	n.a.	T	Helix	AM	CSM ranging
259.7	n.a.	247 Hz 31.6 kHz TONES		R			
231.9	10w	FM/PCM	72 kb/s	T		ATM	ATM telemetry,
237.0	10w	FM/PCM	72 kb/s	T		Solar array	real time or recorded
450.0	n.a.	FM	200 b/s	R		ATM solar array	ATM ground command
243.0		ICW		T		CM	Recovery beacon
259.7	7.6w	AM	n.a.	T			
259.7	n.a.	AM	n.a.	R	Scimitar	SM	Voice ranging to Skylab
296.8	7.6w	AM	n.a.	T			
296.8	n.a.	AM	n.a.	R			
2106.4	250mn 2.8w	PM/PCM	200 b/s	R			Voice, range code to Gnd,
2287.5	11.2w	PM/PCM	51.2 kb/s	T	OMNI	CM	up data down
2272.5	selectable	FM	2 MHz	T			telemetry TV, TM

If the RFI receivers described in Section 4.4.2 are not ready for transfer to the Skylab by October of 1973, it may be possible to use a less sophisticated RFI receiver such as a standard frequency analyzer whose output could be used to modulate the FM transmitter in the downlink, tuned specifically to Space Shuttle-oriented frequencies such as S-band. The system could be calibrated by transmitting a known signal level to Skylab, which in turn would receive the signal and return it to the ground via the spectrum analyzer link.

5. HARDWARE DESIGNS

We are required to provide for NASA several hardware designs for items which may potentially have application to the multipath and RFI tests described in this report. Specifically, we have designed an adaptive delta modulation system for voice. This adaptive delta mod system operates at a data rate of 24.0 kb/s. We have also designed a convolutional encoder (K=5, rate 1/2) and maximum likelihood (Viterbi) decoder forward error control unit. The forward error control unit will operate at a clock rate sufficient to accommodate the 24.0 kb/s data stream. We have also designed a pseudonoise coder which will accommodate data rates of 2.0 kb/s, 6.0 kb/s, and 24.0 kb/s. The 2.0 kb/s data rate is representative of a telemetry link operating at a data rate required by the Space Shuttle. The 6.0 kb/s data rate satisfies the 2.0 kb/s data rate convolutionally encoded with a rate 1/3 code. Finally, the 24.0 kb/s data rate represents the uncoded delta modulated voice channel for the Space Shuttle. The pseudonoise transmission system can also be operated in a clear mode. This clear mode is the equivalent of a standard phase shift keying (PSK) modem. A simplified block diagram of the interface of the Adaptive Delta Modulator for voice, the Forward Error Control Unit, and the PN/PSK integrated modem is shown in Figure 5-1.

We have also provided a design, in block diagram form, for a wideband frequency modulation (WBFM) system. The design which we present is based primarily upon the work conducted for NASA Goddard Space Flight Center, Greenbelt, Maryland, by Teledyne ADCOM, Inc., Cambridge, Massachusetts, as reported, for example, in References 10 and 35. We do not present designs in great detail for this system, such as we did for the pseudonoise receiver/transmitter system. The reasons for not presenting such detailed designs for

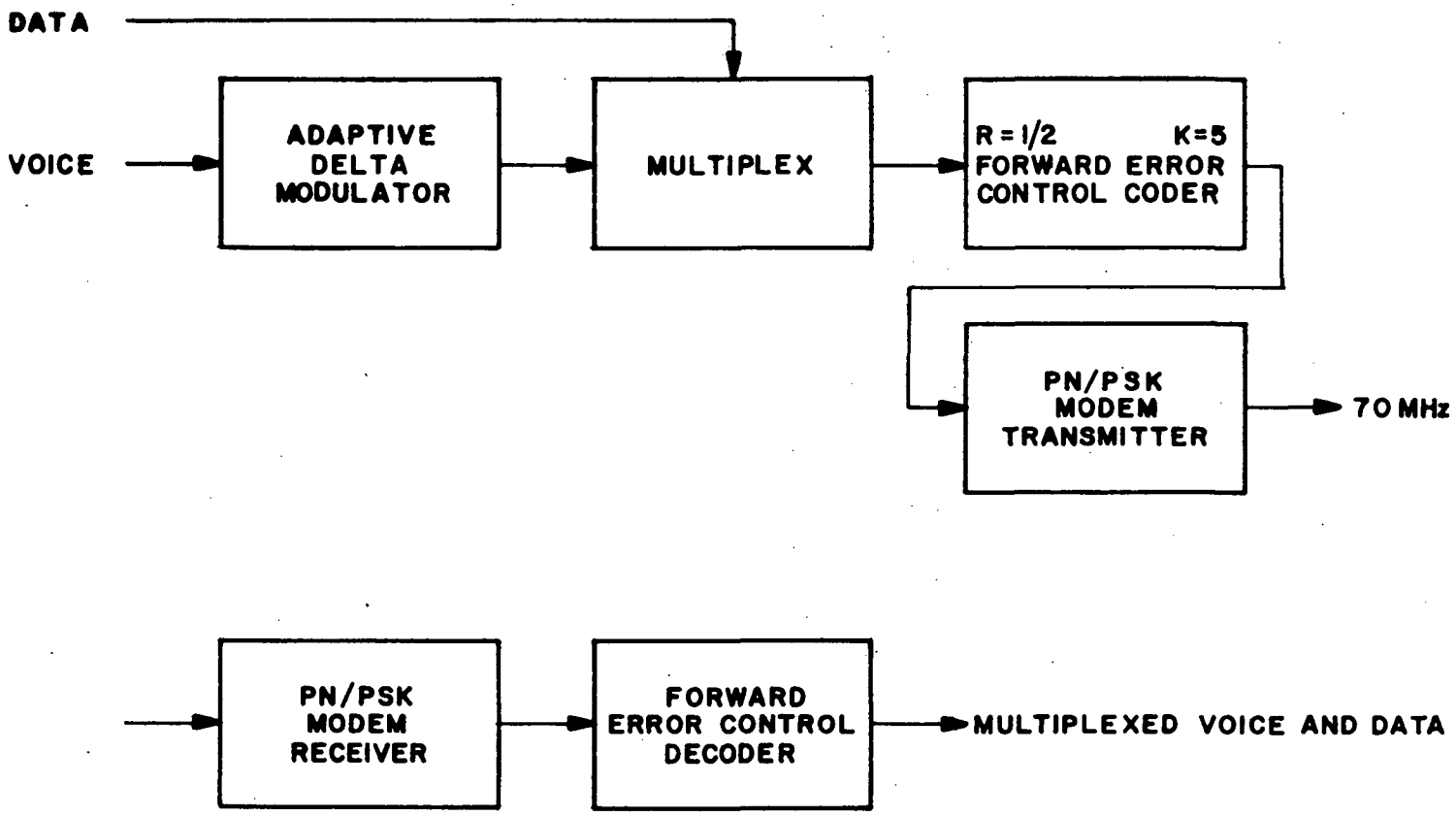

FIGURE 5-1 INTERFACE OF COMMUNICATIONS EQUIPMENTS

the wideband frequency modulation system are based upon conclusions arrived at through the analysis of the performance of the wideband FM system in the presence of RFI and multipath. It will be shown that the wideband high modulation index FM system is severely degraded in the presence of RFI and multipath, thus making the need for a detailed design of equipment questionable.

5.1 ADAPTIVE DELTA MODULATION FOR VOICE COMMUNICATIONS

It has been decided that 24.0 kb/s adaptive delta modulation will be the coding scheme for a voice channel between the Space Shuttle and the relay satellite. The 24.0 kb/s data stream representing a voice channel must be compatible with a clear mode PSK transmission, a pseudo-noise coded transmission and a forward error control coded signal and forward error control coding. It must also be compatible with the high modulation index FM system.

Based on a rather complete survey of existing adaptive delta modulation technology, we have concluded that one implementation provides superior performance. This implementation is based on the work of the British Post Office. Schematics of the British delta mod are given in Figures 5-2 and 5-3.

Figure 5-4 shows the measured PB word intelligibility for adaptive delta mod as a function of the carrier-to-noise density for PSK and delta coded PSK wherein the carrier reference is recovered by a Costas loop. In principle, adaptive delta mod can enjoy the performance of PSK since an inversion in the received bit stream resulting from the ambiguity in the recovered carrier simply serves to change the sign of the reconstructed analog voice signal. However, if the delta mod voice is differentially

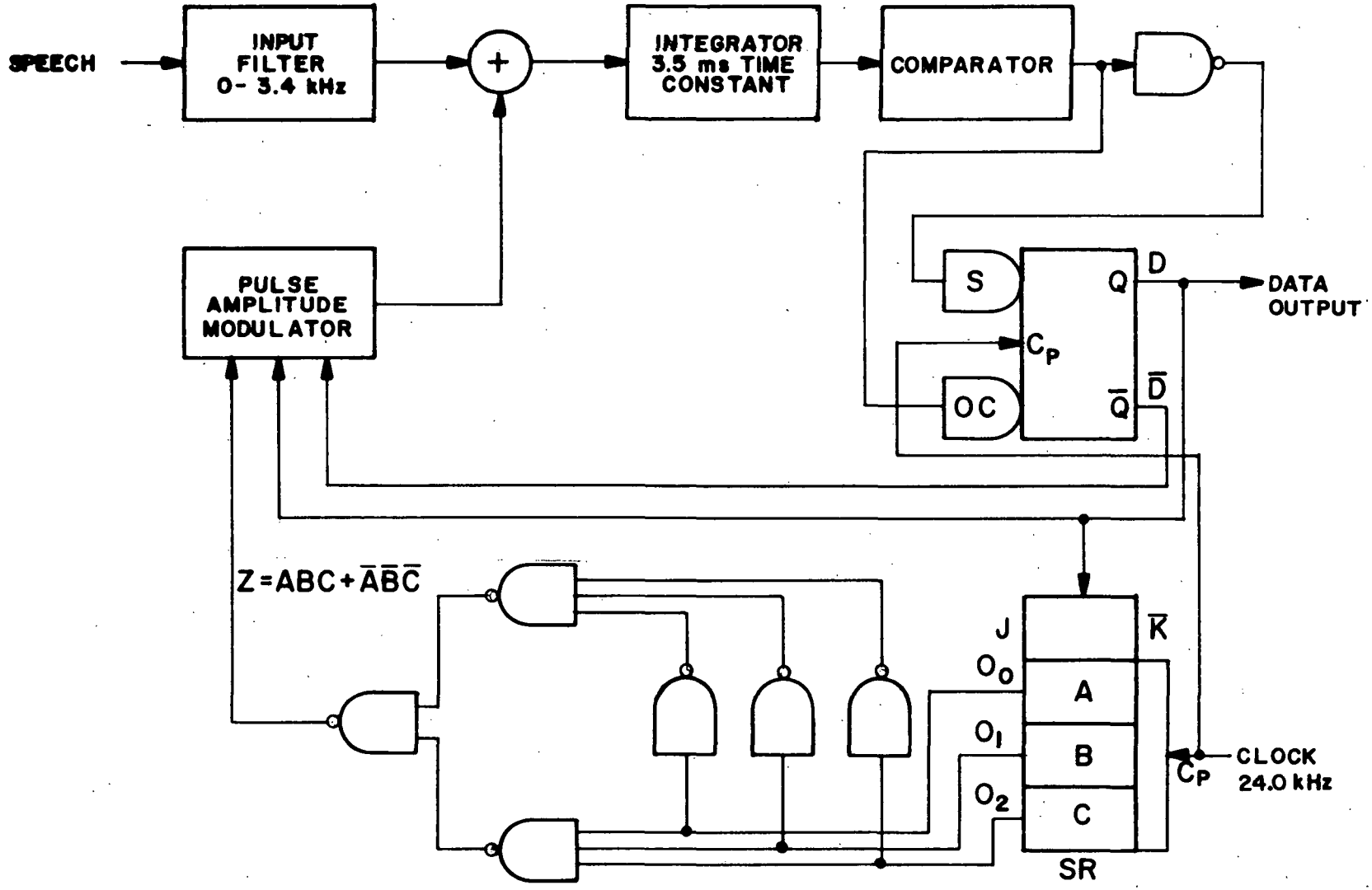

FIGURE 5-2 BRITISH POST OFFICE ADAPTIVE DELTA MODULATION TRANSMITTER

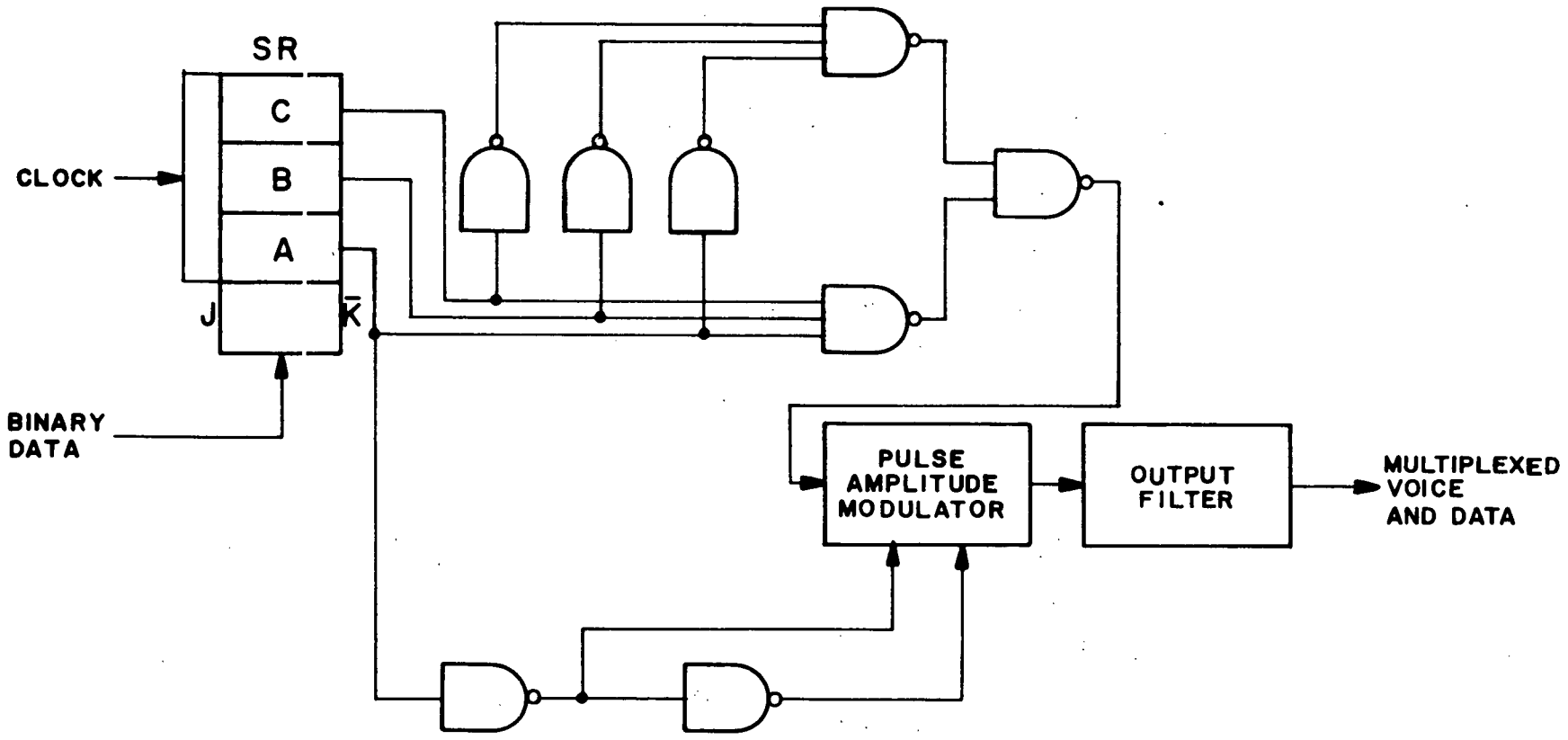

FIGURE 5-3 BRITISH POST OFFICE ADAPTIVE DELTA MODULATION RECEIVER

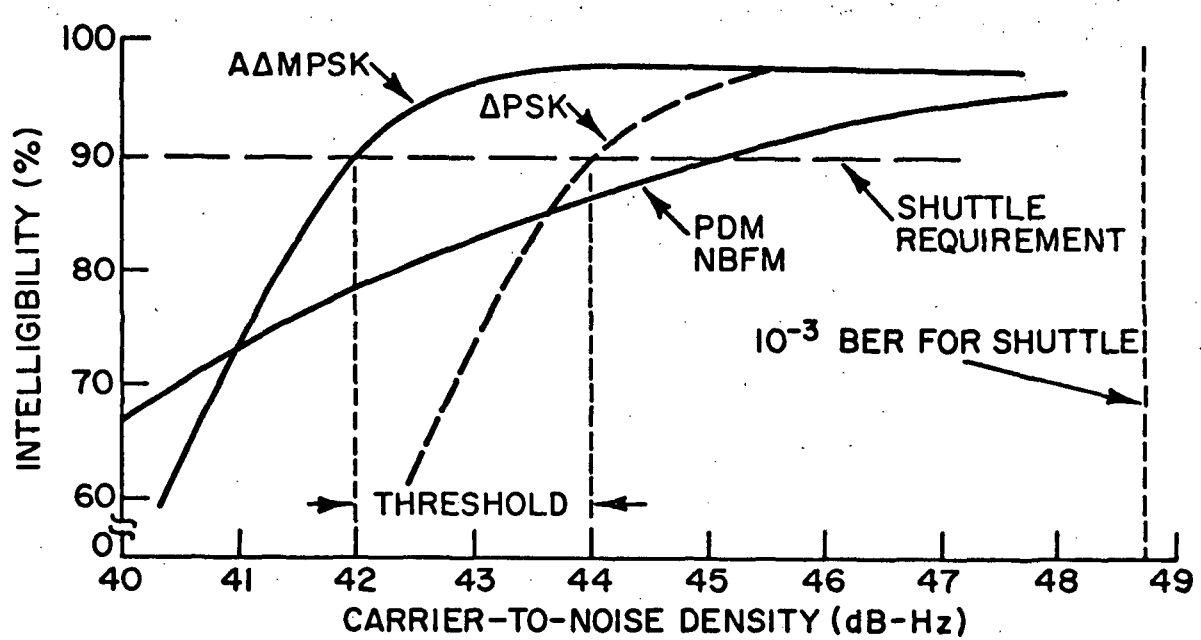

FIGURE 5-4 COMPARISON OF PDM AND ADAPTIVE DELTA MODULATION VOICE

encoded and differentially decoded the performance will be degraded as shown in Figure 5-5.

In addition to adaptive delta modulation, there are a number of digital voice coding techniques which might be evaluated for application to the Space Shuttle program. The most promising of these is predictive coding. There are a number of contracts being supported by DOD to develop high quality predictive voice coders at bit rates between 3.6 and 9.6 kb/s. The predictive voice coding rate may be 4 kb/s or 8 kb/s to be compatible with the proposed changes in the DCA transmission rate standards. These proposed changes would modify transmission rates existing now at 75×2^n b/s to multiples of 2000 b/s, e.g., 4000, 8000, 16000 and 32000. This may be done to be compatible with AT&T's standard sampling rate of 8 kilosamples/second for their digital systems.

Computer generated tapes based on predictive voice coding algorithms are now available from a number of sources with DOD. The results of the computer generated tapes are impressive and illustrate that high quality voice can be obtained at 3.6 kb/s using predictive voice coding techniques. The ultimate costs of implementing the techniques are not known and the performance of the predictive voice coder in the presence of errors is not established at this time. It is anticipated, however, that the performance of the predictive voice coder will remain acceptable at error probabilities of 10^{-2} to 10^{-3}.

5.2 FORWARD ERROR CONTROL UNIT

The error correction unit will consist of a rate 1/2 convolutional encoder with a Viterbi (Maximum Likelihood) decoder. The decoder unit can

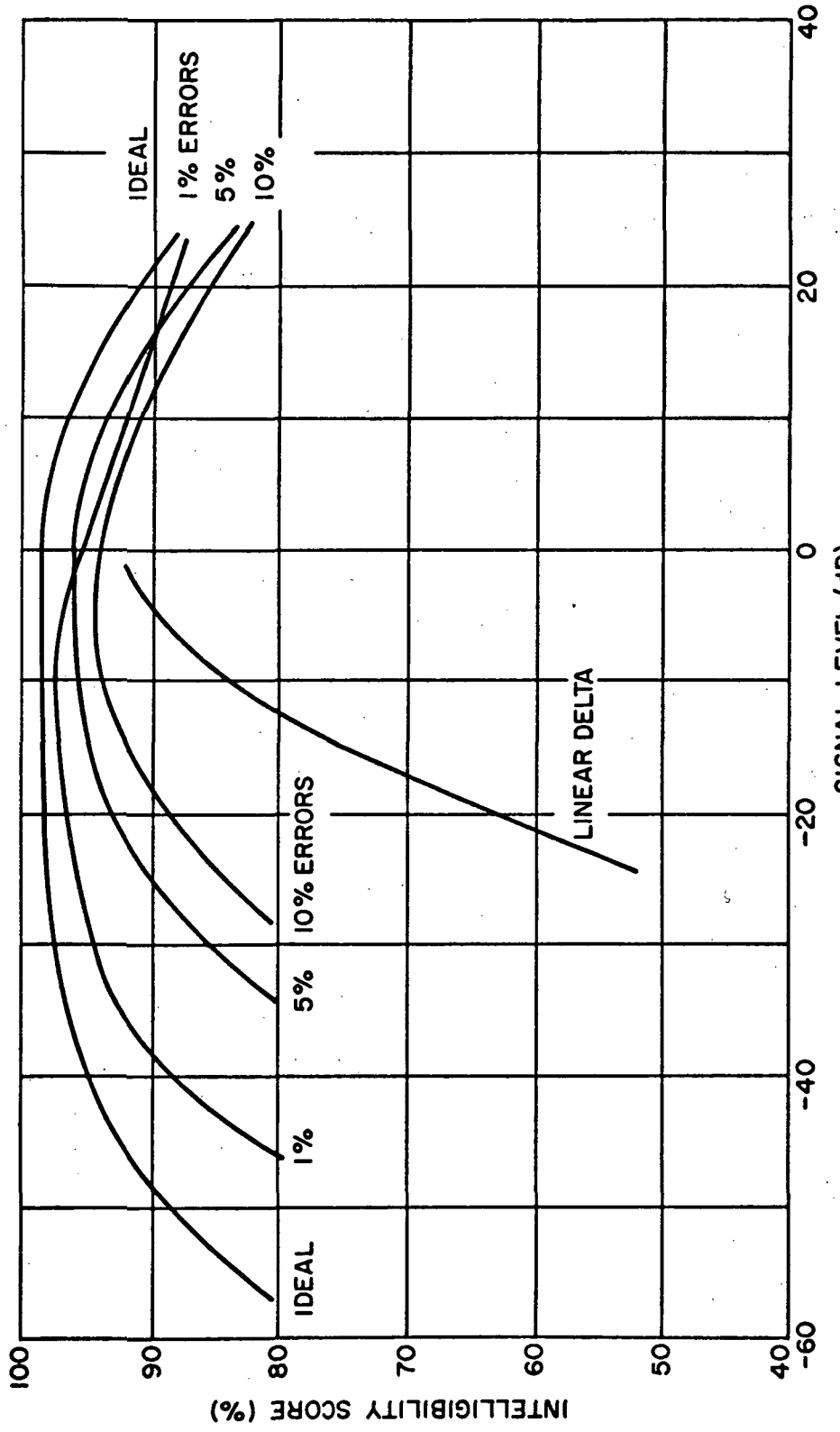

FIGURE 5-5 PERFORMANCE OF TYPICAL ADAPTIVE DELTA MODULATOR

be built on a module which contains its own power supply.

The encoder/decoder designs will accommodate bit rates from 20 kb/s to 1000 kb/s, thus the desired operating rate of 125 kb/s will be covered with leeway for any adjustment in the rate. The units can use large scale integrated (LSI) circuitry.

The performance of Viterbi decoding when used with optimal (maximum distance) codes is shown in Table 5-1 along with the non-optimal transparent code chosen for the present application. The values in the table were obtained by computer simulation.

For reasons to be discussed later, a nonoptimal code was decided upon precisely because it is transparent, i.e., complemented code words due to Costas loop demodulation phase ambiguity result in complemented sequences which can be delta decoded to retrieve the original information. Before delta decoding there is only a 0.2 dB degradation between the transparent code and the otpimal non transparent one. After delta decoding the degradation is only 0.4 dB in the probability region of interest, i.e. 10^{-3} and 10^{-4}, when compared with the K=5 optimal code used without delta coding and decoding.

The error correction unit which will be discussed is a K=5, nonsystematic, transparent, and noncatastrophic convolutional code with the corresponding Viterbi decoder. This decision was based on the following factors:

1) The required value of E_b/N_o can be obtained by the encoder/decoder design.

2) Low power considerations can be met with an LSI design.

TABLE 5-1

VITERBI DECODING OUTPUT ERROR RATE PERFORMANCE

Soft Decision Q = 8

(No Δ-decoding except the K=5 transparent code)

Output Error Rate	Uncoded CPSK E_b/N_0	Uncoded DCPSK E_b/N_0	K = 7		K = 6		K = 5 Optimal Code		
			E_b/N_0	Coding Gain over CPSK	E_b/N_0	Coding Gain over CPSK	E_b/N_0	Coding Gain over CPSK	Coding Gain over DCPSK
1×10^{-5}	9.6	9.9	4.4	5.2	4.9	4.7	5.2	4.4	4.7
1×10^{-4}	8.4	8.8	3.7	4.7	4.1	4.3	4.4	4.0	4.4
1×10^{-3}	6.8	7.3	3.0	3.8	3.3	3.5	3.5	3.3	3.8
1×10^{-2}	4.3	5.2	2.1	2.2	2.3	2.0	2.4	1.9	2.8

K = 5 Transparent Code (Δ-Decoded)			
Output Error Rate	E_b/N_0	Coding Gain over CPSK	Coding Gain over DCPSK
1×10^{-5}	5.6	4.0	4.3
1×10^{-4}	4.8	3.6	4.0
1×10^{-3}	3.9	2.9	3.4
1×10^{-2}	2.8	1.5	2.4

3) The transparency of the code offers little degradation in E_b/N_o when used with differential encoding and decoding.

4) The K=5 specification requires the least amount of complexity in hardware.

5) The unit can be implemented with approximately 20 CMOS MSI or 4 custom LSI chips due to the low data rate.

The following sections describe the Viterbi algorithm and offer trade-off performance curves for the constraint lengths of five, six, and seven. Interface considerations are offered in the following sections together with the hardware approach and some design results for the coder/decoder unit.

5.2.1 PERFORMANCE OF THE MAXIMUM LIKELIHOOD DECODER

In this section, the performance of the maximum likelihood decoder for K=5, 6 and 7; rate 0.5; convolutional codes will be presented. The codes studied are listed in Table 5-2. The contraint length 5 and 6 optimal codes are nontransparent to phase reversals while the constraint length 5 nonoptimal and constraint length 7 optimal codes are transparent.

TABLE 5-2

CONVOLUTIONAL CODES STUDIED

CONSTRAINT LENGTH	CODE POLYNOMIAL
5 (transparent)	{10011} {11001}
5 (optimal)	{10011} {11101}
6 (optimal)	{111101} {101011}
7 (optimal)	{1111001} {1011011}

A code is transparent if the coded output sequences of two complementary information input sequences are themselves complements of one another. Transparency of the code can be useful in a system which may have a phase polarity ambiguity but it is in no way a requirement, e.g., a phase reversal detector can be incorporated into the decoder itself in lieu of the transparency.

The codes shown in Table 5-2 are the optimal codes for their constraint length except the K=5 transparent code. Optimality is defined here as possessing the largest minimum free distance among all codes of identical constraint length.

From a hardware standpoint, it is desirable to use a code of short constraint length (K). As the constraint length of the code is increased, the hardware growth is exponential.

Another hardware problem is to choose the length of the path memory truncation or decoding delay. The problem here is to determine the minimum number of bits to be retained in the path memory without a significant loss in performance. Since there are 2^{K-1} path memories, storage must be allocated for $N \cdot 2^{K-1}$ bits where N is the number of bits retained in each path.

The channel will be modeled as an Additive White Gaussian Noise Channel for all simulations in this section. This is an adequate model for satellite links. As a reference, the probability of a bit error as a

function of the signal-to-noise ratio (E_b/N_o) for ideal CPSK and differentially encoded PSK (DCPSK) is shown in Figure 5-6. A typical error rate of interest is 10^{-5} which for CPSK is achieved at E_b/N_o = 9.6 dB; and for DCPSK, at 9.9 dB.

5.2.1.1 Soft-Decision Decoder

The performance as a function of code constraint length and decoding delay is considered in this section. For the results presented in this section, the decision statistic for the most delayed bit in the path memory is the most likely path metric. Also, the allocated metric storage is four bits with provisions for clamping and resetting.

The performance curves for the soft-decision maximum likelihood decoders for constraint length 5, 6, and 7 codes are shown in Figures 5-7, 5-8, and 5-9. The soft-decision inputs are uniformly quantized to three bits.

Figure 5-7 shows the performance of the constraint length 5 soft-decision maximum likelihood decoder for various decoding delays. The performance of the soft-decision decoder improves with increasing decoding delay. However, for a decoding delay greater than 5 constraint lengths, the return is insignificant. An average error rate of 10^{-5} for the constraint length five optimal code with a decoding delay of five constraint lengths is achieved at E_b/N_o = 5.25 dB. This represents a coding gain of 4.4 dB over ideal two-phase PSK.

In the case of the transparent code there is a 0.2 dB loss over the optimal code shown in Figure 5-7 because the distance is 6 as opposed

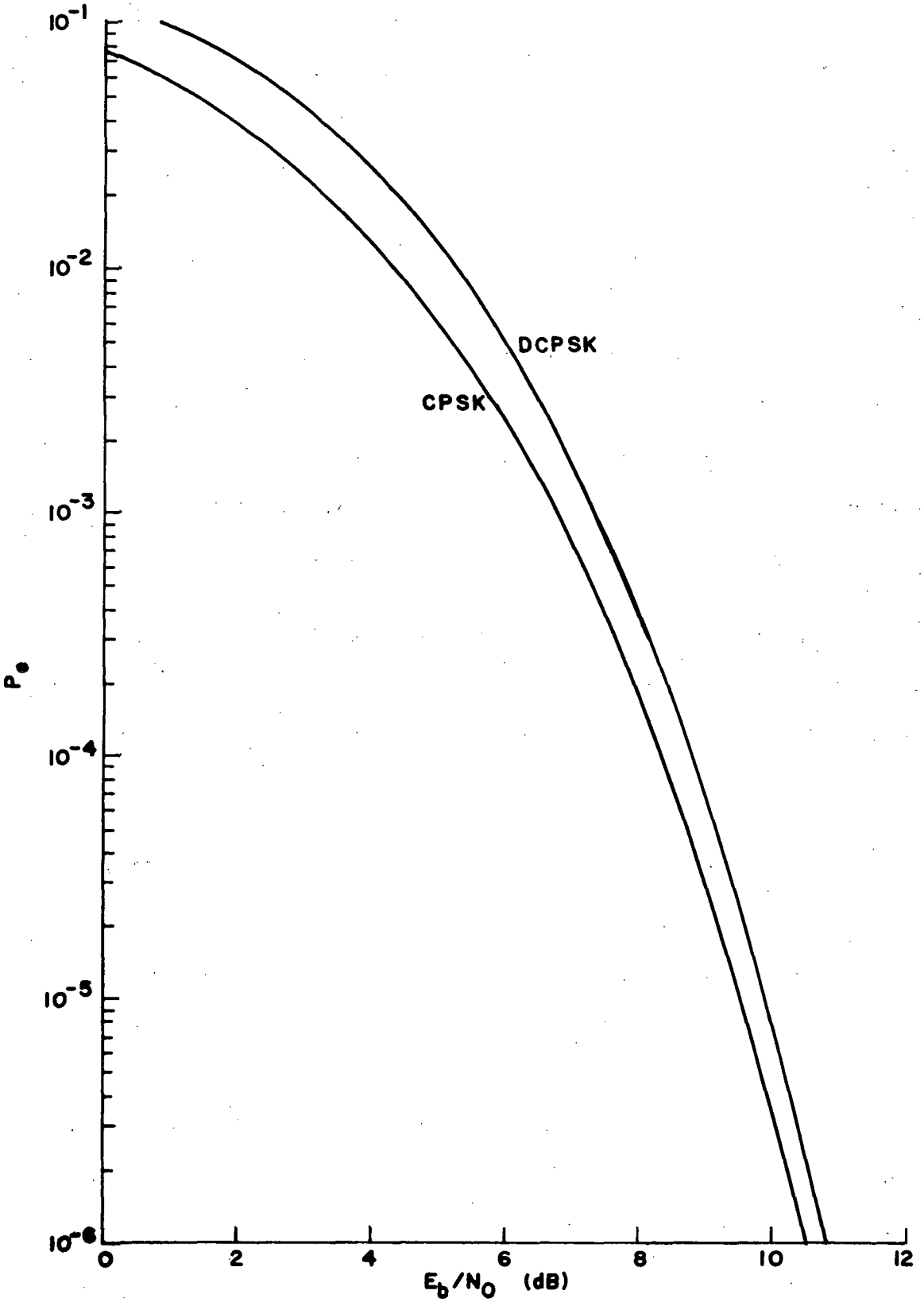

FIGURE 5-6 PROBABILITY OF A RAW BIT ERROR VS. E_b/N_0 FOR IDEAL CPSK AND DCPSK ON THE ADDITIVE GAUSSIAN NOISE CHANNEL

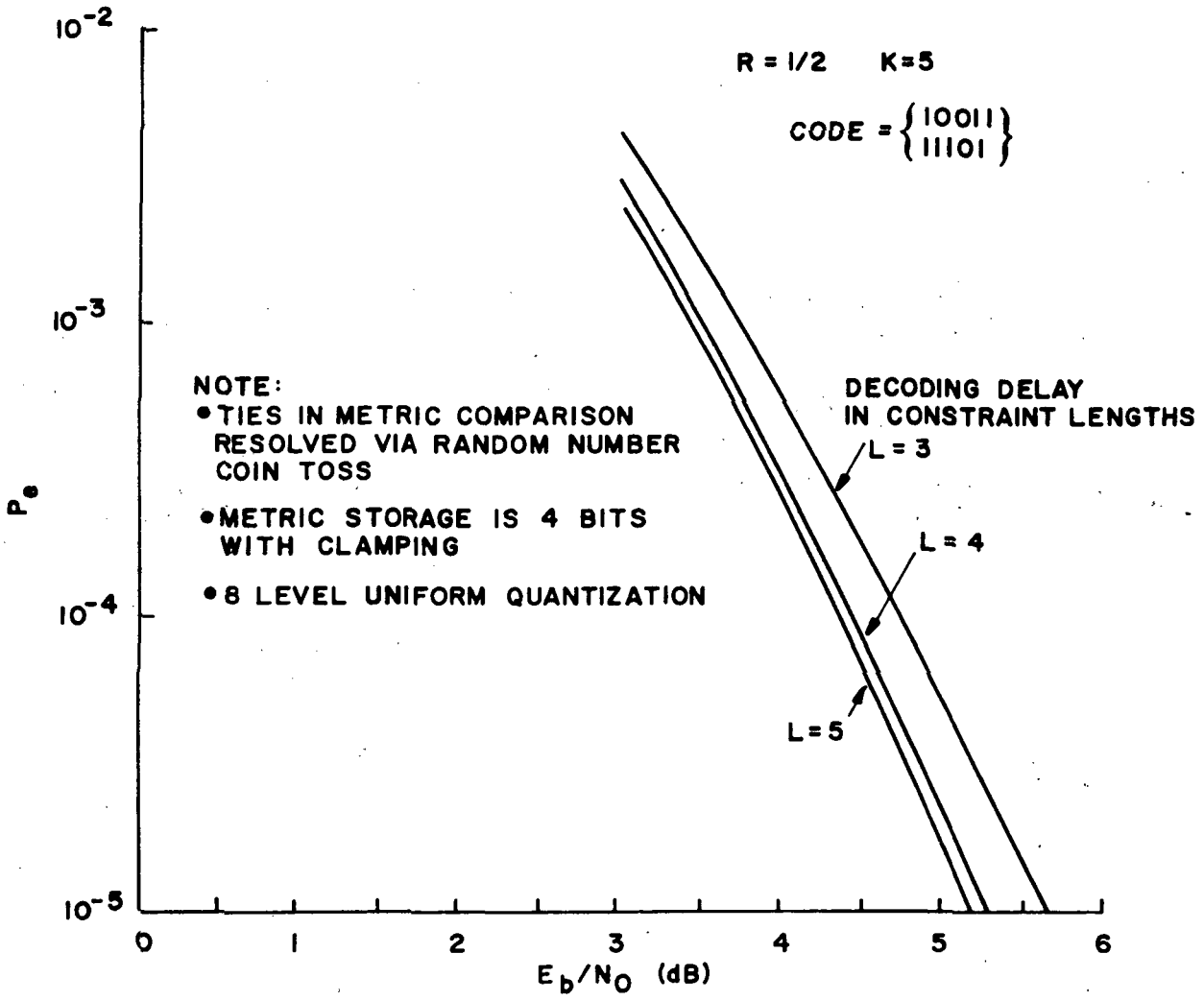

FIGURE 5-7 SOFT DECISION MAXIMUM LIKELIHOOD (K=5) DECODER PERFORMANCE USING MOST LIKELY PATH DECISION RULE ON THE ADDITIVE GAUSSIAN CHANNEL

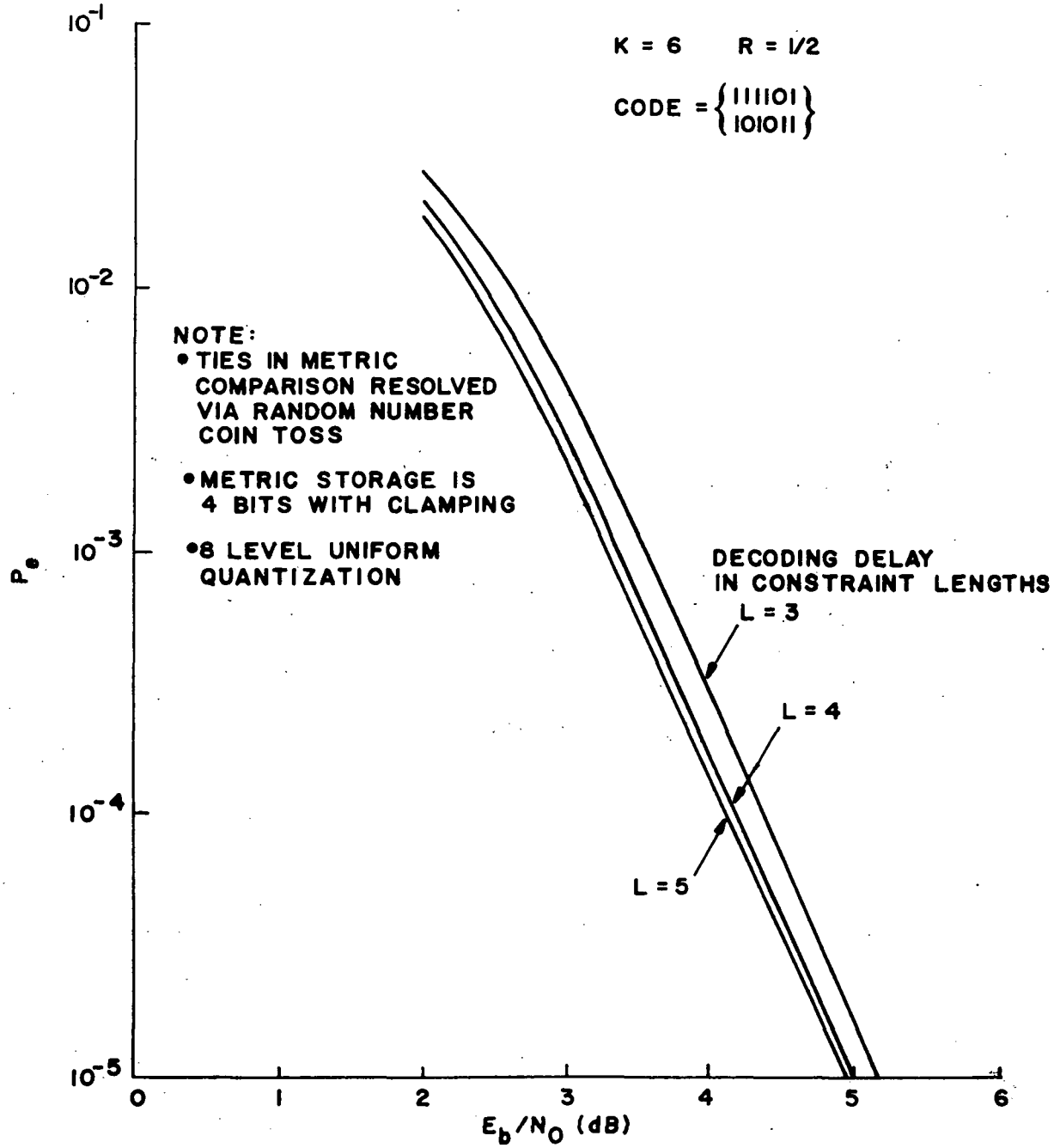

FIGURE 5-8 SOFT DECISION MAXIMUM LIKELIHOOD (K=6) DECODER PERFORMANCE USING MOST LIKELY PATH DECISION RULE ON THE ADDITIVE GAUSSIAN NOISE CHANNEL

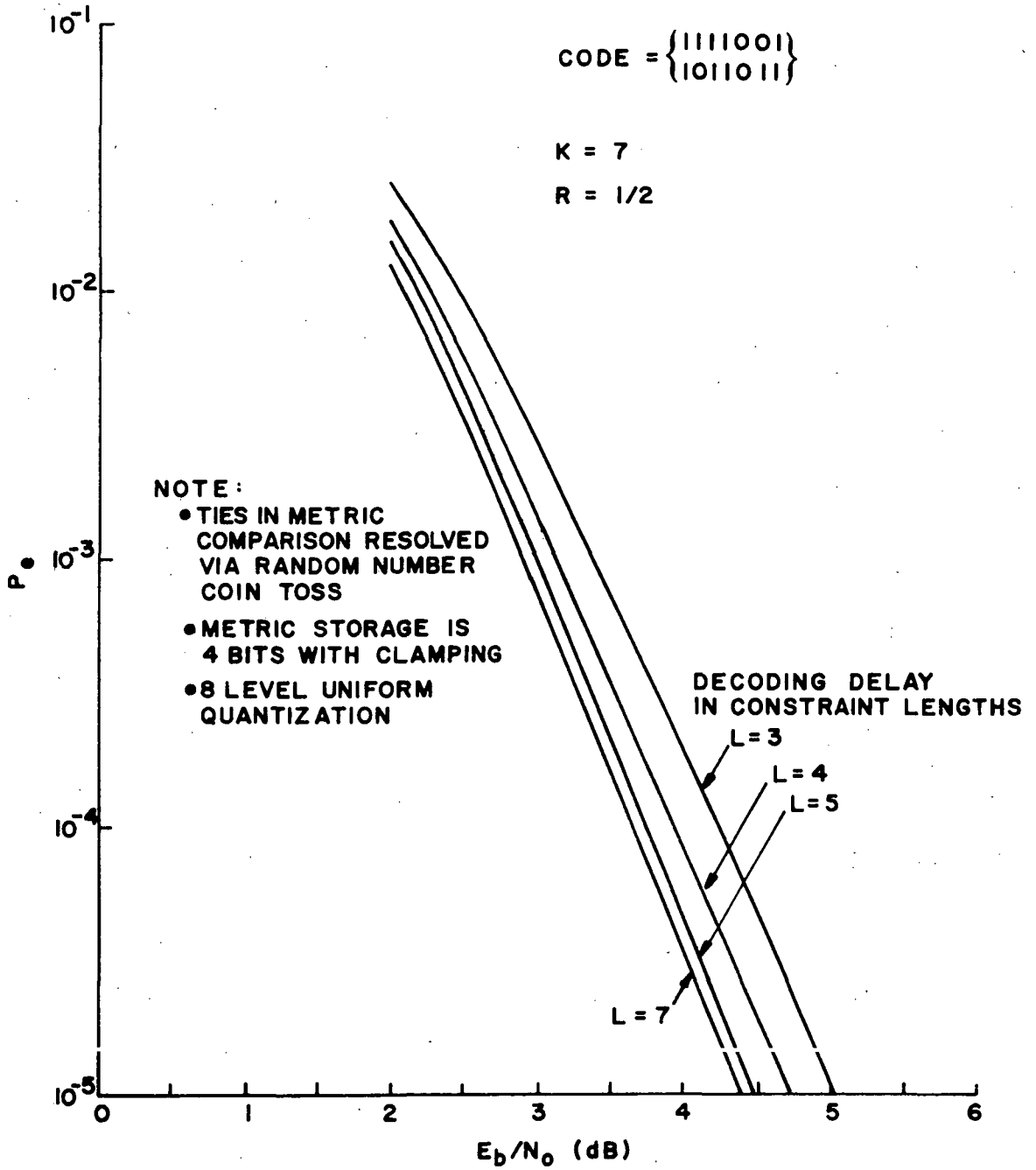

FIGURE 5-9 SOFT DECISION MAXIMUM LIKELIHOOD (K=7) DECODER PERFORMANCE USING MOST LIKELY PATH DECISION STATISTIC ON THE ADDITIVE GAUSSIAN NOISE CHANNEL

to the optimal of 7; also there is a 0.2 dB loss due to the delta decoding needed at the output of the error correction decoder. At 10^{-5} bit error rate, then, the coding gain is only 4.0 dB over coherent PSK.

Figure 5-8 shows the results of the simulation of the soft-decision maximum likelihood decoder for the constraint length six code with variable decoding delay. The chosen decoding delay is five constraint lengths. For a decoding delay of five constraint lengths, the constraint length six soft-decision maximum likelihood decoder achieves an average error rate of 10^{-5} at E_b/N_o = 4.9 dB for a coding gain of 4.75 dB over ideal two-phase PSK.

Figure 5-9 shows the result of the simulation of the constraint length seven soft-decision maximum likelihood decoder with variable decoding delay. To attain a coding gain of 5.0 dB or greater over ideal two-phase PSK, the decoding delay necessary is five constraint lengths. For a decoding delay of five constraint lengths, the system performs at E_b/N_o = 4.4 dB for a coding gain of 5.25 dB.

5.2.1.2 System Interface Considerations

The influence of the system interface on the coder/decoder is summarized in the synchronization, inversions due to phase slips in the PSK demodulator, and the quantization of the inputs to the decoder.

5.2.1.3 Quantization

One of the most critical parts of the system is the quantization of the soft decisions. The equally spaced quantizer is shown in Figure 5-10

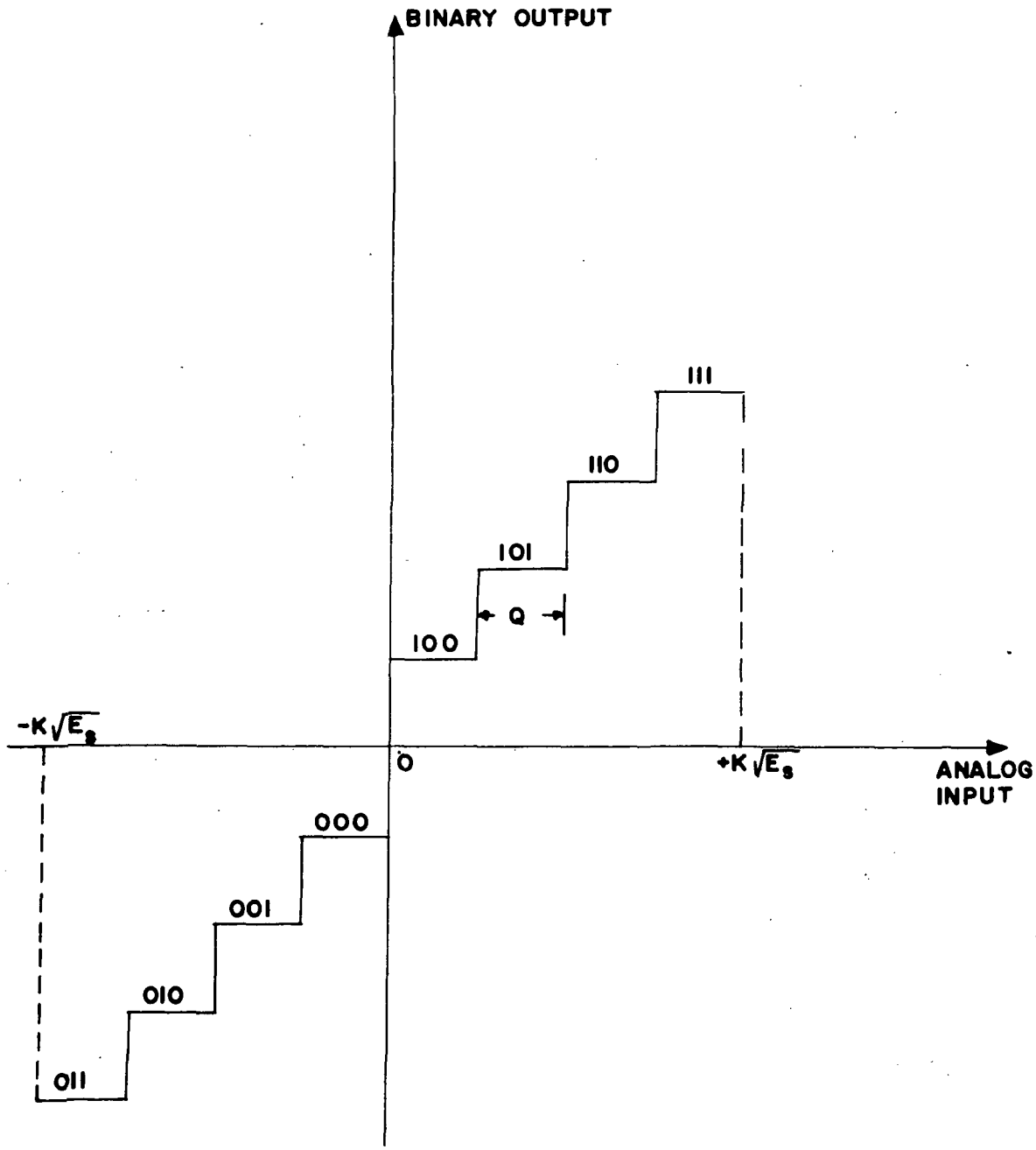

FIGURE 5-10 UNIFORM QUANTIZER (N=8 LEVELS)

for eight levels. The input analog voltage is limited to a maximum signal excursion of $\pm K\sqrt{E_s}$ where $\sqrt{E_s}$ is the mean value of magnitude of the received waveform. The spacing between the levels is given by

$$Q = \frac{2K\sqrt{E_s}}{N} \qquad (5\text{-}1)$$

The output of the quantizer is a three-bit binary number. The sign bit represents the hard decision on the received channel symbol and the remaining two bits represent the magnitude of the associated confidence level.

The error performance of the decoder is sensitive to the spacing Q selected. Since the level of quantization is fixed to be three bits and to be uniformly spaced, the problem is the selection of the optimum signal excursion as input to the quantizer.

Figure 5-11 shows the results of the optimization procedure simulated on a computer for a constraint length 5 optimal code with soft-decision inputs of 3 bits, 4 bits and 5 bits of quantization.

In the case of 3-bit quantization and constraint length of 5, both of which will be assigned parameters of the error correction unit, the optimal level of the quantization setting is $1.8\sqrt{E_s}$.

5.2.1.4 Node Synchronization and Phase-Flips

5.2.1.4.1 Node Synchronization on Code Symbols

At the receiver (decoder) two timing problems arise during the transmission of data by a two-phase PSK system. They are the initial node synchronization on the code symbol pair of the rate 1/2 convolutional code

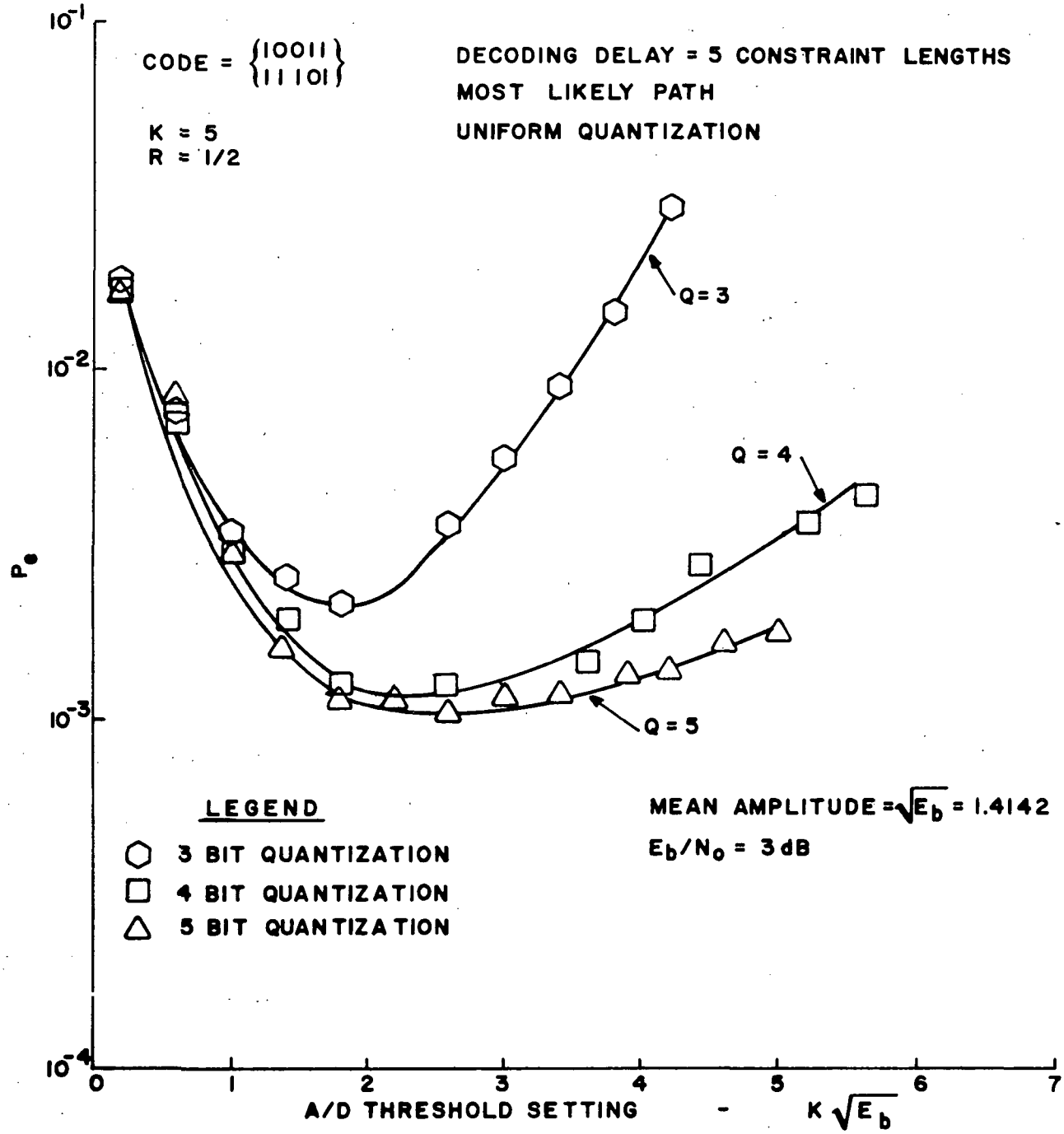

FIGURE 5-11 COMPARISON OF THE EFFECTS OF SOFT-DECISION QUANTIZATION ON A/D THRESHOLD SETTING AND ERROR PERFORMANCE OF A MAXIMUM LIKELIHOOD DECODER

and the monitoring of this synchronization. To monitor sync, the receiver is required to detect when a sync error (bit slip) has occurred and initiate action to recover from the sync error.

Code symbol (node) synchronization within a branch is necessary. Clearly, if the wrong decision of code symbol pairs is made, the decoder will constantly make errors thereafter. This situation can be detected because the mismatch of code symbols will cause all path metrics to be large since there will be correct paths.

A method of detecting this condition is to count the number of metric resets that occur over a specific time interval. If the resets occur too frequently, the decoder can assume that it is out of sync and initiate the appropriate action for correction. Figure 5-12 shows the number of metric resets per bit as a function of E_b/N_o for the constraint length 5 maximum likelihood decoder operating in the out-of-sync and in-sync modes. Note that the number of metric resets is essentially constant for the out-of-sync mode, whereas for the in-sync mode, the number of resets decreases as E_b/N_o increases.

Another method of detecting sync errors is to accumulate the most likely path metric and compare it to a threshold after a specific time interval. This can be considered as a finer grating of the reset counting method.

The first of these methods was chosen for the initial synchronization and monitoring problems.

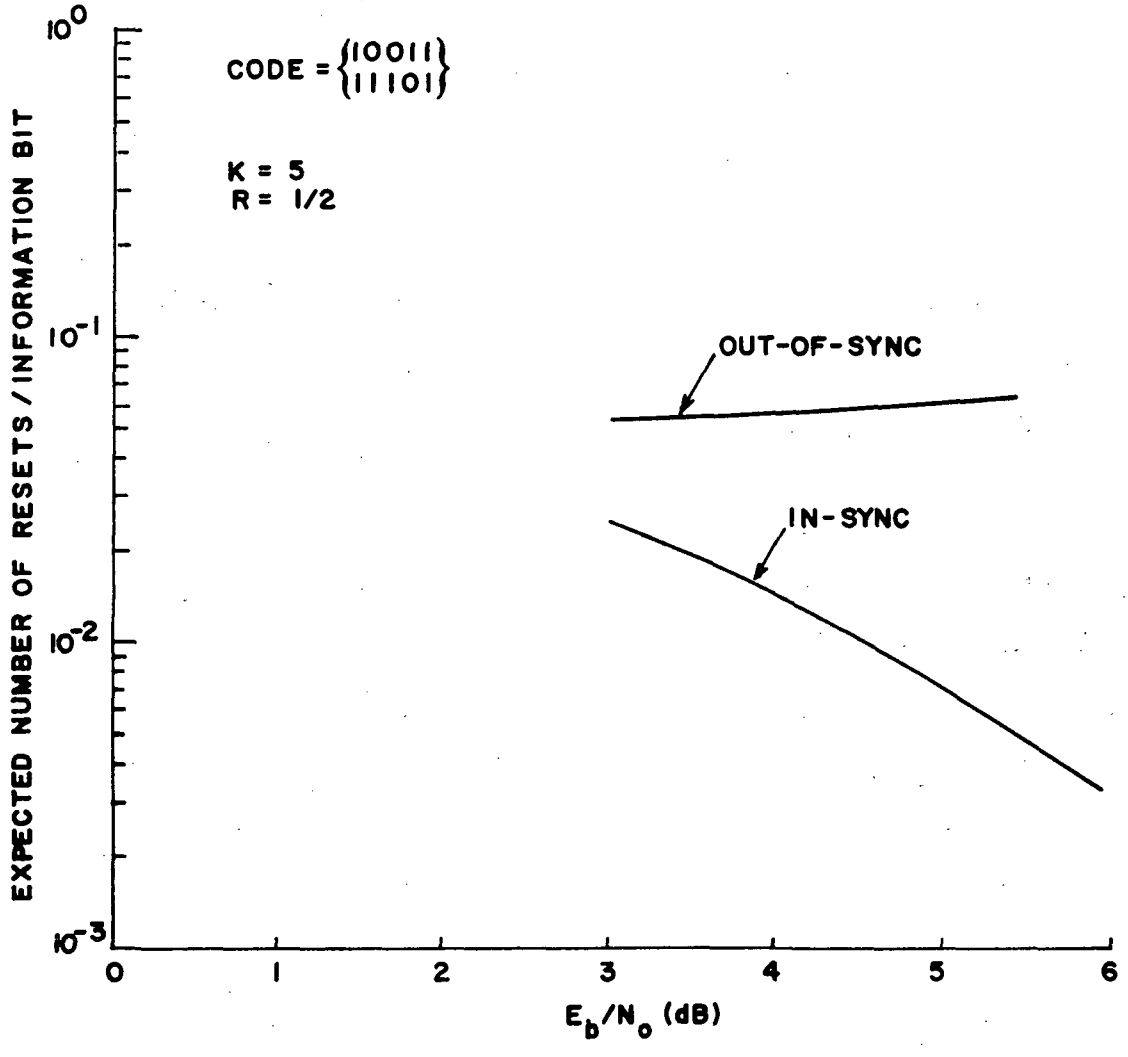

FIGURE 5-12 EXPECTED NUMBER OF RESETS PER INFORMATION BIT VS. E_b/N_0 FOR MOST LIKELY PATH DETECTION RULE USING 4 BITS OF METRIC STORAGE WITH CLAMPING AND 3-BIT UNIFORM QUANTIZATION

5.2.1.4.2 Detection of Phase Flips

The carrier tracking loop introduces another problem. The tracking loop is subject to phase flips which will cause the decisions to be inverted. That is, a zero will be decoded as a one and a one as a zero.

If the convolutional code is transparent, however, the bit inversions can be compensated by the DCPSK encoding. The maximum likelihood decoder will operate without loss of performance after the phase flip has occurred and the decoding memory associated with the actual time of the phase flip is shifted out.

Note that if a nontransparent code was used, the maximum likelihood decoder will act as if it were out of sync. Errors will propagate and the metric will grow rapidly. When a nontransparent code is used, the decoder can be in the following out-of-sync modes:

1) bit inversion and in-sync
2) bit inversion and out-of-sync
3) out-of-sync without a bit inversion

Figure 5-13 applies for conditions 1) and 2) above. Therefore, it may take longer for the decoder to obtain synchronization.

It should be noted also that when a nontransparent code is used bit inversions due to phase flips must be accounted for within the decoder. On the other hand, when a transparent code is used bit inversions are accounted for by external sources, i.e., with DCPSK coding and decoding.

5.2.1.5 Error Rate Indicator

In order to obtain an indication of the decoded error rate (error rate after decoding), one can just integrate the average number of resets

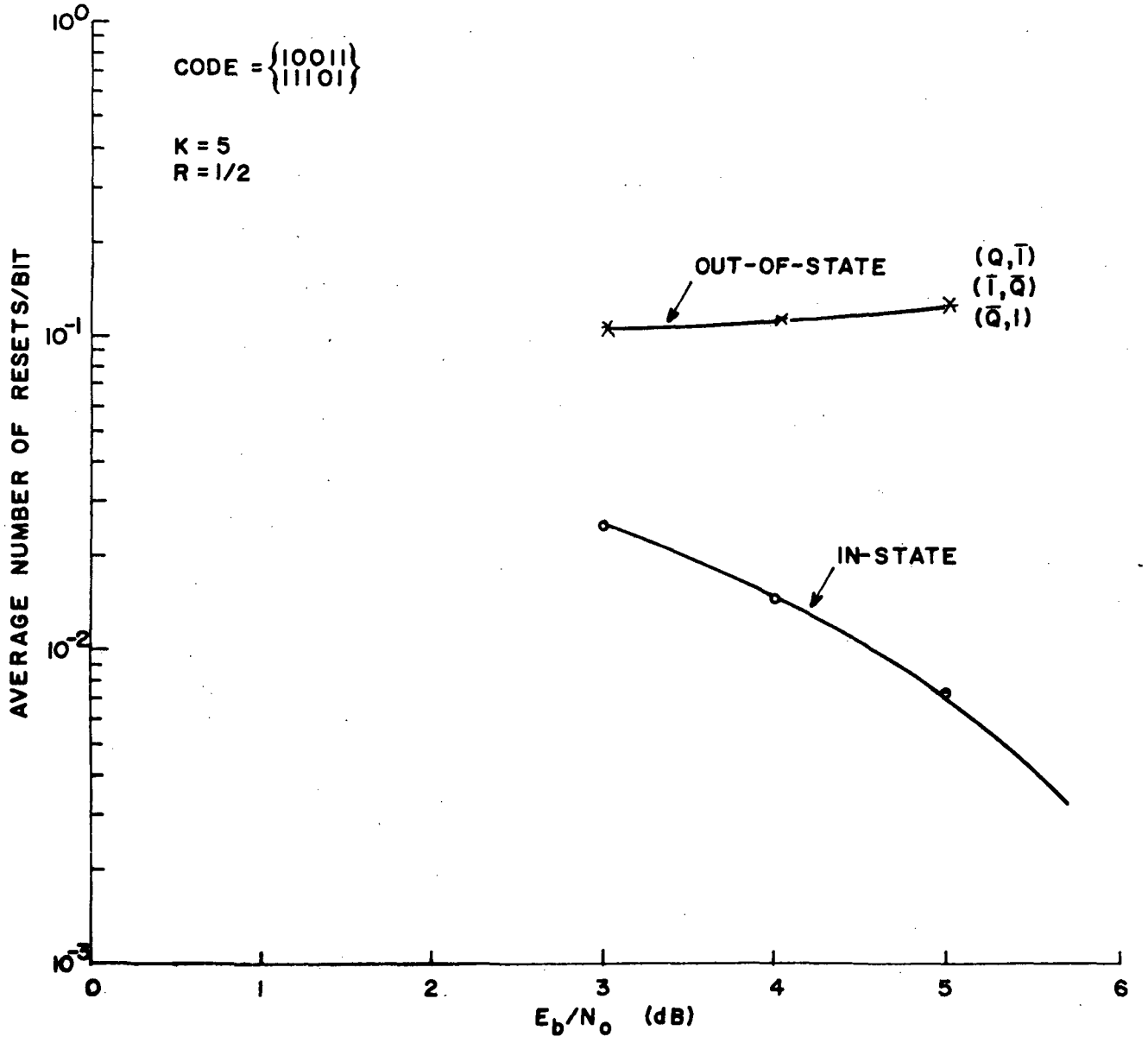

FIGURE 5-13 EXPECTED NUMBER OF METRIC RESETS PER INFORMATION DIGIT VS. E_b/N_o FOR A MOST LIKELY PATH DETECTION RULE USING 4 BITS OF METRIC STORAGE WITH CLAMPING AND 3-BIT UNIFORM QUANTIZATION

which is monotonically related to the probability of an error. Figure 5-14 illustrates this point by plotting the probability of an error as a function of the average of resets.

5.2.2 DESIGN OF A CODER/DECODER WITH CONSTRAINT LENGTH 5

The following section describes the design and development of a convolutional encoder and decoder for transmission of data at rates up to 1 Mb/s, and therefore will more than accommodate the data rates for both the forward and the return links of the Shuttle/TDRS System.

The parameters chosen are given in Table 5-3. The input to the coder will be assumed to be differentially coded.

TABLE 5-3

PARAMETERS FOR CODER/DECODER DESIGN

Code Rate: 1/2
Constraint Length: K=5 bits
Decoder Input Quantization: 3 bits (8 uniformly spaced levels)
Path Delay: 5 constraint lengths
Path Selection: Most likely according to metrics
Metric Storage: 4 bits with clamping

5.2.2.1 Summary of the Decoder Design Considerations and System Interfacing

The models of the maximum likelihood convolutional decoder and encoder are designed to interface with a biphase system.

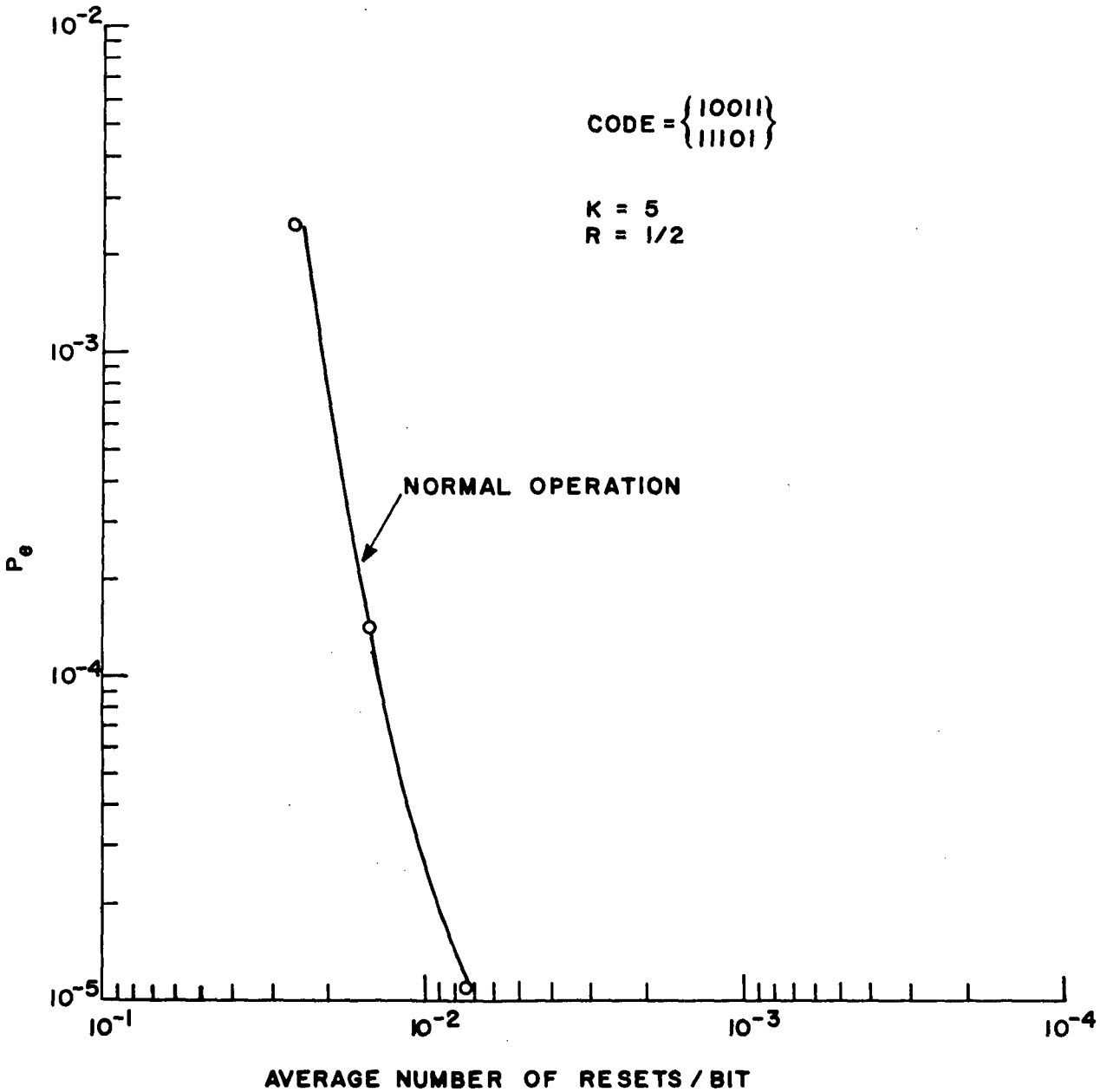

FIGURE 5-14 PROBABILITY OF ERROR VS. AVERAGE NUMBER OF RESETS/INFORMATION BIT USING MOST LIKELY PATH DETECTION RULE WITH 4 BITS OF METRIC STORAGE WITH CLAMPING AND 3-BIT UNIFORM QUANTIZATION

Figure 5-15 is a block diagram showing the inputs and outputs of the convolutional encoder. The encoder operates synchronously with the channel modulator. Clock signals at rates R and 2R are derived from a local reference. Data at clock rate R are fed into the convolutional encoder from a synchronous source. The output of the convolutional encoder is the serial coded data sequence at a clock rate 2R. Output data from the convolutional encoder switch in response to positive-going edges of the clock.

Figure 5-16 shows the configuration for the maximum likelihood convolutional decoder. Three-bit soft-decision statistics are brought from the quantizing unit on three parallel lines, one line for each bit of the soft decisions. The output of the convolutional decoder is the reconstructed delta coded sequence that appeared at the input to the convolutional encoder. It is then delta decoded to recover the original information. The convolutional decoder requires clocks of R and 2R. All output data move in response to the positive edge of clock R.

5.2.2.2 Encoder

Figure 5-17 shows the rate = 1/2, K=5 convolutional encoder. Data bits are entered serially into a five-bit shift register. For each new input data bit two coded bits are generated by the encoder. Each coded bit is generated by a modulo-2 adder that derives its input from three of the five stages of the shift register. In this manner each coded bit is a function of the new data bit in the register and the four data bits preceding the new data bit in time. The four previous data bits which occupy the last four stages of the shift register are by definition the encoder state.

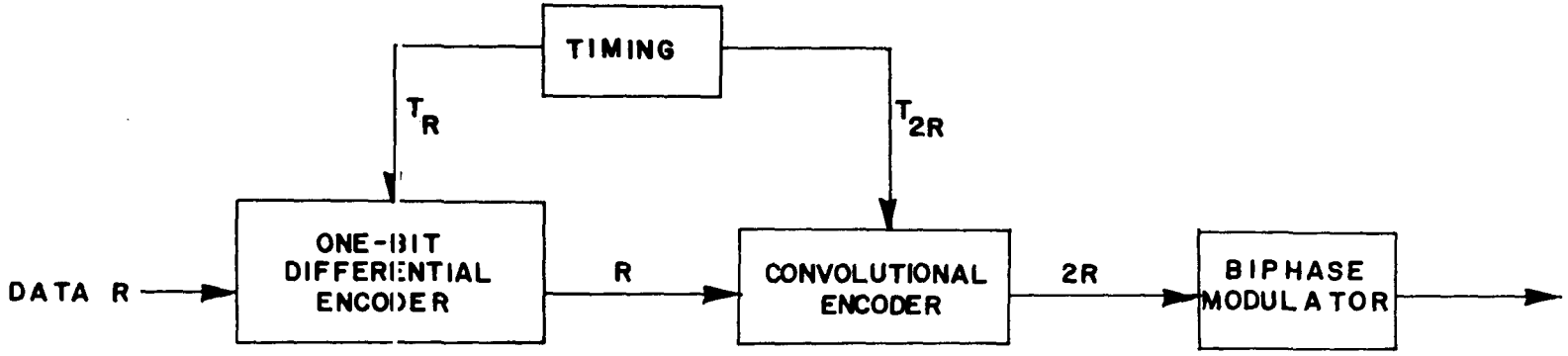

FIGURE 5-15 ENCODER CONFIGURATION

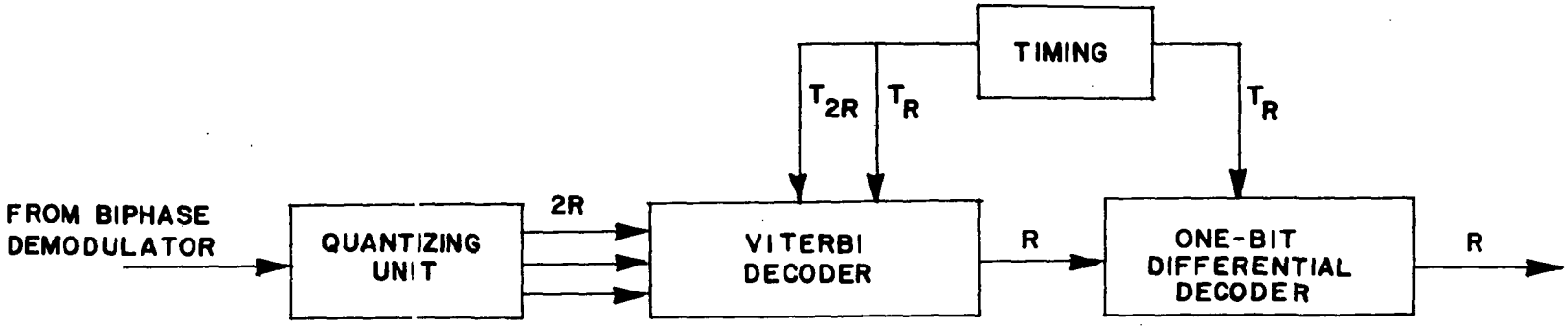

FIGURE 5-16 DECODER CONFIGURATION

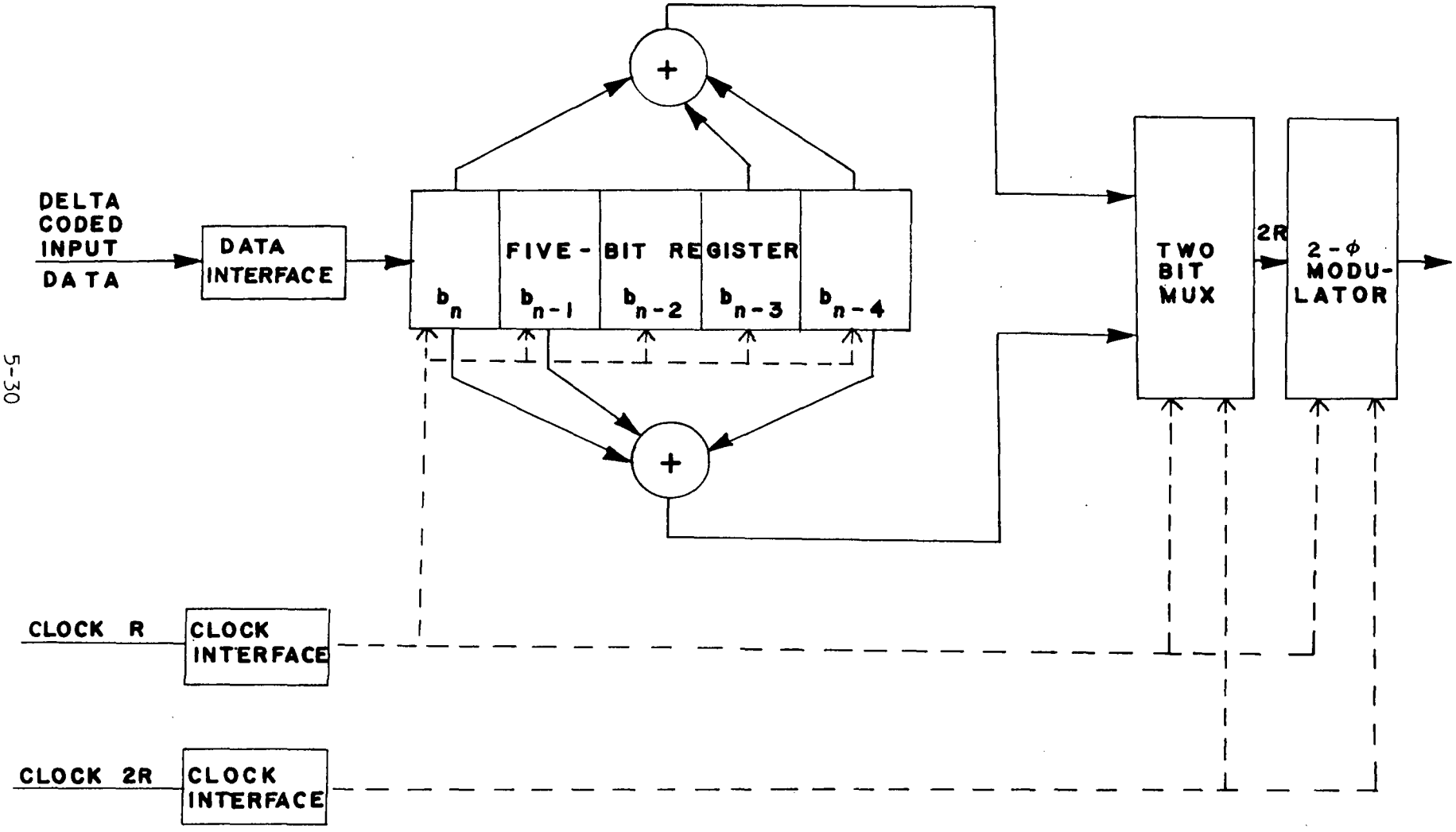

FIGURE 5-17 CONVOLUTIONAL ENCODER R = 1/2, K = 5

The coder bit pair is time-multiplexed into a single line for transmission at twice the data clock rate. Interface circuits are provided at the input and output of the encoder to translate the logic levels of interfacing equipment to that of the logic used in this system.

5.2.2.3 Decoder

The function of the decoder is to reconstruct the data stream fed into the encoder from the soft-decision coded bit pair that the decoder receives from the channel modem. The reconstruction is achieved by determining the most probable sequence of states progressed through by the encoder.

Figure 5-18 is the block diagram for the decoder. The three-bit soft decisions from the quantizing unit are received serially by the Metric Transition Generator at twice the data rate (i.e., at the coded data rate 2R). From each pair of soft-decisions received the Metric Transition Generator calculates a probability measure on each of the four possible magnitude values (i.e., 00, 01, 10, 11) of the associated bit pair. The metric transitions are combined with the metrics from the past in order to generate a new set of metrics.

Each metric indicates the reliability of the most probable data path ending in a specific encoder state. Since for a K=5 code there are 16 encoder states, it is necessary to generate 16 metrics. From an examination of the possible sequence of encoder states, it is known that for each new data bit an encoder state can go to only one of two encoder states and conversely any encoder state can be accessed from only two encoder states. From each metric two new metrics are generated, corresponding to the two new states the old state could have progressed to with a new data bit. The

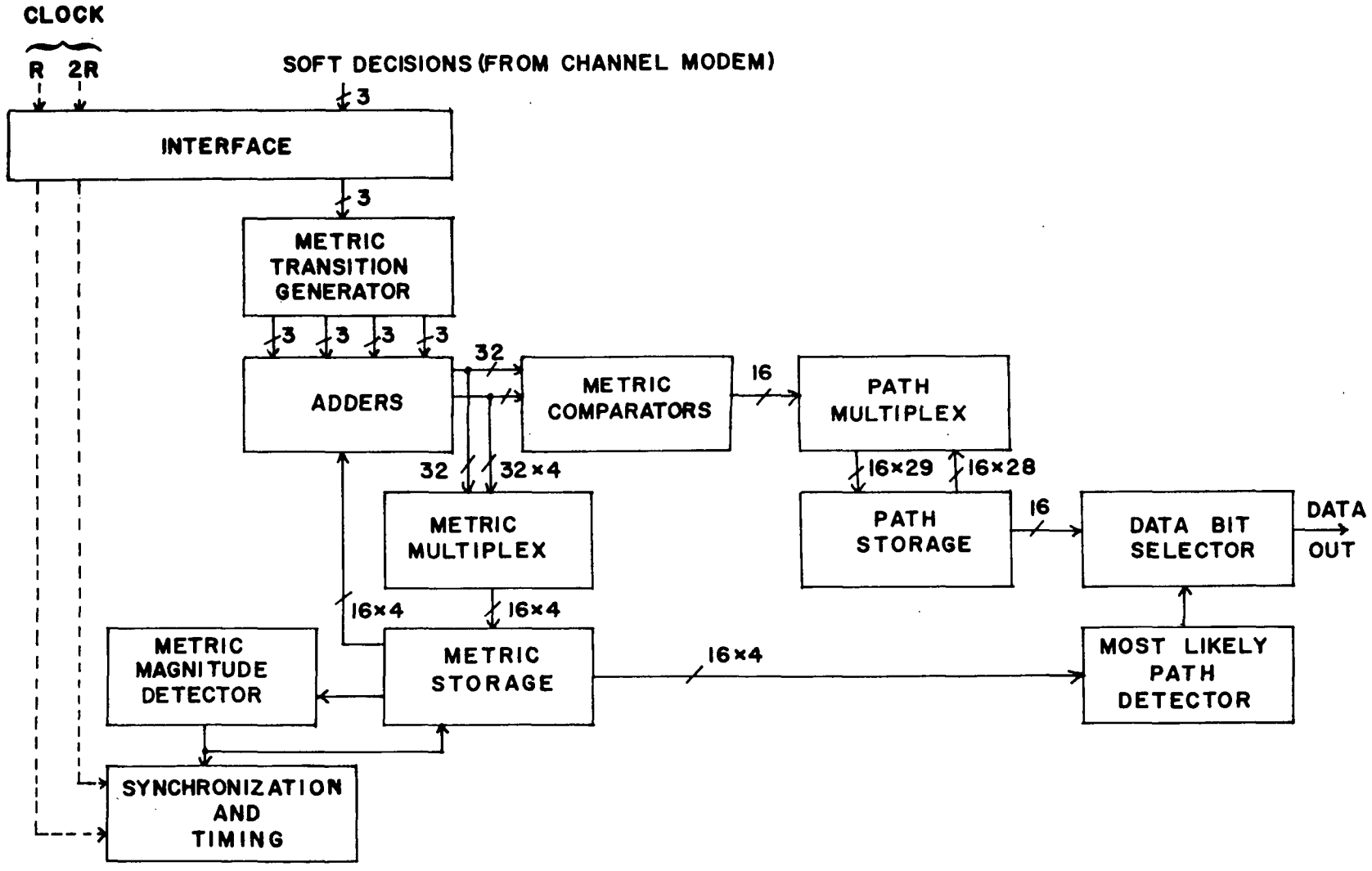

FIGURE 5-18 MAXIMUM LIKELIHOOD CONVOLUTIONAL DECODER

two new metrics are calculated from the old metric in the following manner. The first new metric is the old metric added to the metric transition resulting from a zero (0) as the new data bit in the encoder register. The second new metric is the old metric added to the metric transition if a one (1) had been the new data bit.

In this manner a set of 32 new metrics is generated by the adders. The metric comparators perform pairwise comparisons for each pair of metrics leading to the same states. Each comparison selects the most probable of the two metrics. The most probable metric is indicated by the metric of minimum numerical value. The surviving metrics are then placed via the metric multiplex in the position assigned to their states in the metric storage. The surviving metrics now become the old metrics for the next coded bit pair received.

In addition to determining the surviving metric, each comparison makes a decision on the most delayed bit in the encoder register. This is due to the fact that the states from which each set of parallel paths is derived can only differ in the most delayed bit position. Therefore, each path bit decision from the metric comparisons is, in effect, delayed four bit intervals from the time it was estimated to enter the encoder register. The bits resulting from each comparison are stored in the path storage.

The path storage corresponds to the sequence of bits or path leading to the state of its corresponding metric. When a comparison and a new bit decision are made, that bit must be added to the path associated with the metric from which the new metric was derived. The new path must then be placed in the storage position associated with the new metric.

The result is that the path storage will contain 16 paths, each of which is associated with a metric in the metric storage. The paths are allowed to accumulate for a number of bits equivalent to five constraint lengths of delay from the new data bit positions of the encoder. For any one path five constraint lengths of delay is equivalent to twenty-five minus the four bits represented by the state number itself. Therefore, each path consists of 21 bits.

At each data bit interval the most probable metric in the metric storage is detected. The most delayed bit (i.e., the 21-st bit) in the path associated with that metric is chosen as the decoded data bit by the data bit selector.

5.2.2.3.1 Metric Transition Generation

The metric transition generator calculates a probability measure on the received coded bit pair for each of the four possible received sequences. The four metric transitions ($L_{C_1C_2}$) are defined as follows.

Let r_1, r_2 be the quantized soft decisions on received bits #1 and #2, respectively, of the coded bit pair. Let

$$C_1 = \begin{cases} 0 \text{ if } r_1<0 \\ 1 \text{ if } r_1>0 \end{cases} \quad (5\text{-}2)$$

$$C_2 = \begin{cases} 0 \text{ if } r_2<0 \\ 1 \text{ if } r_2>0 \end{cases} \quad (5\text{-}3)$$

and

$$\alpha_1 = |r_1| \quad (5\text{-}4)$$

$$\alpha_2 = |r_2| \quad (5\text{-}5)$$

Then the metric transitions are given by

$$L_{00} = \alpha_1 \cdot C_1 + \alpha_2 \cdot C_2 \quad (5\text{-}6)$$

$$L_{11} = \alpha_1 \cdot \bar{C}_1 + \alpha_2 \cdot \bar{C}_2 \quad (5\text{-}7)$$

$$L_{10} = \alpha_1 \cdot \bar{C}_1 + \alpha_2 \cdot C_2 \quad (5\text{-}8)$$

$$L_{01} = \alpha_1 \cdot C_1 + \alpha_2 \cdot \bar{C}_2 \quad (5\text{-}9)$$

where a bar over a number indicates its complement and α_i is the absolute value of the soft decision. These metric transitions are chosen such that a positive soft decision represents a received 1 and a negative soft decision represents a 0.

Figure 5-19 is the block diagram for the metric transition generator. The three-bit soft decisions are entered into the r_2 and r_1 registers at the coded data rate. The least significant two bits of r_1 and r_2 (i.e., α_1, α_2) are fed to the inputs of four two-bit adders via NAND gates. The NAND gates will allow or block the adder inputs as dictated by the most significant bit (i.e., sign) of r_1 and r_2, and the metric transition equations. Four three-bit registers store the adder results for each metric transition. These registers are loaded at one-half the coded data rate.

5.2.2.3.2 Metric Generation

Each data bit interval, a new set of 16 metrics is generated from the new set of 4 metric transitions and the 16 metrics of the past bit interval. There are 16 metric computation cells, one for each encoder state. The cells differ only in the inputs required to calculate the different metrics. Two four-bit metrics of the old states and the three-bit metric transitions associated with the transition to the new states are added

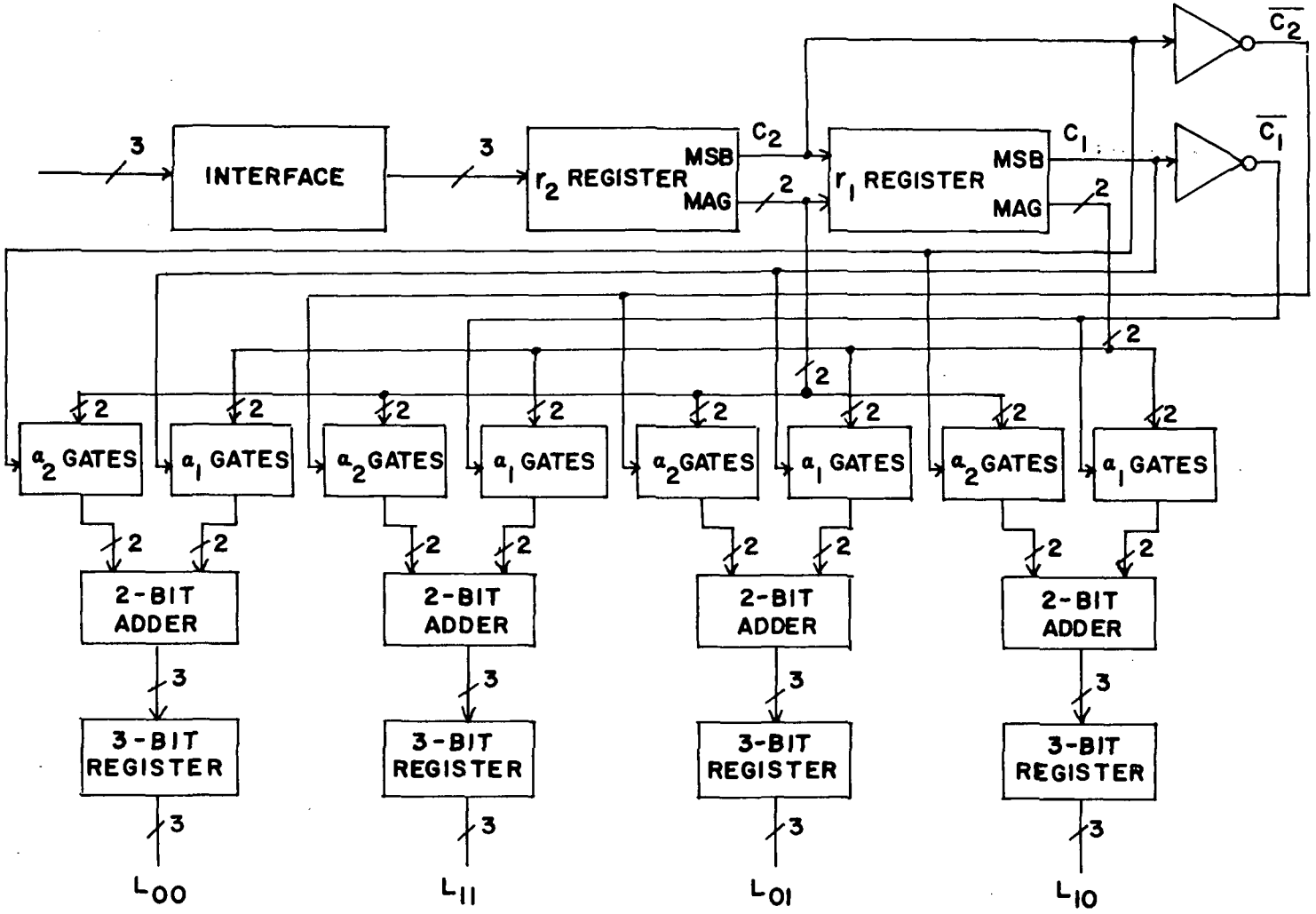

FIGURE 5-19 METRIC TRANSITION GENERATOR

together in two four-bit adders. The output of each adder is a four-bit number representing one of two metrics leading to the same state. The two metrics together with the carries of the adders are compared in a five-bit comparator. The comparator indicates the lesser of the two metrics since that metric indicates the more probable of the two parallel paths. The comparator output also causes a multiplexer to select the indicated metric as the new metric. The output of the multiplexer, which is the new metric, is placed in the four-bit storage register of the new state.

Since both the metrics and the metric transitions are positive numbers, care must be taken to avoid destruction of the metrics by overflows in the addition process. Overflow protection is provided by two mechanisms in the metric calculation. One mechanism detects that both adder outputs being compared have overflowed and causes a maximum number to be substituted for the winning metric in the metric register. This is accomplished by detecting that both adders have produced carries and causing the multiplexer to give a maximum output in place of either of its two inputs. The second overflow mechanism detects when all the new metrics are greater in magnitude than one-half the maximum number capable of being stored in a four-bit register. When this condition is satisfied a constant equal to one-half the maximum number for a four-bit register is subtracted from all the metrics. This is accomplished by detecting when the most significant bits of all metrics are set and then causing them all to reset at the same time. By employing these overflow protections it is possible to limit the metric storage for each metric to four bits and still obtain a performance which is essentially the same as that possible for infinite metric storage.

5.2.2.3.4 Path Generation

For each encoder state, there is a path memory which contains a record of the surviving path leading to that encoder state. Hence there are 16 path memories for the constraint length 5 code. Each comparison between parallel paths leading to the new encoder state, in addition to determining the surviving metric, also determines the surviving path and the newest member of that path. The newest member is a zero or a one depending on the old state from which the transition occurred. If the old state has a zero (one) in the most delayed state position, a zero (one) is appended to the surviving path. The choice of the most probable of the two metric states dictates the selection of this bit.

The path delay or word length is 2 bits long. The select signal from the comparator associated with the path is inserted in the first bit position and is the new member of the path.

5.2.2.3.5 Most Likely Path Selection

Selection of the most likely path is made on the basis of comparison of magnitudes of the metrics; the path register output corresponding to the lowest metric is selected. The most likely path is obtained by selecting one of eight paths, using three levels of comparison and selection logic; then extending this comparison to one more level, selection of one of 16 paths is accomplished. The path register final stage outputs are connected to the first level inputs. A typical "cell" contains a four-bit parallel comparator, a two-input four-bit multiplexer and an AND-OR-INVERT circuit which serves as a two-input one-bit multiplexer. Each comparator produces a logic ONE at the output opposite the input of smaller magnitude, or at both outputs if the inputs are equal. The smaller metric input to each cell

thus appears at an input to the following cell. At the same time, the path register output corresponding to the smaller metric is routed through the AND-OR-INVERT circuit. Note that if the metric inputs to a cell are equal, both path register outputs are OR-gated; a logic ONE at either produces a ONE at the output, an acceptable situation since either choice of path is equally good in such a case.

5.2.2.3.6 Synchronization

The input to the decoder consists of a succession of soft decision A/D outputs following the integrate-and-dump circuit of the quantization unit. The soft decisions are processed in pairs, each pair corresponding to the pair of coded bits generated by the encoder each time a new data bit is generated.

Computer simulation shows that the metric corresponding to the most likely path increases in magnitude considerably faster when out of synchronization than when properly synchronized. Therefore, resetting of the most significant bit of all metrics (which occurs at times determined by the smallest metric, which is by definition that corresponding to the most likely path) occurs more frequently in the out-of-synchronization condition.

5.2.2.3.7 Phase Slips

As seen in Section 5.2.1.4.2 a phase reversal can cause node synchronization difficulty; the decoder must monitor the metrics to recoginize a two-correct-out-of-four condition. Table 5-4 summarizes this. The metric resets provide the clue to any difficulty.

TABLE 5-4

SYNCHRONIZATION AND PHASE REFERENCE MODES

SYNC	PHASE SLIP	CORRECT/INCORRECT
in	0 radians	correct
out	0 radians	incorrect
in	π radians	correct
out	π radians	incorrect

5.3 THE DESIGN OF A HIGH INDEX FM SYSTEM

The design of a high index wideband FM system for the rejection of multipath and RFI is detailed in this section. The design and the performance evaluation are based primarily on a research conducted by ADCOM under NASA contract NAS5-20225 (Reference 35).

The ADCOM wideband FM system was designed to interface with the Tracking and Data Relay Satellite System. As such, it was designed to handle data rates in the forward and return links typical of the TDRS system.

The ADCOM design was chosen for this study since it has been well documented. We do not claim that the ADCOM design is an optimum FM system; but in order to achieve optimality, a departure from a conventional approach is required and the design will actually be in the category of chirp or M-ary frequency agile systems. It was concluded then that the ADCOM design represents a good example of a conventional FM approach.

The wideband FM multiple access system designed by ADCOM was intended to provide:

- command data to the user spacecraft via the TDRS
- telemetry data from the user through the TDRS to the ground station
- multiple access capability so that any one or of several TDRS satellites could access a particular user
- multiple access for the return link so that all users in view of a TDRS could utilize the TDRS as a repeater
- two-way range and range rate measurements
- resistance to RFI and multipath
- resistance to interference from other user's signals

The wideband FM system which is discussed here will follow closely the designs advocated by ADCOM. The above requirements have been modified, however, to reflect current Shuttle requirements. For example, we do not anticipate a multiple access requirement for Space Shuttle on the return link; that is, Space Shuttle will be serviced separately, either at VHF/UHF or at S-band. Therefore the wideband FM system will be evaluated in the forward link against multipath, noise and RFI. In the return link the interference is a single multipath signal, RFI and noise.

The basic signal format for the wideband FM system is as follows:

a) ranging information is carried in a cluster of range tones designed to yield the desired range measurement accuracy and ambiguity resolution

b) data, that is for commands on the uplink and telemetry on the downlink is carried in a split phase format which, along with the ranging tones, phase modulates the carrier

c) spectrum spreading is accomplished by frequency modulating the UHF carrier in the forward link and VHF or S-band carrier in the return link by a sinusoidal subcarrier using a wide frequency deviation, e.g., mod index 5.52.

The system configuration is illustrated in Figure 5-20. Commands are sent from the ground station through the relay satellite to the user, and the signal is coherently transponded back to the ground station via the relay satellite. Both command data and telemetry data are inserted at the ground station and user spacecraft respectively. The UHF signal from the relay satellite to the user, e.g. Space Shuttle or aircraft, is described as follows: first, command data in the form of split phase binary signals is used to modulate the carrier. In addition to the split phase command data, ranging tones also phase modulate the carrier. This composite signal is then wideband frequency modulated by a sinusoidal subcarrier with a modulation index of 5.52.* The frequency relationship of the ranging tones is illustrated in Figure 5-21. The tone ranging signals are generated as:

$$\phi_R(t) = \rho_1 \sin \omega_1 t + [\rho_2 + 2\rho_A(\sin \omega_3 t + \sin \omega_4 t)] \cos(\omega_1 - \omega_2)t \quad (5\text{-}10)$$

with

$$\rho_1 = 0.5$$
$$\rho_2 = 0.48$$
$$\rho_A = 0.375.$$

The circuitry required to generate the ranging tones is shown in Figure 5-22. The composite VHF uplink signals can be written as

$$e_{up}(t) = \sin [2\pi f_o t + \delta \sin \omega_{sc} t + \phi_R(t) + \phi_D(t)] \quad (5\text{-}11)$$

where f_o = 401 MHz and $\delta \sin \omega_{sc} t$ is the wideband FM subcarrier.

---

*This modulation index was chosen as near optimum for the TDRS channel.

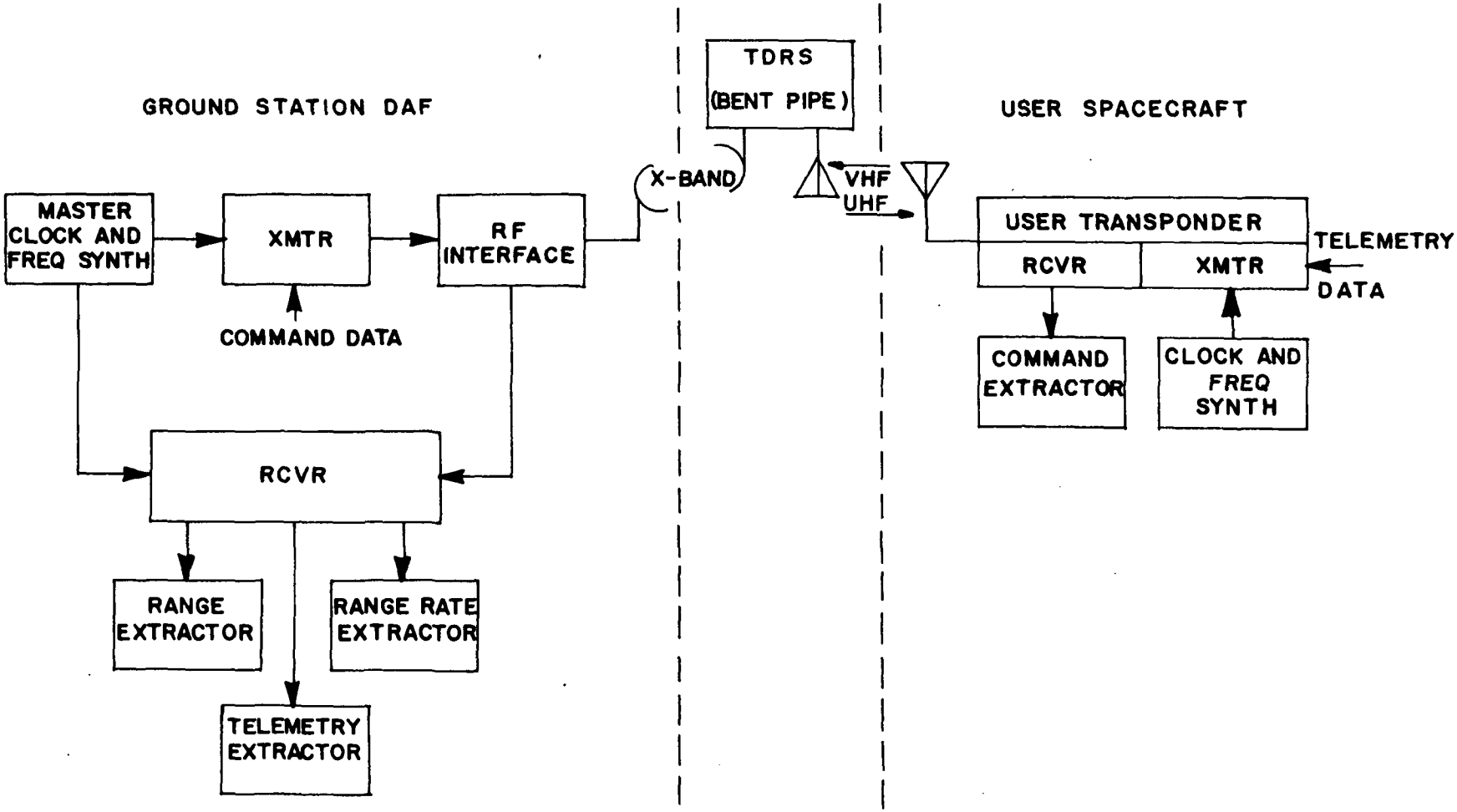

FIGURE 5-20 SYSTEM CONFIGURATION, SINGLE USER AND SINGLE TDRS

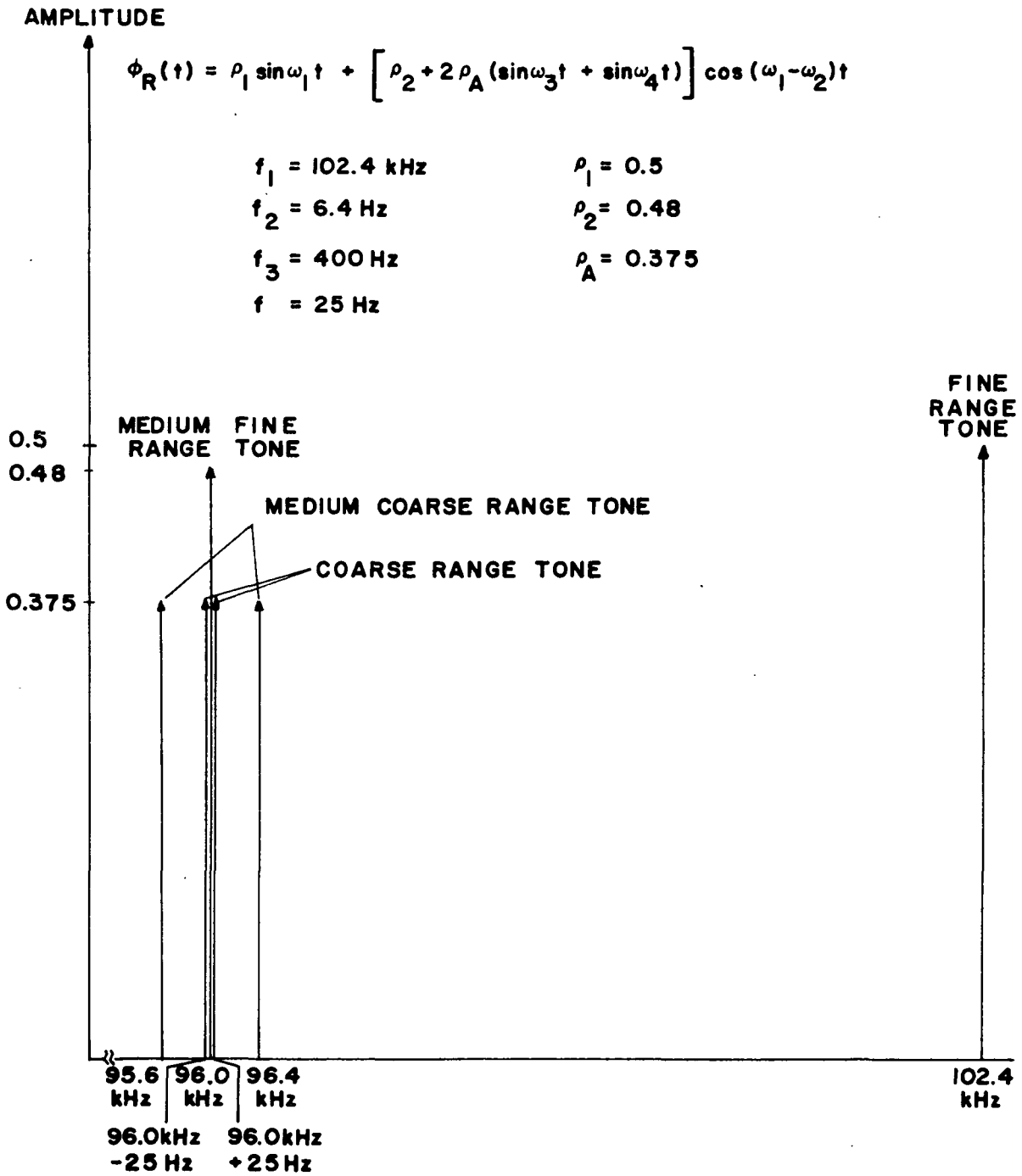

FIGURE 5-21 RANGING SIDETONE SIGNAL STRUCTURE

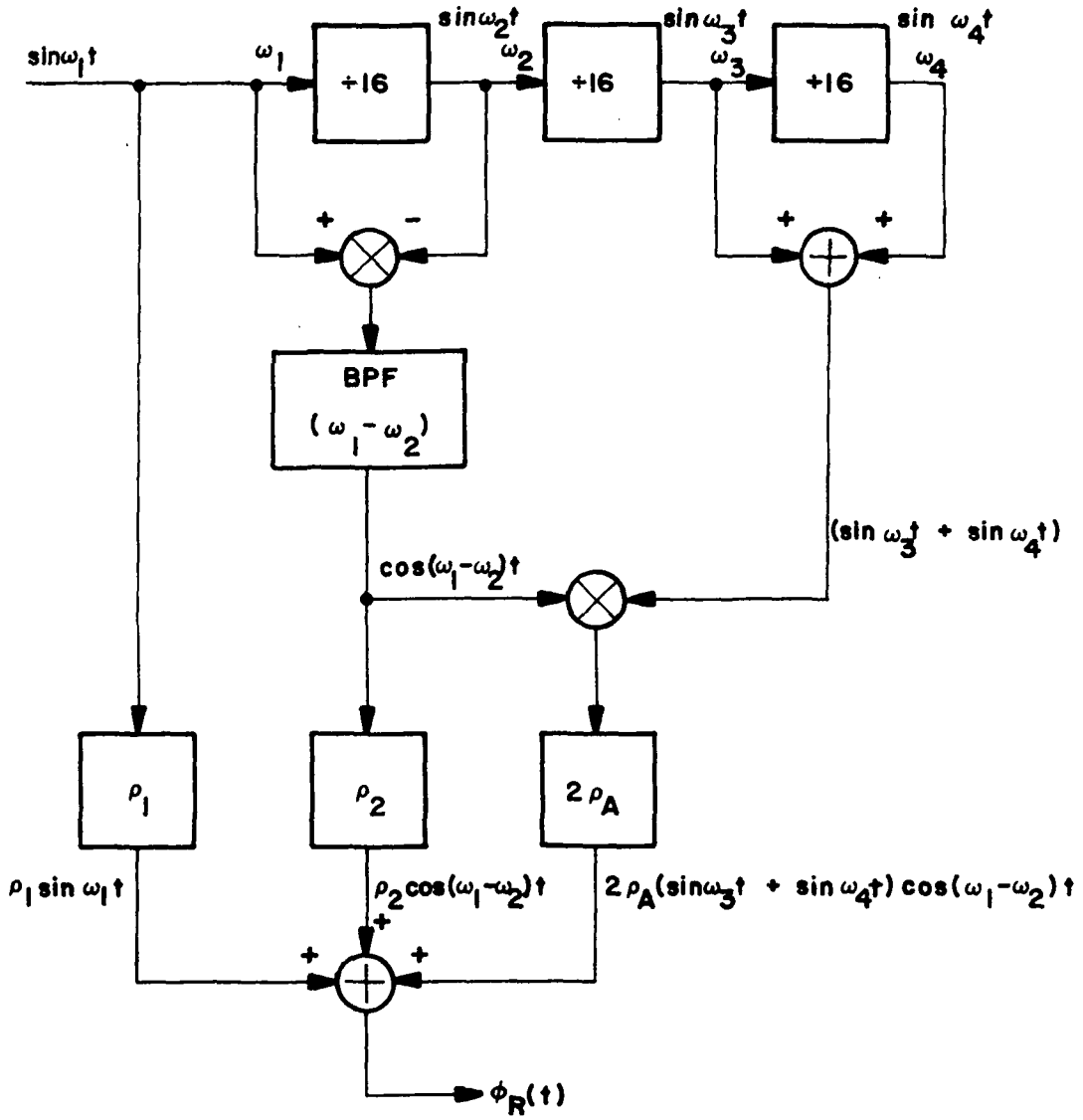

FIGURE 5-22 RANGING SIDETONE SIGNAL GENERATOR

The distribution of the sideband power in the wideband FM signal is illustrated in Figure 5-23 for a modulation index δ = 5.52 radians.

The ground station UHF transmitter is illustrated in Figure 5-24 for a forward link frequency of 401 MHz. A similar implementation would exist for S-band. The component labeled "coherent wideband FM modulator" has been broken down in more detail in Figure 5-25. The basic source at frequency f_o and the subcarrier are coherently locked together as illustrated in Figure 5-26. The choice of the subcarrier for the wideband FM deviation is somewhat arbitrary but a value of 112 kHz is typical.

The user transponder must first acquire the wideband FM signal, coherently track the carrier, and properly demodulate the data. It must also provide for turning around the ranging tones, generating the downlink subcarrier frequency, and coherently generating the downlink carrier. In addition to these functions it must be capable of phase modulating telemetry data and ranging tone on the newly created downlink carrier, and also be capable of providing wideband FM deviation for the downlink carrier.

A functional block diagram of the user transponder is illustrated in Figure 5-27. The user transponder consists of the compound phase lock loop comprised of a carrier tracking phase lock loop and a subcarrier tracking feedback phase lock loop, a wideband FM reference signal generator, and a carrier phase demodulator. The output from the subcarrier loop is used to modulate the carrier loop VCO to permit compression of the wideband FM spectrum. This is illustrated in more detail in Figure 5-27. The loop gain is adjusted to full compression with a modulation index set at 5.52. The basic idea is to provide a compressive FM feedback so as to optimize the operation in the presence of noise and interference. The compression occurs

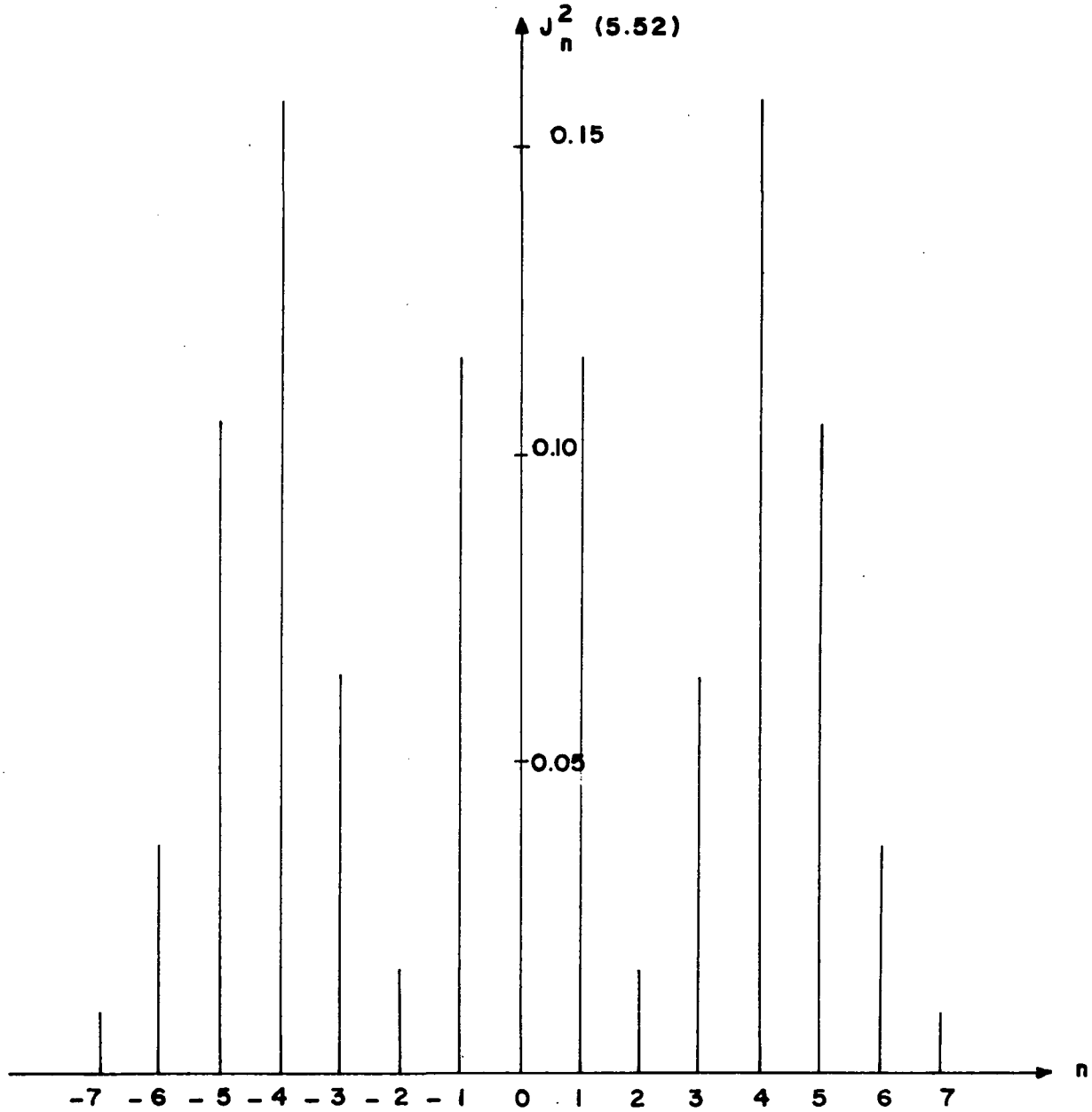

FIGURE 5-23 DISTRIBUTION OF WIDEBAND FM SIGNAL POWER IN VARIOUS SUBCARRIER SIDEBANDS FOR $\delta = 5.52$

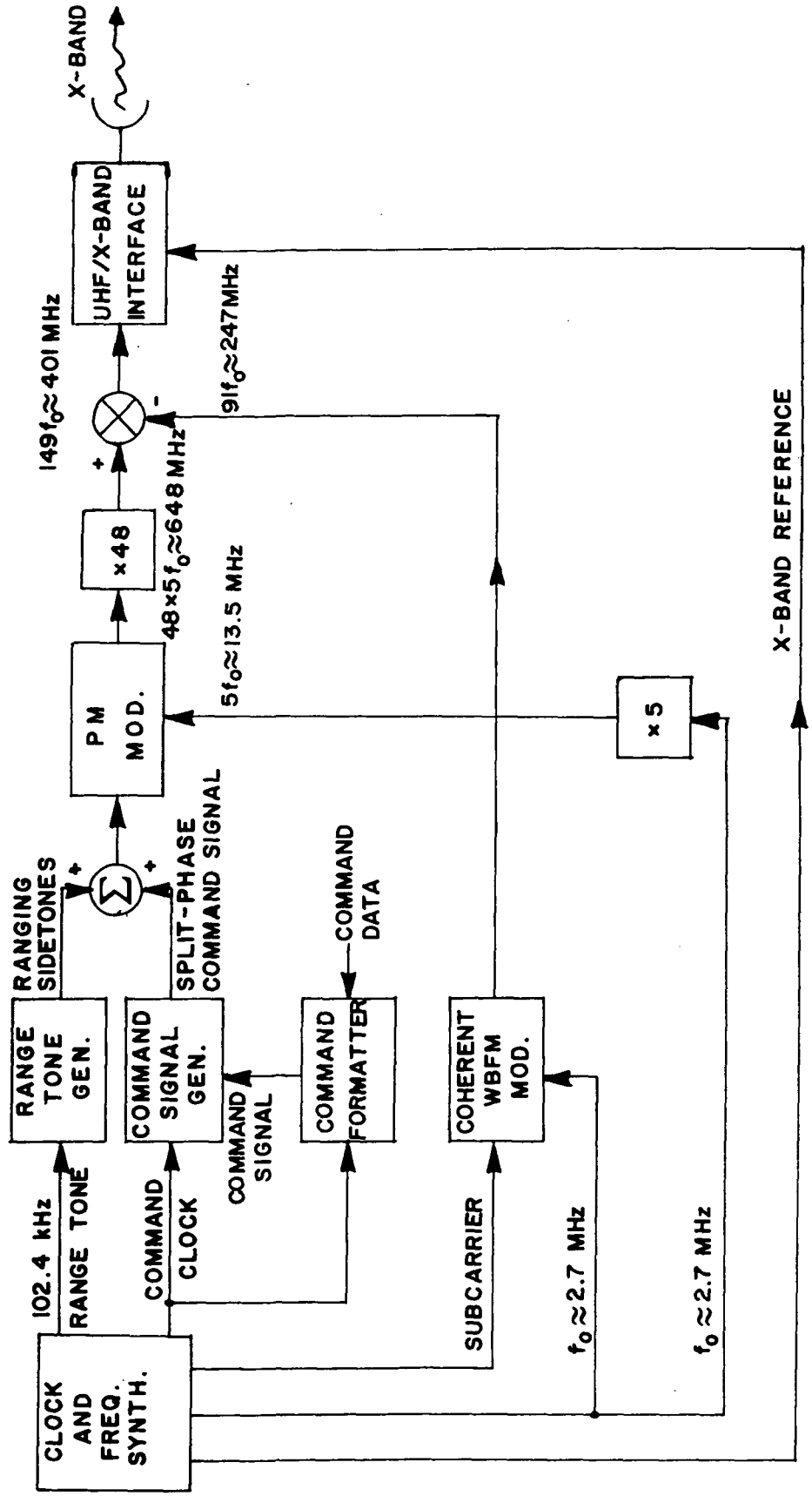

FIGURE 5-24 DAF TRANSMITTER

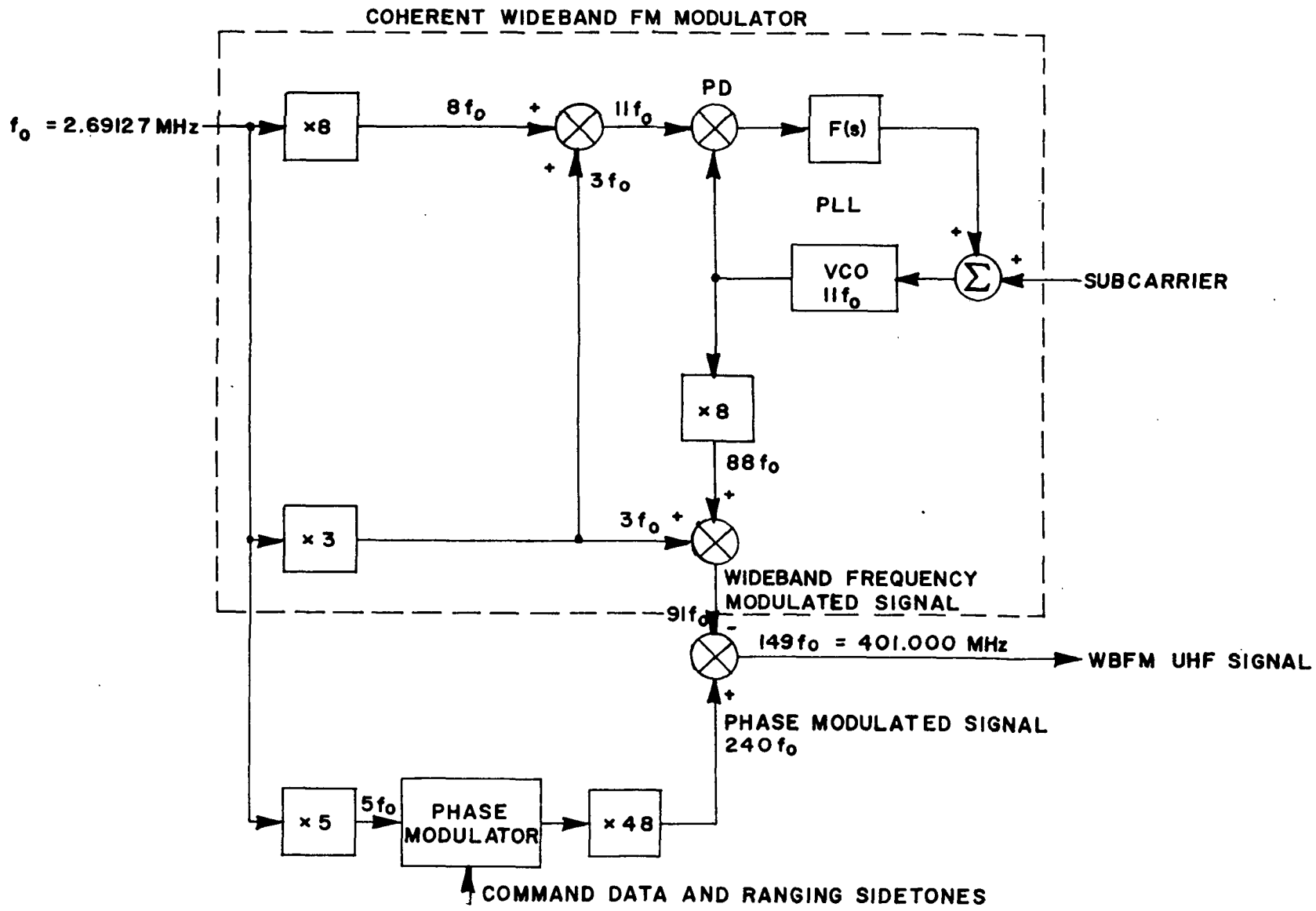

FIGURE 5-25 DAF UHF SIGNAL GENERATOR

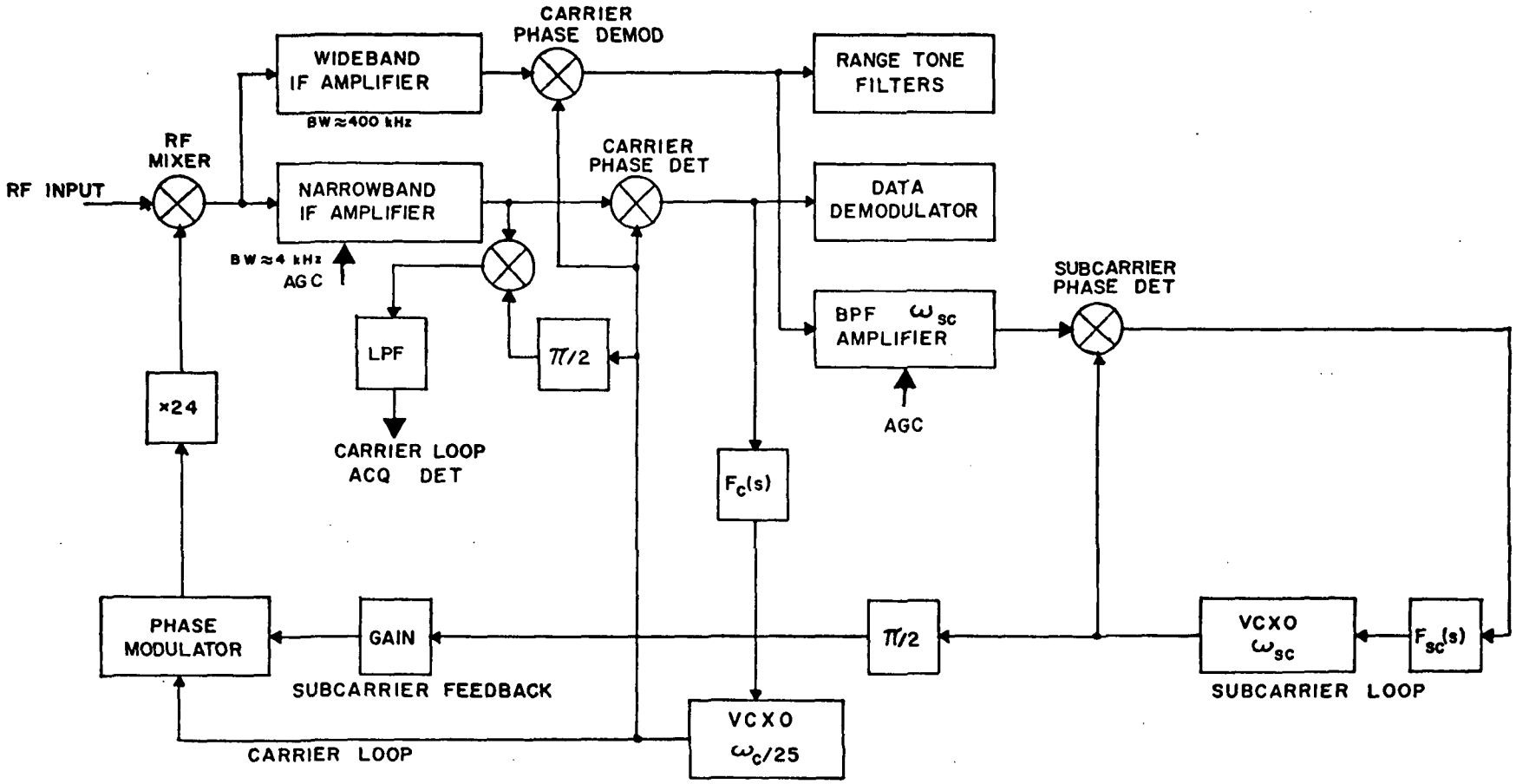

FIGURE 5-26 BLOCK DIAGRAM OF TRACKING PORTION OF WIDEBAND FM COMPOUND PLL

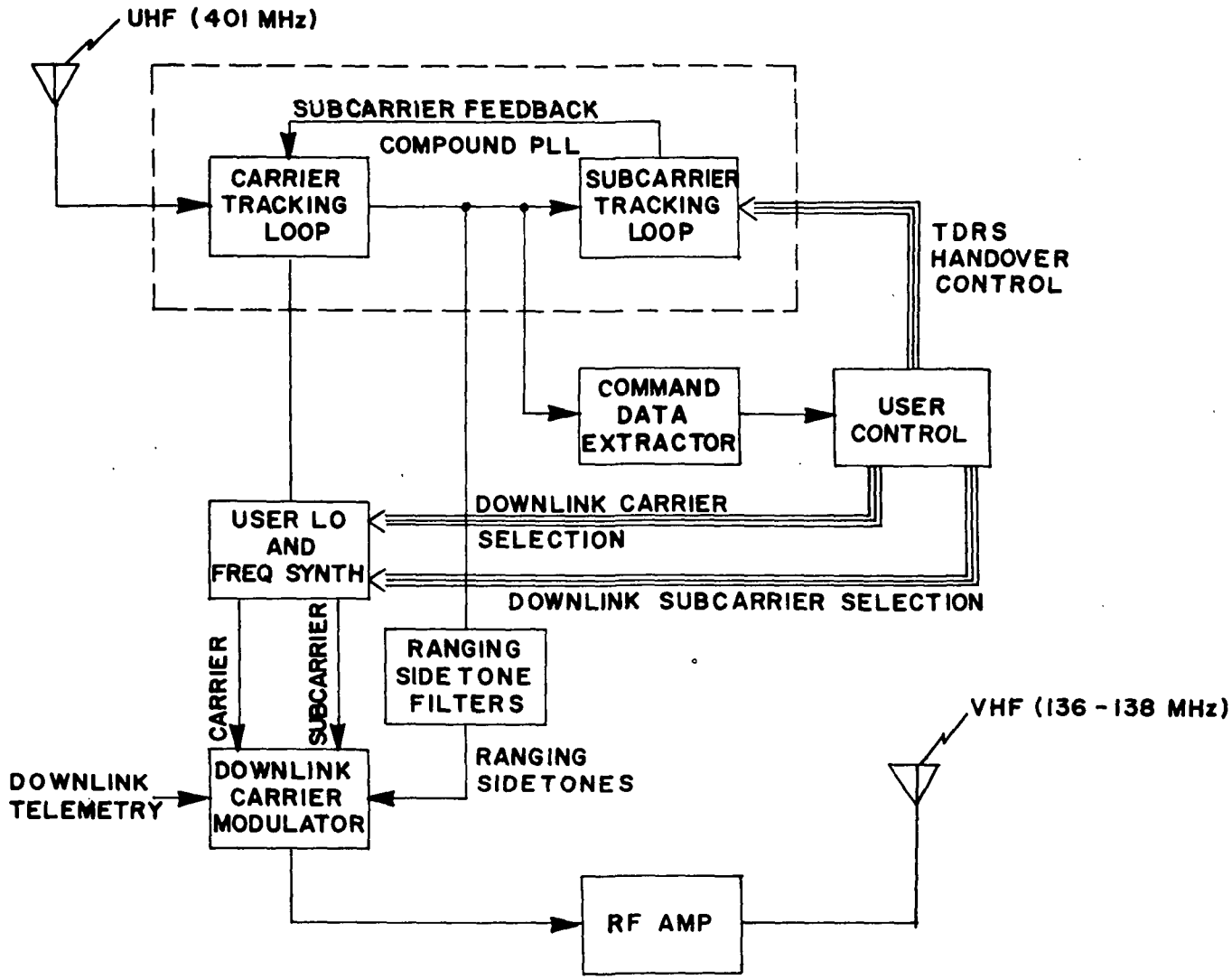

FIGURE 5-27 USER TRANSPONDER FUNCTIONAL BLOCK DIAGRAM

at the first RF mixer and the narrowband frequency compressed carrier is passed through a bandpass filter approximately 4 kHz in bandwidth. In addition to the narrowband IF filter, a wideband IF filter is used to pass the ranging sidetones and the first order subcarrier sidebands. Once the carrier is coherently demodulated by the carrier phase reference demodulator, narrowband filtering is provided for the extraction of the range tones. The coarse and the medium range tones are filtered through a 1 to 2 kHz bandpass filter centered at 96 kHz, and the fine range tone is filtered via a narrow filter centered at 102.4 kHz. The filtered tones are then combined and used to phase modulate the downlink carrier.

Likewise the data is extracted from the output of the narrowband IF filters. Crucial to the performance of this system is the acquisition in the forward link. A block diagram of the forward link proposed acquisition method is illustrated in Figure 5-28. The acquisition scheme is as follows.

1) With the carrier and subcarrier loops unlocked, the carrier loop VCXO is swept until the error frequency is less than about 200 Hz. This is the coarse frequency search.

2) The carrier loop sweep generator continues to sweep in the same direction for a short time and is then switched to its fine frequency search mode in which the sweep is reversed and swept slowly until the error frequency is less than about 20 Hz.

3) At this time the carrier loop is switched from the sweep mode to the acquisition mode, and the carrier loop error frequency is forced to zero.

4) Meanwhile, the subcarrier loop, which is in the acquisition mode, acquires frequency lock.

5) As the carrier loop error frequency goes to zero, the phasing error on the subcarrier signal into the subcarrier acquisition becomes negligibly

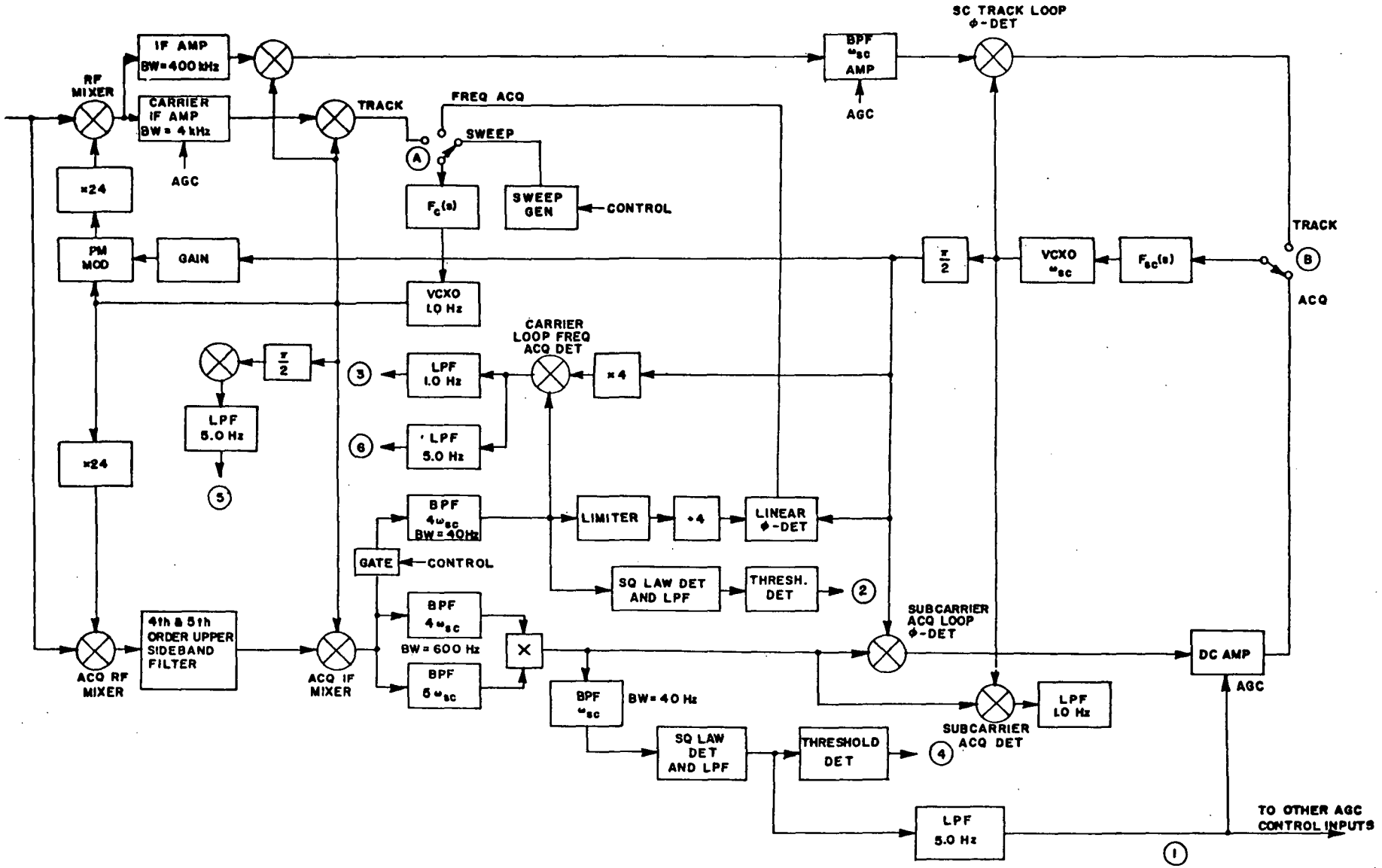

FIGURE 5-28 UPLINK ACQUISITION SCHEME

small, thereby enabling the subcarrier loop VCXO to acquire the proper phase for wideband FM compression.

6) With the subcarrier loop properly phased and the carrier loop frequency acquired, the carrier loop is switched to the track mode.

7) Meanwhile, the gain of the carrier loop IF amplifier is adjusted by an AGC signal derived from the acquisition subcarrier signal so that when the carrier loop is switched to the track mode, its loop noise bandwidth is already set at the proper value. This not only saves acquisition time, but also helps prevent the carrier loop from locking onto a CW RFI component that may be close to one of the subcarrier sidebands but which lies further away from the sideband than several times the carrier loop noise bandwidth. The carrier loop new now only acquire phase lock. The gain of the subcarrier tracking loop is adjusted in a similar fashion.

8) Phase lock is detected by a coherent carrier loop lock indicator, and is verified by checking to see that the upper 4th order subcarrier sideband lies where it should. This permits detection of false lock by the carrier loop on a CW RFI component that may fall within the carrier loop noise bandwidth but which may lie more than a few Hertz away from the particular subcarrier sideband with which it interferes.

9) Finally, when proper carrier lock is verified, the subcarrier loop may be switched to the track mode.

10) The in-lock condition is constantly monitored, so that if the carrier or subcarrier tracking loop falls out of lock, a reacquisition procedure may be initiated. In particular, the subcarrier loop would be immediately switched to the acquisition mode, since, if the carrier loop VCO has not drifted too far in frequency from the frequency of the input carrier, subcarrier loop acquisition could take place rather quickly, and the carrier loop could reacquire without having to switch out of the track mode. Consequently, reacquisition could take place in one or two seconds if the in-lock condition is constantly monitored. This is important since it means that the communications link would only be out of service for a short time should loss of lock occur.

Implementation of the user transmitter is very similar to that of the ground station transmitter except that the return link carrier frequency is coherently synthesized from the forward link carrier frequency and the range tones are filtered and turned around in the transponder and applied to the phase modulator.

5.4 PSEUDONOISE MODEM DESIGN

The pseudonoise modem selected for use with the SATS is designed to operate at data rates of 2, 6, and 24 kb/s with a PN chip rate of 1150 kchips/sec. Schematics of the PN modem design are presented in Appendix B.

The transmitter consists of three boards, namely: the Coder (Board 1A3), Frequency Synthesizer (Board 1A2) and the Data Processor (Board 1A1). The block diagrams in Appendix B show the fundamental implementation. The transmitter unit can be packaged in a 20.3 cm x 22.9 cm x 30.4 cm (8 in x 9 in x 12 in) chassis.

The Receiver consists of six boards, namely

1) Data Processing and error detection (2A1)
2) RF Frequency Synthesizer (2A2)
3) 13 Stage PN Coder (2A3)
4) Code Clock Synthesizer (2A4)
5) Costas Loop and Synchronization Circuit (2A5)
6) 70 MHz IF Amplifier (2A6)

The unit can be packaged in a unit similar to that used for the transmitter. The receiver has a long loop for coherent PSK demodulation and a τ-jitter loop for code clock tracking. The coder's all-ones vector is used for data clock (2, 6, and 24 kb/s) phasing in the PN mode, and code synchronization by sequential decision method.

6. EFFECTS OF MULTIPATH AND RFI ON PSK, PN, AND WIDEBAND FM SYSTEMS

In this section we evaluate the clear mode PSK, the wideband FM, and the PN systems in the presence of multipath and RFI. Aspects of the evaluation include data, range, and range rate performances.

6.1 CLEAR MODE ΔPSK ANALYSIS

This analysis considers the combined effects of specular and diffuse multipath and ever present Gaussian noise on the performance of a ΔPSK transmission.

6.1.1 EFFECTS OF MULTIPATH ON ΔPSK

It has been shown* that the conditional bit error probability for a coherent reference PSK transmission can be expressed as:

$$P_\varepsilon(F,\eta) = \frac{1}{2}\,\text{erfc}\,\sqrt{E/N_o}\,(1 + F\cos\eta) \qquad (6\text{-}1)$$

where

$$F = \sqrt{\frac{P_{ind}}{P_{dir}}}\left|\frac{\sin\frac{\Delta\omega T}{2}}{\frac{\Delta\omega T}{2}}\right|$$

$\Delta\omega$ = differential Doppler

η is a random phase angle uniformly distributed over $[-\pi,\pi]$.

The value of F in the above equation represents the instantaneous ratio of the multipath signal to the desired signal. In practice the multipath signal can consist of a specular component, which is essentially a delayed replica of the direct path signal, and a diffuse component which occupies a bandwidth equal to the fading bandwidth plus the original data bandwidth. The envelope statistics associated with the indirect signal should follow a Rician proba-

---

* Appendix I of Reference 2.

bility density. Thus we argue that F itself will follow a Rician density which is normalized to the power in the direct path. The average bit error probability using equation 6-1 can be calculated to be:

$$\overline{P}_\varepsilon = \int_0^\infty \left[\frac{1}{\pi} \int_0^\pi P_\varepsilon(F,\eta) d\eta \right] P(F) dF \qquad (6\text{-}2)$$

Equation 6-2 can be simplified by considering the diffuse component as Gaussian noise and by considering the specular component as narrowband constant envelope interference; that is, we assume that these components are separable. Under the validity of such assumptions we may restate the above average bit error probability in the following terms:

$$\overline{P}_\varepsilon = \frac{1}{\pi} \int_0^\infty \frac{1}{2} \operatorname{erfc} \left[\sqrt{\frac{P_{dir}}{N_g + P_{diff}}} \left(1 + \sqrt{\frac{P_{spec}}{P_{dir}}} \cos \eta \right) \right] d\eta \qquad (6\text{-}3)$$

where P_{dir} = direct power

P_{spec} = specular power

P_{diff} = diffuse power

N_g = Gaussian Noise power density.

We have considered the diffuse component as noise and the specular component as constant envelope interference with a uniform random phase angle.

The results of equation 6-3 have been obtained by a computer and are included as Table 6-1. In this table K2 is defined as $P_{direct}/(P_{specular} + P_{diffuse})$. Note that the effects of differential Doppler between the direct and the indirect paths have been embedded in the value of F. Furthermore, the frequency weighting effects of the integrate and dump circuit have not been utilized in calculating the noise power due to the diffuse component; thus the results obtained from equation 6-3 can be considered worst case, e.g. when

TABLE 6-1

PROBABILITY OF BIT ERROR FOR PSK IN PRESENCE OF MULTIPATH

K2=	1
SPEC/DIFF=	0
PE	S/N
.160362	1
.125433	2
.104049	4
9.21817 E-2	8
8.59379 E-2	16
8.27378 E-2	32
8.11183 E-2	64
8.03037 E-2	128
SPEC/DIFF=	.25
PE	S/N
.160841	1
.126103	2
.104807	4
9.29558 E-2	8
8.67029 E-2	16
8.34918 E-2	32
8.18649 E-2	64
8.10461 E-2	128
SPEC/DIFF=	.666667
PE	S/N
.162082	1
.127836	2
.106666	4
9.47038 E-2	8
8.82997 E-2	16
8.49777 E-2	32
8.32844 E-2	64
8.24294 E-2	128
SPEC/DIFF=	1.5
PE	S/N
.164237	1
.130763	2
.109499	4
9.69318 E-2	8
8.99247 E-2	16
8.61886 E-2	32
8.42536 E-2	64
8.32681 E-2	128
SPEC/DIFF	4.
PE	S/N
.167483	1
.134974	2
.112933	4
9.85627 E-2	8
8.98025 E-2	16
8.48247 E-2	32
8.21434 E-2	64
8.07473 E-2	128
SPEC/DIFF=	1073741823
PE	S/N
.160916	1
.129523	2
.105562	4
8.63878 E-2	8
7.07379 E-2	16
5.78294 E-2	32
4.71138 E-2	64
UNDERFLOW IN	601
3.81821 E-2	128

K2=	2
SPEC/DIFF=	0
PE	S/N
.125433	1
7.94859 E-2	2
5.17826 E-2	4
3.72165 E-2	8
2.99965 E-2	16
2.64596 E-2	32
2.47191 E-2	64
2.38573 E-2	128
SPEC/DIFF=	.25
PE	S/N
.125645	1
7.97384 E-2	2
5.19484 E-2	4
3.72322 E-2	8
.029885	16
2.62672 E-2	32
2.44815 E-2	64
2.35958 E-2	128
SPEC/DIFF=	.666667
PE	S/N
.126103	1
8.02236 E-2	2
5.20191 E-2	4
3.66864 E-2	8
.028842	16
2.49186 E-2	32
.022966	64
2.19936 E-2	128
SPEC/DIFF=	1.5
PE	S/N
.126827	1
8.08732 E-2	2
5.16366 E-2	4
3.48683 E-2	8
2.59162 E-2	16
2.13418 E-2	32
1.90469 E-2	64
1.79011 E-2	128
SPEC/DIFF=	4.
PE	S/N
.127836	1
8.15688 E-2	2
5.02333 E-2	4
3.06271 E-2	8
1.95497 E-2	16
1.38201 E-2	32
1.09839 E-2	64
9.59318 E-3	128
SPEC/DIFF=	1073741823
PE	S/N
.129144	1
8.21254E-2	2
4.68614 E-2	4
2.16161 E-2	8
6.72768 E-3	16
1.00304 E-3	32
UNDERFLOW IN	601
3.64049 E-5	64
UNDERFLOW IN	601

Note: $K2 = P_{direct}/(P_{specular} + P_{diffuse})$

TABLE 6-1 (Cont.)

PROBABILITY OF BIT ERROR FOR PSK IN PRESENCE OF MULTIPATH

K2=	4
SPEC/DIFF=	0
PE	S/N
.104049	1
5.17826 E-2	2
2.30016 E-2	4
1.05831 E-2	8
5.77662 E-3	16
3.87969 E-3	32
.003075	64
2.71011 E-3	128
SPEC/DIFF=	.25
PE	S/N
.104136	1
5.18611 E-2	2
2.29756 E-2	4
1.04341 E-2	8
5.56084 E-3	16
3.64142 E-3	32
2.29756 E-3	64
2.46584 E-3	128
SPEC/DIFF=	.666667
PE	S/N
.104291 E-2	1
5.19484 E-2	2
2.27155 E-2	4
9.81307 E-3	8
4.79670 E-3	16
2.86996 E-3	32
2.08424 E-3	64
1.73931 E-3	128
SPEC/DIFF=	1.5
PE	S/N
.104514	1
5.20141 E-2	2
2.21094 E-2	4
8.60223 E-3	8
3.48003 E-3	16
1.68286 E-3	32
1.02819 E-3	64
7.66035 E-4	128
SPEC/DIFF=	4.
PE	S/N
.104807	1
5.20191 E-2	2
2.10246 E-2	4
6.72169 E-2	8
1.78659 E-3	16
4.79340 E-4	32
1.63245 E-4	64
7.80157 E-5	128
SPEC/DIFF=	1073741823
PE	S/N
.105169	1
.051914	2
1.93043 E-2	4
4.19845 E-3	8
3.22473 E-4	16
3.24875 E-6	32
5.89810 E-10	64
UNDERFLOW IN 601	
3.58368 E-17	128

K2=	8
SPEC/DIFF=	0
PE	S/N
9.21817 E-2	1
3.72165 E-2	2
1.05831 E-2	4
2.37056 E-3	8
5.54043 E-4	16
1.76392 E-4	32
8.27755 E-5	64
5.31459 E-5	128
SPEC/DIFF=	.25
PE	S/N
9.22192 E-2	1
3.72449 E-2	2
1.05596 E-2	4
2.31393 E-3	8
5.07753 E-4	16
1.46857 E-4	32
6.28050 E-5	64
3.77107 E-5	128
SPEC/DIFF=	.666667
PE	S/N
9.22738 E-2	1
3.72615 E-2	2
1.04341 E-2	4
2.12714 E-3	8
3.85616 E-4	16
8.41449 E-5	32
2.73939 E-5	64
1.34774 E-5	128
SPEC/DIFF=	1.5
PE	S/N
9.23455 E-2	1
3.72597 E-2	2
1.01905 E-2	4
1.82306 E-3	8
2.32045 E-4	16
2.86446 E-5	32
5.04403 E-6	64
1.51917 E-6	128
SPEC/DIFF=	4.
PE	S/N
9.24342 E-2	1
3.72322 E-2	2
9.81307 E-3	4
1.42735 E-3	8
9.64957 E-5	16
3.34865 E-6	32
1.02192 E-7	64
9.43950 E-9	128
SPEC/DIFF=	1073741823
PE	S/N
9.25398 E-2	1
.037171	2
9.28771 E-3	4
9.81677 E-4	8
1.90005 E-5	16
1.27600 E-8	32
1.06338 E-14	64
1.38477 E-26	128

TABLE 6-1 (Cont.)

PROBABILITY OF BIT ERROR FOR PSK IN PRESENCE OF MULTIPATH

K2=	16
SPEC/DIFF=	0
PE	S/N
8.59379 E-2	1
2.99965 E-2	2
5.77662 E-3	4
5.54043 E-4	8
3.23324 E-5	16
1.98018 E-6	32
2.16365 E-7	64
4.97987 E-8	128
SPEC/DIFF=	.25
PE	S/N
8.59549 E-2	1
3.00097 E-2	2
5.77015 E-3	4
5.42781 E-4	8
2.88794 E-5	16
1.41729 E-6	32
1.14323 E-7	64
1.99554 E-8	128
SPEC/DIFF=	.666667
PE	S/N
8.59762 E-2	1
3.00174 E-2	2
5.73305 E-3	4
5.07753 E-4	8
2.10232 E-5	16
5.90709 E-7	32
2.24036 E-8	64
1.93714 E-9	128
SPEC/DIFF=	1.5
PE	S/N
8.60018 E-2	1
3.00185 E-2	2
5.66372 E-3	4
4.53595 E-4	8
1.24960 E-5	16
1.34123 E-7	32
1.16581 E-9	64
2.11989 E-11	128
SPEC DIFF=	4.
PE	S/N
8.60315 E-2	1
.030012	2
5.56084 E-3	4
3.85616 E-4	8
5.77027 E-6	16
1.13311 E-8	32
3.58344 E-12	64
7.00000 E-16	128
SPEC/DIFF=	1073741823
PE	S/N
8.60655 E-2	1
2.99966 E-2	2
5.42329 E-3	4
3.09685 E-4	8
1.84541 E-6	16
1.21160 E-10	32
9.81373 E-19	64
UNDERFLOW IN 601	
1.21685 E-34	128

K2=	32
SPEC/DIFF=	0
PE	S/N
8.27378 E-2	1
2.64596 E-2	2
3.87969 E-3	4
1.76392 E-4	8
1.98018 E-6	16
7.98724 E-9	32
3.39239 E-11	64
4.38747 E-13	128
SPEC/DIFF=	.25
PE	S/N
8.27459 E-2	1
2.64663 E-2	2
3.87903 E-3	4
1.74537 E-4	8
1.80870 E-6	16
5.34239 E-9	32
1.17985 E-11	64
6.67345 E-14	128
SPEC/DIFF=	.666667
PE	S/N
.082755	1
2.64713 E-2	2
3.87025 E-3	4
1.68537 E-4	8
1.41729 E-6	16
2.06165 E-9	32
1.11254 E-12	64
1.02378 E-15	128
SPEC/DIFF=	1.5
PE	S/N
8.27653 E-2	1
2.64744 E-2	2
3.85322 E-3	4
1.59078 E-4	8
9.76453 E-7	16
4.88669 E-10	32
2.52639 E-14	64
7.04302 E-19	128
SPEC/DIFF=	4.
PE	S/N
8.27765 E-2	1
2.64755 E-2	2
3.82784 E-3	4
1.46857 E-4	8
5.90709 E-7	16
6.24733 E-11	32
5.20284 E-17	64
5.27819 E-25	128
SPEC/DIFF=	1073741823
PE	S/N
8.27888 E-2	1
2.64743 E-2	2
3.79401 E-3	4
1.32574 E-4	8
3.08273 E-7	16
3.17529 E-12	32
6.41234 E-22	64
UNDERFLOW IN 601	

TABLE 6-1 (Cont.)

PROBABILITY OF BIT ERROR FOR PSK IN PRESENCE OF MULTIPATH

K2=	64
SPEC/DIFF=	0
PE	S/N
8.11183 E-2	1
2.47191 E-2	2
.003075	4
8.27755 E-5	8
2.16365 E-7	16
3.39239 E-11	32
6.59984 E-16	64
1.35334 E-20	128
SPEC/DIFF=	.25
PE	S/N
8.11222 E-2	1
2.47226 E-2	2
3.07544 E-3	4
8.24754 E-5	8
2.06198 E-7	16
2.45849 E-11	32
1.93540 E-16	64
7.20916 E-22	128
SPEC/DIFF=	.666667
PE	S/N
8.11264 E-2	1
2.47256 E-2	2
3.07381 E-3	4
8.13792 E-5	8
1.80607 E-7	16
1.17985 E-11	32
1.60155 E-17	64
2.26380 E-24	128
SPEC/DIFF=	1.5
PE	S/N
8.11309 E-2	1
2.47281 E-2	2
3.07011 E-3	4
7.95727 E-5	8
1.48002 E-7	16
4.20541 E-12	32
4.53054 E-19	64
3.02472 E-28	128
SPEC/DIFF=	4.
PE	S/N
8.11356 E-2	1
.02473	2
3.06432 E-3	4
7.71405 E-5	8
1.14323 E-7	16
1.11254 E-12	32
3.12827 E-21	64
1.68830 E-34	128
SPEC/DIFF=	1073741823
PE	S/N
8.11406 E-2	1
2.47315 E-2	2
3.05643 E-3	4
7.41664 E-5	8
8.34165 E-8	16
2.08315 E-13	32
2.50946 E-24	64
6.96880 E-46	128

K2=	128
SPEC/DIFF=	0
PE	S/N
8.03037 E-2	1
2.38573 E-2	2
2.71011 E-3	4
5.31459 E-5	8
4.97987 E-8	16
4.38747 E-13	32
1.35334 E-20	64
6.13867 E-30	128
SPEC/DIFF=	.25
PE	S/N
8.03037 E-2	1
.023859	2
2.71054 E-3	4
5.31029 E-5	8
4.88931 E-8	16
3.66938 E-13	32
5.00824 E-21	64
2.18830 E-31	128
SPEC/DIFF	.666667
PE	S/N
8.03077 E-2	1
2.38607 E-2	2
2.71044 E-3	4
5.28903 E-5	8
4.63052 E-8	16
2.41279 E-13	32
7.20916 E-22	64
5.60420 E-34	128
SPEC/DIFF	1.5
PE	S/N
8.11309 E-2	1
2.38622 E-2	2
2.70982 E-3	4
5.25186 E-5	8
4.25898 E-8	16
1.35551 E-13	32
5.57262 E-23	64
1.48177 E-37	128
SPEC/DIFF=	4.
PE	S/N
8.03119 E-2	1
2.38636 E-2	2
2.70868 E-3	4
5.19981 E-5	8
3.81996 E-8	16
6.67345 E-14	32
2.26330 E-24	64
1.78446 E-42	128
SPEC/DIFF=	1073741823
PE	S/N
8.03141 E-2	1
2.38649 E-2	2
2.70702 E-3	4
5.13389 E-5	8
3.34957 E-8	16
2.89510 E-14	32
4.27210 E-26	64
1.79481 E-49	128

low differential Doppler exists and the fading bandwidth is well within the limits of the data bandwidths.

There are several conclusions which can be drawn from the above analysis:

1) Diffuse multipath creates an irreducible bit error probability at high desired signal-to-Gaussian noise ratios whereas specular multipath can be overcome by sufficiently high desired signal-to-Gaussian noise ratios.

2) At low desired signal-to-Gaussian noise ratios both specular and diffuse multipath serve to create essentially equal bit error probabilities.

The actual bit error probability for ΔPSK is $2P_\varepsilon(1-P_\varepsilon)$ where P_ε is the bit error probability associated with the PSK transmission. For bit error probabilities on the order of 0.1 and less, the above equation for the bit error probability associated with the ΔPSK system is given as $2P_\varepsilon$.

Figure 6-1 is a plot of optimum binary PSK performance vs. E/N_o and ΔPSK performance vs. E/N_o for comparison. Figure 6-2 is a plot of optimum PSK performance in the presence of specular or diffuse multipath.

Complete listings of P_ε vs. S/N for various ratios of $\frac{P_{specular}}{P_{diffuse}}$ are given in Table 6-1.

Perhaps a more valuable way of illustrating the performance of PSK (or ΔPSK) in the presence of multipath is to determine the percentage of time the bit error probability is greater than some desired value. This time is referred to as the outage time.

Shown in Figures 6-3, 6-4, 6-5, and 6-6 are outage times for ΔPSK. In these curves E_b/N_o is the usual energy per bit-to-noise density ratio and

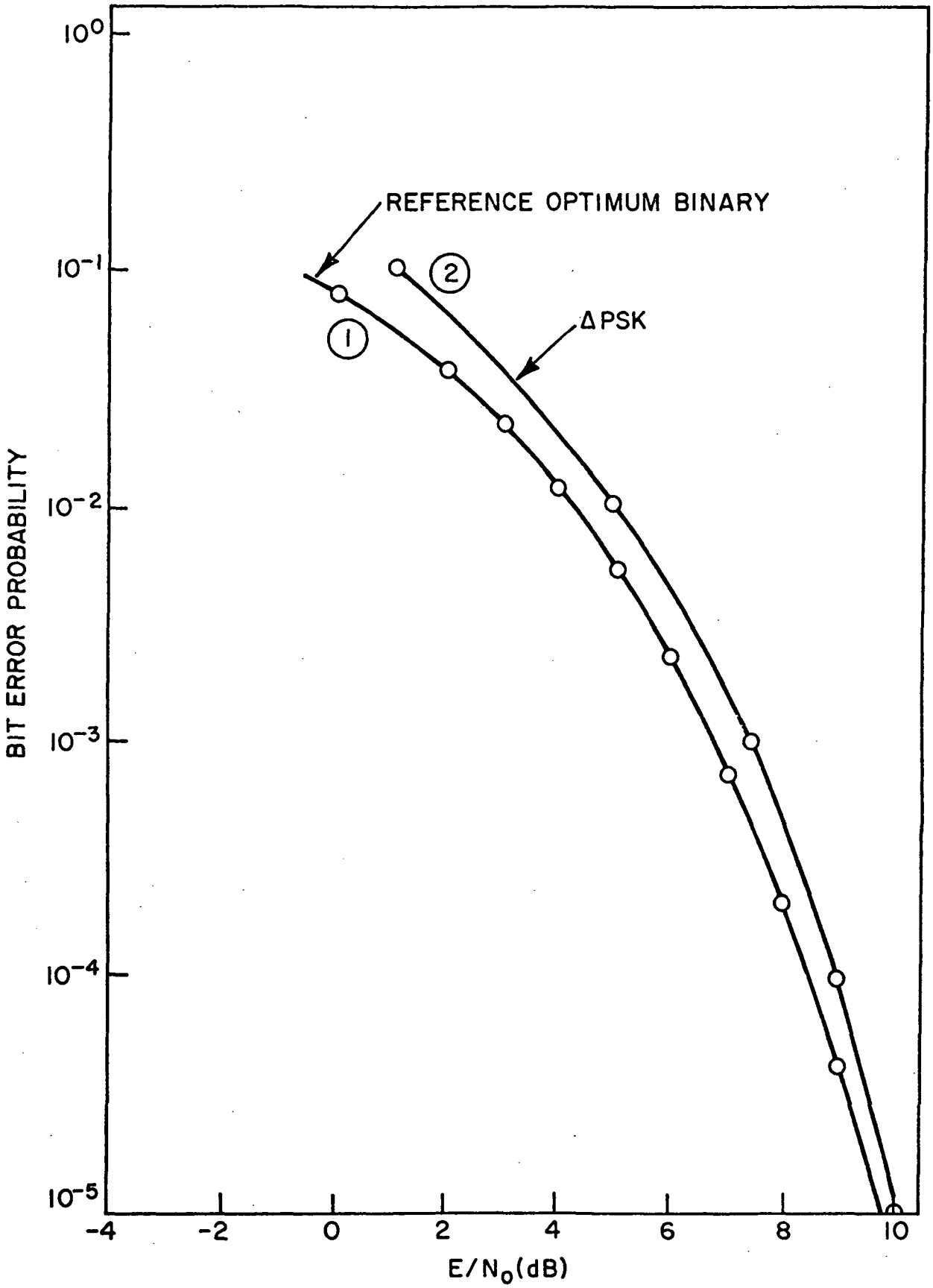

FIGURE 6-1 OPTIMUM BINARY PSK AND ΔPSK PERFORMANCE AS A FUNCTION OF E/No

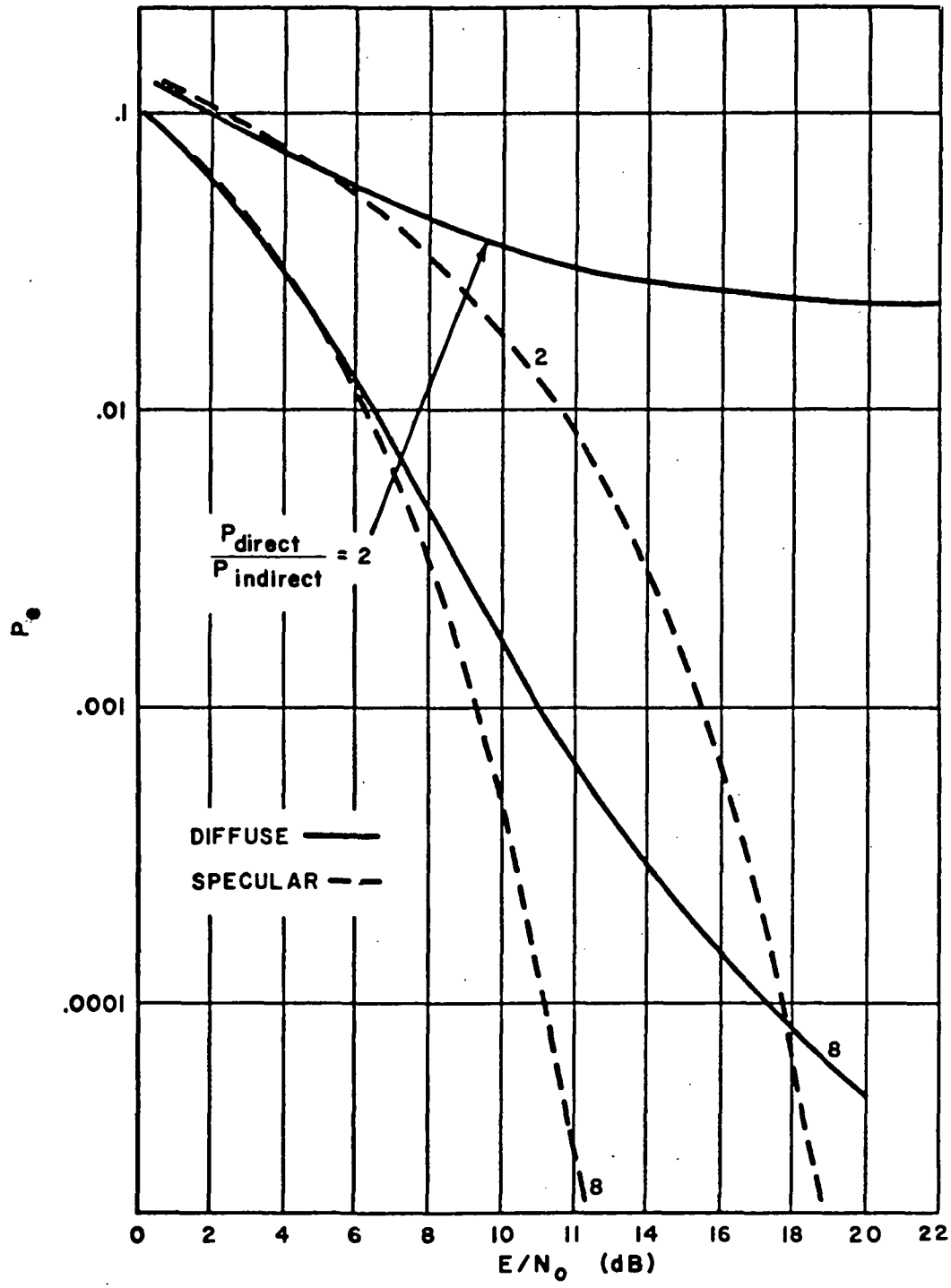

FIGURE 6-2 PERFORMANCE OF OPTIMUM PSK IN THE PRESENCE OF SPECULAR OR DIFFUSE MULTIPATH

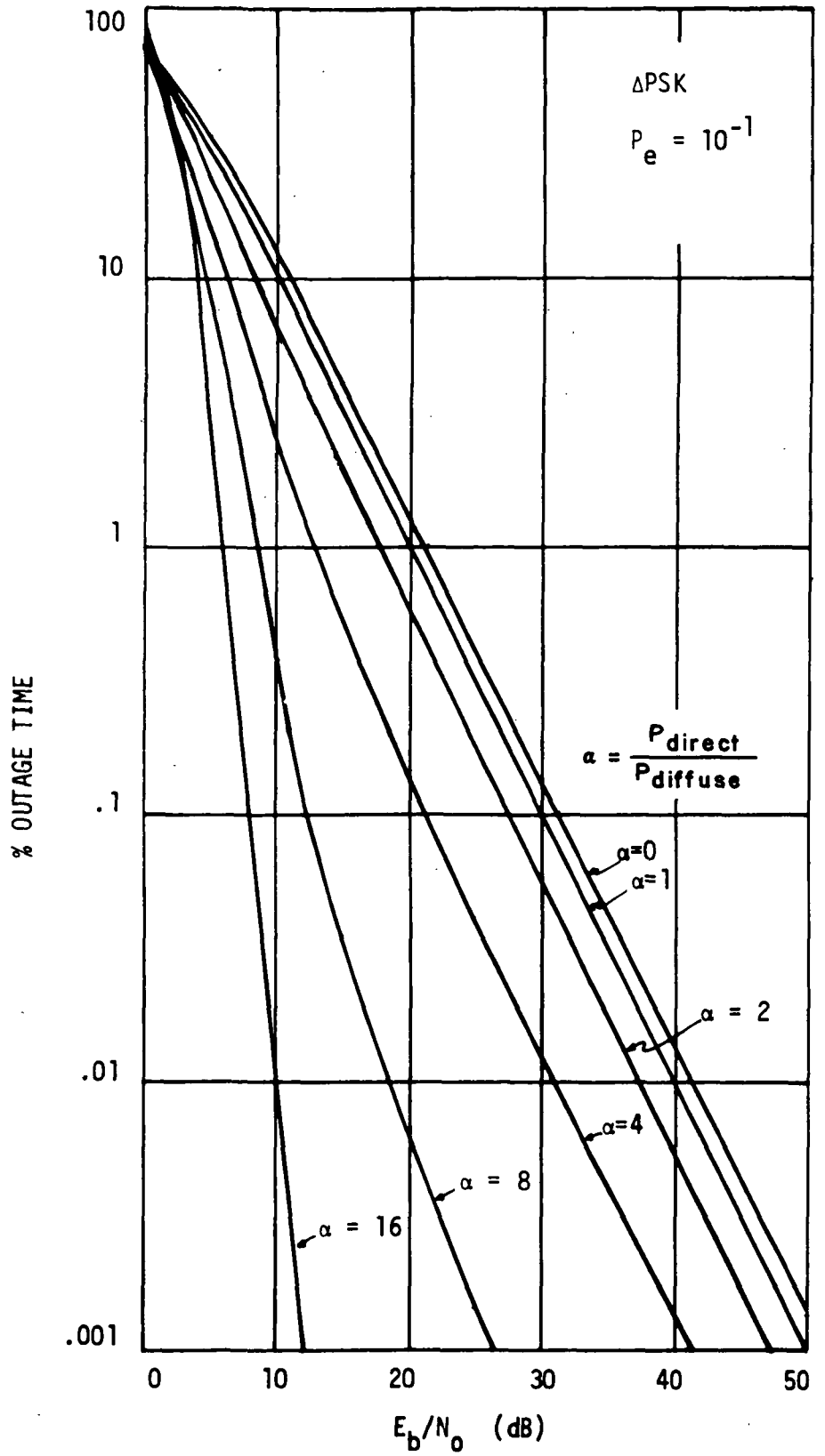

FIGURE 6-3 OUTAGE TIME IN PERCENT VS. E_b / N_o FOR ΔPSK AT $P_e = 10^{-1}$

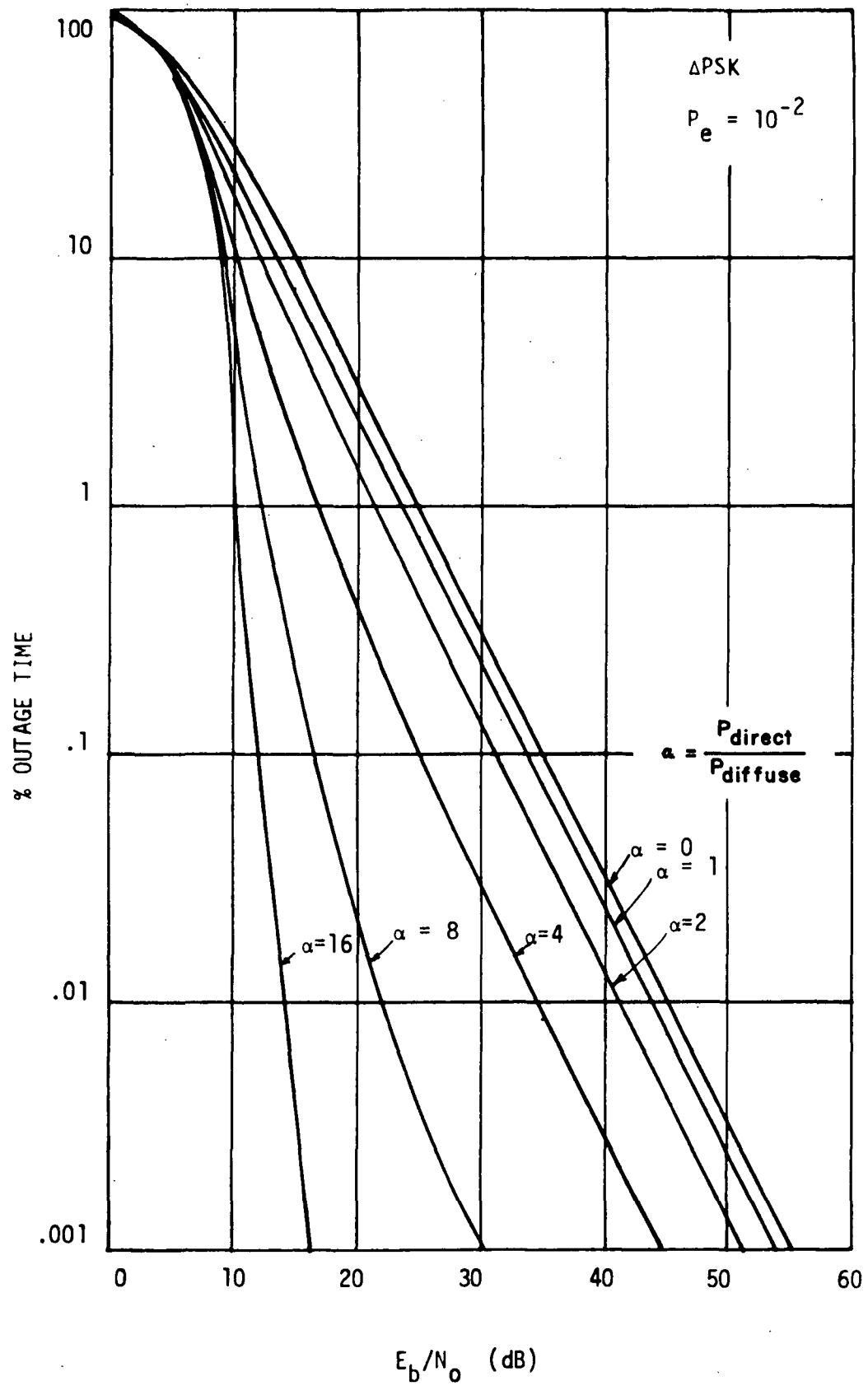

FIGURE 6-4 OUTAGE TIME IN PERCENT VS. E_b/N_o FOR ΔPSK AT $P_e = 10^{-2}$

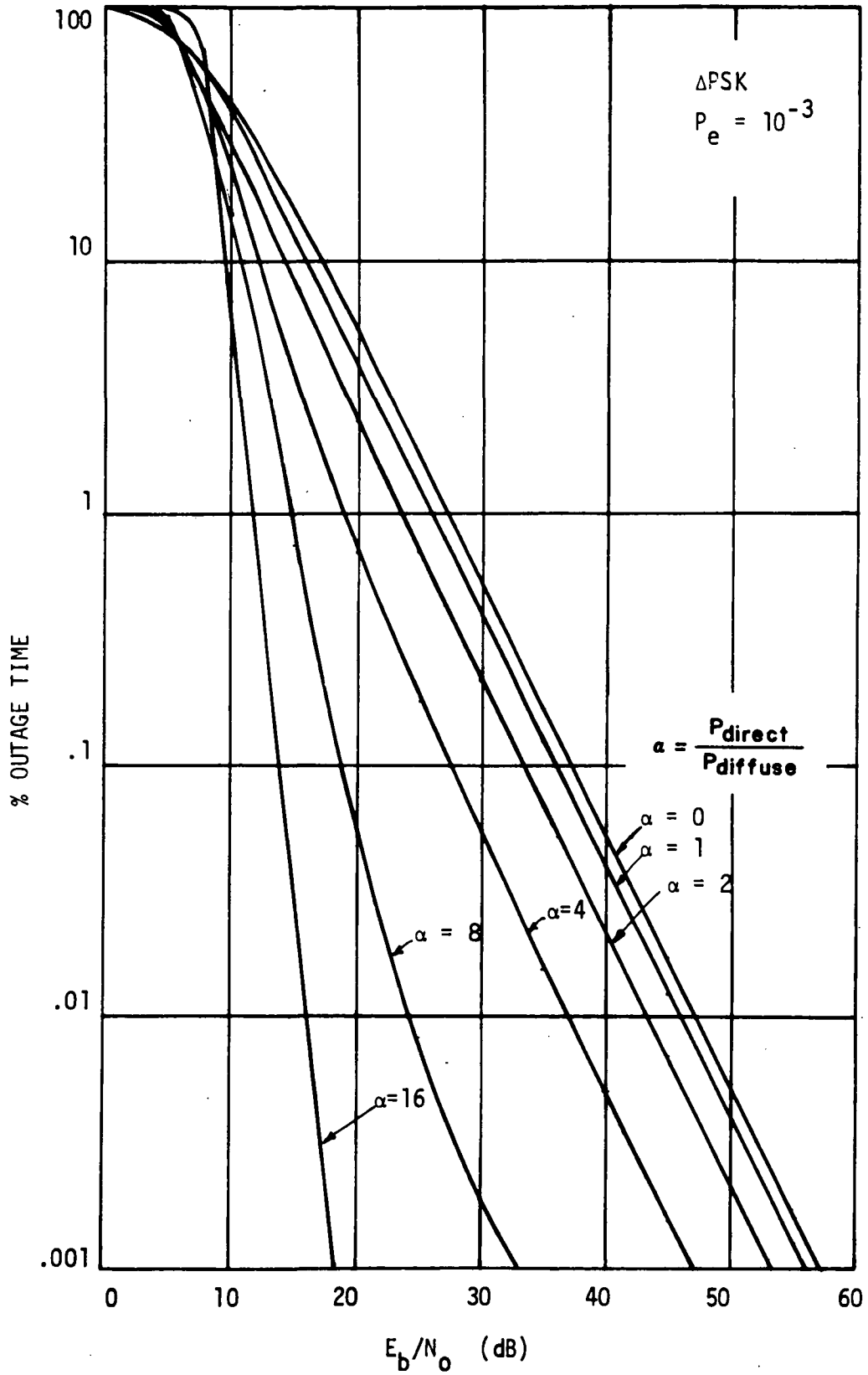

FIGURE 6-5 OUTAGE TIME IN PERCENT VS. E_b/N_o FOR ΔPSK AT $P_e = 10^{-3}$

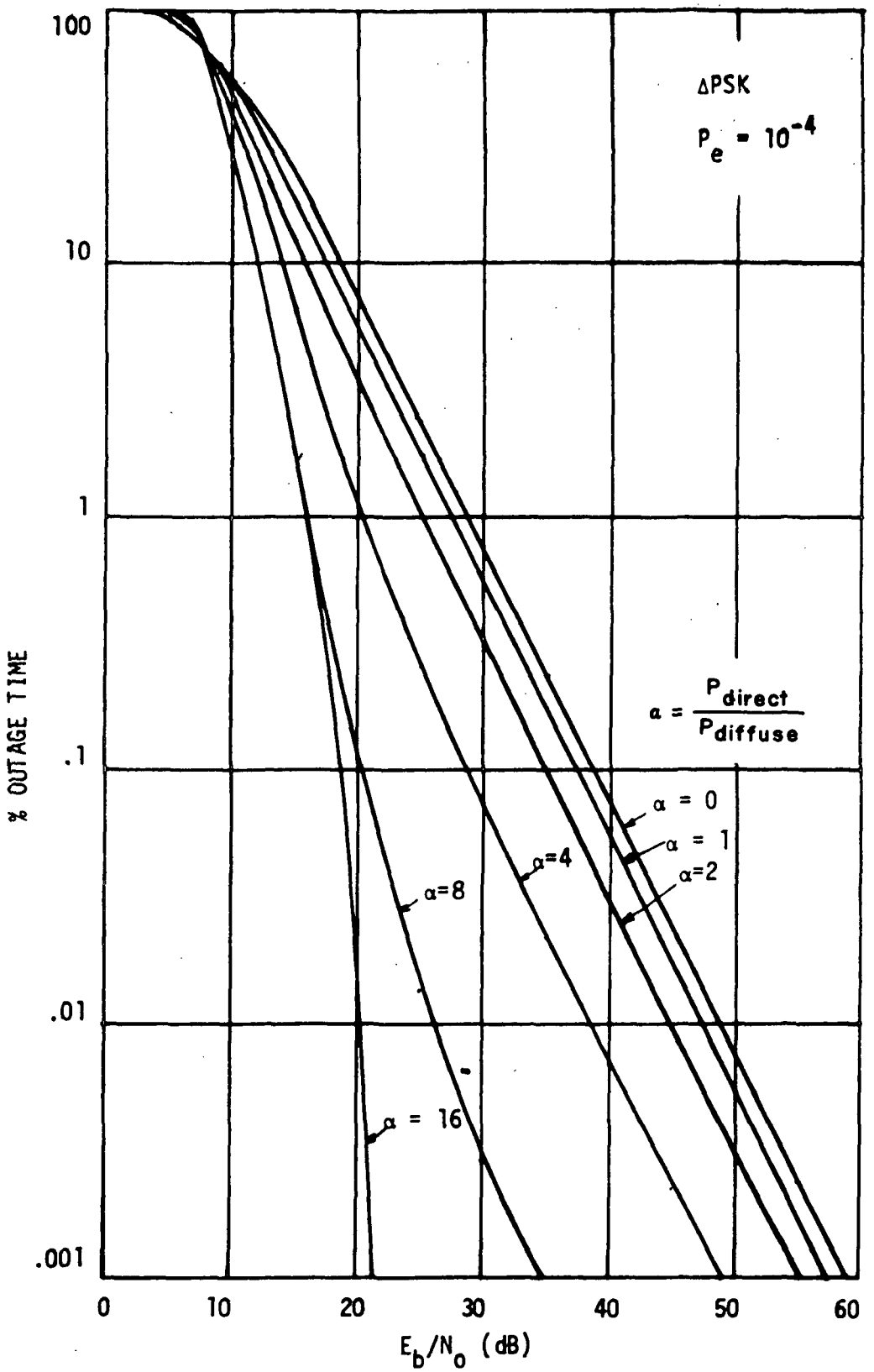

FIGURE 6-6 OUTAGE TIME IN PERCENT VS. E_b/N_0 FOR ΔPSK AT $P_e = 10^{-4}$

$\alpha = P_{direct}/P_{diffuse}$. For these curves $P_{specular} = 0$ is assumed, which will be the case for most frequencies of interest. The parameter P_e is the threshold used to define an outage, i.e. an outage occurs when the actual error rate exceeds the specified P_e. The curves in Figures 6-3 through 6-6 can be used to determine the desired amount of multipath suppression required of an antenna to achieve a specific outage time.

6.1.2 EFFECTS OF RFI ON ΔPSK

We have taken some liberties in the following analysis in that it is assumed the interference is a constant amplitude CW signal. The reader is advised that if such interference is amplitude modulated then the results of the following analyses must be averaged over the amplitude modulation statistics. The input to the coherent detector of Figure 6-7 is a phase-reversal-keyed signal in the presence of an interfering tone and an associated bandpass Gaussian noise. It is assumed that the reference in the receiver is phase-aligned with the desired signal, and that the reference is unaffected by the presence of the interference. It follows that the output

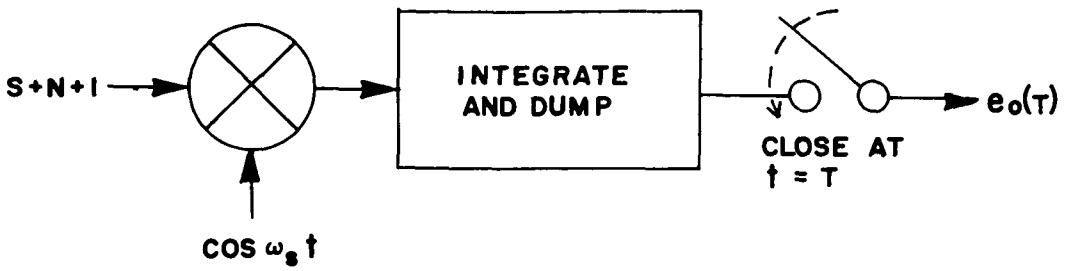

$S = A \cos \omega_s t$ (SIGNAL)

$N = x_c \cos \omega_s t + x_s \sin \omega_s t$ (NOISE)

$I = B \cos[(\omega_s + \Delta\omega)t + \theta]$ (INTERFERENCE)

FIGURE 6-7 COHERENT DETECTOR

from the integrate and dump at the sampling instant is given by:

$$e_0(T) = AT + \int_0^T \left[x_c(t) + B\cos(\Delta\omega t + \theta_D)\right] dt \qquad (6\text{-}4)$$

This results in a conditional binary error probability given by:

$$P_e(\theta) \doteq \frac{1}{2}\,\mathrm{erfc}\left[\frac{A}{\sqrt{2\sigma}}\left(1 + \frac{B}{A}\left|\frac{\sin\frac{\Delta\omega T}{2}}{\frac{\Delta\omega T}{2}}\right|\cos m\right)\right] \qquad (6\text{-}5)$$

where:

$$m = \theta_D - \frac{\Delta\omega T}{2}$$

$$\frac{A}{\sqrt{2\sigma}} = \sqrt{E/N_o}$$

E/N_o = energy to noise density.

Equation 6-5 assumes that the probabilities of 1 and 0 are equal. Under the assumption that the phase angle θ_D is a random variable, we are free to determine the average binary error probability by averaging the conditional density over a uniform density in θ_D or m:

$$\overline{P}_e = \frac{1}{2\pi}\int_{-\pi}^{\pi} \frac{1}{2}\,\mathrm{erfc}\left[\frac{A}{\sqrt{2\sigma}}\,(1 + K_D\cos m)\right] dm \qquad (6\text{-}6)$$

Equation 6-6 has been programmed on a digital computer and the results are shown in Figure 6-8 for various values of K_D as a function of the signal-to-noise ratio.

The value of K_D is seen to be the ratio of the interference to the signal level times a weighting factor which is a function of frequency and duration of the binary symbol. Interference which is well inside the bandwidth occupied by the data transmission is unaffected by the frequency weighting of the integrate and dump filter.

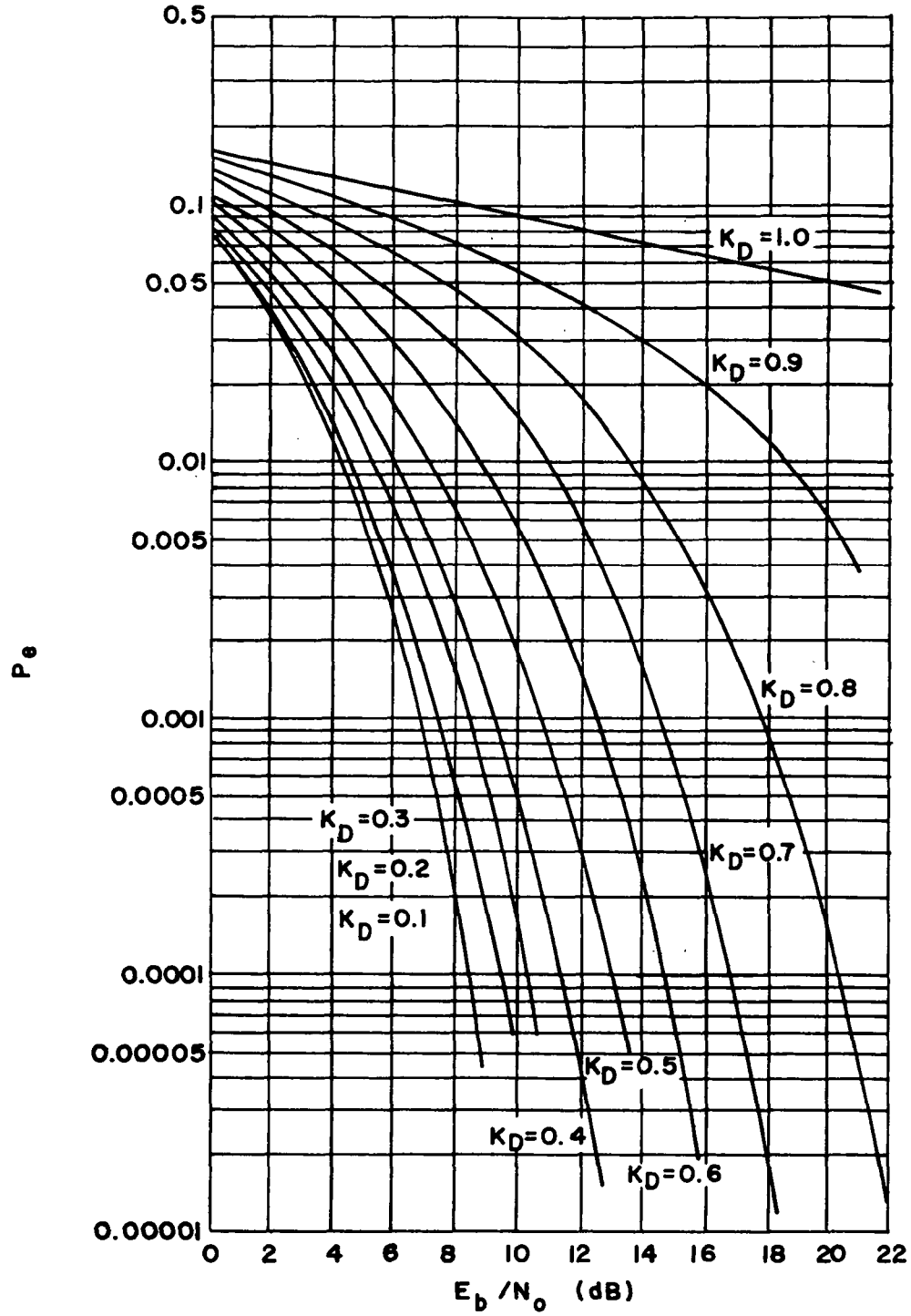

FIGURE 6-8 AVERAGE BINARY ERROR PROBABILITY FOR COHERENT PSK IN THE PRESENCE OF CW INTERFERENCE AND GAUSSIAN NOISE

We see from Figure 6-8 that an interference-to-signal ratio of -3 dB will cause an 8^{+} dB degradation in system performance at 10^{-4} bit error probability. Interference-to-signal ratios less than -20 dB are of little concern.

The primary result of the analysis is to point out that small amounts of narrowband interference can dramatically degrade the performance of narrowband signals or, in effect, require more power from the user craft to maintain a desired bit error probability.

For ΔPSK the results shown in Figure 6-8 are of value since the bit error probability for ΔPSK is approximately $2P_e$ where P_e is the coherent PSK error probability in the presence of CW interference.

For a 400 MHz forward link signal originating at a 30.0 dBw EIRP level from a TDRS, the received C/N_o at a SATS or Shuttle with a +3 dB antenna is approximately 57 dBHz (-115 dBm signal with N_o = -172 dBm/Hz). The path loss at 400 MHz between the ground and a 300 km altitude spacecraft is 135 dB. Thus a 20 dBm signal on the ground will arrive at the spacecraft at -115 dBm and render the data signal useless if the spacecraft antenna cannot discriminate against it. If the spacecraft antenna rejection of RFI is 20 dB, then a ten watt signal on the ground will equal the desired signal level at the spacecraft.

6.2 THE PERFORMANCE OF A PN/PSK SYSTEM IN THE PRESENCE OF MULTIPATH AND RFI

In addition to the Gaussian noise, multipath can produce non-Gaussian noise at the output of the PN correlator. For example, if the multipath signal is essentially specular and the differential time delay between the direct and the indirect signal paths is less than the duration

of a PN chip, the output of the correlation receiver will consist of two components, one of which is Gaussian and the other is non-Gaussian. The portion of the reflected signal within the correlation aperture will produce a randomly phased component which can be represented as a CW term whose power is proportional to the square of the correlation coefficient between paths times the power in the reflected path. That portion of the reflected signal which remains outside the correlation aperture produces essentially Gaussian noise which is suppressed by an amount equal to the processing gain (P.G.) of the receiver; this noise can be added directly to the Gaussian noise resulting from ambient noise and interference.

When the reflection is specular there will exist a differential Doppler between the direct and the indirect paths, reinforcing the postulation that the non-Gaussian component at the output of the correlation receiver will be a randomly phased CW component.

When the reflection from the earth's surface is completely diffuse and the differential time delay between the direct and indirect path is less than a PN chip length, the output components of a correlation receiver will be all Gaussian. The ambient noise and interference will be reduced by the P.G. of the receiver as will the Gaussian noise produced by the reflected signal which lies outside the correlation aperture. That portion of the reflected signal which lies inside the correlation apertures will produce a Gaussian noise component whose power is proportional to the square of the correlation coefficient between the direct and indirect paths times the amount of power in the indirect path; this term will not be diminished by the P.G. of the receiver.

In the analysis which is to follow, the above model of the output of a correlation receiver will be utilized to obtain expressions and curves for the performance of a PN system in both specular and diffuse multipath. This performance will be measured in terms of the expected binary error probability and the rms time jitter for an optimum code tracking system for navigation purposes.

6.2.1 SPECULAR MULTIPATH

When we consider the indirect path to be a perfect reflection, we are able to approach a reasonably accurate solution to the degradations imposed on PN systems by multipath. The model is illustrated in Figure 6-9.

For the purpose of analysis let us assume that the data is PSK and that the system is a two-phase PN coded system. The amount of noise power which will be found in the post-correlation filter is given by:

$$\text{Noise in post-correlation terms} = \underbrace{\frac{N_{in}}{P.G.} + \frac{(1-\rho^2)P_{ind}}{P.G.}}_{\sigma^2 = \text{Gaussian terms}} + \underbrace{\rho^2 P_{ind}}_{\text{C.W.}} \qquad (6\text{-}7)$$

where P_{ind} is the power in the indirect path.

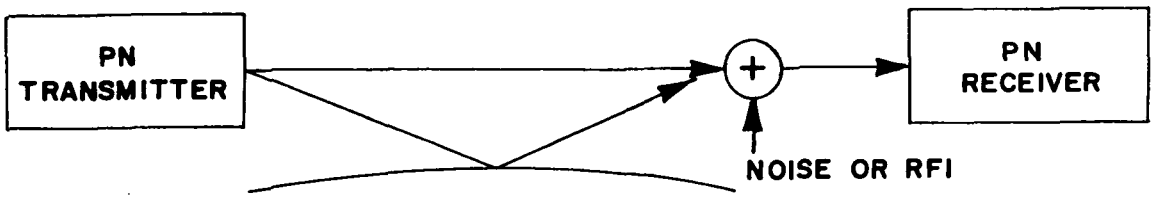

FIGURE 6-9 SIMPLIFIED MULTIPATH PN SYSTEM GEOMETRY

The noise power is seen to consist of the ambient Gaussian noise reduced by the processing gain plus a Gaussian noise term resulting from partial decorrelation with the reflected path diminished by the processing gain and finally a CW term which represents the partial correlation ρ of the direct and indirect path The factor ρ is a number which lies between 0 and 1.

After a few algebraic manipulations a conditional binary error probability is obtained as:

$$P_e(\theta) = \frac{1}{2}\,\mathrm{erfc}\left[\sqrt{\frac{P_{dir}T}{\frac{N_{in}}{CR} + \frac{(1-\rho^2)P_{ind}}{CR}}}\left(1 + \underbrace{\frac{\rho\sqrt{2P_{ind}}}{\sqrt{P_{dir}}}\left|\frac{\sin\Delta\omega\frac{T}{2}}{\Delta\omega\frac{T}{2}}\right|}_{K}\cos\phi\right)\right] \quad (6\text{-}8)$$

where

$\phi = \theta - \Delta\omega T/2$

θ = random phase angle

$\sqrt{2P_{dir}}$ = signal strength of the direct path

$\sqrt{2P_{ind}}$ = signal strength of the indirect path

T = duration of the binary symbol

$\Delta\omega$ = differential Doppler radian frequency

CR = chip rate

$$N_o = \frac{N_{in}}{CR} + \frac{(1-\rho^2)P_{ind}}{CR}$$

Under the assumption that the phase angle θ associated with the specular multipath interference is a random variable we are free to determine the average binary error probability by averaging the conditional density

over a uniform density in phase. This results in

$$P_\varepsilon = \frac{1}{2\pi}\int_{-\pi}^{\pi} \frac{1}{2}\,\mathrm{erfc}\left[\sqrt{\frac{P_{dir}T}{N_o}}\,(1+K_D\cos\phi)\right]d\phi \qquad (6\text{-}9)$$

The above equation has been programmed on a digital computer and the results are shown in Figure 6-8 for various values of K_D in terms of direct path energy per bit $(P_{dir}T/N_o)(E/N_o)$. K_D is the ratio of the signal strength of the reflected path to that of the direct path weighted by the correlation coefficient ρ.* Using the results shown in Figure 6-8, it is now possible to determine the resultant average bit error probability as a function of the correlation coefficient ρ given that the ratio of the direct to the indirect path is fixed. For example, the average bit error probability vs. ρ is illustrated in Figure 6-10 under the assumption that the direct path to indirect path signal ratio is unity, the input signal to Gaussian noise ratio is unity, and the processing gain is 12 dB. Note that the noise power from the interfering path changes as a function of ρ, that is, the Gaussian noise contribution resulting from partial correlation approaches zero as correlation between direct and indirect paths increases. A conservative upper bound on the system performance can be obtained, in most cases, by simply drawing a straight line of Figure 6-8 between the average bit error probability curve for zero correlation and the K_D value associated with maximum correlation. Keep in mind that K_D is the product of the ratio of direct and indirect signal strength times the correlation coefficient ρ.

6.2.2 DIFFUSE MULTIPATH

In the previous section, the effects of specular multipath on a two-phase PN system were evaluated. It is also of interest to evaluate the effects of diffuse scattering on PN systems since diffuse scattering

* This is true when $\Delta\omega T/2$ is small.

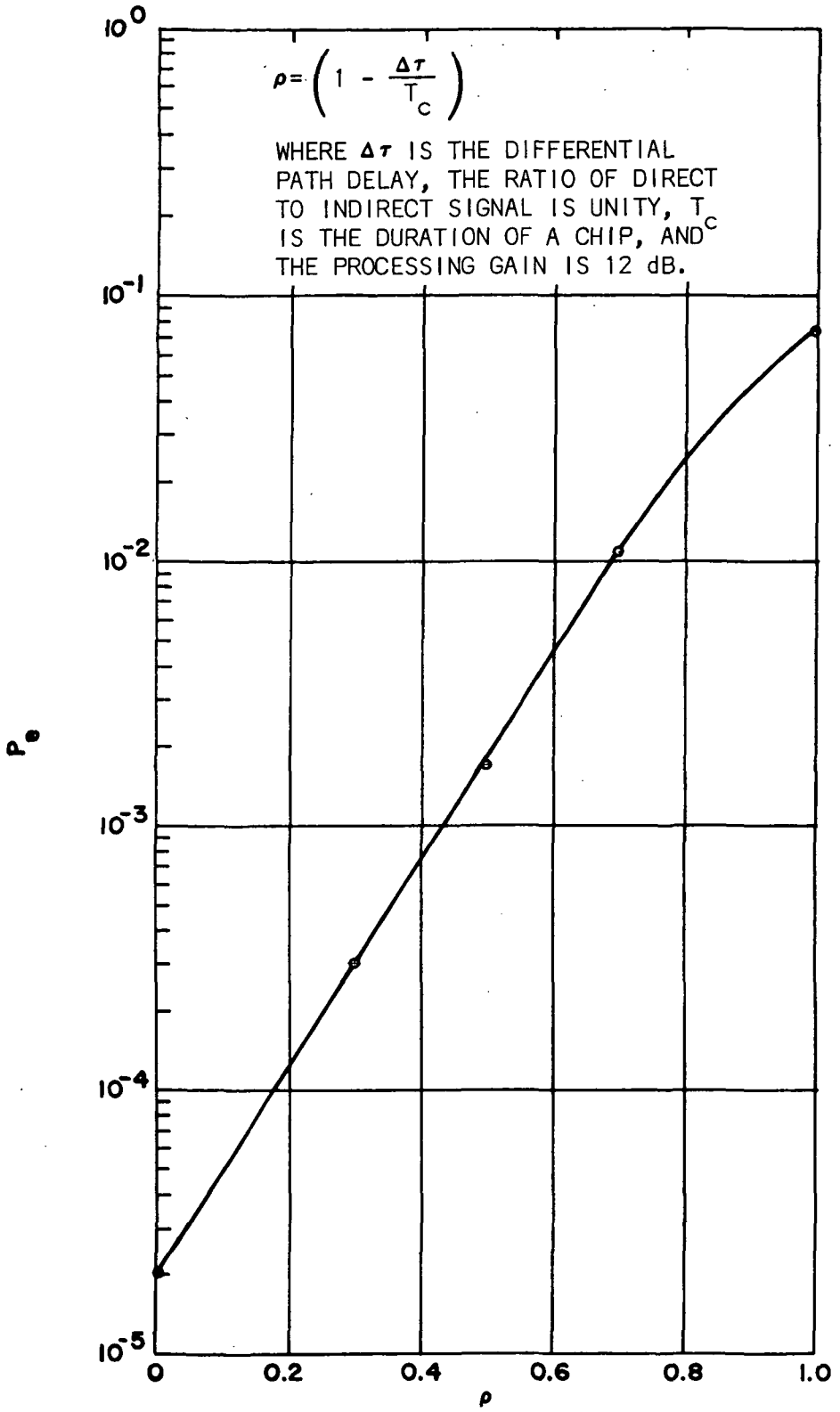

FIGURE 6-10 AVERAGE ERROR PROBABILITY VS. CORRELATION BETWEEN DIRECT AND INDIRECT PATHS

will probably predominate for many frequencies.

In order to carry out this evaluation we assume that the diffuse reflected energy can be broken down into essentially discrete paths. Each path will assume to be fading according to a Rayleigh amplitude statistic and that the paths will be essentially uncorrelated.

Either the total time spread in the indirect path is assumed to be equal to the duration of one PN chip or the time spread is assumed to be much greater than the duration of a chip. Furthermore, it is assumed that each of the paths associated with the indirect path contains equal power and that the sum total of the powers associated with each of the subpaths equal the total power contained in the reflected path. With these assumptions it is possible to determine the performance of a PN system in diffuse multipath interference.

Case 1 - The time spread in the indirect path is assumed to be such that the indirect signal is diffuse and is confined to the original correlation window of the PN sequence. Under these circumstances the amount of noise power produced at the correlator output and seen by a detector (PSK) is given by

$$\text{Total Noise} = \overbrace{\underbrace{\frac{N_{in}}{P.G.} + \frac{(1+\rho^2)P_{ind}}{P.G.} + \rho^2 P_{ind}}_{\text{All Gaussian noise terms}}}^{N} \qquad (6\text{-}10)$$

where

ρ = degree of correlation or signal overlap, $0 \leq \rho \leq 1$

P_{ind} = amount of power in the indirect path

P.G. = Processing Gain

N_{in} = Additive Gaussian noise

We see that as the indirect path and the direct path become more and more correlated the amount of noise power which confronts a binary decision increases as the square of the correlation coefficient and that the noise will be essentially Gaussian since the diffuse path is fading according to a Rayleigh statistic. The amount of interference due to the reflected energy associated with the indirect path which remains uncorrelated is suppressed by the P.G. of the system as is the input noise which is always associated with the system. The post-correlation or predetection signal-to-noise ratio, therefore, will in effect approach 0 dB when the correlation coefficient is 1 and the direct and indirect paths are essentially equal.

The resulting binary error probability for PSK in the presence of diffuse multipath with no time spreading is given by:

$$P_\varepsilon = \frac{1}{2}\,\mathrm{erfc}\sqrt{\frac{P_{direct}}{\frac{N_{in}}{P.G.} + \frac{(1-\rho^2)P_{ind}}{P.G.} + \rho^2 P_{ind}}} \qquad (6\text{-}11)$$

where P_{direct} is the signal power in the direct path. Equation 6-11 has been plotted in Figure 6-11 for various values of $\sqrt{P_{ind}/P_{direct}}$. The figure shows that an irreducible error probability exists due to the diffuse multipath.

Case 2 - Now let us assume that the multipath signal is time spread such that the total reflected signal is distributed over a spread in time which is large compared with the correlation window of the binary sequence. We can expect that only a fraction of the reflected power will be contributed directly in terms of Gaussian noise in the receiver; the rest will remain uncorrelated and suppressed by the P.G. Thus, as a function of the correlation coefficient we have noise terms which have the form:

$$N_{total} = \frac{N_{in}}{P.G.} + \frac{\left(1-\rho^2\,\frac{\Delta}{T_{spread}}\right)P_{ind}}{P.G.} + \rho^2 P_{ind}\left(\frac{\Delta}{T_{spread}}\right) \qquad (6\text{-}12)$$

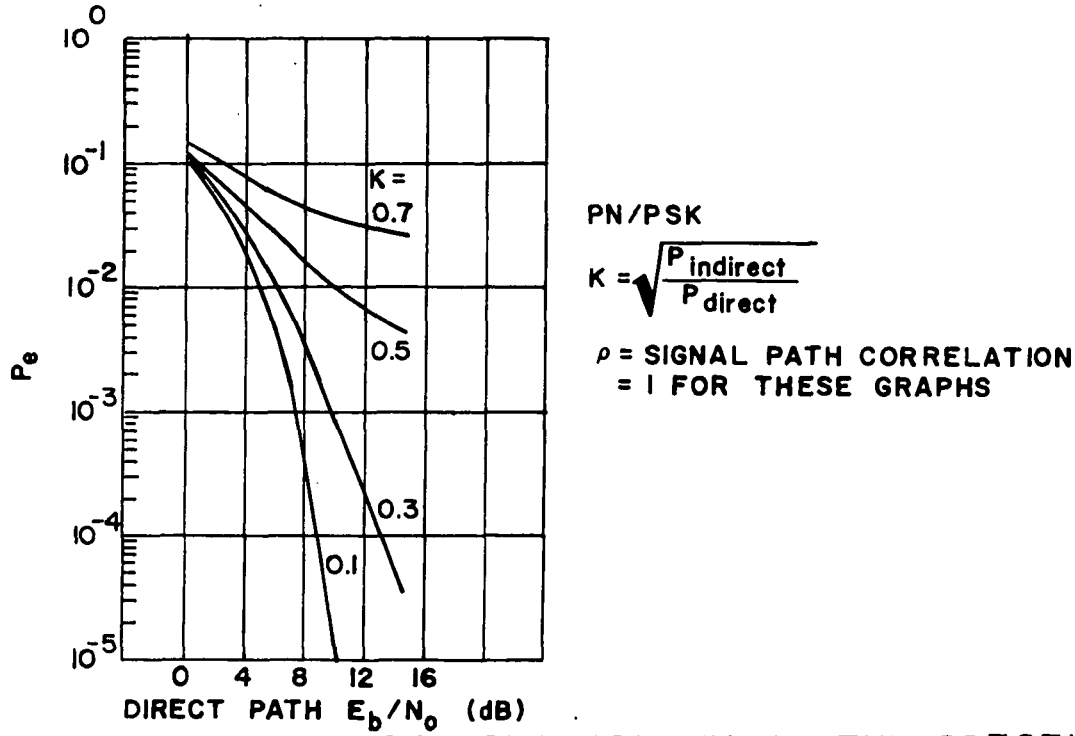

FIGURE 6-11 AVERAGE ERROR PROBABILITY IN THE PRESENCE OF DIFFUSE MULTIPATH

where

Δ = the duration of a PN chip

T_{spread} = the multipath time spread

ρ = the overlap or correlation between direct and indirect paths

P_{ind} = the total power in the indirect signal.

Time smear in the indirect path will be advantageous since it forces more of the reflected energy to be decorrelated in the receiver and to be subject to the suppression by the processing gain of the receiver.

6.2.3 THE EFFECTS OF RFI ON PN SYSTEMS

It has been established through theory and numerous experiments that the performance of a PN system in the presence of constant envelope

interference is completely determined by the well-known output vs input signal-to-noise ratio

$$\left(\frac{S}{N}\right)_{out} = \left(\frac{S}{N}\right)_{in} \text{P.G.} \qquad (6\text{-}13)$$

where N_{in} = ambient noise and RFI.

Therefore

$$\left(\frac{S}{N}\right)_{out} = \left[\frac{S}{N_o W_s + RFI}\right] \frac{W_s}{BR} \qquad (6\text{-}14)$$

where W_s = chip rate

BR = bit rate = 1/T

N_o = noise density.

6.2.4 DETERMINATION OF THE EFFECTS OF MULTIPATH ON THE TRACKING PERFORMANCE OF PN SYSTEMS

6.2.4.1 Effects of Diffuse Correlated Multipath

The coherent delay lock loop discriminator is a device which is utilized to track PN codes in a correlation receiver. It is the basis for measuring a signal's time of arrival for range measurements. A simplified coherent delay lock loop for PN sequence tracking is illustrated in Figure 6-12. For the purpose of analysis we will assume that the code tracking device is coherent and is operating at base band and that a one chip delay is utilized in the shift register to realize the error tracking voltage curve, or discriminator characteristics.

We assume that the phase-lock loop associated with the tracking device has a one-sided bandwidth B_L and that the PN sequence has a minimum chip duration of T_c. It follows for an unrestricted predetection bandwidth

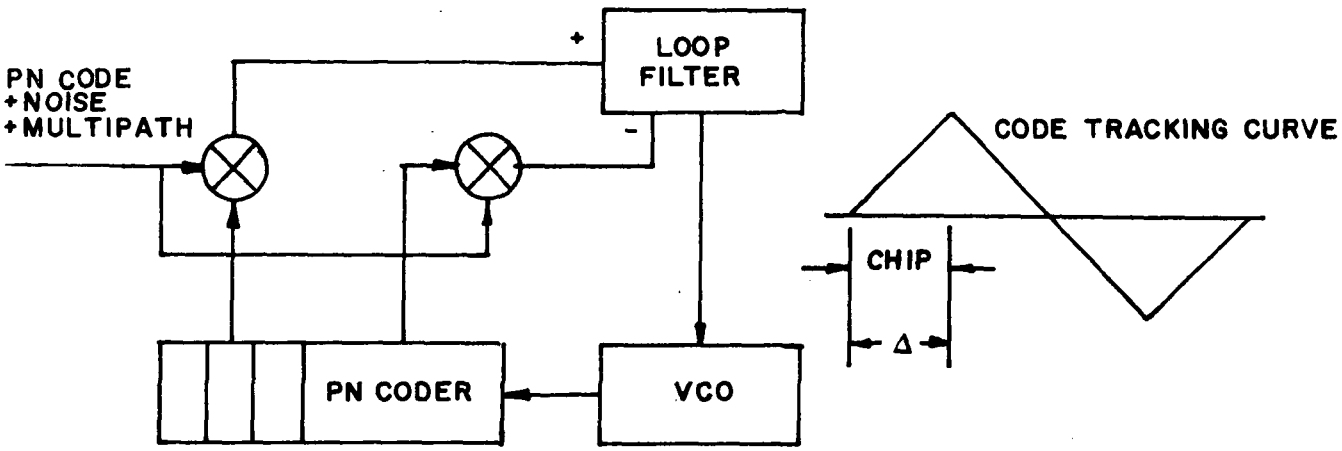

FIGURE 6-12 LOW PASS COHERENT DELAY LOCK LOOP

that the rms range error ΔR for the coherent binary delay lock loop is given by:

$$\Delta R = \frac{\pi}{5} \frac{T_c c}{\sqrt{2\left(\frac{S}{N}\right)_{CL}}} \tag{6-15}$$

where $\left(\frac{S}{N}\right)_{CL}$ = loop SNR in code tracking loop

T_c = chip duration

c = speed of light

We desire to know the performance of a similar system in the presence of diffuse correlated multipath. The rms error of the tracking loop takes the following form in the presence of correlated diffuse multipath:

$$\Delta R = \frac{\pi}{5} \frac{T_c c}{\sqrt{2}} \sqrt{\frac{\frac{N_{in}}{P.G.} + \frac{(1-\rho^2)P_{ind}}{P.G.} + \rho^2 P_{ind}}{P_{direct}}} \tag{6-16}$$

where

P.G. = processing gain

ρ = correlation between the direct and indirect paths

P_{direct} = direct signal power

P_{ind} = power in the indirect path

We see that the input noise level is suppressed by the P.G., there is a Gaussian term showing partial correlation suppressed by the P.G., and a Gaussian term showing partial correlation which is unaffected by the P.G. The sum of these three terms represents the noise which is present in a correlation delay lock loop implementation.

When the P.G. is large it is evident from Equation 6-16 that there exists a lower bound on the tracking error given by

$$\Delta R \approx \frac{\pi}{5} \frac{T_c\, c}{\sqrt{2}} \rho \sqrt{\frac{P_{ind}}{P_{direct}}} \qquad (6\text{-}17)$$

Rearranging terms and taking the ratio of the rms range error without multipath to the rms range error of the loop in the presence of diffuse multipath, we obtain an equation which indicates the relative performance of the delay lock discriminator in the presence of correlated diffuse multipath:

$$\frac{\Delta R_{noise}}{\Delta R_{\substack{diffuse \\ + noise}}} = \frac{\sqrt{N_{in}/P.G.}}{\sqrt{\frac{N_{in}}{P.G.} + \frac{(1-\rho^2)P_{ind}}{P.G.} + \rho^2 P_{ind}}} \qquad (6\text{-}18)$$

In conclusion we see that the multipath can dramatically affect the rms performance of a delay lock loop relative to its performance without multipath. In fact, there is an asymptotic tracking error which is determined

by the degree of correlation between the direct and indirect paths and the ratio of the powers received via the two paths.

6.2.4.2 Specular Multipath

The effects of specular fading on the tracking error in a conventional coherent binary delay lock loop are of interest. In order to determine the tracking loop error resulting from specular multipath, we assume that a portion of the received signal is correlated with the direct path and that this term will show up as a randomly phased CW component at the output of the delay lock loop and will remain within the loop bandwidth of the VCO.

In lieu of a sophisticated analysis we utilize the experimental results obtained by Britt and Palmer (Reference 36) and find that the phase error in a conventional second order phase lock loop resulting from CW interference is given by:

$$\sigma^2_{\phi error} \approx \frac{N/P_{direct}}{1+I/P_{direct}} + \frac{I}{2P_{direct}} \text{ (in radians)} \qquad (6\text{-}19)$$

where P_{direct} is the desired signal power, I is the CW interference power, and N is the noise power in the loop.

We can expect that the rms range error for the coherent delay loop can be written as

$$\Delta R = \frac{\pi}{5} T_c \, c \, \sigma_{\phi error} \qquad (6\text{-}20)$$

where T_c is the duration of a PN chip. In terms of equation 6-20 and the parameters governing multipath, i.e.

$$I = \rho^2 P_{ind}$$

P_{ind} = power in the indirect path

$$N = \frac{N_{in} + (1-\rho^2)P_{ind}}{P.G.}$$

ρ = correlation coefficient between the signal path

P.G. = the processing gain of the tracking loop,

the range error may be written as:

$$\Delta R = \frac{\pi}{5} T_c c \sqrt{\left[\frac{\left[N_{in}+(1-\rho^2)P_{ind}\right]\frac{1}{P.G.}}{P_{direct}+\rho^2 P_{indirect}} + \frac{\rho^2 P_{ind}}{2P_{direct}}\right]} \qquad (6\text{-}21)$$

which for large P.G. reduces to Equation 6-17, the rms bound on the tracking error:

$$\Delta R = \frac{\pi}{5} \frac{T_c c \rho}{\sqrt{\frac{2P_{direct}}{P_{indirect}}}} \qquad (6\text{-}17)$$

The result is not surprising in that a similar equation was derived for the rms range error for a coherent delay lock loop in the presence of correlated diffuse multipath.

6.2.4.3 Combined Effects of Multipath and RFI

In practice ρ is essentially equal to zero. For example, if the differential time delay τ_d between the direct and indirect paths

$$\tau_d \approx \frac{2h}{c} \sin \psi \qquad (6\text{-}22)$$

is large that the duration of a PN chip T_c then ρ=0. For most cases the condition $\tau_d > T_c$ holds and therefore $\rho = 0$.

The multipath, RFI, and noise then become additive and the output signal to noise ratio $\left(\frac{S}{N}\right)_{out}$ for a PN system becomes

$$\left(\frac{S}{N}\right)_{out} = \frac{S_{in}\ (P.G.)}{N_o W_s + RFI + Multipath} = \frac{P_{direct}\ (P.G.)}{N_o W_s + RFI + P_{diff} + P_{specular}} \qquad (6\text{-}23)$$

Equation 6-23 will be used in subsequent paragraphs to determine the performance of a PN system in a synchronous relay satellite (TDRS) and Space Shuttle configuration.

In the previous sections we discussed the performance of the pseudonoise system in the presence of RFI and multipath. In the latter case the multipath was assumed to be correlated in the sense that the differential time delay τ_d between the direct and the indirect paths was so short that it was less than 1 PN chip duration. The analysis was meant to be general and in practice the differential time delay should be greater than the duration of a single pseudonoise chip. In such instances the received signal and the multipath signal become uncorrelated and the multipath signal and the RFI appear to be interfering noise sources which are suppressed by the processing gain of the correlation receiver.

We have generated by computer the performance which can be expected in the forward link between a relay satellite and the Shuttle or SATS. At 400 MHz the expected performance has also been evaluated for the pseudonoise system in the return link at a nominal frequency of 137 MHz.

In the forward link it is assumed that the noise density is -171.8 dBm/Hz. This is based on our best estimates of noise density at the Shuttle or SATS at an altitude of 300 to 500 kilometers. Free space and

other losses are set at 178.8 dB, and it is assumed that the antenna on the Shuttle or SATS is circularly polarized with a nominal 3 dB gain (see Section 7.1 for circularly polarized antenna patterns). A system design margin of 3 dB is also included for the forward link analysis.

In the return link the performance is based upon an ambient noise level of -168.4 dBm/Hz with the free space losses and other losses set at 167.5 dB. Again, a system design margin of 3 dB is included.

In the forward link it is assumed that the digital data has been ΔPSK coded and the design goal of 10^{-4} bit error probability is used. It is understood that, based upon current TDRS designs, an additional 6 dB of power in the forward link is available upon demand for voice signals (if required). Forward error control is also incorporated in the performance curves as will be shown. A nominal 4.0 dB forward error control coding gain is shown in the performance curves to illustrate the potential benefits of forward error control for the forward link. Forward error control coding is also illustrated for the return link.

The system performance in the forward link is based on three equations. The carrier-to-noise density available in the presence of noise, RFI, and multipath is determined by:

$$\frac{C}{N_o} = \frac{P_{received}}{\frac{N}{CR} + \frac{RFI}{CR} + \frac{Multipath}{CR}} \qquad (6\text{-}24)$$

where CR is the chip rate. The range and range rate accuracies are determined from the C/N_o values determined from equation 6-24 by the relationships

$$\Delta R = \frac{\pi}{5} \frac{T_c \, c}{\sqrt{\frac{C}{N_o B_{CL}}}} \qquad (6\text{-}25)$$

where B_{CL} = PN code loop bandwidth

and

$$\Delta \dot{R} = \frac{c}{2\sqrt{2}\,\pi f_c \, T_{obs} \sqrt{\frac{C}{N_o B_{LC}}}} \qquad (6\text{-}26)$$

where B_{LC} = carrier loop bandwidth.

From the calculation of C/N_o, an achievable bit rate is calculated for a given BEP. Shown in Figure 6-13 is the expected performance in the forward link for 400 MHz center frequency. The user altitude is set at 300 kilometers. The pseudonoise chip rates range from 45 to 333 kilochips/sec. This is done to insure that the flux density measured on the earth will meet IRAC standards which are discussed in Section 2.1.2. Not shown in Figure 6-13 is the performance of the forward link with an increased EIRP to 36 dBw for voice operation. However, a curve is shown in Figure 6-13 which reflects the improvement that one can obtain through forward error control in the forward link. A coding gain of 4.0 dB is assumed for a rate $\frac{1}{2}$, K=5 convolutional encoder with maximum likelihood decoding (soft decisions). This forward error control encoder/decoder is discussed in more detail in Section 5.2. Figure 6-14 shows the expected performance for the TDRS-to-Shuttle forward link at S-Band for two TDRS power levels with and without forward error control.

The expected results for the range and the range rate performance in the forward link are shown in Figures 6-15 and 6-16.

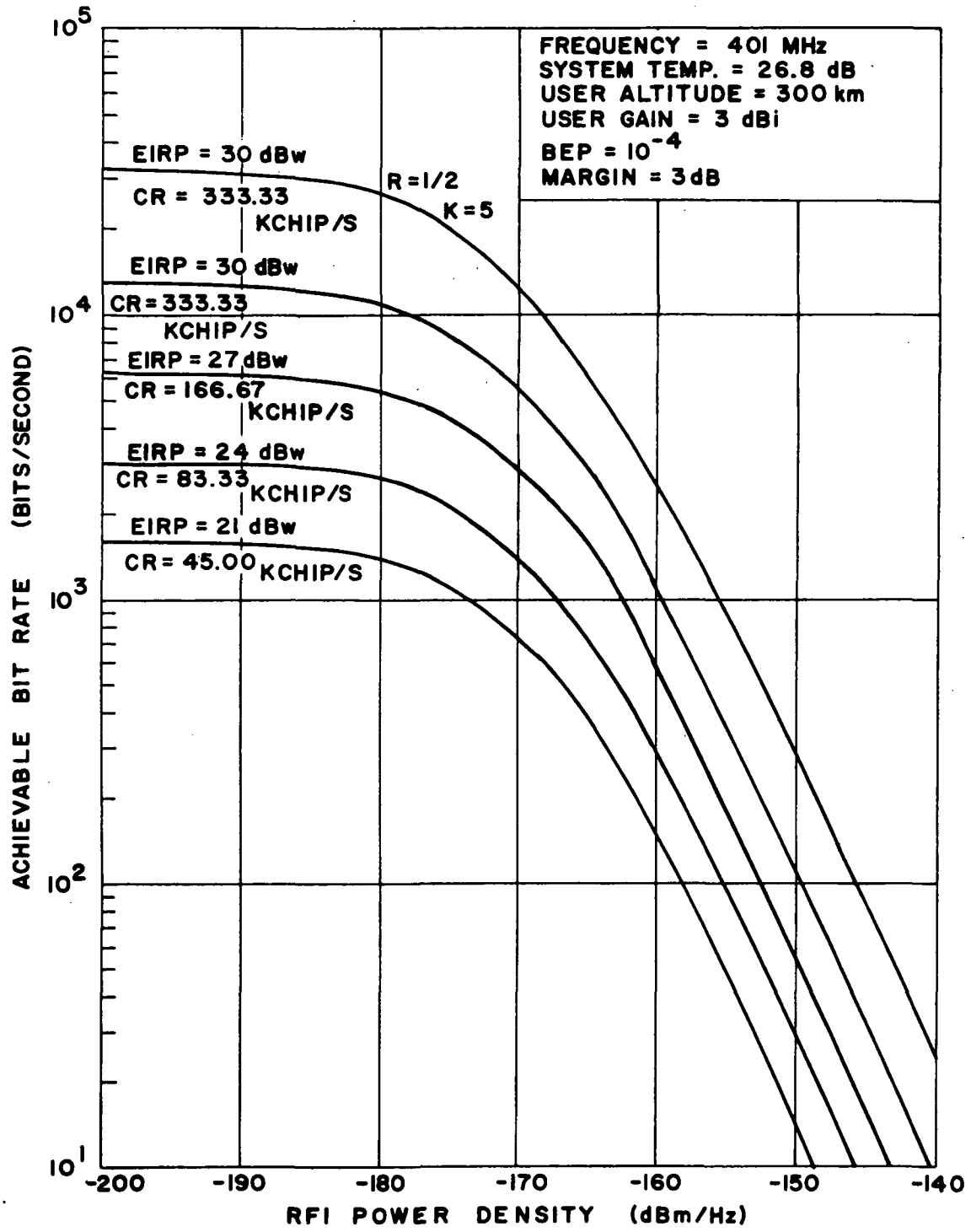

FIGURE 6-13 FORWARD LINK PERFORMANCE

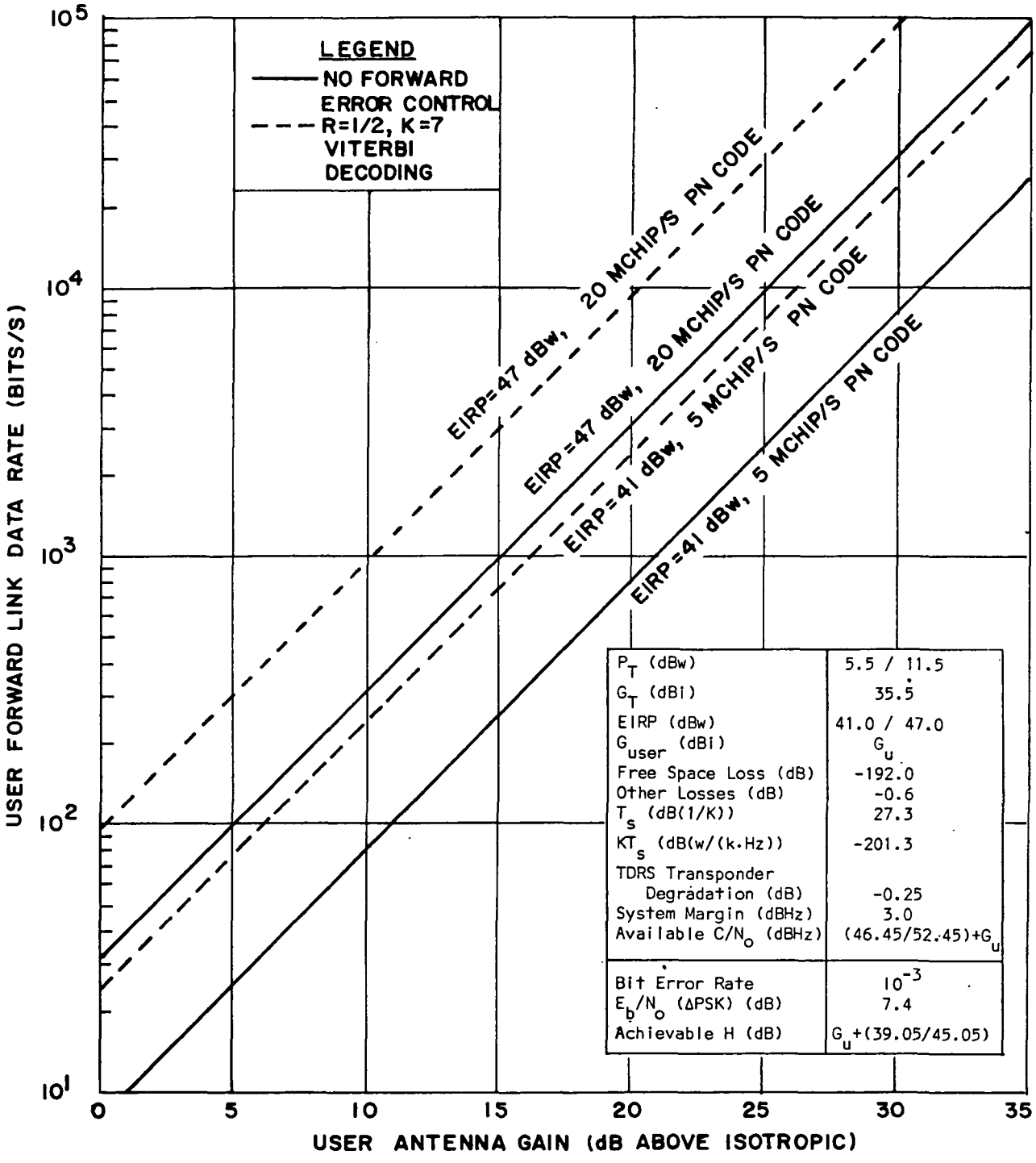

FIGURE 6-14 FORWARD LINK PERFORMANCE FOR S-BAND TDRS/SHUTTLE LINK

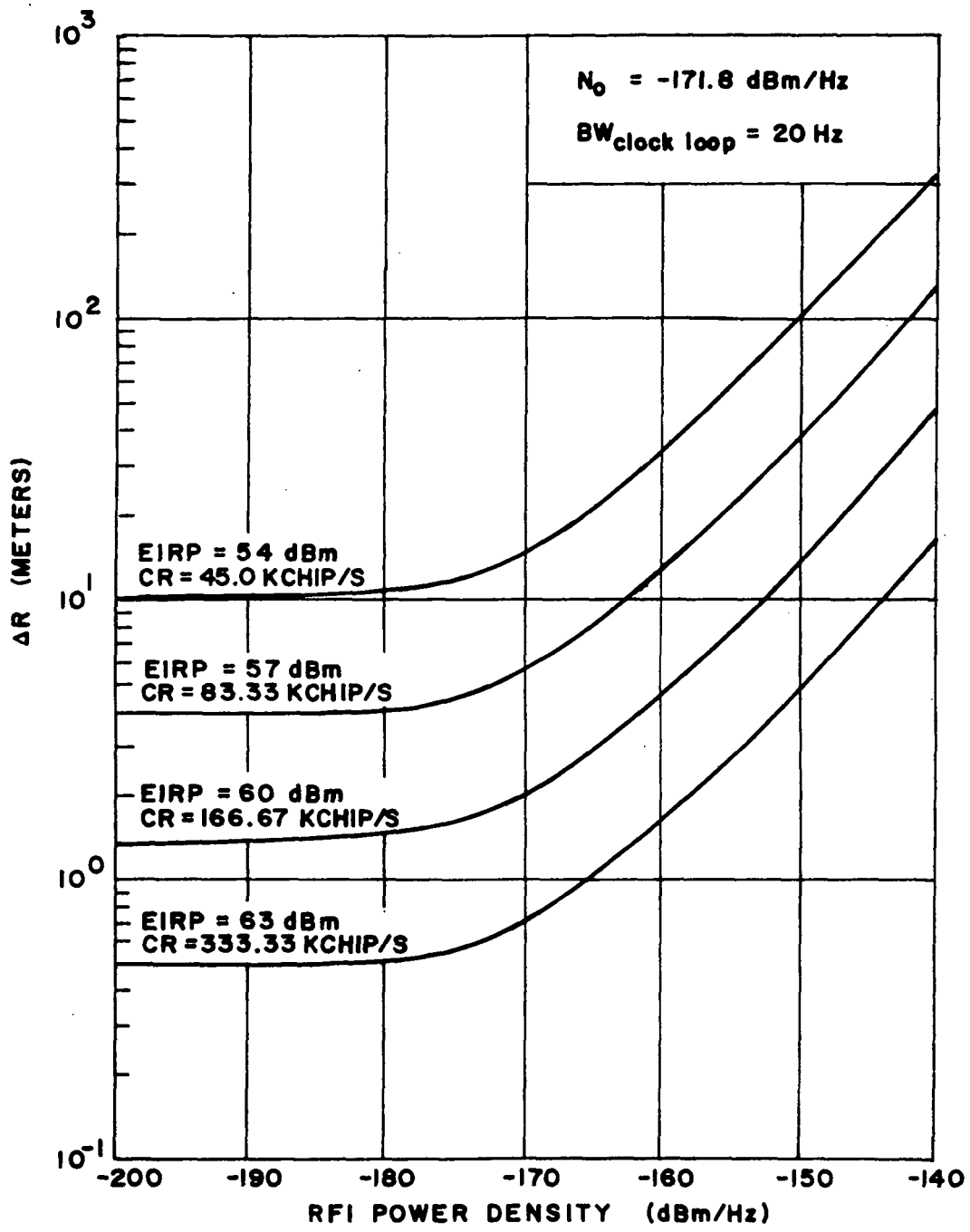

FIGURE 6-15 FORWARD LINK RANGING PERFORMANCE

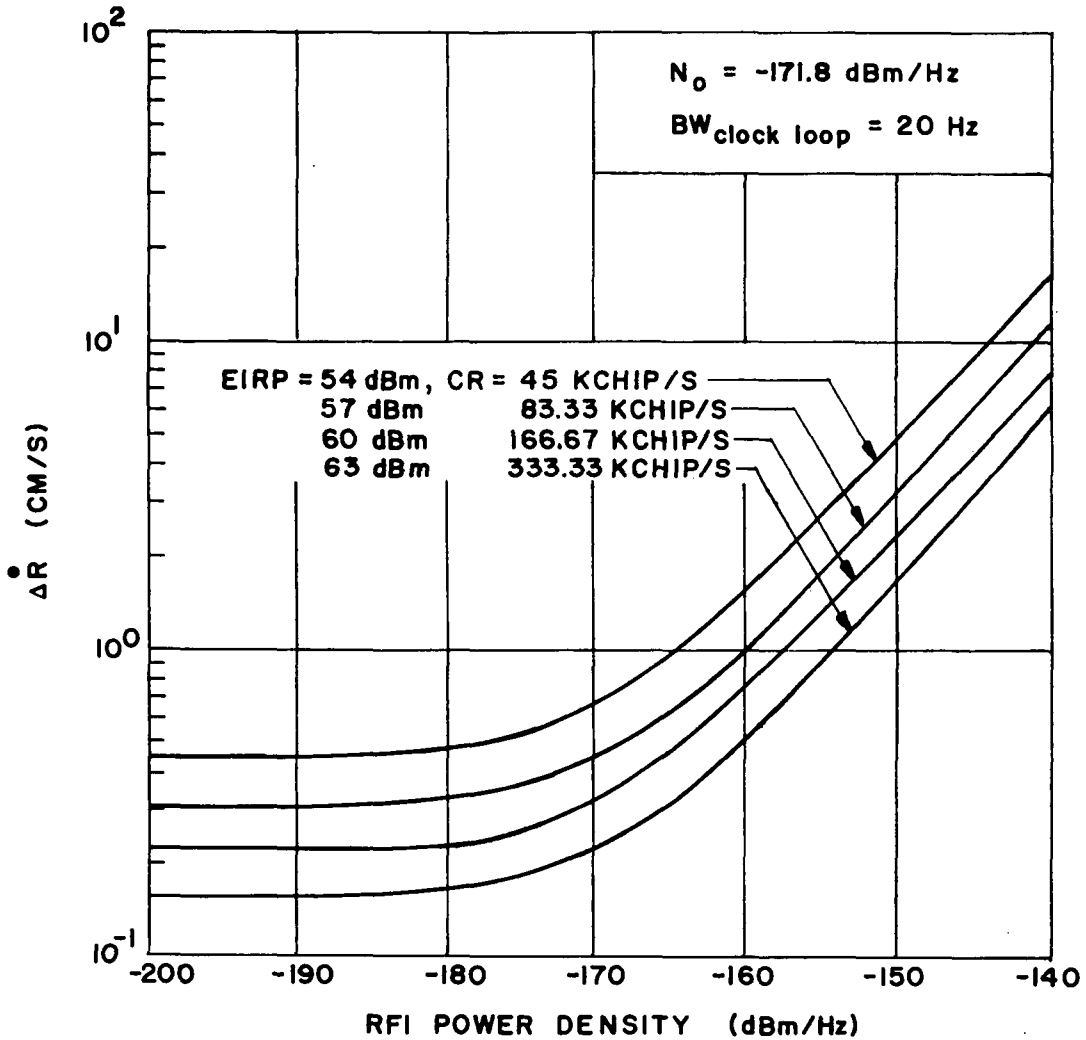

FIGURE 6-16 FORWARD LINK RANGE RATE PERFORMANCE

From Figure 6-14 it is obvious that the multipath in the forward link can be made inconsequential by increasing the PN chip rate so that the multipath is suppressed below the noise level.

Figures 6-17, 6-18, and 6-19 show the expected performance in the return link for a VHF transmission as a function of the EIRP transmitted from the Shuttle to the relay satellite. It is assumed that the relay satellite in this instance has a nominal antenna gain of 15 dB. Curves in Figures 6-17 through 6-19 are drawn for different chip rates, i.e., from 100 kilochips/sec to as high as 1 megachip/sec for the return link. If the AGIPA is used in the return link, an average of 5 to 15 dB improvement in the presence of RFI can be assumed. The AGIPA does not, however, improve the performance of the system in the presence of Gaussian noise. Furthermore, in Figures 6-17 through 6-19 no forward error control encoding is assumed. In addition to AGIPA benefits, the forward error control in the return link could provide an additional 4.7 dB of performance improvement at 10^{-4} bit error probability for a $R=\frac{1}{2}$ K=7 PSK transmission. It can be seen from Figures 6-17 through 6-19 that multipath can be made inconsequential in the return link. An altitude of 300 kilometers is considered worst case in that multipath will be reduced as the user or space shuttle altitude is increased.

Finally, the ΔR and $\Delta \dot{R}$ ranging performance for both the forward and return link are shown in Figures 6-20 and 6-21. The results are based upon the constraint presented above.

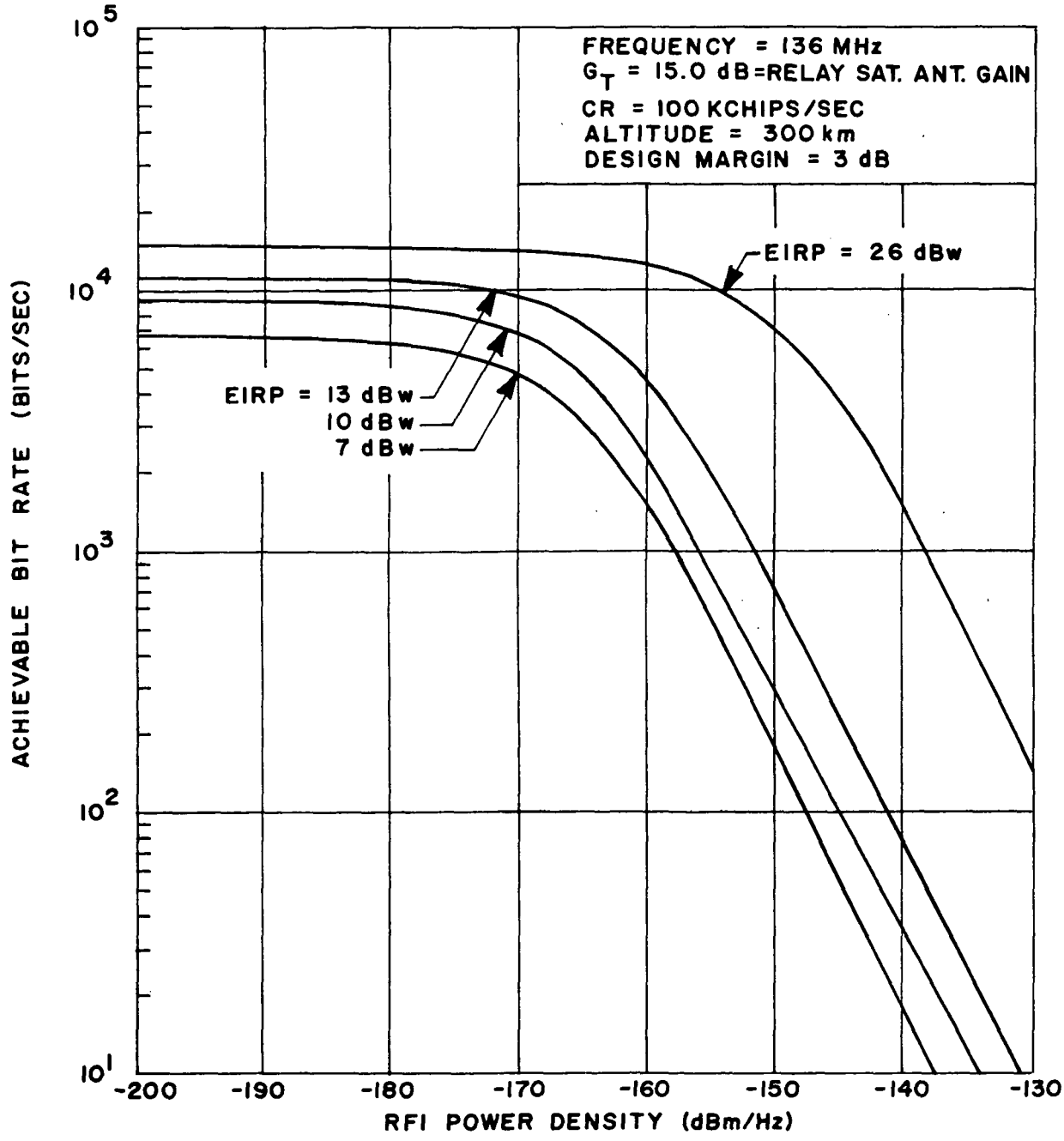

FIGURE 6-17 RETURN LINK PERFORMANCE FOR A CHIP RATE OF 100 KILOCHIPS/SECOND

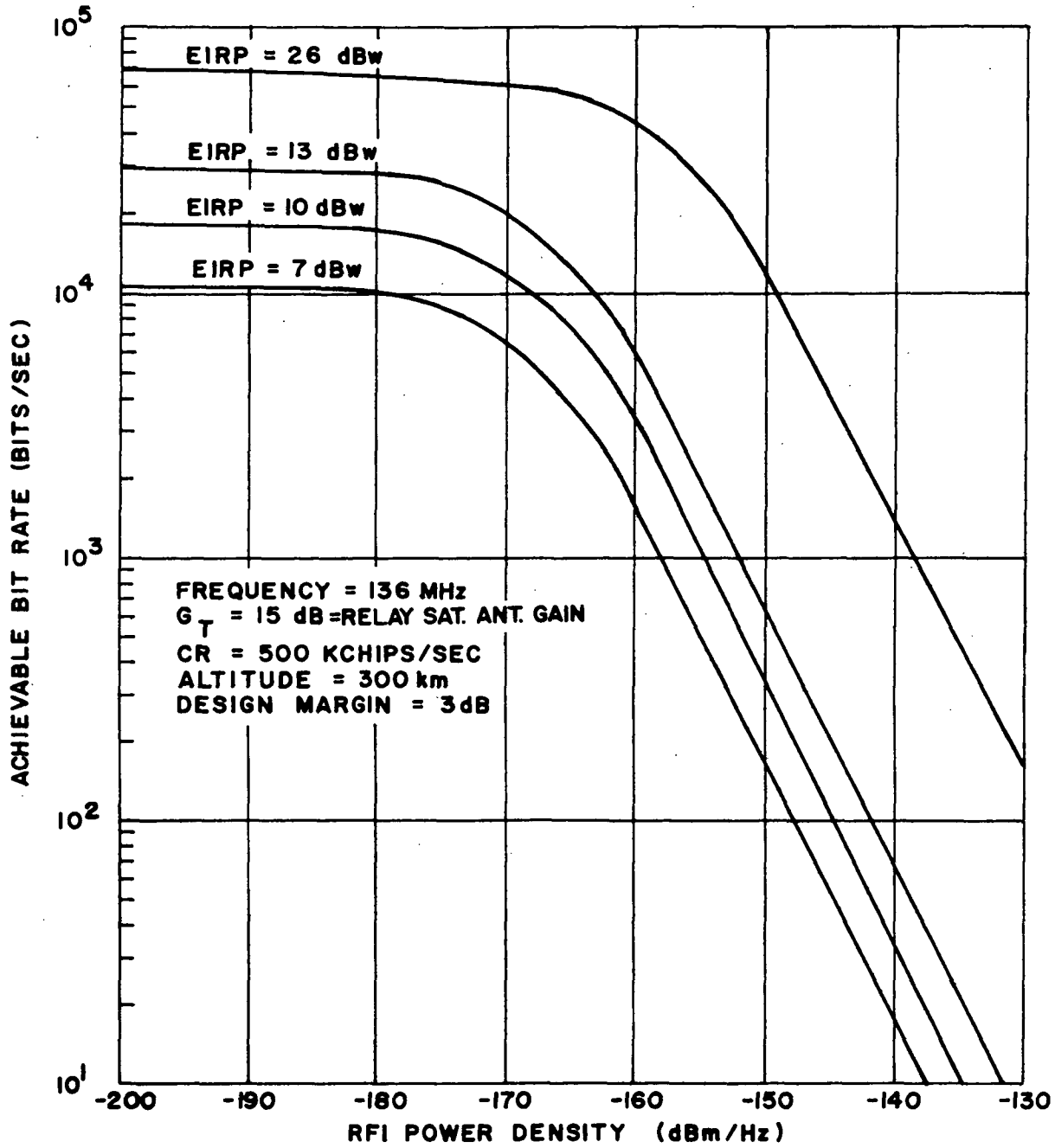

FIGURE 6-18 RETURN LINK PERFORMANCE FOR A CHIP RATE OF 500 KILOCHIPS/SECOND

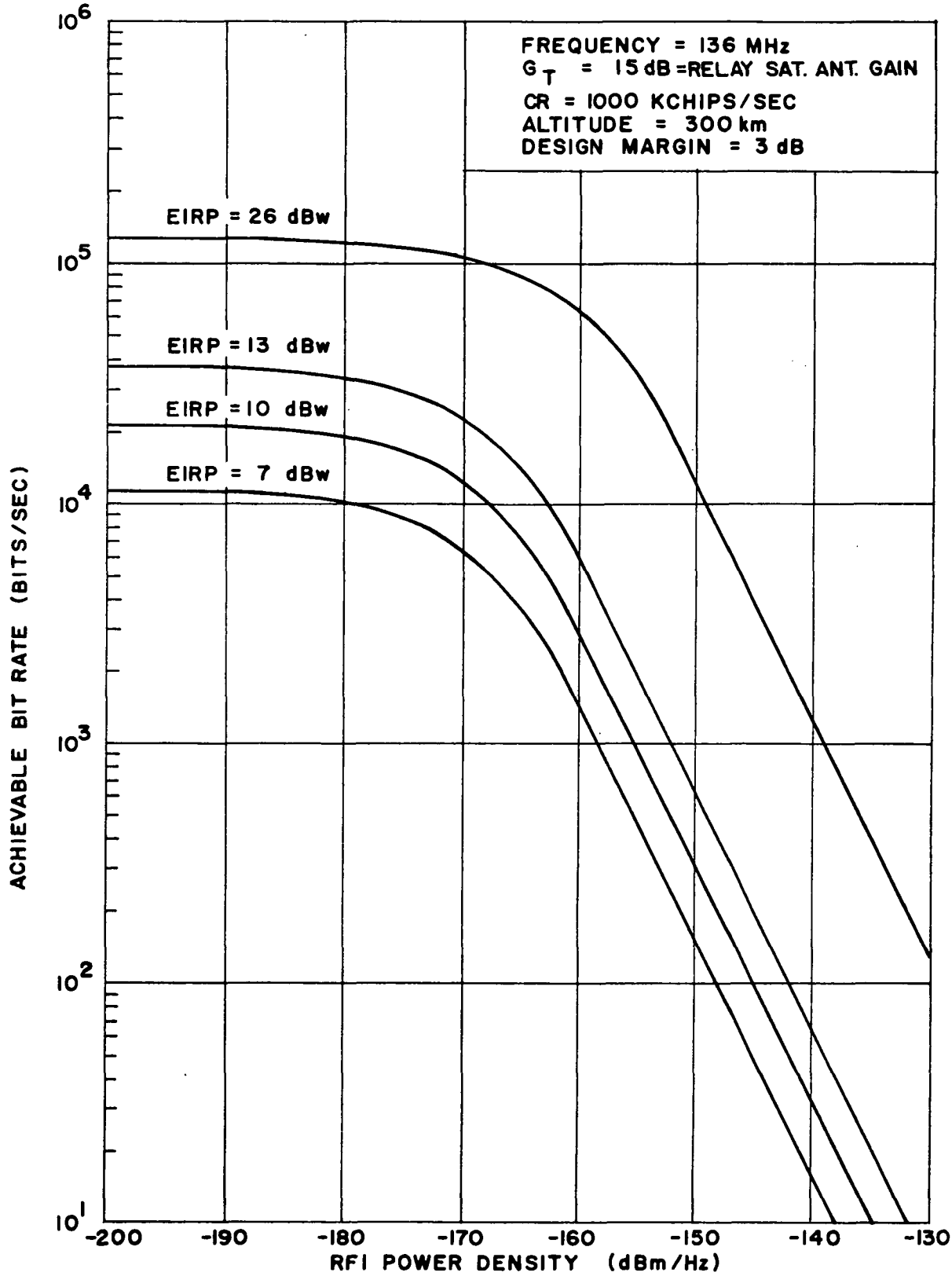

FIGURE 6-19 RETURN LINK PERFORMANCE FOR A CHIP RATE OF 1000 KILOCHIPS/SECOND

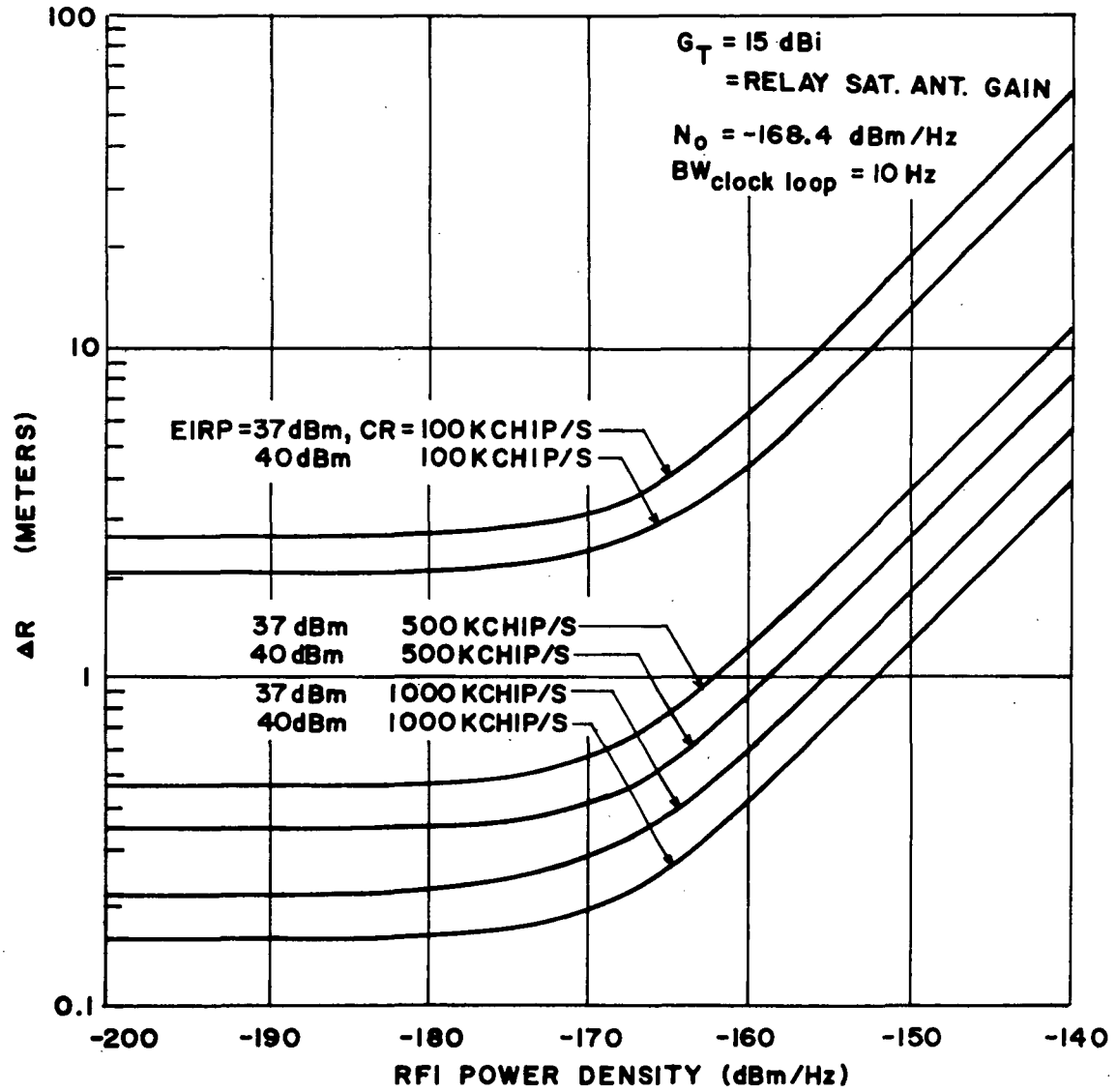

FIGURE 6-20 RETURN LINK RANGING PERFORMANCE

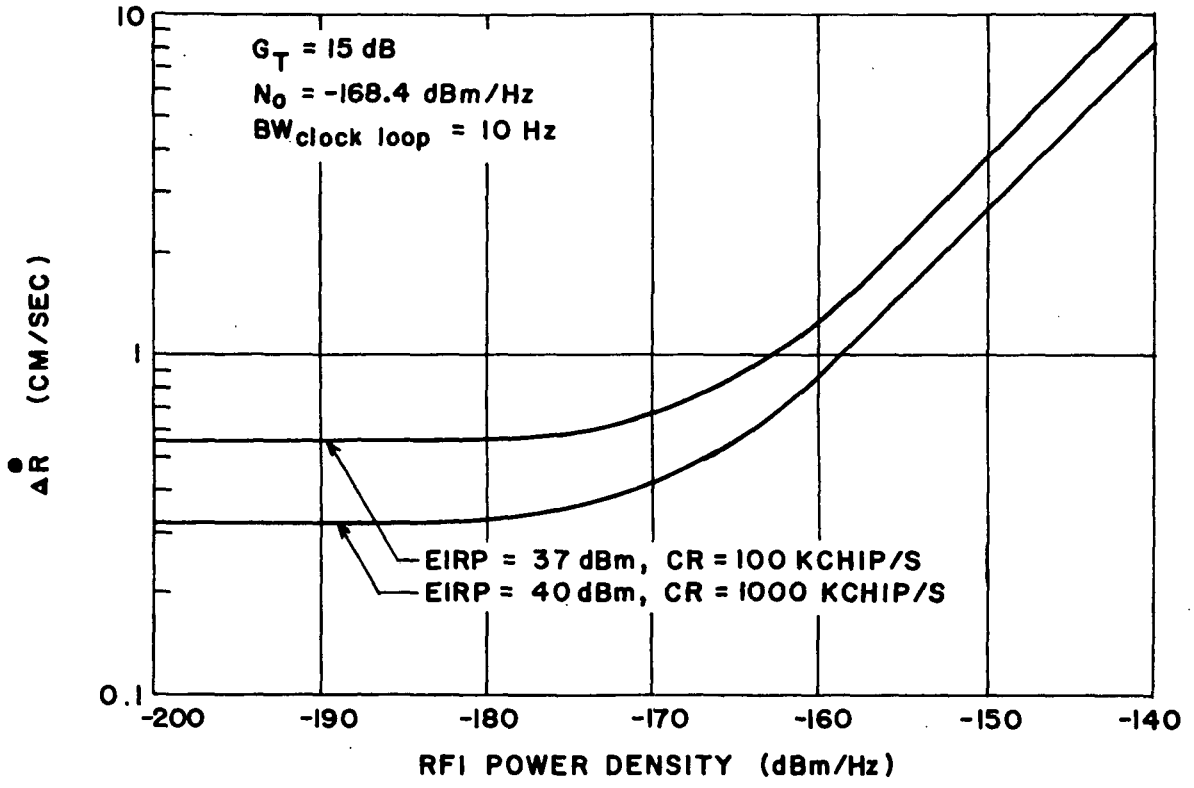

FIGURE 6-21 RETURN LINK RANGE RATE PERFORMANCE

6.3 PERFORMANCE EVALUATION OF THE WIDEBAND FM SYSTEM

The wideband FM system described previously will now be discussed in terms of its performance in the presence of additive noise, CW interference, narrowband RFI, and of course, multipath. To evaluate the wideband FM system properly it is necessary to assess the performance of the system with regard to acquisition, compound phase lock loop tracking, data demodulation, ranging sidetone performance, and Doppler extraction.

In the presence of white Gaussian noise the uplink signal as received by the user will have the form:

$$e_{up}(t) = \sqrt{2P_u} \sin \{\omega_c t + \theta_c(t) + \delta \sin[\omega_{sc} t + \theta_{sc}(t)] + \phi_m(t)\} \quad (6\text{-}27)$$

where P_u = uplink power at user

ω_c = uplink carrier frequency

$\theta_c(t)$ = uplink carrier phase plus Doppler dynamics

δ = wideband FM subcarrier mod index

ω_{sc} = wideband FM subcarrier frequency

$\theta_{sc}(t)$ = wideband FM subcarrier phase

$$\phi_m(t) = \beta d(t) + \rho_1 \sin[\omega_1 t + \theta_1(t)] + \rho_2 \cos[(\omega_1 - \omega_2)t + \theta_1(t) - \theta_2(t)]$$

$$+ 2\rho_A \left(\sin[\omega_3 t + \theta_3(t)] + \sin[\omega_4 t + \theta_4(t)]\right) \cos[(\omega_1 - \omega_2)t + \theta_1(t) - \theta_2(t)]$$

β = peak deviation of the data ~ 1 radian

ρ_1 ~ .5 radian

ρ_2 < 1 radian

ρ_A < 1 radian.

If the compound phase lock loop is tracking properly, a reference signal is generated for the input to the first RF mixer of Figure 5-26. The reference signal has the form:

$$e_{ref}(t) = \sqrt{2} \cos[\omega_c t + \hat{\theta}_c(t) + \delta \sin \omega_{sc} t + \hat{\theta}_{sc}(t))] \qquad (6\text{-}28)$$

Under normal operation the WBFM received signal is compressed into its phase modulated form carrying only the split phase command data and the ranging tones. In these circumstances it is easy to evaluate the performance of the system in the presence of Gaussian noise. To do this we rely upon the well-known work provided by Lindsey (Reference 37).

Based upon Lindsey's formulation the generalized form of an uplink angle modulated carrier by data streams and subcarriers is given by

$$e_{up}(t) = \sqrt{2P} \sin [\omega_c t + \theta(t)] \qquad (6\text{-}29)$$

where P = total power

$\theta(t)$ = composite angle modulation $= \sum_{n=1}^{N} \rho_n \cos \omega_n t + \sum_{m=1}^{M} \beta_m sq_m$

ρ_n = peak phase deviation for the sine wave subcarriers

β_m = peak phase deviation for the square wave (sq_m) subcarriers

Both the sine wave subcarriers and square wave subcarriers are modulated by independent binary data sources.

The above RF signal can be rewritten in a more useful form:

$$e_{up}(t) = \sqrt{2P}\ Im[\exp(j\omega_c t)\ \exp(j\theta(t))] \qquad (6\text{-}30)$$

where $Im[\cdot]$ denotes the imaginary parts of the quantity contained within

the brackets. Furthermore, the exponential modulation may be expanded by the well-known form (Reference 37):

$$\exp(j\theta(t)) = \prod_{n=1}^{N} \prod_{m=1}^{M} \exp(j\rho_n \cos \omega_n t) \exp(j\beta_m sq_m) \tag{6-31}$$

Furthermore,

$$\exp(jZ \cos \theta) = \sum_{\ell=-\infty}^{\infty} j^{\ell} J_{\ell}(Z) \exp(j\ell\theta) \tag{6-32}$$

With the above expression and the fact that both sine wave and square wave subcarriers are assumed to be biphase modulated by the data, the power in the residual carrier and respective channels can be calculated.

Very often the power which remains in the residual carrier is of interest, and it follows from Equation 6-32 that the ratio of the residual power to the total power for a generalized square wave and sine wave frequency modulated PM carrier is

$$\frac{P_c}{P} = \prod_{n=1}^{N} J_0^2(\rho_n) \prod_{m=1}^{M} \cos^2\beta_m \tag{6-33}$$

Furthermore, the power in each of the sine wave subcarriers is given by

$$\frac{P_n(j)}{P} = 2 J_1^2(\rho_n(j)) \prod_{\substack{n=1 \\ n\neq j}}^{N} J_0^2(\rho_n) \prod_{m=1}^{M} \cos^2\beta_m \tag{6-34}$$

for zero phase error in the carrier recovery loop, while the power in the binary square wave subcarriers is:

$$\frac{P_m(j)}{P} = \sin^2\beta_m(j) \prod_{n=1}^{N} J_0^2(\rho_n) \prod_{\substack{m=1 \\ m\neq j}}^{M} \cos^2\beta_m \tag{6-35}$$

for zero phase error in the carrier recovery loop.

Unfortunately some power is lost as a result of intermodulation terms if conventional detectors are employed in the receiver. However, if more sophisticated approaches are taken some of the intermodulation losses can be retrieved and the efficiency of the system improved. In most conventional systems, though, the intermodulation losses are not retrieved, but are lost in the detection process. The cross modulation terms do not interfere with detection but serve to reduce the power available for the detection process; thus, they serve to reduce the overall efficiency of the systems.

The power lost due to cross modulation terms is

$$\frac{P_{cm}}{P} = 1 - \frac{P_c}{P} - \sum_{j=1}^{N} \frac{P_n(j)}{P} - \sum_{j=1}^{M} \frac{P_m(j)}{P} \qquad (6\text{-}36)$$

The modulation indices recommended for the data and the sine wave ranging tones are given in Reference 35 as:

β = 1 radian

ρ_1 = .5 radian

ρ_2 = .16 radian

ρ_A = .11 radian

Based upon the above recommended modulation indices, we can now calculate the amount of power,and therefore signal-to-noise ratio,available to the data signal and to each of the sidetone ranging signals:

$$\frac{P_c}{P_{total}} = \cos^2\beta \; J_o^2(\rho_1) \; J_o^2(\rho_2) \; J_o^2(\rho_A) \qquad (6\text{-}37)$$

$$\frac{P_{data}}{P_{total}} = \sin^2\beta \; J_o^2(\rho_1) \; J_o^2(\rho_2) \; J_o^2(\rho_A) \qquad (6\text{-}38)$$

$$\frac{P_{\text{tone \#1}}}{P_{\text{total}}} = 2J_1^2(\rho_1)\cos^2\beta\, J_o^2(\rho_2)\, J_o^2(\rho_A) \qquad (6\text{-}39)$$

$$\frac{P_{\text{tone \#2}}}{P_{\text{total}}} = 2J_1^2(\rho_2)\cos^2\beta\, J_o^2(\rho_1)\, J_o^2(\rho_A) \qquad (6\text{-}40)$$

$$\frac{P_A}{P_{\text{total}}} = 2J_1^2(\rho_A)\cos^2\beta\, J_o^2(\rho_1)\, J_o^2(\rho_2) \qquad (6\text{-}41)$$

It follows from equation 6-38 that, based upon PSK transmission, the bit error probability can be calculated as

$$P_e = \frac{1}{2}\,\text{erfc}\sqrt{\frac{P_{\text{total}}\sin^2\beta\, J_o^2(\rho_1)\, J_o^2(\rho_2)\, J_o^2(\rho_A)\, T}{N_o}} \qquad (6\text{-}42)$$

It is seen that relative to a standard PSK transmission the proposed wideband FM system, in the presence of Gaussian noise, is inferior by 3.7 dB. The unavoidable sharing of power among the range tones and data channels steals power from the data channel producing the 3.7 dB loss relative to an ideal PSK signal.

6.3.1 THE EFFECTS OF CW INTERFERENCE ON THE DATA CHANNEL OF A WIDEBAND FM SYSTEM

In addition to the effects of Gaussian noise, there is a potential degradation to the WBFM system from CW interference. Specifically, if CW interference falls close to one of the wideband FM subcarrier sidebands, potentially severe degradation can occur in the form of an increase in the

variance of the carrier phase error. Measurements by Britt and Palmer (Reference 36) indicate that for a second order phase lock loop the variance as a function of the interference power to signal power is:

$$\sigma_\theta^2 = \frac{N/P_{direct}}{1 + I/P_{ind}} + \frac{I}{2P_{direct}} \qquad (6\text{-}43)$$

The interference power I is taken as the CW power falling within the loop bandwidth; P is the carrier power; and N is the noise power within the loop bandwidth. For interference-to-signal levels which are small, the above equation reduces to

$$\sigma_\theta^2 = \frac{N}{S} \qquad (6\text{-}44)$$

which is a standard result for Gaussian noise interference.

To evaluate I/S in the carrier loop we must consider what happens when a CW interference (or narrowband interference) is near one of the subcarrier sidebands as shown in Figure 6-22.

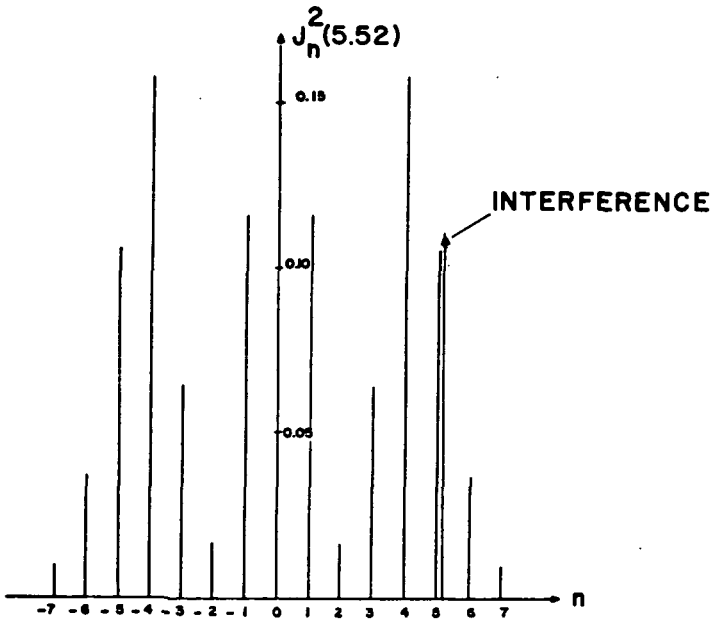

FIGUR E 6-22 INTERFERENCE NEAR SUBCARRIER SIDEBAND

The output of the first mixer, assuming proper carrier tracking, is

$$\sqrt{2I}\cos\Delta\omega t \quad J_n(5.52) \qquad (6\text{-}45)$$

where n denotes the order of the subcarrier sideband; $J_n^2(5.52)$ can take on values of 0.1156 for n=1, 0.01516 for n=2, etc. Note that if the interference is near n=5, the interference is suppressed only by 8 dB. However, the data and range tone modulation indices suppress the carrier component after the mixer by approximately 6 dB. Thus an interfering signal with power equal to the total uplink power at the spacecraft will be suppressed only 2 dB relative to the carrier compressed component. Likewise if the CW interference is separated from an n=5 sideband by the nominal tone frequency, the interference will show up in the range tone filter which can rob power and/or increase the range tone phase error.

Another potential source of degradation to the wideband FM system is CW interference which is close to or is overlapping the spectrum of the data around any of the wideband FM subcarrier sidebands at the RF input to the receiver. To evaluate the effect of CW interference on the data demodulation, we use the model as illustrated in Figure 6-23.

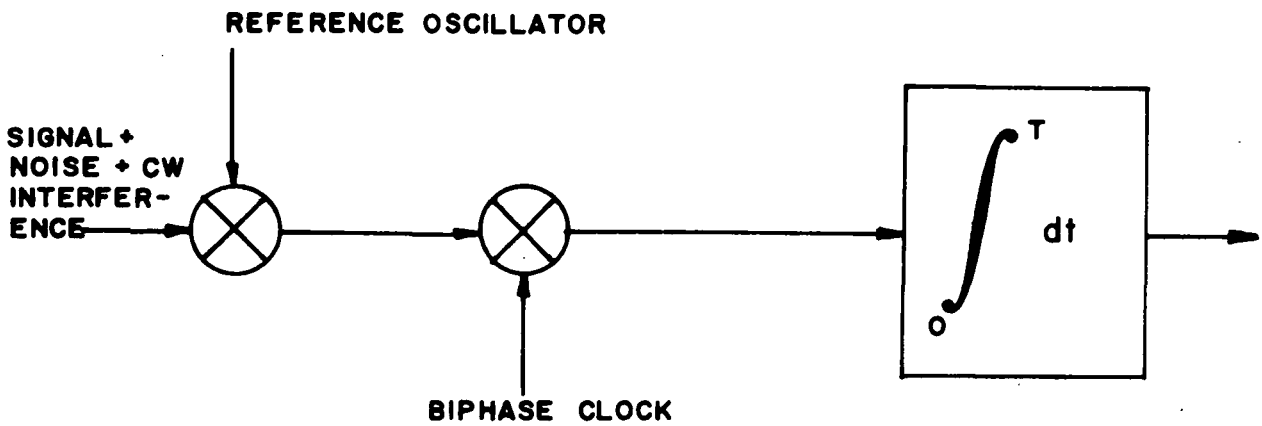

FIGURE 6-23 DATA DEMODULATOR

The receiver consists of a matched filter, i.e. a bi-phase clock signal which multiplies the incoming signal plus noise plus interference followed by an integrate and dump (I&D) over the interval of the data bit. The following mathematical derivation illustrates the effect of the bi-phase coding and the integrate and dump circuit on the CW interference.

Let the CW interference be $B \sin(\Delta\omega t + \omega_o t + \theta)$; the signal, $\pm\sqrt{2P_{data}} \cos \omega_o t$; and the noise, white with density N_o watts per Hertz. The output of the I&D will consist of the signal energy $E = P_{data}T$, N_o (the noise density), and a term associated with the interference. The interference term, however, is dramatically affected by the bi-phase decoder and the integrate and dump.

The interference is offset from the carrier by $\Delta\omega$ and the phase angle is θ. The output of the I&D due to the CW interference is easily shown to be

$$\frac{B}{\sqrt{2P_{data}}} \frac{\sin^2(\Delta\omega T/4)}{(\Delta\omega T/4)^2} \left|\frac{\Delta\omega T}{4}\right| \cos\left(\theta - \frac{\Delta\omega T}{2}\right) . \qquad (6\text{-}46)$$

Thus the error probability can be written as

$$P_e = \frac{1}{2\pi} \int_{-\pi}^{\pi} \frac{1}{2} \operatorname{erfc}\left\{\sqrt{\frac{P_{data}T}{N_o}\left[1 + \frac{B}{\sqrt{2P_{data}}} \frac{\sin^2(\Delta\omega T/4)}{(\Delta\omega T/4)^2} \cdot \left|\frac{\Delta\omega T}{4}\right| \cos\psi\right]}\right\} d\psi \qquad (6\text{-}47)$$

where T is the duration of the binary symbol and

$$P_{data} = P_{total} \sin^2\beta \, J_o^2(\rho_1) \, J_o^2(\rho_2) \, J_o^2(\rho_A).$$

Equation 6-47 has been evaluated on a digital computer with results illustrated in Figure 6-8 where $0.1 \leq K_D \leq 1.0$ where K_D is the coefficient of

cos ψ in equation 6-47. A small amount of interference can serve to degrade the performance of the data channel dramatically. Also, equation 6-47 illustrates that the I&D transfer function (preceded by the multiplication of the signal, noise, and interference by the bi-phase signal) will diminish the effects of the interference depending upon its separation $\Delta\omega$ relative to the carrier reference frequency.

The amount of spectrum which is actually susceptible to interference can be determined from the fact that approximately 12 significant sidebands exist in the wideband FM spectrum for $\delta = 5.52$. The data bandwidth, if it is split phase coded, will have a bandwidth approximately twice the data rate. This means that the spectrum bandwidth which is susceptible to interference is given by

$$4 \times \text{Bit Rate} \times 12 = 48 \times \text{Bit Rate} \qquad (6\text{-}48)$$

The susceptible bandwidth can be considerable at the higher bit rates.

6.3.2 THE EFFECTS OF CW INTERFERENCE ON RANGE TONE TURNAROUND PROCESSING

The interference which lies near a ranging sidetone in the RF spectrum can have a degrading effect on the ranging performance for a number of reasons. If the CW interference lies close enough to the ranging sidetones, a phase error, as given by equation 6-46, is generated. Furthermore, if the CW interference is within the sidetone ranging spectrum such that the CW interference is turned around, and if the CW interference is significant, it will suppress the amount of power in the ranging signals, thus degrading the performance in the return link. Another problem occurs when CW interference is near the ranging tones so that false lock can result in the ground station equipment.

6.3.3 EFFECTS OF NARROWBAND RFI ON THE WIDEBAND FM SYSTEM

First we define what is meant by narrowband RFI. Typically, in the bands of interest, RFI takes the form of modulated carriers having bandwidths of 15 kHz to 75 kHz. This constitutes narrowband RFI.

To evaluate the impact of narrowband RFI on the carrier tracking, we assume that the RFI signal power is distributed uniformly across its information bandwidth B_I. If this is the case, then with the narrow bandwidths associated with the carrier tracking loops, we can assume that the interference will appear as Gaussian noise. In such a case, equation 6-43 for the phase error in the carrier or sidetone loops becomes

$$\sigma_\theta^2 = \frac{N + I(B_L/B_I)}{S} \tag{6-49}$$

where B_L = Loop bandwidth.

Narrowband RFI can also adversely effect data demodulation. The narrowband RFI has a bandwidth B_I which can be less than, equal to, or greater than the bandwidth of the data. In Section 6.1.2 we derived the bit error probability for a bi-phase coded signal in the presence of CW interference. Obviously CW interference sets an upper bound on the bit error probability since all of the interference is contained within the detection bandwidth. In the case of narrowband RFI, the interfering signal power is distributed over a wider bandwidth and thus the post detection integrate and dump bandwidth can discriminate against some of the interference. Without an exact knowledge of the modulation process involved with the narrowband RFI, it is difficult to determine a precise formula for the bit error probability. However it can be bounded between two extremes, i.e., the bandwidth of the RFI much less than the data bandwidth and the bandwidth of the RFI greater than the bandwidth of the data. These bounds are:

$$\frac{1}{2}\,\mathrm{erfc}\sqrt{\frac{P_{data}\,T}{N_o + I/B_I}} < P_\varepsilon < \frac{1}{2\pi}\int_{-\pi}^{\pi} \frac{1}{2}\,\mathrm{erfc}\left\{\sqrt{\frac{P_{data}\,T}{N_o}} \cdot \left[1 + \sqrt{\frac{I}{P_{data}}}\left(\frac{\sin(\Delta\omega T/4)}{\Delta\omega T/4}\right)^2 \left|\frac{\Delta\omega T}{4}\right| \cos\psi\right]\right\} d\psi \qquad (6\text{-}50)$$

6.3.4 THE EFFECTS OF SPECULAR AND DIFFUSE MULTIPATH ON THE WIDEBAND FM SYSTEM

One major problem which confronts the successful operation of the wideband FM system is that the multipath in its entirety competes with the direct path signal under certain conditions of delay between the direct path and the reflected signal. For example, when the multipath time spread is relatively small, the multipath signal can overlay the signal arriving by the direct path. This overlay condition depends upon the period of the subcarrier used in the modulation process. For example, if a 120 kHz subcarrier is employed with a modulation index of 5.52, and if the time delay between the direct and the indirect paths is 8 microseconds, then the multipath signal will completely overlay in both time and frequency the signal received via the direct path, as shown in Figure 6-24. This situation can occur quite frequently, and establishes the upper bound on the performance of the system.

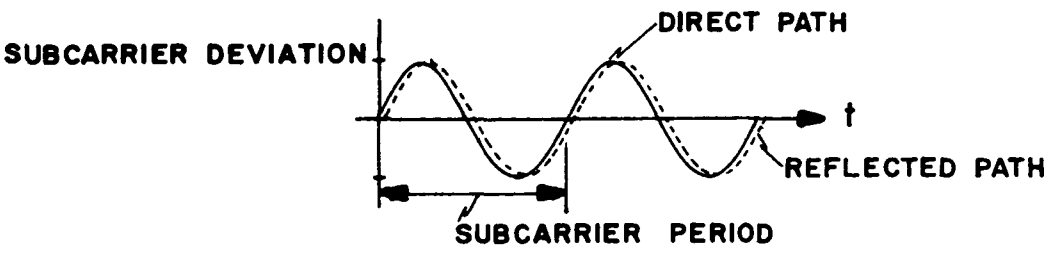

FIGURE 6-24 MULTIPATH OVERLAYS DIRECT SIGNAL

When the multipath overlays the direct path signal in both time and frequency, the frequency compressive action at the receiver simply folds the multipath signal in with the direct path signal and the system is equivalent to a PM modulated system consisting of a data transmission channel and ranging sidetones in the presence of multipath signals as,illustrated in Figure 6-25.

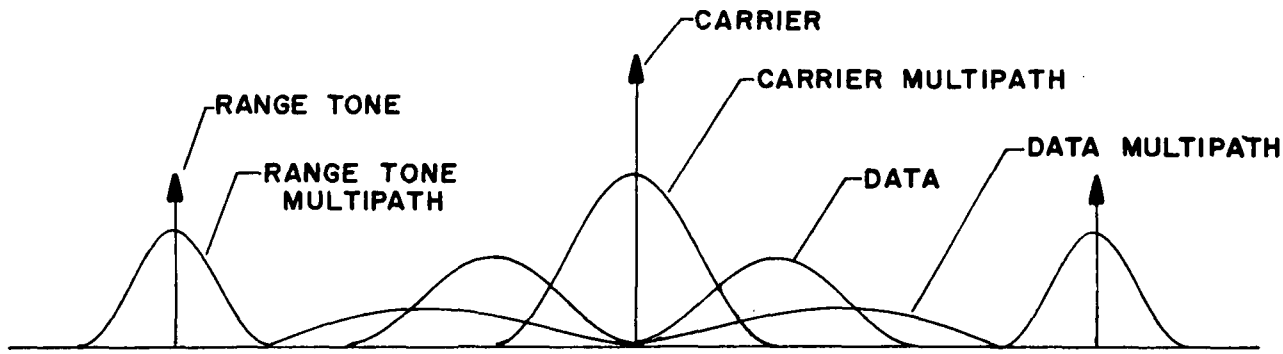

FIGURE 6-25 COMPOSITE PM SPECTRUM INCLUDING MULTIPATH

The model that we will use to evaluate the performance of the system consists of multipath which is noiselike representing diffuse components, and specular reflection representing a reflected version of the signal in the case of data transmission, and CW components in the case of the rangetones. These components will be offset in frequency relative to the direct path by the differential Doppler.

The degrading effects of both specular and diffuse multipath on the PSK data transmission have already been assessed in Section 6.1.1. Therefore, the evaluation of the effects of both specular and diffuse multipath on the wideband FM data channel will not be carried out here.

It is evident from Figure 6-25 that the multipath can interfere with the carrier and interfere with the sidetone associated with the wideband system. Furthermore, the multipath can serve to rob power from the range tone signals when the signals are turned around in the user transponder.

Assuming that the multipath consists of both specular and diffuse components, the carrier phase error can be determined to be

$$\sigma^2_{\theta_{\substack{\text{carrier}\\ \text{max}}}} = \frac{\left[N_o B_{CL} + \frac{B_{CL}}{B_F} P_{diff}\right] \frac{1}{P_{direct}}}{1 + \frac{P_{spec}}{P_{direct}}} + \frac{P_{spec}}{2P_{direct}} \qquad (6\text{-}51)$$

where B_{CL}=carrier loop bandwidth and B_F =fading bandwidth. The diffuse power acts as a noise-like component which falls within the loop bandwidth while the specular multipath acts like CW interference which also increases the phase error of the carrier. Equation 6-51 is the maximum carrier phase error resulting from multipath. When the differential Doppler is moderate to large the specular power can fall outside the loop bandwidth and only diffuse multipath contributes to the carrier phase error.

In like manner the same effect is true for the range tone. That is, the phase error σ^2_θ of a single range tone subcarrier has the same form as Equation 6-51. The actual equivalent rms range error

contributed by multipath, both specular and diffuse, and by ambient noise can be determined to be

$$\Delta R = \frac{c}{4\pi f_R} \sqrt{\frac{N_o B_L + \frac{B_L}{B_F} P_{diff} \frac{1}{P_{direct}} + \frac{P_{spec}}{2P_{direct}}}{1 + \frac{P_{spec}}{P_{direct}}}} \qquad (6\text{-}52)$$

where f_R is the range tone frequency. It is evident from equation 6-52 that a small amount of multipath can dramatically effect the performance of the sidetone ranging system depending upon the intensity of the multipath components, differential Doppler, and the fading bandwidth. The differential Doppler will determine whether the multipath specular component falls within the carrier loop bandwidth or falls within the sidetone ranging loop bandwidth. The ratio of the carrier loop bandwidth to the fading bandwidth will determine the amount of diffuse power which appears in the loop to increase the phase error.

In addition to increasing phase error on both the carrier and subcarrier, the multipath signal will compete for power with the sidetone signals in the turnaround mode. The percentage of power which will be devoted to the sidetone signals in the presence of multipath and noise is given by

$$\frac{\sum P_{sidetones}}{\sum P_{sidetone} + P_{specular} + P_{diffuse}} \times 100\% \qquad (6\text{-}53)$$

If the multipath signal is of the same order of magnitude as the direct path signal then power suppression of at least 3 dB will occur when the sidetone signals are turned around in the user transponder for the downlink transmission.

Multipath incurred on the downlink will serve to increase the carrier and subcarrier phase errors discussed above. Since this multipath energy is uncorrelated with the uplink or forward link multipath, the rms phase errors will increase as the square root of the sum of the squares of the uplink and downlink phase errors.

6.3.5 CONCLUSIONS CONCERNING PERFORMANCE OF THE WIDEBAND FM SYSTEM IN THE PRESENCE OF NOISE, RFI, AND MULTIPATH

In the previous section it has been shown that the wideband FM system is susceptible to noise; interference; and, in some instances, multipath. In addition to these degredations outlined above, false lock problems are of real concern. If the bit rates which are used are typical of Shuttle requirements, then the bandwidth which is susceptible to RFI is 48 times the bit rate. If this bit rate is equivalent to one voice channel and one telemetry channel, then the bandwidth which is susceptible to RFI is approximately 1 MHz. In other words, the wideband FM system is extremely susceptible to RFI for any reasonable data rates.

Table 6-2 gives a qualitative evaluation of the wideband FM system's performance for RFI and multipath.

TABLE 6-2
QUALITATIVE EVALUATION OF
PERFORMANCE OF WIDEBAND FM SYSTEM

MODE	RFI	MULTIPATH
Data	severe	severe
Carrier Tracking	can be severe depending on bandwidth of interference	narrow loop bandwidth makes problem not severe
Ranging	severe	can rob power from sidetones in turnaround operation

7. MULTIPATH MEASUREMENT TECHNIQUES

There are a large number of techniques for measuring multipath. These techniques have been evolved over the past ten years and most of them have been applied to multipath measurements in the HF, troposcatter, and aircraft-to-satellite links. Shown in Table 7-1 are several approaches which represent basic techniques for multipath measurements.

TABLE 7-1

MULTIPATH MEASUREMENT TECHNIQUES

1) Antenna Discrimination (AD)
2) Short Pulse (Single Frequency)
3) Short Pulse (Multiple Frequency)
4) Combination of 2, 3, and 1
5) CW or Multitone Transmission with AD
6) Wideband Probe Signals

In the first approach, the direct path signal and the reflected signal are separated spatially via separate antennas. We refer to this as spatial discrimination of the direct and the indirect paths. This approach can be common to a variety of multipath signal processing measurement techniques such as pulse, CW, wideband signals, etc. The basic advantages of the antenna discrimination approach is that the direct path can be measured separately from the reflected signal and vice versa, that is, the reflected signal can be measured independent of the direct path if the antenna patterns provide sufficient isolation between the two signal paths. Furthermore, the reflected signal's polarization can be determined if both right- and left-hand polarization senses are available at the antenna which is monitoring the reflected signal.

Another advantage of the antenna discrimination technique is that moderate (5-7 dB) gain, which is often required when measuring multipath from high altitude platforms such as satellites, can be provided for both the direct path and the reflected signal path.

The basic disadvantage of the antenna technique is that in certain cases special antenna designs are required in order to point the respective patterns at the direct path signal source and at the reflected signal source. To date, this has been accomplished effectively by the FAA and its contractor, Boeing, who have used the antenna discrimination technique to measure multipath from the ATS-5 satellite using a KC-135 at L-band. The tests have been conducted for grazing angles of nominally 0.19 to 0.38 radian (10° to 20°). Note that if polarization of the reflected signal is to be measured, then some form of antenna spatial discrimination will be required.

7.1 LOW GAIN ANTENNA PATTERNS FOR ANTENNA DISCRIMINATION

In order to separate the direct path from the reflected signal, circularly polarized antennas on the platform will probably be used on the low altitude platform (SATS, aircraft, balloons, etc.). These antennas might be directive as they are on board the Boeing KC-135 aircraft used in the ATS-5/aircraft tests for the FAA at L-band. More than likely, however, antennas on balloons, U-2 aircraft,etc., will not be directive. Therefore, antennas must be selected which have moderate gain, good front to back ratios, circular polarization, and uniform gain patterns.

Shown in Figures 7-1 and 7-2 are the measured patterns for a crossed dipole and a crossed slot antenna. Table 7-2 shows the measured results for

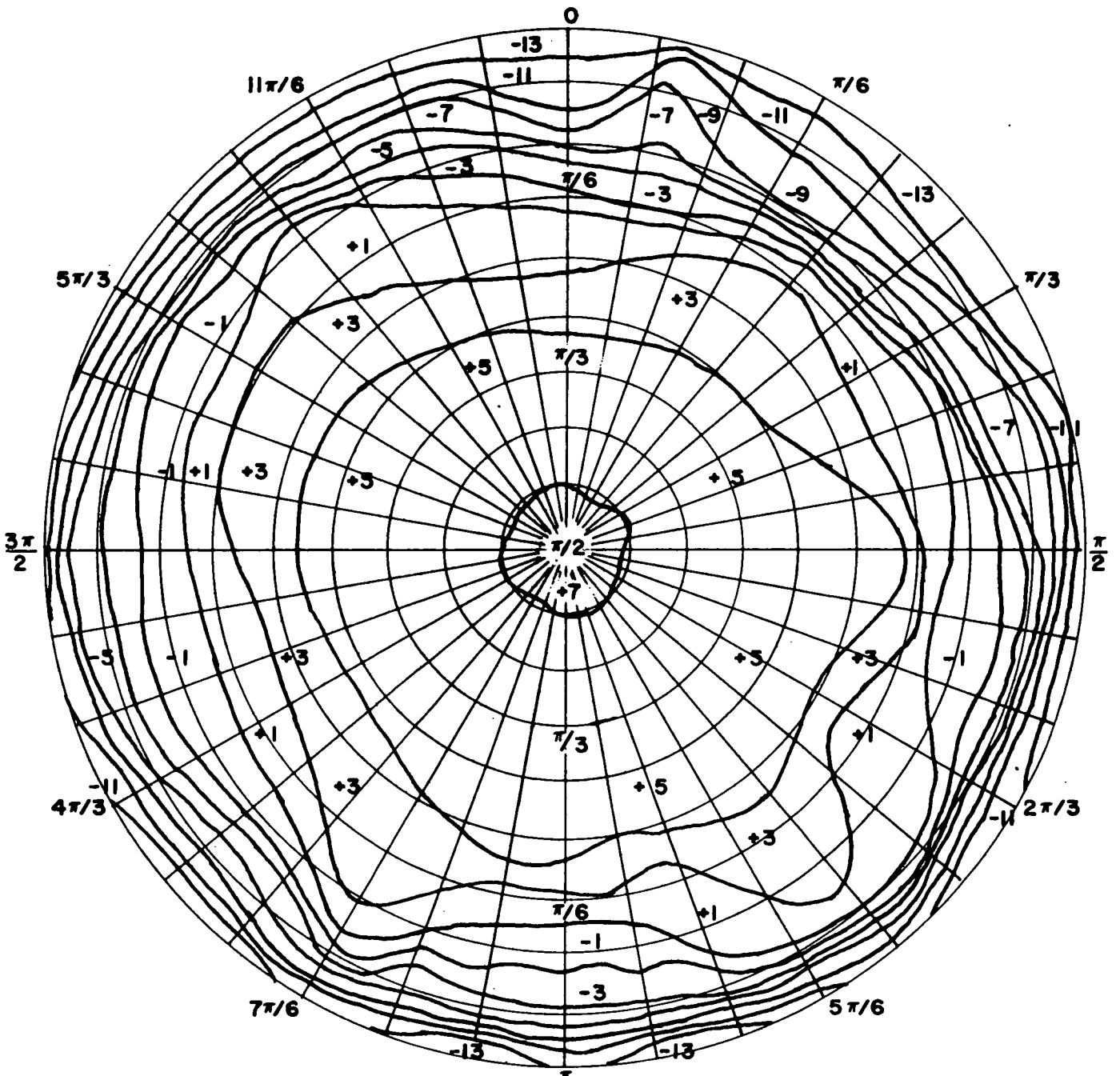

NOTE: SIGNED NUMBERS ARE GAINS IN dB

FIGURE 7-1 CONSTANT GAIN CONTOURS FOR UHF CROSSED DIPOLE ANTENNA

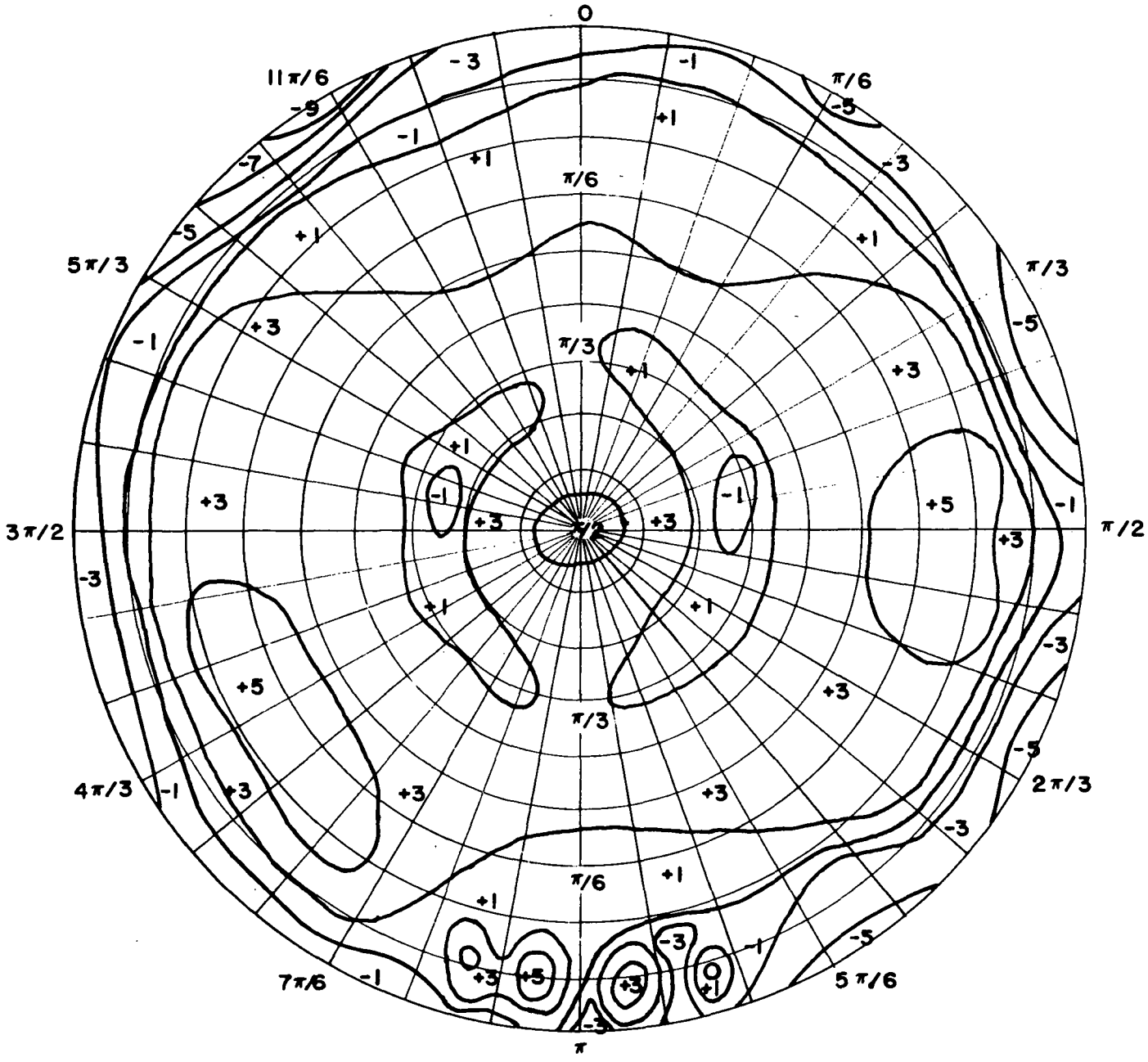

NOTE: SIGNED NUMBERS ARE GAINS IN dB

FIGURE 7-2 CONSTANT GAIN CONTOURS FOR UHF CROSSED SLOT ANTENNA

TABLE 7-2

AVERAGE GAIN FOR TWO UHF AIRBORNE ANTENNAS

Elevation Angle	Crossed Slot	Crossed Dipole
0-0.174 rad. (0-10 deg.)	-0.9 dB	-7.5 dB
0.174-0.349 rad. (10-20 deg.)	+1.1	-2.1
0.349-0.524 rad. (20-30 deg.)	+3.0	+0.5
0.524-0.698 rad. (30-40 deg.)	+2.9	+2.8
0.698-0.872 rad. (40-50 deg.)	+3.0	+4.2
0.872-1.05 rad. (50-60 deg.)	+2.5	+4.9
1.05 -1.22 rad. (60-70 deg.)	+1.4	+5.0
1.22 -1.40 rad. (70-80 deg.)	+3.0	+5.0
1.40 -1.57 rad. (80-90 deg.)	+4.1	+7.0
0-0.174 rad. (0-10 deg.)	-0.9	-7.5
0.174-0.349 rad. (10-20 deg.)	+0.6	-4.6
0.349-0.524 rad. (20-30 deg.)	+1.4	-2.1
0.524-0.698 rad. (30-40 deg.)	+1.8	-0.4
0.698-0.872 rad. (40-50 deg.)	+2.0	+0.5
0.872-1.05 rad. (50-60 deg.)	+2.1	+1.7
1.05 -1.22 rad. (60-70 deg.)	+2.0	+1.9
1.22 -1.40 rad. (70-80 deg.)	+2.1	+2.1
1.40 -1.57 rad. (80-90 deg.)	+2.1	+2.2

Gain computed relative to circularly polarized isotropic antenna.

these antennas. It is apparent that the crossed dipole antenna gives good performance in terms of the desired characteristic. Other antennas which exhibit circular polarization are listed in Table 7-3. The cavity backed dual planar spiral, which can be flush mounted, may be attractive as a Space Shuttle antenna at UHF or S-band since it does not protrude and has moderate gain.

7.2 SHORT PULSE TECHNIQUES

A traditional technique for measuring multipath utilizes a low duty cycle pulse transmission. In this scheme a narrow pulse is transmitted and not retransmitted until the multipath signal has arrived at the receiver. In this way the direct signal and multipath signal can be separated in time to avoid overlap. The pulse width must be narrow enough so that the multipath signal can be resolved accurately. While the approach is simple, most emitters are peak-power limited (e.g., SATS). Another problem facing the low duty factor high peak power pulse technique for measuring multipath is that the rate at which the pulses are transmitted should be at least twice the expected rate of the fading bandwidth of the reflected signal. This requirement is based upon the Nyquist sampling rate required to describe a signal of a specific bandwidth. It also follows that the transmission period of pulses must be greater than the differential time delay T_d plus the time delay spread T_s in the reflected path, as shown in Figure 7-3. Therefore, when a single frequency pulse transmission is used, the repetition rate of the pulses can be related to the sum of the differential time delay and multipath spread by:

$$\text{Pulse Period} > T_d + T_s \qquad (7\text{-}1)$$

TABLE 7-3

CIRCULARLY POLARIZED ANTENNAS

ANTENNA TYPE	GEOMETRY (Not to Scale)	PATTERN SHAPE	DIRECTIVITY (dBi)	BANDWIDTH	COMPLEXITY (Rel. Cost)	MECHANICAL STRENGTH	COMMENTS	REFERENCE
Turnstile		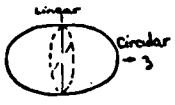	2.15 dB 5.15 dB with gnd. plane	Depends on elements and feed	3	5	-Circularly polarized only along axis (z-direction); elliptically polarized off axis, linearly polarized in plane of dipoles. - Directive arrays can be used for elements. -Dipole elements can be bent to steer antenna.	Kraus, Antennas Reed & Russel, UHF Propagation
Normal Mode Helix	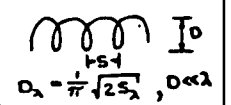		+2.15 dB 5.15 dB with gnd. plane	small because of size	1	1	-Circular polarized at all angles with proper geometry -Poor impedance bandwidth because of small size -Circular polarization condition only at design freq., elliptical polarization at other freq.	Kraus, Antennas Wolff, Antenna Analysis
Axial Mode Helix	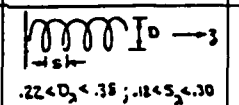		+8 - 23 dB for length .7λ - 10λ	Approx. 1.7:1 depending on dimensions	2	3	-Too directive	Kraus, Antennas Jasik, Antenna Engineering Handbook Wolff, Antenna Analysis
Planar Spiral		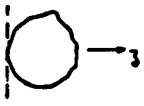	+5 - 7 dB	Large-depends on feed region & ant. dimensions	4	1	-Cavity backing gives unidirectional patterns -Elements can be etched or deposited -Suitable for flush mounting -See "Normal Mode Spiral" below for omni-pattern technique	Wolff, Antenna Analysis Curtis, "Spiral Antennas," IRE Trans.AP May 1960
Conical Spiral		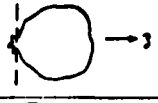	+6 - 9 dB	Large-depends on feed region & ant. dimensions	3	2	-Elements can be etched or deposited -See "Normal Mode Spiral" below for omni-pattern technique	Wolff, Antenna Analysis Dyson (Note 1)
Normal Mode Spiral	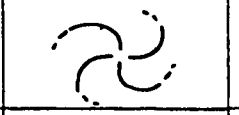	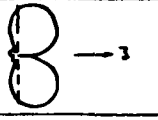	+4 - 5 dB	Large	3-4	1-2	-Can be either planar or conical spiral -Can also be fed for beam mode or two modes combined	Dyson & Mayes (Note 2)
Slot-Fed Biconical		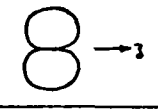	+1.5 - 2 dB	Narrow	5	4	-Required considerable experimental design effort -Suitable for mounting on end of a mast/feed -Very broad pattern coverage	Jasik, Antenna Engineering Handbook
Dual-Mode Horn	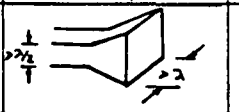		Large-depends on horn size	Narrow	6	6	-Not considered a candidate for this application	Jasik, Antenna Engineering Handbook
Cross-slotted TE_{11} circular wave guide	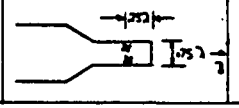	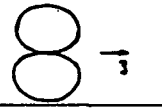	+1.5 dB	Narrow	7	7	-Narrow band -Requires large feed volume	Galindo & Green, company report - The Dalmo-Victor Co.

NOTES 1. Dyson, "The Characteristics and Design of the Conical Log Spiral," Univ. of Illinois Ant. Rept. 65-9.

2. Dyson & Mayes, "New Circularly Polarized Frequency Independent Antennas with Conical Beam or Omni-directional Patterns," IRE Trans. on AP, July 1961.

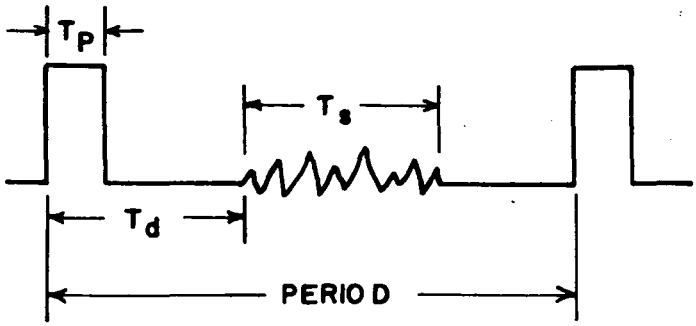

FIGURE 7-3 PULSE PERIOD TO AVOID DIRECT PATH / MULTIPATH OVERLAP

This means that the total delay, that is differential time delay T_d and multipath spread T_s, must be less than $\frac{1}{2B_F}$, i.e.,

$$\frac{1}{2B_F} > T_d + T_s. \tag{7-2}$$

This requirement is true if a pulse is transmitted repeatedly on a single frequency. If more than one non-overlapping frequency is used in a frequency hopping mode, then the above equation can be modified to reflect the increased number of frequency channels:

$$T_d + T_s < \frac{N}{2B_F} \tag{7-3}$$

where N = number of frequencies

The number of non-overlapping frequency slots N is in turn related to the duration of the pulse and the total bandwidths available:

$$N \simeq 2 \times BW \text{ total} \times T_p \tag{7-4}$$

Very often, therefore, it may be impossible to adjust the repetition interval to resolve the fading bandwidth, depending upon the differential time delay and multipath spread. Furthermore, the bandwidths required to satisfy equation 7-4 may not be available because of the desire to resolve

multipath spread. In conclusion, the high peak power, low duty cycle pulse technique suffers from peak power limited channels, potentially unfavorable geometry which may not allow fading bandwidth to be measured, and availability of bandwidths. These comments for the narrow pulse technique are valid only for antenna systems which do not discriminate against direct and indirect paths. If the above technique is coupled with an antenna system which is capable of separating the direct path from the indirect path then the repetition rate of the pulses must be twice the fading bandwidth and the highest rate at which they can occur is determined solely by the multipath spread in the reflected signals. This means that the period must be equal to or greater than the multipath spread for each frequency used. The technique still suffers from a peak power limitation; however, added moderate gain to the system may be accomplished if antennas with gain are used to discriminate between the direct and the indirect paths.

7.3 CW OR MULTITONE APPROACH

A popular method for measuring multipath parameters utilizes the transmission of a CW signal or a transmission of a multitone signal. In theory and in practice all multipath parameters can be measured using this technique.

First consider the transmission of a CW signal from a spacecraft to a low altitude platform. The signal received at the platform will have three components in addition to Gaussian noise: the signal received via direct path and the reflected signal which can consist of both specular and diffuse components. After translation to low frequency, a Fourier transform of the received signal will provide the amplitude of the component received via the direct path, the amplitude of the specular component, the

fading bandwidth of the diffuse component, its intensity, and the differential Doppler. The instrumentation required to accomplish this is illustrated in Figure 7-4. In addition to these parameters the direct path Doppler is also available.

There are a wide variety of equipments on the market for signal analysis. For example, all-digital fast Fourier transform devices are available from Hewlett-Packard which have the capability of real time spectrum analysis providing correlation function generation; power spectrum

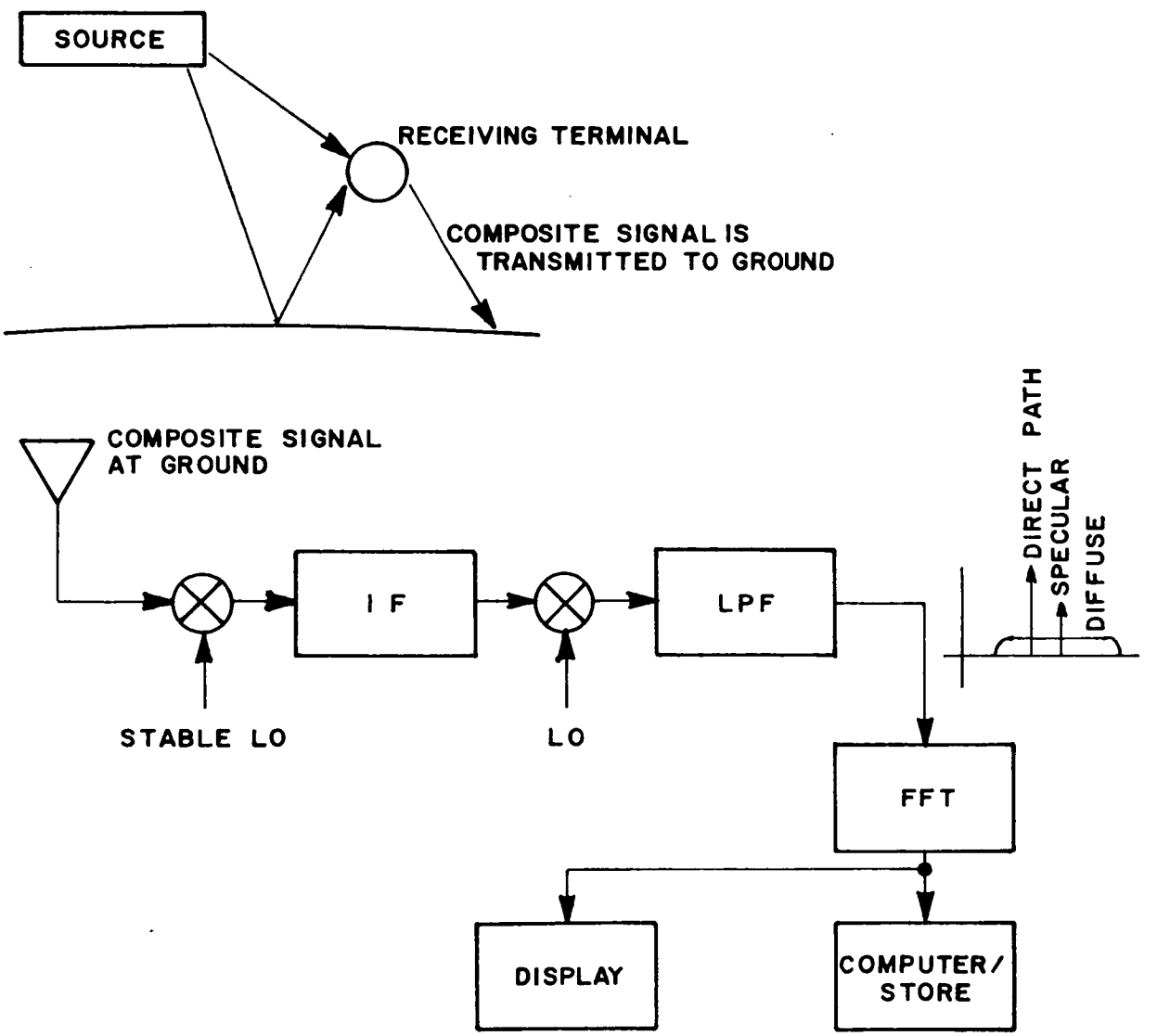

FIGURE 7-4 CW TECHNIQUE FOR MULTIPATH MEASUREMENT

measurements; and peak, average, and total signal power measurements. Equipment is available which has the capability of providing in real time these measurements and computations. The cost of the equipment will run approximately $75,000. This includes the analyzers, computers, display and interface equipment. Equipments of this type are available from Hewlett-Packard; Interstate Electronics; Federal Scientific; and Computer Signal Processing, Inc.

Such equipment when used with the CW or multitone approach will allow measurement of direct signal power, diffuse and specular power, fading bandwidth, correlation bandwidth, etc.

In the following paragraphs we describe in more detail how the multipath parameters can be measured assuming that CW or multitone signals with antenna discrimination are used.

Noncoherent processing techniques for multitone signals are attractive for determining statistical multipath parameters. Specifically, the Rician channel is of interest since it is assumed that a specular plus diffuse multipath waveform is received. This assumption implies that the system temperature is negligible compared with the received power and that a directive antenna is used to reject all but the indirect signal referred to above.

The characteristics to be ascertained are:

- the fading bandwidth
- the specular power
- the diffuse power
- the correlation bandwidth

The fading bandwidth is the amount of frequency spread of the random part of the received signal and is due to the rough surface reflection of the incident multipath sine wave. The following development presents a way of calculating the fading bandwidth from parameters that can be measured at the receiver.

Assume that the signal $s(t) = A \cos \omega_c t + B \cos(\omega_c t + \theta)$ is received, where A is the specular amplitude, ω_c is the carrier frequency, B is the diffuse amplitude, and θ is the diffuse phase. The joint density function of the envelope ($E(t)$) of $s(t)$ with its derivative ($\dot{E}(t)$) is

$$P(E,\dot{E}) = \frac{E}{\sigma_1^2 \sqrt{2\pi}\, \sigma_2} I_o\left(\frac{AE}{\sigma_1^2}\right) e^{-\left(\frac{E^2+A^2}{2\sigma_1^2}\right)} e^{-\left(\frac{\dot{E}^2}{2\sigma_2^2}\right)}$$

$$= p_E(E)\left[\frac{e^{-\dot{E}^2/2\sigma_2^2}}{\sqrt{2\pi}\, \sigma_2}\right], \qquad (7\text{-}5)$$

where σ_1^2 is the diffuse power (variance) in $s(t)$, i.e., $\sigma_1^2 = N_s B_F$; N_s is the single sided diffuse density; B_F is the fading bandwidth; σ_2^2 is the variance of the derivative of $s(t)$; and $I_o(\cdot)$ is the modified Bessel function of order zero.

If a level crossing device is placed at the output of the envelope detector then the average number of level crossing per second at a level chosen to be $\bar{E}$ (the mean of the envelope) is given by

$$\overline{n_o(\bar{E})} = \overline{n_o}\Big|_{E=\bar{E}} = \int_{-\infty}^{\infty} |\dot{E}| P(E,\dot{E}) d\dot{E}\Big|_{E=\bar{E}} \qquad (7\text{-}6)$$

Solving equation 7-6 yields

$$\overline{n_o(\bar{E})} = \left(\sigma_2\sqrt{\frac{2}{\pi}}\right)\frac{\bar{E}}{\sigma_1^2}\, e^{-\left(\frac{(\bar{E})^2+A^2}{2\sigma_1^2}\right)} I_o\left(\frac{A\bar{E}}{\sigma_1^2}\right) = \left(\sigma_2\sqrt{\frac{2}{\pi}}\right)p_E(\bar{E}) \qquad (7\text{-}7)$$

where $p_E(\bar{E})$ is the density function of the envelope of s(t) evaluated at $\bar{E}$. Note that the mean of E(t) was chosen because it can be measured quite readily. The parameter σ_2^2 is found by evaluating its autocorrelation function $R_s^{\cdot}(\tau)$ at $\tau = 0$ and subtracting the mean squared of $\dot{E}(t)$:

$$R_s^{\cdot}(\tau) = F^{-1}\{S_s(f)|j2\pi f|^2\} \qquad (7\text{-}8)$$

where $F^{-1}\{X\}$ is the inverse Fourier transform of X, and $S_s(f)$ is the power density of s(t). Then

$$\sigma_2^2 = R_s^{\cdot}(0) - R_s^{\cdot}(\infty) = \left(\frac{2\pi B_F}{\sqrt{3}}\right)^2\sigma_1^2, \qquad \sigma_2^2 = \dot{\sigma}_I^2 \qquad (7\text{-}9,\ 7\text{-}10)$$

and

$$\overline{n_o(\bar{E})} = B_F\, K(A^2,\sigma_1^2), \qquad (7\text{-}11)$$

where B_F is the fading bandwidth; and

$$K(A^2,\sigma_1^2) \triangleq \left[2\sqrt{\frac{2\pi\sigma_1^2}{3}}\right]\left[\frac{\bar{E}}{\sigma_1^2}\, e^{-\left(\frac{(\bar{E})^2+A^2}{2\sigma_1^2}\right)} I_o\left(\frac{A\bar{E}}{\sigma_1^2}\right)\right]$$

$$= \left[2\sqrt{\frac{2\pi\sigma_1^2}{3}}\right]p_E(\bar{E}).$$

Since $\overline{n_o(\bar{E})}$ and $\bar{E}$ can be measured, only σ_1^2 and A^2 need be known in order to calculate the fading bandwidth, B_F. Below σ_1^2 and A^2 are found in terms of measurable quantities.

The output of a square law detector with s(t) as an input is the square of the envelope. Defining

$$Z = \overline{E^2(t)} \tag{7-12}$$

the following relations hold:

$$\bar{Z} = A^2 + 2\sigma_1^2 \tag{7-13}$$

$$\sigma_Z^2 = 4\sigma_1^2 \, (\sigma_1^2 + A^2) \tag{7-14}$$

Solving for A^2 and σ_1^2 gives

$$A^2 = \sqrt{(\bar{Z})^2 - \sigma_Z^2} = \sqrt{2(\bar{Z})^2 - \overline{Z^2}} \tag{7-15}$$

$$\sigma_1^2 = \frac{\bar{Z} - A^2}{2} . \tag{7-16}$$

A mechanization for finding A^2, σ_1^2, and B_F according to the above equations is shown in Figure 7-5.

The correlation bandwidth B_c is a measure of the frequency separation necessary to obtain independent fading of two sine wave signals reflected from a surface. A simple way of measuring B_c is to calculate the correlation function of the envelope; when it drops to one half of its peak value with frequency as the adjustable parameter, then the correlation bandwidth is the frequency separation present at that time. The correlation bandwidth is defined by

$$\rho(f) = \frac{\overline{E_1(f)E_2(f+\Delta f)} - \overline{E}_1\overline{E}_2}{E_1(f)E_2(f)} \tag{7-17}$$

where E_1 = envelope of frequency #1
E_2 = envelope of frequency #2
$\Delta f = f_2 - f_1$.

A mechanization for measuring correlation bandwidth is shown in Figure 7-6.

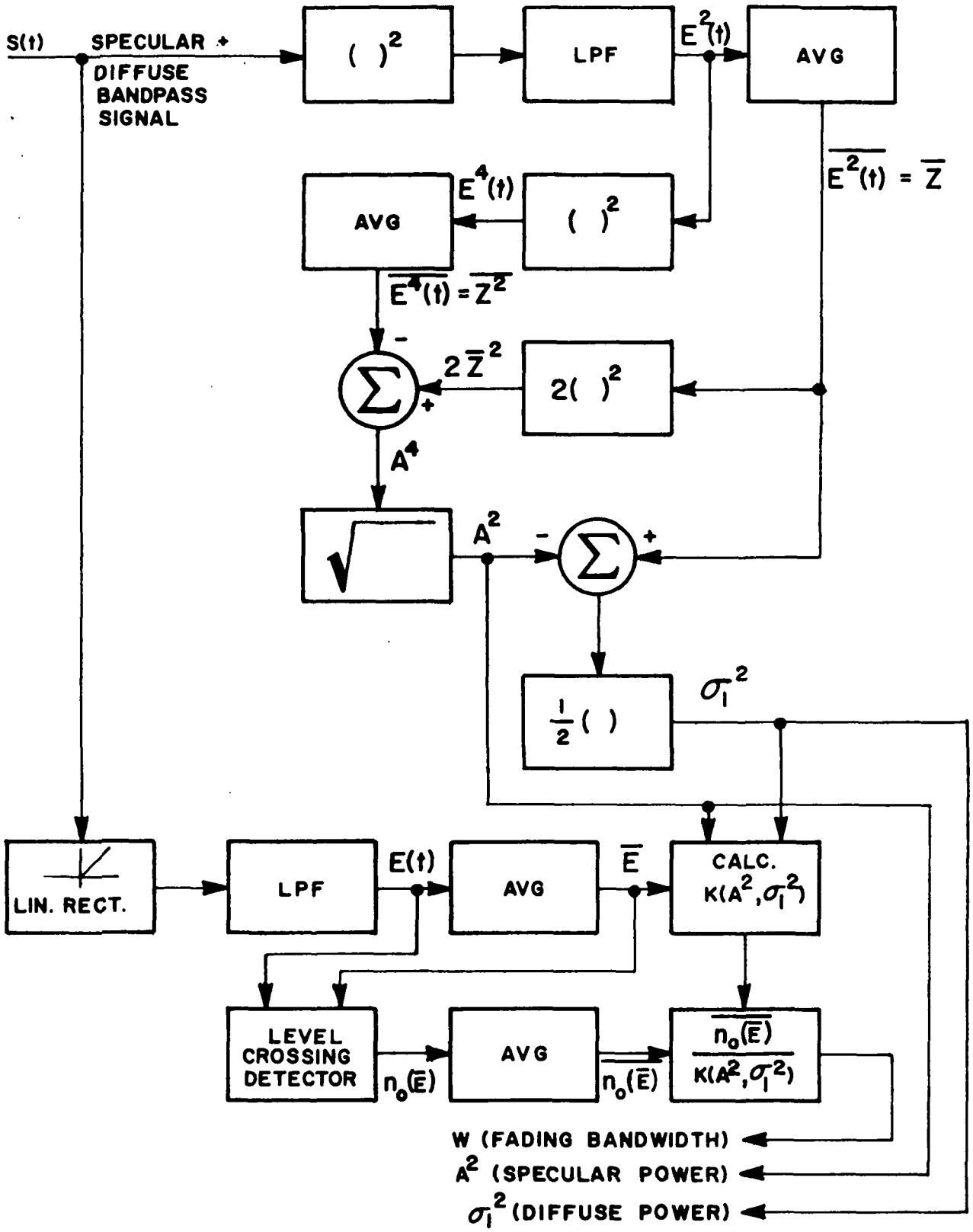

FIGURE 7-5 MECHANIZATION FOR MEASURING FADING BANDWIDTH

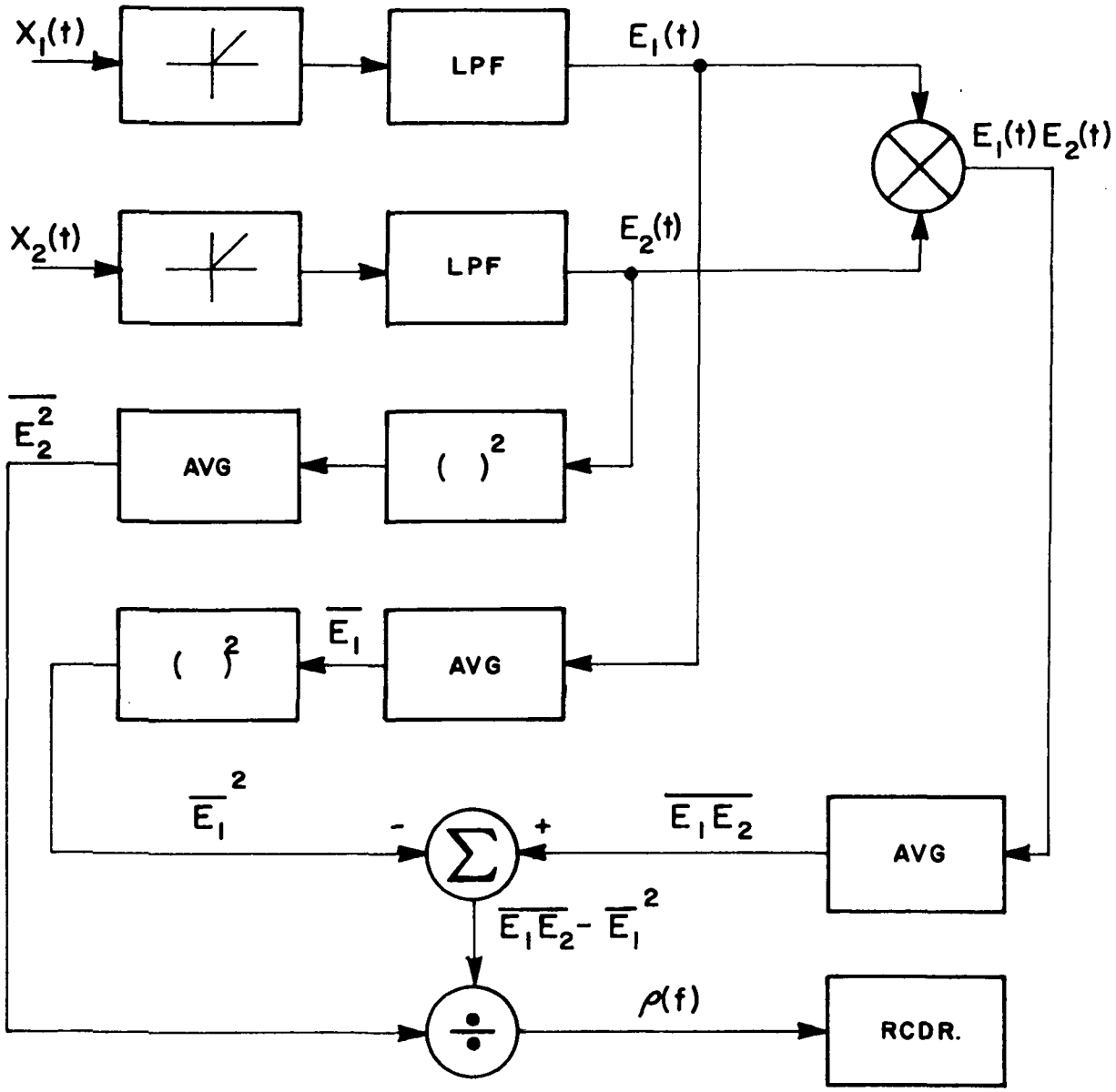

FIGURE 7-6 MECHANIZATION FOR MEASURING CORRELATION BANDWIDTH

An alternate approach to measuring B_F, B_c, P, $P_{specular}$, $P_{diffuse}$, etc., is to use the system shown in Figure 7-7.

This alternate approach is possible since for a Rician variate the joint density in E and $\dot{E}$, $p(E,\dot{E})$, can be written as $P(E)P(\dot{E})$ and $P(\dot{E}) = (2\pi\dot{\sigma}_1^2)^{-1/2} \exp(-\dot{E}^2/2\dot{\sigma}_1^2)$ is Gaussian with zero mean and variance $\dot{\sigma}_1^2$.

In order to measure the correlation bandwidth B_c one need only calculate $\overline{[\dot{E}(f)\dot{E}(f+\Delta f)]}/\dot{\sigma}^2 = 1/2$. This means that the alternate method for measuring B_c can be realized by the system shown in Figure 7-8.

7.4 WIDEBAND SIGNAL APPROACH

Another approach for measuring multipath is to use a wideband signal such as a pseudonoise transmission for the purpose of measuring the direct path and the parameters associated with the reflected signal. The basis for this technique is the autocorrelation properties of a pseudonoise sequence. With sufficient processing gain, defined here as the chip rate divided by the integration bandwidth, it is possible to lock to the direct signal while discriminating against the reflected signal or to lock to the indirect signal and discriminate against the direct signal. This concept is illustrated in Figure 7-9. This approach is particularly attractive if multipath measurements are to be made so that data can be used to program a multipath simulator. In effect, a wideband probe signal like pseudonoise is ideal for gathering all the parameters associated with the multipath channel. These parameters in turn can be recorded or digitized for use with a real time tapped delay line multipath simulator.

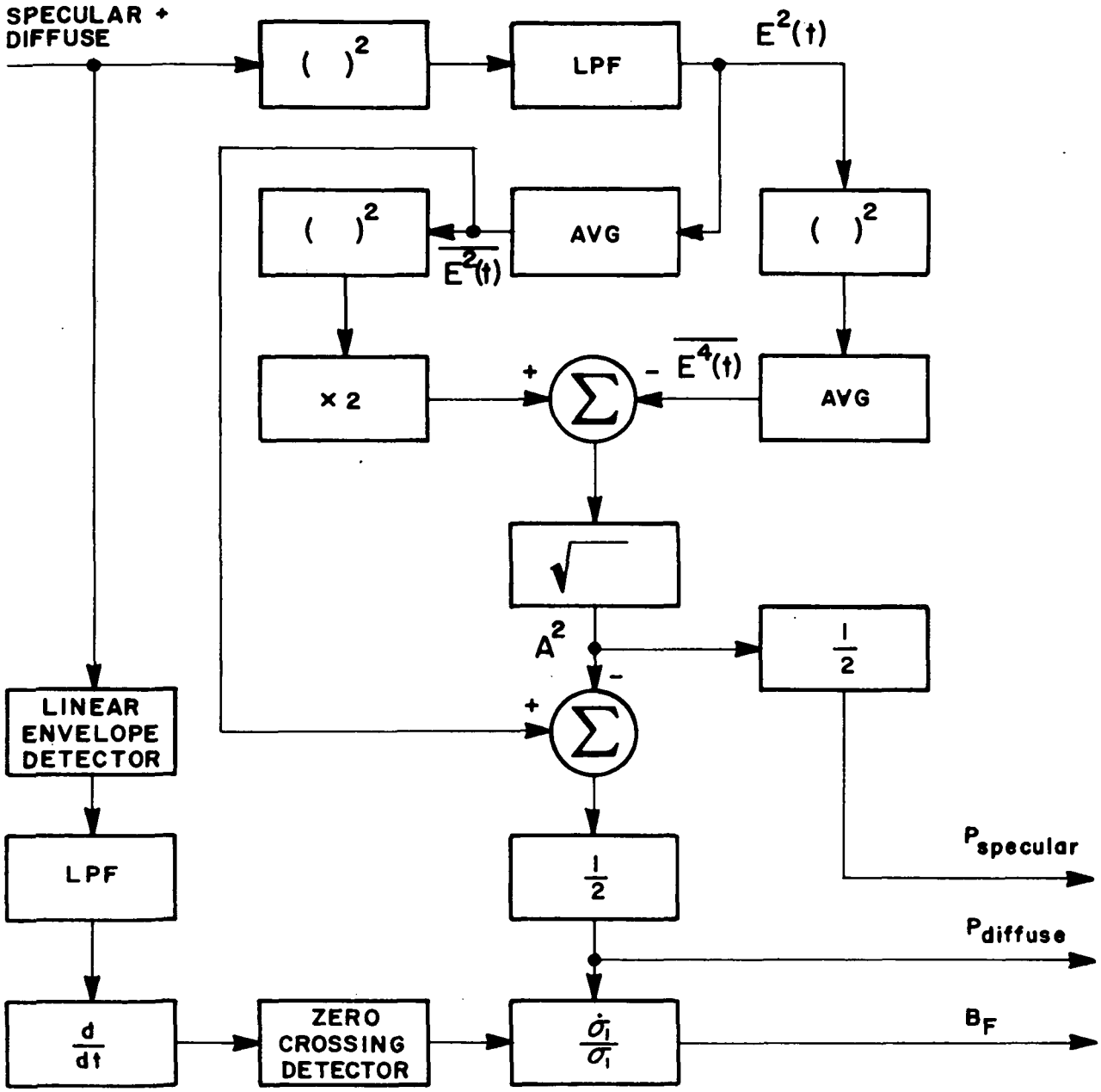

FIGURE 7-7 MECHANIZATION OF NONCOHERENT MULTIPATH MEASUREMENT TECHNIQUE

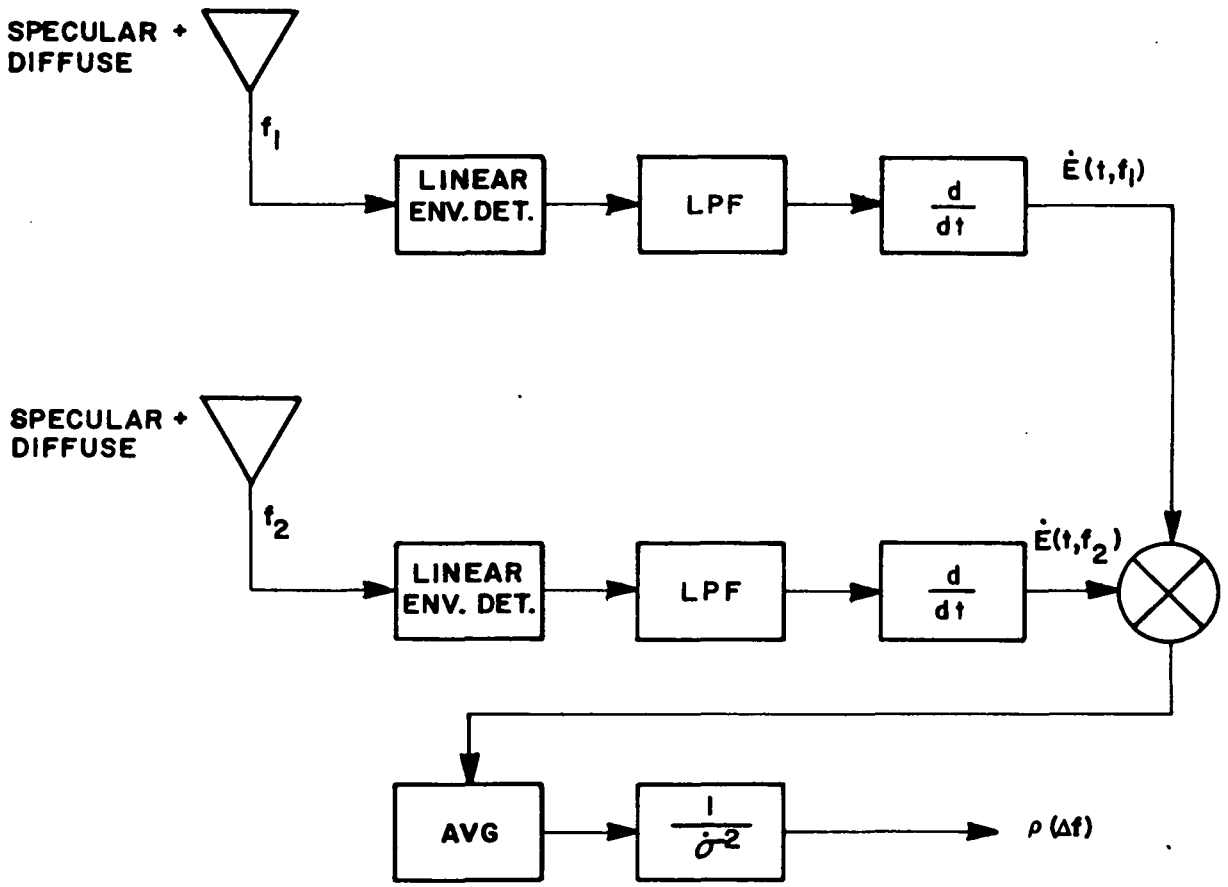

WHEN $\rho(\Delta f) = 1/2$, THEN $\Delta f = B_C$

FIGURE 7-8 ALTERNATE METHOD OF MEASURING CORRELATION BANDWIDTH

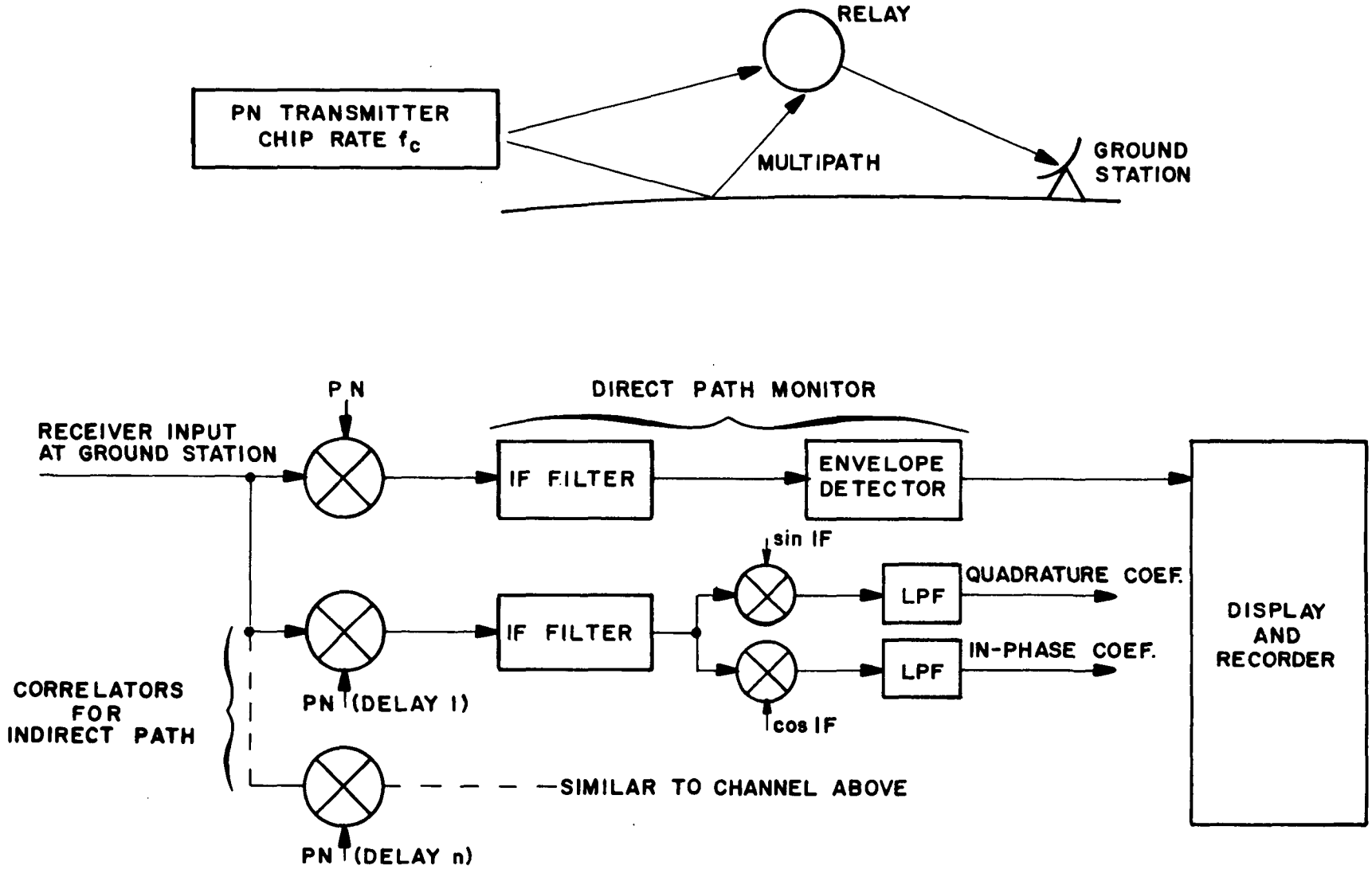

FIGURE 7-9 MULTIPATH ANALYZER

One is tempted to employ a wideband probe signal technique with multiple correlators to measure simultaneously all the parameters associated with both the direct signal and the reflected signal. Unfortunately it may not be possible to measure the direct and the reflected signals with a dual channel pseudonoise receiver, as illustrated in Figure 7-10. For example, if the reflected signal to be measured is some 20 dB below the direct signal level, the output signal-to-noise ratio, as measured in the integration bandwidth of the channel which is used to measure the direct signal strength, is given by

$$\left(\frac{S}{N}\right)_o = \frac{P_d}{P_{diffuse} + P_{specular}} (P.G.) . \qquad (7\text{-}18)$$

There appears to be no problem associated with measuring the direct path signal even if the multipath signal to direct path signal ratio is unity. This is true because sufficient processing gain (P.G.) can be provided in the direct path channel measurement since essentially no time spread exists in that channel.

However, in the multipath channels, i.e. the channels used to measure the properties of the reflected signal, a real problem exists. First, there is time spread in the reflected signal. Second, in order to measure the fading bandwidth the integration time of the post-correlation filter must be inversely proportional to the fading bandwidth. For a given chip rate $1/T_c$ this sets an upper bound on the achievable processing gain in the channel used to measure the properties of the reflected signal. In

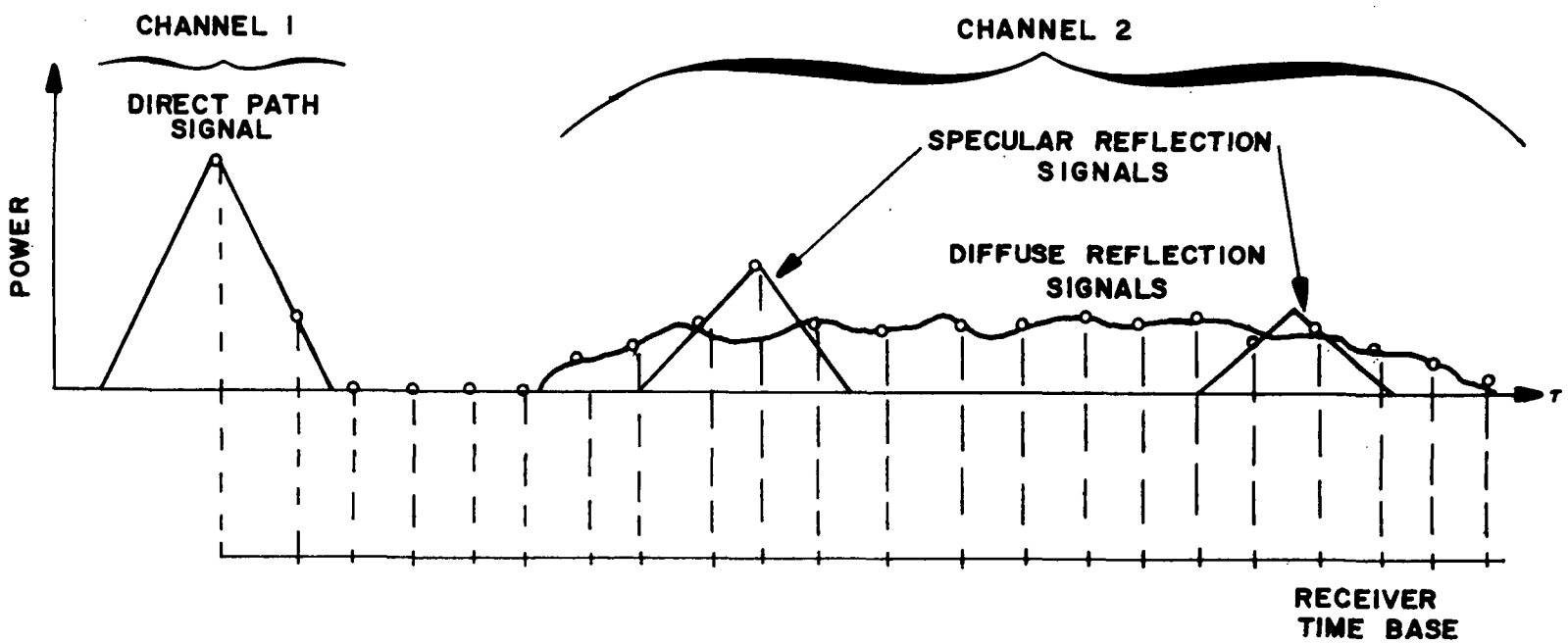

FIGURE 7-10 DUAL CHANNEL CORRELATOR OUTPUT

fact, the output signal-to-noise ratio from a single correlator within the bank of correlators can be shown to be given by

$$\left(\frac{S}{N}\right)_{out} = \frac{P_{diffuse}}{[P_d + (1-T_c/T_s)P_{diffuse}]B_F T_s} \qquad (7\text{-}19)$$

for one multipath channel. As shown in equation 7-19, if the reflected signal is 10 to 20 dB below the direct signal, and the fading bandwidth time spread product is large, then the output signal-to-noise ratio that one can achieve from a single correlator is unacceptably low. In general, the time spread is not a function of the carrier frequency. However, the fading bandwidth is directly proportional to the carrier frequency. It may be difficult to obtain sufficient dynamic range in the multipath channel outputs when the multipath time spread is significant. Thus, as in the other techniques, it is advisable to utilize antenna patterns to separate the direct signal from the reflected signal when using the pseudonoise probe technique.

If AD techniques are not used, then the PN multiple correlator approach can be used when the product $B_F T_s$ is low, which occurs for aircraft platforms (e.g. U-2) to C-118 or for balloon to C-118 (or Sabreliner).

It is not necessary to use a bank of PN correlators to measure the statistics of the reflected signal. Instead of a bank of correlators a single sliding correlator can be used to monitor the reflected signal. The correlator is programmed to slide or pass through the time spread T_s in a slow manner. The correlator can be stopped to measure the B_F as well. The sliding correlator is not a real time device and therefore cannot be used to derive real time data for use with a channel simulator. However,

it is an effective means of measuring all the multipath parameters, especially since the magnitude of the parameters of interest do not change rapidly with time.

7.5 MULTIMODE TRANSPONDER AS A MULTIPATH ANALYSIS TOOL

The Multimode Transponder now being fabricated for NASA/Goddard by Magnavox can be configured to measure multipath as described above.

The Multimode Transponder is a device intended for installation and use on board an aircraft simulating a user spacecraft as part of a Tracking and Data Relay Satellite (TDRS) system. All user spacecraft may utilize the return link simultaneously transmitting telemetry data in a single shared VHF band at 137 MHz. A relay satellite will transmit commands and/or ranging signals over the forward link to only one user spacecraft at a time in an assigned VHF or UHF band. Both the forward and the return links employ polarization diversity reception.

The Multimode Transponder (MMT) along with the associated ground support equipment (MTAR) was designed in order to demonstrate the following modulation techniques:

- Conventional PSK command and telemetry
- Narrowband pseudo-random noise (PN) mode
- Wideband PN mode

The following functions can be simulated with various combinations of the transponder subunits and associated ground equipment:

- Reception, demodulation, and delivery to the user spacecraft of command signals received by the transponder via the forward link

- Acceptance, modulation, and transmission via the return link of the telemetry data generated by the spacecraft user
- Reception via forward link, processing on board, and retransmission via return link of coded signals suitable for ranging and range-rate determination.

The roles and functional interactions of various subunits of the transponder during equipment operation in each of the above modes are described in Figure 7-11 and are discussed in more detail below.

The multimode transponder unit consists of two parallel receivers and a transmit channel.

The inputs for the two receivers are provided by orthogonally polarized antenna elements. The outputs of the two receivers are, after coherent detection, summed to provide a diversity combined output data signal. The receiver will operate in any one of three frequency bands: 127.750 MHz, 149 MHz, or 401 MHz.

In a similar manner, the transmitter is connected via quadriplexers to the polarization diversity antennas. However, in contrast to the receivers, which are always connected to their respective antennas, RF input to the transmitter is selected from the synthesizer of the receiver which is receiving with the highest signal-to-noise ratio. This procedure optimizes the coherent transponding signal radiation strategy. The transmitter will operate in one frequency band at 137 MHz.

In the conventional mode, the received command and the transmitted telemetry data are modulated, respectively, on the incoming and the outgoing carriers as a differential phase shift keying (ΔPSK) with a phase shift of

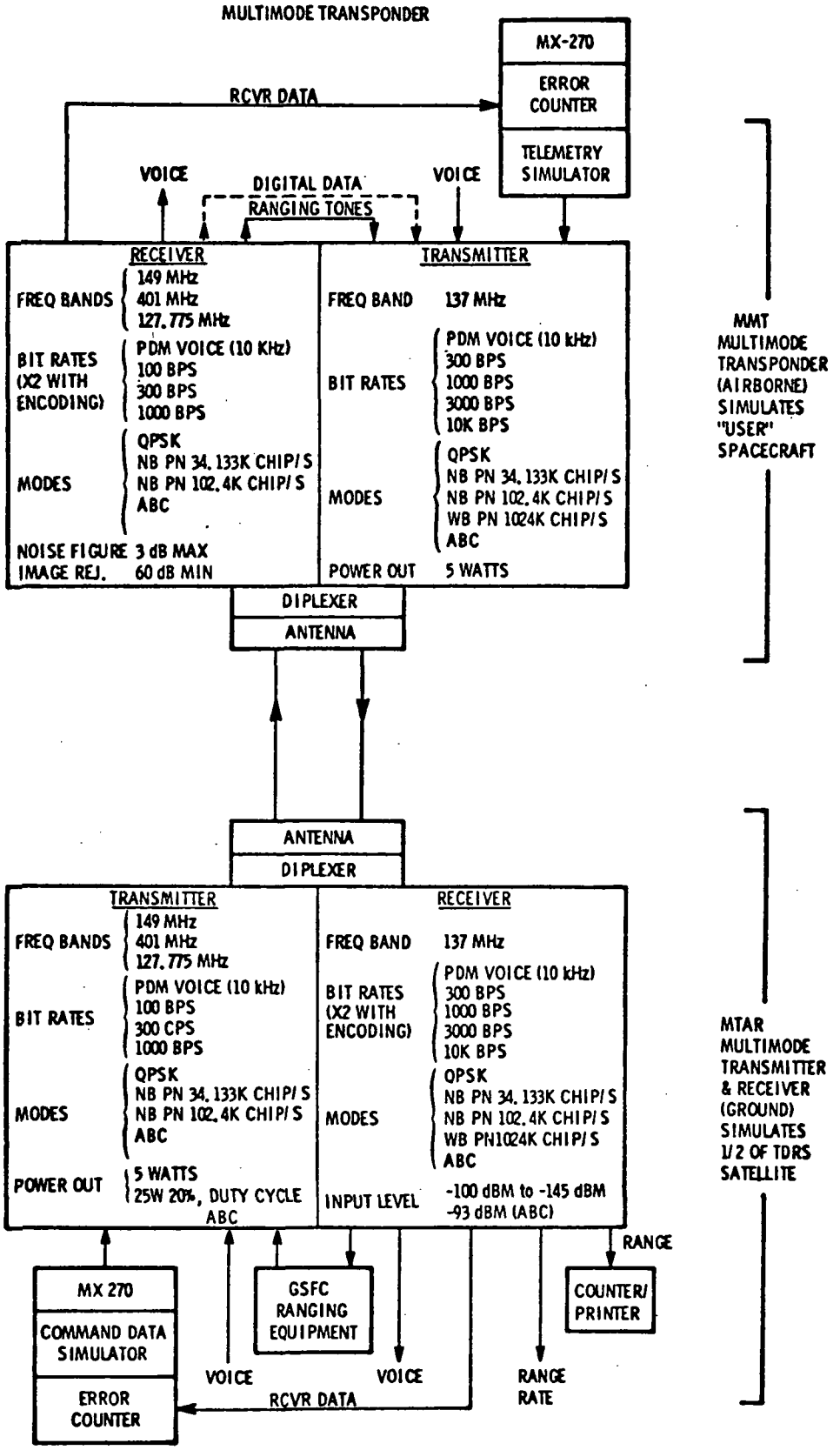

FIGURE 7-11 MULTIMODE TRANSPONDER EQUIPMENT CHARACTERISTICS

±1.57 radians (90 deg.). Essentially, this conventional mode is the basic, most fundamental mode of operation against which the performance improvements in all the other modes will be compared.

In the narrowband PN mode, the forward commands and the return telemetry data will be superimposed on PN binary codes clocked at rates consistent with 50 kHz and 150 kHz channel bandwidths. Specifically, the chips rates will be 34.133 or 102.4 kilochips/second, respectively.

The major additional subunits added to the transponder for this mode of operation are:

- Receiver coder
- Transmitter coder
- Code clock
- Variable time sequential detector
- Search logic
- Code error tracking loop (includes code error combiner).

The transponder configuration in the wideband PN mode (return link only) mode is identical to the one in the narrowband PN mode with the exception of the rate at which the transmitter coder is clocked. The chip rate for the wideband transmit mode is 1024 kilochips/second. Also, to provide for an extended code length, a special switching arrangement is used to extend the repetition period of the wideband code by a factor of 20. Since the receiver portion of the transponder is not modified when the wideband transmission is used, the receiver code search and tracking functions are the same as described above.

The Multimode Transponder will be used to evaluate the TDRS modulation modes by being installed in an aircraft which will simulate a user spacecraft. In the PSK mode of operation the transponder will attempt to acquire a conventional PSK signal which represents an uplink command and demodulate it. Simultaneously it will be required to recover the GRARR ranging signal. All of the above will be done in a series of controlled experiments, namely, various levels of RFI and multipath signals will be induced in order to evaluate the performance of the transponder under adverse conditions such as those predicted for the TDRS system.

It is believed, due to link calculations, that the conventional PSK mode of operation will not be satisfactory under even moderate levels of RFI, multipath, etc.; however, this mode will serve as a basis of comparison for the wideband and narrowband pseudonoise (PN) modes.

In the downlink the conventional PSK mode will return the GRARR ranging signals recovered in the uplink and simultaneously will send down simulated telemetry and/or voice. The telemetry has the option of incorporating forward error control encoding (convolutional code) or not, and thus this function can be tested.

In the PN mode of operation the Multimode Transponder will be required to recover a PN coded uplink command signal. The PN code itself will, in the process of tracking it, be used to synchronize a downlink code, and thus it will replace the GRARR ranging signal used in the PSK mode.

As stated above, in the uplink the PN chip rate will be lower than an optional wide band PN downlink mode; thus the effect of chip rate can be evaluated on the downlink. Concerning the downlink, the telemetry

(forward error control encoded or not) and/or voice will be PN coded prior to PSK modulation.

The following are design factors which are to be tested together with the method for testing them:

- PN Processing Gain - compare PSK and PN-PSK receiver margins under various RFI and multipath conditions.
- Acquisition Time - monitor time to obtain carrier lock in PSK and PN-PSK modes under various RFI and multipath conditions.
- Range and Range Rate (RARR) Accuracy - compare RARR in PSK and PN-PSK modes with known position of the aircraft (radar track, optical track, etc.).
- Telemetry Bit Error Rate - using pseudo-random data check on a bit by bit basis the received telemetry under various RFI and multipath conditions.
- Voice Quality Check- monitor received signal-to-noise ratio and compare with specified voice quality thresholds.
- Command Data Error Rate - same test as Bit Error Rate with the data simulator on the ground and the data recorder on the aircraft.
- Forward Error Control Gain - operating with the convolutional code option the Bit Error Rate Test will be repeated. A comparison with the uncoded (error control) results will yield the coding gain.

All the above tests will be carried out with simulated space loss (appropriate attenuation), several RFI levels (ground transmitters), and varied multipath conditions (choice of terrain for the experiments). Also the bit rates, chip rates, and carrier frequencies will be changed appropriately so as to gather data under the widest set of parameter variations.

Since the Multimode Transponder is a dual channel receiver, it can be made to function as a multipath analysis tool with some modifications to the present design. For example, the PN reference code in the receiver is supplied to both channels simultaneously so that diversity operation is possible. To make a dual channel sliding correlator receiver for multipath measurements, the second channel of the Multimode Transponder would be supplied with a delayed PN code replica. This PN code reference is still derived from the original PN code reference generator. The delayed reference is slewed so that it is programmed to pass through the reflected signal (see Figure 7-10). It is estimated that such a modification will be of minimal cost impact.

7.6 TEST RESULTS OF CURRENT MULTIPATH PROGRAMS

7.6.1 TESTS BY BOEING FOR THE FAA

Under contract to the FAA, the Boeing Company has recently concluded a series of tests using an aircraft and ATS-5 to determine the multipath properties of the aircraft to synchronous satellite link. The investigations were carried out to evaluate multipath problems at low grazing angles between 0.157 radian (9 deg.) and 0.524 radian (30 deg.). The aircraft used in the test was a KC-135 outfitted with directive antennas placed above and below the aircraft so that the directive beams could be steered to isolate the direct from the indirect paths, as shown in Figure 7-12. A test signal at L-band was transmitted from NASA's Rosman Ground Station via the satellite to the aircraft. Directional antennas on board the airplane received the direct and the sea reflected signals via separate RF channels. The tests were designed to measure the intensity of the signal reflected off the ocean, the polarization sense of the reflected signal, the power spectral density of

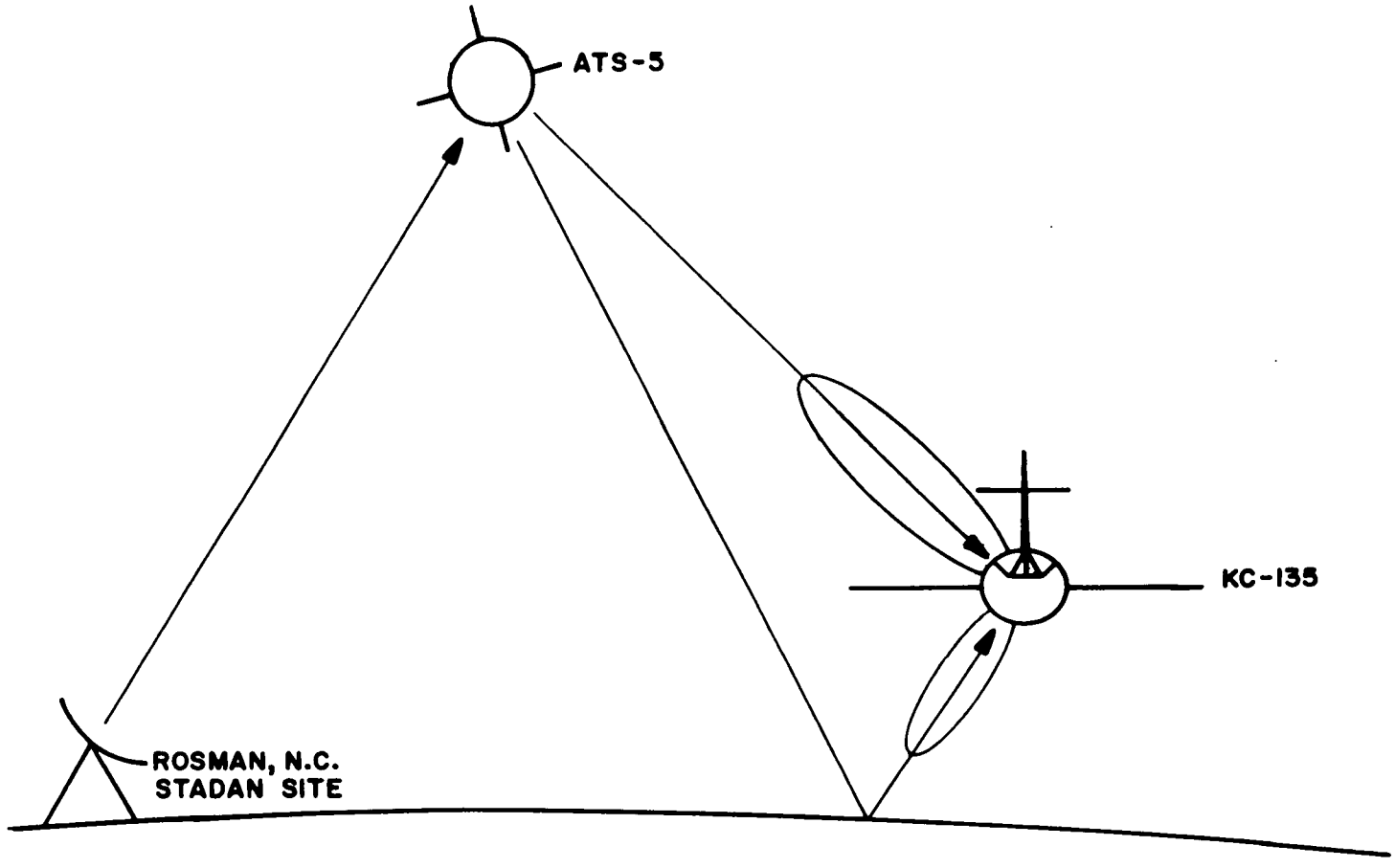

FIGURE 7-12 CONFIGURATION USED BY BOEING AIRCRAFT COMPANY FOR MEASURING MULTIPATH

the reflected signal, and its coherence bandwidth. As backup to the multipath tests, the Naval Research Laboratories provided photographic equipment to provide sea state data to determine the surface RMS slope, wave height spectrum, and RMS slope positional variations. All of this data is required to match the theoretical models with the experimental data. The antenna patterns which were used to separate the direct and indirect paths were calibrated precisely. The off-line equipment which was used to determine the power spectral density of the reflected signal is based upon a fast Fourier transform algorithm. Equipments involved in these off-line measurements are illustrated in Figures 7-13 and 7-14. Tapes taken on board the aircraft are used as inputs to this power spectrum density analyzer. Experimental data are shown in Figure 7-15 which indicates that the reflected signal can be described by a Rician density. The two curves shown in Figure 7-15 are for lefthand circularly polarized reception and righthand circularly polarized reception. As anticipated from theory, a reversal in the sense in polarization occurs in the path reflected off the surface of the ocean and thus one would expect that in switching from a lefthand to a righthand circularly polarized antenna a decrease would be anticipated as the result of the polarization reversal. A 6 dB net difference was noted in these measurements.

The results of the fading bandwidth measurements in terms of its power spectral density are illustrated in Figure 7-16. Also shown in Figure 7-16 is a theoretical curve which shows that the measured values and theory agree. No data is currently available on the coherent bandwidth measurements since sidetone signals could not be separated sufficiently in frequency to obtain accurate coherent bandwidth measurements.

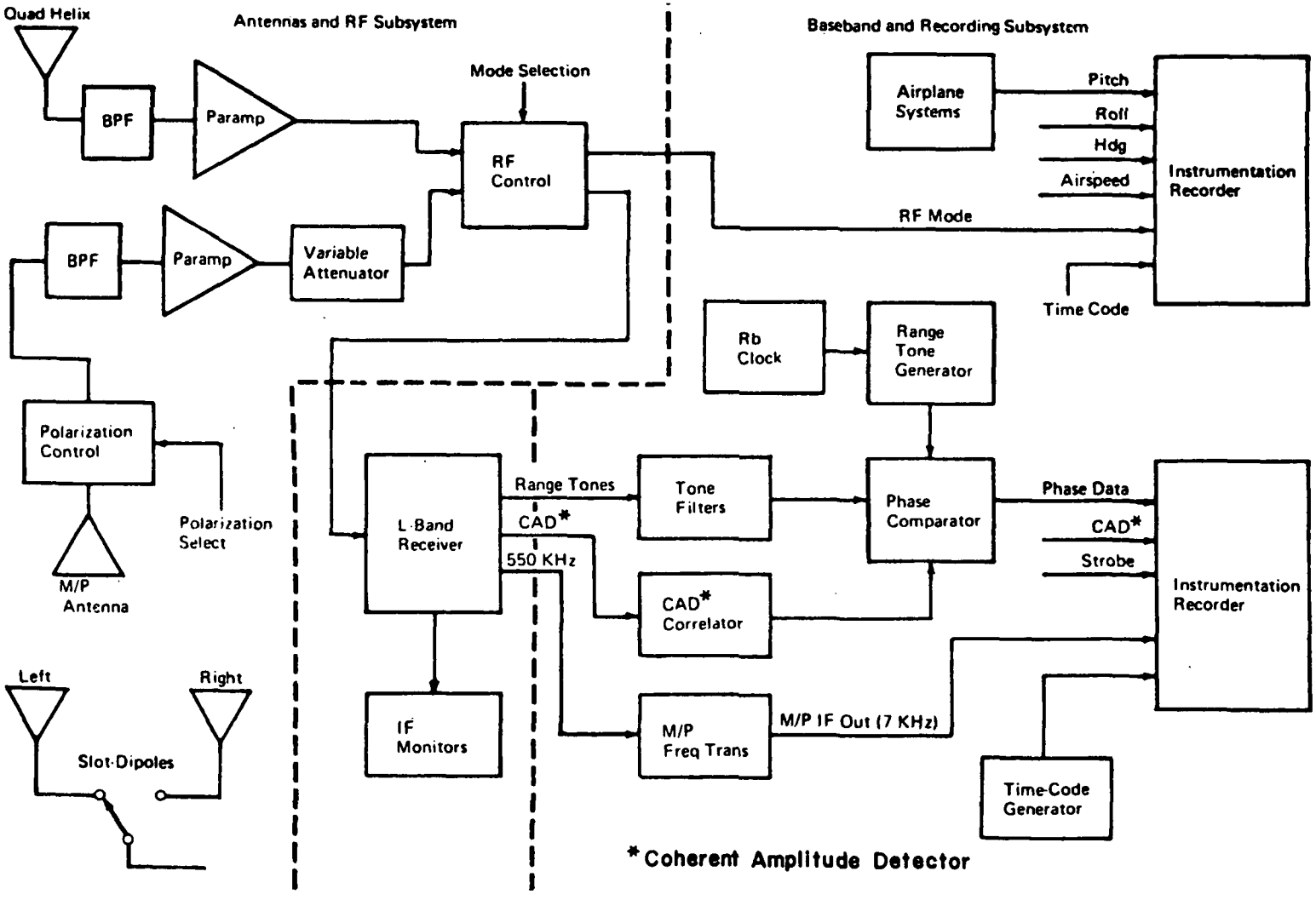

FIGURE 7-13 KC-135 TERMINAL

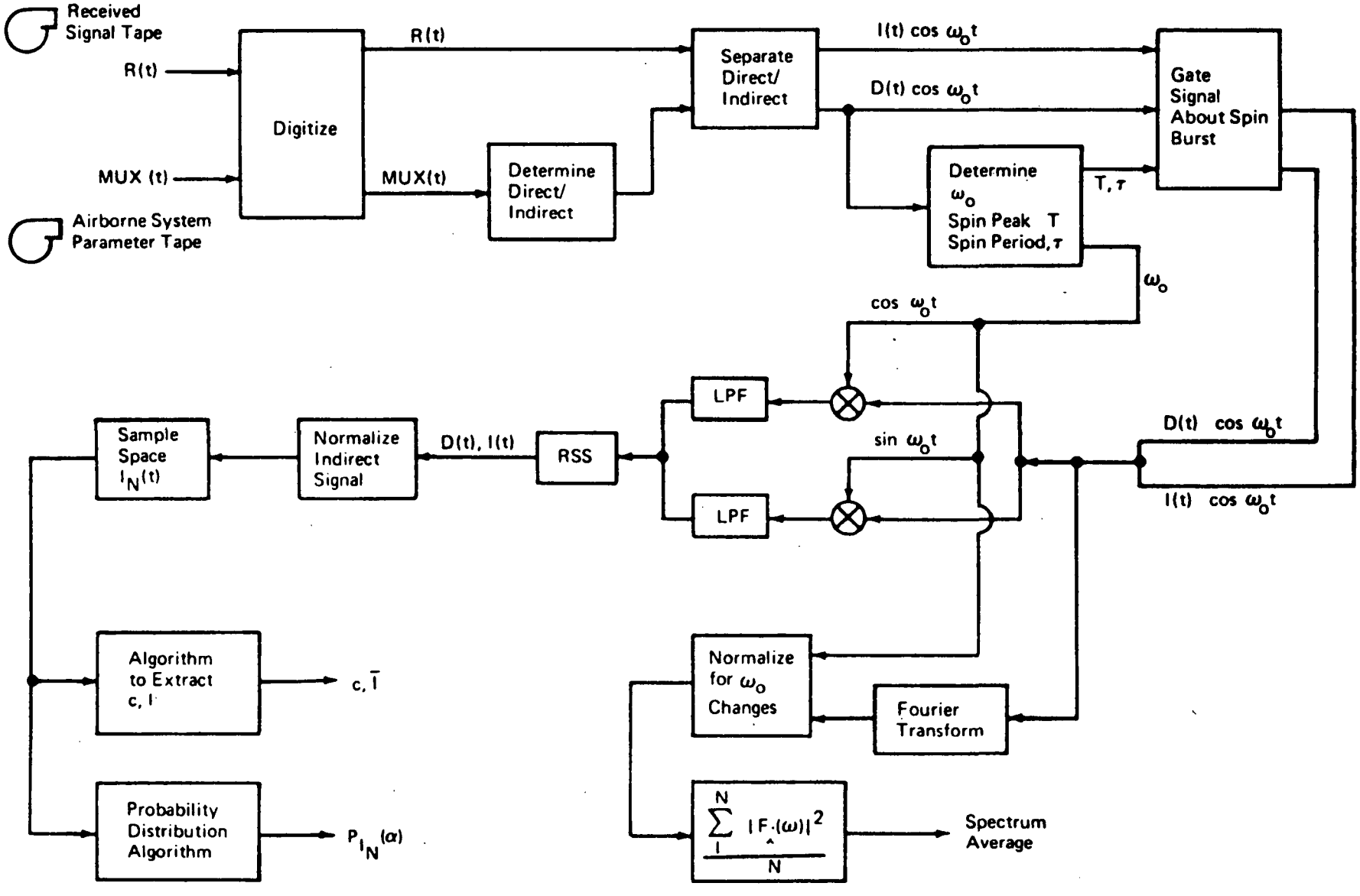

FIGURE 7-14 AMPLITUDE STATISTICS AND POWER SPECTRAL DENSITY DATA REDUCTION AS DONE BY BOEING

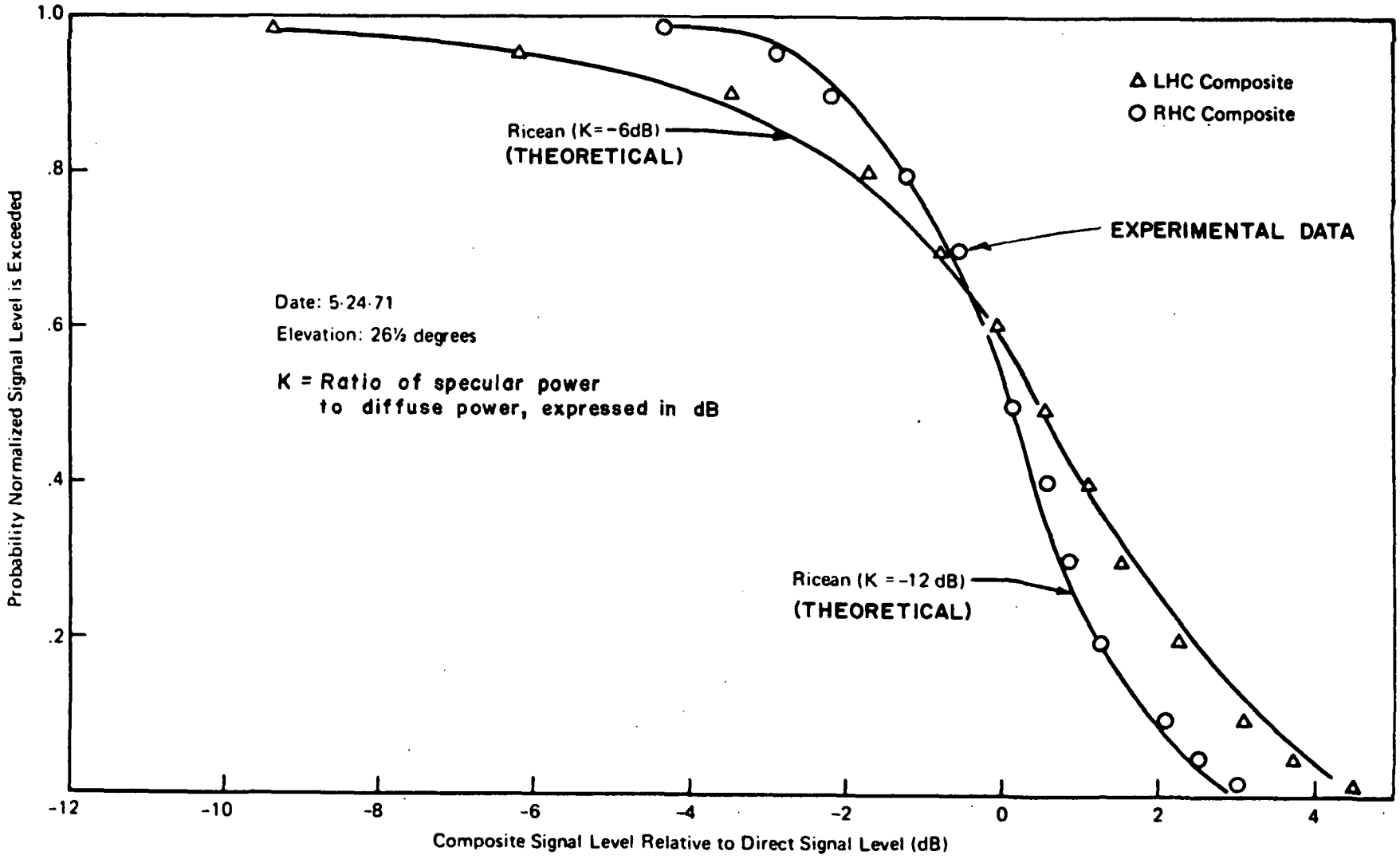

FIGURE 7-15 AMPLITUDE DISTRIBUTION OF COMPOSITE SIGNAL

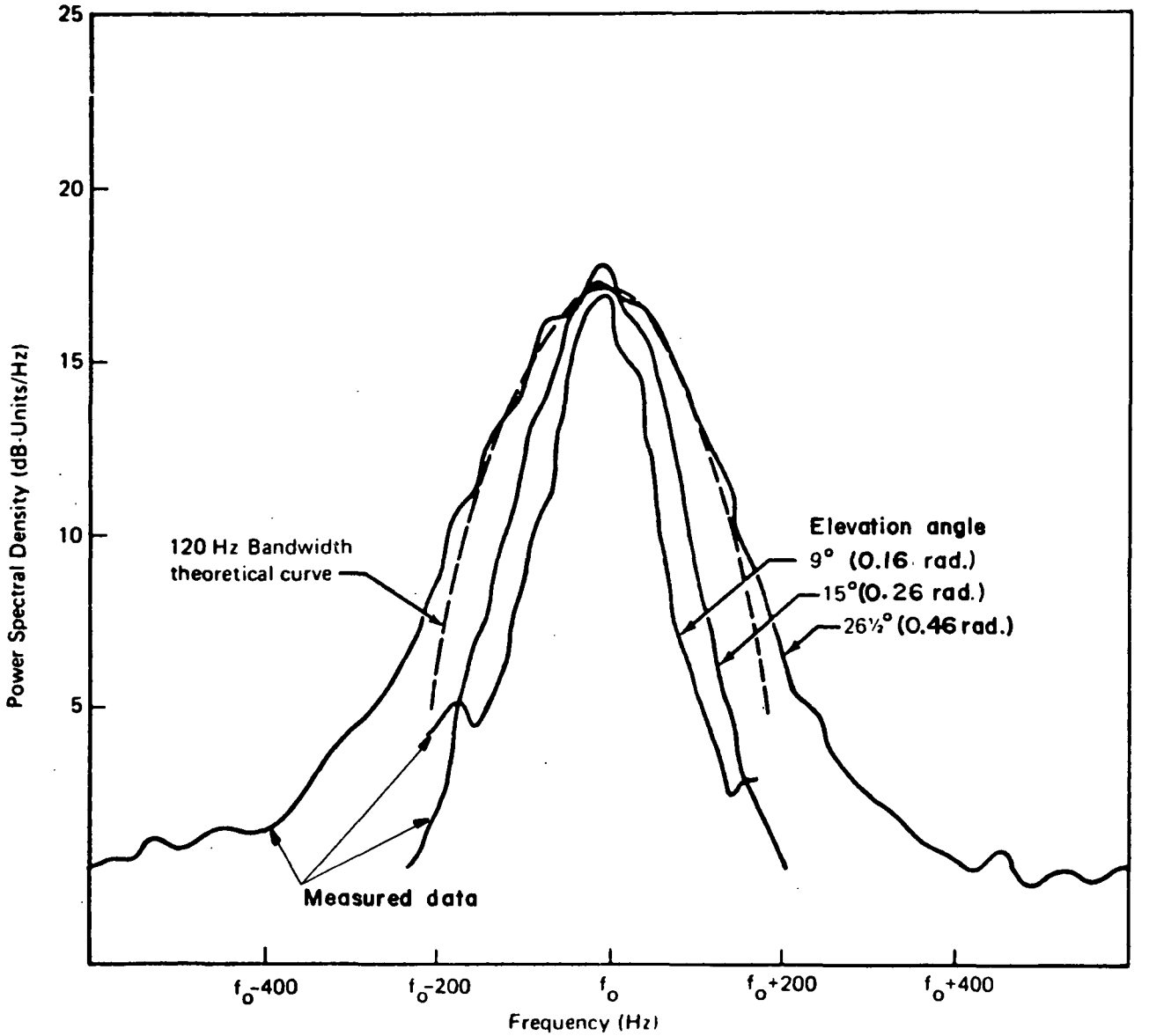

FIGURE 7-16 HORIZONTAL POWER SPECTRAL DENSITIES

L-band ranging tests were conducted using sidetone ranging techniques. The tone frequencies were 8 kHz and 10 kHz. These tone frequencies were selected to provide aircraft position location accuracies of 1 to 2 kilometers for a two-satellite ranging system. Figure 7-17 shows the standard deviations and range error as a function of the suppression of the reflected signal relative to the direct path. These tests are valid for an elevation angle of 0.2 radian (11.5 degrees). The results of these tests indicate that the multipath signal, when comparable to the direct path signal, can severely degrade the performance of a sidetone ranging system. It is understood that tests have been completed by Boeing over marsh land conditions as well as mountainous terrain. The results indicate that much less reflected signal is observed than theory would predict.

Expenditures to date for this extensive multipath measurement program are $1.5 million. This amount represents the expenditures by the government for all of the instrumentation and software involved in making the tests. This amount does not include aircraft support or the cost of making the flights, nor does it include the cost of providing sea state data which was handled by the Naval Research Labs. The total costs of the program are given in Table 7-4.

TABLE 7-4

TOTAL COSTS TO DATE FOR MULTIPATH MEASUREMENT PROGRAMS

° $1.5 x 10^6 for instrumentation, software, and data reduction
° $500,000 for 30 flights
° $100,000 for NRL sea state data measurements
° $300,000 extraneous costs

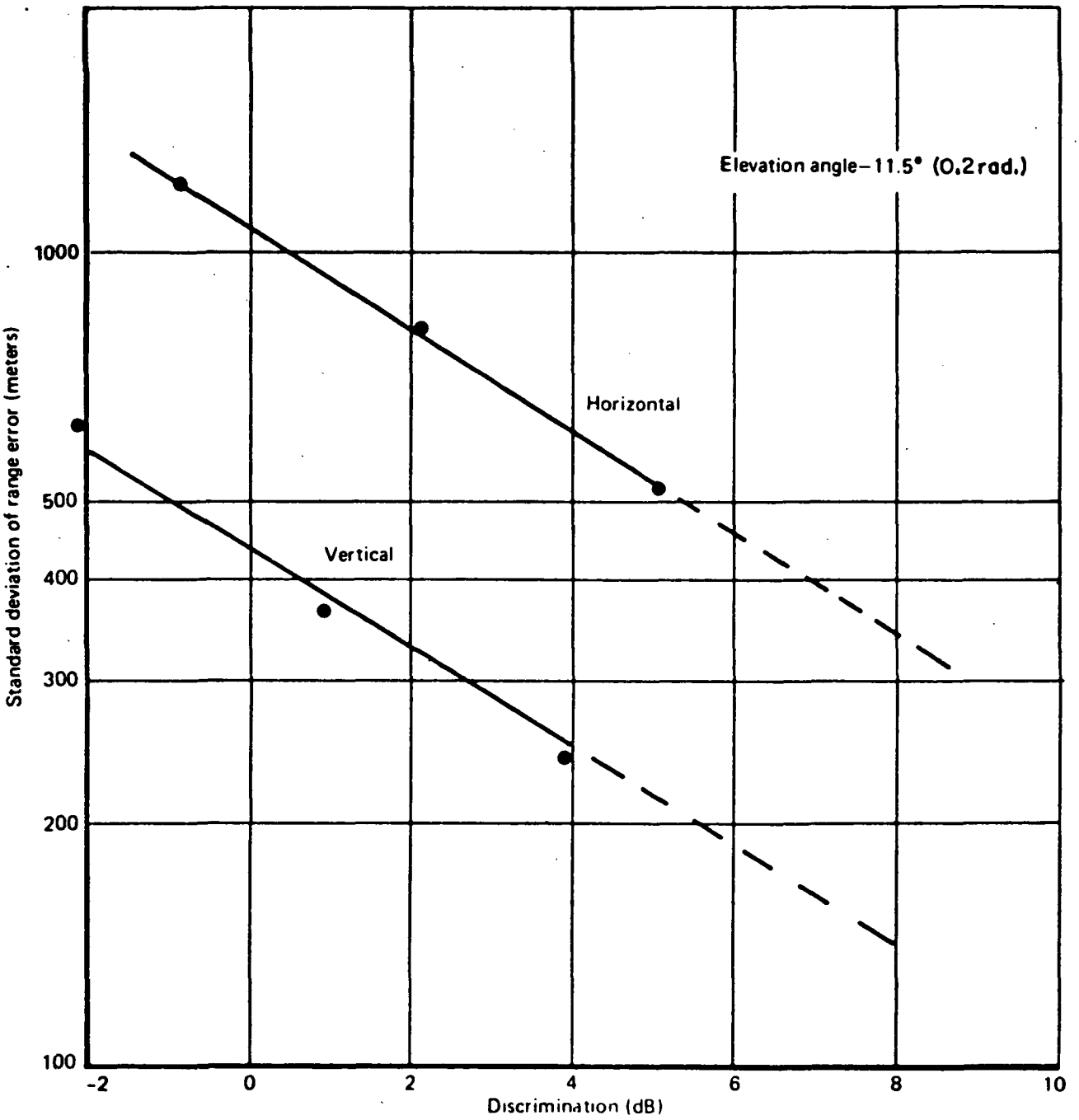

FIGURE 7-17 MULTIPATH RANGE ERROR VS. DISCRIMINATION

The FAA provided the KC-135 at an operating cost of $1,000/hr.

There is a test plan developed by the FAA to run additional multipath measurements and data tests using the ATS-F satellite. Furthermore, in the spring of 1973 data tests will be conducted with ATS-5. Modulation techniques to be tested include coherent PSK and noncoherent delta PSK. Measurements will be made to determine the true effects of multipath on the performance of a satellite-to-aircraft link.

7.6.2 CANADIAN TESTS

During the past year the Canadians have been using a spacecraft, specifically ATS-5, and an aircraft, a KC-135, to determine the multipath parameters associated with this synchronous satellite to aircraft link. Using the C-band to L-band mode of the ATS-5 satellite, the Canadians employed a pseudonoise transmission as a probe signal. There are two antennas mounted on the aircraft: one, a top mounted quad helix steerable antenna which is pointed directly at the satellite; the other, a squared array mounted on the fuselage under the left wing. The receiver/demodulator on board the aircraft is illustrated in Figure 7-18. Since the energy reflected from the surface of the earth is delayed, relative to the direct path, the locally generated pseudonoise code will correlate with the reflected signal at a different time than the correlation occurring with a direct signal. Through this technique the measurement of the direct path signal strength, the multipath signal strength, and the time spread can be obtained. Since the ATS-5 satellite is spinning with a period of 780 milliseconds, the signal is received at the aircraft intermittently.

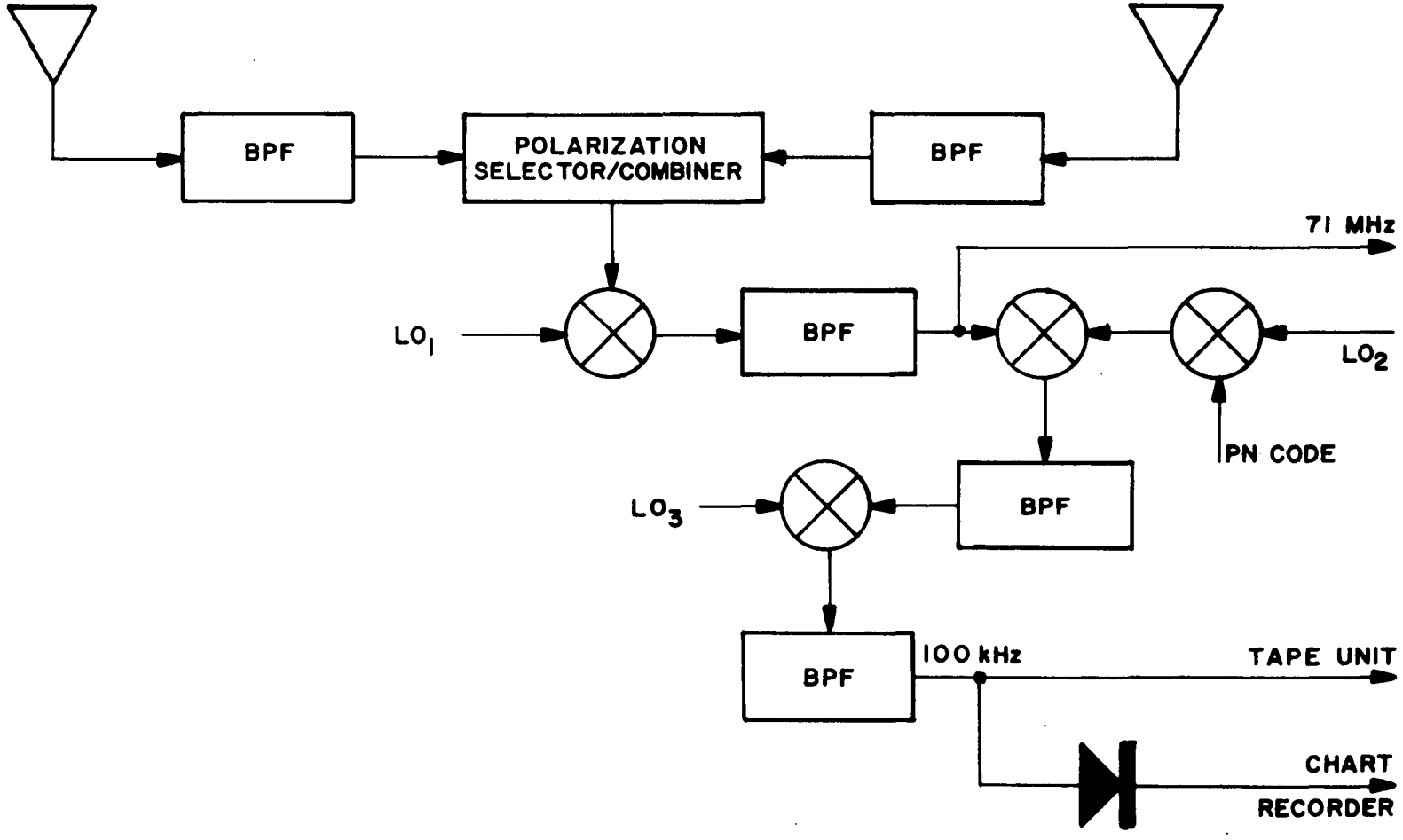

FIGURE 7-18 AIRCRAFT RECEIVER USED IN CANADIAN MULTIPATH EXPERIMENTS

The Canadians have found that for the KC-135 platform and grazing angles of between 0.174 radian (10°) and 0.349 radian (20°), the received multipath spread is on the order of 6 microseconds, which is in general agreement with the Lincoln Laboratories model. The relative amplitudes of the direct and multipath signals and fading bandwidth measurements were consistent with the Boeing results already discussed.

7.6.3 AIR FORCE AIRBORNE COMMUNICATION TESTS USING A SYNCHRONOUS SATELLITE

Over the past four years the United States Air Force at Wright-Patternson Air Force Base, Ohio, has conducted extensive measurements between an aircraft and a synchronous satellite. The synchronous satellites were LES-6 and a TACSAT satellite. The aircraft is an Air Force KC-135.

The aircraft was outfitted with a full complement of UHF and X-band transmitter/receiver and antennas. Multipath measurements, as well as RFI and simulated RFI measurements, have been conducted. A variety of modulation techniques have been employed including a variable data rate PSK modem, a pulse duration modulation voice modem, the TATS modem, and a three frequency diversity FSK modem. Extensive measurements have been made at very low grazing angles to determine the effects of multipath on the variety of modulation systems. The multipath measurements and the effect on data follow closely predictions based on theory. Like the FAA measurements, the Air Force has observed that the use of circular polarization will indeed suppress the multipath by some 6 to 8 dB. This arises as the result of the π radians (180°) phase shift and polarization reversal of the signal reflected off the surface.

The Air Force has estimated that the aircraft cost of these experiments is approximately a thousand dollars per flight hour which is in line with estimates for a commercially available aircraft. These costs, of course, do not include instrumentations or man-hours for collecting and reducing the data.

The Air Force programs will probably be extended for another year. During the forthcoming months additional tests will be conducted with frequency hopping and pseudonoise wideband signals so that a comparison between the two can be performed. The AN/URC-61 has already been tested by the Air Force and it is anticipated that the AN/USC-28 will also be tested during the forthcoming year. Both the AN/URC-61 and AN/USC-28 are wideband pseudonoise systems, the AN/URC-61 operating at a 10 Mchip/sec rate and the AN/USC-28 operating as high as 40 Mchip/sec.

Further airborne multipath fading measurements by the USAF from 250 to 8000 MHz show deep fading for shallow angles using linear polarization, but only moderate fading when circular polarization is employed. These measurements, reported in Reference 38, are summarized below for the frequency range of 100 MHz to 400 MHz.

Extensive measurements of an air-to-air and air-to-ground communications system in the frequency range of 100 MHz to 400 MHz have been made using linear polarized antennas both for transmission and for reception. The angle between the two communicating terminals and the reflection point was very small, on the order of .017 radian to .087 radian (1° to 5°) for the air-to-air and air-to-ground situation. Due to the shallow angle a

large amount of energy was expected to be reflected and extensive multipath could be the result. Over water specular reflection occurred and coherent fading of 10 to 15 dB in depth was regularly experienced, as shown in Figure 7-19. Over land or mountainous terrain the rms irregularities of reflecting surface were greater and random fading resulted. The level of multipath fading still reached 10 to 15 dB, but the fading exhibited a sporadic appearance rather than a regular, continuous cyclical multipath fading.

In the case of air-to-satellite-to-air or air-to-satellite-to-ground, the elevation angle between the reflecting point and the satellite repeater can vary from 0 to 1.57 radians (0° to 90°). A series of propagation measurements was made using the LES-3 satellite at a frequency of approximately 225 MHz. Both the satellite antenna and the airborne receive antenna were linearly polarized. Over water a very regular specular reflection was noted which was extremely angle dependent. For low elevation angles the reflection coefficient of the water is very high and extremely deep fading (20 to 25 dB) occurred, as shown in Figure 7-20. When the elevation angle was greater, the fading began to decrease, dropping from the 25 dB fades at 7° (.12 radian) to a few dB at 30° (.52 radian). Over either fresh water ice or salt water ice, the fading was still specular and as deep as over water. Over land the fading tended to be irregular, but occasionally it was as deep as over water. It exhibited the random occasional specular appearance with fading varying from 0 to 25 dB.

Later tests with the LES-5, LES-6, and TACSAT satellites in the 250 MHz frequency range utilizing circularly polarized receive and transmit antennas showed a considerably different result than the previous LES-3

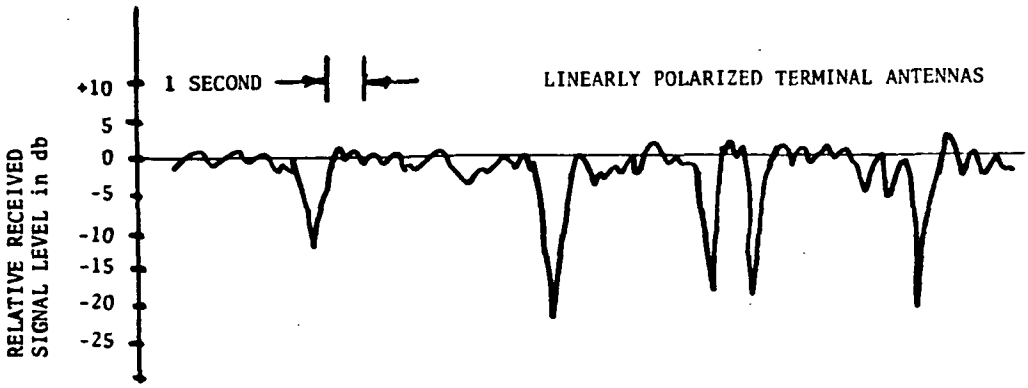

FIGURE 7-19 AIR-TO-AIR MULTIPATH OVER LAND AT 250 MHz

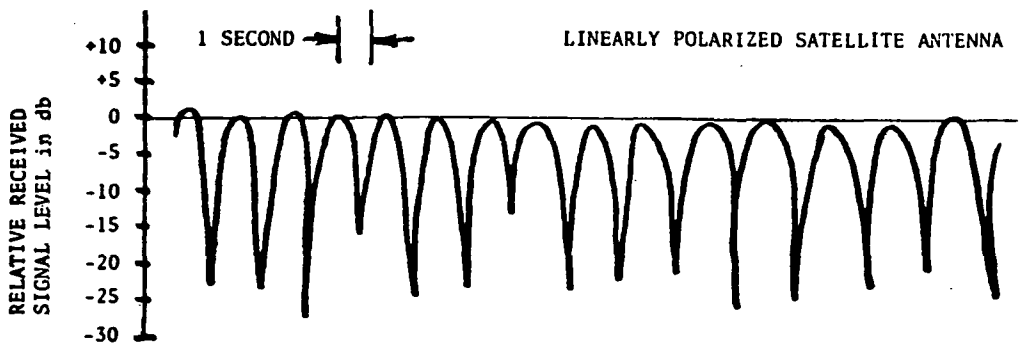

FIGURE 7-20 AIR-TO-SATELLITE MULTIPATH OVER WATER AT 225 MHz WITH LINEAR POLARIZATION

linearly polarized satellite antenna test. As the angle between the aircraft-to-reflecting surface and the aircraft-to-satellite varied from 0 to .26 radian (0° to 15°), regular multipath fading was experienced when the reflection point was over water. This fading usually varied from 5 to 10 dB in depth, as shown in Figure 7-21, compared with the 25 dB in fading previously noted on the LES-3 linearly polarized satellite. Above the .26 radian (15°) angle the fading was usually below 3 dB and often nonexistent. The fading over water clearly exhibited a specular reflection following a two ray multipath model. Over land the fading was irregular, sometimes being specular, but usually being quite random or diffuse and varying from 0 to 10 dB, as shown in Figure 7-22. Both linear and circularly polarized aircraft antennas were tested and the results were quite similar as long as the satellite antenna was circularly polarized.

The availability of the Air Force platform and instrumentation is subject to their own priorities and the compatibility of tests; that is, if NASA is interested in the test results from the Air Force, this can be made available, or if specific tests are desired, then the Air Force may be willing to accommodate these tests if they follow closely the established routine.

7.6.4 LINCOLN LABORATORIES MULTIPATH MEASUREMENTS

Lincoln Laboratories, in 1966, conducted a series of multipath measurements using the LES-3 satellite and an instrumented C-135 jet aircraft. Their results, reported in Reference 19, are summarized in this section.

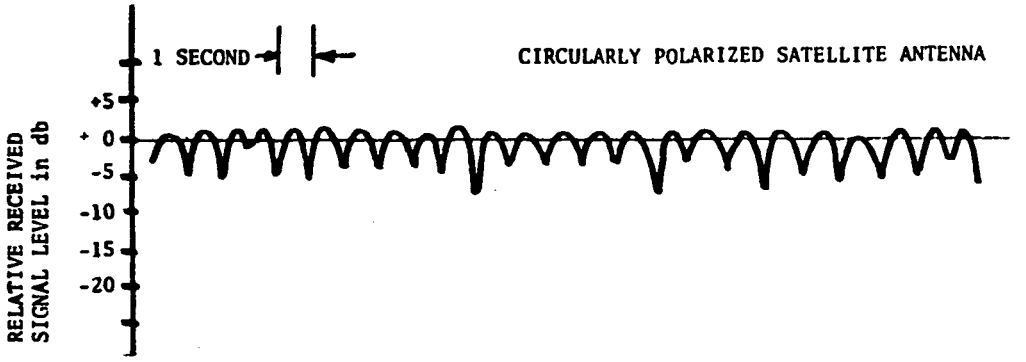

FIGURE 7-21 AIR-TO-SATELLITE MULTIPATH OVER WATER AT 250 MHz WITH CIRCULAR POLARIZATION

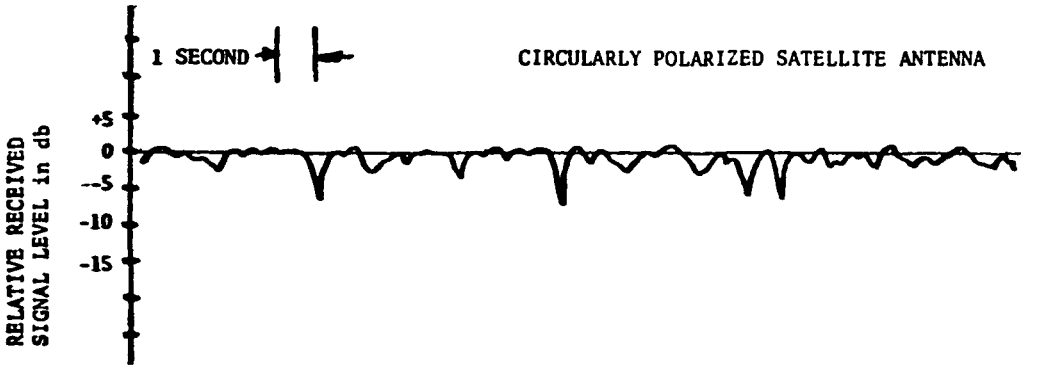

FIGURE 7-22 AIR-TO-SATELLITE MULTIPATH OVER LAND AT 250 MHz

The majority of the Lincoln Labs measurements were taken over the ocean surface, although some were taken over land, ice, and snow. Measurements were made over a variety of satellite elevation angles.

The LES-3 satellite was launched into an elliptical orbit with apogee near synchronous altitude. The satellite used two monopole antennas which radiated a linearly polarized wave. The carrier frequency was approximately 230 MHz with phase reversal keying at a 100 kHz rate according to a maximal length shift-register sequence of length 15.

The C-135 aircraft was equipped with separate horizontally and vertically polarized, forward-looking Yagi antennas mounted in the nose cone. It also had two pads on top capable of accepting experimental omnidirectional antennas.

The aircraft instrumentation consisted of the necessary filters, low-noise preamplifiers, and frequency conversion equipment to permit direct IF recording of the signals as received on each of the four antennas. In-flight monitoring was provided for any one of the four channels.

The data recorded at IF was passed through a 20-channel correlation receiver, each channel corresponding to a different delay. The channel outputs were digitized and rerecorded. A Fourier analysis was made of the digital data. Statistics such as the correlation of fading across the frequency band, correlation of fading with time, and the fading probability distribution were also determined.

The Lincoln Labs multipath measurements over the ocean have been consistent with theory, with the exception of the relative amount of diffuse component when the ocean surface is rough. This is shown in Figure 7-23. The theoretical values given by Equation 3-70 (in Section 3.4.7) are also shown for comparison. The reasons for the discrepancy are not known with certainty. They could be due to any of a number of factors; e.g., high ocean absorption, multiple scattering, etc.

7.7 COMPARISON OF MEASURED DATA WITH A COMPUTER SOLUTION TO DIFFUSE REFLECTION PROBLEM

A computer solution of the surface integral defining the ratio of diffuse multipath signal to direct path signal was undertaken by Deal (Reference 39). His program evaluates the integral

$$\left.\frac{P_R}{P_D}\right|_{a,b} = \frac{1}{4\pi}\int_{\alpha=0}^{\leq\pi/2}\int_{\beta=0}^{2\pi}\frac{1}{r_2^2(\alpha,\beta)}\,G(\alpha,\beta)\left|R_{ab}(\alpha,\beta)\right|^2\sigma(\alpha,\beta)\,d\beta\,d\alpha \qquad (7\text{-}20)$$

where $G(\alpha,\beta)$ = antenna gain function

$R_{ab}(\alpha,\beta)$ = reflection coefficient

$\sigma(\alpha,\beta)$ = scattering coefficient function, based on the link geometrical approximation $[r/r_1r_2]^2 \simeq 1/r_2^2$.

The diffuse multipath power reflected from the rough ocean surface was determined from the computer solution by summing together the contributions from segments of annular rings. The aircraft "look" angles α and β describe the incremental areas, and the summation is performed for equal increments of α and β for the entire surface out to the aircraft's local horizon. The scattering coefficient, σ, is a sensitive function of α and β

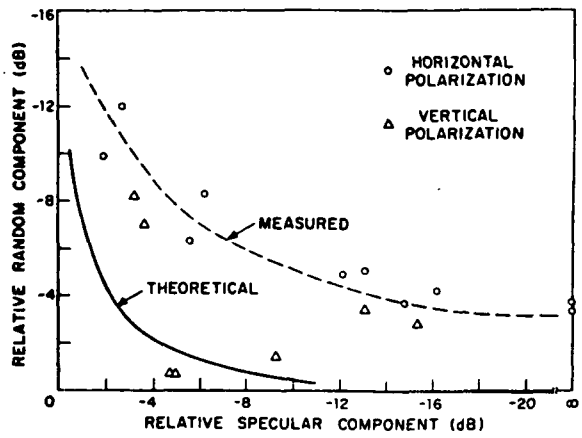

FIGURE 7-23 LINCOLN LABORATORIES MULTIPATH MEASUREMENTS AT 230 MHz OVER WATER

and dominates in determining the contribution from a particular incremental area. To account for the aircraft antenna pattern, the contributions from different segments, determined by α and β, are weighted according to the antenna gain, G, in that direction.

Since shadowing only has a significant effect near grazing incidence, the shadowing effect was omitted from Deal's computer solution. Also omitted was accounting for the curvature of the earth surface by a separate divergence term as is customary in the smooth-surface solution. Rather, the divergence of the reflected radiation due to the curvature of the individual tangent planes is acccounted for in the scattering coefficient.

A comparison of the computer solution with data measured by Boeing (Reference 40) and with an approximate solution by the method of steepest descent is shown in Figure 7-24. The Boeing tests results shown in this figure were conducted by transmitting a CW signal at 1551.7 MHz from the Rosman, North Carolina, STADAN ground station to a KC-135 airplane, via the ATS-5 satellite. It is noted that sea-state information is not available for the Boeing results, and that the computer solution approaches the results by the method of steepest descent as the rms roughness parameter is decreased.

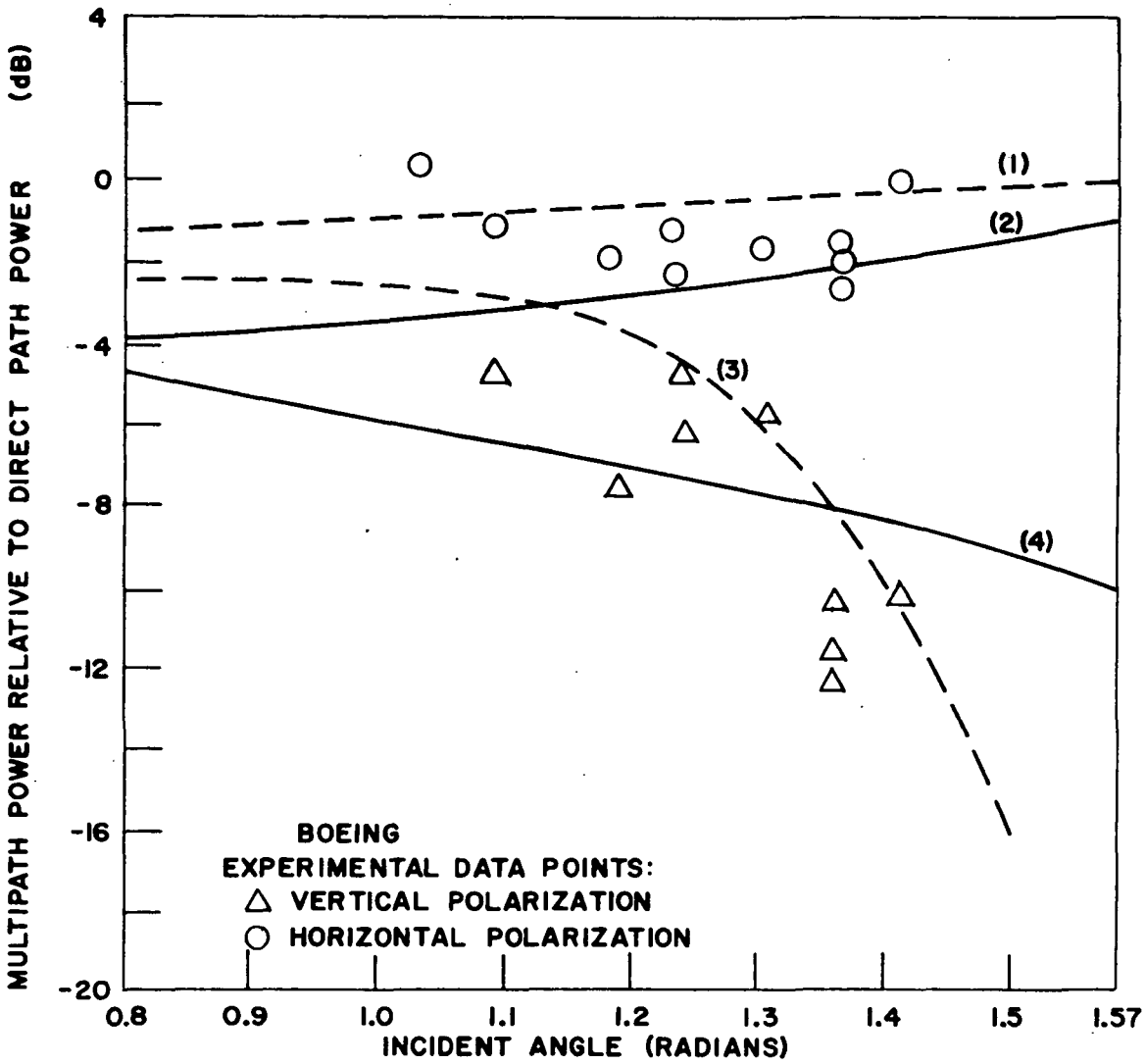

(1) METHOD OF STEEPEST DESCENT, HORIZONTAL POLARIZATION
(2) COMPUTER SOLUTION, HORIZONTAL POLARIZATION
(3) METHOD OF STEEPEST DESCENT, VERTICAL POLARIZATION
(4) COMPUTER SOLUTION, VERTICAL POLARIZATION

FIGURE 7-24 COMPARISON OF COMPUTER SOLUTION OF MULTIPATH POWER TO DIRECT POWER RATIO WITH APPROXIMATE SOLUTION BY THE METHOD OF STEEPEST DESCENT AND WITH EXPERIMENTAL DATA

8. SURVEY OF OTHER SATELLITES AND LOW ALTITUDE PLATFORMS FOR RFI AND MULTIPATH EXPERIMENTS

8.1 SATELLITE SURVEY

In addition to SATS, we have surveyed both "approved" and "probable" satellites now in orbit or to be launched through 1980 to determine if any of these satellites have application to multipath and RFI measurements. Specifically, we have looked at these satellites for their compatibility with SATS, aircraft, balloons, other satellites, etc. and if they can serve as relays or signal sources.

Shown in Tables 8-1, 8-2, and 8-3 is the most up to date listing of "approved" and "probable" satellites. Certain satellites, e.g. C-2 and Transit, are not shown in the Tables but are discussed separately.

We note from Table 8-3 that the SATS launches, occurring no earlier than 1976, may be too late for use in assessing the effects of RFI and multipath on the Space Shuttle communications.

Of the satellites surveyed, Table 8-4 lists satellites which were most promising. This selection is based on EIRP, frequency, launch dates, and bandwidth. Due to the lack of VHF and UHF equipments on commercial satellites (e.g. INTELSAT III and IV), none were found suitable for further consideration.

8.2 SATELLITE DESCRIPTIONS

8.2.1 ITOS-F AND -G FOR RFI EXPERIMENTS

In an attempt to establish the possibility of placing an RFI experiment on board an ITOS series satellite the following spacecraft

TABLE 8-1 APPROVED MISSIONS

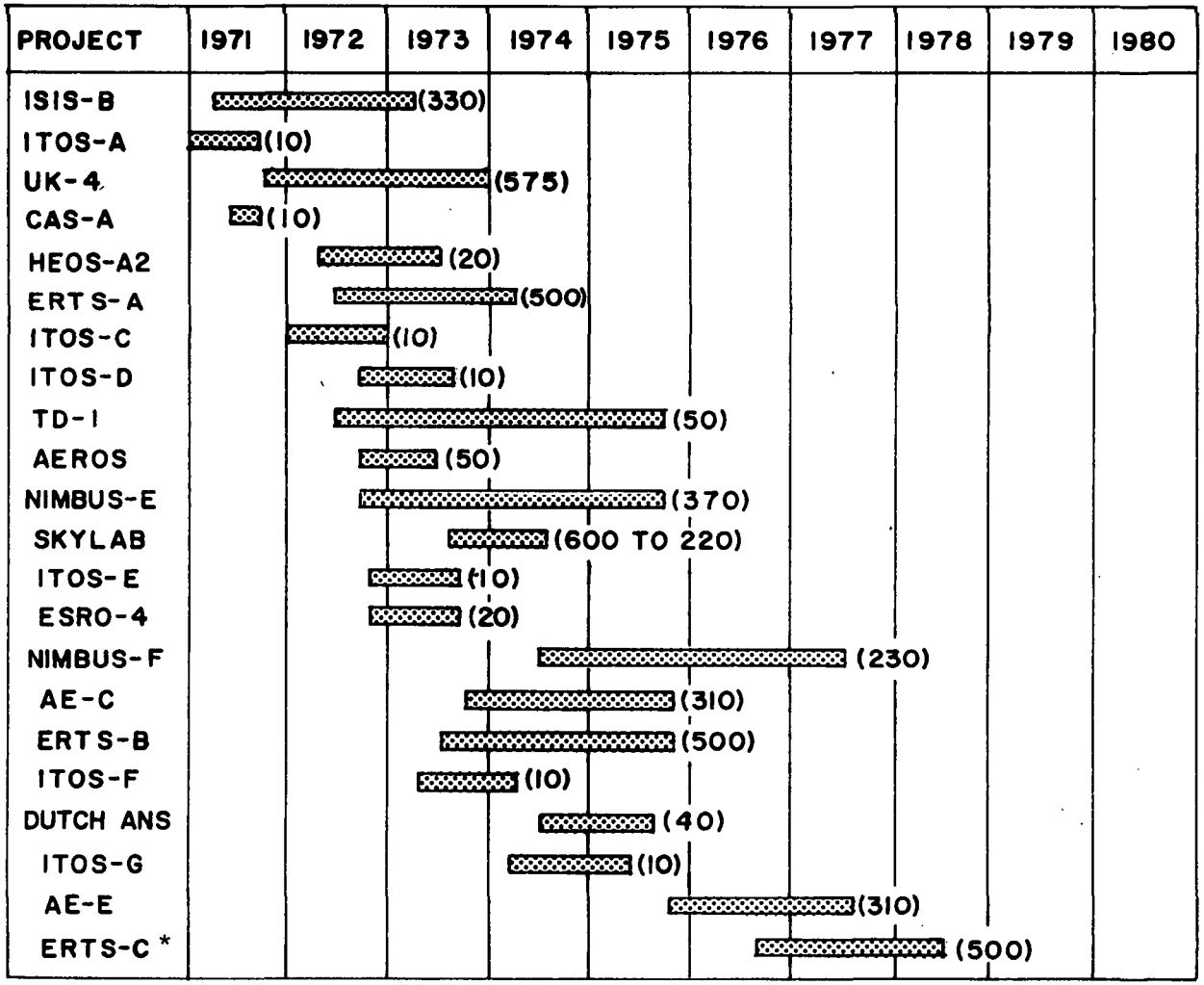

THE NUMBER IN PARENTHESES IS THE MINIMUM LINK DATA HOURS REQUIRED PER QUARTER YEAR.

* THESE MISSIONS MAY NOT BE APPROVED.

TABLE 8-1 (CONT.) APPROVED MISSIONS

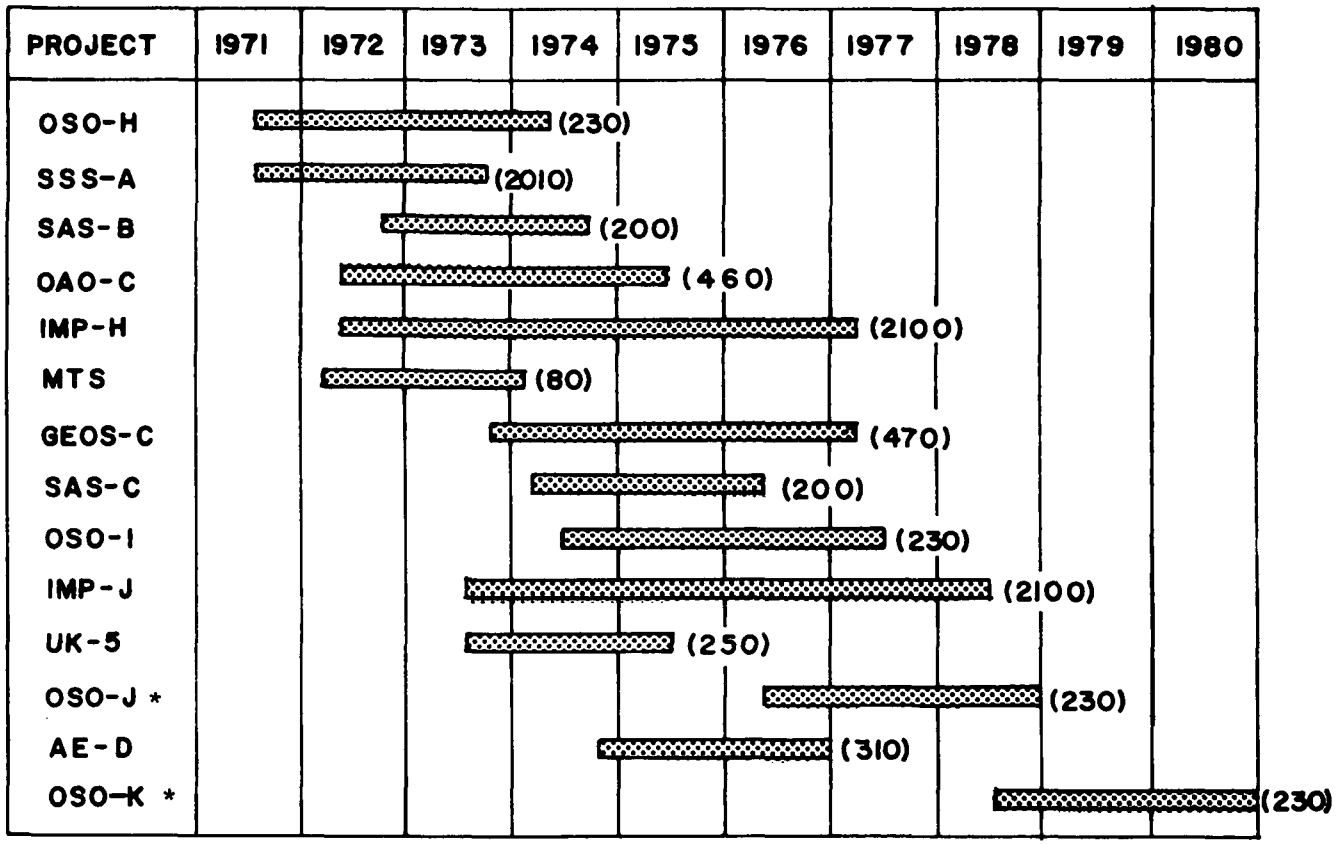

THE NUMBER IN PARENTHESES IS THE MINIMUM LINK DATA HOURS REQUIRED PER QUARTER YEAR.

* THESE MISSIONS MAY NOT BE APPROVED.

TABLE 8-2 FUTURE APPROVED MISSIONS-EARTH SYNCHRONOUS

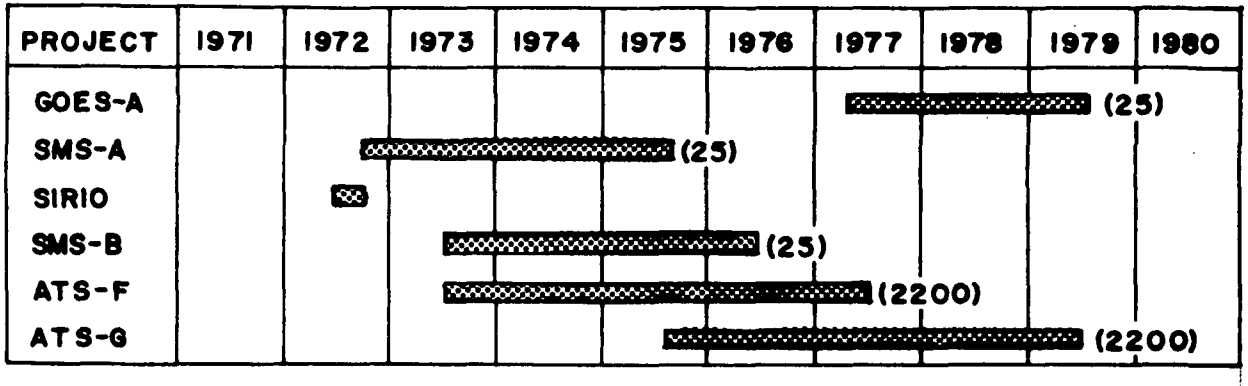

THE NUMBER IN PARENTHESES IS THE MINIMUM LINK DATA HOURS REQUIRED PER QUARTER YEAR.

TABLE 8-3 FUTURE MISSIONS MOST LIKELY TO BE APPROVED

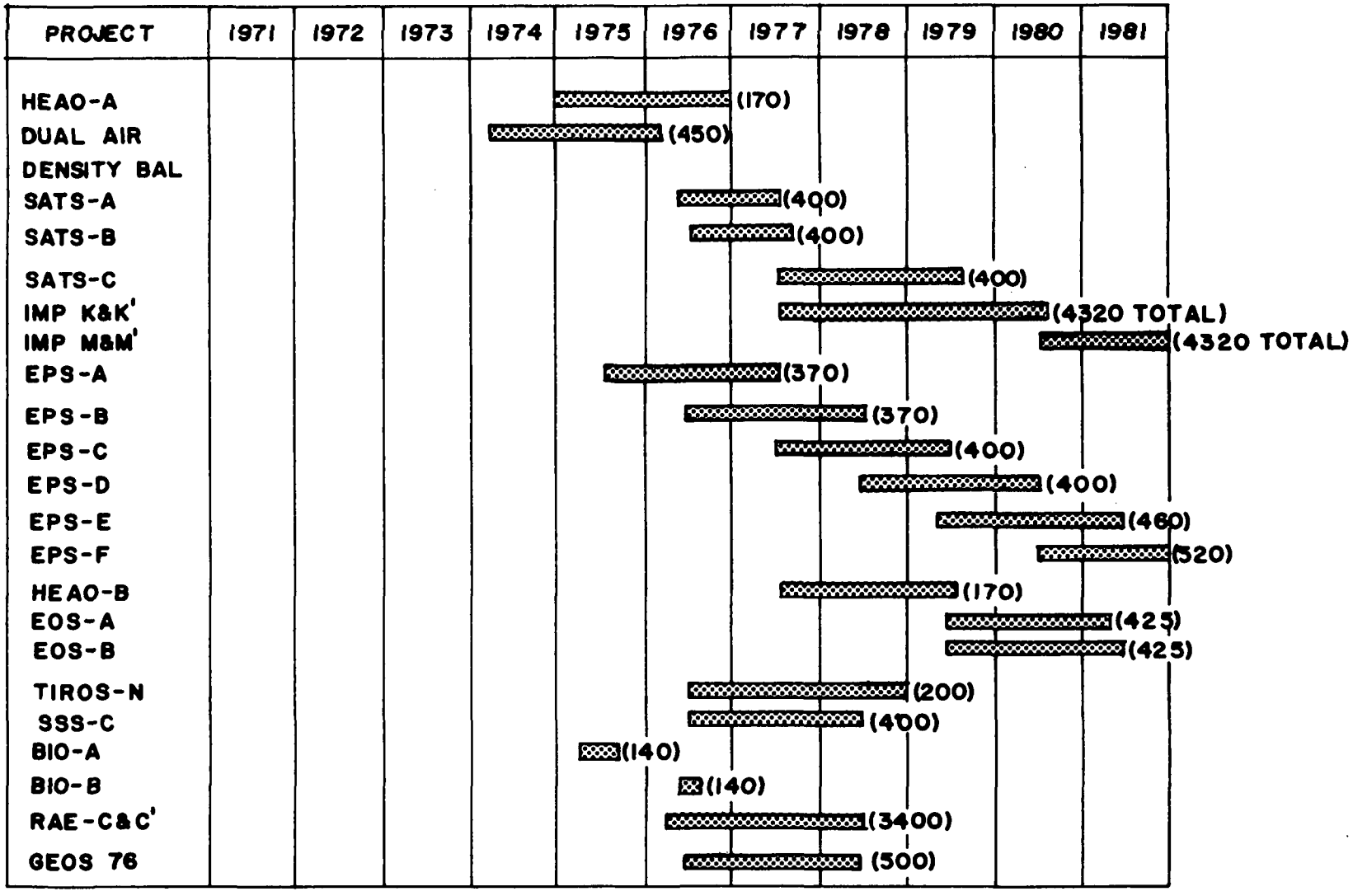

THE NUMBER IN PARENTHESES IS THE MINIMUM LINK DATA HOURS REQUIRED PER QUARTER YEAR.

TABLE 8-3 (CONT.) FUTURE MISSIONS MOST LIKELY TO BE APPROVED

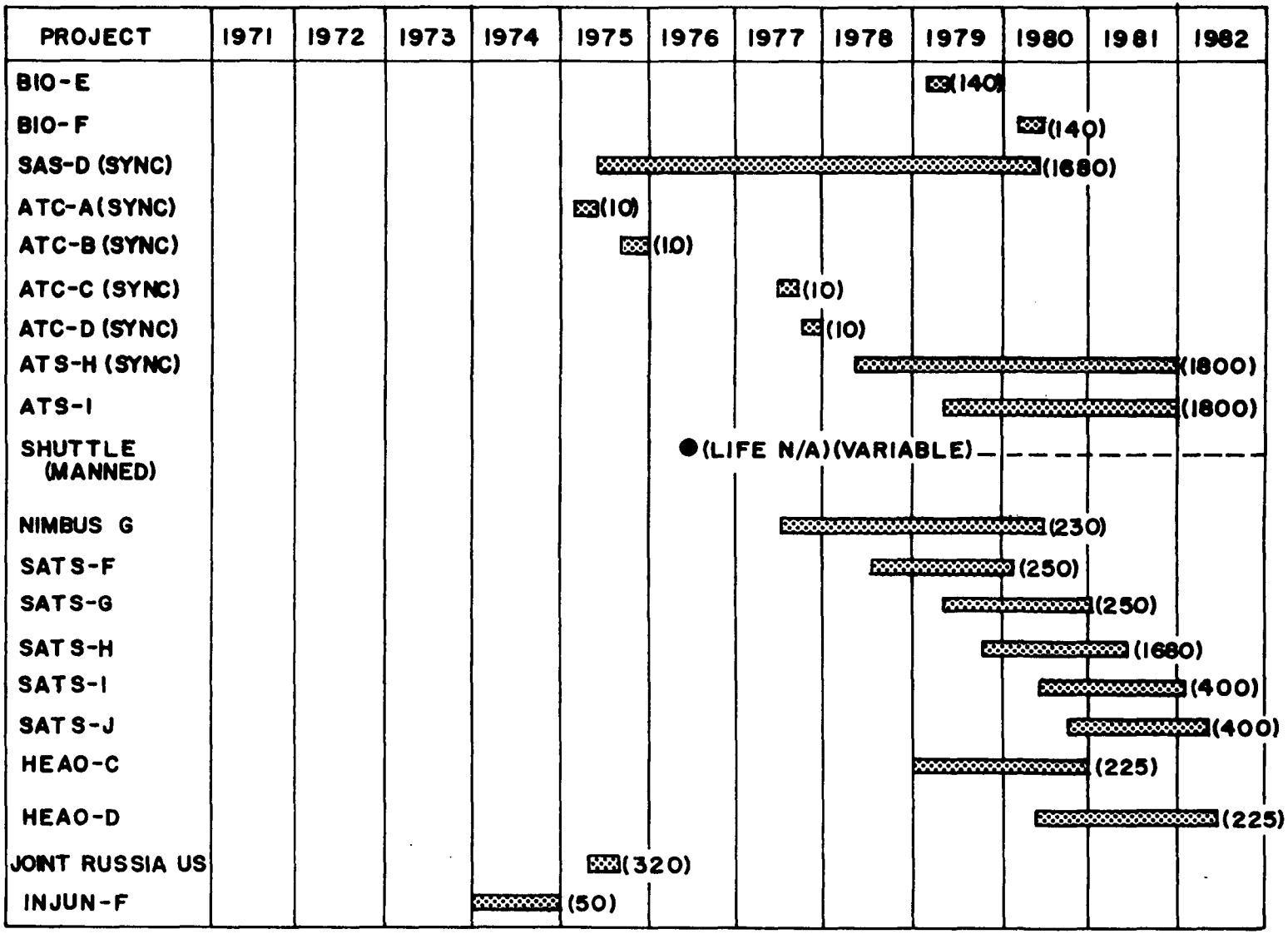

THE NUMBER IN PARENTHESES IS THE MINIMUM LINK DATA HOURS REQUIRED PER QUARTER YEAR.

TABLE 8-3 (CONT.) FUTURE MISSIONS MOST LIKELY TO BE APPROVED

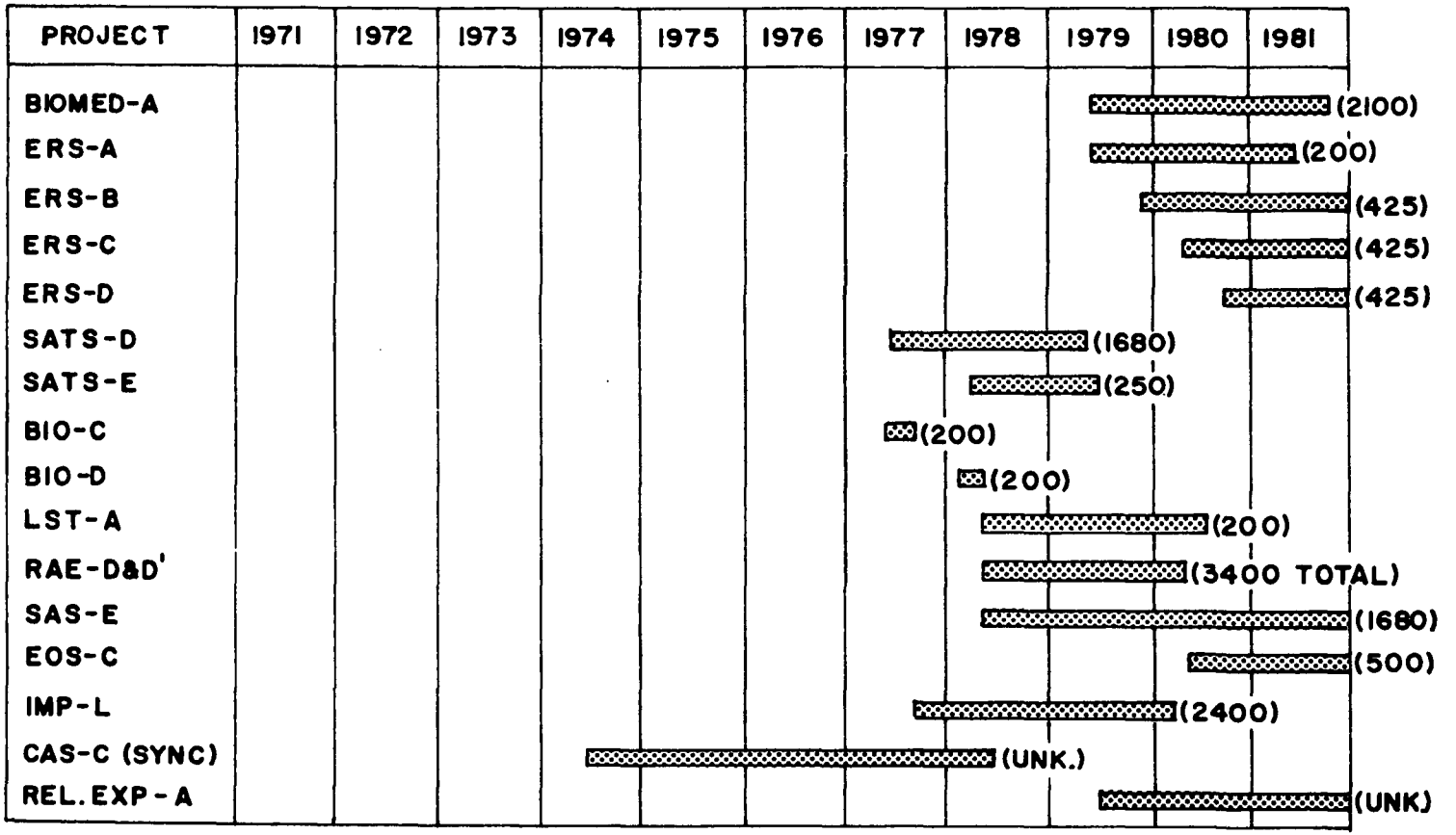

THE NUMBER IN PARENTHESES IS THE MINIMUM LINK DATA HOURS REQUIRED PER QUARTER YEAR.

TABLE 8-4

MOST PROMISING ALTERNATIVE SATELLITES

ITOS-F and -G
ERTS-B
SAS-C
SMS
ATS-F
TRANSIT
C-2
SAS-D (Synchronous)(Probable)
Skylab

characteristics were evaluated. Table 8-5 lists the parameters related to the ITOS-F and -G satellites.

Assuming an RFI experiment would require 40 watts of DC power and an additional payload weight of 35 pounds, an analysis of existing experimental requirements reveals that it is not possible to support an additional experiment of this magnitude. The available power on ITOS-F and -G is 9 watts and is not capable of supporting an RFI experimental package (Reference 41).

8.2.2 SAS-C CHARACTERISTICS

The SAS-C satellite will utilize telemetry data rates of nominally 1 kilobit/second, but will be programmable from 16 kb/s to approximately 125 b/s in binary steps.

SAS-C will accept one command every two seconds and will use the standard PCM VHF standard for commands, but also has stored command capability for those commands which it executes during the latter portion of the orbit. An upper bound on the number of commands per orbit is six.

TABLE 8-5

CHARACTERISTICS OF ITOS-F AND -G SATELLITES

ITOS-F	
Launch	June 1974
Apogee	1460 km
Perigee	1460 km
Period	115 minutes
Inclination	102 degrees
Tracking Frequency	136.77 MHz @ .25 w
Telemetry Frequency	136.77 MHz @ .25 w @ 30 kHz bandwidth 137.5 MHz @ .5 w @ 30 kHz bandwidth 1697.5 MHz @ 4.0 w @ 360 kHz bandwidth
Modulation/ Subcarrier	136.77 MHz FM/PM 137.5 MHz AM/FM 1697.5 MHz FM/FM
Command Frequency	148.56 MHz
ITOS-G	
Launch	June 1975
Apogee	1460 km
Perigee	1460 km
Period	115 minutes
Inclination	102 degrees
Tracking Frequency	136.77 MHz @ .25 w
Telemetry Frequency	136.77 MHz @ .25 w @ 30 kHz bandwidth 137.62 MHz @ .5 w @ 30 kHz bandwidth 1697.5 MHz @ 4.0 w @ 360 kHz bandwidth
Modulation/ Subcarrier	136.77 MHz FM/PM 137.62 MHz AM/FM 1697.5 MHz FM/FM
Command Frequency	148.56 MHz

At VHF, SAS has one quarter or two watt transmitter power capability. It has a 4 watt capability at S-band.

SAS-C has been designed for a 555 km circular equatorial orbit. Since it is an astronomical satellite it can take on random orientations,

commandable from the ground. It also has the capability to lock on the earth with IR sensors.

SAS-C is equipped with two VHF turnstile antennas and two S-band helices. The S-band helices are combined to form an omni-directional pattern, whereas the VHF turnstiles are used as inputs to two independent VHF command receivers. They also act as transmitting antennas. There is space available on SAS for a directional S-band antenna.

8.2.3 CHARACTERISTICS OF THE C-2 SATELLITE

In support of the Maritime Satellite Program, NASA is contemplating launching a synchronous C-2 satellite which has been built by Hughes under the ATS program. Basically the C-2 satellite is an ATS-3 configuration and will have the capability of operating primarily at L-band. It will transmit at 1540 to 1560 MHz and will receive at 1640 to 1660 MHz. It will have an L-band to L-band and L-band to C-band cross strap capability, but no C-band receiver will be available on the C-2 satellite. The C-band transmitter will operate at 4012 MHz. With a phased array antenna a 17 dB gain earth coverage antenna pattern is produced at L-band. Actually the antenna pattern will be warped to maximize coverage, i.e. ± 6 degrees (0.105 radian) in the latitude and ± 8 degrees (0.140 radian) in the longitude. The off-axis gain will be approximately 14.5 dB at the beam edges. It is anticipated that a total power of 40 to 50 watts will be available for L-band transmissions and the goal for the output EIRP is 30 dBw at beam center. The spacecraft will have a lifetime goal of 3 years and should be launched no later than January of 1974. The spacecraft will utilize a translating hard-limiting repeater.

8.2.4 SYNCHRONOUS METEOROLOGICAL SATELLITE

The SMS or GOES satellite is scheduled for launch late in 1973. It is a geosynchronous sensor-ladened satellite which will also serve as a relay for meteorological data. The relay functions are at S-band and UHF.

The UHF relay capability is of particular interest. The SMS transmits on 466 MHz and receives on 401.7 to 402 MHz. The receiver bandwidth is 300 kHz, while the transmitter bandwidth is 100 kHz. The maximum EIRP available from the satellite at UHF is 24 dBw.

8.2.5 TRANSIT

Four TRANSIT satellites are in circular polar orbits at altitudes of 964 km (600 miles). They are used to provide precise position location for near-earth platforms with low velocities, e.g. ships. This is accomplished by transmitting two carriers, one at 150 MHz and one at 400 MHz, from the satellite to the platforms. The Doppler on these signals is precisely measured at the platform and, along with satellite emphemeris data which is transmitted to the platform, is used to compute the platform's position. The TRANSIT satellites are gravity-gradient stabilized and use an earth-directed antenna to transmit the signals. The dual channel approach is used to calibrate out ionospheric effects.

It may be possible to use the signals transmitted from TRANSIT to obtain multipath data from an elevated platform such as a balloon or high flying aircraft, e.g. U-2, KC-135, C-121, etc. Figure 8-1 presents a possible test configuration showing how the TRANSIT satellite signal at 400 MHz or 150 MHz could be received and relayed to the ground for processing.

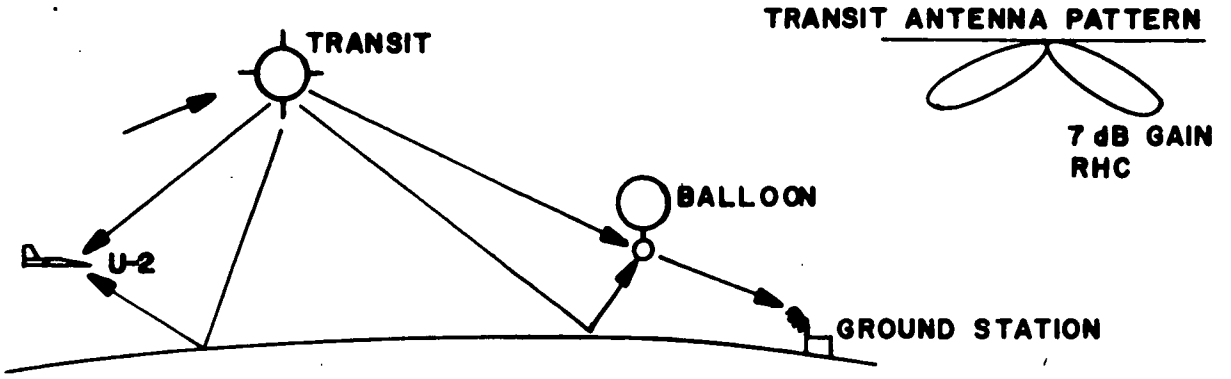

FIGURE 8-1 TRANSIT SATELLITE AND BALLOON OR U-2 USED FOR MULTIPATH MEASUREMENT

To isolate the direct path from the reflected signal a top and bottom mounted antenna configuration would be employed. Commands from the ground could be used to switch the bottom mounted antenna from RHC to LHC to measure the polarization sense of the reflected signal.

The balloon package is envisioned as a simple translating repeater with a command receiver which performs gain control, antenna switching, on-off and package release functions. The balloon package contains a standard beacon for tracking from the ground.

The 400 MHz signal from TRANSIT is right hand circularly (RHC) polarized. The transmitted EIRP is only 1.2 watts at 400 MHz, which produces a signal level of -125 dBm to -130 dBm (measured) on the ground at a slant range of 3860 km (2400 miles). Plans call for increasing the EIRP from new TRANSITS to 3 watts. The transmit antenna patterns on TRANSIT (see Figure 8-1) are designed to favor low elevation angles. Thus the received signal from the satellite at high elevation angle is <u>not</u> increased by as much as 16 times.

A "one in view" TRANSIT system is now being planned. This new concept may be implemented in time to serve as a means of gathering multipath data. The current TRANSIT system gives only periodic service because of the limited number of satellites involved. The new scheme places many more satellites in orbit so that a satellite is visible to a user even at the equator. The same frequencies and orbits are used but obviously co-channel interference is greatest at higher latitudes when more than one satellite is in view. To resolve this problem each satellite is given a unique PN code. Through correlation techniques the satellite signals can be separated in the ground equipment and only one satellite's signal is used for position location calculations. If the chip rates associated with the PN code are sufficiently high, then a dual channel receiver might be used in conjunction with top- and bottom-mounted antennas and the balloon configuration of Figure 8-1 to measure all of the multipath parameters if an adequate S/N ratio is available at the balloon platform.

The received signal at a balloon with a typical circularly polarized antenna can be as high as -117 dBm or as low as -122 dBm at a slant range of 3860 km with 3 watts transmitted from TRANSIT. If the noise density is taken at -174 dBm/Hz the C/N_o value realized will be between 57 dBHz and 52 dBHz. This range of received C/N_o is marginal if multipath signals 20 dB below the direct path are to be measured with a fading bandwidth of approximately 6 kHz at 400 MHz.

8.2.6 ATS-F SATELLITE

ATS-F is configured to transmit at UHF (860 MHz) with an effective EIRP of 48 dBw (80 watts into a 9.14 m (30 foot) parabolic

antenna). ATS-F will also have a 40-watt capability at L-band and a 20-watt capability at S-band.

At UHF the antenna pattern will have a field of view of 0.049 radian (2.8 degrees). This means that when looking directly at the equator an area of 1770 km (1100 miles) on a side will be illuminated from synchronous altitudes. In order to illuminate areas at higher latitudes mechanical slewing of the ATS-F antenna will be required. The present design calls for a slew capability of $\pm$0.175 radian ($\pm$10 degrees) off axis. At S-band and at L-band the present design for ATS-F calls for electronic steering of the beam with a maximum deviation of $\pm$0.088 radian ($\pm$5 degrees). At the above mentioned power levels, an omnidirectional receiving antenna with a 300 K noise temperature near the earth would have available 69 dBHz C/N_o at UHF, 66 dBHz at L-band, and 63 dBHz at S-band. These signal levels are adequate for making multipath measurements, especially if antenna discrimination techniques are employed.

If multipath measurements are made using an ATS-F/SATS configuration consideration must be given to the narrow beam width associated with ATS-F. At UHF (860 MHz) the beam width is 0.049 radian (2.8°); and at L-band, ~0.026 radian (~1.5°). Therefore certain geometries between SATS and ATS-F at L- and S-band will provide only marginal measurements since the ATS-F beam width is so narrow that the simultaneous reception over the direct path and the reflected path is not possible.

While the UHF beam width is adequate to provide simultaneous reception of both signals by a SATS, even at 1.05 radian (60°) inclin-

ation angle, the beam width at L-band is considered marginal. At S-band the beam width constraints are such that either the direct path or the reflected path can be measured, but not both, for certain geometries.

8.2.7 ATS-3

ATS-3 is located at 65°W and is still considered operational. As shown in Table 8-6, ATS-3 operates at VHF, transmitting at 135.6 MHz with a bandwidth of 100 kHz.

Assuming that the ATS-3 transmitter power is 25 dBw the expected received signal level at a low altitude SATS would be -107 dBm if a 5 dB upward looking antenna is used on SATS.

If the SATS receives at 136.5 MHz and if RFI is not present, a noise density at the SATS of -174 dBm/Hz is reasonable. Thus the received C/N_o is approximately 67 dBHz, a respectable signal to noise density for multipath measurements.

8.3 BALLOONS AND AIRCRAFT AS PLATFORMS FOR THE SATS RFI/MULTIPATH EXPERIMENTS

It is well known that NASA conducts many experiments and measurements with balloons which are capable of carrying payloads to altitudes in excess of 30 km (100,000 feet). For example, a relatively small balloon, one which has a capacity of 28300 m^3 (10^6 ft^3) of gas, can be launched for approximately $10,000 and would provide upwards of ten hours of usable data. This balloon has a maximum altitude of 36.6 km (120,000 feet) and a payload capacity of 226 kg (500 pounds). For a cost of between $25,000 and $30,000, a balloon with a gas capacity of 283,000 m^3 (10,000,000 ft^3) and payloads on the order of several thousand kilograms can be obtained.

TABLE 8-6 VHF REPEATER CHARACTERISTICS

CHARACTERISTIC	ATS-1	ATS-3
Transmitter output power (5 watts), dBw	7.0	8.0
Total output power (40 watts), dBw	16.0	17.0
Antenna	Phased array	Phased array
Antenna gain, transmit, dB	9.5	10.5
Antenna gain, receive, dB	>7.5	>7.5
Antenna polarization	Linear	Linear
Transmitter losses (diplexer and cables), dB	2.4	1.7
ERP, dBw	23.1	25.8
Receiver losses (diplexer and cables), dB	<1.4	<1.3
Receiver noise figure, dB	4.0	3.5
Receiver bandwidth, kHz	100.0	100.0
Transmitter frequency, MHz	135.6	135.6
Receiver frequency, MHz	149.22	149.22
DC power required, watts	<90.0	<105.0
Third and fifth IM level, dB below carrier	>9.5	>16.0

Normally the balloons are tracked via a beacon and the payload package retrieved by means of a parachute. Depending upon the altitude, drift rates on the order of 2.5 to 7.5 m/s (5 to 15 knots) will be incurred. It is standard practice not to launch these balloons over populated areas, thus restricting to some extent their flexibility. Furthermore, appropriate weather conditions must prevail for launches so that abnormally high drift rates do not carry the balloon far from the desired area.

The balloon can carry a relatively simple translating repeater which can be made coherent with the ground if required. Signals emanate from the balloon and are received by a lower altitude aircraft. The direct path signal and the multipath signal arrive at the aircraft and are separated by top- and bottom-mounted antennas on the aircraft. An attractive feature of the balloon/aircraft configuration is that the aircraft can easily track the balloon and compensate for drifts over a long term period. The primary disadvantages of the balloon as an active relay are that proper weather conditions and restricted geographical areas must be used in the test. In addition to these factors, it is often difficult to retrieve the repeater package after the balloon mission is spent. Thus, the repeater must be low cost or expendable.

8.4 NASA U-2 AIRCRAFT FOR RFI AND MULTIPATH MEASUREMENTS

NASA owns two high altitude U-2 aircraft. Landing facilities are provided at Moffett Field, California and Wallops Island, Virginia. Routine flights are conducted along the East and West Coasts and across the United States. The NASA U-2 aircraft can carry a payload of up to 210 kg (460 pounds) in the equipment bay for a distance of 2800 km (1,500 n.m.)

at a velocity of 240 m/s (.7 mach) and an altitude of approximately 20 km (65,000 feet).

The availability of flights by the U-2 depends primarily on the pilot and ground crew availability. Both pilot and ground crews are provided by Lockheed. It is recommended that the number of hours per day per flight not exceed 6.5 hours and not to exceed 26 flights per week or 100 flights per month.

The general configuration of the U-2 is shown in Figure 8-2.

The attitude control of the aircraft is quite adequate. The U-2 can turn at a bank angle of 0.45 radian (26 degrees) at 20 km (65,000 feet) which represents a turn rate of 0.023 radian/sec (1.34 degrees/sec).

A U-2 is outfitted with a complete compliment of communications and navigation equipment. On board radio and navigation equipment consists of low frequency receivers from 0.19 to 1.75 MHz, high frequency receivers from 2-30 MHz, VHF receivers from 108 to 152 MHz, ultra-high frequency receivers from 225 to 400 MHz, and radar receivers from 1030 to 1090 MHz.

The equipment bays are maintained at a pressure of between 37900 N/m^2 (5.5 psi) and 31000 N/m^2 (4.5 psi) between altitudes of 15 km (50,000 ft.) and 21 km (70,000 ft.). The temperatures of the equipment bay ranges between 278 K (5 C) and 298 K (25 C), depending upon the location within the bay.

It is understood that the nose cone of the U-2 is plexiglass and could be used to house antennas if necessary.

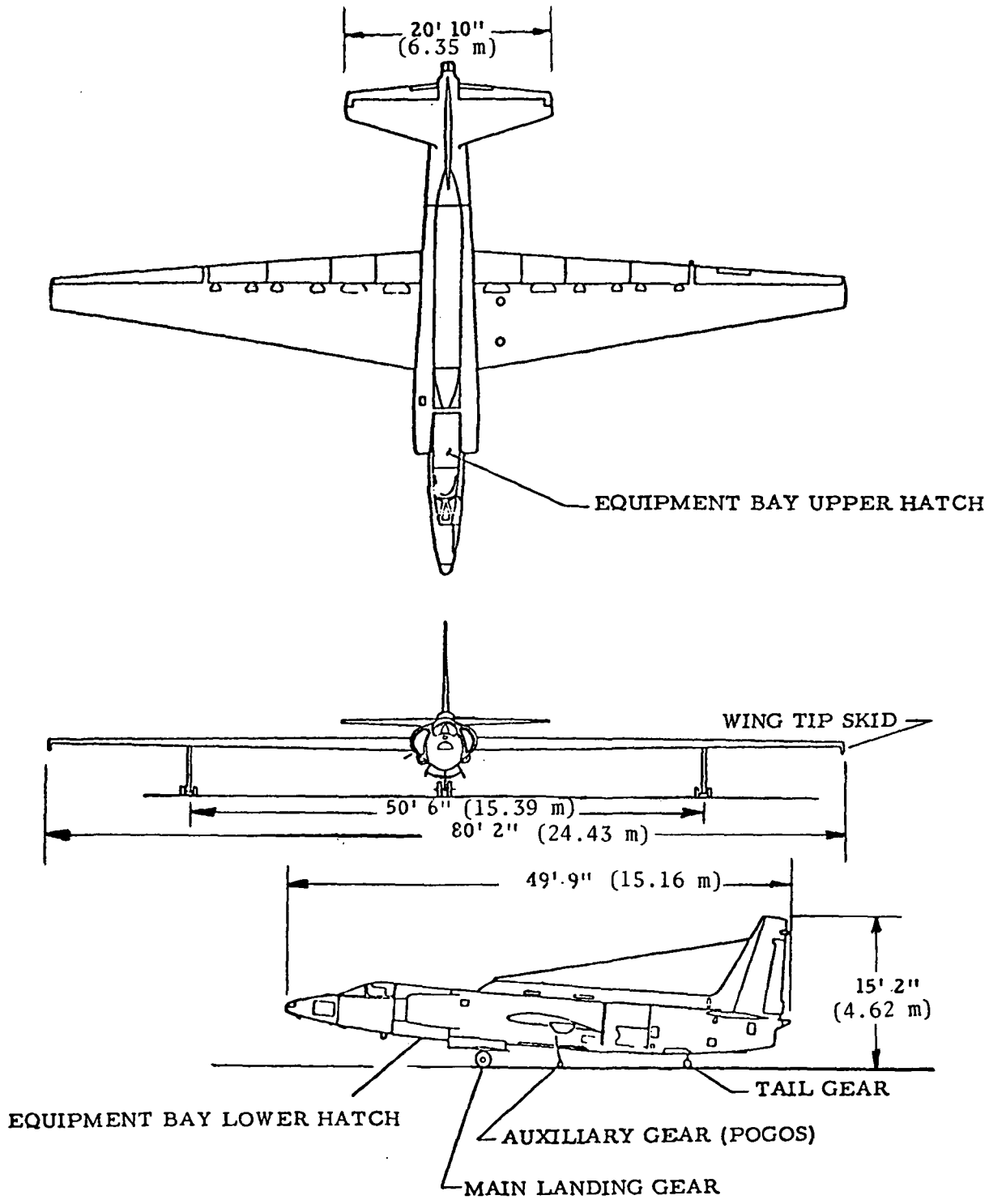

FIGURE 8-2 GENERAL CONFIGURATION OF U-2 AIRCRAFT

The most attractive features of the U-2 are its altitude capability, its equipment capacity, and its cost of operation. The flight cost is very low. The main disadvantages are scheduling of flights and the severe constraints on modifying the aircraft for special antennas, etc.

8.5 NASA C-118/C-121 TEST AIRCRAFT

After December 1972 a NASA test aircraft will be available. These aircraft, the C-118 and C-121, have a maximum altitude of 6.1 km (20,000 feet). Hourly operations cost for these aircraft is on the order of $650. These aircraft are outfitted with about 6 racks of equipment plus a Honeywell DDP-516 computer. Receivers are available at 136 MHz, 400 MHz, and 1700 MHz. All necessary testing equipment for monitoring the performance of the receivers and transmitters is also available. Aircraft attitude and heading information are available from a circular flight path unit and the attitude read-out unit. A full compliment of Hewlett-Packard test equipment and signal generators is also provided.

In addition to a complete compliment of test equipment, chart recorders and wideband analog tape recorders (FR-1300) are available.

The advantages of the NASA C-118/121 aircraft are its availability and its instrumentation, as well as its relatively low cost of operation. The major drawback associated with the aircraft is its maximum altitude limitation of 6.1 km (20,000 feet).

9. CONCLUSIONS AND RECOMMENDATIONS

In this study we have attempted to define the time varying channel which can exist between a synchronous relay satellite and a lower altitude platform, such as SATS, Space Shuttle, aircraft, etc. We have defined all of the parameters which we consider significant in the description of this channel. These parameters include RFI originating on the surface of the earth.

We have surveyed a number of multipath models, and of these models we have selected Painter's model and Lincoln Laboratories' model as being most representative of a synchronous satellite to low altitude aircraft link. Both these models are substantially the same and have been verified by experiments conducted between a synchronous satellite and a low altitude aircraft. These experiments have been conducted at VHF, UHF, and L-band. The model which seems the most appropriate for a synchronous satellite to low altitude satellite (e.g. shuttle or SATS) is the multipath model developed by ESL, Inc., Sunnyvale, California. This model has not been verified by experiments. However, we are confident that the theoretical predictions for this link should follow closely experimental results. Furthermore, we believe that the results obtained by multipath measurements using lower altitude aircraft from the synchronous relay satellite can be extended to the synchronous relay to low altitude satellite link. For these reasons, in order of priority, we consider multipath measurements to be less important than RFI measurements. Furthermore, it has been shown in Section 6.2.4 that a low altitude satellite, when operated with a synchronous relay satellite, can function with little or no degradation in the presence of multipath if proper coding is employed (e.g. pseudonoise spread spectrum modulation). In other words,

multipath problems can be circumvented. More will be said later in this section when specific recommendations and conclusions concerning multipath measurements and RFI measurements are addressed.

9.1 CONCLUSIONS AND RECOMMENDATIONS REGARDING HARDWARE DESIGNS

We have designed in this study several pieces of hardware. First, we have provided a detailed block diagram of an adaptive delta modulator for voice. The adaptive delta modulator is based upon a British Post Office design which was judged the best adaptive delta mod available for practical military use under the MALLARD program. The unit as originally designed operates at 19.2 kb/s, but this rate can be increased to 24 kb/s with only minor modifications to the time constant associated with the encoder. The cost of this unit should not exceed $10K for a breadboard development while the cost in production is trivial.

In addition to the adaptive delta modulator for voice, it is recommended that predictive coding be studied for Space Shuttle applications. Very high quality voice has been demonstrated using predictive coding at data rates as low as 3.6 kb/s. This represents a substantial savings in bandwidth relative to a delta mod if bandwidth is a commodity. The lower data rate associated with predictive coding also implies that the predictive coded voice could be transmitted over NASCOM network lines to central points where the voice could be reconstructed in its analog form. The lower data rate also implies that if the requirement remains to transmit voice with a speedup factor of 2, as was required in the Apollo program, then the use of lower data rates allows this to be done using conventional data modems over voice-bandwidth transmission lines.

A rate $\frac{1}{2}$, constraint length 5 convolutional encoder/maximal likelihood decoder forward error control unit has been designed in this study. A transparent code has been devised for this rate and constraint length. Performance curves indicate that for a 10^{-4} bit error probability 4 dB coding gain can be achieved. Soft decisions (8 quantizing levels) are employed in the decoder. The unit is designed to operate as high as 1 megabit/sec and to interface between a data source or voice coder and the multipath encoding system (e.g. high index wideband FM or pseudonoise transmitters).

A high index wideband FM system has been designed in block diagram form and follows closely the design advocated by ADCOM. Subsequent analysis has shown that this approach is highly susceptible to the degrading effects of both RFI and multipath; therefore, we recommend that the FM system not be considered or pursued for application to the relay satellite to Space Shuttle link.

A spread spectrum pseudonoise modem which will interface with the forward error control encoder and decoder has been designed in this study. Detailed schematics are provided for this unit. The unit can accommodate data rates up to 76.8 kb/s and can be operated in a clear PSK mode. The cost to develop this unit is placed between \$50K and \$60K. We hasten to point out that similar pseudonoise equipment is being designed for NASA Goddard and for MSC. These facts make the pursuit of the development of another pseudonoise equipment questionable. Performance of the pseudonoise system in the presence of RFI and multipath is analyzed in Section 6.2.4 of this report.

Of the two systems for combatting multipath that have been considered in this report, we recommend that pseudonoise be used for the link between a relay satellite and Shuttle. The pseudonoise spread spectrum waveform provides in a single waveform range, range rate, and data signals while combatting the effects of multipath and RFI. The pseudonoise waveform also minimizes the flux density incident on the earth.

Unlike the pseudonoise system, the wideband high index FM system is penalized for many reasons. The data and ranging signals are separate, thus dividing the useful power between a number of channels. The resulting spectrum is not uniform across the band and could present flux density problems.

9.2 CONCLUSIONS AND RECOMMENDATIONS CONCERNING MULTIPATH AND RFI MEASUREMENT

It is obvious that there are a large number of candidate configurations which utilize SATS and other platforms such as aircraft, balloons, and other satellites for the purpose of measuring multipath and RFI. In order to focus on those configurations which are most probable, we attempt to provide in the following paragraphs a capsule narrative of the pros and cons of the various platforms.

9.2.1 CONCLUSIONS AND RECOMMENDATIONS CONCERNING MULTIPATH MEASUREMENT

First of all we contend that for multipath measurements involving platforms with low power sources (low to moderate EIRP) the receiving platform should be equipped with antennas which are capable of separating the direct path from the indirect path. For example, if SATS is used in a low

altitude configuration in conjunction with a high altitude aircraft such as a U-2, SATS, because of this limited power, would transmit to the aircraft and the aircraft would be equipped with both bottom- and top-mounted antennas so as to separate the reflected path from the direct path.

Consider first multipath measurements where the probe signals are transmitted from synchronous altitude spacecraft. For reasons given above, it is doubtful that a synchronous satellite should be used to receive the multipath signals, since the signals could not be spatially separated effectively. Thus we discount the possibility of using a synchronous satellite as a receiver and relay of signals emanating from a lower altitude platform. Rather, a synchronous satellite is more likely to serve as the signal source for the multipath measurements.

Again, because of its limited EIRP at synchronous altitudes, the SATS satellite is not considered a prime candidate for transmitting signals for multipath measurements. Therefore, we look to higher power spacecraft for this purpose. For the same reasons just given, the Synchronous Meteorological Satellite is not considered a candidate for transmitting multipath probe signals to a lower altitude receiving platform. Satellites such as ATS-F, ATS-3, and the C-2 satellite are, however, prime candidates owing to their relatively high EIRP.

As mentioned previously, the C-2 satellite will have an approximate EIRP of 34 dBw, and will transmit at L-band frequencies. The ATS-F will have the capability of transmitting 40 watts at L-band into a 9.14m (30-foot) parabolic dish with an equivalent EIRP of 50 dBw. At UHF (860 MHz) the EIRP for ATS-F is 48 dBw and at S-band the EIRP is approximately 48 dBw.

The ATS-3, on the other hand, has a 25 dBw EIRP, transmits at 137 MHz, and provides a high signal-to-noise ratio for a near-earth platform. Furthermore, the 25 dBw from ATS-3, which is located at 65 degrees West, consists of a 10.5 dB antenna driven at a 15 dBw power level.

To operate ATS-F at UHF for multipath measurements would require mechanical slewing of the entire spacecraft in order to achieve a variety of grazing angles for a low altitude platform. It is not known whether sufficient propellent can be allocated to perform an adequate number of multipath measurements at UHF, because of the mechanical steering requirement. If it is impossible to mechanically slew the ATS-F, to conduct an adequate number of multipath measurements at UHF the most logical choice for multipath measurement is at L-band. The L-band antenna beamwidth is approximately 0.026 radian (1.5 degrees) and the antenna can be electronically steered to provide multipath measurements at low grazing angles. At S-band the antenna beamwidth is so narrow that certain geometries (low grazing angles) will not provide adequate multipath measurements. However, it may be possible to transmit from ATS-F to a low altitude SATS (to simulate a Shuttle at S-band) if grazing angles of $\pi/4$ radians (45 degrees) or less are considered appropriate.

It appears that the synchronous satellites which offer the best transmitting sources for multipath measurements are ATS-3 and ATS-F. The military satellites, LES-6 and TACSAT, are also adequate but because of scheduling problems these satellites were not considered as candidates. The C-2 satellite at L-band has a lower EIRP than the ATS-F (at L-band) and would be considered as a multipath measurement source if the ATS-F L-band transmitter were not available.

SATS launched into a low altitude orbit, e.g. 500 km, with an appropriate inclination angle, i.e. 0.87 to 1.05 radians (50-60 degrees), could be outfitted with top- and bottom-mounted antennas for the purpose of isolating the direct path from the indirect paths. Signals would be received by SATS at L-band from ATS-F or at VHF from ATS-3. The isolation between the top-mounted and bottom-mounted antennas should be on the order of 20 dB.

At S-band the fading bandwidth of the reflected signal (which will be completely diffuse), could occupy a bandwidth of from 0 to 40 kHz at the subsatellite point. Thus even though the transmitted power from ATS-F is high and the received signal level is on the order of -110 dBm (assuming a 5 dB receiving antenna), the multipath signal can be spread over a 40 kHz bandwidth and radiometric techniques would be required to measure the multipath energy distributed over this bandwidth. Standard frequency analysis techniques such as swept analyzers, FFT's, etc., would probably not be adequate because of the low signal density relative to the expected noise density. At lower grazing angles where the fading bandwidth is expected to be reduced, then standard frequency analysis techniques of the reflected signal should render a good estimate of the multipath intensity, fading bandwidth, etc.

Of the two satellites which are prime candidates for transmitting multipath probe signals from synchronous altitudes, ATS-3 appears to be the best choice. This comes about because multipath parameters such as fading bandwidth, differential doppler, etc., are proportional to the carrier frequencies, and therefore the reflected signal dispersion or fading bandwidth will be narrower at VHF than at S-band. This means that a high signal-

to-noise ratio exists, and simple analysis techniques can be applied. Observing a VHF signal would also guarantee some percentage of specular reflection in the multipath signal while at S-band the probability of having specular energy is quite small.

Obviously if it is decided not to use a SATS for the low altitude platform, an aircraft such as a U-2, C-118, KC-135, Sabreliner, or a balloon could serve as replacements. All of these platforms would be outfitted with top- and bottom-mounted antennas for signal separation purposes. However, it is also obvious that many multipath measurements have already been conducted by the FAA, the Air Force, Lincoln Laboratories, and Canada, from synchronous satellites to aircraft. Furthermore, the measurements that have been conducted are in agreement with theoretical predictions. Thus it is recommended that if multipath data is to be gathered from a low altitude platform other than SATS, then MSC would be well advised to monitor or influence tests that will be conducted by the Air Force and by the FAA in the near future. The FAA plans to conduct tests both with the C-2 satellite at L-band and with the ATS-F satellite. Furthermore, MSC should monitor and/or influence the PLACE experiments between the ATS-F satellite and aircraft which will attempt to simulate air traffic control (over the ocean and over the land) by synchronous satellites.

While it is our opinion that many multipath measurements have been conducted, and that these measurements have and will provide data which is meaningful to the evaluation of the performance of the Space Shuttle when operating with a synchronous relay satellite, if it is still desirable to conduct multipath measurements with an aircraft, then the following configurations should be considered. North American Rockwell, which operates the

Sabreliner at very low cost to the government, could provide this aircraft for multipath measurements. The Sabreliner would be outfitted with NASA's Multimode Transponder, which is a dual channel receiver, as described in more detail in Section 7.5. The Multimode Transponder receives on 127.775 MHz, 149 MHz, and 401 MHz. It has both a clear mode operation and a pseudo-noise mode, either one of which could be used to receive the direct and the reflected signals if top- and bottom-mounted antennas were provided on the Sabreliner. The Sabreliner would be used to receive multipath probe signals transmitted from either a higher altitude aircraft such as a U-2 or from a balloon at an altitude of 37 km (120000 ft.). Signals from the ground station would be transmitted to the U-2 or balloon which would retransmit the signals that are subsequently received by the Sabreliner. This would represent a very low cost method of measuring multipath since the U-2 flight costs are inconsequential, the costs of the Sabreliner are minimal ($750/hr.), and the Multimode Transponder is under development via a NASA contract. The primary cost involved would be in modification of the Multimode Transponder, installation cost, and data reduction cost. It may be desirable to use a balloon rather than the U-2 aircraft for these measurements. In such an instance the cost of the balloon and its transponder would be additional. The Sabreliner/U-2 test would be representative of a synchronous satellite/Shuttle link during the Shuttle landing phase.

If the Sabreliner was outfitted with a Multimode Transponder, it would be possible to receive multipath probe signals from ATS-F or the ATS-3 satellites. In order to receive these signals without substantial modification to the Multimode Transponder, additional front-end circuitry would be provided. VHF and UHF signals from ATS-3 and ATS-F, respectively, would

be received and translated to the 401 MHz receive frequency of the Multimode Transponder, as shown in Figure 9-1 . Furthermore, the channel in the Multimode Transponder which is used to monitor the reflected signal would have to be modified so that it could be programmed to scan through the reflected signal. This would represent a minor modification to the Multimode Transponder now under development.

Our conclusions are that ATS-F and ATS-3 can serve as synchronous satellite multipath signal sources at UHF, L-band or S-band from the ATS-F satellite and VHF from the ATS-3 satellite. Furthermore, a low altitude SATS satellite can best serve as a low altitude receiver or a low altitude transmitter (to an aircraft, etc.) for multipath measurements. It is doubtful that SATS can be used as either a synchronous relay or a synchronous altitude transmitter.

Furthermore, if platforms such as aircraft and/or balloons are to be used in the multipath measurements, much data already exists for measurements with synchronous satellites, thus making the need for additional measurements questionable.

Now let us turn our attention to the use of SATS as a low altitude spacecraft for transmitting multipath probe signals. If SATS is placed in a low orbit, e.g. 500 km, then the SATS could be configured to transmit multipath probe signals to a lower altitude platform such as a balloon or aircraft. In this circumstance, the dynamics of the spacecraft and the lower altitude platform would be representative of the dynamics associated with Space Shuttle and a synchronous relay satellite. If the SATS were placed in a low orbit, e.g. 500 km, and equipped to transmit multipath probe signals at a power level of 5 watts into an earth-directed antenna with a nominal

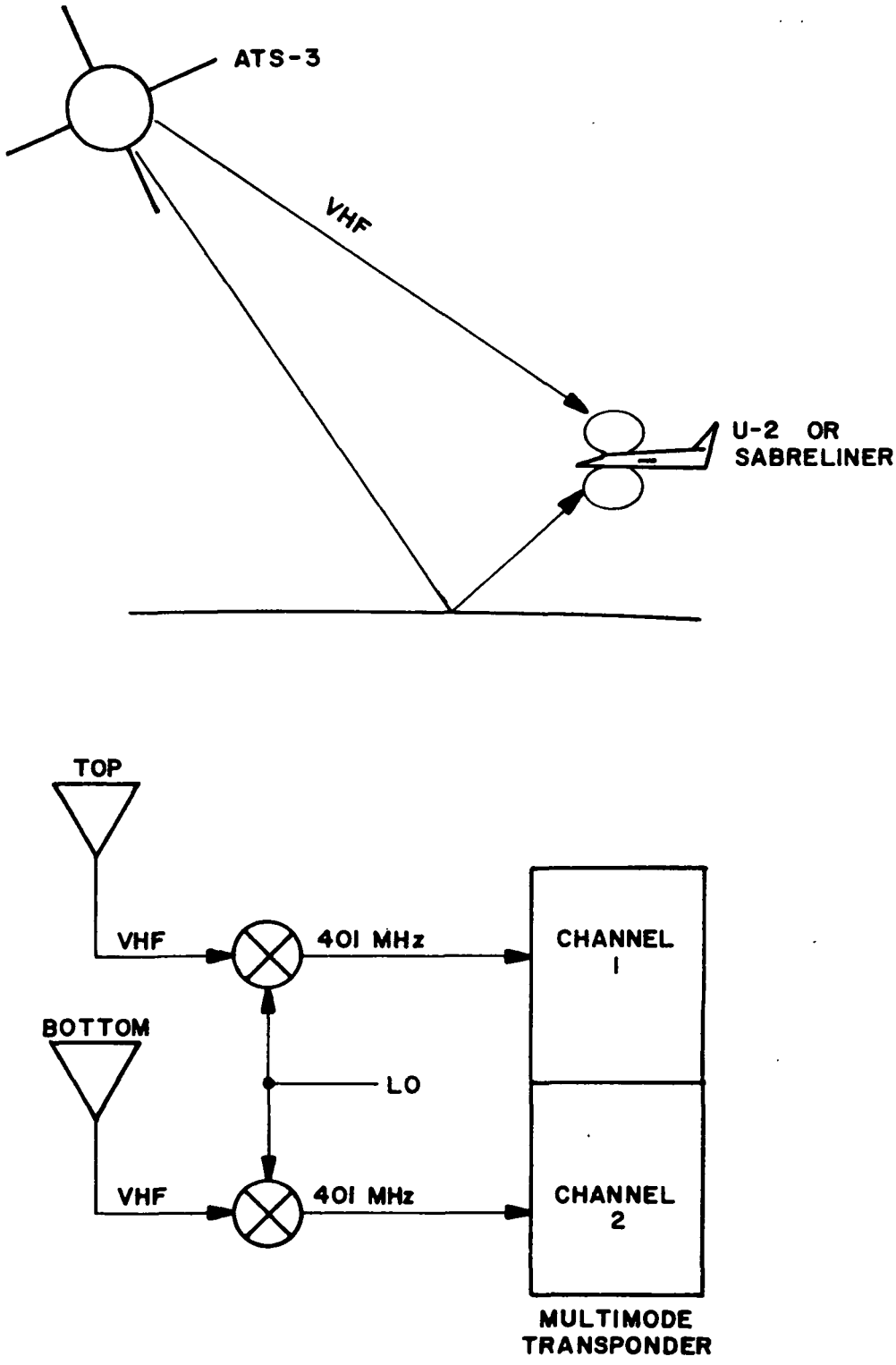

FIGURE 9-1 USE OF MULTIMODE TRANSPONDER FOR MULTIPATH MEASUREMENTS

gain of 3 dB, then at 400 MHz the received signal level at a lower altitude platform is approximately -95 dBm. This substantial signal level could be received by a U-2 aircraft, a KC-135, a C-118, or a Sabreliner, properly outfitted with top- and bottom-mounted antennas to separate the direct signal from the reflected signal to provide multipath measurements. An aircraft, as opposed to a balloon, is more suitable for these measurements since an aircraft can maneuver between satellite passes, thus guaranteeing that multiple satellite passes can be observed.

9.2.2 CONCLUSIONS AND RECOMMENDATIONS CONCERNING RFI MEASUREMENT

RFI measurements can be made by aircraft such as the U-2, Sabreliner (North American Rockwell), and NASA C-118 and by high altitude balloons. These low altitude platforms have one major drawback, i.e. it is highly desirable to produce a world-wide RFI map since Shuttle will be confronted with a world-wide RFI problem. The lower altitude platforms are useful in that they can determine signal duty factors and actual usage of frequency by licensed operators. In order to obtain a composite RFI picture as seen by a Space Shuttle or SATS satellite in a low orbit, or for that matter a synchronous relay satellite, it would be necessary to make many measurements from the lower altitude platforms and to superimpose them on a statistical basis to arrive at a meaningful RFI mapping of the earth. North American Rockwell and NASA have made a significant beginning by measuring RFI along the West Coast of the United States, particularly over San Francisco, Los Angeles, and San Diego, and then developing a composite RFI map of these three major urban areas. These measurements were conducted using a Sabreliner and a downward looking antenna over the VHF band from an altitude of 10.6 km (35,000 feet).

Thus the low altitude platforms for RFI measurements are a useful but a second choice. Our first choice is an RFI measurement conducted with platforms which will be representative of the Space Shuttle, e.g. SATS, Skylab, etc.

In Section 4.4.2 we discussed in some detail an RFI receiver which is now under development by NASA. The RFI receiver being designed is to operate over several bands of interest, with exception of S-band. Therefore, it is recommended that serious consideration be given to modifying this RFI receiver to include S-band frequencies of interest to Shuttle. The RFI receiver is being designed to be compatible with a SATS satellite and an RFI experiment has already been proposed and discussed in Section 4.5.

We have also discussed two RFI analyzers, one developed by North American Rockwell and the second developed by Hughes under NASA contract. The latter is to be used with ATS-F for RFI measurements. The equipment is to be placed at an ATS ground station and RFI relayed through ATS-F to the ground at C-band. The processing equipment, however, should be compatible with most any properly calibrated RFI input spectra. Thus we are recommending that the RFI receiver now being built by AIL and the RFI analyzers (North American Rockwell and Hughes) be interfaced to provide a low cost RFI analysis system. The receiver would be placed on board SATS in the proposed orbit, i.e. 500 km and 1.05 radian (60 degree) angle of inclination. The RFI data from all the bands of interest would be transmitted to the ground, recorded, and interfaced with either the Hughes analyzer or the North American Rockwell analyzer.

9.2.3 CONCLUSIONS CONCERNING COMBINED MULTIPATH AND RFI MEASUREMENT

We have concluded that SATS, equipped with the RFI receiver now under development by NASA, is the preferred method of measuring RFI on a world-wide basis. This option would be to equip SATS with a multipath probe signal transmitter or transmitters at the carrier frequencies of interest, UHF and S-band, etc. The control of the transmitters would be provided from command signals from the ground station in view of the SATS which has been placed in a 500 km orbit at 1.05 radian (60°) inclination, for the RFI measurements. These multipath probe signals would be received by a low altitude aircraft such as NASA's C-118, the U-2, or the North American Rockwell Sabreliner. With this configuration, RFI measurements and multipath measurements could be provided from a single SATS experiment. The signals received by the low altitude platform are separated by top- and bottom-mounted antennas, recorded, and processed off line. The aircraft, because of its maneuverability, could observe many satellite passes over a variety of terrain, thus accumulating a great deal of multipath data.

9.3 SUMMARY OF CONCLUSIONS AND RECOMMENDATIONS

In summary, then, we have concluded that these choices of models, hardware, and further studies are the most cost-effective compromise optimum choices:

- Use Painter's model or Lincoln Labs model for satellite to aircraft links
- Use ESL's model for satellite (SATS) to relay satellite link
- Extend voice coding studies
- No forward error control equipment development; C-MOS/LSI implementation urged

- Wideband FM system not recommended
- PN/PSK is recommended but no development is required
- Unless SATS launches are advanced in time, they may occur too late to use results of SATS-based experiments in design of Shuttle communications systems.

With regard to multipath and its effects on communication system performance, we conclude and recommend that:

- Multipath can be effectively coded against.
- Many tests have been and will be made.
- Much multipath measurement equipment exists.
- Tests confirm theory.
- Test data is sufficient to predict the performance of Shuttle/Relay link.
- The need for more tests is questionable.
- NASA should monitor FAA, Canadian, and U.S.A.F.* forthcoming tests.
- NASA should monitor or participate in the 621-B program if test cluster is approved for 1974.*

With regard to the preferred multipath test configuration we recommend:

- ATS-3 or ATS-F transmitting to SATS
  - SATS have top and bottom antennas
  - SATS have dual channel receiver
  - Dual channels transmitted to ground station for analysis
  - PN or Multitone CW probe signals

* Information on participating in the DOD Space Experiments Support Program may be found in "Space Experiments Support Program (SESP) Management," AFM 80-2, AR 70-43, OPNAV 76P-2, 8 April 1970. The request channels outlined therein should also apply to other DOD activities in which NASA may wish to participate.

- o SATS (low orbit) transmits to aircraft
  - ° Aircraft have AD dual channel receiver
  - ° PN probe signal
  - ° Aircraft record and/or display multipath measurements
  - ° Multimode Transponder is a possible receiver

As an alternate multipath test, we recommend:

- ° U-2 or balloon as high altitude source
- ° Sabreliner, C-118, etc. serve as receiving platform
- ° AD with dual channel receiver on the receiving platform.

With regard to RFI measurement, we recommend, as the preferred experiment:

- ° RFI test should take priority over multipath tests
- ° Modify GSFC RFI receiver for S-band
- ° Fly RFI receiver in a SATS in a 500 km circular orbit at 50°- 60° inclination
- ° Interface RFI receiver outputs with North American Rockwell or Hughes RFI data reduction equipment.

As an alternative RFI measurement experiment, we recommend:

- ° Sabreliner fly the East and West coasts of the U.S.A. and the West coast of Europe.
- ° Many flights, i.e. 60-80 hrs.
- ° Make composite RFI map
- ° Establish duty factors
- ° Up-date ESL model
- ° Use Skylab as possible platform

With regard to making combined RFI and multipath tests, we recommend that NASA:

- Fly SATS RFI experiment
- Place multipath probe transmitter on board SATS
- Receive on Sabreliner, C-118, etc.
- Use AD with Multimode Transponder or Canadian type PN analyzer

9.4 COST ANALYSIS

In this section we document the expected cost for individual platforms and selected experiments. Also included are availability and altitude limits of each platform.

The costs and availability of the various candidate platforms are summarized in Table 9-1.

The costs of performing an RFI collection experiment using a Sabreliner aircraft as the platform are presented in Table 9-1. These costs include aircraft, operators, instrumentation, and data reduction. The costs of an RFI experiment using SATS are presented in Table 9-3.

The costs of performing a multipath experiment using the U-2 and the Sabreliner are summarized in Table 9-4.

TABLE 9-1

COST OF PLATFORMS

PLATFORM	EXPERIMENT	COST	AVAILABILITY	ALTITUDE
C-118	RFI/Multipath	$650/hr	yes	6.1 km
U-2	RFI/Multipath	$ 0	maybe	19.6 km
Sabreliner	RFI/Multipath	$750/hr	yes	10.6 km
Balloons	RFI/Multipath	$5000/launch	yes	36.6 km
KC-135 USAF	RFI/Multipath	$1000/hr	no	9.1 km
KC-135 FAA	RFI/Multipath	$1000/hr	no	9.1 km
KC-135 Boeing	RFI/Multipath	$2000/hr	yes	9.1 km

TABLE 9-2

COSTS FOR AIRCRAFT RFI EXPERIMENT

PLATFORM: SABRELINER

COST - $75K for 20 hrs East Coast of U.S.A.

- $125K for 40 hrs East and West Coast U.S.A.

- $200K for 60 hrs U.S.A. and West Coast of Europe

Cost includes: Aircraft, operators, instrumentation, data reduction

TABLE 9-3

COST FOR SATS RFI EXPERIMENT

SATS: $6 million

Receiver: $0.5 million

Launch Cost: $9.2K/kg for 500 km orbit at 60° inclination

$6.7K/kg for synchronous orbit

SATS Weight: 163 kg Scout (500 km orbit)

670 kg Delta (synchronous orbit)

Launch Cost ~ $1.5 million for Scout

~ $4.5 million for Delta

Support and Data Reduction for 6 months Program } ~ $200K

TABLE 9-4

COST OF MULTIPATH EXPERIMENT

PLATFORMS: U-2, SABRELINER

U-2 Costs	$0/flight hr
U-2 Costs for Modifications	$10K
PN Transmitter	$15K
Dual Channel PN Receiver	$60K
Instrumentation	$20K
Sabreliner Mods	$10K
Data Reduction and Testing	$20K
	$135K total less flight time
10 hrs flight time	7.5K
	$142.5K

10. REFERENCES

1. E. J. Baghdady and R. H. Wachsman, "Mathematical Models of TDRS Multipath Environment," Tech. Memo. G-161-6, ADCOM, Cambridge, Mass., July 1970.

2. J. N. Birch, "Multipath/Modulation Study for the Tracking and Data Relay Satellite System," Final Report, The Magnavox Company, Silver Spring, Maryland, undated.

3. S. H. Duranni and H. Staras, "Multipath Problems in Communications Between Low Altitude Spacecraft and Stationary Satellites," RCA Review, March 1968.

4. D. Eggert, "Multipath Study for a Low Altitude Satellite Utilizing a Data Relay Satellite System," N71-13478, Hughes Aircraft Company, Culver City, California, October 1970, under contract NAS5-11602.

5. -----, "Phase III Final Report, Vol. I, a VHF Communication System for a Low Altitude Satellite Utilizing a Data Relay Satellite System," Hughes Aircraft Company, Culver City, California, November 1970, under Contract NAS5-11602.

6. J. A. Jenny and F. J. Weiss, "The Effects of Multipath and RFI on the Tracking and Data Relay Satellite System," ESL-TM215, X71-10576, ESL, Incorporated, Sunnyvale, California, 18 March 1971, under NASA Contract NAS5-20125.

7. J. A. Jenny, D. Gaushell, and P. D. Shaft, "Communication Performance Over the TDRS Multipath/Interference Channel," ESL-TM239, ESL, Incorporated, Sunnyvale, California, 19 August 1971, under Contract NAS5-20228.

8. J. A. Jenny and P. Shaft, "The Effects of Multipath and RFI on the TDRSS Command and Telemetry Links - A Final Report," ESL, Incorporated, Sunnyvale, California, 9 March 1972, under NASA Contract NAS5-20228.

9. J. L. Massey and J. J. Uhran, Jr., "Final Report for Multipath Study," University of Notre Dame, Notre Dame, Indiana, 1969, under Contract NAS5-10786.

10. S. J. Sohn and A. F. Ghais, "Multipath Performance of a TDRS System Employing Wideband FM VHF Signals," Technical Memorandum G-161-2, Teledyne ADCOM, Cambridge, Massachusetts, 26 December 1969, prepared under Contract NAS5-10797.

11. Anon., "Small Applications Technology Satellite Interim Systems Definition Report," NASA Goddard Spaceflight Center, June 1972.

12. T. Golden, "Range and Velocity Components of TDRS Multipath Signals," X-520-69-38, NASA Goddard Space Flight Center, February 1968.

13. C. C. Johnson, Field and Wave Electrodynamics, New York: McGraw-Hill, 1965.

14. A. D. Poularikas and T. S. Golden, "A Note on the Effects of the Ionosphere on Satellite Orbital Corrections in Near-Real Time," IEEE Trans. on Aerospace and Electronic Systems (Correspondence), Vol. AES-5, No. 5, September 1969, pp. 865-867.

15. D. E. Kerr, Propagation of Short Radio Waves, New York: Dover Publications, 1951.

16. P. Beckmann and A. Spizzichino, The Scattering of Electromagnetic Waves from Rough Surfaces, New York: MacMillan, 1963.

17. J. H. Painter, "Modeling, Experimentation, and Estimation for Multipath Signals," Ph.D. Dissertation, Southern Methodist University, Dallas, Texas, August 15, 1972.

18. H. Staras, "Rough Surface Scattering on a Communication Link," Radio Science, Vol. 3 (new series), No. 6, June 1968, pp. 623-631.

19. I. L. Lebow, K. L. Jordan, Jr., and P. R. Drouilhet, Jr., "Satellite Communications to Mobile Platforms," Proc. IEEE, Volume 59, No. 2, February 1971, pp. 139-159.

20. International Frequency Registration Board, "Preface to the International Frequency List," 5th Edition, Geneva: International Telecommunication Union, 1 February 1969.

21. -----, "Supplement No. 1 to the Preface to the International Frequency List (5th Edition)," Geneva: International Telecommunication Union, 1 May 1969.

22. -----, "Supplement No. 2 to the Preface to the International Frequency List (5th Edition)," Geneva: International Telecommunication Union, 1 August 1969.

23. -----, "Supplement No. 3 to the Preface to the International Frequency List (5th Edition)," Geneva: International Telecommunication Union, 1 November 1969.

24. -----, "Supplement No. 4 to the Preface to the International Frequency List (5th Edition)," Geneva: International Telecommunication Union, 1 February 1970.

25. -----, "Supplement No. 5 to the Preface to the International Frequency List (5th Edition)," Geneva: International Telecommunication Union, 1 May 1970.

26. -----, "Supplement No. 6 to the Preface to the International Frequency List (5th Edition)," Geneva: International Telecommunication Union, 1 August 1970.

27. -----, "Supplement No. 7 to the Preface to the International Frequency List (5th Edition)," Geneva: International Telecommunication Union, 1 November 1970.

28. -----, "International Frequency List. Volume IV, Part b) Particulars of frequency assignments in Region 1 in the bands between 50 Mc/s and 40000 Mc/s, and of assignments to broadcasting stations in Region 1 in the bands between 28 Mc/s and 50 Mc/s," 5th Edition, Geneva: International Telecommunication Union, 1 February 1969.

29. -----, "International Frequency List. Volume IV, Part c) Particulars of frequency assignments in Region 2 in the bands between 50 Mc/s and 40000 Mc/s," 5th Edition, Geneva: International Telecommunication Union, 1 February 1969.

30. -----, "International Frequency List. Volume IV, Part d) Particulars of frequency assignments in Region 3 in the bands between 50 Mc/s and 40000 Mc/s, and of assignments to broadcasting stations in Region 3 in the bands between 28 Mc/s and 50 Mc/s," 5th Edition, Geneva: International Telecommunication Union, 1 February 1969.

31. -----, "Recapitulative Supplement No. 7 to the International Frequency List (5th Edition) Volume IV, Part b) Particulars of frequency assignments in Region 1 in the bands between 50 Mc/s and 40000 Mc/s, and of assignments to broadcasting stations in Region 1 in the bands between 28 Mc/s and 50 Mc/s,"Geneva: International Telecommunication Union, 1 November 1970.

32. -----, "Recapitulative Supplement No. 7 to the International Frequency List (5th Edition) Volume IV, Part c) Particulars of frequency assignments in Region 2 in the bands between 50 Mc/s and 40000 Mc/s,"Geneva: International Telecommunication Union, 1 November 1970.

33. -----, "Recapitulative Supplement No. 7 to the International Frequency List (5th Edition) Volume IV, Part d) Particulars of frequency assignments in Region 3 in the bands between 50 Mc/s and 40000 Mc/s, and of assignments to broadcasting stations in Region 3 in the bands between 28 Mc/s and 50 Mc/s," Geneva: International Telecommunication Union, 1 November 1970.

34. G. Ploussios, "Noise Temperature of Airborne Antennas at UHF," Technical Note 1966-59, AD-644849, Massachusetts Institute of Technology Lincoln Laboratory, Lexington, Massachusetts, 6 December 1966.

35. R. H. Wachsman and A. F. Ghais, "Design and Performance Evaluation of a Wideband FM Spread Spectrum Multiple Access System," Teledyne ADCOM, Cambridge, Massachusetts, July 1971, under Contract NAS5-20225.

36. C. L. Britt and D. F. Palmer, "Effects of CW Interference on Narrow-Band Second-Order Phase-Lock Loops," IEEE Trans. on Aerospace and Electronic Systems, Vol. AES-3, No. 1, January 1967, pp. 128-135.

37. W. C. Lindsey, "Design of Block Coded Communication Systems," IEEE Trans. on Communication Technology, Vol. COM-15, No. 4, August 1967, pp. 525-534.

38. A. L. Johnson, "Measurement of Airborne Propagation Anomalies," National Telecommunications Conf. 1972 Record, IEEE, 1972.

39. J. H. Deal, "Multipath Propagation Study for L-Band, Over-Ocean, Satellite-Aircraft Communication Link," X-752-72-335 (Preprint), NASA/Goddard Space Flight Center, August 1972.

40. Commercial Airplane Group, "ATS-5 Multipath/Ranging Experimental Program - Interim Results," D6-60149, DOT FA69WA-2109, Boeing Aircraft Company, Seattle, Washington, December 1971.

41. Private Communication, ITOS Project Office, NASA Goddard Space Flight Center.

APPENDIX A

REFLECTED POWER FOR A ROUGH, SPHERICAL EARTH

This Appendix presents an extensive tabulation of the ratio of reflected power to direct power for the geometry of a low altitude platform communicating with a synchronous relay satellite. The method used is that of the Magnavox Model discussed in Section 3.4.2 of this report, with the divergence factor and the reflection coefficients calculated using the equations given by Kerr (Reference 15).

In the following printouts, PSI represents the grazing angle. The complex reflection coefficient is taken as $\varepsilon = 80 - j7.2 \times 10^{10} f^{-1}$. The tabulations presented cover VHF (137 MHz), UHF (400 MHz), and S-band (2000 MHz) for surface roughnesses of 0.15 m, 1.5 m, and 15.0 m. Tabulations run from grazing angles of 0 to 90 degrees (0 to 1.57 radians) in steps of 10 degrees. A supplementary table is included for 2000 MHz covering the range of grazing angles 0.1 degree to 12 degrees in steps of 0.1 degree to show more clearly the peaks of the curve.

A listing of the computer program used to generate these tables is presented at the end of the Appendix.

FREQUENCY = 137.0 MHZ
SIGMA = 0.15 METERS
PLATFORM ALTITUDE = 6.0960 KM

PSI (DEGREES)	SPECULAR VERTICAL	SPECULAR HORIZONTAL	DIFFUSE VERTICAL	DIFFUSE HORIZONTAL
0.0	0.0	0.0	0.0	0.0
2.0	0.67237139E-01	0.45088947E 00	0.67297935E-01	0.45129716E 00
4.0	0.13896507E 00	0.72477078E 00	0.13946772E 00	0.72739232E 00
6.0	0.25517505E 00	0.83630353E 00	0.25725222E 00	0.84311116E 00
8.0	0.35670626E 00	0.88118809E 00	0.36186981E 00	0.89394385E 00
10.0	0.43546808E 00	0.89798123E 00	0.44532102E 00	0.91829902E 00
12.0	0.49492222E 00	0.90113443E 00	0.51105392E 00	0.93050635E 00
14.0	0.53942919E 00	0.89672166E 00	0.56337065E 00	0.93652081E 00
16.0	0.57245916E 00	0.88762105E 00	0.60565788E 00	0.93909699E 00
18.0	0.59657621E 00	0.87536800E 00	0.64037973E 00	0.93964171E 00
20.0	0.61365479E 00	0.86086631E 00	0.66929811E 00	0.93892562E 00
30.0	0.63265151E 00	0.77046728E 00	0.76159787E 00	0.92750311E 00
40.0	0.59591299E 00	0.67191422E 00	0.80970472E 00	0.91297245E 00
50.0	0.54212356E 00	0.58197898E 00	0.83791369E 00	0.89951479E 00
60.0	0.49025941E 00	0.50923562E 00	0.85528207E 00	0.88838702E 00
70.0	0.44967324E 00	0.45709896E 00	0.86585724E 00	0.88015568E 00
80.0	0.42441356E 00	0.42612606E 00	0.87160027E 00	0.87511718E 00
90.0	0.50842047E 01	0.50842018E 01	0.10677464E 02	0.10677457E 02

FREQUENCY = 137.0 MHZ
SIGMA = 0.15 METERS
PLATFORM ALTITUDE = 15.2400 KM

PSI (DEGREES)	SPECULAR VERTICAL	SPECULAR HORIZONTAL	DIFFUSE VERTICAL	DIFFUSE HORIZONTAL
0.0	0.0	0.0	0.0	0.0
2.0	0.43184806E-01	0.28959560E 00	0.43223850E-01	0.28985745E 00
4.0	0.10400158E 00	0.54241949E 00	0.10437781E 00	0.54438150E 00
6.0	0.21277392E 00	0.69733953E 00	0.21450597E 00	0.70301598E 00
8.0	0.31637710E 00	0.78156102E 00	0.32095689E 00	0.79287463E 00
10.0	0.40033078E 00	0.82552451E 00	0.40938872E 00	0.84420288E 00
12.0	0.46510589E 00	0.84684592E 00	0.48026574E 00	0.87444836E 00
14.0	0.51420957E 00	0.85479772E 00	0.53703171E 00	0.89273620E 00
16.0	0.55101049E 00	0.85436410E 00	0.58296537E 00	0.90391135E 00
18.0	0.57817262E 00	0.84836411E 00	0.62062484E 00	0.91065508E 00
20.0	0.59771150E 00	0.83850026E 00	0.65190917E 00	0.91453153E 00
30.0	0.62380022E 00	0.75968778E 00	0.75094253E 00	0.91452658E 00
40.0	0.59015471E 00	0.66542161E 00	0.80188060E 00	0.90415049E 00
50.0	0.53796458E 00	0.57751429E 00	0.83148551E 00	0.89261413E 00
60.0	0.48700756E 00	0.50585794E 00	0.84960908E 00	0.88249451E 00
70.0	0.44694436E 00	0.45432496E 00	0.86060274E 00	0.87481433E 00
80.0	0.42195922E 00	0.42366189E 00	0.86655998E 00	0.87005657E 00
90.0	0.49371204E 01	0.49371176E 01	0.10368569E 02	0.10368562E 02

FREQUENCY = 137.0 MHZ
SIGMA = 0.15 METERS
PLATFORM ALTITUDE = 30.4800 KM

PSI	SPECULAR		DIFFUSE	
(DEGREES)	VERTICAL	HORIZONTAL	VERTICAL	HORIZONTAL
0.0	0.0	0.0	0.0	0.0
2.0	0.30039228E-01	0.20144188E 00	0.30066390E-01	0.20162404E 00
4.0	0.77205479E-01	0.40266472E 00	0.77484787E-01	0.40412122E 00
6.0	0.17063725E 00	0.55924171E 00	0.17202628E 00	0.56379402E 00
8.0	0.26920915E 00	0.66503990E 00	0.27310616E 00	0.67466676E 00
10.0	0.35486460E 00	0.73176843E 00	0.36289382E 00	0.74832547E 00
12.0	0.42393780E 00	0.77188879E 00	0.43775582E 00	0.79704803E 00
14.0	0.47784573E 00	0.79434812E 00	0.49905396E 00	0.82960367E 00
16.0	0.51913738E 00	0.80494350E 00	0.54924381E 00	0.85162473E 00
18.0	0.55022728E 00	0.80735928E 00	0.59062761E 00	0.86663949E 00
20.0	0.57311499E 00	0.80399501E 00	0.62508237E 00	0.87689751E 00
30.0	0.60959584E 00	0.74238920E 00	0.73384303E 00	0.89370221E 00
40.0	0.58078510E 00	0.65485692E 00	0.78914952E 00	0.88979560E 00
50.0	0.53115493E 00	0.57020402E 00	0.82096046E 00	0.88131523E 00
60.0	0.48166615E 00	0.50030977E 00	0.84029067E 00	0.87281543E 00
70.0	0.44245511E 00	0.44976163E 00	0.85195857E 00	0.86602747E 00
80.0	0.41791809E 00	0.41960442E 00	0.85826087E 00	0.86172402E 00
90.0	0.47086954E 01	0.47086916E 01	0.98888474E 01	0.98888397E 01

FREQUENCY = 137.0 MHZ
SIGMA = 0.15 METERS
PLATFORM ALTITUDE = 160.9344 KM

PSI	SPECULAR		DIFFUSE	
(DEGREES)	VERTICAL	HORIZONTAL	VERTICAL	HORIZONTAL
0.0	0.0	0.0	0.0	0.0
2.0	0.12419317E-01	0.83283365E-01	0.12430549E-01	0.83358705E-01
4.0	0.32688521E-01	0.17048657E 00	0.32806758E-01	0.17110324E 00
6.0	0.78271806E-01	0.25652599E 00	0.78908980E-01	0.25861418E 00
8.0	0.13624871E 00	0.33658159E 00	0.13822103E 00	0.34145385E 00
10.0	0.19748867E 00	0.40724260E 00	0.20195711E 00	0.41645694E 00
12.0	0.25640053E 00	0.46684372E 00	0.26475775E 00	0.48206019E 00
14.0	0.30990195E 00	0.51516646E 00	0.32365632E 00	0.53803110E 00
16.0	0.35660094E 00	0.55292422E 00	0.37728137E 00	0.58499002E 00
18.0	0.39615315E 00	0.58128327E 00	0.42524064E 00	0.62396389E 00
20.0	0.42881221E 00	0.60155970E 00	0.46769488E 00	0.65610629E 00
30.0	0.51053470E 00	0.62174875E 00	0.61459136E 00	0.74847293E 00
40.0	0.51070869E 00	0.57584321E 00	0.69393229E 00	0.78243464E 00
50.0	0.47852683E 00	0.51370686E 00	0.73961776E 00	0.79399246E 00
60.0	0.43968052E 00	0.45669895E 00	0.76704460E 00	0.79673421E 00
70.0	0.40684414E 00	0.41356260E 00	0.78338873E 00	0.79632533E 00
80.0	0.38571846E 00	0.38727486E 00	0.79213387E 00	0.79533017E 00
90.0	0.33383226E 01	0.33383207E 01	0.70108948E 01	0.70108900E 01

FREQUENCY = 137.0 MHZ
SIGMA = 0.15 METERS
PLATFORM ALTITUDE = 321.8688 KM

PSI (DEGREES)	SPECULAR VERTICAL	SPECULAR HORIZONTAL	DIFFUSE VERTICAL	DIFFUSE HORIZONTAL
0.0	0.0	0.0	0.0	0.0
2.0	0.86402819E-02	0.57941392E-01	0.86480938E-02	0.57993781E-01
4.0	0.22444986E-01	0.11706150E 00	0.22526171E-01	0.11748493E 00
6.0	0.53639546E-01	0.17579663E 00	0.54076180E-01	0.17722768E 00
8.0	0.94089091E-01	0.23243272E 00	0.95451117E-01	0.23579735E 00
10.0	0.13839716E 00	0.28538960E 00	0.14152855E 00	0.29184687E 00
12.0	0.18312919E 00	0.33343422E 00	0.18909818E 00	0.34430230E 00
14.0	0.22604865E 00	0.37577266E 00	0.23608136E 00	0.39245057E 00
16.0	0.26574081E 00	0.41204196E 00	0.28115201E 00	0.43593758E 00
18.0	0.30139267E 00	0.44223940E 00	0.32352239E 00	0.47471076E 00
20.0	0.33262491E 00	0.46662325E 00	0.36278582E 00	0.50893444E 00
30.0	0.42577511E 00	0.51852524E 00	0.51255620E 00	0.62421054E 00
40.0	0.44349968E 00	0.50006258E 00	0.60261118E 00	0.67946672E 00
50.0	0.42508644E 00	0.45633769E 00	0.65701956E 00	0.70532185E 00
60.0	0.39572728E 00	0.41104454E 00	0.69036603E 00	0.71708775E 00
70.0	0.36894298E 00	0.37503552E 00	0.71040910E 00	0.72214049E 00
80.0	0.35116178E 00	0.35257876E 00	0.72116619E 00	0.72407615E 00
90.0	0.24124422E 01	0.24124403E 01	0.50664301E 01	0.50664263E 01

FREQUENCY = 137.0 MHZ
SIGMA = 0.15 METERS
PLATFORM ALTITUDE = 643.7376 KM

PSI	SPECULAR		DIFFUSE	
(DEGREES)	VERTICAL	HORIZONTAL	VERTICAL	HORIZONTAL
0.0	0.0	0.0	0.0	0.0
2.0	0.60219094E-02	0.40382694E-01	0.60273558E-02	0.40419206E-01
4.0	0.15381306E-01	0.80220938E-01	0.15436944E-01	0.80511153E-01
6.0	0.36356650E-01	0.11915421E 00	0.36652599E-01	0.12012416E 00
8.0	0.63442171E-01	0.15672427E 00	0.64360559E-01	0.15899301E 00
10.0	0.93321621E-01	0.19243920E 00	0.95433176E-01	0.19679338E 00
12.0	0.12403250E 00	0.22583336E 00	0.12807530E 00	0.23319429E 00
14.0	0.15430558E 00	0.25651038E 00	0.16115415E 00	0.26789510E 00
16.0	0.18327427E 00	0.28417426E 00	0.19390297E 00	0.30065447E 00
18.0	0.21034193E 00	0.30863887E 00	0.22578627E 00	0.33130062E 00
20.0	0.23511374E 00	0.32982963E 00	0.25643277E 00	0.35973704E 00
30.0	0.32020223E 00	0.38995463E 00	0.38546556E 00	0.46943480E 00
40.0	0.34915721E 00	0.39368790E 00	0.47442210E 00	0.53492874E 00
50.0	0.34480721E 00	0.37015653E 00	0.53293884E 00	0.57211912E 00
60.0	0.32708424E 00	0.33974457E 00	0.57061481E 00	0.59270138E 00
70.0	0.30843252E 00	0.31352580E 00	0.59389466E 00	0.60370195E 00
80.0	0.29536349E 00	0.29655528E 00	0.60657561E 00	0.60902315E 00
90.0	0.14966230E 01	0.14966221E 01	0.31430960E 01	0.31430941E 01

FREQUENCY = 137.0 MHZ
SIGMA = 0.15 METERS
PLATFORM ALTITUDE = 1287.4750 KM

PSI	SPECULAR		DIFFUSE	
(DEGREES)	VERTICAL	HORIZONTAL	VERTICAL	HORIZONTAL
0.0	0.0	0.0	0.0	0.0
2.0	0.41878410E-02	0.28083522E-01	0.41916296E-02	0.28108913E-01
4.0	0.10493144E-01	0.54726891E-01	0.10531101E-01	0.54924842E-01
6.0	0.24408340E-01	0.79995155E-01	0.24607029E-01	0.80646336E-01
8.0	0.42052913E-01	0.10388523E 00	0.42661656E-01	0.10538906E 00
10.0	0.61271615E-01	0.12634850E 00	0.62657952E-01	0.12920731E 00
12.0	0.80907822E-01	0.14731365E 00	0.83544970E-01	0.15211529E 00
14.0	0.10028189E 00	0.16670400E 00	0.10473275E 00	0.17410284E 00
16.0	0.11895823E 00	0.18444961E 00	0.12585700E 00	0.19514644E 00
18.0	0.13664037E 00	0.20049518E 00	0.14667320E 00	0.21521652E 00
20.0	0.15312386E 00	0.21481001E 00	0.16700846E 00	0.23428798E 00
30.0	0.21439528E 00	0.26109880E 00	0.25809312E 00	0.31431568E 00
40.0	0.24173808E 00	0.27256876E 00	0.32846487E 00	0.37035650E 00
50.0	0.24546856E 00	0.26351476E 00	0.37939966E 00	0.40729207E 00
60.0	0.23760545E 00	0.24680233E 00	0.41451460E 00	0.43055904E 00
70.0	0.22705907E 00	0.23080862E 00	0.43720806E 00	0.44442791E 00
80.0	0.21907383E 00	0.21995783E 00	0.44990277E 00	0.45171815E 00
90.0	0.79096782E 00	0.79096735E 00	0.16611309E 01	0.16611300E 01

FREQUENCY = 137.0 MHZ
SIGMA = 1.50 METERS
PLATFORM ALTITUDE = 6.0960 KM

PSI (DEGREES)	SPECULAR VERTICAL	SPECULAR HORIZONTAL	DIFFUSE VERTICAL	DIFFUSE HORIZONTAL
0.0	0.0	0.0	0.0	0.0
2.0	0.61482728E-01	0.41230059E 00	0.67297935E-01	0.45129716E 00
4.0	0.97200990E-01	0.50695068E 00	0.13946772E 00	0.72739232E 00
6.0	0.11435854E 00	0.37479556E 00	0.25725222E 00	0.84311116E 00
8.0	0.85978985E-01	0.21239793E 00	0.36186981E 00	0.89394385E 00
10.0	0.47532208E-01	0.98016441E-01	0.44532102E 00	0.91829902E 00
12.0	0.20677201E-01	0.37648216E-01	0.51105392E 00	0.93050635E 00
14.0	0.73251799E-02	0.12177031E-01	0.56337065E 00	0.93652081E 00
16.0	0.21574665E-02	0.33452390E-02	0.60565788E 00	0.93909699E 00
18.0	0.53613726E-03	0.78668469E-03	0.64037973E 00	0.93964171E 00
20.0	0.11378196E-03	0.15961916E-03	0.66929811E 00	0.93892562E 00
30.0	0.66928045E-08	0.81507530E-08	0.76159787E 00	0.92750311E 00
40.0	0.39259943E-13	0.44267060E-13	0.80970472E 00	0.91297245E 00
50.0	0.10306215E-18	0.11063897E-18	0.83791369E 00	0.89951479E 00
60.0	0.58044790E-24	0.60291500E-24	0.85528207E 00	0.88838702E 00
70.0	0.30374997E-28	0.30876605E-28	0.86585724E 00	0.88015568E 00
80.0	0.48697063E-31	0.48893556E-31	0.87160027E 00	0.87511718E 00
90.0	0.63673379E-31	0.63673332E-31	0.10677464E 02	0.10677457E 02

FREQUENCY = 137.0 MHZ
SIGMA = 1.50 METERS
PLATFORM ALTITUDE = 15.2400 KM

PSI	SPECULAR		DIFFUSE	
(DEGREES)	VERTICAL	HORIZONTAL	VERTICAL	HORIZONTAL
0.0	0.0	0.0	0.0	0.0
2.0	0.39488882E-01	0.26481086E 00	0.43223850E-01	0.28985745E 00
4.0	0.72745323E-01	0.37940264E 00	0.10437781E 00	0.54438150E 00
6.0	0.95356166E-01	0.31251782E 00	0.21450597E 00	0.70301598E 00
8.0	0.76258183E-01	0.18838423E 00	0.32095689E 00	0.79287463E 00
10.0	0.43696906E-01	0.90107620E-01	0.40938872E 00	0.84420288E 00
12.0	0.19431517E-01	0.35380114E-01	0.48026574E 00	0.87444836E 00
14.0	0.69827102E-02	0.11607729E-01	0.53703171E 00	0.89273620E 00
16.0	0.20766316E-02	0.32199011E-02	0.58296537E 00	0.90391135E 00
18.0	0.51959814E-03	0.76241652E-03	0.62062484E 00	0.91065508E 00
20.0	0.11082580E-03	0.15547211E-03	0.65190917E 00	0.91453153E 00
30.0	0.65991657E-08	0.80367180E-08	0.75094253E 00	0.91452658E 00
40.0	0.38880577E-13	0.43839312E-13	0.80188060E 00	0.90415049E 00
50.0	0.10227147E-18	0.10979024E-18	0.83148551E 00	0.89261413E 00
60.0	0.57659786E-24	0.59891597E-24	0.84960908E 00	0.88249451E 00
70.0	0.30190673E-28	0.30689224E-28	0.86060274E 00	0.87481433E 00
80.0	0.48415459E-31	0.48610817E-31	0.86655998E 00	0.87005657E 00
90.0	0.61831332E-31	0.61831285E-31	0.10368569E 02	0.10368562E 02

FREQUENCY = 137.0 MHZ
SIGMA = 1.50 METERS
PLATFORM ALTITUDE = 30.4800 KM

PSI (DEGREES)	SPECULAR VERTICAL	SPECULAR HORIZONTAL	DIFFUSE VERTICAL	DIFFUSE HORIZONTAL
0.0	0.0	0.0	0.0	0.0
2.0	0.27468354E-01	0.18420172E 00	0.30066390E-01	0.20162404E 00
4.0	0.54002449E-01	0.28164929E 00	0.77484787E-01	0.40412122E 00
6.0	0.76472342E-01	0.25062829E 00	0.17202628E 00	0.56379402E 00
8.0	0.64889014E-01	0.16029847E 00	0.27310616E 00	0.67466676E 00
10.0	0.38734179E-01	0.79873979E-01	0.36289382E 00	0.74832547E 00
12.0	0.17711569E-01	0.32248504E-01	0.43775582E 00	0.79704803E 00
14.0	0.64889081E-02	0.10786850E-01	0.49905396E 00	0.82960367E 00
16.0	0.19565092E-02	0.30336464E-02	0.54924381E 00	0.85162473E 00
18.0	0.49448386E-03	0.72556594E-03	0.59062761E 00	0.86663949E 00
20.0	0.10626520E-03	0.14907426E-03	0.62508237E 00	0.87689751E 00
30.0	0.64489001E-08	0.78537177E-08	0.73384303E 00	0.89370221E 00
40.0	0.38263290E-13	0.43143291E-13	0.78914952E 00	0.88979560E 00
50.0	0.10097694E-18	0.10840047E-18	0.82096046E 00	0.88131523E 00
60.0	0.57027381E-24	0.59234712E-24	0.84029067E 00	0.87281543E 00
70.0	0.29887423E-28	0.30380979E-28	0.85195857E 00	0.86602747E 00
80.0	0.47951779E-31	0.48145269E-31	0.85826087E 00	0.86172402E 00
90.0	0.58970602E-31	0.58970555E-31	0.98888474E 01	0.98888397E 01

FREQUENCY = 137.0 MHZ
SIGMA = 1.50 METERS
PLATFORM ALTITUDE = 160.9344 KM

PSI	SPECULAR		DIFFUSE	
(DEGREES)	VERTICAL	HORIZONTAL	VERTICAL	HORIZONTAL
0.0	0.0	0.0	0.0	0.0
2.0	0.11356425E-01	0.76155663E-01	0.12430549E-01	0.83358705E-01
4.0	0.22864427E-01	0.11924911E 00	0.32806758E-01	0.17110324E 00
6.0	0.35078101E-01	0.11496401E 00	0.78908980E-01	0.25861418E 00
8.0	0.32840833E-01	0.81128240E-01	0.13822103E 00	0.34145385E 00
10.0	0.21556284E-01	0.44451345E-01	0.20195711E 00	0.41645694E 00
12.0	0.10712076E-01	0.19504119E-01	0.26475775E 00	0.48206019E 00
14.0	0.42083114E-02	0.69957040E-02	0.32365632E 00	0.53803110E 00
16.0	0.13439467E-02	0.20838438E-02	0.37728137E 00	0.58499002E 00
18.0	0.35601901E-03	0.52239350E-03	0.42524064E 00	0.62396389E 00
20.0	0.79509016E-04	0.11153932E-03	0.46769488E 00	0.65610629E 00
30.0	0.54009313E-08	0.65774621E-08	0.61459136E 00	0.74847293E 00
40.0	0.33646517E-13	0.37937708E-13	0.69393229E 00	0.78243464E 00
50.0	0.90971876E-19	0.97659890E-19	0.73961776E 00	0.79399246E 00
60.0	0.52056443E-24	0.54071366E-24	0.76704460E 00	0.79673421E 00
70.0	0.27481937E-28	0.27935758E-28	0.78338873E 00	0.79632533E 00
80.0	0.44257207E-31	0.44435788E-31	0.79213387E 00	0.79533017E 00
90.0	0.41808379E-31	0.41808352E-31	0.70108948E 01	0.70108900E 01

FREQUENCY = 137.0 MHZ
SIGMA = 1.50 METERS
PLATFORM ALTITUDE = 321.8688 KM

PSI	SPECULAR		DIFFUSE	
(DEGREES)	VERTICAL	HORIZONTAL	VERTICAL	HORIZONTAL
0.0	0.0	0.0	0.0	0.0
2.0	0.79008117E-02	0.52982543E-01	0.86480938E-02	0.57993781E-01
4.0	0.15699446E-01	0.81880212E-01	0.22526171E-01	0.11748493E 00
6.0	0.24038956E-01	0.78784525E-01	0.54076180E-01	0.17722768E 00
8.0	0.22678852E-01	0.56024626E-01	0.95451117E-01	0.23579735E 00
10.0	0.15106324E-01	0.31150844E-01	0.14152855E 00	0.29184687E 00
12.0	0.76508969E-02	0.13930444E-01	0.18909818E 00	0.34430230E 00
14.0	0.30696285E-02	0.51028058E-02	0.23608136E 00	0.39245057E 00
16.0	0.10015159E-02	0.15528912E-02	0.28115201E 00	0.43593758E 00
18.0	0.27085864E-03	0.39743609E-03	0.32352239E 00	0.47471076E 00
20.0	0.61674276E-04	0.86519824E-04	0.36278582E 00	0.50893444E 00
30.0	0.45042619E-08	0.54854645E-08	0.51255620E 00	0.62421054E 00
40.0	0.29218652E-13	0.32945126E-13	0.60261118E 00	0.67946672E 00
50.0	0.80812444E-19	0.86753565E-19	0.65701956E 00	0.70532185E 00
60.0	0.46852554E-24	0.48666057E-24	0.69036603E 00	0.71708775E 00
70.0	0.24921750E-28	0.25333297E-28	0.71040910E 00	0.72214049E 00
80.0	0.40292182E-31	0.40454764E-31	0.72116619E 00	0.72407615E 00
90.0	0.30212867E-31	0.30212844E-31	0.50664301E 01	0.50664263E 01

FREQUENCY = 137.0 MHZ
SIGMA = 1.50 METERS
PLATFORM ALTITUDE = 643.7376 KM

PSI	SPECULAR		DIFFUSE	
(DEGREES)	VERTICAL	HORIZONTAL	VERTICAL	HORIZONTAL
0.0	0.0	0.0	0.0	0.0
2.0	0.55065304E-02	0.36926586E-01	0.60273558E-02	0.40419206E-01
4.0	0.10758661E-01	0.56111652E-01	0.15436944E-01	0.80511153E-01
6.0	0.16293500E-01	0.53399846E-01	0.36652599E-01	0.12012416E 00
8.0	0.15291844E-01	0.37776183E-01	0.64360559E-01	0.15899301E 00
10.0	0.10186244E-01	0.21005124E-01	0.95433176E-01	0.19679338E 00
12.0	0.51819161E-02	0.94350204E-02	0.12807530E 00	0.23319429E 00
14.0	0.20953936E-02	0.34832840E-02	0.16115415E 00	0.26789510E 00
16.0	0.69071865E-03	0.10709874E-02	0.19390297E 00	0.30065447E 00
18.0	0.18903227E-03	0.27737068E-03	0.22578627E 00	0.33130062E 00
20.0	0.43594060E-04	0.61155981E-04	0.25643277E 00	0.35973704E 00
30.0	0.33874121E-08	0.41253188E-08	0.38546556E 00	0.46943480E 00
40.0	0.23003182E-13	0.25936952E-13	0.47442210E 00	0.53492874E 00
50.0	0.65550703E-19	0.70369806E-19	0.53293884E 00	0.57211912E 00
60.0	0.38725488E-24	0.40224422E-24	0.57061481E 00	0.59270138E 00
70.0	0.20834325E-28	0.21178368E-28	0.59389466E 00	0.60370195E 00
80.0	0.33869905E-31	0.34026653E-31	0.60657561E 00	0.60902315E 00
90.0	0.18743363E-31	0.18743351E-31	0.31430960E 01	0.31430941E 01

FREQUENCY = 137.0 MHZ
SIGMA = 1.50 METERS
PLATFORM ALTITUDE = 1287.4750 KM

PSI (DEGREES)	SPECULAR VERTICAL	SPECULAR HORIZONTAL	DIFFUSE VERTICAL	DIFFUSE HORIZONTAL
0.0	0.0	0.0	0.0	0.0
2.0	0.38294313E-02	0.25680024E-01	0.41916296E-02	0.28108913E-01
4.0	0.73395707E-02	0.38279463E-01	0.10531101E-01	0.54924842E-01
6.0	0.10938775E-01	0.35850421E-01	0.24607029E-01	0.80646336E-01
8.0	0.10136258E-01	0.25040071E-01	0.42661656E-01	0.10538906E 00
10.0	0.66879168E-02	0.13791192E-01	0.62657952E-01	0.12920731E 00
12.0	0.33802232E-02	0.61545707E-02	0.83544970E-01	0.15211529E 00
14.0	0.13617789E-02	0.22637579E-02	0.10473275E 00	0.17410284E 00
16.0	0.44832611E-03	0.69514802E-03	0.12585700E 00	0.19514644E 00
18.0	0.12279741E-03	0.18018309E-03	0.14667320E 00	0.21521652E 00
20.0	0.28391747E-04	0.39829392E-04	0.16700846E 00	0.23428798E 00
30.0	0.22680826E-08	0.27621578E-08	0.25809312E 00	0.31431568E 00
40.0	0.15926191E-13	0.17957380E-13	0.32846487E 00	0.37035650E 00
50.0	0.46665608E-19	0.50096333E-19	0.37939966E 00	0.40729207E 00
60.0	0.28131554E-24	0.29220429E-24	0.41451460E 00	0.43055904E 00
70.0	0.15337625E-28	0.15590908E-28	0.43720806E 00	0.44442791E 00
80.0	0.25136457E-31	0.25237884E-31	0.44990277E 00	0.45171815E 00
90.0	0.99058938E-32	0.99058880E-32	0.16611309E 01	0.16611300E 01

FREQUENCY = 137.0 MHZ
SIGMA = 15.00 METERS
PLATFORM ALTITUDE = 6.0960 KM

PSI (DEGREES)	SPECULAR VERTICAL	SPECULAR HORIZONTAL	DIFFUSE VERTICAL	DIFFUSE HORIZONTAL
0.0	0.0	0.0	0.0	0.0
2.0	0.80009695E-05	0.53654163E-04	0.67297935E-01	0.45129716E 00
4.0	0.29119259E-16	0.15187123E-15	0.13946772E 00	0.72739232E 00
6.0	0.15897184E-35	0.52100996E-35	0.25725222E 00	0.84311116E 00
8.0	0.13884516E-62	0.34299562E-62	0.36186981E 00	0.89394385E 00
10.0	0.0	0.0	0.44532102E 00	0.91829902E 00
12.0	0.0	0.0	0.51105392E 00	0.93050635E 00
14.0	0.0	0.0	0.56337065E 00	0.93652081E 00
16.0	0.0	0.0	0.60565788E 00	0.93909699E 00
18.0	0.0	0.0	0.64037973E 00	0.93964171E 00
20.0	0.0	0.0	0.66929811E 00	0.93892562E 00
30.0	0.0	0.0	0.76159787E 00	0.92750311E 00
40.0	0.0	0.0	0.80970472E 00	0.91297245E 00
50.0	0.0	0.0	0.83791369E 00	0.89951479E 00
60.0	0.0	0.0	0.85528207E 00	0.88838702E 00
70.0	0.0	0.0	0.86585724E 00	0.88015568E 00
80.0	0.0	0.0	0.87160027E 00	0.87511718E 00
90.0	0.0	0.0	0.10677464E 02	0.10677457E 02

FREQUENCY = 137.0 MHZ
SIGMA = 15.00 METERS
PLATFORM ALTITUDE = 15.2400 KM

PSI (DEGREES)	SPECULAR VERTICAL	SPECULAR HORIZONTAL	DIFFUSE VERTICAL	DIFFUSE HORIZONTAL
0.0	0.0	0.0	0.0	0.0
2.0	0.51388306E-05	0.34460798E-04	0.43223850E-01	0.28985745E 00
4.0	0.21792887E-16	0.11366065E-15	0.10437781E 00	0.54438150E 00
6.0	0.13255636E-35	0.43443657E-35	0.21450597E 00	0.70301598E 00
8.0	0.12314735E-62	0.30421657E-62	0.32095689E 00	0.79287463E 00
10.0	0.0	0.0	0.40938872E 00	0.84420288E 00
12.0	0.0	0.0	0.48026574E 00	0.87444836E 00
14.0	0.0	0.0	0.53703171E 00	0.89273620E 00
16.0	0.0	0.0	0.58296537E 00	0.90391135E 00
18.0	0.0	0.0	0.62062484E 00	0.91065508E 00
20.0	0.0	0.0	0.65190917E 00	0.91453153E 00
30.0	0.0	0.0	0.75094253E 00	0.91452658E 00
40.0	0.0	0.0	0.80188060E 00	0.90415049E 00
50.0	0.0	0.0	0.83148551E 00	0.89261413E 00
60.0	0.0	0.0	0.84960908E 00	0.88249451E 00
70.0	0.0	0.0	0.86060274E 00	0.87481433E 00
80.0	0.0	0.0	0.86655998E 00	0.87005657E 00
90.0	0.0	0.0	0.10368569E 02	0.10368562E 02

FREQUENCY = 137.0 MHZ
SIGMA = 15.00 METERS
PLATFORM ALTITUDE = 30.4800 KM

PSI	SPECULAR		DIFFUSE	
(DEGREES)	VERTICAL	HORIZONTAL	VERTICAL	HORIZONTAL
0.0	0.0	0.0	0.0	0.0
2.0	0.35745561E-05	0.23970832E-04	0.30066390E-01	0.20162404E 00
4.0	0.16177932E-16	0.84375903E-16	0.77484787E-01	0.40412122E 00
6.0	0.10630554E-35	0.34840278E-35	0.17202628E 00	0.56379402E 00
8.0	0.10478759E-62	0.25886156E-62	0.27310616E 00	0.67466676E 00
10.0	0.0	0.0	0.36289382E 00	0.74832547E 00
12.0	0.0	0.0	0.43775582E 00	0.79704803E 00
14.0	0.0	0.0	0.49905396E 00	0.82960367E 00
16.0	0.0	0.0	0.54924381E 00	0.85162473E 00
18.0	0.0	0.0	0.59062761E 00	0.86663949E 00
20.0	0.0	0.0	0.62508237E 00	0.87689751E 00
30.0	0.0	0.0	0.73384303E 00	0.89370221E 00
40.0	0.0	0.0	0.78914952E 00	0.88979560E 00
50.0	0.0	0.0	0.82096046E 00	0.88131523E 00
60.0	0.0	0.0	0.84029067E 00	0.87281543E 00
70.0	0.0	0.0	0.85195857E 00	0.86602747E 00
80.0	0.0	0.0	0.85826087E 00	0.86172402E 00
90.0	0.0	0.0	0.98888474E 01	0.98888397E 01

FREQUENCY = 137.0 MHZ
SIGMA = 15.00 METERS
PLATFORM ALTITUDE = 160.9344 KM

PSI	SPECULAR		DIFFUSE	
(DEGREES)	VERTICAL	HORIZONTAL	VERTICAL	HORIZONTAL
0.0	0.0	0.0	0.0	0.0
2.0	0.14778525E-05	0.99104145E-05	0.12430549E-01	0.83358705E-01
4.0	0.68496775E-17	0.35724409E-16	0.32806758E-01	0.17110324E 00
6.0	0.48762684E-36	0.15981349E-35	0.78908980E-01	0.25861418E 00
8.0	0.53033766E-63	0.13101180E-62	0.13822103E 00	0.34145385E 00
10.0	0.0	0.0	0.20195711E 00	0.41645694E 00
12.0	0.0	0.0	0.26475775E 00	0.48206019E 00
14.0	0.0	0.0	0.32365632E 00	0.53803110E 00
16.0	0.0	0.0	0.37728137E 00	0.58499002E 00
18.0	0.0	0.0	0.42524064E 00	0.62396389E 00
20.0	0.0	0.0	0.46769488E 00	0.65610629E 00
30.0	0.0	0.0	0.61459136E 00	0.74847293E 00
40.0	0.0	0.0	0.69393229E 00	0.78243464E 00
50.0	0.0	0.0	0.73961776E 00	0.79399246E 00
60.0	0.0	0.0	0.76704460E 00	0.79673421E 00
70.0	0.0	0.0	0.78338873E 00	0.79632533E 00
80.0	0.0	0.0	0.79213387E 00	0.79533017E 00
90.0	0.0	0.0	0.70108948E 01	0.70108900E 01

FREQUENCY = 137.0 MHZ
SIGMA = 15.00 METERS
PLATFORM ALTITUDE = 321.8688 KM

PSI (DEGREES)	SPECULAR VERTICAL	SPECULAR HORIZONTAL	DIFFUSE VERTICAL	DIFFUSE HORIZONTAL
0.0	0.0	0.0	0.0	0.0
2.0	0.10281610E-05	0.68948093E-05	0.86480938E-02	0.57993781E-01
4.0	0.47032075E-17	0.24529505E-16	0.22526171E-01	0.11748493E 00
6.0	0.33416977E-36	0.10951978E-35	0.54076180E-01	0.17722768E 00
8.0	0.36623455E-63	0.90472638E-63	0.95451117E-01	0.23579735E 00
10.0	0.0	0.0	0.14152855E 00	0.29184687E 00
12.0	0.0	0.0	0.18909818E 00	0.34430230E 00
14.0	0.0	0.0	0.23608136E 00	0.39245057E 00
16.0	0.0	0.0	0.28115201E 00	0.43593758E 00
18.0	0.0	0.0	0.32352239E 00	0.47471076E 00
20.0	0.0	0.0	0.36278582E 00	0.50893444E 00
30.0	0.0	0.0	0.51255620E 00	0.62421054E 00
40.0	0.0	0.0	0.60261118E 00	0.67946672E 00
50.0	0.0	0.0	0.65701956E 00	0.70532185E 00
60.0	0.0	0.0	0.69036603E 00	0.71708775E 00
70.0	0.0	0.0	0.71040910E 00	0.72214049E 00
80.0	0.0	0.0	0.72116619E 00	0.72407615E 00
90.0	0.0	0.0	0.50654301E 01	0.50664263E 01

FREQUENCY = 137.0 MHZ
SIGMA = 15.00 METERS
PLATFORM ALTITUDE = 643.7376 KM

PSI	SPECULAR		DIFFUSE	
(DEGREES)	VERTICAL	HORIZONTAL	VERTICAL	HORIZONTAL
0.0	0.0	0.0	0.0	0.0
2.0	0.71658496E-06	0.48053898E-05	0.60273558E-02	0.40419206E-01
4.0	0.32230580E-17	0.16809806E-16	0.15436944E-01	0.80511153E-01
6.0	0.22649880E-36	0.74232066E-36	0.36652599E-01	0.12012416E 00
8.0	0.24694373E-63	0.61003734E-63	0.64360559E-01	0.15899301E 00
10.0	0.0	0.0	0.95433176E-01	0.19679338E 00
12.0	0.0	0.0	0.12807530E 00	0.23319429E 00
14.0	0.0	0.0	0.16115415E 00	0.26789510E 00
16.0	0.0	0.0	0.19390297E 00	0.30065447E 00
18.0	0.0	0.0	0.22578627E 00	0.33130062E 00
20.0	0.0	0.0	0.25643277E 00	0.35973704E 00
30.0	0.0	0.0	0.38546556E 00	0.46943480E 00
40.0	0.0	0.0	0.47442210E 00	0.53492874E 00
50.0	0.0	0.0	0.53293884E 00	0.57211912E 00
60.0	0.0	0.0	0.57061481E 00	0.59270138E 00
70.0	0.0	0.0	0.59389466E 00	0.60370195E 00
80.0	0.0	0.0	0.60657561E 00	0.60902315E 00
90.0	0.0	0.0	0.31430960E 01	0.31430941E 01

FREQUENCY = 137.0 MHZ
SIGMA = 15.00 METERS
PLATFORM ALTITUDE = 1287.4750 KM

PSI (DEGREES)	SPECULAR VERTICAL	SPECULAR HORIZONTAL	DIFFUSE VERTICAL	DIFFUSE HORIZONTAL
0.0	0.0	0.0	0.0	0.0
2.0	0.49833773E-06	0.33418337E-05	0.41916296E-02	0.28108913E-01
4.0	0.21987735E-17	0.11467681E-16	0.10531101E-01	0.54924842E-01
6.0	0.15206187E-36	0.49836303E-36	0.24607029E-01	0.80646336E-01
8.0	0.16368770E-63	0.40436534E-63	0.42661656E-01	0.10538906E 00
10.0	0.0	0.0	0.62657952E-01	0.12920731E 00
12.0	0.0	0.0	0.83544970E-01	0.15211529E 00
14.0	0.0	0.0	0.10473275E 00	0.17410284E 00
16.0	0.0	0.0	0.12585700E 00	0.19514644E 00
18.0	0.0	0.0	0.14667320E 00	0.21521652E 00
20.0	0.0	0.0	0.16700846E 00	0.23428798E 00
30.0	0.0	0.0	0.25809312E 00	0.31431568E 00
40.0	0.0	0.0	0.32846487E 00	0.37035650E 00
50.0	0.0	0.0	0.37939966E 00	0.40729207E 00
60.0	0.0	0.0	0.41451460E 00	0.43055904E 00
70.0	0.0	0.0	0.43720806E 00	0.44442791E 00
80.0	0.0	0.0	0.44990277E 00	0.45171815E 00
90.0	0.0	0.0	0.16611309E 01	0.16611300E 01

FREQUENCY = 400.0 MHZ
SIGMA = 0.15 METERS
PLATFORM ALTITUDE = 6.0960 KM

PSI	SPECULAR		DIFFUSE	
(DEGREES)	VERTICAL	HORIZONTAL	VERTICAL	HORIZONTAL
0.0	0.0	0.0	0.0	0.0
2.0	0.90882123E-01	0.44615877E 00	0.91585040E-01	0.44960928E 00
4.0	0.62076483E-01	0.70008212E 00	0.64016819E-01	0.72196472E 00
6.0	0.97915947E-01	0.77803111E 00	0.10492235E 00	0.83370334E 00
8.0	0.15293276E 00	0.77913535E 00	0.17286551E 00	0.88068497E 00
10.0	0.20057201E 00	0.74482554E 00	0.24271882E 00	0.90133786E 00
12.0	0.23312914E 00	0.69227463E 00	0.30643845E 00	0.90996587E 00
14.0	0.25023949E 00	0.63017851E 00	0.36235094E 00	0.91250890E 00
16.0	0.25406837E 00	0.56383133E 00	0.41082722E 00	0.91171223E 00
18.0	0.24750412E 00	0.49686146E 00	0.45279408E 00	0.90897846E 00
20.0	0.23343635E 00	0.43185848E 00	0.48922718E 00	0.90507293E 00
30.0	0.12639827E 00	0.18081820E 00	0.61446863E 00	0.87902385E 00
40.0	0.50208759E-01	0.62441919E-01	0.68515450E 00	0.85208964E 00
50.0	0.17795078E-01	0.20242348E-01	0.72832775E 00	0.82849121E 00
60.0	0.65763853E-02	0.70460066E-02	0.75554931E 00	0.80950332E 00
70.0	0.28981946E-02	0.29857042E-02	0.77236199E 00	0.79568309E 00
80.0	0.16934078E-02	0.17058421E-02	0.78156608E 00	0.78730494E 00
90.0	0.17171111E-01	0.17171115E-01	0.95903940E 01	0.95903959E 01

FREQUENCY = 400.0 MHZ
SIGMA = 0.15 METERS
PLATFORM ALTITUDE = 15.2400 KM

PSI (DEGREES)	SPECULAR VERTICAL	SPECULAR HORIZONTAL	DIFFUSE VERTICAL	DIFFUSE HORIZONTAL
0.0	0.0	0.0	0.0	0.0
2.0	0.58371458E-01	0.28655708E 00	0.58822893E-01	0.28877330E 00
4.0	0.46458144E-01	0.52394253E 00	0.47910295E-01	0.54031950E 00
6.0	0.81645787E-01	0.64874989E 00	0.87487996E-01	0.69517136E 00
8.0	0.13564223E 00	0.69104642E 00	0.15332139E 00	0.78111488E 00
10.0	0.18438816E 00	0.68472672E 00	0.22313422E 00	0.82861030E 00
12.0	0.21908438E 00	0.65056878E 00	0.28797722E 00	0.85514534E 00
14.0	0.23854011E 00	0.60071611E 00	0.34541011E 00	0.86984688E 00
16.0	0.24454904E 00	0.54270601E 00	0.39543450E 00	0.87755269E 00
18.0	0.23986894E 00	0.48153400E 00	0.43882602E 00	0.88093776E 00
20.0	0.22737145E 00	0.42063844E 00	0.47651660E 00	0.88155836E 00
30.0	0.12462986E 00	0.17828840E 00	0.60587180E 00	0.86672562E 00
40.0	0.49723595E-01	0.61838549E-01	0.67853391E 00	0.84385598E 00
50.0	0.17658558E-01	0.20087056E-01	0.72274023E 00	0.82213533E 00
60.0	0.65327659E-02	0.69992729E-02	0.75053787E 00	0.80413401E 00
70.0	0.28806068E-02	0.29675851E-02	0.76767486E 00	0.79085439E 00
80.0	0.16836151E-02	0.16959775E-02	0.77704644E 00	0.78275210E 00
90.0	0.16674358E-01	0.16674362E-01	0.93129473E 01	0.93129492E 01

FREQUENCY = 400.0 MHZ
SIGMA = 0.15 METERS
PLATFORM ALTITUDE = 30.4800 KM

PSI	SPECULAR		DIFFUSE	
(DEGREES)	VERTICAL	HORIZONTAL	VERTICAL	HORIZONTAL
0.0	0.0	0.0	0.0	0.0
2.0	0.40603019E-01	0.19932830E 00	0.40917039E-01	0.20086992E 00
4.0	0.34488179E-01	0.38894838E 00	0.35566181E-01	0.40110582E 00
6.0	0.65477014E-01	0.52027458E 00	0.70162237E-01	0.55750299E 00
8.0	0.11541963E 00	0.58801985E 00	0.13046300E 00	0.66466022E 00
10.0	0.16344690E 00	0.60696131E 00	0.19779253E 00	0.73450381E 00
12.0	0.19969243E 00	0.59298486E 00	0.26248735E 00	0.77945364E 00
14.0	0.22167104E 00	0.55823463E 00	0.32098341E 00	0.80833304E 00
16.0	0.23040313E 00	0.51131320E 00	0.37256068E 00	0.82679069E 00
18.0	0.22827512E 00	0.45825952E 00	0.41761577E 00	0.83835852E 00
20.0	0.21801484E 00	0.40332872E 00	0.45690739E 00	0.84528124E 00
30.0	0.12179196E 00	0.17422867E 00	0.59207565E 00	0.84698969E 00
40.0	0.48934158E-01	0.60856763E-01	0.66776115E 00	0.83045840E 00
50.0	0.17435037E-01	0.19832794E-01	0.71359175E 00	0.81172866E 00
60.0	0.64611174E-02	0.69225058E-02	0.74230611E 00	0.79531437E 00
70.0	0.28516729E-02	0.29377781E-02	0.75996411E 00	0.78291088E 00
80.0	0.16674909E-02	0.16797350E-02	0.76960462E 00	0.77525562E 00
90.0	0.15902884E-01	0.15902888E-01	0.88820648E 01	0.88820667E 01

FREQUENCY = 400.0 MHZ
SIGMA = 0.15 METERS
PLATFORM ALTITUDE = 160.9344 KM

PSI	SPECULAR		DIFFUSE	
(DEGREES)	VERTICAL	HORIZONTAL	VERTICAL	HORIZONTAL
0.0	0.0	0.0	0.0	0.0
2.0	0.16786773E-01	0.82409561E-01	0.16916599E-01	0.83046913E-01
4.0	0.14602151E-01	0.16467911E 00	0.15058573E-01	0.16982651E 00
6.0	0.30034535E-01	0.23865163E 00	0.32183666E-01	0.25572842E 00
8.0	0.58414735E-01	0.29760116E 00	0.66028297E-01	0.33638942E 00
10.0	0.90961218E-01	0.33778512E 00	0.11007518E 00	0.40876490E 00
12.0	0.12077534E 00	0.35864127E 00	0.15875417E 00	0.47141892E 00
14.0	0.14376253E 00	0.36203742E 00	0.20817053E 00	0.52423620E 00
16.0	0.15826637E 00	0.35122645E 00	0.25591588E 00	0.56793129E 00
18.0	0.16435373E 00	0.32993811E 00	0.30067539E 00	0.60360211E 00
20.0	0.16312158E 00	0.30177587E 00	0.34186417E 00	0.63245058E 00
30.0	0.10200042E 00	0.14591599E 00	0.49586159E 00	0.70935136E 00
40.0	0.43029856E-01	0.53513911E-01	0.58719039E 00	0.73025697E 00
50.0	0.15707530E-01	0.17867714E-01	0.64288741E 00	0.73130065E 00
60.0	0.58979169E-02	0.63190870E-02	0.67760104E 00	0.72598875E 00
70.0	0.26221564E-02	0.27013312E-02	0.69879848E 00	0.71989834E 00
80.0	0.15390147E-02	0.15503154E-02	0.71030837E 00	0.71552402E 00
90.0	0.11274666E-01	0.11274669E-01	0.62971172E 01	0.62971182E 01

FREQUENCY = 400.0 MHZ
SIGMA = 0.15 METERS
PLATFORM ALTITUDE = 321.8688 KM

PSI	SPECULAR		DIFFUSE	
(DEGREES)	VERTICAL	HORIZONTAL	VERTICAL	HORIZONTAL
0.0	0.0	0.0	0.0	0.0
2.0	0.11678778E-01	0.57333469E-01	0.11769101E-01	0.57776876E-01
4.0	0.10026306E-01	0.11307395E 00	0.10339700E-01	0.11660832E 00
6.0	0.20582609E-01	0.16354740E 00	0.22055402E-01	0.17525011E 00
8.0	0.40339388E-01	0.20551401E 00	0.45597076E-01	0.23229998E 00
10.0	0.63744247E-01	0.23671484E 00	0.77139020E-01	0.28645641E 00
12.0	0.86261451E-01	0.25615269E 00	0.11338711E 00	0.33670199E 00
14.0	0.10486323E 00	0.26407725E 00	0.15184373E 00	0.38238829E 00
16.0	0.11794090E 00	0.26173574E 00	0.19070983E 00	0.42322528E 00
18.0	0.12504005E 00	0.25101638E 00	0.22875339E 00	0.45921957E 00
20.0	0.12653160E 00	0.23408425E 00	0.26518029E 00	0.49058503E 00
30.0	0.85066140E-01	0.12169081E 00	0.41353804E 00	0.59158397E 00
40.0	0.37367154E-01	0.46471510E-01	0.50991648E 00	0.63415557E 00
50.0	0.13953362E-01	0.15872303E-01	0.57109171E 00	0.64963126E 00
60.0	0.53083226E-02	0.56873932E-02	0.60986388E 00	0.65341443E 00
70.0	0.23778789E-02	0.24496780E-02	0.63369912E 00	0.65283340E 00
80.0	0.14011336E-02	0.14114219E-02	0.64667153E 00	0.65141988E 00
90.0	0.81476495E-02	0.81476495E-02	0.45506182E 01	0.45506182E 01

FREQUENCY = 400.0 MHZ
SIGMA = 0.15 METERS
PLATFORM ALTITUDE = 643.7376 KM

PSI (DEGREES)	SPECULAR		DIFFUSE	
	VERTICAL	HORIZONTAL	VERTICAL	HORIZONTAL
0.0	0.0	0.0	0.0	0.0
2.0	0.81396103E-02	0.39958991E-01	0.82025640E-02	0.40268030E-01
4.0	0.68709180E-02	0.77488363E-01	0.70856847E-02	0.79910457E-01
6.0	0.13950802E-01	0.11085171E 00	0.14949057E-01	0.11878377E 00
8.0	0.27199972E-01	0.13857359E 00	0.30745115E-01	0.15663481E 00
10.0	0.42983018E-01	0.15961760E 00	0.52015163E-01	0.19315857E 00
12.0	0.58424488E-01	0.17349094E 00	0.76796532E-01	0.22804660E 00
14.0	0.71581841E-01	0.18026477E 00	0.10365176E 00	0.26102644E 00
16.0	0.81340671E-01	0.18051207E 00	0.13152742E 00	0.29188710E 00
18.0	0.87265432E-01	0.17518431E 00	0.15964699E 00	0.32048935E 00
20.0	0.89438021E-01	0.16546088E 00	0.18744093E 00	0.34676683E 00
30.0	0.63973606E-01	0.91517031E-01	0.31099945E 00	0.44489813E 00
40.0	0.29418312E-01	0.36585964E-01	0.40144569E 00	0.49925631E 00
50.0	0.11318214E-01	0.12874756E-01	0.46323884E 00	0.52694589E 00
60.0	0.43875389E-02	0.47008544E-02	0.50407654E 00	0.54007280E 00
70.0	0.19878822E-02	0.20479055E-02	0.52976590E 00	0.54576194E 00
80.0	0.11784986E-02	0.11871522E-02	0.54391783E 00	0.54791170E 00
90.0	0.50546117E-02	0.50546154E-02	0.28230972E 01	0.28230991E 01

FREQUENCY = 400.0 MHZ
SIGMA = 0.15 METERS
PLATFORM ALTITUDE = 1287.4750 KM

PSI	SPECULAR		DIFFUSE	
(DEGREES)	VERTICAL	HORIZONTAL	VERTICAL	HORIZONTAL
0.0	0.0	0.0	0.0	0.0
2.0	0.56605674E-02	0.27788866E-01	0.57043470E-02	0.28003782E-01
4.0	0.46873465E-02	0.52862670E-01	0.48338622E-02	0.54515008E-01
6.0	0.93659833E-02	0.74421167E-01	0.10036170E-01	0.79746425E-01
8.0	0.18029608E-01	0.91853976E-01	0.20379521E-01	0.10382593E 00
10.0	0.28221074E-01	0.10479903E 00	0.34151252E-01	0.12682080E 00
12.0	0.38110994E-01	0.11317015E 00	0.50095297E-01	0.14875746E 00
14.0	0.46520483E-01	0.11715263E 00	0.67362428E-01	0.16963899E 00
16.0	0.52795958E-01	0.11716539E 00	0.85370779E-01	0.18945581E 00
18.0	0.56688584E-01	0.11380160E 00	0.10370839E 00	0.20819330E 00
20.0	0.58248840E-01	0.10776067E 00	0.12207574E 00	0.22584081E 00
30.0	0.42834327E-01	0.61276346E-01	0.20823342E 00	0.29788685E 00
40.0	0.20367689E-01	0.25330190E-01	0.27793986E 00	0.34565872E 00
50.0	0.80574453E-02	0.91655478E-02	0.32978010E 00	0.37513322E 00
60.0	0.31872627E-02	0.34148658E-02	0.36617887E 00	0.39232779E 00
70.0	0.14634214E-02	0.15076087E-02	0.38999832E 00	0.40177417E 00
80.0	0.87410351E-03	0.88052172E-03	0.40342891E 00	0.40639120E 00
90.0	0.26713717E-02	0.26713717E-02	0.14920120E 01	0.14920120E 01

FREQUENCY = 400.0 MHZ
SIGMA = 1.50 METERS
PLATFORM ALTITUDE = 6.0960 KM

PSI (DEGREES)	SPECULAR VERTICAL	SPECULAR HORIZONTAL	DIFFUSE VERTICAL	DIFFUSE HORIZONTAL
0.0	0.0	0.0	0.0	0.0
2.0	0.42387944E-01	0.20809084E 00	0.91585040E-01	0.44960928E 00
4.0	0.29484797E-02	0.33252172E-01	0.64016819E-01	0.72196472E 00
6.0	0.10457016E-03	0.83090481E-03	0.10492235E 00	0.83370334E 00
8.0	0.82591890E-06	0.42077472E-05	0.17286551E 00	0.88068497E 00
10.0	0.12641315E-08	0.46943605E-08	0.24271882E 00	0.90133786E 00
12.0	0.40895304E-12	0.12143819E-11	0.30643845E 00	0.90996587E 00
14.0	0.30322919E-16	0.76362270E-16	0.36235094E 00	0.91250890E 00
16.0	0.55309444E-21	0.12274334E-20	0.41082722E 00	0.91171223E 00
18.0	0.26549684E-26	0.53298154E-26	0.45279408E 00	0.90897846E 00
20.0	0.35916760E-32	0.66446229E-32	0.48922718E 00	0.90507293E 00
30.0	0.12959356E-68	0.18538916E-68	0.61446863E 00	0.87902385E 00
40.0	0.0	0.0	0.68515450E 00	0.85208964E 00
50.0	0.0	0.0	0.72832775E 00	0.82849121E 00
60.0	0.0	0.0	0.75554931E 00	0.80950332E 00
70.0	0.0	0.0	0.77236199E 00	0.79568309E 00
80.0	0.0	0.0	0.78156608E 00	0.78730494E 00
90.0	0.0	0.0	0.95903940E 01	0.95903959E 01

FREQUENCY = 400.0 MHZ
SIGMA = 1.50 METERS
PLATFORM ALTITUDE = 15.2400 KM

PSI	SPECULAR		DIFFUSE	
(DEGREES)	VERTICAL	HORIZONTAL	VERTICAL	HORIZONTAL
0.0	0.0	0.0	0.0	0.0
2.0	0.27224768E-01	0.13365179E 00	0.58822893E-01	0.28877330E 00
4.0	0.22066473E-02	0.24885979E-01	0.47910295E-01	0.54031950E 00
6.0	0.87194334E-04	0.69283787E-03	0.87487996E-01	0.69517136E 00
8.0	0.73254074E-06	0.37320196E-05	0.15332139E 00	0.78111488E 00
10.0	0.11621306E-08	0.43155772E-08	0.22313422E 00	0.82861030E 00
12.0	0.38431590E-12	0.11412217E-11	0.28797722E 00	0.85514534E 00
14.0	0.28905251E-16	0.72792145E-16	0.34541011E 00	0.86984688E 00
16.0	0.53237130E-21	0.11814447E-20	0.39543450E 00	0.87755269E 00
18.0	0.25730665E-26	0.51653965E-26	0.43882602E 00	0.88093776E 00
20.0	0.34983623E-32	0.64719898E-32	0.47651660E 00	0.88155836E 00
30.0	0.12778045E-68	0.18279542E-68	0.60587180E 00	0.86672562E 00
40.0	0.0	0.0	0.67853391E 00	0.84385598E 00
50.0	0.0	0.0	0.72274023E 00	0.82213533E 00
60.0	0.0	0.0	0.75053787E 00	0.80413401E 00
70.0	0.0	0.0	0.76767486E 00	0.79085439E 00
80.0	0.0	0.0	0.77704644E 00	0.78275210E 00
90.0	0.0	0.0	0.93129473E 01	0.93129492E 01

FREQUENCY = 400.0 MHZ
SIGMA = 1.50 METERS
PLATFORM ALTITUDE = 30.4800 KM

PSI (DEGREES)	SPECULAR VERTICAL	SPECULAR HORIZONTAL	DIFFUSE VERTICAL	DIFFUSE HORIZONTAL
0.0	0.0	0.0	0.0	0.0
2.0	0.18937472E-01	0.92967808E-01	0.40917039E-01	0.20086992E 00
4.0	0.16381033E-02	0.18474087E-01	0.35566181E-01	0.40110582E 00
6.0	0.69926726E-04	0.55563147E-03	0.70162237E-01	0.55750299E 00
8.0	0.62332771E-06	0.31756208E-05	0.13046300E 00	0.66466022E 00
10.0	0.10301457E-08	0.38254520E-08	0.19779253E 00	0.73450381E 00
12.0	0.35029873E-12	0.10402087E-11	0.26248735E 00	0.77945364E 00
14.0	0.26861122E-16	0.67644422E-16	0.32098341E 00	0.80833304E 00
16.0	0.50157639E-21	0.11131040E-20	0.37256068E 00	0.82679069E 00
18.0	0.24486996E-26	0.49157343E-26	0.41761577E 00	0.83835852E 00
20.0	0.33543995E-32	0.62056610E-32	0.45690739E 00	0.84528124E 00
30.0	0.12487079E-68	0.17863305E-68	0.59207565E 00	0.84698969E 00
40.0	0.0	0.0	0.66776115E 00	0.83045840E 00
50.0	0.0	0.0	0.71359175E 00	0.81172866E 00
60.0	0.0	0.0	0.74230611E 00	0.79531437E 00
70.0	0.0	0.0	0.75996411E 00	0.78291088E 00
80.0	0.0	0.0	0.76960462E 00	0.77525562E 00
90.0	0.0	0.0	0.88820648E 01	0.88820667E 01

FREQUENCY = 400.0 MHZ
SIGMA = 1.50 METERS
PLATFORM ALTITUDE = 160.9344 KM

PSI	SPECULAR		DIFFUSE	
(DEGREES)	VERTICAL	HORIZONTAL	VERTICAL	HORIZONTAL
0.0	0.0	0.0	0.0	0.0
2.0	0.78294426E-02	0.38436275E-01	0.16916599E-01	0.83046913E-01
4.0	0.69356617E-03	0.78218505E-02	0.15058573E-01	0.16982651E 00
6.0	0.32075637E-04	0.25486993E-03	0.32183666E-01	0.25572842E 00
8.0	0.31547074E-06	0.16072054E-05	0.66028297E-01	0.33638942E 00
10.0	0.57329497E-09	0.21289350E-08	0.11007518E 00	0.40876490E 00
12.0	0.21186308E-12	0.62912539E-12	0.15875417E 00	0.47141892E 00
14.0	0.17420503E-16	0.43870100E-16	0.20817053E 00	0.52423620E 00
16.0	0.34453809E-21	0.76460307E-21	0.25591588E 00	0.56793129E 00
18.0	0.17630171E-26	0.35392337E-26	0.30067539E 00	0.60360211E 00
20.0	0.25098077E-32	0.46431557E-32	0.34186417E 00	0.63245058E 00
30.0	0.10457892E-68	0.14960465E-68	0.49586159E 00	0.70935136E 00
40.0	0.0	0.0	0.58719039E 00	0.73025697E 00
50.0	0.0	0.0	0.64288741E 00	0.73130065E 00
60.0	0.0	0.0	0.67760104E 00	0.72598875E 00
70.0	0.0	0.0	0.69879848E 00	0.71989834E 00
80.0	0.0	0.0	0.71030837E 00	0.71552402E 00
90.0	0.0	0.0	0.62971172E 01	0.62971182E 01

FREQUENCY = 400.0 MHZ
SIGMA = 1.50 METERS
PLATFORM ALTITUDE = 321.8688 KM

PSI	SPECULAR		DIFFUSE	
(DEGREES)	VERTICAL	HORIZONTAL	VERTICAL	HORIZONTAL
0.0	0.0	0.0	0.0	0.0
2.0	0.54470450E-02	0.26740644E-01	0.11769101E-01	0.57776876E-01
4.0	0.47622458E-03	0.53707324E-02	0.10339700E-01	0.11660832E 00
6.0	0.21981366E-04	0.17466187E-03	0.22055402E-01	0.17525011E 00
8.0	0.21785422E-06	0.11098855E-05	0.45597076E-01	0.23229998E 00
10.0	0.40175641E-09	0.14919261E-08	0.77139020E-01	0.28645641E 00
12.0	0.15131912E-12	0.44934081E-12	0.11338711E 00	0.33670199E 00
14.0	0.12706869E-16	0.31999727E-16	0.15184373E 00	0.38238829E 00
16.0	0.25675153E-21	0.56978608E-21	0.19070983E 00	0.42322528E 00
18.0	0.13413006E-26	0.26926444E-26	0.22875339E 00	0.45921957E 00
20.0	0.19468304E-32	0.36016471E-32	0.26518029E 00	0.49058503E 00
30.0	0.87216597E-69	0.12476710E-68	0.41353804E 00	0.59158397E 00
40.0	0.0	0.0	0.50991648E 00	0.63415557E 00
50.0	0.0	0.0	0.57109171E 00	0.64963126E 00
60.0	0.0	0.0	0.60986388E 00	0.65341443E 00
70.0	0.0	0.0	0.63369912E 00	0.65283340E 00
80.0	0.0	0.0	0.64667153E 00	0.65141988E 00
90.0	0.0	0.0	0.45506182E 01	0.45506182E 01

FREQUENCY = 400.0 MHZ
SIGMA = 1.50 METERS
PLATFORM ALTITUDE = 643.7376 KM

PSI (DEGREES)	SPECULAR VERTICAL	SPECULAR HORIZONTAL	DIFFUSE VERTICAL	DIFFUSE HORIZONTAL
0.0	0.0	0.0	0.0	0.0
2.0	0.37963605E-02	0.18637091E-01	0.82025640E-02	0.40268030E-01
4.0	0.32635150E-03	0.36805074E-02	0.70856847E-02	0.79910457E-01
6.0	0.14898879E-04	0.11838505E-03	0.14949057E-01	0.11878377E 00
8.0	0.14689437E-06	0.74837163E-06	0.30745115E-01	0.15663481E 00
10.0	0.27090596E-09	0.10060111E-08	0.52015163E-01	0.19315857E 00
12.0	0.10248768E-12	0.30433631E-12	0.76796532E-01	0.22804660E 00
14.0	0.86739797E-17	0.21843696E-16	0.10365176E 00	0.26102644E 00
16.0	0.17707471E-21	0.39296612E-21	0.13152742E 00	0.29188710E 00
18.0	0.93609363E-27	0.18791965E-26	0.15964699E 00	0.32048935E 00
20.0	0.13761040E-32	0.25458008E-32	0.18744093E 00	0.34676683E 00
30.0	0.65590857E-69	0.93830548E-69	0.31099945E 00	0.44489813E 00
40.0	0.0	0.0	0.40144569E 00	0.49925631E 00
50.0	0.0	0.0	0.46323884E 00	0.52694589E 00
60.0	0.0	0.0	0.50407654E 00	0.54097280E 00
70.0	0.0	0.0	0.52976590E 00	0.54576194E 00
80.0	0.0	0.0	0.54391783E 00	0.54791170E 00
90.0	0.0	0.0	0.28230972E 01	0.28230991E 01

FREQUENCY = 400.0 MHZ
SIGMA = 1.50 METERS
PLATFORM ALTITUDE = 1287.4750 KM

PSI	SPECULAR		DIFFUSE	
(DEGREES)	VERTICAL	HORIZONTAL	VERTICAL	HORIZONTAL
0.0	0.0	0.0	0.0	0.0
2.0	0.26401205E-02	0.12960877E-01	0.57043470E-02	0.28003782E-01
4.0	0.22263751E-03	0.25108464E-02	0.48338622E-02	0.54515008E-01
6.0	0.10002483E-04	0.79478748E-04	0.10036170E-01	0.79746425E-01
8.0	0.97369480E-07	0.49606075E-06	0.20379521E-01	0.10382593E 00
10.0	0.17786704E-09	0.66050987E-09	0.34151252E-01	0.12682080E 00
12.0	0.66853966E-13	0.19852213E-12	0.50095297E-01	0.14875746E 00
14.0	0.56371482E-17	0.14196034E-16	0.67362428E-01	0.16963899E 00
16.0	0.11493424E-21	0.25506324E-21	0.85370779E-01	0.18945581E 00
18.0	0.60809639E-27	0.12207461E-26	0.10370839E 00	0.20819330E 00
20.0	0.89622316E-33	0.16580181E-32	0.12207574E 00	0.22584081E 00
30.0	0.43917142E-69	0.62825363E-69	0.20823342E 00	0.29788685E 00
40.0	0.0	0.0	0.27793986E 00	0.34565872E 00
50.0	0.0	0.0	0.32978010E 00	0.37513322E 00
60.0	0.0	0.0	0.36617887E 00	0.39232779E 00
70.0	0.0	0.0	0.38999832E 00	0.40177417E 00
80.0	0.0	0.0	0.40342891E 00	0.40639120E 00
90.0	0.0	0.0	0.14920120E 01	0.14920120E 01

FREQUENCY = 400.0 MHZ
SIGMA = 15.00 METERS
PLATFORM ALTITUDE = 6.0960 KM

PSI	SPECULAR		DIFFUSE	
(DEGREES)	VERTICAL	HORIZONTAL	VERTICAL	HORIZONTAL
0.0	0.0	0.0	0.0	0.0
2.0	0.31884171E-34	0.15652577E-33	0.91585040E-01	0.44960928E 00
4.0	0.0	0.0	0.64016819E-01	0.72196472E 00
6.0	0.0	0.0	0.10492235E 00	0.83370334E 00
8.0	0.0	0.0	0.17286551E 00	0.88068497E 00
10.0	0.0	0.0	0.24271882E 00	0.90133786E 00
12.0	0.0	0.0	0.30643845E 00	0.90996587E 00
14.0	0.0	0.0	0.36235094E 00	0.91250890E 00
16.0	0.0	0.0	0.41082722E 00	0.91171223E 00
18.0	0.0	0.0	0.45279408E 00	0.90897846E 00
20.0	0.0	0.0	0.48922718E 00	0.90507293E 00
30.0	0.0	0.0	0.61446863E 00	0.87902385E 00
40.0	0.0	0.0	0.68515450E 00	0.85208964E 00
50.0	0.0	0.0	0.72832775E 00	0.82849121E 00
60.0	0.0	0.0	0.75554931E 00	0.80950332E 00
70.0	0.0	0.0	0.77236199E 00	0.79568309E 00
80.0	0.0	0.0	0.78156608E 00	0.78730494E 00
90.0	0.0	0.0	0.95903940E 01	0.95903959E 01

FREQUENCY = 400.0 MHZ
SIGMA = 15.00 METERS
PLATFORM ALTITUDE = 15.2400 KM

PSI	SPECULAR		DIFFUSE	
(DEGREES)	VERTICAL	HORIZONTAL	VERTICAL	HORIZONTAL
0.0	0.0	0.0	0.0	0.0
2.0	0.20478443E-34	0.10053277E-33	0.58822893E-01	0.28877330E 00
4.0	0.0	0.0	0.47910295E-01	0.54031950E 00
6.0	0.0	0.0	0.87487996E-01	0.69517136E 00
8.0	0.0	0.0	0.15332139E 00	0.78111488E 00
10.0	0.0	0.0	0.22313422E 00	0.82861030E 00
12.0	0.0	0.0	0.28797722E 00	0.85514534E 00
14.0	0.0	0.0	0.34541011E 00	0.86984688E 00
16.0	0.0	0.0	0.39543450E 00	0.87755269E 00
18.0	0.0	0.0	0.43882602E 00	0.88093776E 00
20.0	0.0	0.0	0.47651660E 00	0.88155836E 00
30.0	0.0	0.0	0.60587180E 00	0.86672562E 00
40.0	0.0	0.0	0.67853391E 00	0.84385598E 00
50.0	0.0	0.0	0.72274023E 00	0.82213533E 00
60.0	0.0	0.0	0.75053787E 00	0.80413401E 00
70.0	0.0	0.0	0.76767486E 00	0.79085439E 00
80.0	0.0	0.0	0.77704644E 00	0.78275210E 00
90.0	0.0	0.0	0.93129473E 01	0.93129492E 01

FREQUENCY = 400.0 MHZ
SIGMA = 15.00 METERS
PLATFORM ALTITUDE = 30.4800 KM

PSI (DEGREES)	SPECULAR VERTICAL	SPECULAR HORIZONTAL	DIFFUSE VERTICAL	DIFFUSE HORIZONTAL
0.0	0.0	0.0	0.0	0.0
2.0	0.14244742E-34	0.69930320E-34	0.40917039E-01	0.20086992E 00
4.0	0.0	0.0	0.35566181E-01	0.40110582E 00
6.0	0.0	0.0	0.70162237E-01	0.55750299E 00
8.0	0.0	0.0	0.13046300E 00	0.66466022E 00
10.0	0.0	0.0	0.19779253E 00	0.73450381E 00
12.0	0.0	0.0	0.26248735E 00	0.77945364E 00
14.0	0.0	0.0	0.32098341E 00	0.80833304E 00
16.0	0.0	0.0	0.37256068E 00	0.82679069E 00
18.0	0.0	0.0	0.41761577E 00	0.83835852E 00
20.0	0.0	0.0	0.45690739E 00	0.84528124E 00
30.0	0.0	0.0	0.59207565E 00	0.84698969E 00
40.0	0.0	0.0	0.66776115E 00	0.83045840E 00
50.0	0.0	0.0	0.71359175E 00	0.81172866E 00
60.0	0.0	0.0	0.74230611E 00	0.79531437E 00
70.0	0.0	0.0	0.75996411E 00	0.78291088E 00
80.0	0.0	0.0	0.76960462E 00	0.77525562E 00
90.0	0.0	0.0	0.88820648E 01	0.88820667E 01

FREQUENCY = 400.0 MHZ
SIGMA = 15.00 METERS
PLATFORM ALTITUDE = 160.9344 KM

PSI (DEGREES)	SPECULAR		DIFFUSE	
	VERTICAL	HORIZONTAL	VERTICAL	HORIZONTAL
0.0	0.0	0.0	0.0	0.0
2.0	0.58892999E-35	0.28911731E-34	0.16916599E-01	0.83046913E-01
4.0	0.0	0.0	0.15058573E-01	0.16982651E 00
6.0	0.0	0.0	0.32183666E-01	0.25572842E 00
8.0	0.0	0.0	0.66028297E-01	0.33638942E 00
10.0	0.0	0.0	0.11007518E 00	0.40876490E 00
12.0	0.0	0.0	0.15875417E 00	0.47141892E 00
14.0	0.0	0.0	0.20817053E 00	0.52423620E 00
16.0	0.0	0.0	0.25591588E 00	0.56793129E 00
18.0	0.0	0.0	0.30067539E 00	0.60360211E 00
20.0	0.0	0.0	0.34186417E 00	0.63245058E 00
30.0	0.0	0.0	0.49586159E 00	0.70935136E 00
40.0	0.0	0.0	0.58719039E 00	0.73025697E 00
50.0	0.0	0.0	0.64288741E 00	0.73130065E 00
60.0	0.0	0.0	0.67760104E 00	0.72598875E 00
70.0	0.0	0.0	0.69879848E 00	0.71989834E 00
80.0	0.0	0.0	0.71030837E 00	0.71552402E 00
90.0	0.0	0.0	0.62971172E 01	0.62971182E 01

FREQUENCY = 400.0 MHZ
SIGMA = 15.00 METERS
PLATFORM ALTITUDE = 321.8688 KM

PSI (DEGREES)	SPECULAR VERTICAL	SPECULAR HORIZONTAL	DIFFUSE VERTICAL	DIFFUSE HORIZONTAL
0.0	0.0	0.0	0.0	0.0
2.0	0.40972629E-35	0.20114281E-34	0.11769101E-01	0.57776876E-01
4.0	0.0	0.0	0.10339700E-01	0.11660832E 00
6.0	0.0	0.0	0.22055402E-01	0.17525011E 00
8.0	0.0	0.0	0.45597076E-01	0.23229998E 00
10.0	0.0	0.0	0.77139020E-01	0.28645641E 00
12.0	0.0	0.0	0.11338711E 00	0.33670199E 00
14.0	0.0	0.0	0.15184373E 00	0.38238829E 00
16.0	0.0	0.0	0.19070983E 00	0.42322528E 00
18.0	0.0	0.0	0.22875339E 00	0.45921957E 00
20.0	0.0	0.0	0.26518029E 00	0.49058503E 00
30.0	0.0	0.0	0.41353804E 00	0.59158397E 00
40.0	0.0	0.0	0.50991648E 00	0.63415557E 00
50.0	0.0	0.0	0.57109171E 00	0.64963126E 00
60.0	0.0	0.0	0.60986388E 00	0.65341443E 00
70.0	0.0	0.0	0.63369912E 00	0.65283340E 00
80.0	0.0	0.0	0.64667153E 00	0.65141988E 00
90.0	0.0	0.0	0.45506182E 01	0.45506182E 01

FREQUENCY = 400.0 MHZ
SIGMA = 15.00 METERS
PLATFORM ALTITUDE = 643.7376 KM

PSI	SPECULAR		DIFFUSE	
(DEGREES)	VERTICAL	HORIZONTAL	VERTICAL	HORIZONTAL
0.0	0.0	0.0	0.0	0.0
2.0	0.28556183E-35	0.14018803E-34	0.82025640E-02	0.40268030E-01
4.0	0.0	0.0	0.70856847E-02	0.79910457E-01
6.0	0.0	0.0	0.14949057E-01	0.11878377E 00
8.0	0.0	0.0	0.30745115E-01	0.15663481E 00
10.0	0.0	0.0	0.52015163E-01	0.19315857E 00
12.0	0.0	0.0	0.76796532E-01	0.22804660E 00
14.0	0.0	0.0	0.10365176E 00	0.26102644E 00
16.0	0.0	0.0	0.13152742E 00	0.29188710E 00
18.0	0.0	0.0	0.15964699E 00	0.32048935E 00
20.0	0.0	0.0	0.18744093E 00	0.34676683E 00
30.0	0.0	0.0	0.31099945E 00	0.44489813E 00
40.0	0.0	0.0	0.40144569E 00	0.49925631E 00
50.0	0.0	0.0	0.46323884E 00	0.52694589E 00
60.0	0.0	0.0	0.50407654E 00	0.54007280E 00
70.0	0.0	0.0	0.52976590E 00	0.54576194E 00
80.0	0.0	0.0	0.54391783E 00	0.54791170E 00
90.0	0.0	0.0	0.28230972E 01	0.28230991E 01

FREQUENCY = 400.0 MHZ
SIGMA = 15.00 METERS
PLATFORM ALTITUDE = 1287.4750 KM

PSI (DEGREES)	SPECULAR VERTICAL	SPECULAR HORIZONTAL	DIFFUSE VERTICAL	DIFFUSE HORIZONTAL
0.0	0.0	0.0	0.0	0.0
2.0	0.19858960E-35	0.97491623E-35	0.57043470E-02	0.28003782E-01
4.0	0.0	0.0	0.48338622E-02	0.54515008E-01
6.0	0.0	0.0	0.10036170E-01	0.79746425E-01
8.0	0.0	0.0	0.20379521E-01	0.10382593E 00
10.0	0.0	0.0	0.34151252E-01	0.12682080E 00
12.0	0.0	0.0	0.50095297E-01	0.14875746E 00
14.0	0.0	0.0	0.67362428E-01	0.16963899E 00
16.0	0.0	0.0	0.85370779E-01	0.18945581E 00
18.0	0.0	0.0	0.10370839E 00	0.20819330E 00
20.0	0.0	0.0	0.12207574E 00	0.22584081E 00
30.0	0.0	0.0	0.20823342E 00	0.29788685E 00
40.0	0.0	0.0	0.27793986E 00	0.34565872E 00
50.0	0.0	0.0	0.32978010E 00	0.37513322E 00
60.0	0.0	0.0	0.36617887E 00	0.39232779E 00
70.0	0.0	0.0	0.38999832E 00	0.40177417E 00
80.0	0.0	0.0	0.40342891E 00	0.40639120E 00
90.0	0.0	0.0	0.14920120E 01	0.14920120E 01

FREQUENCY = 2000.0 MHZ
SIGMA = 0.15 METERS
PLATFORM ALTITUDE = 6.0960 KM

PSI	SPECULAR		DIFFUSE	
(DEGREES)	VERTICAL	HORIZONTAL	VERTICAL	HORIZONTAL
0.0	0.0	0.0	0.0	0.0
2.0	0.99338591E-01	0.36851203E 00	0.12043804E 00	0.44678372E 00
4.0	0.18331781E-01	0.33026934E 00	0.39571185E-01	0.71292299E 00
6.0	0.16818591E-02	0.14536005E 00	0.94657429E-02	0.81810707E 00
8.0	0.12360143E-02	0.40152103E-01	0.26437286E-01	0.85881901E 00
10.0	0.55071758E-03	0.74205324E-02	0.64827263E-01	0.87350166E 00
12.0	0.11886015E-03	0.94198622E-03	0.11058766E 00	0.87642545E 00
14.0	0.15036496E-04	0.83544568E-04	0.15721309E 00	0.87349468E 00
16.0	0.12227720E-05	0.52543419E-05	0.20186675E 00	0.86743605E 00
18.0	0.67360418E-07	0.23787680E-06	0.24342722E 00	0.85963929E 00
20.0	0.26063709E-08	0.78760216E-08	0.28157198E 00	0.85086405E 00
30.0	0.28899995E-17	0.54427955E-17	0.42646509E 00	0.80317044E 00
40.0	0.21798530E-28	0.31979706E-28	0.51722938E 00	0.75880522E 00
50.0	0.28808168E-40	0.36108144E-40	0.57574385E 00	0.72163695E 00
60.0	0.19103068E-51	0.21553944E-51	0.61381924E 00	0.69257104E 00
70.0	0.14530585E-60	0.15306332E-60	0.63778257E 00	0.67183191E 00
80.0	0.16160075E-66	0.16368037E-66	0.65104067E 00	0.65941894E 00
90.0	0.16891216E-67	0.16891220E-67	0.80108137E 01	0.80108156E 01

FREQUENCY = 2000.0 MHZ
SIGMA = 0.15 METERS
PLATFORM ALTITUDE = 15.2400 KM

PSI	SPECULAR		DIFFUSE	
(DEGREES)	VERTICAL	HORIZONTAL	VERTICAL	HORIZONTAL
0.0	0.0	0.0	0.0	0.0
2.0	0.63802719E-01	0.23668647E 00	0.77354431E-01	0.28695852E 00
4.0	0.13719536E-01	0.24717408E 00	0.29615138E-01	0.53355265E 00
6.0	0.14023939E-02	0.12120634E 00	0.78928731E-02	0.68216670E 00
8.0	0.10962710E-02	0.35612512E-01	0.23448296E-01	0.76172107E 00
10.0	0.50628115E-03	0.68217777E-02	0.59596464E-01	0.80302012E 00
12.0	0.11169947E-03	0.88523678E-03	0.10392535E 00	0.82362556E 00
14.0	0.14333504E-04	0.79638645E-04	0.14986300E 00	0.83265668E 00
16.0	0.11769580E-05	0.50574745E-05	0.19430333E 00	0.83493531E 00
18.0	0.65282450E-07	0.23053866E-06	0.23591781E 00	0.83312058E 00
20.0	0.25386548E-08	0.76713960E-08	0.27425647E 00	0.82875794E 00
30.0	0.28495661E-17	0.53666461E-17	0.42049849E 00	0.79193348E 00
40.0	0.21587893E-28	0.31670690E-28	0.51223141E 00	0.75147289E 00
50.0	0.28587167E-40	0.35831136E-40	0.57132691E 00	0.71610087E 00
60.0	0.18976353E-51	0.21410980E-51	0.60974789E 00	0.68797737E 00
70.0	0.14442402E-60	0.15213443E-60	0.63391209E 00	0.66775483E 00
80.0	0.16066621E-66	0.16273384E-66	0.64727581E 00	0.65560567E 00
90.0	0.16402559E-67	0.16402563E-67	0.77790642E 01	0.77790661E 01

FREQUENCY = 2000.0 MHZ
SIGMA = 0.15 METERS
PLATFORM ALTITUDE = 30.4800 KM

PSI	SPECULAR		DIFFUSE	
(DEGREES)	VERTICAL	HORIZONTAL	VERTICAL	HORIZONTAL
0.0	0.0	0.0	0.0	0.0
2.0	0.44381078E-01	0.16463846E 00	0.53807583E-01	0.19960755E 00
4.0	0.10184687E-01	0.18348950E 00	0.21984775E-01	0.39608240E 00
6.0	0.11246710E-02	0.97203195E-01	0.63298084E-02	0.54707360E 00
8.0	0.93283039E-03	0.30303121E-01	0.19952442E-01	0.64815778E 00
10.0	0.44878200E-03	0.60470179E-02	0.52828003E-01	0.71181995E 00
12.0	0.10181256E-03	0.80688135E-03	0.94726563E-01	0.75072372E 00
14.0	0.13319868E-04	0.74006763E-04	0.13926500E 00	0.77377290E 00
16.0	0.11088769E-05	0.47649255E-05	0.18306386E 00	0.78663856E 00
18.0	0.62127071E-07	0.21939582E-06	0.22451496E 00	0.79285258E 00
20.0	0.24341862E-08	0.73557089E-08	0.26297051E 00	0.79465359E 00
30.0	0.27846795E-17	0.52444442E-17	0.41092348E 00	0.77390063E 00
40.0	0.21245150E-28	0.31167866E-28	0.50409895E 00	0.73954207E 00
50.0	0.28225304E-40	0.35377586E-40	0.56409496E 00	0.70703632E 00
60.0	0.18768232E-51	0.21176158E-51	0.60306025E 00	0.68043172E 00
70.0	0.14297343E-60	0.15060634E-60	0.62754494E 00	0.66104776E 00
80.0	0.15912752E-66	0.16117535E-66	0.64107686E 00	0.64932686E 00
90.0	0.15643661E-67	0.15643666E-67	0.74191494E 01	0.74191523E 01

FREQUENCY = 2000.0 MHZ
SIGMA = 0.15 METERS
PLATFORM ALTITUDE = 160.9344 KM

PSI	SPECULAR		DIFFUSE	
(DEGREES)	VERTICAL	HORIZONTAL	VERTICAL	HORIZONTAL
0.0	0.0	0.0	0.0	0.0
2.0	0.18348757E-01	0.68067491E-01	0.22246022E-01	0.82525015E-01
4.0	0.43121539E-02	0.77688634E-01	0.93082637E-02	0.16769964E 00
6.0	0.51589031E-03	0.44587437E-01	0.29035048E-02	0.25094444E 00
8.0	0.47211233E-03	0.15336633E-01	0.10098077E-01	0.32803744E 00
10.0	0.24975534E-03	0.33652787E-02	0.29399760E-01	0.39614093E 00
12.0	0.61576953E-04	0.48800744E-03	0.57291292E-01	0.45404291E 00
14.0	0.86384662E-05	0.47996335E-04	0.90318918E-01	0.50182259E 00
16.0	0.76169931E-06	0.32730777E-05	0.12574846E 00	0.54035038E 00
18.0	0.44730339E-07	0.15796076E-06	0.16164649E 00	0.57083869E 00
20.0	0.18212900E-08	0.55036367E-08	0.19675797E 00	0.59457034E 00
30.0	0.23321605E-17	0.43922066E-17	0.34414715E 00	0.64813948E 00
40.0	0.18681749E-28	0.27407211E-28	0.44327533E 00	0.65031040E 00
50.0	0.25428674E-40	0.31872293E-40	0.50820315E 00	0.63698155E 00
60.0	0.17132238E-51	0.19330275E-51	0.55049294E 00	0.62112010E 00
70.0	0.13146621E-60	0.13848481E-60	0.57703704E 00	0.60784334E 00
80.0	0.14686713E-66	0.14875714E-66	0.59168339E 00	0.59929770E 00
90.0	0.11090885E-67	0.11090890E-67	0.52599545E 01	0.52599564E 01

FREQUENCY = 2000.0 MHZ
SIGMA = 0.15 METERS
PLATFORM ALTITUDE = 321.8688 KM

PSI	SPECULAR		DIFFUSE	
(DEGREES)	VERTICAL	HORIZONTAL	VERTICAL	HORIZONTAL
0.0	0.0	0.0	0.0	0.0
2.0	0.12765471E-01	0.47355503E-01	0.15476849E-01	0.57413775E-01
4.0	0.29608628E-02	0.53343546E-01	0.63913502E-02	0.11514795E 00
6.0	0.35353843E-03	0.30555662E-01	0.19897651E-02	0.17197162E 00
8.0	0.32602577E-03	0.10590997E-01	0.69734156E-02	0.22653240E 00
10.0	0.17502499E-03	0.23583372E-02	0.20602919E-01	0.27760965E 00
12.0	0.43980166E-04	0.34855003E-03	0.40919214E-01	0.32429147E 00
14.0	0.63010639E-05	0.35009478E-04	0.65880358E-01	0.36603934E 00
16.0	0.56762224E-06	0.24391138E-05	0.93708396E-01	0.40267181E 00
18.0	0.34030762E-07	0.12017631E-06	0.12298036E 00	0.43429321E 00
20.0	0.14127546E-08	0.42691113E-08	0.15262300E 00	0.46120167E 00
30.0	0.19449721E-17	0.36630064E-17	0.28701144E 00	0.54053456E 00
40.0	0.16223251E-28	0.23800438E-28	0.38494056E 00	0.56472993E 00
50.0	0.22588877E-40	0.28312885E-40	0.45144862E 00	0.56584543E 00
60.0	0.15419604E-51	0.17397902E-51	0.49546224E 00	0.55902910E 00
70.0	0.11921897E-60	0.12558371E-60	0.52328092E 00	0.55121732E 00
80.0	0.13370922E-66	0.13542991E-66	0.53867418E 00	0.54560637E 00
90.0	0.80148398E-68	0.80148420E-68	0.38011112E 01	0.38011122E 01

FREQUENCY = 2000.0 MHZ
SIGMA = 0.15 METERS
PLATFORM ALTITUDE = 643.7376 KM

PSI	SPECULAR		DIFFUSE	
(DEGREES)	VERTICAL	HORIZONTAL	VERTICAL	HORIZONTAL
0.0	0.0	0.0	0.0	0.0
2.0	0.88969879E-02	0.33004776E-01	0.10786705E-01	0.40014964E-01
4.0	0.20290478E-02	0.36555752E-01	0.43799244E-02	0.78909636E-01
6.0	0.23962690E-03	0.20710502E-01	0.13486543E-02	0.11656165E 00
8.0	0.21983229E-03	0.71412772E-02	0.47020242E-02	0.15274584E 00
10.0	0.11802001E-03	0.15902354E-02	0.13892625E-01	0.18719321E 00
12.0	0.29787552E-04	0.23607125E-03	0.27714387E-01	0.21964103E 00
14.0	0.43012433E-05	0.23898217E-04	0.44971369E-01	0.24986625E 00
16.0	0.39147392E-06	0.16821914E-05	0.64628184E-01	0.27771193E 00
18.0	0.23750072E-07	0.83871043E-07	0.85828006E-01	0.30309319E 00
20.0	0.99859654E-09	0.30175953E-08	0.10788059E 00	0.32599747E 00
30.0	0.14627076E-17	0.27547480E-17	0.21584564E 00	0.40650666E 00
40.0	0.12772190E-28	0.18737541E-28	0.30305499E 00	0.44459909E 00
50.0	0.18322886E-40	0.22965891E-40	0.36619079E 00	0.45898330E 00
60.0	0.12744914E-51	0.14380062E-51	0.40951914E 00	0.46205968E 00
70.0	0.99665813E-61	0.10498667E-60	0.43745738E 00	0.46081197E 00
80.0	0.11246333E-66	0.11391061E-66	0.45308083E 00	0.45891154E 00
90.0	0.49722200E-68	0.49722222E-68	0.23581209E 01	0.23581219E 01

FREQUENCY = 2000.0 MHZ
SIGMA = 0.15 METERS
PLATFORM ALTITUDE = 1287.4750 KM

PSI	SPECULAR		DIFFUSE	
(DEGREES)	VERTICAL	HORIZONTAL	VERTICAL	HORIZONTAL
0.0	0.0	0.0	0.0	0.0
2.0	0.61872751E-02	0.22952661E-01	0.75014494E-02	0.27827788E-01
4.0	0.13842192E-02	0.24938386E-01	0.29879906E-02	0.53832270E-01
6.0	0.16087545E-03	0.13904165E-01	0.90542994E-03	0.78254640E-01
8.0	0.14571662E-03	0.47336183E-02	0.31167534E-02	0.10124809E 00
10.0	0.77487610E-04	0.10440901E-02	0.91213882E-02	0.12290418E 00
12.0	0.19430765E-04	0.15399205E-03	0.18078417E-01	0.14327443E 00
14.0	0.27953429E-05	0.15531245E-04	0.29226527E-01	0.16238600E 00
16.0	0.25409486E-06	0.10918639E-05	0.41948359E-01	0.18025512E 00
18.0	0.15428306E-07	0.54483561E-07	0.55754814E-01	0.19689268E 00
20.0	0.65036154E-09	0.19652866E-08	0.70259983E-01	0.21231425E 00
30.0	0.97937357E-18	0.18444746E-17	0.14452207E 00	0.27218139E 00
40.0	0.88427975E-29	0.12972884E-28	0.20981932E 00	0.30781698E 00
50.0	0.13044074E-40	0.16349431E-40	0.26069146E 00	0.32675058E 00
60.0	0.92583492E-52	0.10446178E-51	0.29748899E 00	0.33565629E 00
70.0	0.73371065E-61	0.77288135E-61	0.32204348E 00	0.33923644E 00
80.0	0.83415079E-67	0.84488531E-67	0.33605427E 00	0.34037894E 00
90.0	0.26278250E-68	0.26278272E-68	0.12462702E 01	0.12462711E 01

FREQUENCY = 2000.0 MHZ
SIGMA = 1.50 METERS
PLATFORM ALTITUDE = 6.0960 KM

PSI (DEGREES)	SPECULAR		DIFFUSE	
	VERTICAL	HORIZONTAL	VERTICAL	HORIZONTAL
0.0	0.0	0.0	0.0	0.0
2.0	0.52023696E-09	0.19299009E-08	0.12043804E 00	0.44678372E 00
4.0	0.15133663E-34	0.27265132E-33	0.39571185E-01	0.71292299E 00
6.0	0.87010031E-77	0.75201267E-75	0.94657429E-02	0.81810707E 00
8.0	0.0	0.0	0.26437286E-01	0.85881901E 00
10.0	0.0	0.0	0.64827263E-01	0.87350166E 00
12.0	0.0	0.0	0.11058766E 00	0.87642545E 00
14.0	0.0	0.0	0.15721309E 00	0.87349468E 00
16.0	0.0	0.0	0.20186675E 00	0.86743605E 00
18.0	0.0	0.0	0.24342722E 00	0.85963929E 00
20.0	0.0	0.0	0.28157198E 00	0.85086405E 00
30.0	0.0	0.0	0.42646509E 00	0.80317044E 00
40.0	0.0	0.0	0.51722938E 00	0.75880522E 00
50.0	0.0	0.0	0.57574385E 00	0.72163695E 00
60.0	0.0	0.0	0.61331924E 00	0.69257104E 00
70.0	0.0	0.0	0.63778257E 00	0.67183191E 00
80.0	0.0	0.0	0.65104067E 00	0.65941894E 00
90.0	0.0	0.0	0.80108137E 01	0.80108156E 01

FREQUENCY = 2000.0 MHZ
SIGMA = 1.50 METERS
PLATFORM ALTITUDE = 15.2400 KM

PSI	SPECULAR		DIFFUSE	
(DEGREES)	VERTICAL	HORIZONTAL	VERTICAL	HORIZONTAL
0.0	0.0	0.0	0.0	0.0
2.0	0.33413561E-09	0.12395294E-08	0.77354431E-01	0.28695852E 00
4.0	0.11326060E-34	0.20405259E-33	0.29615138E-01	0.53355265E 00
6.0	0.72552127E-77	0.62705481E-75	0.78928731E-02	0.68216670E 00
8.0	0.0	0.0	0.23448296E-01	0.76172107E 00
10.0	0.0	0.0	0.59596464E-01	0.80302012E 00
12.0	0.0	0.0	0.10392535E 00	0.82362556E 00
14.0	0.0	0.0	0.14986300E 00	0.83265668E 00
16.0	0.0	0.0	0.19430333E 00	0.83493531E 00
18.0	0.0	0.0	0.23591781E 00	0.83312058E 00
20.0	0.0	0.0	0.27425647E 00	0.82875794E 00
30.0	0.0	0.0	0.42049849E 00	0.79193348E 00
40.0	0.0	0.0	0.51223141E 00	0.75147289E 00
50.0	0.0	0.0	0.57132691E 00	0.71610087E 00
60.0	0.0	0.0	0.60974789E 00	0.68797737E 00
70.0	0.0	0.0	0.63391209E 00	0.66775483E 00
80.0	0.0	0.0	0.64727581E 00	0.65560567E 00
90.0	0.0	0.0	0.77790642E 01	0.77790661E 01

FREQUENCY = 2000.0 MHZ
SIGMA = 1.50 METERS
PLATFORM ALTITUDE = 30.4800 KM

PSI (DEGREES)	SPECULAR VERTICAL	SPECULAR HORIZONTAL	DIFFUSE VERTICAL	DIFFUSE HORIZONTAL
0.0	0.0	0.0	0.0	0.0
2.0	0.23242411E-09	0.86221319E-09	0.53807583E-01	0.19960755E 00
4.0	0.84078912E-35	0.15147837E-33	0.21984775E-01	0.39608240E 00
6.0	0.58184269E-77	0.50287576E-75	0.63298084E-02	0.54707360E 00
8.0	0.0	0.0	0.19952442E-01	0.64815778E 00
10.0	0.0	0.0	0.52828003E-01	0.71181995E 00
12.0	0.0	0.0	0.94726563E-01	0.75072372E 00
14.0	0.0	0.0	0.13926500E 00	0.77377290E 00
16.0	0.0	0.0	0.18306386E 00	0.78663856E 00
18.0	0.0	0.0	0.22451496E 00	0.79285258E 00
20.0	0.0	0.0	0.26297051E 00	0.79465359E 00
30.0	0.0	0.0	0.41092348E 00	0.77390063E 00
40.0	0.0	0.0	0.50409895E 00	0.73954207E 00
50.0	0.0	0.0	0.56409496E 00	0.70703632E 00
60.0	0.0	0.0	0.60306025E 00	0.68043172E 00
70.0	0.0	0.0	0.62754494E 00	0.66104776E 00
80.0	0.0	0.0	0.64107686E 00	0.64932686E 00
90.0	0.0	0.0	0.74191494E 01	0.74191523E 01

FREQUENCY = 2000.0 MHZ
SIGMA = 1.50 METERS
PLATFORM ALTITUDE = 160.9344 KM

PSI (DEGREES)	SPECULAR VERTICAL	SPECULAR HORIZONTAL	DIFFUSE VERTICAL	DIFFUSE HORIZONTAL
0.0	0.0	0.0	0.0	0.0
2.0	0.96092620E-10	0.35647019E-09	0.22246022E-01	0.82525015E-01
4.0	0.35598667E-35	0.64135305E-34	0.93082637E-02	0.16769964E 00
6.0	0.26689319E-77	0.23067067E-75	0.29035048E-02	0.25094444E 00
8.0	0.0	0.0	0.10098077E-01	0.32803744E 00
10.0	0.0	0.0	0.23997760E-01	0.39614093E 00
12.0	0.0	0.0	0.57291292E-01	0.45404291E 00
14.0	0.0	0.0	0.90318918E-01	0.50182259E 00
16.0	0.0	0.0	0.12574846E 00	0.54035038E 00
18.0	0.0	0.0	0.16164649E 00	0.57083869E 00
20.0	0.0	0.0	0.19675797E 00	0.59457034E 00
30.0	0.0	0.0	0.34414715E 00	0.64813948E 00
40.0	0.0	0.0	0.44327533E 00	0.65031040E 00
50.0	0.0	0.0	0.50820315E 00	0.63698155E 00
60.0	0.0	0.0	0.55049294E 00	0.62112010E 00
70.0	0.0	0.0	0.57703704E 00	0.60784334E 00
80.0	0.0	0.0	0.59168339E 00	0.59929770E 00
90.0	0.0	0.0	0.52599545E 01	0.52599564E 01

FREQUENCY = 2000.0 MHZ
SIGMA = 1.50 METERS
PLATFORM ALTITUDE = 321.8688 KM

PSI	SPECULAR		DIFFUSE	
(DEGREES)	VERTICAL	HORIZONTAL	VERTICAL	HORIZONTAL
0.0	0.0	0.0	0.0	0.0
2.0	0.66852898E-10	0.24800118E-09	0.15476849E-01	0.57413775E-01
4.0	0.24443180E-35	0.44037359E-34	0.63913502E-02	0.11514795E 00
6.0	0.18290132E-77	0.15807802E-75	0.19897651E-02	0.17197162E 00
8.0	0.0	0.0	0.69734156E-02	0.22653240E 00
10.0	0.0	0.0	0.20602919E-01	0.27760965E 00
12.0	0.0	0.0	0.40919214E-01	0.32429147E 00
14.0	0.0	0.0	0.65880358E-01	0.36603934E 00
16.0	0.0	0.0	0.93708396E-01	0.40267181E 00
18.0	0.0	0.0	0.12298036E 00	0.43429321E 00
20.0	0.0	0.0	0.15262300E 00	0.46120167E 00
30.0	0.0	0.0	0.28701144E 00	0.54053456E 00
40.0	0.0	0.0	0.38494056E 00	0.56472993E 00
50.0	0.0	0.0	0.45144862E 00	0.56584543E 00
60.0	0.0	0.0	0.49546224E 00	0.55902910E 00
70.0	0.0	0.0	0.52328092E 00	0.55121732E 00
80.0	0.0	0.0	0.53867418E 00	0.54560637E 00
90.0	0.0	0.0	0.38011112E 01	0.38011122E 01

FREQUENCY = 2000.0 MHZ
SIGMA = 1.50 METERS
PLATFORM ALTITUDE = 643.7376 KM

PSI (DEGREES)	SPECULAR		DIFFUSE	
	VERTICAL	HORIZONTAL	VERTICAL	HORIZONTAL
0.0	0.0	0.0	0.0	0.0
2.0	0.46593618E-10	0.17284631E-09	0.10786705E-01	0.40014964E-01
4.0	0.16750651E-35	0.30178315E-34	0.43799244E-02	0.78909636E-01
6.0	0.12396971E-77	0.10714471E-75	0.13486543E-02	0.11656165E 00
8.0	0.0	0.0	0.47020242E-02	0.15274584E 00
10.0	0.0	0.0	0.13892625E-01	0.18719321E 00
12.0	0.0	0.0	0.27714387E-01	0.21964103E 00
14.0	0.0	0.0	0.44971369E-01	0.24986625E 00
16.0	0.0	0.0	0.64628184E-01	0.27771193E 00
18.0	0.0	0.0	0.85828006E-01	0.30309319E 00
20.0	0.0	0.0	0.10788059E 00	0.32599747E 00
30.0	0.0	0.0	0.21584564E 00	0.40650666E 00
40.0	0.0	0.0	0.30305499E 00	0.44459909E 00
50.0	0.0	0.0	0.36619079E 00	0.45898330E 00
60.0	0.0	0.0	0.40951914E 00	0.46205968E 00
70.0	0.0	0.0	0.43745738E 00	0.46081197E 00
80.0	0.0	0.0	0.45308083E 00	0.45891154E 00
90.0	0.0	0.0	0.23581209E 01	0.23581219E 01

FREQUENCY = 2000.0 MHZ
SIGMA = 1.50 METERS
PLATFORM ALTITUDE = 1287.4750 KM

PSI	SPECULAR		DIFFUSE	
(DEGREES)	VERTICAL	HORIZONTAL	VERTICAL	HORIZONTAL
0.0	0.0	0.0	0.0	0.0
2.0	0.32402817E-10	0.12020329E-09	0.75014494E-02	0.27827788E-01
4.0	0.11427313E-35	0.20587693E-34	0.29879906E-02	0.53832270E-01
6.0	0.83228079E-78	0.71932489E-76	0.90542994E-03	0.78254640E-01
8.0	0.0	0.0	0.31167534E-02	0.10124809E 00
10.0	0.0	0.0	0.91213882E-02	0.12290418E 00
12.0	0.0	0.0	0.18078417E-01	0.14327443E 00
14.0	0.0	0.0	0.29226527E-01	0.16238600E 00
16.0	0.0	0.0	0.41948359E-01	0.18025512E 00
18.0	0.0	0.0	0.55754814E-01	0.19689268E 00
20.0	0.0	0.0	0.70259988E-01	0.21231425E 00
30.0	0.0	0.0	0.14452207E 00	0.27218139E 00
40.0	0.0	0.0	0.20981932E 00	0.30781698E 00
50.0	0.0	0.0	0.26069146E 00	0.32675058E 00
60.0	0.0	0.0	0.29748899E 00	0.33565629E 00
70.0	0.0	0.0	0.32204348E 00	0.33923644E 00
80.0	0.0	0.0	0.33605427E 00	0.34037894E 00
90.0	0.0	0.0	0.12462702E 01	0.12462711E 01

FREQUENCY = 2000.0 MHZ
SIGMA = 15.00 METERS
PLATFORM ALTITUDE = 6.0960 KM

PSI	SPECULAR		DIFFUSE	
(DEGREES)	VERTICAL	HORIZONTAL	VERTICAL	HORIZONTAL
0.0	0.0	0.0	0.0	0.0
2.0	0.0	0.0	0.12043804E 00	0.44678372E 00
4.0	0.0	0.0	0.39571185E-01	0.71292299E 00
6.0	0.0	0.0	0.94657429E-02	0.81810707E 00
8.0	0.0	0.0	0.26437286E-01	0.85881901E 00
10.0	0.0	0.0	0.64827263E-01	0.87350166E 00
12.0	0.0	0.0	0.11058766E 00	0.87642545E 00
14.0	0.0	0.0	0.15721309E 00	0.87349468E 00
16.0	0.0	0.0	0.20186675E 00	0.86743605E 00
18.0	0.0	0.0	0.24342722E 00	0.85963929E 00
20.0	0.0	0.0	0.28157198E 00	0.85086405E 00
30.0	0.0	0.0	0.42646509E 00	0.80317044E 00
40.0	0.0	0.0	0.51722938E 00	0.75880522E 00
50.0	0.0	0.0	0.57574385E 00	0.72163695E 00
60.0	0.0	0.0	0.61381924E 00	0.69257104E 00
70.0	0.0	0.0	0.63778257E 00	0.67183191E 00
80.0	0.0	0.0	0.65104067E 00	0.65941894E 00
90.0	0.0	0.0	0.80108137E 01	0.80108156E 01

FREQUENCY = 2000.0 MHZ
SIGMA = 15.00 METERS
PLATFORM ALTITUDE = 15.2400 KM

PSI (DEGREES)	SPECULAR		DIFFUSE	
	VERTICAL	HORIZONTAL	VERTICAL	HORIZONTAL
0.0	0.0	0.0	0.0	0.0
2.0	0.0	0.0	0.77354431E-01	0.28695852E 00
4.0	0.0	0.0	0.29615138E-01	0.53355265E 00
6.0	0.0	0.0	0.78928731E-02	0.68216670E 00
8.0	0.0	0.0	0.23448296E-01	0.76172107E 00
10.0	0.0	0.0	0.59596464E-01	0.80302012E 00
12.0	0.0	0.0	0.10392535E 00	0.82362556E 00
14.0	0.0	0.0	0.14986300E 00	0.83265668E 00
16.0	0.0	0.0	0.19430333E 00	0.83493531E 00
18.0	0.0	0.0	0.23591781E 00	0.83312058E 00
20.0	0.0	0.0	0.27425647E 00	0.82875794E 00
30.0	0.0	0.0	0.42049849E 00	0.79193348E 00
40.0	0.0	0.0	0.51223141E 00	0.75147289E 00
50.0	0.0	0.0	0.57132691E 00	0.71610087E 00
60.0	0.0	0.0	0.60974789E 00	0.68797737E 00
70.0	0.0	0.0	0.63391209E 00	0.66775483E 00
80.0	0.0	0.0	0.64727581E 00	0.65560567E 00
90.0	0.0	0.0	0.77790642E 01	0.77790661E 01

FREQUENCY = 2000.0 MHZ
SIGMA = 15.00 METERS
PLATFORM ALTITUDE = 30.4800 KM

PSI (DEGREES)	SPECULAR VERTICAL	SPECULAR HORIZONTAL	DIFFUSE VERTICAL	DIFFUSE HORIZONTAL
0.0	0.0	0.0	0.0	0.0
2.0	0.0	0.0	0.53807583E-01	0.19960755E 00
4.0	0.0	0.0	0.21984775E-01	0.39608240E 00
6.0	0.0	0.0	0.63298084E-02	0.54707360E 00
8.0	0.0	0.0	0.19952442E-01	0.64815778E 00
10.0	0.0	0.0	0.52828003E-01	0.71181995E 00
12.0	0.0	0.0	0.94726563E-01	0.75072372E 00
14.0	0.0	0.0	0.13926500E 00	0.77377290E 00
16.0	0.0	0.0	0.18306386E 00	0.78663856E 00
18.0	0.0	0.0	0.22451496E 00	0.79285258E 00
20.0	0.0	0.0	0.26297051E 00	0.79465359E 00
30.0	0.0	0.0	0.41092348E 00	0.77390063E 00
40.0	0.0	0.0	0.50409895E 00	0.73954207E 00
50.0	0.0	0.0	0.56409496E 00	0.70703632E 00
60.0	0.0	0.0	0.60306025E 00	0.68043172E 00
70.0	0.0	0.0	0.62754494E 00	0.66104776E 00
80.0	0.0	0.0	0.64107686E 00	0.64932686E 00
90.0	0.0	0.0	0.74191494E 01	0.74191523E 01

FREQUENCY = 2000.0 MHZ
SIGMA = 15.00 METERS
PLATFORM ALTITUDE = 160.9344 KM

PSI (DEGREES)	SPECULAR VERTICAL	SPECULAR HORIZONTAL	DIFFUSE VERTICAL	DIFFUSE HORIZONTAL
0.0	0.0	0.0	0.0	0.0
2.0	0.0	0.0	0.22246022E-01	0.82525015E-01
4.0	0.0	0.0	0.93082637E-02	0.16769964E 00
6.0	0.0	0.0	0.29035048E-02	0.25094444E 00
8.0	0.0	0.0	0.10098077E-01	0.32803744E 00
10.0	0.0	0.0	0.29399760E-01	0.39614093E 00
12.0	0.0	0.0	0.57291292E-01	0.45404291E 00
14.0	0.0	0.0	0.90318918E-01	0.50182259E 00
16.0	0.0	0.0	0.12574846E 00	0.54035038E 00
18.0	0.0	0.0	0.16164649E 00	0.57083869E 00
20.0	0.0	0.0	0.19675797E 00	0.59457034E 00
30.0	0.0	0.0	0.34414715E 00	0.64813948E 00
40.0	0.0	0.0	0.44327533E 00	0.65031040E 00
50.0	0.0	0.0	0.50820315E 00	0.63698155E 00
60.0	0.0	0.0	0.55049294E 00	0.62112010E 00
70.0	0.0	0.0	0.57703704E 00	0.60784334E 00
80.0	0.0	0.0	0.59168339E 00	0.59929770E 00
90.0	0.0	0.0	0.52599545E 01	0.52599564E 01

FREQUENCY = 2000.0 MHZ
SIGMA = 15.00 METERS
PLATFORM ALTITUDE = 321.8688 KM

PSI (DEGREES)	SPECULAR VERTICAL	SPECULAR HORIZONTAL	DIFFUSE VERTICAL	DIFFUSE HORIZONTAL
0.0	0.0	0.0	0.0	0.0
2.0	0.0	0.0	0.15476849E-01	0.57413775E-01
4.0	0.0	0.0	0.63913502E-02	0.11514795E 00
6.0	0.0	0.0	0.19897651E-02	0.17197162E 00
8.0	0.0	0.0	0.69734156E-02	0.22653240E 00
10.0	0.0	0.0	0.20602919E-01	0.27760965E 00
12.0	0.0	0.0	0.40919214E-01	0.32429147E 00
14.0	0.0	0.0	0.65880358E-01	0.36603934E 00
16.0	0.0	0.0	0.93708396E-01	0.40267181E 00
18.0	0.0	0.0	0.12298036E 00	0.43429321E 00
20.0	0.0	0.0	0.15262300E 00	0.46120167E 00
30.0	0.0	0.0	0.28701144E 00	0.54053456E 00
40.0	0.0	0.0	0.38494056E 00	0.56472993E 00
50.0	0.0	0.0	0.45144862E 00	0.56584543E 00
60.0	0.0	0.0	0.49546224E 00	0.55902910E 00
70.0	0.0	0.0	0.52328092E 00	0.55121732E 00
80.0	0.0	0.0	0.53867418E 00	0.54560637E 00
90.0	0.0	0.0	0.38011112E 01	0.38011122E 01

FREQUENCY = 2000.0 MHZ
SIGMA = 15.00 METERS
PLATFORM ALTITUDE = 643.7376 KM

PSI (DEGREES)	SPECULAR VERTICAL	SPECULAR HORIZONTAL	DIFFUSE VERTICAL	DIFFUSE HORIZONTAL
0.0	0.0	0.0	0.0	0.0
2.0	0.0	0.0	0.10786705E-01	0.40014964E-01
4.0	0.0	0.0	0.43799244E-02	0.78909636E-01
6.0	0.0	0.0	0.13486543E-02	0.11656165E 00
8.0	0.0	0.0	0.47020242E-02	0.15274584E 00
10.0	0.0	0.0	0.13892625E-01	0.18719321E 00
12.0	0.0	0.0	0.27714387E-01	0.21964103E 00
14.0	0.0	0.0	0.44971369E-01	0.24986625E 00
16.0	0.0	0.0	0.64628184E-01	0.27771193E 00
18.0	0.0	0.0	0.85828006E-01	0.30309319E 00
20.0	0.0	0.0	0.10788059E 00	0.32599747E 00
30.0	0.0	0.0	0.21584564E 00	0.40650666E 00
40.0	0.0	0.0	0.30305499E 00	0.44459909E 00
50.0	0.0	0.0	0.36619079E 00	0.45898330E 00
60.0	0.0	0.0	0.40951914E 00	0.46205968E 00
70.0	0.0	0.0	0.43745738E 00	0.46081197E 00
80.0	0.0	0.0	0.45308083E 00	0.45891154E 00
90.0	0.0	0.0	0.23581209E 01	0.23581219E 01

FREQUENCY = 2000.0 MHZ
SIGMA = 15.00 METERS
PLATFORM ALTITUDE = 1287.4750 KM

PSI	SPECULAR		DIFFUSE	
(DEGREES)	VERTICAL	HORIZONTAL	VERTICAL	HORIZONTAL
0.0	0.0	0.0	0.0	0.0
2.0	0.0	0.0	0.75014494E-02	0.27827788E-01
4.0	0.0	0.0	0.29879906E-02	0.53832270E-01
6.0	0.0	0.0	0.90542994E-03	0.78254640E-01
8.0	0.0	0.0	0.31167534E-02	0.10124809E 00
10.0	0.0	0.0	0.91213882E-02	0.12290418E 00
12.0	0.0	0.0	0.18078417E-01	0.14327443E 00
14.0	0.0	0.0	0.29226527E-01	0.16238600E 00
16.0	0.0	0.0	0.41948359E-01	0.18025512E 00
18.0	0.0	0.0	0.55754814E-01	0.19689268E 00
20.0	0.0	0.0	0.70259988E-01	0.21231425E 00
30.0	0.0	0.0	0.14452207E 00	0.27218139E 00
40.0	0.0	0.0	0.20981932E 00	0.30781698E 00
50.0	0.0	0.0	0.26069146E 00	0.32675058E 00
60.0	0.0	0.0	0.29748899E 00	0.33565629E 00
70.0	0.0	0.0	0.32204348E 00	0.33923644E 00
80.0	0.0	0.0	0.33605427E 00	0.34037894E 00
90.0	0.0	0.0	0.12462702E 01	0.12462711E 01

FREQUENCY = 2000.0 MHZ
SIGMA = 0.15 METERS
PLATFORM ALTITUDE = 0.0960 KM

PSI (DEGREES)	SPECULAR VERTICAL	SPECULAR HORIZONTAL	DIFFUSE VERTICAL	DIFFUSE HORIZONTAL
0.1	0.19185506E-01	0.20444792E-01	0.19194752E-01	0.20454645E-01
0.2	0.36564734E-01	0.41523363E-01	0.36635257E-01	0.41603450E-01
0.3	0.52143648E-01	0.63107073E-01	0.52370198E-01	0.63381255E-01
0.4	0.65938532E-01	0.85055053E-01	0.66448689E-01	0.85713148E-01
0.5	0.77979863E-01	0.10721999E 00	0.78924596E-01	0.10851896E 00
0.6	0.88304281E-01	0.12944096E 00	0.89848876E-01	0.13170511E 00
0.7	0.96969566E-01	0.15156364E 00	0.99285305E-01	0.15518343E 00
0.8	0.10403496E 00	0.17342007E 00	0.10729200E 00	0.17884934E 00
0.9	0.10958445E 00	0.19486308E 00	0.11394435E 00	0.20261580E 00
1.0	0.11369836E 00	0.21573019E 00	0.11930871E 00	0.22637516E 00
1.1	0.11648023E 00	0.23589146E 00	0.12347025E 00	0.25004733E 00
1.2	0.11803240E 00	0.25521523E 00	0.12650901E 00	0.27354378E 00
1.3	0.11846089E 00	0.27357841E 00	0.12850606E 00	0.29677707E 00
1.4	0.11787701E 00	0.29087573E 00	0.12954599E 00	0.31967032E 00
1.5	0.11639476E 00	0.30702156E 00	0.12971568E 00	0.34215891E 00
1.6	0.11412650E 00	0.32194251E 00	0.12910038E 00	0.36418271E 00
1.7	0.11118692E 00	0.33559602E 00	0.12778932E 00	0.38570702E 00
1.8	0.10767370E 00	0.34791768E 00	0.12585425E 00	0.40666294E 00
1.9	0.10369146E 00	0.35888934E 00	0.12337756E 00	0.42702532E 00
2.0	0.99538591E-01	0.36851203E 00	0.12043804E 00	0.44678372E 00
2.1	0.94695628E-01	0.37675476E 00	0.11709690E 00	0.46588004E 00
2.2	0.89852452E-01	0.38366735E 00	0.11343122E 00	0.48434782E 00
2.3	0.84877133E-01	0.38924897E 00	0.10949582E 00	0.50215083E 00
2.4	0.79834282E-01	0.39352542E 00	0.10534590E 00	0.51927918E 00
2.5	0.74784577E-01	0.39654976E 00	0.10103655E 00	0.53575236E 00
2.6	0.69779515E-01	0.39837271E 00	0.96616089E-01	0.55158311E 00
2.7	0.64861298E-01	0.39904088E 00	0.92125297E-01	0.56677479E 00
2.8	0.60063373E-01	0.39858723E 00	0.87597370E-01	0.58130592E 00
2.9	0.55421617E-01	0.39710855E 00	0.83073974E-01	0.59524399E 00
3.0	0.50956707E-01	0.39464140E 00	0.78579307E-01	0.60856855E 00
3.1	0.46690434E-01	0.39126843E 00	0.74143291E-01	0.62132496E 00
3.2	0.42634368E-01	0.38703173E 00	0.69784105E-01	0.63349515E 00
3.3	0.38800653E-01	0.38201493E 00	0.65524638E-01	0.64512813E 00

3.4	0.35195354E-01	0.37628204E 00	0.61381210E-01	0.65624136E 00
3.5	0.31820340E-01	0.36988604E 00	0.57306051E-01	0.66683555E 00
3.6	0.28676238E-01	0.36289841E 00	0.53491786E-01	0.67693973E 00
3.7	0.25761001E-01	0.35538459E 00	0.49768794E-01	0.68658298E 00
3.8	0.23069531E-01	0.34740412E 00	0.46203919E-01	0.69578493E 00
3.9	0.20595759E-01	0.33901364E 00	0.42803362E-01	0.70455879E 00
4.0	0.18331781E-01	0.33026934E 00	0.39571185E-01	0.71292299E 00
4.1	0.16268946E-01	0.32122827E 00	0.36510866E-01	0.72090232E 00
4.2	0.14397003E-01	0.31192988E 00	0.33623088E-01	0.72848821E 00
4.3	0.12706343E-01	0.30243963E 00	0.30910302E-01	0.73573500E 00
4.4	0.11186104E-01	0.29280049E 00	0.28372161E-01	0.74265188E 00
4.5	0.98252073E-02	0.28305250E 00	0.26007514E-01	0.74924546E 00
4.6	0.86124018E-02	0.27322602E 00	0.23814287E-01	0.75550145E 00
4.7	0.75371577E-02	0.26337802E 00	0.21791667E-01	0.76148850E 00
4.8	0.65834216E-02	0.25353301E 00	0.19936461E-01	0.76718664E 00
4.9	0.57558386E-02	0.24372894E 00	0.18246144E-01	0.77262658E 00
5.0	0.50291450E-02	0.23399186E 00	0.16717236E-01	0.77780533E 00
5.1	0.43986402E-02	0.22435313E 00	0.15346445E-01	0.78274679E 00
5.2	0.38549415E-02	0.21483636E 00	0.14129907E-01	0.78746164E 00
5.3	0.33893285E-02	0.20546699E 00	0.13064004E-01	0.79196268E 00
5.4	0.29933952E-02	0.19625926E 00	0.12144189E-01	0.79624695E 00
5.5	0.26591065E-02	0.18723255E 00	0.11366576E-01	0.80032343E 00
5.6	0.23797345E-02	0.17841071E 00	0.10727271E-01	0.80423272E 00
5.7	0.21482136E-02	0.16980016E 00	0.10221694E-01	0.80794829E 00
5.8	0.19584033E-02	0.16141343E 00	0.98456554E-02	0.81148809E 00
5.9	0.18046915E-02	0.15326542E 00	0.95951483E-02	0.81487870E 00
6.0	0.16818591E-02	0.14536005E 00	0.94657429E-02	0.81810707E 00
6.1	0.15852581E-02	0.13770562E 00	0.94533265E-02	0.82118678E 00
6.2	0.15135999E-02	0.13030666E 00	0.95537528E-02	0.82412118E 00
6.3	0.14641810E-02	0.12316859E 00	0.97630732E-02	0.82692868E 00
6.4	0.14325879E-02	0.11629152E 00	0.10077070E-01	0.82959646E 00
6.5	0.13828600E-02	0.10967797E 00	0.10491949E-01	0.83214176E 00
6.6	0.13623927E-02	0.10332775E 00	0.11003911E-01	0.83456832E 00
6.7	0.13489400E-02	0.97242236E-01	0.11609461E-01	0.83690172E 00
6.8	0.13403763E-02	0.91415048E-01	0.12304358E-01	0.83910739E 00
6.9	0.13353792E-02	0.85840722E-01	0.13065593E-01	0.84122610E 00
7.0	0.13322362E-02	0.80531836E-01	0.13949353E-01	0.84323859E 00
7.1	0.13297719E-02	0.75465977E-01	0.14892250E-01	0.84515113E 00
7.2	0.13271391E-02	0.70645630E-01	0.15911300E-01	0.84698272E 00
7.3	0.13235123E-02	0.66064715E-01	0.17003044E-01	0.84872806E 00
7.4	0.13162783E-02	0.61716110E-01	0.18164441E-01	0.85038084E 00
7.5	0.13109986E-02	0.57595078E-01	0.19392733E-01	0.85196579E 00
7.6	0.13013328E-02	0.53694285E-01	0.20684663E-01	0.85346967E 00
7.7	0.12890480E-02	0.50007097E-01	0.22037894E-01	0.85490894E 00

7.8	0.12741317E-02	0.46525985E-01	0.23449592E-01	0.85628146E 00
7.9	0.12564207E-02	0.43243211E-01	0.24916656E-01	0.85757589E 00
8.0	0.12360143E-02	0.40152103E-01	0.26437286E-01	0.85881901E 00
8.1	0.12129885E-02	0.37244551E-01	0.28008468E-01	0.85999388E 00
8.2	0.11874870E-02	0.34513224E-01	0.29627986E-01	0.86111015E 00
8.3	0.11596838E-02	0.31950384E-01	0.31293657E-01	0.86216986E 00
8.4	0.11297981E-02	0.29549051E-01	0.33003502E-01	0.86318272E 00
8.5	0.10980291E-02	0.27301015E-01	0.34755092E-01	0.86413842E 00
8.6	0.10646251E-02	0.25199428E-01	0.36546413E-01	0.86504507E 00
8.7	0.10298258E-02	0.23236904E-01	0.38375683E-01	0.86590576E 00
8.8	0.99387502E-03	0.21406434E-01	0.40240761E-01	0.86671883E 00
8.9	0.95701596E-03	0.19701026E-01	0.42140059E-01	0.86749077E 00
9.0	0.91948081E-03	0.18113855E-01	0.44071723E-01	0.86821675E 00
9.1	0.88130636E-03	0.16638681E-01	0.46034057E-01	0.86890584E 00
9.2	0.84329303E-03	0.15268717E-01	0.48025206E-01	0.86954731E 00
9.3	0.80506573E-03	0.13998363E-01	0.50044391E-01	0.87016439E 00
9.4	0.76699886E-03	0.12821373E-01	0.52089293E-01	0.87073958E 00
9.5	0.72926958E-03	0.11732113E-01	0.54158613E-01	0.87127584E 00
9.6	0.69204229E-03	0.10725278E-01	0.56251328E-01	0.87178361E 00
9.7	0.65545272E-03	0.97955354E-02	0.58365669E-01	0.87225640E 00
9.8	0.61962940E-03	0.89379326E-02	0.60500689E-01	0.87270087E 00
9.9	0.58468617E-03	0.81477985E-02	0.62654674E-01	0.87311387E 00
10.0	0.55071758E-03	0.74205324E-02	0.64827263E-01	0.87350166E 00
10.1	0.51779207E-03	0.67516975E-02	0.67016006E-01	0.87384856E 00
10.2	0.48598996E-03	0.61374791E-02	0.69220662E-01	0.87417525E 00
10.3	0.45536068E-03	0.55740215E-02	0.71440339E-01	0.87447941E 00
10.4	0.42595714E-03	0.50575286E-02	0.73674500E-01	0.87476200E 00
10.5	0.39778627E-03	0.45846365E-02	0.75920880E-01	0.87501645E 00
10.6	0.37087500E-03	0.41521192E-02	0.78178683E-01	0.87524891E 00
10.7	0.34523499E-03	0.37569352E-02	0.80447972E-01	0.87545520E 00
10.8	0.32086112E-03	0.33962207E-02	0.82727015E-01	0.87564099E 00
10.9	0.29774752E-03	0.30673160E-02	0.85015535E-01	0.87580770E 00
11.0	0.27587824E-03	0.27677247E-02	0.87312102E-01	0.87595069E 00
11.1	0.25523151E-03	0.24951075E-02	0.89616179E-01	0.87607449E 00
11.2	0.23578233E-03	0.22472916E-02	0.91927469E-01	0.87618029E 00
11.3	0.21749854E-03	0.20222489E-02	0.94245434E-01	0.87627131E 00
11.4	0.20034371E-03	0.18180900E-02	0.96567988E-01	0.87634039E 00
11.5	0.18428040E-03	0.16330483E-02	0.98895967E-01	0.87639207E 00
11.6	0.16926802E-03	0.14655169E-02	0.10122800E 00	0.87642866E 00
11.7	0.15526451E-03	0.13139893E-02	0.10356414E 00	0.87645382E 00
11.8	0.14222509E-03	0.11770609E-02	0.10590255E 00	0.87645400E 00
11.9	0.13010440E-03	0.10534485E-02	0.10824323E 00	0.87643987E 00
12.0	0.11886015E-03	0.94198622E-03	0.11058766E 00	0.87642545E 00

FREQUENCY = 2000.0 MHZ
SIGMA = 0.15 METERS
PLATFORM ALTITUDE = 15.2400 KM

PSI (DEGREES)	SPECULAR VERTICAL	SPECULAR HORIZONTAL	DIFFUSE VERTICAL	DIFFUSE HORIZONTAL
0.1	0.12090951E-01	0.12884565E-01	0.12096778E-01	0.12890775E-01
0.2	0.22899207E-01	0.26004620E-01	0.22943374E-01	0.26054777E-01
0.3	0.32477267E-01	0.39305784E-01	0.32618370E-01	0.39476555E-01
0.4	0.40880173E-01	0.52731883E-01	0.41196458E-01	0.53139862E-01
0.5	0.48103727E-01	0.66223562E-01	0.48747230E-01	0.67025900E-01
0.6	0.54385401E-01	0.79720795E-01	0.55336695E-01	0.81115305E-01
0.7	0.59604924E-01	0.93162715E-01	0.61028458E-01	0.95387757E-01
0.8	0.63881099E-01	0.10648590E 00	0.65881014E-01	0.10981965E 00
0.9	0.67275882E-01	0.11962998E 00	0.69952488E-01	0.12438953E 00
1.0	0.69850802E-01	0.13253427E 00	0.73297560E-01	0.13907403E 00
1.1	0.71668029E-01	0.14513952E 00	0.75968862E-01	0.15384936E 00
1.2	0.72788715E-01	0.15738726E 00	0.78016162E-01	0.16869020E 00
1.3	0.73274791E-01	0.16922367E 00	0.79488277E-01	0.18357337E 00
1.4	0.73186219E-01	0.18059593E 00	0.80431163E-01	0.19847363E 00
1.5	0.72582781E-01	0.19145608E 00	0.80889583E-01	0.21336746E 00
1.6	0.71522295E-01	0.20175910E 00	0.80906332E-01	0.22823071E 00
1.7	0.70062037E-01	0.21147054E 00	0.80524385E-01	0.24304718E 00
1.8	0.68254292E-01	0.22054499E 00	0.79778969E-01	0.25778365E 00
1.9	0.66151142E-01	0.22895765E 00	0.78710139E-01	0.27242583E 00
2.0	0.63802719E-01	0.23668647E 00	0.77354431E-01	0.28695852E 00
2.1	0.61252844E-01	0.24369961E 00	0.75742841E-01	0.30134934E 00
2.2	0.58546465E-01	0.24999154E 00	0.73909998E-01	0.31559336E 00
2.3	0.55723082E-01	0.25554758E 00	0.71885586E-01	0.32966930E 00
2.4	0.52818600E-01	0.26035744E 00	0.69697142E-01	0.34355646E 00
2.5	0.49868055E-01	0.26442844E 00	0.67373455E-01	0.35725194E 00
2.6	0.46901632E-01	0.26776254E 00	0.64939559E-01	0.37074149E 00
2.7	0.43946356E-01	0.27036750E 00	0.62418886E-01	0.38401455E 00
2.8	0.41024055E-01	0.27224410E 00	0.59831001E-01	0.39704508E 00
2.9	0.38159829E-01	0.27342373E 00	0.57199497E-01	0.40984726E 00
3.0	0.35368245E-01	0.27391434E 00	0.54540653E-01	0.42239773E 00
3.1	0.32666001E-01	0.27374268E 00	0.51872831E-01	0.43469685E 00
3.2	0.30065592E-01	0.27293319E 00	0.49211483E-01	0.44673818E 00
3.3	0.27577564E-01	0.27151722E 00	0.46571638E-01	0.45852494E 00

3.4	0.25209378E-01	0.26951951E 00	0.43965522E-01	0.47004598E 00
3.5	0.22966862E-01	0.26697183E 00	0.41404895E-01	0.48129964E 00
3.6	0.20853568E-01	0.26390231E 00	0.38899612E-01	0.49227536E 00
3.7	0.18872704E-01	0.26035738E 00	0.36460996E-01	0.50299579E 00
3.8	0.17023832E-01	0.25636190E 00	0.34095522E-01	0.51344448E 00
3.9	0.15306979E-01	0.25195831E 00	0.31811893E-01	0.52363515E 00
4.0	0.13719536E-01	0.24717408E 00	0.29615138E-01	0.53355265E 00
4.1	0.12258962E-01	0.24205166E 00	0.27511634E-01	0.54321373E 00
4.2	0.10921072E-01	0.23661923E 00	0.25505319E-01	0.55260605E 00
4.3	0.97015391E-02	0.23091853E 00	0.23600612E-01	0.56174797E 00
4.4	0.85952356E-02	0.22498351E 00	0.21800745E-01	0.57064259E 00
4.5	0.75964779E-02	0.21884549E 00	0.20108022E-01	0.57928824E 00
4.6	0.66992417E-02	0.21253163E 00	0.18524181E-01	0.58767438E 00
4.7	0.58975182E-02	0.20608300E 00	0.17051127E-01	0.59583503E 00
4.8	0.51848814E-02	0.19952250E 00	0.15689366E-01	0.60375178E 00
4.9	0.45550400E-02	0.19288194E 00	0.14439609E-01	0.61144042E 00
5.0	0.40016059E-02	0.18618619E 00	0.13301823E-01	0.61889595E 00
5.1	0.35185625E-02	0.17946452E 00	0.12275930E-01	0.62613481E 00
5.2	0.30995756E-02	0.17273980E 00	0.11361189E-01	0.63316083E 00
5.3	0.27388525E-02	0.16603398E 00	0.10556776E-01	0.63997006E 00
5.4	0.24306630E-02	0.15936905E 00	0.98614842E-02	0.64657897E 00
5.5	0.21695340E-02	0.15276104E 00	0.92738643E-02	0.65297538E 00
5.6	0.19505585E-02	0.14623505E 00	0.87926500E-02	0.65919274E 00
5.7	0.17686861E-02	0.13980132E 00	0.84158145E-02	0.66520697E 00
5.8	0.16194400E-02	0.13347572E 00	0.81415549E-02	0.67103451E 00
5.9	0.14988445E-02	0.12727410E 00	0.79679638E-02	0.67668855E 00
6.0	0.14023939E-02	0.12120634E 00	0.78928731E-02	0.68216670E 00
6.1	0.13271079E-02	0.11528254E 00	0.79140067E-02	0.68747008E 00
6.2	0.12695390E-02	0.10951245E 00	0.80291741E-02	0.69260901E 00
6.3	0.12267395E-02	0.10390437E 00	0.82360767E-02	0.69759285E 00
6.4	0.11960240E-02	0.98462880E-01	0.85321553E-02	0.70241141E 00
6.5	0.11750283E-02	0.93194306E-01	0.89150965E-02	0.70707786E 00
6.6	0.11616540E-02	0.88103175E-01	0.93825646E-02	0.71160090E 00
6.7	0.11540460E-02	0.83192766E-01	0.99321343E-02	0.71598697E 00
6.8	0.11505587E-02	0.78463376E-01	0.10561086E-01	0.72022295E 00
6.9	0.11496244E-02	0.73918104E-01	0.11267312E-01	0.72433537E 00
7.0	0.11506340E-02	0.69555879E-01	0.12048144E-01	0.72831047E 00
7.1	0.11519874E-02	0.65376461E-01	0.12901224E-01	0.73215801E 00
7.2	0.11530630E-02	0.61379272E-01	0.13824273E-01	0.73588669E 00
7.3	0.11531732E-02	0.57562061E-01	0.14814712E-01	0.73949462E 00
7.4	0.11517867E-02	0.53921700E-01	0.15870366E-01	0.74298233E 00
7.5	0.11485063E-02	0.50456423E-01	0.16989093E-01	0.74636841E 00
7.6	0.11430164E-02	0.47161985E-01	0.18168226E-01	0.74963892E 00
7.7	0.11351358E-02	0.44034962E-01	0.19406002E-01	0.75281078E 00

7.8	0.11247331E-02	0.41070584E-01	0.20700004E-01	0.75587821E 00
7.9	0.11117714E-02	0.38264707E-01	0.22048049E-01	0.75884485E 00
8.0	0.10962710E-02	0.35612512E-01	0.23448296E-01	0.76172107E 00
8.1	0.10782969E-02	0.33108864E-01	0.24898376E-01	0.76449901E 00
8.2	0.10579657E-02	0.30748803E-01	0.26396405E-01	0.76718736E 00
8.3	0.10354235E-02	0.28526895E-01	0.27940538E-01	0.76978821E 00
8.4	0.10108578E-02	0.26438259E-01	0.29529031E-01	0.77231061E 00
8.5	0.98443986E-03	0.24476767E-01	0.31159736E-01	0.77474469E 00
8.6	0.95639401E-03	0.22637628E-01	0.32831058E-01	0.77710366E 00
8.7	0.92692906E-03	0.20915154E-01	0.34541313E-01	0.77938753E 00
8.8	0.89625642E-03	0.19303869E-01	0.36288269E-01	0.78158879E 00
8.9	0.86460332E-03	0.17798629E-01	0.38070876E-01	0.78372300E 00
9.0	0.83218492E-03	0.16394120E-01	0.39887536E-01	0.78578800E 00
9.1	0.79921051E-03	0.15085325E-01	0.41736409E-01	0.78778642E 00
9.2	0.76586450E-03	0.13866790E-01	0.43615680E-01	0.78970820E 00
9.3	0.73236180E-03	0.12734197E-01	0.45524981E-01	0.79158163E 00
9.4	0.69886143E-03	0.11682373E-01	0.47461879E-01	0.79338652E 00
9.5	0.66553685E-03	0.10706812E-01	0.49425550E-01	0.79513264E 00
9.6	0.63253334E-03	0.98030083E-02	0.51414255E-01	0.79681873E 00
9.7	0.59999037E-03	0.89666620E-02	0.53426936E-01	0.79844844E 00
9.8	0.56802877E-03	0.81936121E-02	0.55462386E-01	0.80002517E 00
9.9	0.53676078E-03	0.74799359E-02	0.57519015E-01	0.80154610E 00
10.0	0.50628115E-03	0.68217777E-02	0.59596464E-01	0.80302012E 00
10.1	0.47666137E-03	0.62153786E-02	0.61692595E-01	0.80443436E 00
10.2	0.44798059E-03	0.56574643E-02	0.63806891E-01	0.80580556E 00
10.3	0.42029956E-03	0.51447600E-02	0.65938592E-01	0.80713445E 00
10.4	0.39364980E-03	0.46739392E-02	0.68086565E-01	0.80841500E 00
10.5	0.36806986E-03	0.42421445E-02	0.70249259E-01	0.80964929E 00
10.6	0.34358352E-03	0.38465785E-02	0.72425961E-01	0.81084222E 00
10.7	0.32020779E-03	0.34845863E-02	0.74616075E-01	0.81199145E 00
10.8	0.29794476E-03	0.31536559E-02	0.76818526E-01	0.81310093E 00
10.9	0.27679210E-03	0.28514378E-02	0.79032183E-01	0.81416821E 00
11.0	0.25674421E-03	0.25757649E-02	0.81256390E-01	0.81519777E 00
11.1	0.23778576E-03	0.23245579E-02	0.83490610E-01	0.81619167E 00
11.2	0.21989703E-03	0.20958851E-02	0.85734069E-01	0.81714952E 00
11.3	0.20305363E-03	0.18879431E-02	0.87986231E-01	0.81807458E 00
11.4	0.18722631E-03	0.16990507E-02	0.90245247E-01	0.81896210E 00
11.5	0.17238314E-03	0.15276172E-02	0.92511177E-01	0.81981140E 00
11.6	0.15849275E-03	0.13722251E-02	0.94784021E-01	0.82063705E 00
11.7	0.14551722E-03	0.12314990E-02	0.97062528E-01	0.82143134E 00
11.8	0.13341942E-03	0.11041849E-02	0.99345744E-01	0.82218969E 00
11.9	0.12215924E-03	0.98911673E-03	0.10163307E 00	0.82291758E 00
12.0	0.11169947E-03	0.88523678E-03	0.10392535E 00	0.82362556E 00

FREQUENCY = 2000.0 MHZ
SIGMA = 0.15 METERS
PLATFORM ALTITUDE = 30.4800 KM

PSI (DEGREES)	SPECULAR VERTICAL	SPECULAR HORIZONTAL	DIFFUSE VERTICAL	DIFFUSE HORIZONTAL
0.1	0.85502643E-02	0.91114156E-02	0.85543245E-02	0.91158077E-02
0.2	0.16137917E-01	0.18326420E-01	0.16169041E-01	0.18361766E-01
0.3	0.22815511E-01	0.27612593E-01	0.22914637E-01	0.27732562E-01
0.4	0.28635520E-01	0.36937349E-01	0.28857071E-01	0.37223127E-01
0.5	0.33649422E-01	0.46266951E-01	0.34057084E-01	0.46827473E-01
0.6	0.37907654E-01	0.55566940E-01	0.38570706E-01	0.56538902E-01
0.7	0.41460942E-01	0.64803600E-01	0.42451147E-01	0.66351295E-01
0.8	0.44357810E-01	0.73941708E-01	0.45746509E-01	0.76256633E-01
0.9	0.46646055E-01	0.82949460E-01	0.48503969E-01	0.86249650E-01
1.0	0.48377883E-01	0.91791630E-01	0.50765030E-01	0.96320987E-01
1.1	0.49594283E-01	0.10043645E 00	0.52570432E-01	0.10646367E 00
1.2	0.50342467E-01	0.10885274E 00	0.53957857E-01	0.11667013E 00
1.3	0.50665725E-01	0.11700934E 00	0.54962032E-01	0.12693143E 00
1.4	0.50606646E-01	0.12487799E 00	0.55616334E-01	0.13723999E 00
1.5	0.50205760E-01	0.13243067E 00	0.55951603E-01	0.14758688E 00
1.6	0.49502362E-01	0.13964248E 00	0.55997271E-01	0.15796417E 00
1.7	0.48533700E-01	0.14648950E 00	0.55780720E-01	0.16836321E 00
1.8	0.47335081E-01	0.15295011E 00	0.55327523E-01	0.17877549E 00
1.9	0.45940243E-01	0.15900493E 00	0.54662105E-01	0.18919241E 00
2.0	0.44381076E-01	0.16463846E 00	0.53807583E-01	0.19960755E 00
2.1	0.42686690E-01	0.16983253E 00	0.52784674E-01	0.21000820E 00
2.2	0.40885437E-01	0.17457956E 00	0.51614434E-01	0.22039205E 00
2.3	0.39002355E-01	0.17886579E 00	0.50315004E-01	0.23074591E 00
2.4	0.37061516E-01	0.18268639E 00	0.48904773E-01	0.24106508E 00
2.5	0.35084173E-01	0.18603587E 00	0.47399923E-01	0.25134093E 00
2.6	0.33090363E-01	0.18891364E 00	0.45816630E-01	0.26156807E 00
2.7	0.31097561E-01	0.19131899E 00	0.44169191E-01	0.27173853E 00
2.8	0.29121276E-01	0.19325197E 00	0.42470928E-01	0.28184175E 00
2.9	0.27176041E-01	0.19472247E 00	0.40735401E-01	0.29187834E 00
3.0	0.25273528E-01	0.19573432E 00	0.38973793E-01	0.30183798E 00
3.1	0.23424257E-01	0.19629651E 00	0.37197161E-01	0.31171417E 00
3.2	0.21637179E-01	0.19642061E 00	0.35415825E-01	0.32150209E 00
3.3	0.19919585E-01	0.19611984E 00	0.33639222E-01	0.33119762E 00

3.4	0.18277399E-01	0.19540811E 00	0.31876050E-01	0.34079462E 00
3.5	0.16715195E-01	0.19430107E 00	0.30134328E-01	0.35028803E 00
3.6	0.15236340E-01	0.19281626E 00	0.28421409E-01	0.35967368E 00
3.7	0.13843250E-01	0.19097388E 00	0.26744377E-01	0.36895078E 00
3.8	0.12536772E-01	0.18879128E 00	0.25108792E-01	0.37811333E 00
3.9	0.11317451E-01	0.18628931E 00	0.23520615E-01	0.38715774E 00
4.0	0.10184687E-01	0.18348950E 00	0.21984775E-01	0.39608240E 00
4.1	0.91372468E-02	0.18041384E 00	0.20505864E-01	0.40488583E 00
4.2	0.81730708E-02	0.17708027E 00	0.19087579E-01	0.41355741E 00
4.3	0.72898604E-02	0.17351520E 00	0.17733805E-01	0.42210478E 00
4.4	0.64847358E-02	0.16974044E 00	0.16447730E-01	0.43052554E 00
4.5	0.57543963E-02	0.16577733E 00	0.15232004E-01	0.43881571E 00
4.6	0.50952211E-02	0.16164452E 00	0.14088877E-01	0.44696581E 00
4.7	0.45034662E-02	0.15736932E 00	0.13020601E-01	0.45499218E 00
4.8	0.39750859E-02	0.15296769E 00	0.12028549E-01	0.46287763E 00
4.9	0.35060633E-02	0.14846307E 00	0.11114303E-01	0.47063154E 00
5.0	0.30922787E-02	0.14387494E 00	0.10278951E-01	0.47825044E 00
5.1	0.27295782E-02	0.13922238E 00	0.95232390E-02	0.48573375E 00
5.2	0.24138365E-02	0.13452345E 00	0.88476799E-02	0.49308246E 00
5.3	0.21411015E-02	0.12979734E 00	0.82527734E-02	0.50029767E 00
5.4	0.19073579E-02	0.12505800E 00	0.77383742E-02	0.50737494E 00
5.5	0.17088850E-02	0.12032300E 00	0.73046088E-02	0.51431942E 00
5.6	0.15420504E-02	0.11560881E 00	0.69511943E-02	0.52113688E 00
5.7	0.14033858E-02	0.11092705E 00	0.66776313E-02	0.52781653E 00
5.8	0.12896012E-02	0.10629010E 00	0.64833276E-02	0.53436190E 00
5.9	0.11976564E-02	0.10171229E 00	0.63676760E-02	0.54078197E 00
6.0	0.11246710E-02	0.97203195E-01	0.63298084E-02	0.54707360E 00
6.1	0.10679783E-02	0.92772543E-01	0.63687265E-02	0.55323511E 00
6.2	0.10251350E-02	0.88429749E-01	0.64834468E-02	0.55927187E 00
6.3	0.99389325E-03	0.84182441E-01	0.66727959E-02	0.56518364E 00
6.4	0.97220996E-03	0.80037355E-01	0.69355182E-02	0.57096779E 00
6.5	0.95825270E-03	0.76001346E-01	0.72703920E-02	0.57663250E 00
6.6	0.95057627E-03	0.72079301E-01	0.76760948E-02	0.58217734E 00
6.7	0.94711967E-03	0.68275869E-01	0.81512518E-02	0.58760661E 00
6.8	0.94717881E-03	0.64593732E-01	0.86942427E-02	0.59291190E 00
6.9	0.94945496E-03	0.61037093E-01	0.93038604E-02	0.59811211E 00
7.0	0.95296395E-03	0.57606697E-01	0.99783577E-02	0.60319197E 00
7.1	0.95688296E-03	0.54304127E-01	0.10716230E-01	0.60815740E 00
7.2	0.96053793E-03	0.51130887E-01	0.11516057E-01	0.61301702E 00
7.3	0.96335285E-03	0.48086952E-01	0.12376107E-01	0.61776876E 00
7.4	0.96487720E-03	0.45171391E-01	0.13294958E-01	0.62241262E 00
7.5	0.96475030E-03	0.42383622E-01	0.14270913E-01	0.62695283E 00
7.6	0.96271420E-03	0.39722558E-01	0.15302327E-01	0.63138932E 00
7.7	0.95859636E-03	0.37186522E-01	0.16387928E-01	0.63573158E 00

7.8	0.95226300E-03	0.34772724E-01	0.17525814E-01	0.63997006E 00
7.9	0.94367703E-03	0.32479271E-01	0.18714491E-01	0.64411128E 00
8.0	0.93283039E-03	0.30303121E-01	0.19952442E-01	0.64815778E 00
8.1	0.91978163E-03	0.28241694E-01	0.21238185E-01	0.65211380E 00
8.2	0.90460270E-03	0.26291445E-01	0.22569977E-01	0.65597558E 00
8.3	0.88740769E-03	0.24448920E-01	0.23946386E-01	0.65974545E 00
8.4	0.86835166E-03	0.22711109E-01	0.25366165E-01	0.66343367E 00
8.5	0.84757170E-03	0.21073733E-01	0.26827551E-01	0.66703099E 00
8.6	0.82525029E-03	0.19533485E-01	0.28329168E-01	0.67054474E 00
8.7	0.80156052E-03	0.18086486E-01	0.29869780E-01	0.67397934E 00
8.8	0.77669718E-03	0.16728766E-01	0.31447466E-01	0.67732620E 00
8.9	0.75083645E-03	0.15456647E-01	0.33061415E-01	0.68059891E 00
9.0	0.72416040E-03	0.14266144E-01	0.34710091E-01	0.68379182E 00
9.1	0.69687166E-03	0.13153650E-01	0.36392063E-01	0.68691051E 00
9.2	0.66912151E-03	0.12115154E-01	0.38106207E-01	0.68995327E 00
9.3	0.64108591E-03	0.11147104E-01	0.39851099E-01	0.69292504E 00
9.4	0.61292644E-03	0.10245856E-01	0.41625757E-01	0.69582820E 00
9.5	0.58478606E-03	0.94077326E-02	0.43428663E-01	0.69865781E 00
9.6	0.55680354E-03	0.86293481E-02	0.45258716E-01	0.70141989E 00
9.7	0.52910298E-03	0.79072751E-02	0.47114678E-01	0.70411384E 00
9.8	0.50179986E-03	0.72382838E-02	0.48995793E-01	0.70674670E 00
9.9	0.47499756E-03	0.66192448E-02	0.50900515E-01	0.70931512E 00
10.0	0.44878200E-03	0.60470179E-02	0.52828003E-01	0.71181995E 00
10.1	0.42322977E-03	0.55186637E-02	0.54777142E-01	0.71426094E 00
10.2	0.39841072E-03	0.50314553E-02	0.56746554E-01	0.71664172E 00
10.3	0.37438911E-03	0.45827813E-02	0.58735959E-01	0.71896887E 00
10.4	0.35119941E-03	0.41699074E-02	0.60744248E-01	0.72123665E 00
10.5	0.32888353E-03	0.37905076E-02	0.62770188E-01	0.72345018E 00
10.6	0.30746753E-03	0.34422402E-02	0.64812839E-01	0.72560942E 00
10.7	0.28697331E-03	0.31229197E-02	0.66871643E-01	0.72771454E 00
10.8	0.26740786E-03	0.28304344E-02	0.68945289E-01	0.72976536E 00
10.9	0.24877838E-03	0.25628495E-02	0.71033478E-01	0.73176795E 00
11.0	0.23108182E-03	0.23183080E-02	0.73134542E-01	0.73371583E 00
11.1	0.21431241E-03	0.20950867E-02	0.75248718E-01	0.73562050E 00
11.2	0.19845630E-03	0.18915285E-02	0.77374697E-01	0.73747444E 00
11.3	0.18349729E-03	0.17061131E-02	0.79512179E-01	0.73928487E 00
11.4	0.16941300E-03	0.15374029E-02	0.81659317E-01	0.74104595E 00
11.5	0.15618240E-03	0.13840499E-02	0.83816886E-01	0.74276459E 00
11.6	0.14377652E-03	0.12448120E-02	0.85983217E-01	0.74443966E 00
11.7	0.13216729E-03	0.11185198E-02	0.88157892E-01	0.74607223E 00
11.8	0.12132563E-03	0.10040959E-02	0.90340555E-01	0.74766213E 00
11.9	0.11121741E-03	0.90052164E-03	0.92529774E-01	0.74920881E 00
12.0	0.10181256E-03	0.80688135E-03	0.94726563E-01	0.75072372E 00

FREQUENCY = 2000.0 MHZ
SIGMA = 0.15 METERS
PLATFORM ALTITUDE = 160.9344 KM

PSI (DEGREES)	SPECULAR VERTICAL	SPECULAR HORIZONTAL	DIFFUSE VERTICAL	DIFFUSE HORIZONTAL
0.1	0.37534540E-02	0.39998144E-02	0.37552626E-02	0.40017441E-02
0.2	0.70477910E-02	0.80035590E-02	0.70613846E-02	0.80189966E-02
0.3	0.99146329E-02	0.11999238E-01	0.99577121E-02	0.12051374E-01
0.4	0.12384597E-01	0.15975058E-01	0.12480415E-01	0.16098656E-01
0.5	0.14436820E-01	0.19918948E-01	0.14662329E-01	0.20160265E-01
0.6	0.16249515E-01	0.23819365E-01	0.16533747E-01	0.24236009E-01
0.7	0.17699633E-01	0.27664613E-01	0.18122353E-01	0.28325323E-01
0.8	0.18802952E-01	0.31443402E-01	0.19453492E-01	0.32427792E-01
0.9	0.19764386E-01	0.35145018E-01	0.20550720E-01	0.36543280E-01
1.0	0.20427302E-01	0.38758557E-01	0.21435264E-01	0.40671051E-01
1.1	0.20874307E-01	0.42273864E-01	0.22126973E-01	0.44810716E-01
1.2	0.21126740E-01	0.45681227E-01	0.22643976E-01	0.48961867E-01
1.3	0.21204822E-01	0.48971262E-01	0.23002930E-01	0.53123880E-01
1.4	0.21127902E-01	0.52135635E-01	0.23219410E-01	0.57296682E-01
1.5	0.20913873E-01	0.55165790E-01	0.23307383E-01	0.61479289E-01
1.6	0.20579878E-01	0.58054306E-01	0.23280043E-01	0.65671265E-01
1.7	0.20142008E-01	0.60794678E-01	0.23149602E-01	0.69872499E-01
1.8	0.19615006E-01	0.63380361E-01	0.22926964E-01	0.74082017E-01
1.9	0.19012935E-01	0.65806091E-01	0.22622589E-01	0.78299582E-01
2.0	0.18348757E-01	0.68067491E-01	0.22246022E-01	0.82525015E-01
2.1	0.17634314E-01	0.70159554E-01	0.21805894E-01	0.86756527E-01
2.2	0.16880691E-01	0.72079957E-01	0.21310456E-01	0.90994895E-01
2.3	0.16097974E-01	0.73825657E-01	0.20767201E-01	0.95238864E-01
2.4	0.15295512E-01	0.75394750E-01	0.20183034E-01	0.99487722E-01
2.5	0.14481064E-01	0.76786578E-01	0.19564416E-01	0.10374135E 00
2.6	0.13662737E-01	0.78000784E-01	0.18917296E-01	0.10799915E 00
2.7	0.12847036E-01	0.79037666E-01	0.18247195E-01	0.11226064E 00
2.8	0.12039885E-01	0.79897940E-01	0.17559160E-01	0.11652446E 00
2.9	0.11246547E-01	0.80583990E-01	0.16857959E-01	0.12079102E 00
3.0	0.10471445E-01	0.81097543E-01	0.16147807E-01	0.12505889E 00
3.1	0.97165560E-02	0.81441939E-01	0.15432838E-01	0.12932789E 00
3.2	0.89911632E-02	0.81621051E-01	0.14716774E-01	0.13359773E 00
3.3	0.82919039E-02	0.81638575E-01	0.14002964E-01	0.13786727E 00

3.4	0.76229982E-02	0.81499279E-01	0.13294619E-01	0.14213592E 00
3.5	0.69661375E-02	0.81208348E-01	0.12594681E-01	0.14640331E 00
3.6	0.63625585E-02	0.80771387E-01	0.11905834E-01	0.15066850E 00
3.7	0.58131218E-02	0.80194652E-01	0.11230629E-01	0.15493155E 00
3.8	0.52781776E-02	0.79484046E-01	0.10571193E-01	0.15919161E 00
3.9	0.47779344E-02	0.78646481E-01	0.99297985E-02	0.16344798E 00
4.0	0.43121539E-02	0.77688634E-01	0.93082637E-02	0.16769964E 00
4.1	0.38804025E-02	0.76618016E-01	0.87084211E-02	0.17194664E 00
4.2	0.34819674E-02	0.75441301E-01	0.81318654E-02	0.17618746E 00
4.3	0.31159574E-02	0.74166775E-01	0.75800866E-02	0.18042308E 00
4.4	0.27812978E-02	0.72801471E-01	0.70544146E-02	0.18465191E 00
4.5	0.24767865E-02	0.71353197E-01	0.65561011E-02	0.18887341E 00
4.6	0.22011076E-02	0.69829464E-01	0.60863160E-02	0.19308656E 00
4.7	0.19527767E-02	0.68237841E-01	0.56459419E-02	0.19729191E 00
4.8	0.17303370E-02	0.66586077E-01	0.52359700E-02	0.20148838E 00
4.9	0.15322168E-02	0.64881146E-01	0.48571639E-02	0.20567489E 00
5.0	0.13568602E-02	0.63130796E-01	0.45102984E-02	0.20985126E 00
5.1	0.12026685E-02	0.61342195E-01	0.41959956E-02	0.21401709E 00
5.2	0.10680379E-02	0.59521917E-01	0.39147884E-02	0.21817172E 00
5.3	0.95143123E-03	0.57677381E-01	0.36672466E-02	0.22231472E 00
5.4	0.85126795E-03	0.55814270E-01	0.34536936E-02	0.22644502E 00
5.5	0.76607266E-03	0.53939361E-01	0.32745693E-02	0.23056316E 00
5.6	0.69438620E-03	0.52058712E-01	0.31301274E-02	0.23466820E 00
5.7	0.63482556E-03	0.50178193E-01	0.30206463E-02	0.23875934E 00
5.8	0.58604497E-03	0.48302360E-01	0.29462760E-02	0.24283475E 00
5.9	0.54679856E-03	0.46437468E-01	0.29072079E-02	0.24689782E 00
6.0	0.51589031E-03	0.44587437E-01	0.29035048E-02	0.25094444E 00
6.1	0.49221003E-03	0.42757049E-01	0.29352203E-02	0.25497514E 00
6.2	0.47472469E-03	0.40950470E-01	0.30023858E-02	0.25899029E 00
6.3	0.46247267E-03	0.39171267E-01	0.31049480E-02	0.26298785E 00
6.4	0.45457995E-03	0.37423369E-01	0.32428675E-02	0.26696950E 00
6.5	0.45023928E-03	0.35709560E-01	0.34160267E-02	0.27093321E 00
6.6	0.44872682E-03	0.34032729E-01	0.36243233E-02	0.27487898E 00
6.7	0.44938852E-03	0.32395460E-01	0.38675985E-02	0.27880692E 00
6.8	0.45163906E-03	0.30799944E-01	0.41456372E-02	0.28271556E 00
6.9	0.45496388E-03	0.29247999E-01	0.44582635E-02	0.28660578E 00
7.0	0.45891479E-03	0.27741406E-01	0.48052371E-02	0.29047656E 00
7.1	0.46309736E-03	0.26281264E-01	0.51862746E-02	0.29432654E 00
7.2	0.46718107E-03	0.24868798E-01	0.56011230E-02	0.29815632E 00
7.3	0.47068857E-03	0.23504999E-01	0.60494654E-02	0.30196661E 00
7.4	0.47396871E-03	0.22190109E-01	0.65310486E-02	0.30575556E 00
7.5	0.47629350E-03	0.20924639E-01	0.70454963E-02	0.30952430E 00
7.6	0.47766068E-03	0.19708760E-01	0.75924098E-02	0.31327039E 00
7.7	0.47798594E-03	0.18542361E-01	0.81715323E-02	0.31699562E 00

7.8	0.47719409E-03	0.17425139E-01	0.87824576E-02	0.32069874E 00
7.9	0.47524250E-03	0.16356789E-01	0.94247535E-02	0.32437897E 00
8.0	0.47211233E-03	0.15336633E-01	0.10098077E-01	0.32803744E 00
8.1	0.46781055E-03	0.14364019E-01	0.10801964E-01	0.33167183E 00
8.2	0.46236231E-03	0.13438143E-01	0.11536010E-01	0.33528376E 00
8.3	0.45580859E-03	0.12557968E-01	0.12299839E-01	0.33887237E 00
8.4	0.44820923E-03	0.11722591E-01	0.13093024E-01	0.34243870E 00
8.5	0.43962360E-03	0.10930654E-01	0.13915077E-01	0.34597981E 00
8.6	0.43013203E-03	0.10181125E-01	0.14765561E-01	0.34949738E 00
8.7	0.41981274E-03	0.94726197E-02	0.15644010E-01	0.35299009E 00
8.8	0.40875515E-03	0.88039078E-02	0.16549971E-01	0.35645884E 00
8.9	0.39704633E-03	0.81735551E-02	0.17483052E-01	0.35990429E 00
9.0	0.38477546E-03	0.75801164E-02	0.18442713E-01	0.36332327E 00
9.1	0.37203706E-03	0.70223026E-02	0.19428533E-01	0.36671901E 00
9.2	0.35891519E-03	0.64985417E-02	0.20440083E-01	0.37008941E 00
9.3	0.34549693E-03	0.60074516E-02	0.21476746E-01	0.37343454E 00
9.4	0.33186772E-03	0.55475980E-02	0.22538181E-01	0.37675488E 00
9.5	0.31810673E-03	0.51175393E-02	0.23623936E-01	0.38004988E 00
9.6	0.30428707E-03	0.47158450E-02	0.24733391E-01	0.38331836E 00
9.7	0.29048021E-03	0.43411367E-02	0.25866207E-01	0.38656229E 00
9.8	0.27674972E-03	0.39920174E-02	0.27021877E-01	0.38978106E 00
9.9	0.26315707E-03	0.36671807E-02	0.28199788E-01	0.39297318E 00
10.0	0.24975554E-03	0.33652787E-02	0.29399760E-01	0.39614093E 00
10.1	0.23659081E-03	0.30850018E-02	0.30621104E-01	0.39928079E 00
10.2	0.22370910E-03	0.28251803E-02	0.31863384E-01	0.40239674E 00
10.3	0.21114908E-03	0.25846115E-02	0.33126071E-01	0.40548617E 00
10.4	0.19893938E-03	0.23620734E-02	0.34408998E-01	0.40854949E 00
10.5	0.18710940E-03	0.21565054E-02	0.35711400E-01	0.41158718E 00
10.6	0.17568127E-03	0.19668327E-02	0.37032858E-01	0.41459990E 00
10.7	0.16467439E-03	0.17920285E-02	0.38373049E-01	0.41758525E 00
10.8	0.15409991E-03	0.16311011E-02	0.39731279E-01	0.42054361E 00
10.9	0.14396949E-03	0.14831347E-02	0.41107468E-01	0.42347801E 00
11.0	0.13428895E-03	0.13472415E-02	0.42500786E-01	0.42638528E 00
11.1	0.12506095E-03	0.12225769E-02	0.43911021E-01	0.42926753E 00
11.2	0.11628561E-03	0.11083423E-02	0.45337759E-01	0.43212366E 00
11.3	0.10795944E-03	0.10037806E-02	0.46780474E-01	0.43495345E 00
11.4	0.10007742E-03	0.90818759E-03	0.48238479E-01	0.43775696E 00
11.5	0.92632108E-04	0.82088285E-03	0.49711969E-01	0.44053519E 00
11.6	0.85613996E-04	0.74124290E-03	0.51200066E-01	0.44328833E 00
11.7	0.79012083E-04	0.66867191E-03	0.52702446E-01	0.44601583E 00
11.8	0.72814641E-04	0.60261693E-03	0.54218680E-01	0.44871604E 00
11.9	0.67007262E-04	0.54255407E-03	0.55748172E-01	0.45138991E 00
12.0	0.61576953E-04	0.48800744E-03	0.57291292E-01	0.45404291E 00

FREQUENCY = 2000.0 MHZ
SIGMA = 0.15 METERS
PLATFORM ALTITUDE = 321.8688 KM

PSI (DEGREES)	SPECULAR VERTICAL	SPECULAR HORIZONTAL	DIFFUSE VERTICAL	DIFFUSE HORIZONTAL
0.1	0.26711663E-02	0.28464943E-02	0.26724534E-02	0.28478659E-02
0.2	0.50085038E-02	0.56877173E-02	0.50181635E-02	0.56986883E-02
0.3	0.70360340E-02	0.85153915E-02	0.70666037E-02	0.85523911E-02
0.4	0.87768510E-02	0.11321381E-01	0.88447593E-02	0.11408973E-01
0.5	0.10252856E-01	0.14097374E-01	0.10377072E-01	0.14268164E-01
0.6	0.11485208E-01	0.16835608E-01	0.11686105E-01	0.17130092E-01
0.7	0.12493931E-01	0.19528076E-01	0.12792323E-01	0.19994464E-01
0.8	0.13298225E-01	0.22167344E-01	0.13714552E-01	0.22861332E-01
0.9	0.13916291E-01	0.24745949E-01	0.14469959E-01	0.25730480E-01
1.0	0.14365502E-01	0.27256958E-01	0.15074350E-01	0.28601918E-01
1.1	0.14662305E-01	0.29693544E-01	0.15542187E-01	0.31475451E-01
1.2	0.14822252E-01	0.32049377E-01	0.15886728E-01	0.34351032E-01
1.3	0.14860027E-01	0.34318335E-01	0.16120113E-01	0.37228432E-01
1.4	0.14789563E-01	0.36495026E-01	0.16253624E-01	0.40107768E-01
1.5	0.14623784E-01	0.38574047E-01	0.16297419E-01	0.42988691E-01
1.6	0.14374938E-01	0.40550642E-01	0.16260989E-01	0.45871049E-01
1.7	0.14054447E-01	0.42420607E-01	0.16153049E-01	0.48754822E-01
1.8	0.13672922E-01	0.44180233E-01	0.15981570E-01	0.51639985E-01
1.9	0.13240229E-01	0.45826118E-01	0.15753921E-01	0.54526314E-01
2.0	0.12765471E-01	0.47355503E-01	0.15476849E-01	0.57413775E-01
2.1	0.12257069E-01	0.48765782E-01	0.15156608E-01	0.60301837E-01
2.2	0.11722658E-01	0.50055318E-01	0.14798872E-01	0.63190639E-01
2.3	0.11169381E-01	0.51223062E-01	0.14409069E-01	0.66080332E-01
2.4	0.10603525E-01	0.52267659E-01	0.13991956E-01	0.68970144E-01
2.5	0.10030862E-01	0.53189196E-01	0.13552044E-01	0.71860433E-01
2.6	0.94565824E-02	0.53987771E-01	0.13093498E-01	0.74750960E-01
2.7	0.88852607E-02	0.54664038E-01	0.12620118E-01	0.77641666E-01
2.8	0.83209611E-02	0.55218790E-01	0.12135424E-01	0.80531955E-01
2.9	0.77672079E-02	0.55653762E-01	0.11642624E-01	0.83421946E-01
3.0	0.72270520E-02	0.55970892E-01	0.11144694E-01	0.86311579E-01
3.1	0.67031346E-02	0.56172594E-01	0.10644421E-01	0.89200735E-01
3.2	0.61976053E-02	0.56261394E-01	0.10144267E-01	0.92088878E-01
3.3	0.57122707E-02	0.56240600E-01	0.96466057E-02	0.94976366E-01

3.4	0.52485317E-02	0.56113310E-01	0.91535188E-02	0.97862422E-01
3.5	0.48075095E-02	0.55883564E-01	0.86670332E-02	0.10074747E 00
3.6	0.43899715E-02	0.55555187E-01	0.81889220E-02	0.10363096E 00
3.7	0.39964318E-02	0.55132579E-01	0.77208802E-02	0.10651302E 00
3.8	0.36270618E-02	0.54619938E-01	0.72643198E-02	0.10939342E 00
3.9	0.32819402E-02	0.54021906E-01	0.68207271E-02	0.11227161E 00
4.0	0.29608628E-02	0.53343546E-01	0.63913502E-02	0.11514795E 00
4.1	0.26634631E-02	0.52589692E-01	0.59773587E-02	0.11802208E 00
4.2	0.23891966E-02	0.51765062E-01	0.55797845E-02	0.12089330E 00
4.3	0.21374119E-02	0.50875228E-01	0.51996112E-02	0.12376249E 00
4.4	0.19073323E-02	0.49925134E-01	0.48377104E-02	0.12662888E 00
4.5	0.16980940E-02	0.48920043E-01	0.44948868E-02	0.12949228E 00
4.6	0.15087595E-02	0.47864977E-01	0.41718930E-02	0.13235217E 00
4.7	0.13382896E-02	0.46765205E-01	0.38693133E-02	0.13520932E 00
4.8	0.11856507E-02	0.45625705E-01	0.35877589E-02	0.13806260E 00
4.9	0.10497565E-02	0.44451553E-01	0.33277532E-02	0.14091247E 00
5.0	0.92951627E-03	0.43247744E-01	0.30897779E-02	0.14375854E 00
5.1	0.82382164E-03	0.42019084E-01	0.28742356E-02	0.14660060E 00
5.2	0.73156226E-03	0.40770024E-01	0.26814693E-02	0.14943850E 00
5.3	0.65167272E-03	0.39505493E-01	0.25118417E-02	0.15227205E 00
5.4	0.58306614E-03	0.38229350E-01	0.23655682E-02	0.15510094E 00
5.5	0.52472460E-03	0.36945973E-01	0.22429293E-02	0.15792513E 00
5.6	0.47564739E-03	0.35659686E-01	0.21441050E-02	0.16074532E 00
5.7	0.43488084E-03	0.34374051E-01	0.20692630E-02	0.16355962E 00
5.8	0.40150597E-03	0.33092480E-01	0.20185267E-02	0.16636878E 00
5.9	0.37466339E-03	0.31818707E-01	0.19920038E-02	0.16917306E 00
6.0	0.35353843E-03	0.30555662E-01	0.19897651E-02	0.17197162E 00
6.1	0.33736904E-03	0.29306404E-01	0.20118500E-02	0.17476428E 00
6.2	0.32544881E-03	0.28073717E-01	0.20582946E-02	0.17755157E 00
6.3	0.31711953E-03	0.26859913E-01	0.21290767E-02	0.18033195E 00
6.4	0.31178421E-03	0.25667690E-01	0.22241964E-02	0.18310726E 00
6.5	0.30888943E-03	0.24498757E-01	0.23435857E-02	0.18587536E 00
6.6	0.30794204E-03	0.23355205E-01	0.24872185E-02	0.18863767E 00
6.7	0.30849222E-03	0.22238553E-01	0.26549953E-02	0.19139296E 00
6.8	0.31014089E-03	0.21150343E-01	0.28468135E-02	0.19414097E 00
6.9	0.31253533E-03	0.20091780E-01	0.30625851E-02	0.19688255E 00
7.0	0.31536864E-03	0.19064032E-01	0.33021832E-02	0.19961691E 00
7.1	0.31837029E-03	0.18067844E-01	0.35654625E-02	0.20234364E 00
7.2	0.32131374E-03	0.17104015E-01	0.38522866E-02	0.20506299E 00
7.3	0.32400505E-03	0.16173121E-01	0.41624643E-02	0.20777464E 00
7.4	0.32628886E-03	0.15275445E-01	0.44959076E-02	0.21047902E 00
7.5	0.32803207E-03	0.14411181E-01	0.48523620E-02	0.21317506E 00
7.6	0.32913825E-03	0.13580576E-01	0.52316487E-02	0.21586305E 00
7.7	0.32953336E-03	0.12783483E-01	0.56336224E-02	0.21854329E 00

7.8	0.32916362E-03	0.12019694E-01	0.60580522E-02	0.22121489E 00
7.9	0.32799947E-03	0.11289015E-01	0.65047108E-02	0.22387767E 00
8.0	0.32602577E-03	0.10590997E-01	0.69734156E-02	0.22653240E 00
8.1	0.32324670E-03	0.99252164E-02	0.74639171E-02	0.22917789E 00
8.2	0.31967647E-03	0.92911012E-02	0.79759806E-02	0.23181444E 00
8.3	0.31534256E-03	0.86879805E-02	0.85094087E-02	0.23444217E 00
8.4	0.31028292E-03	0.81152283E-02	0.90639442E-02	0.23706090E 00
8.5	0.30453969E-03	0.75719692E-02	0.96393712E-02	0.23966992E 00
8.6	0.29816548E-03	0.70575066E-02	0.10235418E-01	0.24226993E 00
8.7	0.29121293E-03	0.65709017E-02	0.10851830E-01	0.24485976E 00
8.8	0.28374232E-03	0.61113350E-02	0.11488363E-01	0.24744010E 00
8.9	0.27581211E-03	0.56778379E-02	0.12144774E-01	0.25001097E 00
9.0	0.26748469E-03	0.52694716E-02	0.12820836E-01	0.25257158E 00
9.1	0.25882225E-03	0.48853420E-02	0.13516229E-01	0.25512254E 00
9.2	0.24988339E-03	0.45244060E-02	0.14230765E-01	0.25766313E 00
9.3	0.24072803E-03	0.41857436E-02	0.14964104E-01	0.26019377E 00
9.4	0.23141385E-03	0.38683801E-02	0.15716039E-01	0.26271379E 00
9.5	0.22199539E-03	0.35713483E-02	0.16486306E-01	0.26522326E 00
9.6	0.21252364E-03	0.32936931E-02	0.17274573E-01	0.26772147E 00
9.7	0.20304776E-03	0.30344857E-02	0.18080655E-01	0.27020979E 00
9.8	0.19361197E-03	0.27927849E-02	0.18904291E-01	0.27268779E 00
9.9	0.18425904E-03	0.25677094E-02	0.19745104E-01	0.27515441E 00
10.0	0.17502499E-03	0.23583372E-02	0.20602919E-01	0.27760965E 00
10.1	0.16594359E-03	0.21638048E-02	0.21477487E-01	0.28005356E 00
10.2	0.15704645E-03	0.19833113E-02	0.22368476E-01	0.28248745E 00
10.3	0.14836114E-03	0.18160427E-02	0.23275603E-01	0.28490943E 00
10.4	0.13990786E-03	0.16611724E-02	0.24198774E-01	0.28732008E 00
10.5	0.13170751E-03	0.15179783E-02	0.25137484E-01	0.28971893E 00
10.6	0.12377692E-03	0.13857393E-02	0.26091643E-01	0.29210788E 00
10.7	0.11612964E-03	0.12637519E-02	0.27060967E-01	0.29448426E 00
10.8	0.10877421E-03	0.11513424E-02	0.28045043E-01	0.29684842E 00
10.9	0.10171920E-03	0.10478836E-02	0.29043783E-01	0.29920119E 00
11.0	0.94970062E-04	0.95277838E-03	0.30056853E-01	0.30154258E 00
11.1	0.88528759E-04	0.86544408E-03	0.31083949E-01	0.30387211E 00
11.2	0.82396422E-04	0.78533706E-03	0.32124948E-01	0.30618948E 00
11.3	0.76571213E-04	0.71194023E-03	0.33179477E-01	0.30849457E 00
11.4	0.71050526E-04	0.64477278E-03	0.34247179E-01	0.31078798E 00
11.5	0.65829343E-04	0.58336346E-03	0.35327990E-01	0.31306803E 00
11.6	0.60902355E-04	0.52729039E-03	0.36421672E-01	0.31533754E 00
11.7	0.56262230E-04	0.47614193E-03	0.37527889E-01	0.31759506E 00
11.8	0.51901297E-04	0.42953715E-03	0.38646348E-01	0.31983876E 00
11.9	0.47810259E-04	0.38711703E-03	0.39776798E-01	0.32207060E 00
12.0	0.43980166E-04	0.34855023E-03	0.40919214E-01	0.32429147E 00

FREQUENCY = 2000.0 MHZ
SIGMA = 0.15 METERS
PLATFORM ALTITUDE = 643.7376 KM

PSI	SPECULAR		DIFFUSE	
(DEGREES)	VERTICAL	HORIZONTAL	VERTICAL	HORIZONTAL
0.1	0.19013910E-02	0.20261931E-02	0.19023072E-02	0.20271696E-02
0.2	0.35608048E-02	0.40436871E-02	0.35676723E-02	0.40514879E-02
0.3	0.49962327E-02	0.60467087E-02	0.50179400E-02	0.60729831E-02
0.4	0.62249005E-02	0.80295838E-02	0.62730648E-02	0.80917105E-02
0.5	0.72631240E-02	0.99865794E-02	0.73511191E-02	0.10107569E-01
0.6	0.81265830E-02	0.11912361E-01	0.82687326E-02	0.12120731E-01
0.7	0.88300556E-02	0.13801422E-01	0.90409443E-02	0.14131039E-01
0.8	0.93876719E-02	0.15648682E-01	0.96815713E-02	0.16138591E-01
0.9	0.98128431E-02	0.17449196E-01	0.10203253E-01	0.18143423E-01
1.0	0.10118183E-01	0.19198138E-01	0.10617454E-01	0.20145450E-01
1.1	0.10315757E-01	0.20891089E-01	0.10934807E-01	0.22144761E-01
1.2	0.10416806E-01	0.22523712E-01	0.11164900E-01	0.24141274E-01
1.3	0.10432042E-01	0.24092171E-01	0.11316650E-01	0.26135117E-01
1.4	0.10371413E-01	0.25592718E-01	0.11398111E-01	0.28126210E-01
1.5	0.10244288E-01	0.27021982E-01	0.11416707E-01	0.30114539E-01
1.6	0.10059420E-01	0.28376896E-01	0.11379261E-01	0.32100059E-01
1.7	0.98249987E-02	0.29654849E-01	0.11292063E-01	0.34082893E-01
1.8	0.95485263E-02	0.30853406E-01	0.11160780E-01	0.36062948E-01
1.9	0.92370473E-02	0.31970590E-01	0.10990724E-01	0.38040280E-01
2.0	0.88969879E-02	0.33004776E-01	0.10786705E-01	0.40014964E-01
2.1	0.85342936E-02	0.33954415E-01	0.10553174E-01	0.41986689E-01
2.2	0.81543401E-02	0.34818787E-01	0.10294173E-01	0.43955795E-01
2.3	0.77620745E-02	0.35597082E-01	0.10013469E-01	0.45922033E-01
2.4	0.73619373E-02	0.36289025E-01	0.97144954E-02	0.47885429E-01
2.5	0.69579184E-02	0.36894780E-01	0.94003901E-02	0.49846116E-01
2.6	0.65536015E-02	0.37414648E-01	0.90740547E-02	0.51803969E-01
2.7	0.61521530E-02	0.37849385E-01	0.87381676E-02	0.53759098E-01
2.8	0.57563595E-02	0.38199831E-01	0.83951652E-02	0.55711236E-01
2.9	0.53686164E-02	0.38467370E-01	0.80472641E-02	0.57660483E-01
3.0	0.49910136E-02	0.38653616E-01	0.76965429E-02	0.59606958E-01
3.1	0.46253093E-02	0.38760357E-01	0.73448829E-02	0.61550520E-01
3.2	0.42729676E-02	0.38789682E-01	0.69940127E-02	0.63491106E-01
3.3	0.39351694E-02	0.38744003E-01	0.66455230E-02	0.65428972E-01

3.4	0.36128310E-02	0.38625643E-01	0.63008294E-02	0.67363679E-01
3.5	0.33066741E-02	0.38437501E-01	0.59613064E-02	0.69295526E-01
3.6	0.30171748E-02	0.38182389E-01	0.56281462E-02	0.71224272E-01
3.7	0.27446398E-02	0.37863508E-01	0.53024888E-02	0.73150158E-01
3.8	0.24891340E-02	0.37483875E-01	0.49852654E-02	0.75073123E-01
3.9	0.22506660E-02	0.37046753E-01	0.46774708E-02	0.76992810E-01
4.0	0.20290478E-02	0.36555752E-01	0.43799244E-02	0.78909636E-01
4.1	0.18239799E-02	0.36014240E-01	0.40933862E-02	0.80823362E-01
4.2	0.16350567E-02	0.35425626E-01	0.38185488E-02	0.82733810E-01
4.3	0.14617795E-02	0.34793612E-01	0.35560231E-02	0.84641278E-01
4.4	0.13035827E-02	0.34121737E-01	0.33063751E-02	0.86545527E-01
4.5	0.11598456E-02	0.33413738E-01	0.30701335E-02	0.88446796E-01
4.6	0.10298891E-02	0.32672916E-01	0.28477621E-02	0.90344369E-01
4.7	0.91297436E-03	0.31902995E-01	0.26396259E-02	0.92239141E-01
4.8	0.80837193E-03	0.31107437E-01	0.24461199E-02	0.94130576E-01
4.9	0.71531069E-03	0.30289557E-01	0.22675523E-02	0.96018612E-01
5.0	0.63302577E-03	0.29452879E-01	0.21042223E-02	0.97903430E-01
5.1	0.56074024E-03	0.28600603E-01	0.19563700E-02	0.99784791E-01
5.2	0.49768086E-03	0.27735792E-01	0.18242002E-02	0.10166281E 00
5.3	0.44310489E-03	0.26861776E-01	0.17079273E-02	0.10353744E 00
5.4	0.39625866E-03	0.25981102E-01	0.16076681E-02	0.10540837E 00
5.5	0.35643694E-03	0.25096811E-01	0.15235860E-02	0.10727602E 00
5.6	0.32294798E-03	0.24211679E-01	0.14557729E-02	0.10914046E 00
5.7	0.29513566E-03	0.23328245E-01	0.14043231E-02	0.11100113E 00
5.8	0.27236552E-03	0.22448629E-01	0.13692884E-02	0.11285800E 00
5.9	0.25404920E-03	0.21575406E-01	0.13507239E-02	0.11471170E 00
6.0	0.23962690E-03	0.20710502E-01	0.13486543E-02	0.11656165E 00
6.1	0.22857721E-03	0.19855924E-01	0.13630854E-02	0.11840779E 00
6.2	0.22041713E-03	0.19013513E-01	0.13940230E-02	0.12025052E 00
6.3	0.21469743E-03	0.18184781E-01	0.14414345E-02	0.12208891E 00
6.4	0.21101118E-03	0.17371517E-01	0.15053041E-02	0.12392431E 00
6.5	0.20898151E-03	0.16574819E-01	0.15855706E-02	0.12575537E 00
6.6	0.20827334E-03	0.15796036E-01	0.16822030E-02	0.12758303E 00
6.7	0.20858113E-03	0.15036166E-01	0.17951238E-02	0.12940663E 00
6.8	0.20963394E-03	0.14296170E-01	0.19242496E-02	0.13122588E 00
6.9	0.21119362E-03	0.13576873E-01	0.20695196E-02	0.13304192E 00
7.0	0.21305104E-03	0.12878928E-01	0.22308289E-02	0.13485354E 00
7.1	0.21502524E-03	0.12202907E-01	0.24080893E-02	0.13666159E 00
7.2	0.21696129E-03	0.11549167E-01	0.26011863E-02	0.13846499E 00
7.3	0.21872971E-03	0.10918159E-01	0.28100009E-02	0.14026463E 00
7.4	0.22022489E-03	0.10309972E-01	0.30344592E-02	0.14206022E 00
7.5	0.22135828E-03	0.97247511E-02	0.32744061E-02	0.14385182E 00
7.6	0.22206421E-03	0.91625825E-02	0.35297065E-02	0.14563912E 00
7.7	0.22229269E-03	0.86233206E-02	0.38002606E-02	0.14742219E 00

7.8	0.22200836E-03	0.81068203E-02	0.40859245E-02	0.14920098E 00
7.9	0.22119179E-03	0.76129287E-02	0.43865554E-02	0.15097547E 00
8.0	0.21983229E-03	0.71412772E-02	0.47020242E-02	0.15274584E 00
8.1	0.21793286E-03	0.66915788E-02	0.50321706E-02	0.15451169E 00
8.2	0.21550368E-03	0.62634163E-02	0.53768493E-02	0.15627319E 00
8.3	0.21256272E-03	0.58563016E-02	0.57359301E-02	0.15803027E 00
8.4	0.20913631E-03	0.54698065E-02	0.61092600E-02	0.15978324E 00
8.5	0.20525185E-03	0.51033087E-02	0.64966828E-02	0.16153121E 00
8.6	0.20094505E-03	0.47563203E-02	0.68980344E-02	0.16327488E 00
8.7	0.19625183E-03	0.44282116E-02	0.73131770E-02	0.16501397E 00
8.8	0.19121241E-03	0.41183941E-02	0.77419430E-02	0.16674852E 00
8.9	0.18586533E-03	0.38262045E-02	0.81841648E-02	0.16847837E 00
9.0	0.18025318E-03	0.35510033E-02	0.86397305E-02	0.17020345E 00
9.1	0.17441754E-03	0.32921801E-02	0.91084391E-02	0.17192435E 00
9.2	0.16839738E-03	0.30490120E-02	0.95901638E-02	0.17364001E 00
9.3	0.16223302E-03	0.28208822E-02	0.10084707E-01	0.17535132E 00
9.4	0.15596322E-03	0.26071263E-02	0.10591950E-01	0.17705810E 00
9.5	0.14962407E-03	0.24070742E-02	0.11111710E-01	0.17875940E 00
9.6	0.14324982E-03	0.22200872E-02	0.11643786E-01	0.18045551E 00
9.7	0.13687379E-03	0.20455346E-02	0.12188107E-01	0.18214732E 00
9.8	0.13052505E-03	0.18827773E-02	0.12744479E-01	0.18383455E 00
9.9	0.12423249E-03	0.17312195E-02	0.13312690E-01	0.18551660E 00
10.0	0.11802001E-03	0.15902354E-02	0.13892625E-01	0.18719321E 00
10.1	0.11191057E-03	0.14592460E-02	0.14484186E-01	0.18886501E 00
10.2	0.10592468E-03	0.13377052E-02	0.15087117E-01	0.19053233E 00
10.3	0.10008139E-03	0.12250654E-02	0.15701246E-01	0.19219410E 00
10.4	0.94393778E-04	0.11207683E-02	0.16326558E-01	0.19385058E 00
10.5	0.88876142E-04	0.10243503E-02	0.16962759E-01	0.19550204E 00
10.6	0.83539315E-04	0.93526044E-03	0.17609730E-01	0.19714892E 00
10.7	0.78392710E-04	0.85308915E-03	0.18267367E-01	0.19879007E 00
10.8	0.73442090E-04	0.77736238E-03	0.18935431E-01	0.20042586E 00
10.9	0.68693058E-04	0.70765754E-03	0.19613862E-01	0.20205677E 00
11.0	0.64149135E-04	0.64357044E-03	0.20302411E-01	0.20368212E 00
11.1	0.59811966E-04	0.58471318E-03	0.21000996E-01	0.20530272E 00
11.2	0.55682016E-04	0.53071696E-03	0.21709461E-01	0.20691741E 00
11.3	0.51758296E-04	0.48123603E-03	0.22427659E-01	0.20852691E 00
11.4	0.48038914E-04	0.43594581E-03	0.23155313E-01	0.21013099E 00
11.5	0.44520653E-04	0.39453106E-03	0.23892466E-01	0.21172923E 00
11.6	0.41199761E-04	0.35670609E-03	0.24638854E-01	0.21332234E 00
11.7	0.38071594E-04	0.32219617E-03	0.25394421E-01	0.21491057E 00
11.8	0.35130972E-04	0.29074540E-03	0.26158955E-01	0.21649259E 00
11.9	0.32371579E-04	0.26211073E-03	0.26932251E-01	0.21806896E 00
12.0	0.29787552E-04	0.23607125E-03	0.27714387E-01	0.21964103E 00

FREQUENCY = 2000.0 MHZ
SIGMA = 0.15 METERS
PLATFORM ALTITUDE = 1287.4750 KM

PSI	SPECULAR		DIFFUSE	
(DEGREES)	VERTICAL	HORIZONTAL	VERTICAL	HORIZONTAL
0.1	0.13504180E-02	0.14390557E-02	0.13510687E-02	0.14397493E-02
0.2	0.25260167E-02	0.28685760E-02	0.25308887E-02	0.28741085E-02
0.3	0.35401699E-02	0.42845085E-02	0.35555509E-02	0.43031238E-02
0.4	0.44056550E-02	0.56829117E-02	0.44397414E-02	0.57268813E-02
0.5	0.51345564E-02	0.70598572E-02	0.51967613E-02	0.71453899E-02
0.6	0.57383925E-02	0.84116273E-02	0.58387667E-02	0.85587613E-02
0.7	0.62280372E-02	0.97344518E-02	0.63767806E-02	0.99669397E-02
0.8	0.66138767E-02	0.11024937E-01	0.68209358E-02	0.11370093E-01
0.9	0.69056600E-02	0.12279648E-01	0.71804076E-02	0.12768202E-01
1.0	0.71125999E-02	0.13495374E-01	0.74635632E-02	0.14161289E-01
1.1	0.72434619E-02	0.14669191E-01	0.76781437E-02	0.15549488E-01
1.2	0.73063821E-02	0.15798204E-01	0.78310966E-02	0.16932767E-01
1.3	0.73090531E-02	0.16879827E-01	0.79288408E-02	0.18311188E-01
1.4	0.72586834E-02	0.17911669E-01	0.79772398E-02	0.19684795E-01
1.5	0.71619786E-02	0.18891588E-01	0.79816394E-02	0.21053653E-01
1.6	0.70252158E-02	0.19817613E-01	0.79469532E-02	0.22417765E-01
1.7	0.68541877E-02	0.20688031E-01	0.78776516E-02	0.23777157E-01
1.8	0.66542923E-02	0.21501489E-01	0.77778585E-02	0.25131978E-01
1.9	0.64304620E-02	0.22256639E-01	0.76513030E-02	0.26482116E-01
2.0	0.61872751E-02	0.22952661E-01	0.75014494E-02	0.27827788E-01
2.1	0.59289187E-02	0.23588706E-01	0.73314682E-02	0.29168859E-01
2.2	0.56591369E-02	0.24164353E-01	0.71441866E-02	0.30505467E-01
2.3	0.53814240E-02	0.24679363E-01	0.69423094E-02	0.31837624E-01
2.4	0.50988458E-02	0.25133632E-01	0.67282207E-02	0.33165254E-01
2.5	0.48141815E-02	0.25527496E-01	0.65041259E-02	0.34488525E-01
2.6	0.45299307E-02	0.25861464E-01	0.62720999E-02	0.35807539E-01
2.7	0.42482391E-02	0.26136097E-01	0.60339570E-02	0.37122212E-01
2.8	0.39710253E-02	0.26352197E-01	0.57914108E-02	0.38432460E-01
2.9	0.36999523E-02	0.26510999E-01	0.55460259E-02	0.39738540E-01
3.0	0.34363931E-02	0.26613623E-01	0.52991919E-02	0.41040327E-01
3.1	0.31815514E-02	0.26661567E-01	0.50522275E-02	0.42337935E-01
3.2	0.29364082E-02	0.26656508E-01	0.48063248E-02	0.43631483E-01
3.3	0.27017170E-02	0.26599981E-01	0.45625269E-02	0.44920743E-01

3.4	0.24781071E-02	0.26494052E-01	0.43218546E-02	0.46206012E-01
3.5	0.22660061E-02	0.26340555E-01	0.40851794E-02	0.47487028E-01
3.6	0.20657252E-02	0.26141789E-01	0.38533409E-02	0.48764102E-01
3.7	0.18774187E-02	0.25899842E-01	0.36270670E-02	0.50037030E-01
3.8	0.17011103E-02	0.25617026E-01	0.34070029E-02	0.51306065E-01
3.9	0.15367649E-02	0.25295697E-01	0.31937980E-02	0.52571058E-01
4.0	0.13842192E-02	0.24938386E-01	0.29879906E-02	0.53832270E-01
4.1	0.12432258E-02	0.24547335E-01	0.27900545E-02	0.55089269E-01
4.2	0.11134886E-02	0.24125189E-01	0.26004666E-02	0.56342516E-01
4.3	0.99462690E-03	0.23674361E-01	0.24195963E-02	0.57591844E-01
4.4	0.88622887E-03	0.23197375E-01	0.22478094E-02	0.58837246E-01
4.5	0.78784488E-03	0.22696871E-01	0.20854406E-02	0.60079049E-01
4.6	0.69898227E-03	0.22175014E-01	0.19327665E-02	0.61316464E-01
4.7	0.61911973E-03	0.21634519E-01	0.17900227E-02	0.62550545E-01
4.8	0.54773479E-03	0.21077689E-01	0.16574366E-02	0.63780725E-01
4.9	0.48428471E-03	0.20506851E-01	0.15351942E-02	0.65007210E-01
5.0	0.42823027E-03	0.19924313E-01	0.14234679E-02	0.66229820E-01
5.1	0.37902850E-03	0.19332368E-01	0.13223945E-02	0.67448795E-01
5.2	0.33613853E-03	0.18733028E-01	0.12320827E-02	0.68664074E-01
5.3	0.29904372E-03	0.18128540E-01	0.11526502E-02	0.69875598E-01
5.4	0.26722183E-03	0.17520674E-01	0.10841505E-02	0.71083426E-01
5.5	0.24018394E-03	0.16911395E-01	0.10266635E-02	0.72287560E-01
5.6	0.21745297E-03	0.16302615E-01	0.98022586E-03	0.73488295E-01
5.7	0.19857696E-03	0.15696008E-01	0.94487472E-03	0.74685216E-01
5.8	0.18312161E-03	0.15093047E-01	0.92062354E-03	0.75878620E-01
5.9	0.17068181E-03	0.14495332E-01	0.90747769E-03	0.77068508E-01
6.0	0.16087545E-03	0.13904165E-01	0.90542994E-03	0.78254640E-01
6.1	0.15334743E-03	0.13320897E-01	0.91446401E-03	0.79437137E-01
6.2	0.14776869E-03	0.12746740E-01	0.93455962E-03	0.80616474E-01
6.3	0.14383353E-03	0.12182631E-01	0.96566882E-03	0.81791699E-01
6.4	0.14126650E-03	0.11629771E-01	0.10077620E-02	0.82964063E-01
6.5	0.13981228E-03	0.11088837E-01	0.10607745E-02	0.84132493E-01
6.6	0.13924456E-03	0.10560695E-01	0.11246644E-02	0.85297704E-01
6.7	0.13935739E-03	0.10045975E-01	0.11993595E-02	0.86459279E-01
6.8	0.13996888E-03	0.95452927E-02	0.12847874E-02	0.87617159E-01
6.9	0.14091867E-03	0.90591498E-02	0.13808843E-02	0.88772058E-01
7.0	0.14206700E-03	0.85879490E-02	0.14875645E-02	0.89923263E-01
7.1	0.14329233E-03	0.81319809E-02	0.16047454E-02	0.91070890E-01
7.2	0.14449237E-03	0.76915398E-02	0.17323440E-02	0.92215240E-01
7.3	0.14558036E-03	0.72668158E-02	0.18702578E-02	0.93356133E-01
7.4	0.14648603E-03	0.68578385E-02	0.20184179E-02	0.94493568E-01
7.5	0.14715156E-03	0.64646862E-02	0.21767153E-02	0.95627844E-01
7.6	0.14753363E-03	0.60873777E-02	0.23450444E-02	0.96758783E-01
7.7	0.14759880E-03	0.57257451E-02	0.25233126E-02	0.97885966E-01

7.8	0.14732513E-03	0.53796954E-02	0.27114262E-02	0.99009931E-01
7.9	0.14670001E-03	0.50490834E-02	0.29092750E-02	0.10013074E 00
8.0	0.14571662E-03	0.47336183E-02	0.31167534E-02	0.10124809E 00
8.1	0.14437815E-03	0.44330955E-02	0.33337583E-02	0.10236228E 00
8.2	0.14269105E-03	0.41471794E-02	0.35601633E-02	0.10347277E 00
8.3	0.14066801E-03	0.38755345E-02	0.37958766E-02	0.10457993E 00
8.4	0.13832739E-03	0.36178515E-02	0.40408000E-02	0.10568416E 00
8.5	0.13568750E-03	0.33736883E-02	0.42948164E-02	0.10678482E 00
8.6	0.13277253E-03	0.31426952E-02	0.45578107E-02	0.10788232E 00
8.7	0.12960612E-03	0.29244213E-02	0.48296750E-02	0.10897636E 00
8.8	0.12621566E-03	0.27184752E-02	0.51103085E-02	0.11006755E 00
8.9	0.12262617E-03	0.25243694E-02	0.53995699E-02	0.11115497E 00
9.0	0.11886671E-03	0.23416833E-02	0.56974106E-02	0.11223942E 00
9.1	0.11496396E-03	0.21699765E-02	0.60036518E-02	0.11332059E 00
9.2	0.11094431E-03	0.20087638E-02	0.63182339E-02	0.11439830E 00
9.3	0.10683422E-03	0.18576174E-02	0.66410154E-02	0.11547297E 00
9.4	0.10265913E-03	0.17160783E-02	0.69719031E-02	0.11654425E 00
9.5	0.98443154E-04	0.15837015E-02	0.73108003E-02	0.11761230E 00
9.6	0.94208473E-04	0.14600430E-02	0.76575540E-02	0.11867678E 00
9.7	0.89977068E-04	0.13446780E-02	0.80121271E-02	0.11973864E 00
9.8	0.85767591E-04	0.12371663E-02	0.83743557E-02	0.12079704E 00
9.9	0.81599166E-04	0.11371104E-02	0.87441243E-02	0.12185216E 00
10.0	0.77487610E-04	0.10440901E-02	0.91213882E-02	0.12290418E 00
10.1	0.73447198E-04	0.95770718E-03	0.95060095E-02	0.12395263E 00
10.2	0.69491885E-04	0.87759993E-03	0.98978840E-02	0.12499851E 00
10.3	0.65633329E-04	0.80339704E-03	0.10296870E-01	0.12604076E 00
10.4	0.61880346E-04	0.73472597E-03	0.10702964E-01	0.12707984E 00
10.5	0.58241916E-04	0.67125959E-03	0.11115961E-01	0.12811553E 00
10.6	0.54725155E-04	0.61267288E-03	0.11535827E-01	0.12914884E 00
10.7	0.51335781E-04	0.55864872E-03	0.11962458E-01	0.13017845E 00
10.8	0.48077287E-04	0.50888327E-03	0.12395676E-01	0.13120443E 00
10.9	0.44953207E-04	0.46309642E-03	0.12835465E-01	0.13222748E 00
11.0	0.41965992E-04	0.42101974E-03	0.13281722E-01	0.13324761E 00
11.1	0.39116159E-04	0.38239360E-03	0.13734348E-01	0.13426489E 00
11.2	0.36403842E-04	0.34697261E-03	0.14193233E-01	0.13527864E 00
11.3	0.33826182E-04	0.31452603E-03	0.14658272E-01	0.13628900E 00
11.4	0.31387928E-04	0.28484059E-03	0.15129350E-01	0.13729656E 00
11.5	0.29080649E-04	0.25770534E-03	0.15606429E-01	0.13830030E 00
11.6	0.26903814E-04	0.23293216E-03	0.16089395E-01	0.13930130E 00
11.7	0.24854191E-04	0.21033867E-03	0.16578183E-01	0.14029956E 00
11.8	0.22928260E-04	0.18975514E-03	0.17072663E-01	0.14129400E 00
11.9	0.21121814E-04	0.17102221E-03	0.17572764E-01	0.14228570E 00
12.0	0.19430765E-04	0.15399205E-03	0.18078417E-01	0.14327443E 00

FREQUENCY = 2000.0 MHZ
SIGMA = 1.50 METERS
PLATFORM ALTITUDE = 6.0960 KM

PSI	SPECULAR		DIFFUSE	
(DEGREES)	VERTICAL	HORIZONTAL	VERTICAL	HORIZONTAL
0.1	0.18292058E-01	0.19492701E-01	0.19194752E-01	0.20454645E-01
0.2	0.30214828E-01	0.34312330E-01	0.36635257E-01	0.41603450E-01
0.3	0.33947460E-01	0.41085061E-01	0.52370198E-01	0.63381255E-01
0.4	0.30744951E-01	0.39658368E-01	0.66448689E-01	0.85713148E-01
0.5	0.23671687E-01	0.32547861E-01	0.78924596E-01	0.10851896E 00
0.6	0.15864454E-01	0.23254935E-01	0.89848876E-01	0.13170511E 00
0.7	0.93726292E-02	0.14649469E-01	0.99285305E-01	0.15518343E 00
0.8	0.49179271E-02	0.81978925E-02	0.10729200E 00	0.17884934E 00
0.9	0.23031419E-02	0.40954426E-02	0.11394435E 00	0.20261580E 00
1.0	0.96582156E-03	0.18325406E-02	0.11930871E 00	0.22637516E 00
1.1	0.36355574E-03	0.73625962E-03	0.12347025E 00	0.25004733E 00
1.2	0.12305514E-03	0.26607560E-03	0.12650901E 00	0.27354378E 00
1.3	0.37503647E-04	0.86612432E-04	0.12850606E 00	0.29677707E 00
1.4	0.10302530E-04	0.25422720E-04	0.12954599E 00	0.31967032E 00
1.5	0.25532399E-05	0.67348356E-05	0.12971568E 00	0.34215891E 00
1.6	0.57125931E-06	0.16114800E-05	0.12910038E 00	0.36418271E 00
1.7	0.11545734E-06	0.34848540E-06	0.12778932E 00	0.38570702E 00
1.8	0.21089132E-07	0.68143606E-07	0.12585425E 00	0.40666294E 00
1.9	0.34828136E-08	0.12054457E-07	0.12337756E 00	0.42702532E 00
2.0	0.52023696E-09	0.19299009E-08	0.12043804E 00	0.44678372E 00
2.1	0.70308995E-10	0.27973024E-09	0.11709690E 00	0.46588004E 00
2.2	0.85997060E-11	0.36720474E-10	0.11343122E 00	0.48434782E 00
2.3	0.95220706E-12	0.43668498E-11	0.10949582E 00	0.50215083E 00
2.4	0.95457984E-13	0.47053908E-12	0.10534590E 00	0.51927918E 00
2.5	0.86663837E-14	0.45954028E-13	0.10103655E 00	0.53575236E 00
2.6	0.71270686E-15	0.40688583E-14	0.96616089E-01	0.55158311E 00
2.7	0.53096591E-16	0.32666164E-15	0.92125297E-01	0.56677479E 00
2.8	0.35838957E-17	0.23783123E-16	0.87597370E-01	0.58130592E 00
2.9	0.21922137E-18	0.15707713E-17	0.83073974E-01	0.59524399E 00
3.0	0.12151322E-19	0.94107615E-19	0.78579307E-01	0.60856855E 00
3.1	0.61048514E-21	0.51158988E-20	0.74143291E-01	0.62132496E 00
3.2	0.27802513E-22	0.25238924E-21	0.69784105E-01	0.63349515E 00
3.3	0.11477311E-23	0.11300085E-22	0.65524638E-01	0.64512813E 00

3.4	0.42956521E-25	0.45925855E-24	0.61381210E-01	0.65624136E 00
3.5	0.14576387E-26	0.16943909E-25	0.57366051E-01	0.66683555E 00
3.6	0.44853813E-28	0.56762606E-27	0.53491786E-01	0.67693973E 00
3.7	0.12517461E-29	0.17268405E-28	0.49768794E-01	0.68658298E 00
3.8	0.31071982E-31	0.47694846E-30	0.46203919E-01	0.69578493E 00
3.9	0.72688787E-33	0.11964837E-31	0.42803362E-01	0.70455879E 00
4.0	0.15133663E-34	0.27265132E-33	0.39571185E-01	0.71292299E 00
4.1	0.28585901E-36	0.56442491E-35	0.36510866E-01	0.72090232E 00
4.2	0.48987040E-38	0.10613686E-36	0.33623088E-01	0.72848821E 00
4.3	0.76176927E-40	0.18131828E-38	0.30910302E-01	0.73573500E 00
4.4	0.10753200E-41	0.28146908E-40	0.28372161E-01	0.74265188E 00
4.5	0.13784292E-43	0.39710903E-42	0.26007514E-01	0.74924546E 00
4.6	0.16051107E-45	0.50921674E-44	0.23814287E-01	0.75550145E 00
4.7	0.16978353E-47	0.59329185E-46	0.21791667E-01	0.76148850E 00
4.8	0.16329472E-49	0.62838401E-48	0.19936461E-01	0.76718664E 00
4.9	0.14284858E-51	0.60488706E-50	0.18246144E-01	0.77262658E 00
5.0	0.11379698E-53	0.52946509E-52	0.16717236E-01	0.77780533E 00
5.1	0.82615851E-56	0.42138288E-54	0.15346445E-01	0.78274679E 00
5.2	0.54693122E-58	0.30480548E-56	0.14129907E-01	0.78746164E 00
5.3	0.33096541E-60	0.20063574E-58	0.13064004E-01	0.79196268E 00
5.4	0.18305351E-62	0.12002101E-60	0.12144189E-01	0.79624695E 00
5.5	0.92721268E-65	0.65282 74E-63	0.11366576E-01	0.80032343E 00
5.6	0.43090883E-67	0.32305620E-65	0.10727271E-01	0.80423272E 00
5.7	0.18406494E-69	0.14548961E-67	0.10221694E-01	0.80794829E 00
5.8	0.72273012E-72	0.59568612E-70	0.98456554E-02	0.81148809E 00
5.9	0.26126455E-74	0.22188186E-72	0.95951483E-02	0.81487870E 00
6.0	0.87010031E-77	0.75201267E-75	0.94657429E-02	0.81810707E 00
6.1	0.0	0.23195059E-77	0.94533265E-02	0.82118678E 00
6.2	0.0	0.0	0.95537528E-02	0.82412118E 00
6.3	0.0	0.0	0.97630732E-02	0.82692868E 00
6.4	0.0	0.0	0.10077070E-01	0.82959646E 00
6.5	0.0	0.0	0.10491949E-01	0.83214176E 00
6.6	0.0	0.0	0.11003911E-01	0.83456832E 00
6.7	0.0	0.0	0.11609461E-01	0.83690172E 00
6.8	0.0	0.0	0.12304358E-01	0.83910739E 00
6.9	0.0	0.0	0.13085593E-01	0.84122610E 00
7.0	0.0	0.0	0.13949353E-01	0.84323859E 00
7.1	0.0	0.0	0.14892250E-01	0.84515113E 00
7.2	0.0	0.0	0.15911300E-01	0.84698272E 00
7.3	0.0	0.0	0.17003044E-01	0.84872806E 00
7.4	0.0	0.0	0.18164441E-01	0.85038084E 00
7.5	0.0	0.0	0.19392733E-01	0.85196579E 00
7.6	0.0	0.0	0.20684663E-01	0.85346967E 00
7.7	0.0	0.0	0.22037894E-01	0.85490894E 00

7.8	0.0	0.0	0.23449592E-01	0.85628146E 00
7.9	0.0	0.0	0.24916656E-01	0.85757589E 00
8.0	0.0	0.0	0.26437286E-01	0.85881901E 00
8.1	0.0	0.0	0.28008468E-01	0.85999388E 00
8.2	0.0	0.0	0.29627986E-01	0.86111015E 00
8.3	0.0	0.0	0.31293657E-01	0.86216986E 00
8.4	0.0	0.0	0.33003502E-01	0.86318272E 00
8.5	0.0	0.0	0.34755092E-01	0.86413842E 00
8.6	0.0	0.0	0.36546413E-01	0.86504507E 00
8.7	0.0	0.0	0.38375683E-01	0.86590576E 00
8.8	0.0	0.0	0.40240761E-01	0.86671883E 00
8.9	0.0	0.0	0.42140059E-01	0.86749077E 00
9.0	0.0	0.0	0.44071723E-01	0.86821675E 00
9.1	0.0	0.0	0.46034057E-01	0.86890584E 00
9.2	0.0	0.0	0.48025206E-01	0.86954731E 00
9.3	0.0	0.0	0.50044391E-01	0.87016439E 00
9.4	0.0	0.0	0.52089293E-01	0.87073958E 00
9.5	0.0	0.0	0.54158613E-01	0.87127584E 00
9.6	0.0	0.0	0.56251328E-01	0.87178361E 00
9.7	0.0	0.0	0.58365669E-01	0.87225640E 00
9.8	0.0	0.0	0.60500689E-01	0.87270087E 00
9.9	0.0	0.0	0.62654674E-01	0.87311387E 00
10.0	0.0	0.0	0.64827263E-01	0.87350166E 00
10.1	0.0	0.0	0.67016006E-01	0.87384856E 00
10.2	0.0	0.0	0.69220662E-01	0.87417525E 00
10.3	0.0	0.0	0.71440339E-01	0.87447941E 00
10.4	0.0	0.0	0.73674500E-01	0.87476200E 00
10.5	0.0	0.0	0.75920880E-01	0.87501645E 00
10.6	0.0	0.0	0.78178883E-01	0.87524891E 00
10.7	0.0	0.0	0.80447972E-01	0.87545520E 00
10.8	0.0	0.0	0.82727015E-01	0.87564099E 00
10.9	0.0	0.0	0.85015535E-01	0.87580770E 00
11.0	0.0	0.0	0.87312102E-01	0.87595069E 00
11.1	0.0	0.0	0.89616179E-01	0.87607449E 00
11.2	0.0	0.0	0.91927469E-01	0.87618029E 00
11.3	0.0	0.0	0.94245434E-01	0.87627131E 00
11.4	0.0	0.0	0.96567988E-01	0.87634039E 00
11.5	0.0	0.0	0.98895967E-01	0.87639207E 00
11.6	0.0	0.0	0.10122800E 00	0.87642866E 00
11.7	0.0	0.0	0.10356414E 00	0.87645382E 00
11.8	0.0	0.0	0.10590255E 00	0.87645400E 00
11.9	0.0	0.0	0.10824323E 00	0.87643987E 00
12.0	0.0	0.0	0.11058766E 00	0.87642545E 00

FREQUENCY = 2000.0 MHZ
SIGMA = 1.50 METERS
PLATFORM ALTITUDE = 15.2400 KM

PSI	SPECULAR		DIFFUSE	
(DEGREES)	VERTICAL	HORIZONTAL	VERTICAL	HORIZONTAL
0.1	0.11527888E-01	0.12284547E-01	0.12096778E-01	0.12890775E-01
0.2	0.18922482E-01	0.21488603E-01	0.22943374E-01	0.26054777E-01
0.3	0.21143910E-01	0.25589529E-01	0.32618370E-01	0.39476555E-01
0.4	0.19061070E-01	0.24587128E-01	0.41196458E-01	0.53139862E-01
0.5	0.14620651E-01	0.20102933E-01	0.48747230E-01	0.67025900E-01
0.6	0.97706988E-02	0.14322381E-01	0.55336695E-01	0.81115305E-01
0.7	0.57611465E-02	0.90046972E-02	0.61028458E-01	0.95387757E-01
0.8	0.30197797E-02	0.50337873E-02	0.65881014E-01	0.10981965E 00
0.9	0.14139402E-02	0.25142687E-02	0.69952488E-01	0.12438953E 00
1.0	0.59335446E-03	0.11258249E-02	0.73297560E-01	0.13907403E 00
1.1	0.22368887E-03	0.45300648E-03	0.75968862E-01	0.15384936E 00
1.2	0.75886215E-04	0.16408473E-03	0.78016162E-01	0.16869020E 00
1.3	0.23198125E-04	0.53574680E-04	0.79488277E-01	0.18357337E 00
1.4	0.63965272E-05	0.15784201E-04	0.80431163E-01	0.19847363E 00
1.5	0.15921778E-05	0.41997873E-05	0.80889583E-01	0.21336746E 00
1.6	0.35800429E-06	0.10099029E-05	0.80906332E-01	0.22823071E 00
1.7	0.72753551E-07	0.21959255E-06	0.80524385E-01	0.24304718E 00
1.8	0.13368393E-07	0.43196270E-07	0.79778969E-01	0.25778365E 00
1.9	0.22219011E-08	0.76902822E-08	0.78710139E-01	0.27242583E 00
2.0	0.33413561E-09	0.12395294E-08	0.77354431E-01	0.28695852E 00
2.1	0.45478593E-10	0.18094050E-09	0.75742841E-01	0.30134934E 00
2.2	0.56034335E-11	0.23926472E-10	0.73909998E-01	0.31559336E 00
2.3	0.62513802E-12	0.28669003E-11	0.71885586E-01	0.32966930E 00
2.4	0.63155264E-13	0.31130984E-12	0.69697142E-01	0.34355646E 00
2.5	0.57789399E-14	0.30643196E-13	0.67373455E-01	0.35725194E 00
2.6	0.47903906E-15	0.27348453E-14	0.64939559E-01	0.37074149E 00
2.7	0.35975236E-16	0.22132751E-15	0.62418886E-01	0.38401455E 00
2.8	0.24478822E-17	0.16244411E-16	0.59831001E-01	0.39704508E 00
2.9	0.15094201E-18	0.10815329E-17	0.57199497E-01	0.40984726E 00
3.0	0.84340402E-20	0.65318576E-19	0.54540653E-01	0.42239773E 00
3.1	0.42711338E-21	0.35792299E-20	0.51872831E-01	0.43469685E 00
3.2	0.19606223E-22	0.17798390E-21	0.49211483E-01	0.44673818E 00
3.3	0.81575026E-24	0.80315372E-23	0.46571638E-01	0.45852494E 00

3.4	0.30768469E-25	0.32895307E-24	0.43965522E-01	0.47004598E 00
3.5	0.10520747E-26	0.12229547E-25	0.41404895E-01	0.48129964E 00
3.6	0.32618019E-28	0.41278168E-27	0.38899612E-01	0.49227536E 00
3.7	0.91703907E-30	0.12650964E-28	0.36460996E-01	0.50299579E 00
3.8	0.23371887E-31	0.35195726E-30	0.34095522E-01	0.51344448E 00
3.9	0.54023039E-33	0.88923855E-32	0.31811893E-01	0.52363515E 00
4.0	0.11320060E-34	0.20405259E-33	0.29615138E-01	0.53355265E 00
4.1	0.21540020E-36	0.42530496E-35	0.27511634E-01	0.54321373E 00
4.2	0.37159885E-38	0.80511749E-37	0.25505319E-01	0.55260605E 00
4.3	0.58162546E-40	0.13844004E-38	0.23600612E-01	0.56174797E 00
4.4	0.82625977E-42	0.21627662E-40	0.21800745E-01	0.57064259E 00
4.5	0.10657492E-43	0.30702968E-42	0.20108022E-01	0.57928824E 00
4.6	0.12485513E-45	0.39609919E-44	0.18524181E-01	0.58767438E 00
4.7	0.13284893E-47	0.46422770E-46	0.17051127E-01	0.59583503E 00
4.8	0.12850779E-49	0.49451845E-48	0.15689366E-01	0.60375178E 00
4.9	0.11304732E-51	0.47869506E-50	0.14439609E-01	0.61144042E 00
5.0	0.90547735E-54	0.42129276E-52	0.13301823E-01	0.61889595E 00
5.1	0.66086089E-56	0.33707262E-54	0.12275930E-01	0.62613481E 00
5.2	0.43976149E-58	0.24507977E-56	0.11361189E-01	0.63316083E 00
5.3	0.26744530E-60	0.16212989E-58	0.10556776E-01	0.63997006E 00
5.4	0.14864552E-62	0.97461024E-61	0.98614842E-02	0.64657897E 00
5.5	0.75602060E-65	0.53265562E-63	0.92738643E-02	0.65297538E 00
5.6	0.35319627E-67	0.26479434E-65	0.87926500E-02	0.65919274E 00
5.7	0.15154597E-69	0.11978576E-67	0.84158145E-02	0.66520697E 00
5.8	0.59764391E-72	0.49258382E-70	0.81415549E-02	0.67103451E 00
5.9	0.21695625E-74	0.18425431E-72	0.79679638E-02	0.67668855E 00
6.0	0.72552127E-77	0.62705481E-75	0.78928731E-02	0.68216670E 00
6.1	0.0	0.19418126E-77	0.79140067E-02	0.68747008E 00
6.2	0.0	0.0	0.80291741E-02	0.69260901E 00
6.3	0.0	0.0	0.82360767E-02	0.69759285E 00
6.4	0.0	0.0	0.85321553E-02	0.70241141E 00
6.5	0.0	0.0	0.89150965E-02	0.70707786E 00
6.6	0.0	0.0	0.93825646E-02	0.71160090E 00
6.7	0.0	0.0	0.99321343E-02	0.71598697E 00
6.8	0.0	0.0	0.10561086E-01	0.72022295E 00
6.9	0.0	0.0	0.11267312E-01	0.72433537E 00
7.0	0.0	0.0	0.12048144E-01	0.72831047E 00
7.1	0.0	0.0	0.12901224E-01	0.73215801E 00
7.2	0.0	0.0	0.13824273E-01	0.73588669E 00
7.3	0.0	0.0	0.14814712E-01	0.73949462E 00
7.4	0.0	0.0	0.15870366E-01	0.74298233E 00
7.5	0.0	0.0	0.16989093E-01	0.74636841E 00
7.6	0.0	0.0	0.18168226E-01	0.74963892E 00
7.7	0.0	0.0	0.19406002E-01	0.75281078E 00

7.8	0.0	0.0	0.20700004E-01	0.75587821E 00
7.9	0.0	0.0	0.22048049E-01	0.75884485E 00
8.0	0.0	0.0	0.23448296E-01	0.76172107E 00
8.1	0.0	0.0	0.24898376E-01	0.76449901E 00
8.2	0.0	0.0	0.26396405E-01	0.76718736E 00
8.3	0.0	0.0	0.27940538E-01	0.76978821E 00
8.4	0.0	0.0	0.29529031E-01	0.77231061E 00
8.5	0.0	0.0	0.31159736E-01	0.77474469E 00
8.6	0.0	0.0	0.32831058E-01	0.77710366E 00
8.7	0.0	0.0	0.34541313E-01	0.77938753E 00
8.8	0.0	0.0	0.36288269E-01	0.78158879E 00
8.9	0.0	0.0	0.38070876E-01	0.78372300E 00
9.0	0.0	0.0	0.39887536E-01	0.78578800E 00
9.1	0.0	0.0	0.41736409E-01	0.78778642E 00
9.2	0.0	0.0	0.43615680E-01	0.78970820E 00
9.3	0.0	0.0	0.45524981E-01	0.79158163E 00
9.4	0.0	0.0	0.47461879E-01	0.79338652E 00
9.5	0.0	0.0	0.49425550E-01	0.79513264E 00
9.6	0.0	0.0	0.51414255E-01	0.79681873E 00
9.7	0.0	0.0	0.53426936E-01	0.79844844E 00
9.8	0.0	0.0	0.55462386E-01	0.80002517E 00
9.9	0.0	0.0	0.57519015E-01	0.80154610E 00
10.0	0.0	0.0	0.59596464E-01	0.80302012E 00
10.1	0.0	0.0	0.61692595E-01	0.80443436E 00
10.2	0.0	0.0	0.63806891E-01	0.80580556E 00
10.3	0.0	0.0	0.65938592E-01	0.80713445E 00
10.4	0.0	0.0	0.68086565E-01	0.80841500E 00
10.5	0.0	0.0	0.70249259E-01	0.80964929E 00
10.6	0.0	0.0	0.72425961E-01	0.81084222E 00
10.7	0.0	0.0	0.74616075E-01	0.81199145E 00
10.8	0.0	0.0	0.76818526E-01	0.81310093E 00
10.9	0.0	0.0	0.79032183E-01	0.81416821E 00
11.0	0.0	0.0	0.81256390E-01	0.81519777E 00
11.1	0.0	0.0	0.83490610E-01	0.81619167E 00
11.2	0.0	0.0	0.85734069E-01	0.81714952E 00
11.3	0.0	0.0	0.87986231E-01	0.81807458E 00
11.4	0.0	0.0	0.90245247E-01	0.81896210E 00
11.5	0.0	0.0	0.92511177E-01	0.81981140E 00
11.6	0.0	0.0	0.94784021E-01	0.82063705E 00
11.7	0.0	0.0	0.97062528E-01	0.82143134E 00
11.8	0.0	0.0	0.99345744E-01	0.82218969E 00
11.9	0.0	0.0	0.10163307E 00	0.82291758E 00
12.0	0.0	0.0	0.10392535E 00	0.82362556E 00

FREQUENCY = 2000.0 MHZ
SIGMA = 1.50 METERS
PLATFORM ALTITUDE = 30.4800 KM

PSI	SPECULAR		DIFFUSE	
(DEGREES)	VERTICAL	HORIZONTAL	VERTICAL	HORIZONTAL
0.1	0.81520304E-02	0.86871088E-02	0.85543245E-02	0.91158077E-02
0.2	0.13335370E-01	0.15143815E-01	0.16169041E-01	0.18361766E-01
0.3	0.14853746E-01	0.17976828E-01	0.22914637E-01	0.27732562E-01
0.4	0.13351794E-01	0.17222062E-01	0.28857071E-01	0.37223127E-01
0.5	0.10214668E-01	0.14044862E-01	0.34057084E-01	0.46827473E-01
0.6	0.68103597E-02	0.99829696E-02	0.38570706E-01	0.56538902E-01
0.7	0.40074289E-02	0.62636286E-02	0.42451147E-01	0.66351295E-01
0.8	0.20968767E-02	0.34953656E-02	0.45746509E-01	0.76256633E-01
0.9	0.98040421E-03	0.17433525E-02	0.48503969E-01	0.86249650E-01
1.0	0.41095028E-03	0.77973260E-03	0.50765030E-01	0.96320987E-01
1.1	0.15479264E-03	0.31348015E-03	0.52570432E-01	0.10646367E 00
1.2	0.52484727E-04	0.11348487E-03	0.53957857E-01	0.11667013E 00
1.3	0.16040300E-04	0.37044098E-04	0.54962032E-01	0.12693143E 00
1.4	0.44230537E-05	0.10914418E-04	0.55616334E-01	0.13723999E 00
1.5	0.11013153E-05	0.29050052E-05	0.55951603E-01	0.14758688E 00
1.6	0.24778365E-06	0.69897936E-06	0.55997271E-01	0.15796417E 00
1.7	0.50397755E-07	0.15211577E-06	0.55780720E-01	0.16836321E 00
1.8	0.92711154E-08	0.29957036E-07	0.55327523E-01	0.17877549E 00
1.9	0.15430515E-08	0.53406950E-08	0.54662105E-01	0.18919241E 00
2.0	0.23242411E-09	0.86221319E-09	0.53807583E-01	0.19960755E 00
2.1	0.31693731E-10	0.12609613E-09	0.52784674E-01	0.21000820E 00
2.2	0.39131112E-11	0.16708857E-10	0.51614434E-01	0.22039205E 00
2.3	0.43755391E-12	0.20066336E-11	0.50315004E-01	0.23074591E 00
2.4	0.44314517E-13	0.21843844E-12	0.48904773E-01	0.24106508E 00
2.5	0.40657141E-14	0.21558706E-13	0.47399923E-01	0.25134093E 00
2.6	0.33797504E-15	0.19295067E-14	0.45816630E-01	0.26156807E 00
2.7	0.25456993E-16	0.15661701E-15	0.44169191E-01	0.27173853E 00
2.8	0.17376244E-17	0.11531070E-16	0.42470928E-01	0.28184175E 00
2.9	0.10749538E-18	0.77022897E-18	0.40735401E-01	0.29187834E 00
3.0	0.60268153E-20	0.46675527E-19	0.38973793E-01	0.30183798E 00
3.1	0.30627594E-21	0.25666096E-20	0.37197161E-01	0.31171417E 00
3.2	0.14109932E-22	0.12808887E-21	0.35415825E-01	0.32150209E 00
3.3	0.58922565E-24	0.58012673E-23	0.33639222E-01	0.33119762E 00

3.4	0.22307871E-25	0.23849888E-24	0.31876050E-01	0.34079462E 00
3.5	0.76569601E-27	0.89006190E-26	0.30134328E-01	0.35028803E 00
3.6	0.23831854E-28	0.30159273E-27	0.28421409E-01	0.35967368E 00
3.7	0.67265412E-30	0.92795683E-29	0.26744377E-01	0.36895078E 00
3.8	0.17211638E-31	0.25919011E-30	0.25108792E-01	0.37811333E 00
3.9	0.39942765E-33	0.65747221E-32	0.23520615E-01	0.38715774E 00
4.0	0.84078912E-35	0.15147837E-33	0.21984775E-01	0.39608240E 00
4.1	0.16054907E-36	0.31700221E-35	0.20505864E-01	0.40488583E 00
4.2	0.27809588E-38	0.60253099E-37	0.19087579E-01	0.41355741E 00
4.3	0.43704091E-40	0.10402565E-38	0.17733805E-01	0.42210478E 00
4.4	0.62337798E-42	0.16317146E-40	0.16447730E-01	0.43052554E 00
4.5	0.80731446E-44	0.23257757E-42	0.15232004E-01	0.43881571E 00
4.6	0.94960668E-46	0.30126014E-44	0.14088877E-01	0.44696581E 00
4.7	0.10144623E-47	0.35449411E-46	0.13020601E-01	0.45499218E 00
4.8	0.98522921E-50	0.37913185E-48	0.12028549E-01	0.46287763E 00
4.9	0.87013585E-52	0.36845616E-50	0.11114303E-01	0.47063154E 00
5.0	0.69970526E-54	0.32555301E-52	0.10278951E-01	0.47825044E 00
5.1	0.51267266E-56	0.26148927E-54	0.95232390E-02	0.48573375E 00
5.2	0.34247018E-58	0.19085915E-56	0.88476799E-02	0.49308246E 00
5.3	0.20907571E-60	0.12674532E-58	0.82527734E-02	0.50029767E 00
5.4	0.11664316E-62	0.76478341E-61	0.77383742E-02	0.50737494E 00
5.5	0.59586334E-65	0.41954889E-63	0.73046088E-02	0.51431942E 00
5.6	0.27922594E-67	0.20933804E-65	0.69511943E-02	0.52113688E 00
5.7	0.12024606E-69	0.95045454E-68	0.66776313E-02	0.52781653E 00
5.8	0.47591928E-72	0.39225702E-70	0.64833276E-02	0.53436190E 00
5.9	0.17338430E-74	0.14724853E-72	0.63676760E-02	0.54078197E 00
6.0	0.58184269E-77	0.50287576E-75	0.63298084E-02	0.54707360E 00
6.1	0.0	0.15626554E-77	0.63687265E-02	0.55323511E 00
6.2	0.0	0.0	0.64834468E-02	0.55927187E 00
6.3	0.0	0.0	0.66727959E-02	0.56518364E 00
6.4	0.0	0.0	0.69355182E-02	0.57096779E 00
6.5	0.0	0.0	0.72703920E-02	0.57663250E 00
6.6	0.0	0.0	0.76760948E-02	0.58217734E 00
6.7	0.0	0.0	0.81512518E-02	0.58760661E 00
6.8	0.0	0.0	0.86942427E-02	0.59291190E 00
6.9	0.0	0.0	0.93038604E-02	0.59811211E 00
7.0	0.0	0.0	0.99783577E-02	0.60319197E 00
7.1	0.0	0.0	0.10716230E-01	0.60815740E 00
7.2	0.0	0.0	0.11516057E-01	0.61301702E 00
7.3	0.0	0.0	0.12376107E-01	0.61776876E 00
7.4	0.0	0.0	0.13294958E-01	0.62241262E 00
7.5	0.0	0.0	0.14270913E-01	0.62695283E 00
7.6	0.0	0.0	0.15302327E-01	0.63138932E 00
7.7	0.0	0.0	0.16387928E-01	0.63573158E 00

7.8	0.0	0.0	0.17525814E-01	0.63997006E 00
7.9	0.0	0.0	0.16714491E-01	0.64411128E 00
8.0	0.0	0.0	0.19952442E-01	0.64815778E 00
8.1	0.0	0.0	0.21238185E-01	0.65211380E 00
8.2	0.0	0.0	0.22569977E-01	0.65597558E 00
8.3	0.0	0.0	0.23946386E-01	0.65974545E 00
8.4	0.0	0.0	0.25366165E-01	0.66343367E 00
8.5	0.0	0.0	0.26827551E-01	0.66703099E 00
8.6	0.0	0.0	0.28329168E-01	0.67054474E 00
8.7	0.0	0.0	0.29869780E-01	0.67397934E 00
8.8	0.0	0.0	0.31447466E-01	0.67732620E 00
8.9	0.0	0.0	0.33061415E-01	0.68059891E 00
9.0	0.0	0.0	0.34710091E-01	0.68379182E 00
9.1	0.0	0.0	0.36392063E-01	0.68691051E 00
9.2	0.0	0.0	0.38106207E-01	0.68995327E 00
9.3	0.0	0.0	0.39851099E-01	0.69292504E 00
9.4	0.0	0.0	0.41625757E-01	0.69582820E 00
9.5	0.0	0.0	0.43428663E-01	0.69865781E 00
9.6	0.0	0.0	0.45258716E-01	0.70141989E 00
9.7	0.0	0.0	0.47114678E-01	0.70411384E 00
9.8	0.0	0.0	0.48995793E-01	0.70674670E 00
9.9	0.0	0.0	0.50900515E-01	0.70931512E 00
10.0	0.0	0.0	0.52828003E-01	0.71181995E 00
10.1	0.0	0.0	0.54777142E-01	0.71426094E 00
10.2	0.0	0.0	0.56746554E-01	0.71664172E 00
10.3	0.0	0.0	0.58735959E-01	0.71896887E 00
10.4	0.0	0.0	0.60744248E-01	0.72123665E 00
10.5	0.0	0.0	0.62770188E-01	0.72345018E 00
10.6	0.0	0.0	0.64812839E-01	0.72560942E 00
10.7	0.0	0.0	0.66871643E-01	0.72771454E 00
10.8	0.0	0.0	0.68945289E-01	0.72976536E 00
10.9	0.0	0.0	0.71033478E-01	0.73176795E 00
11.0	0.0	0.0	0.73134542E-01	0.73371583E 00
11.1	0.0	0.0	0.75248718E-01	0.73562050E 00
11.2	0.0	0.0	0.77374697E-01	0.73747444E 00
11.3	0.0	0.0	0.79512179E-01	0.73928487E 00
11.4	0.0	0.0	0.81659317E-01	0.74104595E 00
11.5	0.0	0.0	0.83816886E-01	0.74276459E 00
11.6	0.0	0.0	0.85983217E-01	0.74443966E 00
11.7	0.0	0.0	0.88157892E-01	0.74607223E 00
11.8	0.0	0.0	0.90340555E-01	0.74766213E 00
11.9	0.0	0.0	0.92529774E-01	0.74920881E 00
12.0	0.0	0.0	0.94726563E-01	0.75072372E 00

FREQUENCY = 2000.0 MHZ
SIGMA = 1.50 METERS
PLATFORM ALTITUDE = 160.9344 KM

PSI (DEGREES)	SPECULAR VERTICAL	SPECULAR HORIZONTAL	DIFFUSE VERTICAL	DIFFUSE HORIZONTAL
0.1	0.35786001E-02	0.38135499E-02	0.37552626E-02	0.40017441E-02
0.2	0.58258544E-02	0.66136420E-02	0.70613846E-02	0.80189966E-02
0.3	0.64547956E-02	0.78119524E-02	0.99577121E-02	0.12051374E-01
0.4	0.57745241E-02	0.74486397E-02	0.12480415E-01	0.16098656E-01
0.5	0.43976381E-02	0.60466230E-02	0.14662329E-01	0.20160265E-01
0.6	0.29193340E-02	0.42793080E-02	0.16533747E-01	0.24236009E-01
0.7	0.17107681E-02	0.26759389E-02	0.18122353E-01	0.28325323E-01
0.8	0.89168712E-03	0.14863885E-02	0.19453492E-01	0.32427792E-01
0.9	0.41538896E-03	0.73864427E-03	0.20550720E-01	0.36543280E-01
1.0	0.17352165E-03	0.32923813E-03	0.21435264E-01	0.40671051E-01
1.1	0.65152440E-04	0.13194430E-03	0.22126973E-01	0.44810716E-01
1.2	0.22025764E-04	0.47625130E-04	0.22643976E-01	0.48961867E-01
1.3	0.67132532E-05	0.15503843E-04	0.23002930E-01	0.53123880E-01
1.4	0.18465920E-05	0.45566885E-05	0.23219410E-01	0.57296682E-01
1.5	0.45876749E-06	0.12101182E-05	0.23307383E-01	0.61479289E-01
1.6	0.10301236E-06	0.29059032E-06	0.23280043E-01	0.65671265E-01
1.7	0.20915061E-07	0.63129619E-07	0.23149602E-01	0.69872499E-01
1.8	0.38418229E-08	0.12413768E-07	0.22926964E-01	0.74082017E-01
1.9	0.63861094E-09	0.22103115E-08	0.22622589E-01	0.78299582E-01
2.0	0.96052620E-10	0.35647019E-09	0.22246022E-01	0.82525015E-01
2.1	0.13093008E-10	0.52091595E-10	0.21805894E-01	0.86756527E-01
2.2	0.16136364E-11	0.68987125E-11	0.21310456E-01	0.90994895E-01
2.3	0.18059762E-12	0.82822497E-12	0.20767201E-01	0.95238864E-01
2.4	0.18288631E-13	0.90149676E-13	0.20183034E-01	0.99487722E-01
2.5	0.16781350E-14	0.88983860E-14	0.19564416E-01	0.10374135E 00
2.6	0.13954705E-15	0.79667620E-15	0.18917296E-01	0.10799915E 00
2.7	0.10516805E-16	0.64701631E-16	0.18247195E-01	0.11226064E 00
2.8	0.71840279E-18	0.47673976E-17	0.17559160E-01	0.11652446E 00
2.9	0.44485961E-19	0.31875177E-18	0.16857959E-01	0.12079102E 00
3.0	0.24970596E-20	0.19338817E-19	0.16147807E-01	0.12505889E 00
3.1	0.12707176E-21	0.10648672E-20	0.15432838E-01	0.12932789E 00
3.2	0.58632749E-23	0.53226351E-22	0.14716774E-01	0.13359773E 00
3.3	0.24527633E-24	0.24148870E-23	0.14002964E-01	0.13786727E 00

3.4	0.93039950E-26	0.99471219E-25	0.13294619E-01	0.14213592E 00
3.5	0.32002369E-27	0.37200246E-26	0.12594681E-01	0.14640331E 00
3.6	0.99832550E-29	0.12633824E-27	0.11905834E-01	0.15066850E 00
3.7	0.28246419E-30	0.38967198E-29	0.11230629E-01	0.15493155E 00
3.8	0.72463673E-32	0.10912307E-30	0.10571193E-01	0.15919161E 00
3.9	0.16862812E-33	0.27756781E-32	0.99297985E-02	0.16344798E 00
4.0	0.35598667E-35	0.64135305E-34	0.93082637E-02	0.16769964E 00
4.1	0.68181892E-37	0.13462424E-35	0.87084211E-02	0.17194664E 00
4.2	0.11847695E-38	0.25669574E-37	0.81318654E-02	0.17618746E 00
4.3	0.18680743E-40	0.44464374E-39	0.75800866E-02	0.18042308E 00
4.4	0.26736615E-42	0.69984082E-41	0.70544146E-02	0.18465191E 00
4.5	0.34748106E-44	0.10010513E-42	0.65561011E-02	0.18887341E 00
4.6	0.41022470E-46	0.13014259E-44	0.60863160E-02	0.19308656E 00
4.7	0.43588737E-48	0.15371425E-46	0.56459419E-02	0.19729191E 00
4.8	0.42886544E-50	0.16503425E-48	0.52359700E-02	0.20148838E 00
4.9	0.38026606E-52	0.16102232E-50	0.48571639E-02	0.20567489E 00
5.0	0.30702354E-54	0.14284917E-52	0.45102984E-02	0.20985126E 00
5.1	0.22588669E-56	0.11521368E-54	0.41959956E-02	0.21401709E 00
5.2	0.15153103E-58	0.84448475E-57	0.39147884E-02	0.21817172E 00
5.3	0.92905970E-61	0.56321192E-59	0.36672466E-02	0.22231472E 00
5.4	0.52058694E-63	0.34132831E-61	0.34536936E-02	0.22644502E 00
5.5	0.26711842E-65	0.18807863E-63	0.32745693E-02	0.23056316E 00
5.6	0.12573563E-67	0.94264978E-66	0.31301274E-02	0.23466820E 00
5.7	0.54393655E-70	0.42994092E-68	0.30206463E-02	0.23875934E 00
5.8	0.21627621E-72	0.17825682E-70	0.29462760E-02	0.24283475E 00
5.9	0.79159836E-75	0.67227343E-73	0.29072079E-02	0.24689782E 00
6.0	0.26689319E-77	0.23067067E-75	0.29035048E-02	0.25094444E 00
6.1	0.0	0.72019684E-78	0.29352203E-02	0.25497514E 00
6.2	0.0	0.0	0.30023858E-02	0.25899029E 00
6.3	0.0	0.0	0.31049480E-02	0.26298785E 00
6.4	0.0	0.0	0.32428675E-02	0.26696950E 00
6.5	0.0	0.0	0.34160267E-02	0.27093321E 00
6.6	0.0	0.0	0.36243233E-02	0.27487898E 00
6.7	0.0	0.0	0.38675985E-02	0.27880692E 00
6.8	0.0	0.0	0.41456372E-02	0.28271556E 00
6.9	0.0	0.0	0.44582635E-02	0.28660578E 00
7.0	0.0	0.0	0.48052371E-02	0.29047656E 00
7.1	0.0	0.0	0.51862746E-02	0.29432654E 00
7.2	0.0	0.0	0.56011230E-02	0.29815632E 00
7.3	0.0	0.0	0.60494654E-02	0.30196661E 00
7.4	0.0	0.0	0.65310486E-02	0.30575556E 00
7.5	0.0	0.0	0.70454963E-02	0.30952430E 00
7.6	0.0	0.0	0.75924098E-02	0.31327039E 00
7.7	0.0	0.0	0.81715323E-02	0.31699562E 00

7.8	0.0	0.0	0.87824576E-02	0.32069874E 00
7.9	0.0	0.0	0.94247535E-02	0.32437897E 00
8.0	0.0	0.0	0.10098077E-01	0.32803744E 00
8.1	0.0	0.0	0.10801964E-01	0.33167183E 00
8.2	0.0	0.0	0.11536010E-01	0.33528376E 00
8.3	0.0	0.0	0.12299839E-01	0.33887237E 00
8.4	0.0	0.0	0.13093024E-01	0.34243870E 00
8.5	0.0	0.0	0.13915077E-01	0.34597981E 00
8.6	0.0	0.0	0.14765561E-01	0.34949738E 00
8.7	0.0	0.0	0.15644010E-01	0.35299009E 00
8.8	0.0	0.0	0.16549971E-01	0.35645884E 00
8.9	0.0	0.0	0.17483052E-01	0.35990429E 00
9.0	0.0	0.0	0.18442713E-01	0.36332327E 00
9.1	0.0	0.0	0.19428533E-01	0.36671901E 00
9.2	0.0	0.0	0.20440083E-01	0.37008941E 00
9.3	0.0	0.0	0.21476746E-01	0.37343454E 00
9.4	0.0	0.0	0.22538181E-01	0.37675488E 00
9.5	0.0	0.0	0.23623936E-01	0.38004988E 00
9.6	0.0	0.0	0.24733391E-01	0.38331836E 00
9.7	0.0	0.0	0.25866207E-01	0.38656229E 00
9.8	0.0	0.0	0.27021877E-01	0.38978106E 00
9.9	0.0	0.0	0.28199788E-01	0.39297318E 00
10.0	0.0	0.0	0.29399760E-01	0.39614093E 00
10.1	0.0	0.0	0.30621104E-01	0.39928079E 00
10.2	0.0	0.0	0.31863384E-01	0.40239674E 00
10.3	0.0	0.0	0.33126071E-01	0.40548617E 00
10.4	0.0	0.0	0.34408998E-01	0.40854949E 00
10.5	0.0	0.0	0.35711400E-01	0.41158718E 00
10.6	0.0	0.0	0.37032858E-01	0.41459990E 00
10.7	0.0	0.0	0.38373049E-01	0.41758525E 00
10.8	0.0	0.0	0.39731279E-01	0.42054361E 00
10.9	0.0	0.0	0.41107468E-01	0.42347801E 00
11.0	0.0	0.0	0.42500786E-01	0.42638528E 00
11.1	0.0	0.0	0.43911021E-01	0.42926753E 00
11.2	0.0	0.0	0.45337759E-01	0.43212366E 00
11.3	0.0	0.0	0.46780474E-01	0.43495345E 00
11.4	0.0	0.0	0.48238479E-01	0.43775696E 00
11.5	0.0	0.0	0.49711969E-01	0.44053519E 00
11.6	0.0	0.0	0.51200066E-01	0.44328833E 00
11.7	0.0	0.0	0.52702446E-01	0.44601583E 00
11.8	0.0	0.0	0.54218680E-01	0.44871604E 00
11.9	0.0	0.0	0.55748172E-01	0.45138991E 00
12.0	0.0	0.0	0.57291292E-01	0.45404291E 00

FREQUENCY = 2000.0 MHZ
SIGMA = 1.50 METERS
PLATFORM ALTITUDE = 321.8688 KM

PSI	SPECULAR		DIFFUSE	
(DEGREES)	VERTICAL	HORIZONTAL	VERTICAL	HORIZONTAL
0.1	0.25467731E-02	0.27139364E-02	0.26724534E-02	0.28478659E-02
0.2	0.41387156E-02	0.46999753E-02	0.50161635E-02	0.56986883E-02
0.3	0.45807175E-02	0.55458392E-02	0.70666037E-02	0.85523911E-02
0.4	0.40923543E-02	0.52787848E-02	0.88447593E-02	0.11408973E-01
0.5	0.31125732E-02	0.42794198E-02	0.10377072E-01	0.14268164E-01
0.6	0.20633945E-02	0.30246296E-02	0.11686105E-01	0.17130092E-01
0.7	0.12076080E-02	0.18874973E-02	0.12792323E-01	0.19994464E-01
0.8	0.62863203E-03	0.10478918E-02	0.13714552E-01	0.22861332E-01
0.9	0.29247929E-03	0.52008661E-03	0.14469959E-01	0.25730480E-01
1.0	0.12202910E-03	0.23153679E-03	0.15074350E-01	0.28601918E-01
1.1	0.45763663E-04	0.92678863E-04	0.15542187E-01	0.31475451E-01
1.2	0.15452999E-04	0.33413191E-04	0.15866728E-01	0.34351032E-01
1.3	0.47045487E-05	0.10864873E-04	0.16120113E-01	0.37228432E-01
1.4	0.12926175E-05	0.31896889E-05	0.16253624E-01	0.40107768E-01
1.5	0.32078788E-06	0.84616175E-06	0.16297419E-01	0.42988691E-01
1.6	0.71953593E-07	0.20297585E-06	0.16260989E-01	0.45871049E-01
1.7	0.14594242E-07	0.44049873E-07	0.16153049E-01	0.48754622E-01
1.8	0.26779963E-08	0.86532026E-08	0.15981570E-01	0.51639985E-01
1.9	0.44471582E-09	0.15392181E-08	0.15753921E-01	0.54526314E-01
2.0	0.66852698E-10	0.24800118E-09	0.15476849E-01	0.57413775E-01
2.1	0.91005476E-11	0.36207287E-10	0.15156608E-01	0.60301837E-01
2.2	0.11219654E-11	0.47907529E-11	0.14798872E-01	0.63190639E-01
2.3	0.12530542E-12	0.57465382E-12	0.14409069E-01	0.66080332E-01
2.4	0.12678653E-13	0.62496503E-13	0.13991956E-01	0.68970144E-01
2.5	0.11624231E-14	0.61638079E-14	0.13552044E-01	0.71860433E-01
2.6	0.96586691E-16	0.55141464E-15	0.13093498E-01	0.74750960E-01
2.7	0.72736283E-17	0.44748923E-16	0.12620118E-01	0.77641666E-01
2.8	0.49649996E-18	0.32948258E-17	0.12135424E-01	0.80531955E-01
2.9	0.30723368E-19	0.22013964E-18	0.11642624E-01	0.83421946E-01
3.0	0.17233896E-20	0.13347021E-19	0.11144694E-01	0.86311579E-01
3.1	0.87644618E-22	0.73486590E-21	0.10644421E-01	0.89200735E-01
3.2	0.40415529E-23	0.36888911E-22	0.10144267E-01	0.92088878E-01
3.3	0.16897021E-24	0.16636083E-23	0.96466057E-02	0.94976366E-01

3.4	0.64059234E-26	0.68487227E-25	0.91535188E-02	0.97862422E-01
3.5	0.22022431E-27	0.25599357E-26	0.86670332E-02	0.10074747E 00
3.6	0.68665572E-29	0.86896406E-28	0.81889220E-02	0.10363096E 00
3.7	0.19418964E-30	0.26789339E-29	0.77208802E-02	0.10651302E 00
3.8	0.49795645E-32	0.74987277E-31	0.72643198E-02	0.10939342E 00
3.9	0.11582978E-33	0.19065997E-32	0.68207271E-02	0.11227161E 00
4.0	0.24443180E-35	0.44037359E-34	0.63913502E-02	0.11514795E 00
4.1	0.46799269E-37	0.92404446E-36	0.59773587E-02	0.11802208E 00
4.2	0.81294491E-39	0.17613509E-37	0.55797845E-02	0.12089330E 00
4.3	0.12814185E-40	0.30500645E-39	0.51996112E-02	0.12376249E 00
4.4	0.18335183E-42	0.47993036E-41	0.48377104E-02	0.12662888E 00
4.5	0.23823438E-44	0.68632450E-43	0.44948868E-02	0.12949228E 00
4.6	0.28119040E-46	0.89206897E-45	0.41718930E-02	0.13235217E 00
4.7	0.30146646E-48	0.10534447E-46	0.38693133E-02	0.13520932E 00
4.8	0.29386454E-50	0.11308373E-48	0.35877589E-02	0.13806260E 00
4.9	0.26052887E-52	0.11031999E-50	0.33277532E-02	0.14091247E 00
5.0	0.21032633E-54	0.97858838E-53	0.30897779E-02	0.14375854E 00
5.1	0.15473123E-56	0.78920746E-55	0.28742356E-02	0.14660060E 00
5.2	0.10379254E-58	0.57843671E-57	0.26814693E-02	0.14943850E 00
5.3	0.63634955E-61	0.38576587E-59	0.25118417E-02	0.15227205E 00
5.4	0.35657004E-63	0.23378895E-61	0.23655682E-02	0.15510094E 00
5.5	0.18296383E-65	0.12882523E-63	0.22429293E-02	0.15792513E 00
5.6	0.86127600E-68	0.64570558E-66	0.21441050E-02	0.16074532E 00
5.7	0.37261820E-70	0.29452646E-68	0.20692630E-02	0.16355962E 00
5.8	0.14817324E-72	0.12212570E-70	0.20185267E-02	0.16636878E 00
5.9	0.54239912E-75	0.46063805E-73	0.19920038E-02	0.16917306E 00
6.0	0.18290132E-77	0.15807802E-75	0.19897651E-02	0.17197162E 00
6.1	0.0	0.0	0.20118500E-02	0.17476428E 00
6.2	0.0	0.0	0.20582946E-02	0.17755157E 00
6.3	0.0	0.0	0.21290767E-02	0.18033195E 00
6.4	0.0	0.0	0.22241964E-02	0.18310726E 00
6.5	0.0	0.0	0.23435857E-02	0.18587536E 00
6.6	0.0	0.0	0.24872185E-02	0.18863767E 00
6.7	0.0	0.0	0.26549953E-02	0.19139296E 00
6.8	0.0	0.0	0.28468135E-02	0.19414097E 00
6.9	0.0	0.0	0.30625851E-02	0.19688255E 00
7.0	0.0	0.0	0.33021832E-02	0.19961691E 00
7.1	0.0	0.0	0.35654625E-02	0.20234364E 00
7.2	0.0	0.0	0.38522866E-02	0.20506299E 00
7.3	0.0	0.0	0.41624643E-02	0.20777464E 00
7.4	0.0	0.0	0.44959076E-02	0.21047902E 00
7.5	0.0	0.0	0.48523620E-02	0.21317506E 00
7.6	0.0	0.0	0.52316487E-02	0.21586305E 00
7.7	0.0	0.0	0.56336224E-02	0.21854329E 00

7.8	0.0	0.0	0.60580522E-02	0.22121489E 00
7.9	0.0	0.0	0.65047108E-02	0.22387767E 00
8.0	0.0	0.0	0.69734156E-02	0.22653240E 00
8.1	0.0	0.0	0.74639171E-02	0.22917789E 00
8.2	0.0	0.0	0.79759806E-02	0.23181444E 00
8.3	0.0	0.0	0.85094087E-02	0.23444217E 00
8.4	0.0	0.0	0.90639442E-02	0.23706090E 00
8.5	0.0	0.0	0.96393712E-02	0.23966992E 00
8.6	0.0	0.0	0.10235418E-01	0.24226993E 00
8.7	0.0	0.0	0.10851830E-01	0.24485976E 00
8.8	0.0	0.0	0.11488363E-01	0.24744010E 00
8.9	0.0	0.0	0.12144774E-01	0.25001097E 00
9.0	0.0	0.0	0.12820836E-01	0.25257158E 00
9.1	0.0	0.0	0.13516229E-01	0.25512254E 00
9.2	0.0	0.0	0.14230765E-01	0.25766313E 00
9.3	0.0	0.0	0.14964104E-01	0.26019377E 00
9.4	0.0	0.0	0.15716039E-01	0.26271379E 00
9.5	0.0	0.0	0.16486306E-01	0.26522326E 00
9.6	0.0	0.0	0.17274573E-01	0.26772147E 00
9.7	0.0	0.0	0.18080655E-01	0.27020979E 00
9.8	0.0	0.0	0.18904291E-01	0.27268779E 00
9.9	0.0	0.0	0.19745104E-01	0.27515441E 00
10.0	0.0	0.0	0.20602919E-01	0.27760965E 00
10.1	0.0	0.0	0.21477487E-01	0.28005356E 00
10.2	0.0	0.0	0.22368476E-01	0.28248745E 00
10.3	0.0	0.0	0.23275603E-01	0.28490943E 00
10.4	0.0	0.0	0.24198774E-01	0.28732008E 00
10.5	0.0	0.0	0.25137484E-01	0.28971893E 00
10.6	0.0	0.0	0.26091643E-01	0.29210788E 00
10.7	0.0	0.0	0.27060967E-01	0.29448426E 00
10.8	0.0	0.0	0.28045043E-01	0.29684842E 00
10.9	0.0	0.0	0.29043783E-01	0.29920119E 00
11.0	0.0	0.0	0.30056853E-01	0.30154258E 00
11.1	0.0	0.0	0.31083949E-01	0.30387211E 00
11.2	0.0	0.0	0.32124948E-01	0.30618948E 00
11.3	0.0	0.0	0.33179477E-01	0.30849457E 00
11.4	0.0	0.0	0.34247179E-01	0.31078798E 00
11.5	0.0	0.0	0.35327990E-01	0.31306803E 00
11.6	0.0	0.0	0.36421672E-01	0.31533754E 00
11.7	0.0	0.0	0.37527889E-01	0.31759506E 00
11.8	0.0	0.0	0.38646348E-01	0.31983870E 00
11.9	0.0	0.0	0.39776798E-01	0.32207060E 00
12.0	0.0	0.0	0.40919214E-01	0.32429147E 00

FREQUENCY = 2000.0 MHZ
SIGMA = 1.50 METERS
PLATFORM ALTITUDE = 643.7376 KM

PSI (DEGREES)	SPECULAR VERTICAL	SPECULAR HORIZONTAL	DIFFUSE VERTICAL	DIFFUSE HORIZONTAL
0.1	0.18128452E-02	0.19318357E-02	0.19023072E-02	0.20271696E-02
0.2	0.29424280E-02	0.33414534E-02	0.35676723E-02	0.40514879E-02
0.3	0.32527340E-02	0.39366335E-02	0.50179400E-02	0.60729831E-02
0.4	0.29024663E-02	0.37439303E-02	0.62730648E-02	0.80917105E-02
0.5	0.22048056E-02	0.30315418E-02	0.73511191E-02	0.10107569E-01
0.6	0.14599953E-02	0.21401357E-02	0.82687326E-02	0.12120731E-01
0.7	0.85347402E-03	0.13339841E-02	0.90409443E-02	0.14131039E-01
0.8	0.44377268E-03	0.73974254E-03	0.96815713E-02	0.16138591E-01
0.9	0.20623699E-03	0.36673038E-03	0.10203253E-01	0.18143423E-01
1.0	0.85949854E-04	0.16308040E-03	0.10617454E-01	0.20145450E-01
1.1	0.32197320E-04	0.65204818E-04	0.10934807E-01	0.22144761E-01
1.2	0.10860083E-04	0.23482178E-04	0.11164900E-01	0.24141274E-01
1.3	0.33026890E-05	0.76273618E-05	0.11316650E-01	0.26135117E-01
1.4	0.90646864E-06	0.22368204E-05	0.11398111E-01	0.28126210E-01
1.5	0.22471909E-06	0.59275521E-06	0.11416707E-01	0.30114539E-01
1.6	0.50352359E-07	0.14204028E-06	0.11379261E-01	0.32100059E-01
1.7	0.10202353E-07	0.30793817E-07	0.11292063E-01	0.34082893E-01
1.8	0.18701884E-08	0.60429919E-08	0.11160780E-01	0.36062948E-01
1.9	0.31025004E-09	0.10738355E-08	0.10990724E-01	0.38040280E-01
2.0	0.46593618E-10	0.17284631E-09	0.10786705E-01	0.40014964E-01
2.1	0.63364878E-11	0.25210251E-10	0.10553174E-01	0.41986689E-01
2.2	0.78044532E-12	0.33324767E-11	0.10294173E-01	0.43955795E-01
2.3	0.87080029E-13	0.39935140E-12	0.10013469E-01	0.45922033E-01
2.4	0.88026815E-14	0.43390848E-13	0.97144954E-02	0.47885429E-01
2.5	0.80631607E-15	0.42755377E-14	0.94003901E-02	0.49846116E-01
2.6	0.66936467E-16	0.38214186E-15	0.90740547E-02	0.51803969E-01
2.7	0.50362594E-17	0.30984148E-16	0.87381676E-02	0.53759098E-01
2.8	0.34347372E-18	0.22793293E-17	0.83951652E-02	0.55711236E-01
2.9	0.21235681E-19	0.15215848E-18	0.80472641E-02	0.57660483E-01
3.0	0.11901750E-20	0.92174804E-20	0.76965429E-02	0.59606958E-01
3.1	0.60476702E-22	0.50679797E-21	0.73448829E-02	0.61550520E-01
3.2	0.27864673E-23	0.25295336E-22	0.69940127E-02	0.63491106E-01
3.3	0.11640318E-24	0.11460555E-23	0.66455230E-02	0.65428972E-01

3.4	0.4405198E-26	0.47143243E-25	0.63008294E-02	0.67363679E-01
3.5	0.15147340E-27	0.17607599E-26	0.59613064E-02	0.69295526E-01
3.6	0.47193010E-29	0.59722823E-28	0.56281462E-02	0.71224272E-01
3.7	0.13336411E-30	0.18398168E-29	0.53024888E-02	0.73150158E-01
3.8	0.34173120E-32	0.51461309E-31	0.49852654E-02	0.75073123E-01
3.9	0.79432940E-34	0.13074941E-32	0.46774708E-02	0.76992810E-01
4.0	0.16750651E-35	0.30178315E-34	0.43799244E-02	0.78909636E-01
4.1	0.32048851E-37	0.63280029E-36	0.40933862E-02	0.80823362E-01
4.2	0.55634212E-39	0.12053874E-37	0.38185488E-02	0.82733810E-01
4.3	0.87636453E-41	0.20859414E-39	0.35560231E-02	0.84641278E-01
4.4	0.12531341E-42	0.32801222E-41	0.33063751E-02	0.86545527E-01
4.5	0.16272074E-44	0.46877855E-43	0.30701335E-02	0.88446796E-01
4.6	0.19194241E-46	0.60893147E-45	0.28477621E-02	0.90344369E-01
4.7	0.20565888E-48	0.71865482E-47	0.26396259E-02	0.92239141E-01
4.8	0.20035575E-50	0.77100061E-49	0.24461199E-02	0.94130576E-01
4.9	0.17752600E-52	0.75172718E-51	0.22675523E-02	0.96018612E-01
5.0	0.14323790E-54	0.66644498E-53	0.21042223E-02	0.97903430E-01
5.1	0.10531897E-56	0.53718001E-55	0.19563700E-02	0.99784791E-01
5.2	0.70609950E-59	0.39350970E-57	0.18242002E-02	0.10166281E 00
5.3	0.43268594E-61	0.26230165E-59	0.17079273E-02	0.10353744E 00
5.4	0.24232925E-63	0.15888563E-61	0.16076681E-02	0.10540837E 00
5.5	0.12428438E-65	0.87508921E-64	0.15235860E-02	0.10727602E 00
5.6	0.58477645E-68	0.43841167E-66	0.14557729E-02	0.10914046E 00
5.7	0.25288057E-70	0.19988299E-68	0.14043231E-02	0.11100113E 00
5.8	0.10051485E-72	0.82845259E-71	0.13692884E-02	0.11285800E 00
5.9	0.36778619E-75	0.31234643E-73	0.13507239E-02	0.11471170E 00
6.0	0.12396971E-77	0.10714471E-75	0.13486543E-02	0.11656165E 00
6.1	0.0	0.0	0.13630854E-02	0.11840779E 00
6.2	0.0	0.0	0.13940230E-02	0.12025052E 00
6.3	0.0	0.0	0.14414345E-02	0.12208891E 00
6.4	0.0	0.0	0.15053041E-02	0.12392431E 00
6.5	0.0	0.0	0.15855706E-02	0.12575537E 00
6.6	0.0	0.0	0.16822030E-02	0.12758303E 00
6.7	0.0	0.0	0.17951238E-02	0.12940663E 00
6.8	0.0	0.0	0.19242496E-02	0.13122588E 00
6.9	0.0	0.0	0.20695196E-02	0.13304192E 00
7.0	0.0	0.0	0.22308289E-02	0.13485354E 00
7.1	0.0	0.0	0.24080893E-02	0.13666159E 00
7.2	0.0	0.0	0.26011863E-02	0.13846499E 00
7.3	0.0	0.0	0.28100009E-02	0.14026463E 00
7.4	0.0	0.0	0.30344592E-02	0.14206022E 00
7.5	0.0	0.0	0.32744061E-02	0.14385182E 00
7.6	0.0	0.0	0.35297065E-02	0.14563912E 00
7.7	0.0	0.0	0.38002606E-02	0.14742219E 00

7.8	0.0	0.0	0.40859245E-02	0.14920098E 00
7.9	0.0	0.0	0.43865554E-02	0.15097547E 00
8.0	0.0	0.0	0.47020242E-02	0.15274584E 00
8.1	0.0	0.0	0.50321706E-02	0.15451169E 00
8.2	0.0	0.0	0.53768493E-02	0.15627319E 00
8.3	0.0	0.0	0.57359301E-02	0.15803027E 00
8.4	0.0	0.0	0.61092600E-02	0.15978324E 00
8.5	0.0	0.0	0.64966828E-02	0.16153121E 00
8.6	0.0	0.0	0.68980344E-02	0.16327488E 00
8.7	0.0	0.0	0.73131770E-02	0.16501397E 00
8.8	0.0	0.0	0.77419430E-02	0.16674852E 00
8.9	0.0	0.0	0.81841648E-02	0.16847837E 00
9.0	0.0	0.0	0.86397305E-02	0.17020345E 00
9.1	0.0	0.0	0.91084391E-02	0.17192435E 00
9.2	0.0	0.0	0.95901638E-02	0.17364001E 00
9.3	0.0	0.0	0.10084707E-01	0.17535132E 00
9.4	0.0	0.0	0.10591950E-01	0.17705810E 00
9.5	0.0	0.0	0.11111710E-01	0.17875940E 00
9.6	0.0	0.0	0.11643786E-01	0.18045551E 00
9.7	0.0	0.0	0.12188107E-01	0.18214732E 00
9.8	0.0	0.0	0.12744479E-01	0.18383455E 00
9.9	0.0	0.0	0.13312690E-01	0.18551660E 00
10.0	0.0	0.0	0.13892625E-01	0.18719321E 00
10.1	0.0	0.0	0.14484186E-01	0.18886501E 00
10.2	0.0	0.0	0.15087117E-01	0.19053233E 00
10.3	0.0	0.0	0.15701246E-01	0.19219410E 00
10.4	0.0	0.0	0.16326558E-01	0.19385058E 00
10.5	0.0	0.0	0.16962759E-01	0.19550204E 00
10.6	0.0	0.0	0.17609730E-01	0.19714892E 00
10.7	0.0	0.0	0.18267367E-01	0.19879007E 00
10.8	0.0	0.0	0.18935431E-01	0.20042586E 00
10.9	0.0	0.0	0.19613862E-01	0.20205677E 00
11.0	0.0	0.0	0.20302411E-01	0.20368212E 00
11.1	0.0	0.0	0.21000996E-01	0.20530272E 00
11.2	0.0	0.0	0.21709461E-01	0.20691741E 00
11.3	0.0	0.0	0.22427659E-01	0.20852691E 00
11.4	0.0	0.0	0.23155313E-01	0.21013099E 00
11.5	0.0	0.0	0.23892466E-01	0.21172923E 00
11.6	0.0	0.0	0.24638854E-01	0.21332234E 00
11.7	0.0	0.0	0.25394421E-01	0.21491057E 00
11.8	0.0	0.0	0.26158955E-01	0.21649259E 00
11.9	0.0	0.0	0.26932251E-01	0.21806896E 00
12.0	0.0	0.0	0.27714387E-01	0.21964103E 00

FREQUENCY = 2000.0 MHZ
SIGMA = 1.50 METERS
PLATFORM ALTITUDE = 1267.4750 KM

PSI	SPECULAR		DIFFUSE	
(DEGREES)	VERTICAL	HORIZONTAL	VERTICAL	HORIZONTAL
0.1	0.12875306E-02	0.13720407E-02	0.13510687E-02	0.14397493E-02
0.2	0.20873435E-02	0.23704129E-02	0.25308887E-02	0.28741085E-02
0.3	0.23047826E-02	0.27893751E-02	0.35555509E-02	0.43031238E-02
0.4	0.20542110E-02	0.26497543E-02	0.44397414E-02	0.57268813E-02
0.5	0.15586535E-02	0.21431015E-02	0.51967613E-02	0.71453899E-02
0.6	0.10309406E-02	0.15112050E-02	0.58387667E-02	0.85587613E-02
0.7	0.60197432E-03	0.94088889E-03	0.63767806E-02	0.99669397E-02
0.8	0.31265034E-03	0.52116928E-03	0.68209358E-02	0.11370093E-01
0.9	0.14513661E-03	0.25808183E-03	0.71804076E-02	0.12768202E-01
1.0	0.60418650E-04	0.11463773E-03	0.74635632E-02	0.14161289E-01
1.1	0.22608147E-04	0.45785171E-04	0.76781437E-02	0.15549488E-01
1.2	0.76172964E-05	0.16470469E-04	0.78310966E-02	0.16932767E-01
1.3	0.23139801E-05	0.53439990E-05	0.79288408E-02	0.18311188E-01
1.4	0.63441371E-06	0.15654914E-05	0.79772398E-02	0.19684795E-01
1.5	0.15710543E-06	0.41440654E-06	0.79816394E-02	0.21053653E-01
1.6	0.35164661E-07	0.99196882E-07	0.79469532E-02	0.22417765E-01
1.7	0.71174391E-08	0.21482606E-07	0.78776516E-02	0.23777157E-01
1.8	0.13033195E-08	0.42113122E-08	0.77778585E-02	0.25131978E-01
1.9	0.21598791E-09	0.74756112E-09	0.76513030E-02	0.26482116E-01
2.0	0.32402817E-10	0.12020329E-09	0.75014494E-02	0.27827788E-01
2.1	0.44020647E-11	0.17513976E-10	0.73314682E-02	0.29168859E-01
2.2	0.54163136E-12	0.23127498E-11	0.71441866E-02	0.30505467E-01
2.3	0.60372334E-13	0.27686924E-12	0.69423094E-02	0.31837624E-01
2.4	0.60967026E-14	0.30052326E-13	0.67282207E-02	0.33165254E-01
2.5	0.55788978E-15	0.29582448E-14	0.65041259E-02	0.34488525E-01
2.6	0.46267335E-16	0.26414108E-15	0.62720999E-02	0.35807539E-01
2.7	0.34776824E-17	0.21395457E-16	0.60339570E-02	0.37122212E-01
2.8	0.23694558E-18	0.15723976E-17	0.57914108E-02	0.38432460E-01
2.9	0.14635239E-19	0.10486479E-18	0.55460259E-02	0.39738540E-01
3.0	0.81945467E-21	0.63463785E-20	0.52991919E-02	0.41040327E-01
3.1	0.41599311E-22	0.34860432E-21	0.50522275E-02	0.42337935E-01
3.2	0.19148762E-23	0.17383112E-22	0.48063248E-02	0.43631483E-01
3.3	0.79917329E-25	0.78683314E-24	0.45625269E-02	0.44920743E-01

3.4	0.30245711E-26	0.32336435E-25	0.43218546E-02	0.46206012E-01
3.5	0.10380209E-27	0.12066182E-26	0.40851794E-02	0.47487028E-01
3.6	0.32310951E-29	0.40889563E-28	0.38533409E-02	0.48764102E-01
3.7	0.91225179E-31	0.12584929E-29	0.36270670E-02	0.50037030E-01
3.8	0.23354411E-32	0.35169416E-31	0.34070029E-02	0.51306065E-01
3.9	0.54237160E-34	0.89276316E-33	0.31937980E-02	0.52571058E-01
4.0	0.11427313E-35	0.20587693E-34	0.29879906E-02	0.53832270E-01
4.1	0.21844517E-37	0.43131716E-36	0.27900545E-02	0.55089269E-01
4.2	0.37887415E-39	0.82088036E-38	0.26004666E-02	0.56342516E-01
4.3	0.59629766E-41	0.14193228E-39	0.24195963E-02	0.57591844E-01
4.4	0.85193199E-43	0.22299633E-41	0.22478094E-02	0.58837246E-01
4.5	0.11053083E-44	0.31842616E-43	0.20854406E-02	0.60079049E-01
4.6	0.13027066E-46	0.41328009E-45	0.19327665E-02	0.61316464E-01
4.7	0.13946448E-48	0.48734465E-47	0.17900227E-02	0.62550545E-01
4.8	0.13575662E-50	0.52241221E-49	0.16574366E-02	0.63780725E-01
4.9	0.12018992E-52	0.50893966E-51	0.15351942E-02	0.65007210E-01
5.0	0.96897832E-55	0.45083742E-53	0.14234679E-02	0.66229820E-01
5.1	0.71189608E-57	0.36310297E-55	0.13223945E-02	0.67448795E-01
5.2	0.47690652E-59	0.26578033E-57	0.12320827E-02	0.68664074E-01
5.3	0.29201233E-61	0.17702278E-59	0.11526502E-02	0.69875598E-01
5.4	0.16341763E-63	0.10714647E-61	0.10841505E-02	0.71083426E-01
5.5	0.83748618E-66	0.58967567E-64	0.10266635E-02	0.72287560E-01
5.6	0.39375158E-68	0.29519872E-66	0.98022586E-03	0.73488295E-01
5.7	0.17014634E-70	0.13448785E-68	0.94487472E-03	0.74685216E-01
5.8	0.67579874E-73	0.55699941E-71	0.92062354E-03	0.75878620E-01
5.9	0.24709541E-75	0.20984844E-73	0.90747769E-03	0.77068508E-01
6.0	0.83228079E-78	0.71932489E-76	0.90542994E-03	0.78254640E-01
6.1	0.0	0.0	0.91446401E-03	0.79437137E-01
6.2	0.0	0.0	0.93455962E-03	0.80616474E-01
6.3	0.0	0.0	0.96566882E-03	0.81791699E-01
6.4	0.0	0.0	0.10077620E-02	0.82964063E-01
6.5	0.0	0.0	0.10607745E-02	0.84132493E-01
6.6	0.0	0.0	0.11246644E-02	0.85297704E-01
6.7	0.0	0.0	0.11993595E-02	0.86459279E-01
6.8	0.0	0.0	0.12847874E-02	0.87617159E-01
6.9	0.0	0.0	0.13808843E-02	0.88772058E-01
7.0	0.0	0.0	0.14875645E-02	0.89923263E-01
7.1	0.0	0.0	0.16047454E-02	0.91070890E-01
7.2	0.0	0.0	0.17323440E-02	0.92215240E-01
7.3	0.0	0.0	0.18702578E-02	0.93356133E-01
7.4	0.0	0.0	0.20184179E-02	0.94493568E-01
7.5	0.0	0.0	0.21767153E-02	0.95627844E-01
7.6	0.0	0.0	0.23450444E-02	0.96758783E-01
7.7	0.0	0.0	0.25233126E-02	0.97885966E-01

7.8	0.0	0.0	0.27114262E-02	0.99009931E-01
7.9	0.0	0.0	0.29092750E-02	0.10013074E 00
8.0	0.0	0.0	0.31167534E-02	0.10124809E 00
8.1	0.0	0.0	0.33337583E-02	0.10236228E 00
8.2	0.0	0.0	0.35601633E-02	0.10347277E 00
8.3	0.0	0.0	0.37958766E-02	0.10457993E 00
8.4	0.0	0.0	0.40408000E-02	0.10568416E 00
8.5	0.0	0.0	0.42948164E-02	0.10678482E 00
8.6	0.0	0.0	0.45578107E-02	0.10788232E 00
8.7	0.0	0.0	0.48296750E-02	0.10897636E 00
8.8	0.0	0.0	0.51103085E-02	0.11006755E 00
8.9	0.0	0.0	0.53995699E-02	0.11115497E 00
9.0	0.0	0.0	0.56974106E-02	0.11223942E 00
9.1	0.0	0.0	0.60036518E-02	0.11332059E 00
9.2	0.0	0.0	0.63182339E-02	0.11439830E 00
9.3	0.0	0.0	0.66410154E-02	0.11547297E 00
9.4	0.0	0.0	0.69719031E-02	0.11654425E 00
9.5	0.0	0.0	0.73108003E-02	0.11761230E 00
9.6	0.0	0.0	0.76575540E-02	0.11867678E 00
9.7	0.0	0.0	0.80121271E-02	0.11973864E 00
9.8	0.0	0.0	0.83743557E-02	0.12079704E 00
9.9	0.0	0.0	0.87441243E-02	0.12185216E 00
10.0	0.0	0.0	0.91213882E-02	0.12290418E 00
10.1	0.0	0.0	0.95060095E-02	0.12395263E 00
10.2	0.0	0.0	0.98978840E-02	0.12499851E 00
10.3	0.0	0.0	0.10296870E-01	0.12604076E 00
10.4	0.0	0.0	0.10702964E-01	0.12707984E 00
10.5	0.0	0.0	0.11115961E-01	0.12811553E 00
10.6	0.0	0.0	0.11535827E-01	0.12914884E 00
10.7	0.0	0.0	0.11962458E-01	0.13017845E 00
10.8	0.0	0.0	0.12395676E-01	0.13120443E 00
10.9	0.0	0.0	0.12835465E-01	0.13222748E 00
11.0	0.0	0.0	0.13281722E-01	0.13324761E 00
11.1	0.0	0.0	0.13734348E-01	0.13426489E 00
11.2	0.0	0.0	0.14193233E-01	0.13527864E 00
11.3	0.0	0.0	0.14658272E-01	0.13628900E 00
11.4	0.0	0.0	0.15129350E-01	0.13729656E 00
11.5	0.0	0.0	0.15606429E-01	0.13830030E 00
11.6	0.0	0.0	0.16089395E-01	0.13930130E 00
11.7	0.0	0.0	0.16578183E-01	0.14029956E 00
11.8	0.0	0.0	0.17072663E-01	0.14129400E 00
11.9	0.0	0.0	0.17572764E-01	0.14228570E 00
12.0	0.0	0.0	0.18078417E-01	0.14327443E 00

FREQUENCY = 2000.0 MHZ
SIGMA = 15.00 METERS
PLATFORM ALTITUDE = 0.0960 KM

PSI (DEGREES)	SPECULAR VERTICAL	SPECULAR HORIZONTAL	DIFFUSE VERTICAL	DIFFUSE HORIZONTAL
0.1	0.15530914E-03	0.16550322E-03	0.19194752E-01	0.20454645E-01
0.2	0.15703279E-09	0.17832838E-09	0.36635257E-01	0.41603450E-01
0.3	0.77876857E-20	0.94250801E-20	0.52370198E-01	0.63381255E-01
0.4	0.22451311E-34	0.28960289E-34	0.66448689E-01	0.85713148E-01
0.5	0.39707136E-53	0.54596125E-53	0.78924596E-01	0.10851896E 00
0.6	0.44132449E-76	0.64691621E-76	0.89848876E-01	0.13170511E 00
0.7	0.0	0.0	0.99285305E-01	0.15518343E 00
0.8	0.0	0.0	0.10729200E 00	0.17884934E 00
0.9	0.0	0.0	0.11394435E 00	0.20261580E 00
1.0	0.0	0.0	0.11930871E 00	0.22637516E 00
1.1	0.0	0.0	0.12347025E 00	0.25004733E 00
1.2	0.0	0.0	0.12650901E 00	0.27354378E 00
1.3	0.0	0.0	0.12850606E 00	0.29677707E 00
1.4	0.0	0.0	0.12954599E 00	0.31967032E 00
1.5	0.0	0.0	0.12971568E 00	0.34215891E 00
1.6	0.0	0.0	0.12910038E 00	0.36418271E 00
1.7	0.0	0.0	0.12778932E 00	0.38570702E 00
1.8	0.0	0.0	0.12585425E 00	0.40666294E 00
1.9	0.0	0.0	0.12337756E 00	0.42702532E 00
2.0	0.0	0.0	0.12043804E 00	0.44678372E 00
2.1	0.0	0.0	0.11709690E 00	0.46588004E 00
2.2	0.0	0.0	0.11343122E 00	0.48434782E 00
2.3	0.0	0.0	0.10949582E 00	0.50215083E 00
2.4	0.0	0.0	0.10534590E 00	0.51927918E 00
2.5	0.0	0.0	0.10103655E 00	0.53575236E 00
2.6	0.0	0.0	0.96616089E-01	0.55158311E 00
2.7	0.0	0.0	0.92125297E-01	0.56677479E 00
2.8	0.0	0.0	0.87597370E-01	0.58130592E 00
2.9	0.0	0.0	0.83073974E-01	0.59524399E 00
3.0	0.0	0.0	0.78579307E-01	0.60856855E 00
3.1	0.0	0.0	0.74143291E-01	0.62132496E 00
3.2	0.0	0.0	0.69784105E-01	0.63349515E 00
3.3	0.0	0.0	0.65524638E-01	0.64512813E 00

3.4	0.0	0.0	0.61381210E-01	0.65624136E 00
3.5	0.0	0.0	0.57366051E-01	0.66683555E 00
3.6	0.0	0.0	0.53491786E-01	0.67693973E 00
3.7	0.0	0.0	0.49768794E-01	0.68658298E 00
3.8	0.0	0.0	0.46203919E-01	0.69578493E 00
3.9	0.0	0.0	0.42803362E-01	0.70455879E 00
4.0	0.0	0.0	0.39571185E-01	0.71292299E 00
4.1	0.0	0.0	0.36510866E-01	0.72090232E 00
4.2	0.0	0.0	0.33623088E-01	0.72848821E 00
4.3	0.0	0.0	0.30910302E-01	0.73573500E 00
4.4	0.0	0.0	0.28372161E-01	0.74265188E 00
4.5	0.0	0.0	0.26007514E-01	0.74924546E 00
4.6	0.0	0.0	0.23814287E-01	0.75550145E 00
4.7	0.0	0.0	0.21791667E-01	0.76148850E 00
4.8	0.0	0.0	0.19936461E-01	0.76718664E 00
4.9	0.0	0.0	0.18246144E-01	0.77262658E 00
5.0	0.0	0.0	0.16717236E-01	0.77780533E 00
5.1	0.0	0.0	0.15346445E-01	0.78274679E 00
5.2	0.0	0.0	0.14129907E-01	0.78746164E 00
5.3	0.0	0.0	0.13064004E-01	0.79196268E 00
5.4	0.0	0.0	0.12144189E-01	0.79624695E 00
5.5	0.0	0.0	0.11366576E-01	0.80032343E 00
5.6	0.0	0.0	0.10727271E-01	0.80423272E 00
5.7	0.0	0.0	0.10221694E-01	0.80794829E 00
5.8	0.0	0.0	0.98456554E-02	0.81148809E 00
5.9	0.0	0.0	0.95951483E-02	0.81487870E 00
6.0	0.0	0.0	0.94657429E-02	0.81810707E 00
6.1	0.0	0.0	0.94533265E-02	0.82118678E 00
6.2	0.0	0.0	0.95537528E-02	0.82412118E 00
6.3	0.0	0.0	0.97630732E-02	0.82692868E 00
6.4	0.0	0.0	0.10077070E-01	0.82959646E 00
6.5	0.0	0.0	0.10491949E-01	0.83214176E 00
6.6	0.0	0.0	0.11003911E-01	0.83456832E 00
6.7	0.0	0.0	0.11609461E-01	0.83690172E 00
6.8	0.0	0.0	0.12304358E-01	0.83910739E 00
6.9	0.0	0.0	0.13085593E-01	0.84122610E 00
7.0	0.0	0.0	0.13949353E-01	0.84323859E 00
7.1	0.0	0.0	0.14892250E-01	0.84515113E 00
7.2	0.0	0.0	0.15911300E-01	0.84698272E 00
7.3	0.0	0.0	0.17003044E-01	0.84872806E 00
7.4	0.0	0.0	0.18164441E-01	0.85038084E 00
7.5	0.0	0.0	0.19392733E-01	0.85196579E 00
7.6	0.0	0.0	0.20684663E-01	0.85346967E 00
7.7	0.0	0.0	0.22037894E-01	0.85490894E 00

7.8	0.0	0.0	0.23449592E-01	0.85628146E 00
7.9	0.0	0.0	0.24916656E-01	0.85757589E 00
8.0	0.0	0.0	0.26437286E-01	0.85881901E 00
8.1	0.0	0.0	0.28008468E-01	0.85999388E 00
8.2	0.0	0.0	0.29627986E-01	0.86111015E 00
8.3	0.0	0.0	0.31293657E-01	0.86216986E 00
8.4	0.0	0.0	0.33003502E-01	0.86318272E 00
8.5	0.0	0.0	0.34755092E-01	0.86413842E 00
8.6	0.0	0.0	0.36546413E-01	0.86504507E 00
8.7	0.0	0.0	0.38375683E-01	0.86590576E 00
8.8	0.0	0.0	0.40240761E-01	0.86671883E 00
8.9	0.0	0.0	0.42140059E-01	0.86749077E 00
9.0	0.0	0.0	0.44071723E-01	0.86821675E 00
9.1	0.0	0.0	0.46034057E-01	0.86890584E 00
9.2	0.0	0.0	0.48025206E-01	0.86954731E 00
9.3	0.0	0.0	0.50044391E-01	0.87016439E 00
9.4	0.0	0.0	0.52089293E-01	0.87073958E 00
9.5	0.0	0.0	0.54158613E-01	0.87127584E 00
9.6	0.0	0.0	0.56251328E-01	0.87178361E 00
9.7	0.0	0.0	0.58365669E-01	0.87225640E 00
9.8	0.0	0.0	0.60500689E-01	0.87270087E 00
9.9	0.0	0.0	0.62654674E-01	0.87311387E 00
10.0	0.0	0.0	0.64827263E-01	0.87350166E 00
10.1	0.0	0.0	0.67016006E-01	0.87384856E 00
10.2	0.0	0.0	0.69220662E-01	0.87417525E 00
10.3	0.0	0.0	0.71440339E-01	0.87447941E 00
10.4	0.0	0.0	0.73674500E-01	0.87476200E 00
10.5	0.0	0.0	0.75920880E-01	0.87501645E 00
10.6	0.0	0.0	0.78178883E-01	0.87524891E 00
10.7	0.0	0.0	0.80447972E-01	0.87545520E 00
10.8	0.0	0.0	0.82727015E-01	0.87564099E 00
10.9	0.0	0.0	0.85015535E-01	0.87580770E 00
11.0	0.0	0.0	0.87312102E-01	0.87595069E 00
11.1	0.0	0.0	0.89616179E-01	0.87607449E 00
11.2	0.0	0.0	0.91927469E-01	0.87618029E 00
11.3	0.0	0.0	0.94245434E-01	0.87627131E 00
11.4	0.0	0.0	0.96567988E-01	0.87634039E 00
11.5	0.0	0.0	0.98895967E-01	0.87639207E 00
11.6	0.0	0.0	0.10122800E 00	0.87642866E 00
11.7	0.0	0.0	0.10356414E 00	0.87645382E 00
11.8	0.0	0.0	0.10590255E 00	0.87645400E 00
11.9	0.0	0.0	0.10824323E 00	0.87643987E 00
12.0	0.0	0.0	0.11058766E 00	0.87642545E 00

FREQUENCY = 2000.0 MHZ
SIGMA = 15.00 METERS
PLATFORM ALTITUDE = 15.2400 KM

PSI (DEGREES)	SPECULAR VERTICAL	SPECULAR HORIZONTAL	DIFFUSE VERTICAL	DIFFUSE HORIZONTAL
0.1	0.97877797E-04	0.10430222E-03	0.12096778E-01	0.12890775E-01
0.2	0.98344111E-10	0.11168079E-09	0.22943374E-01	0.26054777E-01
0.3	0.48504999E-20	0.58703425E-20	0.32618370E-01	0.39476555E-01
0.4	0.13919251E-34	0.17954597E-34	0.41196458E-01	0.53139862E-01
0.5	0.24524835E-53	0.33720877E-53	0.48747230E-01	0.67025900E-01
0.6	0.27180570E-76	0.39842648E-76	0.55336695E-01	0.81115305E-01
0.7	0.0	0.0	0.61028458E-01	0.95387757E-01
0.8	0.0	0.0	0.65881014E-01	0.10981965E 00
0.9	0.0	0.0	0.69952488E-01	0.12438953E 00
1.0	0.0	0.0	0.73297560E-01	0.13907403E 00
1.1	0.0	0.0	0.75968862E-01	0.15384936E 00
1.2	0.0	0.0	0.78016162E-01	0.16869020E 00
1.3	0.0	0.0	0.79488277E-01	0.18357337E 00
1.4	0.0	0.0	0.80431163E-01	0.19847363E 00
1.5	0.0	0.0	0.80889583E-01	0.21336746E 00
1.6	0.0	0.0	0.80906332E-01	0.22823071E 00
1.7	0.0	0.0	0.80524385E-01	0.24304718E 00
1.8	0.0	0.0	0.79778969E-01	0.25778365E 00
1.9	0.0	0.0	0.78710139E-01	0.27242583E 00
2.0	0.0	0.0	0.77354431E-01	0.28695852E 00
2.1	0.0	0.0	0.75742841E-01	0.30134934E 00
2.2	0.0	0.0	0.73909998E-01	0.31559336E 00
2.3	0.0	0.0	0.71885586E-01	0.32966930E 00
2.4	0.0	0.0	0.69697142E-01	0.34355646E 00
2.5	0.0	0.0	0.67373455E-01	0.35725194E 00
2.6	0.0	0.0	0.64939559E-01	0.37074149E 00
2.7	0.0	0.0	0.62418886E-01	0.38401455E 00
2.8	0.0	0.0	0.59831001E-01	0.39704508E 00
2.9	0.0	0.0	0.57199497E-01	0.40984726E 00
3.0	0.0	0.0	0.54540653E-01	0.42239773E 00
3.1	0.0	0.0	0.51872831E-01	0.43469685E 00
3.2	0.0	0.0	0.49211483E-01	0.44673818E 00
3.3	0.0	0.0	0.46571638E-01	0.45852494E 00

3.4	0.0	0.0	0.43965522E-01	0.47004598E 00
3.5	0.0	0.0	0.41404895E-01	0.48129964E 00
3.6	0.0	0.0	0.38899612E-01	0.49227536E 00
3.7	0.0	0.0	0.36460996E-01	0.50299579E 00
3.8	0.0	0.0	0.34095522E-01	0.51344448E 00
3.9	0.0	0.0	0.31811893E-01	0.52363515E 00
4.0	0.0	0.0	0.29615138E-01	0.53355265E 00
4.1	0.0	0.0	0.27511634E-01	0.54321373E 00
4.2	0.0	0.0	0.25505319E-01	0.55260605E 00
4.3	0.0	0.0	0.23600612E-01	0.56174797E 00
4.4	0.0	0.0	0.21800745E-01	0.57064259E 00
4.5	0.0	0.0	0.20108022E-01	0.57928824E 00
4.6	0.0	0.0	0.18524181E-01	0.58767438E 00
4.7	0.0	0.0	0.17051127E-01	0.59583503E 00
4.8	0.0	0.0	0.15689366E-01	0.60375178E 00
4.9	0.0	0.0	0.14439609E-01	0.61144042E 00
5.0	0.0	0.0	0.13301823E-01	0.61889595E 00
5.1	0.0	0.0	0.12275930E-01	0.62613481E 00
5.2	0.0	0.0	0.11361189E-01	0.63316083E 00
5.3	0.0	0.0	0.10556776E-01	0.63997006E 00
5.4	0.0	0.0	0.98614842E-02	0.64657897E 00
5.5	0.0	0.0	0.92738643E-02	0.65297538E 00
5.6	0.0	0.0	0.87926500E-02	0.65919274E 00
5.7	0.0	0.0	0.84158145E-02	0.66520697E 00
5.8	0.0	0.0	0.81415549E-02	0.67103451E 00
5.9	0.0	0.0	0.79679638E-02	0.67668855E 00
6.0	0.0	0.0	0.78928731E-02	0.68216670E 00
6.1	0.0	0.0	0.79140067E-02	0.68747008E 00
6.2	0.0	0.0	0.80291741E-02	0.69260901E 00
6.3	0.0	0.0	0.82360767E-02	0.69759285E 00
6.4	0.0	0.0	0.85321553E-02	0.70241141E 00
6.5	0.0	0.0	0.89150965E-02	0.70707786E 00
6.6	0.0	0.0	0.93825646E-02	0.71160090E 00
6.7	0.0	0.0	0.99321343E-02	0.71598697E 00
6.8	0.0	0.0	0.10561086E-01	0.72022295E 00
6.9	0.0	0.0	0.11267312E-01	0.72433537E 00
7.0	0.0	0.0	0.12048144E-01	0.72831047E 00
7.1	0.0	0.0	0.12901224E-01	0.73215801E 00
7.2	0.0	0.0	0.13824273E-01	0.73588669E 00
7.3	0.0	0.0	0.14814712E-01	0.73949462E 00
7.4	0.0	0.0	0.15870366E-01	0.74298233E 00
7.5	0.0	0.0	0.16989093E-01	0.74636841E 00
7.6	0.0	0.0	0.18168226E-01	0.74963892E 00
7.7	0.0	0.0	0.19406002E-01	0.75281078E 00

7.8	0.0	0.0	0.20700004E-01	0.75587821E 00
7.9	0.0	0.0	0.22048049E-01	0.75884485E 00
8.0	0.0	0.0	0.23448296E-01	0.76172107E 00
8.1	0.0	0.0	0.24898376E-01	0.76449901E 00
8.2	0.0	0.0	0.26396405E-01	0.76718736E 00
8.3	0.0	0.0	0.27940538E-01	0.76978821E 00
8.4	0.0	0.0	0.29529031E-01	0.77231061E 00
8.5	0.0	0.0	0.31159736E-01	0.77474469E 00
8.6	0.0	0.0	0.32831058E-01	0.77710366E 00
8.7	0.0	0.0	0.34541313E-01	0.77938753E 00
8.8	0.0	0.0	0.36288269E-01	0.78158879E 00
8.9	0.0	0.0	0.38070876E-01	0.78372300E 00
9.0	0.0	0.0	0.39887536E-01	0.78578800E 00
9.1	0.0	0.0	0.41736409E-01	0.78778642E 00
9.2	0.0	0.0	0.43615680E-01	0.78970820E 00
9.3	0.0	0.0	0.45524981E-01	0.79158163E 00
9.4	0.0	0.0	0.47461879E-01	0.79338652E 00
9.5	0.0	0.0	0.49425550E-01	0.79513264E 00
9.6	0.0	0.0	0.51414255E-01	0.79681873E 00
9.7	0.0	0.0	0.53426936E-01	0.79844844E 00
9.8	0.0	0.0	0.55462386E-01	0.80002517E 00
9.9	0.0	0.0	0.57519015E-01	0.80154610E 00
10.0	0.0	0.0	0.59596464E-01	0.80302012E 00
10.1	0.0	0.0	0.61692595E-01	0.80443436E 00
10.2	0.0	0.0	0.63806891E-01	0.80580556E 00
10.3	0.0	0.0	0.65938592E-01	0.80713445E 00
10.4	0.0	0.0	0.68086565E-01	0.80841500E 00
10.5	0.0	0.0	0.70249259E-01	0.80964929E 00
10.6	0.0	0.0	0.72425961E-01	0.81084222E 00
10.7	0.0	0.0	0.74616075E-01	0.81199145E 00
10.8	0.0	0.0	0.76818526E-01	0.81310093E 00
10.9	0.0	0.0	0.79032183E-01	0.81416821E 00
11.0	0.0	0.0	0.81256390E-01	0.81519777E 00
11.1	0.0	0.0	0.83490610E-01	0.81619167E 00
11.2	0.0	0.0	0.85734069E-01	0.81714952E 00
11.3	0.0	0.0	0.87986231E-01	0.81807458E 00
11.4	0.0	0.0	0.90245247E-01	0.81896210E 00
11.5	0.0	0.0	0.92511177E-01	0.81981140E 00
11.6	0.0	0.0	0.94784021E-01	0.82063705E 00
11.7	0.0	0.0	0.97062528E-01	0.82143134E 00
11.8	0.0	0.0	0.99345744E-01	0.82218969E 00
11.9	0.0	0.0	0.10163307E 00	0.82291758E 00
12.0	0.0	0.0	0.10392535E 00	0.82362556E 00

FREQUENCY = 2000.0 MHZ
SIGMA = 15.00 METERS
PLATFORM ALTITUDE = 30.4800 KM

PSI (DEGREES)	SPECULAR VERTICAL	SPECULAR HORIZONTAL	DIFFUSE VERTICAL	DIFFUSE HORIZONTAL
0.1	0.69215006E-04	0.73758085E-04	0.85543245E-02	0.91158077E-02
0.2	0.69306727E-10	0.78705584E-10	0.16169041E-01	0.18361766E-01
0.3	0.34075091E-20	0.41239574E-20	0.22914637E-01	0.27732562E-01
0.4	0.97500692E-35	0.12576745E-34	0.28857071E-01	0.37223127E-01
0.5	0.17134189E-53	0.23559004E-53	0.34057084E-01	0.46827473E-01
0.6	0.18945359E-76	0.27771081E-76	0.38570706E-01	0.56538902E-01
0.7	0.0	0.0	0.42451147E-01	0.66351295E-01
0.8	0.0	0.0	0.45746509E-01	0.76256633E-01
0.9	0.0	0.0	0.48503969E-01	0.86249650E-01
1.0	0.0	0.0	0.50765030E-01	0.96320987E-01
1.1	0.0	0.0	0.52570432E-01	0.10646367E 00
1.2	0.0	0.0	0.53957857E-01	0.11667013E 00
1.3	0.0	0.0	0.54962032E-01	0.12693143E 00
1.4	0.0	0.0	0.55616334E-01	0.13723999E 00
1.5	0.0	0.0	0.55951603E-01	0.14758688E 00
1.6	0.0	0.0	0.55997271E-01	0.15796417E 00
1.7	0.0	0.0	0.55780720E-01	0.16836321E 00
1.8	0.0	0.0	0.55327523E-01	0.17877549E 00
1.9	0.0	0.0	0.54662105E-01	0.18919241E 00
2.0	0.0	0.0	0.53807583E-01	0.19960755E 00
2.1	0.0	0.0	0.52784674E-01	0.21000820E 00
2.2	0.0	0.0	0.51614434E-01	0.22039205E 00
2.3	0.0	0.0	0.50315004E-01	0.23074591E 00
2.4	0.0	0.0	0.48904773E-01	0.24106508E 00
2.5	0.0	0.0	0.47399923E-01	0.25134093E 00
2.6	0.0	0.0	0.45816630E-01	0.26156807E 00
2.7	0.0	0.0	0.44169191E-01	0.27173853E 00
2.8	0.0	0.0	0.42470928E-01	0.28184175E 00
2.9	0.0	0.0	0.40735401E-01	0.29187834E 00
3.0	0.0	0.0	0.38973793E-01	0.30183798E 00
3.1	0.0	0.0	0.37197161E-01	0.31171417E 00
3.2	0.0	0.0	0.35415825E-01	0.32150209E 00
3.3	0.0	0.0	0.33639222E-01	0.33119762E 00

3.4	0.0	0.0	0.31876050E-01	0.34079462E 00
3.5	0.0	0.0	0.30134328E-01	0.35028803E 00
3.6	0.0	0.0	0.28421409E-01	0.35967368E 00
3.7	0.0	0.0	0.26744377E-01	0.36895078E 00
3.8	0.0	0.0	0.25108792E-01	0.37811333E 00
3.9	0.0	0.0	0.23520615E-01	0.38715774E 00
4.0	0.0	0.0	0.21984775E-01	0.39608240E 00
4.1	0.0	0.0	0.20505864E-01	0.40488583E 00
4.2	0.0	0.0	0.19087579E-01	0.41355741E 00
4.3	0.0	0.0	0.17733805E-01	0.42210478E 00
4.4	0.0	0.0	0.16447730E-01	0.43052554E 00
4.5	0.0	0.0	0.15232004E-01	0.43881571E 00
4.6	0.0	0.0	0.14088877E-01	0.44696581E 00
4.7	0.0	0.0	0.13020601E-01	0.45499218E 00
4.8	0.0	0.0	0.12028549E-01	0.46287763E 00
4.9	0.0	0.0	0.11114303E-01	0.47063154E 00
5.0	0.0	0.0	0.10278951E-01	0.47825044E 00
5.1	0.0	0.0	0.95252390E-02	0.48573375E 00
5.2	0.0	0.0	0.88476799E-02	0.49308246E 00
5.3	0.0	0.0	0.82527734E-02	0.50029767E 00
5.4	0.0	0.0	0.77383742E-02	0.50737494E 00
5.5	0.0	0.0	0.73046088E-02	0.51431942E 00
5.6	0.0	0.0	0.69511943E-02	0.52113688E 00
5.7	0.0	0.0	0.66776313E-02	0.52781653E 00
5.8	0.0	0.0	0.64833276E-02	0.53436190E 00
5.9	0.0	0.0	0.63676760E-02	0.54078197E 00
6.0	0.0	0.0	0.63298084E-02	0.54707360E 00
6.1	0.0	0.0	0.63687265E-02	0.55323511E 00
6.2	0.0	0.0	0.64834468E-02	0.55927187E 00
6.3	0.0	0.0	0.66727959E-02	0.56518364E 00
6.4	0.0	0.0	0.69355182E-02	0.57096779E 00
6.5	0.0	0.0	0.72703920E-02	0.57663250E 00
6.6	0.0	0.0	0.76760948E-02	0.58217734E 00
6.7	0.0	0.0	0.81512518E-02	0.58760661E 00
6.8	0.0	0.0	0.86942427E-02	0.59291190E 00
6.9	0.0	0.0	0.93038604E-02	0.59811211E 00
7.0	0.0	0.0	0.99783577E-02	0.60319197E 00
7.1	0.0	0.0	0.10716230E-01	0.60815740E 00
7.2	0.0	0.0	0.11516057E-01	0.61301702E 00
7.3	0.0	0.0	0.12376107E-01	0.61776876E 00
7.4	0.0	0.0	0.13294958E-01	0.62241262E 00
7.5	0.0	0.0	0.14270913E-01	0.62695283E 00
7.6	0.0	0.0	0.15302327E-01	0.63138932E 00
7.7	0.0	0.0	0.16387928E-01	0.63573158E 00

7.8	0.0	0.0	0.17525814E-01	0.63997006E 00
7.9	0.0	0.0	0.18714491E-01	0.64411128E 00
8.0	0.0	0.0	0.19952442E-01	0.64815778E 00
8.1	0.0	0.0	0.21238185E-01	0.65211380E 00
8.2	0.0	0.0	0.22569977E-01	0.65597558E 00
8.3	0.0	0.0	0.23946386E-01	0.65974545E 00
8.4	0.0	0.0	0.25366165E-01	0.66343367E 00
8.5	0.0	0.0	0.26827551E-01	0.66703099E 00
8.6	0.0	0.0	0.28329168E-01	0.67054474E 00
8.7	0.0	0.0	0.29869780E-01	0.67397934E 00
8.8	0.0	0.0	0.31447466E-01	0.67732620E 00
8.9	0.0	0.0	0.33061415E-01	0.68059891E 00
9.0	0.0	0.0	0.34710091E-01	0.68379182E 00
9.1	0.0	0.0	0.36392063E-01	0.68691051E 00
9.2	0.0	0.0	0.38106207E-01	0.68995327E 00
9.3	0.0	0.0	0.39851099E-01	0.69292504E 00
9.4	0.0	0.0	0.41625757E-01	0.69582820E 00
9.5	0.0	0.0	0.43428663E-01	0.69865781E 00
9.6	0.0	0.0	0.45258716E-01	0.70141989E 00
9.7	0.0	0.0	0.47114678E-01	0.70411384E 00
9.8	0.0	0.0	0.48995793E-01	0.70674670E 00
9.9	0.0	0.0	0.50900515E-01	0.70931512E 00
10.0	0.0	0.0	0.52828003E-01	0.71181995E 00
10.1	0.0	0.0	0.54777142E-01	0.71426094E 00
10.2	0.0	0.0	0.56746554E-01	0.71664172E 00
10.3	0.0	0.0	0.58735959E-01	0.71896887E 00
10.4	0.0	0.0	0.60744248E-01	0.72123665E 00
10.5	0.0	0.0	0.62770188E-01	0.72345018E 00
10.6	0.0	0.0	0.64812839E-01	0.72560942E 00
10.7	0.0	0.0	0.66871643E-01	0.72771454E 00
10.8	0.0	0.0	0.68945289E-01	0.72976536E 00
10.9	0.0	0.0	0.71033478E-01	0.73176795E 00
11.0	0.0	0.0	0.73134542E-01	0.73371583E 00
11.1	0.0	0.0	0.75248718E-01	0.73562050E 00
11.2	0.0	0.0	0.77374697E-01	0.73747444E 00
11.3	0.0	0.0	0.79512179E-01	0.73928487E 00
11.4	0.0	0.0	0.81659317E-01	0.74104595E 00
11.5	0.0	0.0	0.83816886E-01	0.74276459E 00
11.6	0.0	0.0	0.85983217E-01	0.74443966E 00
11.7	0.0	0.0	0.88157892E-01	0.74607223E 00
11.8	0.0	0.0	0.90340555E-01	0.74766213E 00
11.9	0.0	0.0	0.92529774E-01	0.74920881E 00
12.0	0.0	0.0	0.94726563E-01	0.75072372E 00

FREQUENCY = 2000.0 MHZ
SIGMA = 15.00 METERS
PLATFORM ALTITUDE = 160.9344 KM

PSI	SPECULAR		DIFFUSE	
(DEGREES)	VERTICAL	HORIZONTAL	VERTICAL	HORIZONTAL
0.1	0.30384690E-04	0.3237903CE-C4	0.37552626E-02	0.40017441E-02
0.2	0.30267802E-10	0.34372491E-10	0.70613846E-02	0.80189966E-02
0.3	0.148C7573E-20	0.17920945E-20	0.99577121E-02	0.12051374E-01
0.4	0.42168141E-35	0.54393253E-35	0.12480415E-01	0.16098656E-01
0.5	0.73766441E-54	0.10142669E-53	0.14662329E-01	0.20160265E-01
0.6	0.81211348E-77	0.11904365E-76	0.16533747E-01	0.24236009E-01
0.7	0.0	0.0	0.18122353E-01	0.28325323E-01
0.8	0.0	0.0	0.19453492E-01	0.32427792E-01
0.9	0.0	0.0	0.20550720E-01	0.36543280E-01
1.0	0.0	0.0	0.21435264E-01	0.40671051E-01
1.1	0.0	0.0	0.22126973E-01	0.44810716E-01
1.2	0.0	0.0	0.22643976E-01	0.48961867E-01
1.3	0.0	0.0	0.23002930E-01	0.53123880E-01
1.4	0.0	0.0	0.23219410E-01	0.57296682E-01
1.5	0.0	0.0	0.23307383E-01	0.61479289E-01
1.6	0.0	0.0	0.23280043E-01	0.65671265E-01
1.7	0.0	0.0	0.23149602E-01	0.69872499E-01
1.8	0.0	0.0	0.22926964E-01	0.74082017E-01
1.9	0.0	0.0	0.22622589E-01	0.78299582E-01
2.0	0.0	0.0	0.22246022E-01	0.82525015E-01
2.1	0.0	0.0	0.21805894E-01	0.86756527E-01
2.2	0.0	0.0	0.21310456E-01	0.90994895E-01
2.3	0.0	0.0	0.20767201E-01	0.95238864E-01
2.4	0.0	0.0	0.20183034E-01	0.99487722E-01
2.5	0.0	0.0	0.19564416E-01	0.10374135E 00
2.6	0.0	0.0	0.18917296E-01	0.10799915E 00
2.7	0.0	0.0	0.18247195E-01	0.11226064E 00
2.8	0.0	0.0	0.17559160E-01	0.11652446E 00
2.9	0.0	0.0	0.16857959E-01	0.12079102E 00
3.0	0.0	0.0	0.16147807E-01	0.12505889E 00
3.1	0.0	0.0	0.15432838E-01	0.12932789E 00
3.2	0.0	0.0	0.14716774E-01	0.13359773E 00
3.3	0.0	0.0	0.14002964E-01	0.13786727E 00

3.4	0.0	0.0	0.13294619E-01	0.14213592E 00
3.5	0.0	0.0	0.12594681E-01	0.14640331E 00
3.6	0.0	0.0	0.11905834E-01	0.15066850E 00
3.7	0.0	0.0	0.11230629E-01	0.15493155E 00
3.8	0.0	0.0	0.10571193E-01	0.15919161E 00
3.9	0.0	0.0	0.99297985E-02	0.16344798E 00
4.0	0.0	0.0	0.93082637E-02	0.16769964E 00
4.1	0.0	0.0	0.87084211E-02	0.17194664E 00
4.2	0.0	0.0	0.81318654E-02	0.17618746E 00
4.3	0.0	0.0	0.75800866E-02	0.18042308E 00
4.4	0.0	0.0	0.70544146E-02	0.18465191E 00
4.5	0.0	0.0	0.65561011E-02	0.18887341E 00
4.6	0.0	0.0	0.60863160E-02	0.19308656E 00
4.7	0.0	0.0	0.56459419E-02	0.19729191E 00
4.8	0.0	0.0	0.52359700E-02	0.20148838E 00
4.9	0.0	0.0	0.48571639E-02	0.20567489E 00
5.0	0.0	0.0	0.45102984E-02	0.20985126E 00
5.1	0.0	0.0	0.41959956E-02	0.21401709E 00
5.2	0.0	0.0	0.39147884E-02	0.21817172E 00
5.3	0.0	0.0	0.36672466E-02	0.22231472E 00
5.4	0.0	0.0	0.34536936E-02	0.22644502E 00
5.5	0.0	0.0	0.32745693E-02	0.23056316E 00
5.6	0.0	0.0	0.31301274E-02	0.23466820E 00
5.7	0.0	0.0	0.30206463E-02	0.23875934E 00
5.8	0.0	0.0	0.29462760E-02	0.24283475E 00
5.9	0.0	0.0	0.29072079E-02	0.24689782E 00
6.0	0.0	0.0	0.29035048E-02	0.25094444E 00
6.1	0.0	0.0	0.29352203E-02	0.25497514E 00
6.2	0.0	0.0	0.30023858E-02	0.25899029E 00
6.3	0.0	0.0	0.31049480E-02	0.26298785E 00
6.4	0.0	0.0	0.32428675E-02	0.26696950E 00
6.5	0.0	0.0	0.34160267E-02	0.27093321E 00
6.6	0.0	0.0	0.36243233E-02	0.27487898E 00
6.7	0.0	0.0	0.38675985E-02	0.27880692E 00
6.8	0.0	0.0	0.41456372E-02	0.28271556E 00
6.9	0.0	0.0	0.44582635E-02	0.28660578E 00
7.0	0.0	0.0	0.48052371E-02	0.29047656E 00
7.1	0.0	0.0	0.51862746E-02	0.29432654E 00
7.2	0.0	0.0	0.56011230E-02	0.29815632E 00
7.3	0.0	0.0	0.60494654E-02	0.30196661E 00
7.4	0.0	0.0	0.65310486E-02	0.30575556E 00
7.5	0.0	0.0	0.70454963E-02	0.30952430E 00
7.6	0.0	0.0	0.75924098E-02	0.31327039E 00
7.7	0.0	0.0	0.81715323E-02	0.31699562E 00

7.8	0.0	0.0	0.87824576E-02	0.32069874E 00
7.9	0.0	0.0	0.94247535E-02	0.32437897E 00
8.0	0.0	0.0	0.10098077E-01	0.32803744E 00
8.1	0.0	0.0	0.10801964E-01	0.33167183E 00
8.2	0.0	0.0	0.11536010E-01	0.33528376E 00
8.3	0.0	0.0	0.12299839E-01	0.33887237E 00
8.4	0.0	0.0	0.13093024E-01	0.34243870E 00
8.5	0.0	0.0	0.13915077E-01	0.34597981E 00
8.6	0.0	0.0	0.14765561E-01	0.34949738E 00
8.7	0.0	0.0	0.15644010E-01	0.35299009E 00
8.8	0.0	0.0	0.16549971E-01	0.35645884E 00
8.9	0.0	0.0	0.17483052E-01	0.35990429E 00
9.0	0.0	0.0	0.18442713E-01	0.36332327E 00
9.1	0.0	0.0	0.19428533E-01	0.36671901E 00
9.2	0.0	0.0	0.20440083E-01	0.37008941E 00
9.3	0.0	0.0	0.21476746E-01	0.37343454E 00
9.4	0.0	0.0	0.22538181E-01	0.37675488E 00
9.5	0.0	0.0	0.23623936E-01	0.38004988E 00
9.6	0.0	0.0	0.24733391E-01	0.38331836E 00
9.7	0.0	0.0	0.25866207E-01	0.38656229E 00
9.8	0.0	0.0	0.27021877E-01	0.38978106E 00
9.9	0.0	0.0	0.28199783E-01	0.39297318E 00
10.0	0.0	0.0	0.29399760E-01	0.39614093E 00
10.1	0.0	0.0	0.30621104E-01	0.39928079E 00
10.2	0.0	0.0	0.31863384E-01	0.40239674E 00
10.3	0.0	0.0	0.33126071E-01	0.40548617E 00
10.4	0.0	0.0	0.34408998E-01	0.40854949E 00
10.5	0.0	0.0	0.35711400E-01	0.41158718E 00
10.6	0.0	0.0	0.37032858E-01	0.41459990E 00
10.7	0.0	0.0	0.38373049E-01	0.41758525E 00
10.8	0.0	0.0	0.39731279E-01	0.42054361E 00
10.9	0.0	0.0	0.41107468E-01	0.42347801E 00
11.0	0.0	0.0	0.42500786E-01	0.42638528E 00
11.1	0.0	0.0	0.43911021E-01	0.42926753E 00
11.2	0.0	0.0	0.45337759E-01	0.43212566E 00
11.3	0.0	0.0	0.46780474E-01	0.43495345E 00
11.4	0.0	0.0	0.48238479E-01	0.43775696E 00
11.5	0.0	0.0	0.49711969E-01	0.44053519E 00
11.6	0.0	0.0	0.51200066E-01	0.44328833E 00
11.7	0.0	0.0	0.52702446E-01	0.44601583E 00
11.8	0.0	0.0	0.54218680E-01	0.44871604E 00
11.9	0.0	0.0	0.55748172E-01	0.45138991E 00
12.0	0.0	0.0	0.57291292E-01	0.45404291E 00

FREQUENCY = 2000.0 MHZ
SIGMA = 15.00 METERS
PLATFORM ALTITUDE = 321.8008 KM

PSI	SPECULAR		DIFFUSE	
(DEGREES)	VERTICAL	HORIZONTAL	VERTICAL	HORIZONTAL
0.1	0.21623433E-04	0.23042725E-04	0.26724534E-02	0.28478659E-02
0.2	0.21509766E-10	0.24426766E-10	0.50181635E-02	0.56986883E-02
0.3	0.10538362E-20	0.12717797E-20	0.70666037E-02	0.85523911E-02
0.4	0.29884189E-35	0.38548014E-35	0.88447593E-02	0.11408973E-01
0.5	0.52207275E-54	0.71783415E-54	0.10377072E-01	0.14268164E-01
0.6	0.57400440E-77	0.84140504E-77	0.11686105E-01	0.17130092E-01
0.7	0.0	0.0	0.12792323E-01	0.19994464E-01
0.8	0.0	0.0	0.13714552E-01	0.22861332E-01
0.9	0.0	0.0	0.14469959E-01	0.25730480E-01
1.0	0.0	0.0	0.15074350E-01	0.28601918E-01
1.1	0.0	0.0	0.15542187E-01	0.31475451E-01
1.2	0.0	0.0	0.15886728E-01	0.34351032E-01
1.3	0.0	0.0	0.16120113E-01	0.37228432E-01
1.4	0.0	0.0	0.16253624E-01	0.40107768E-01
1.5	0.0	0.0	0.16297419E-01	0.42988691E-01
1.6	0.0	0.0	0.16260989E-01	0.45871049E-01
1.7	0.0	0.0	0.16153049E-01	0.48754822E-01
1.8	0.0	0.0	0.15981570E-01	0.51639985E-01
1.9	0.0	0.0	0.15753921E-01	0.54526314E-01
2.0	0.0	0.0	0.15476849E-01	0.57413775E-01
2.1	0.0	0.0	0.15156608E-01	0.60301837E-01
2.2	0.0	0.0	0.14798872E-01	0.63190639E-01
2.3	0.0	0.0	0.14409069E-01	0.66080332E-01
2.4	0.0	0.0	0.13991956E-01	0.68970144E-01
2.5	0.0	0.0	0.13552044E-01	0.71860433E-01
2.6	0.0	0.0	0.13093498E-01	0.74750960E-01
2.7	0.0	0.0	0.12620118E-01	0.77641666E-01
2.8	0.0	0.0	0.12135424E-01	0.80531955E-01
2.9	0.0	0.0	0.11642624E-01	0.83421946E-01
3.0	0.0	0.0	0.11144694E-01	0.86311579E-01
3.1	0.0	0.0	0.10644421E-01	0.89200735E-01
3.2	0.0	0.0	0.10144267E-01	0.92088878E-01
3.3	0.0	0.0	0.96466057E-02	0.94976366E-01

3.4	0.0	0.0	0.91535188E-02	0.97862422E-01
3.5	0.0	0.0	0.86670332E-02	0.10074747E 00
3.6	0.0	0.0	0.81889220E-02	0.10363096E 00
3.7	0.0	0.0	0.77208802E-02	0.10651302E 00
3.8	0.0	0.0	0.72643198E-02	0.10939342E 00
3.9	0.0	0.0	0.68207271E-02	0.11227161E 00
4.0	0.0	0.0	0.63913502E-02	0.11514795E 00
4.1	0.0	0.0	0.59773587E-02	0.11802208E 00
4.2	0.0	0.0	0.55797845E-02	0.12089330E 00
4.3	0.0	0.0	0.51996112E-02	0.12376249E 00
4.4	0.0	0.0	0.48377104E-02	0.12662888E 00
4.5	0.0	0.0	0.44948868E-02	0.12949228E 00
4.6	0.0	0.0	0.41718930E-02	0.13235217E 00
4.7	0.0	0.0	0.38693133E-02	0.13520932E 00
4.8	0.0	0.0	0.35877589E-02	0.13806260E 00
4.9	0.0	0.0	0.33277532E-02	0.14091247E 00
5.0	0.0	0.0	0.30897779E-02	0.14375854E 00
5.1	0.0	0.0	0.28742356E-02	0.14660060E 00
5.2	0.0	0.0	0.26814693E-02	0.14943850E 00
5.3	0.0	0.0	0.25118417E-02	0.15227205E 00
5.4	0.0	0.0	0.23655682E-02	0.15510094E 00
5.5	0.0	0.0	0.22429293E-02	0.15792513E 00
5.6	0.0	0.0	0.21441050E-02	0.16074532E 00
5.7	0.0	0.0	0.20692630E-02	0.16355962E 00
5.8	0.0	0.0	0.20185267E-02	0.16636878E 00
5.9	0.0	0.0	0.19920038E-02	0.16917306E 00
6.0	0.0	0.0	0.19897651E-02	0.17197162E 00
6.1	0.0	0.0	0.20118500E-02	0.17476428E 00
6.2	0.0	0.0	0.20582946E-02	0.17755157E 00
6.3	0.0	0.0	0.21290767E-02	0.18033195E 00
6.4	0.0	0.0	0.22241964E-02	0.18310726E 00
6.5	0.0	0.0	0.23435857E-02	0.18587536E 00
6.6	0.0	0.0	0.24872185E-02	0.18863767E 00
6.7	0.0	0.0	0.26549953E-02	0.19139296E 00
6.8	0.0	0.0	0.28468135E-02	0.19414097E 00
6.9	0.0	0.0	0.30625851E-02	0.19688255E 00
7.0	0.0	0.0	0.33021832E-02	0.19961691E 00
7.1	0.0	0.0	0.35654625E-02	0.20234364E 00
7.2	0.0	0.0	0.38522866E-02	0.20506299E 00
7.3	0.0	0.0	0.41624643E-02	0.20777464E 00
7.4	0.0	0.0	0.44959076E-02	0.21047902E 00
7.5	0.0	0.0	0.48523620E-02	0.21317506E 00
7.6	0.0	0.0	0.52316487E-02	0.21586305E 00
7.7	0.0	0.0	0.56336224E-02	0.21854329E 00

7.8	0.0	0.0	0.60580522E-02	0.22121489E 00
7.9	0.0	0.0	0.65047108E-02	0.22387767E 00
8.0	0.0	0.0	0.69734156E-02	0.22653240E 00
8.1	0.0	0.0	0.74639171E-02	0.22917789E 00
8.2	0.0	0.0	0.79759806E-02	0.23181444E 00
8.3	0.0	0.0	0.85094087E-02	0.23444217E 00
8.4	0.0	0.0	0.90639442E-02	0.23706090E 00
8.5	0.0	0.0	0.96393712E-02	0.23966992E 00
8.6	0.0	0.0	0.10235418E-01	0.24226993E 00
8.7	0.0	0.0	0.10851830E-01	0.24485976E 00
8.8	0.0	0.0	0.11488363E-01	0.24744010E 00
8.9	0.0	0.0	0.12144774E-01	0.25001097E 00
9.0	0.0	0.0	0.12820836E-01	0.25257158E 00
9.1	0.0	0.0	0.13516229E-01	0.25512254E 00
9.2	0.0	0.0	0.14230765E-01	0.25766313E 00
9.3	0.0	0.0	0.14964104E-01	0.26019377E 00
9.4	0.0	0.0	0.15716039E-01	0.26271379E 00
9.5	0.0	0.0	0.16486306E-01	0.26522326E 00
9.6	0.0	0.0	0.17274573E-01	0.26772147E 00
9.7	0.0	0.0	0.18080655E-01	0.27020979E 00
9.8	0.0	0.0	0.18904291E-01	0.27268779E 00
9.9	0.0	0.0	0.19745104E-01	0.27515441E 00
10.0	0.0	0.0	0.20602919E-01	0.27760965E 00
10.1	0.0	0.0	0.21477487E-01	0.28005356E 00
10.2	0.0	0.0	0.22368476E-01	0.28248745E 00
10.3	0.0	0.0	0.23275603E-01	0.28490943E 00
10.4	0.0	0.0	0.24198774E-01	0.28732008E 00
10.5	0.0	0.0	0.25137484E-01	0.28971893E 00
10.6	0.0	0.0	0.26091643E-01	0.29210788E 00
10.7	0.0	0.0	0.27060967E-01	0.29448426E 00
10.8	0.0	0.0	0.28045043E-01	0.29684842E 00
10.9	0.0	0.0	0.29043783E-01	0.29920119E 00
11.0	0.0	0.0	0.30056853E-01	0.30154258E 00
11.1	0.0	0.0	0.31083949E-01	0.30387211E 00
11.2	0.0	0.0	0.32124948E-01	0.30618948E 00
11.3	0.0	0.0	0.33179477E-01	0.30849457E 00
11.4	0.0	0.0	0.34247179E-01	0.31078798E 00
11.5	0.0	0.0	0.35327990E-01	0.31306803E 00
11.6	0.0	0.0	0.36421672E-01	0.31533754E 00
11.7	0.0	0.0	0.37527889E-01	0.31759506E 00
11.8	0.0	0.0	0.38646348E-01	0.31983876E 00
11.9	0.0	0.0	0.39776798E-01	0.32207060E 00
12.0	0.0	0.0	0.40919214E-01	0.32429147E 00

FREQUENCY = 2000.0 MHZ
SIGMA = 15.00 METERS
PLATFORM ALTITUDE = 643.7376 KM

PSI	SPECULAR		DIFFUSE	
(DEGREES)	VERTICAL	HORIZONTAL	VERTICAL	HORIZONTAL
0.1	0.15391997E-04	0.16402293E-04	0.19023072E-02	0.20271696E-02
0.2	0.15292406E-10	0.17366233E-10	0.35676723E-02	0.40514879E-02
0.3	0.74619062E-21	0.90308029E-21	0.50179400E-02	0.60729831E-02
0.4	0.21195087E-35	0.27339829E-35	0.62730648E-02	0.80917105E-02
0.5	0.36983640E-54	0.50851404E-54	0.73511191E-02	0.10107569E-01
0.6	0.40614801E-77	0.59535256E-77	0.82687326E-02	0.12120731E-01
0.7	0.0	0.0	0.90409443E-02	0.14131039E-01
0.8	0.0	0.0	0.96815713E-02	0.16138591E-01
0.9	0.0	0.0	0.10203253E-01	0.18143423E-01
1.0	0.0	0.0	0.10617454E-01	0.20145450E-01
1.1	0.0	0.0	0.10934807E-01	0.22144761E-01
1.2	0.0	0.0	0.11164900E-01	0.24141274E-01
1.3	0.0	0.0	0.11316650E-01	0.26135117E-01
1.4	0.0	0.0	0.11398111E-01	0.28126210E-01
1.5	0.0	0.0	0.11416707E-01	0.30114539E-01
1.6	0.0	0.0	0.11379261E-01	0.32100059E-01
1.7	0.0	0.0	0.11292063E-01	0.34082893E-01
1.8	0.0	0.0	0.11160780E-01	0.36062948E-01
1.9	0.0	0.0	0.10990724E-01	0.38040280E-01
2.0	0.0	0.0	0.10786705E-01	0.40014964E-01
2.1	0.0	0.0	0.10553174E-01	0.41986689E-01
2.2	0.0	0.0	0.10294173E-01	0.43955795E-01
2.3	0.0	0.0	0.10013469E-01	0.45922033E-01
2.4	0.0	0.0	0.97144954E-02	0.47885429E-01
2.5	0.0	0.0	0.94003901E-02	0.49846116E-01
2.6	0.0	0.0	0.90740547E-02	0.51803969E-01
2.7	0.0	0.0	0.87381676E-02	0.53759098E-01
2.8	0.0	0.0	0.83951652E-02	0.55711236E-01
2.9	0.0	0.0	0.80472641E-02	0.57660483E-01
3.0	0.0	0.0	0.76965429E-02	0.59606958E-01
3.1	0.0	0.0	0.73448829E-02	0.61550520E-01
3.2	0.0	0.0	0.69940127E-02	0.63491106E-01
3.3	0.0	0.0	0.66455230E-02	0.65428972E-01

3.4	0.0	0.0	0.63008294E-02	0.67363679E-01
3.5	0.0	0.0	0.59613064E-02	0.69295526E-01
3.6	0.0	0.0	0.56281462E-02	0.71224272E-01
3.7	0.0	0.0	0.53024888E-02	0.73150158E-01
3.8	0.0	0.0	0.49852654E-02	0.75073123E-01
3.9	0.0	0.0	0.46774708E-02	0.76992810E-01
4.0	0.0	0.0	0.43799244E-02	0.78909636E-01
4.1	0.0	0.0	0.40933862E-02	0.80823362E-01
4.2	0.0	0.0	0.38185488E-02	0.82733810E-01
4.3	0.0	0.0	0.35560231E-02	0.84641278E-01
4.4	0.0	0.0	0.33063751E-02	0.86545527E-01
4.5	0.0	0.0	0.30701335E-02	0.88446796E-01
4.6	0.0	0.0	0.28477621E-02	0.90344369E-01
4.7	0.0	0.0	0.26396259E-02	0.92239141E-01
4.8	0.0	0.0	0.24461199E-02	0.94130576E-01
4.9	0.0	0.0	0.22675523E-02	0.96018612E-01
5.0	0.0	0.0	0.21042223E-02	0.97903430E-01
5.1	0.0	0.0	0.19563700E-02	0.99784791E-01
5.2	0.0	0.0	0.18242002E-02	0.10166281E 00
5.3	0.0	0.0	0.17079273E-02	0.10353744E 00
5.4	0.0	0.0	0.16076681E-02	0.10540837E 00
5.5	0.0	0.0	0.15235860E-02	0.10727602E 00
5.6	0.0	0.0	0.14557729E-02	0.10914046E 00
5.7	0.0	0.0	0.14043231E-02	0.11100113E 00
5.8	0.0	0.0	0.13692884E-02	0.11285800E 00
5.9	0.0	0.0	0.13507239E-02	0.11471170E 00
6.0	0.0	0.0	0.13486543E-02	0.11656165E 00
6.1	0.0	0.0	0.13630854E-02	0.11840779E 00
6.2	0.0	0.0	0.13940230E-02	0.12025052E 00
6.3	0.0	0.0	0.14414345E-02	0.12208891E 00
6.4	0.0	0.0	0.15053041E-02	0.12392431E 00
6.5	0.0	0.0	0.15855706E-02	0.12575537E 00
6.6	0.0	0.0	0.16822030E-02	0.12758303E 00
6.7	0.0	0.0	0.17951238E-02	0.12940663E 00
6.8	0.0	0.0	0.19242496E-02	0.13122588E 00
6.9	0.0	0.0	0.20695196E-02	0.13304192E 00
7.0	0.0	0.0	0.22308289E-02	0.13485354E 00
7.1	0.0	0.0	0.24080893E-02	0.13666159E 00
7.2	0.0	0.0	0.26011863E-02	0.13846499E 00
7.3	0.0	0.0	0.28100009E-02	0.14026463E 00
7.4	0.0	0.0	0.30344592E-02	0.14206022E 00
7.5	0.0	0.0	0.32744061E-02	0.14385182E 00
7.6	0.0	0.0	0.35297065E-02	0.14563912E 00
7.7	0.0	0.0	0.38002606E-02	0.14742219E 00

7.8	0.0	0.0	0.40859245E-02	0.14920098E 00
7.9	0.0	0.0	0.43865554E-02	0.15097547E 00
8.0	0.0	0.0	0.47020242E-02	0.15274584E 00
8.1	0.0	0.0	0.50321706E-02	0.15451169E 00
8.2	0.0	0.0	0.53768493E-02	0.15627319E 00
8.3	0.0	0.0	0.57359301E-02	0.15803027E 00
8.4	0.0	0.0	0.61092600E-02	0.15978324E 00
8.5	0.0	0.0	0.64966828E-02	0.16153121E 00
8.6	0.0	0.0	0.68980344E-02	0.16327488E 00
8.7	0.0	0.0	0.73131770E-02	0.16501397E 00
8.8	0.0	0.0	0.77419430E-02	0.16674852E 00
8.9	0.0	0.0	0.81841648E-02	0.16847837E 00
9.0	0.0	0.0	0.86397305E-02	0.17020345E 00
9.1	0.0	0.0	0.91084391E-02	0.17192435E 00
9.2	0.0	0.0	0.95901638E-02	0.17364001E 00
9.3	0.0	0.0	0.10084707E-01	0.17535132E 00
9.4	0.0	0.0	0.10591950E-01	0.17705810E 00
9.5	0.0	0.0	0.11111710E-01	0.17875940E 00
9.6	0.0	0.0	0.11643786E-01	0.18045551E 00
9.7	0.0	0.0	0.12188107E-01	0.18214732E 00
9.8	0.0	0.0	0.12744479E-01	0.18383455E 00
9.9	0.0	0.0	0.13312690E-01	0.18551660E 00
10.0	0.0	0.0	0.13892625E-01	0.18719321E 00
10.1	0.0	0.0	0.14484186E-01	0.18886501E 00
10.2	0.0	0.0	0.15087117E-01	0.19053233E 00
10.3	0.0	0.0	0.15701246E-01	0.19219410E 00
10.4	0.0	0.0	0.16326558E-01	0.19385058E 00
10.5	0.0	0.0	0.16962759E-01	0.19550204E 00
10.6	0.0	0.0	0.17609730E-01	0.19714892E 00
10.7	0.0	0.0	0.18267367E-01	0.19879007E 00
10.8	0.0	0.0	0.18935431E-01	0.20042586E 00
10.9	0.0	0.0	0.19613862E-01	0.20205677E 00
11.0	0.0	0.0	0.20302411E-01	0.20368212E 00
11.1	0.0	0.0	0.21000996E-01	0.20530272E 00
11.2	0.0	0.0	0.21709461E-01	0.20691741E 00
11.3	0.0	0.0	0.22427659E-01	0.20852691E 00
11.4	0.0	0.0	0.23155313E-01	0.21013099E 00
11.5	0.0	0.0	0.23892466E-01	0.21172923E 00
11.6	0.0	0.0	0.24638854E-01	0.21332234E 00
11.7	0.0	0.0	0.25394421E-01	0.21491057E 00
11.8	0.0	0.0	0.26158955E-01	0.21649259E 00
11.9	0.0	0.0	0.26932251E-01	0.21806896E 00
12.0	0.0	0.0	0.27714387E-01	0.21964103E 00

FREQUENCY = 2000.0 MHZ
SIGMA = 15.00 METERS
PLATFORM ALTITUDE = 1287.4750 KM

PSI	SPECULAR		DIFFUSE	
(DEGREES)	VERTICAL	HORIZONTAL	VERTICAL	HORIZONTAL
0.1	0.10931807E-04	0.11649342E-04	0.13510687E-02	0.14397493E-02
0.2	0.10848361E-10	0.12319534E-10	0.25308887E-02	0.28741085E-02
0.3	0.52872654E-21	0.63989408E-21	0.35555C9E-02	0.43031238E-02
0.4	0.15000754E-35	0.19349667E-35	0.44397414E-02	0.57268813E-02
0.5	0.26145019E-54	0.35948613E-54	0.51967613E-02	0.71453899E-02
0.6	0.28679164E-77	0.42039382E-77	0.58387667E-02	0.85587613E-02
0.7	0.0	0.0	0.63767806E-02	0.99669397E-02
0.8	0.0	0.0	0.68209358E-02	0.11370093E-01
0.9	0.0	0.0	0.71804076E-02	0.12768202E-01
1.0	0.0	0.0	0.74635632E-02	0.14161289E-01
1.1	0.0	0.0	0.76781437E-02	0.15549488E-01
1.2	0.0	0.0	0.78310966E-02	0.16932767E-01
1.3	0.0	0.0	0.79288408E-02	0.18311188E-01
1.4	0.0	0.0	0.79772398E-02	0.19684795E-01
1.5	0.0	0.0	0.79816394E-02	0.21053653E-01
1.6	0.0	0.0	0.79469532E-02	0.22417765E-01
1.7	0.0	0.0	0.78776516E-02	0.23777157E-01
1.8	0.0	0.0	0.77778585E-02	0.25131978E-01
1.9	0.0	0.0	0.76513030E-02	0.26482116E-01
2.0	0.0	0.0	0.75014494E-02	0.27827788E-01
2.1	0.0	0.0	0.73314682E-02	0.29168859E-01
2.2	0.0	0.0	0.71441866E-02	0.30505467E-01
2.3	0.0	0.0	0.69423094E-02	0.31837624E-01
2.4	0.0	0.0	0.67282207E-02	0.33165254E-01
2.5	0.0	0.0	0.65041259E-02	0.34488525E-01
2.6	0.0	0.0	0.62720999E-02	0.35807539E-01
2.7	0.0	0.0	0.60339570E-02	0.37122212E-01
2.8	0.0	0.0	0.57914108E-02	0.38432460E-01
2.9	0.0	0.0	0.55460259E-02	0.39738540E-01
3.0	0.0	0.0	0.52991919E-02	0.41040327E-01
3.1	0.0	0.0	0.50522275E-02	0.42337935E-01
3.2	0.0	0.0	0.48063248E-02	0.43631483E-01
3.3	0.0	0.0	0.45625269E-02	0.44920743E-01

3.4	0.0	0.0	0.43218546E-02	0.46206012E-01
3.5	0.0	0.0	0.40851794E-02	0.47487028E-01
3.6	0.0	0.0	0.38533409E-02	0.48764102E-01
3.7	0.0	0.0	0.36270670E-02	0.50037030E-01
3.8	0.0	0.0	0.34070029E-02	0.51306065E-01
3.9	0.0	0.0	0.31937980E-02	0.52571058E-01
4.0	0.0	0.0	0.29879906E-02	0.53832270E-01
4.1	0.0	0.0	0.27900545E-02	0.55089269E-01
4.2	0.0	0.0	0.26004666E-02	0.56342516E-01
4.3	0.0	0.0	0.24195963E-02	0.57591844E-01
4.4	0.0	0.0	0.22478094E-02	0.58837246E-01
4.5	0.0	0.0	0.20854406E-02	0.60079049E-01
4.6	0.0	0.0	0.19327665E-02	0.61316464E-01
4.7	0.0	0.0	0.17900227E-02	0.62550545E-01
4.8	0.0	0.0	0.16574366E-02	0.63780725E-01
4.9	0.0	0.0	0.15351942E-02	0.65007210E-01
5.0	0.0	0.0	0.14234679E-02	0.66229820E-01
5.1	0.0	0.0	0.13223945E-02	0.67448795E-01
5.2	0.0	0.0	0.12320827E-02	0.68664074E-01
5.3	0.0	0.0	0.11526502E-02	0.69875598E-01
5.4	0.0	0.0	0.10841505E-02	0.71083426E-01
5.5	0.0	0.0	0.10266635E-02	0.72287560E-01
5.6	0.0	0.0	0.98022586E-03	0.73488295E-01
5.7	0.0	0.0	0.94487472E-03	0.74685216E-01
5.8	0.0	0.0	0.92062354E-03	0.75878620E-01
5.9	0.0	0.0	0.90747769E-03	0.77068508E-01
6.0	0.0	0.0	0.90542994E-03	0.78254640E-01
6.1	0.0	0.0	0.91446401E-03	0.79437137E-01
6.2	0.0	0.0	0.93455962E-03	0.80616474E-01
6.3	0.0	0.0	0.96566882E-03	0.81791699E-01
6.4	0.0	0.0	0.10077620E-02	0.82964063E-01
6.5	0.0	0.0	0.10607745E-02	0.84132493E-01
6.6	0.0	0.0	0.11246644E-02	0.85297704E-01
6.7	0.0	0.0	0.11993595E-02	0.86459279E-01
6.8	0.0	0.0	0.12847674E-02	0.87617159E-01
6.9	0.0	0.0	0.13808843E-02	0.88772058E-01
7.0	0.0	0.0	0.14875645E-02	0.89923263E-01
7.1	0.0	0.0	0.16047454E-02	0.91070890E-01
7.2	0.0	0.0	0.17323440E-02	0.92215240E-01
7.3	0.0	0.0	0.18702578E-02	0.93356133E-01
7.4	0.0	0.0	0.20184179E-02	0.94493568E-01
7.5	0.0	0.0	0.21767153E-02	0.95627844E-01
7.6	0.0	0.0	0.23450444E-02	0.96758783E-01
7.7	0.0	0.0	0.25233126E-02	0.97885966E-01

7.8	0.0	0.0	0.27114262E-02	0.99009931E-01
7.9	0.0	0.0	0.29092750E-02	0.10013074E 00
8.0	0.0	0.0	0.31167534E-02	0.10124609E 00
8.1	0.0	0.0	0.33337583E-02	0.10236228E 00
8.2	0.0	0.0	0.35601633E-02	0.10347277E 00
8.3	0.0	0.0	0.37958766E-02	0.10457993E 00
8.4	0.0	0.0	0.40408000E-02	0.10568416E 00
8.5	0.0	0.0	0.42948164E-02	0.10678482E 00
8.6	0.0	0.0	0.45578107E-02	0.10788232E 00
8.7	0.0	0.0	0.48296750E-02	0.10897636E 00
8.8	0.0	0.0	0.51103085E-02	0.11006755E 00
8.9	0.0	0.0	0.53995699E-02	0.11115497E 00
9.0	0.0	0.0	0.56974106E-02	0.11223942E 00
9.1	0.0	0.0	0.60036518E-02	0.11332059E 00
9.2	0.0	0.0	0.63182339E-02	0.11439830E 00
9.3	0.0	0.0	0.66410154E-02	0.11547297E 00
9.4	0.0	0.0	0.69719031E-02	0.11654425E 00
9.5	0.0	0.0	0.73108003E-02	0.11761230E 00
9.6	0.0	0.0	0.76575540E-02	0.11867678E 00
9.7	0.0	0.0	0.80121271E-02	0.11973864E 00
9.8	0.0	0.0	0.83743557E-02	0.12079704E 00
9.9	0.0	0.0	0.87441243E-02	0.12185216E 00
10.0	0.0	0.0	0.91213882E-02	0.12290418E 00
10.1	0.0	0.0	0.95060095E-02	0.12395263E 00
10.2	0.0	0.0	0.98978840E-02	0.12499851E 00
10.3	0.0	0.0	0.10296870E-01	0.12604076E 00
10.4	0.0	0.0	0.10702964E-01	0.12707984E 00
10.5	0.0	0.0	0.11115961E-01	0.12811553E 00
10.6	0.0	0.0	0.11535827E-01	0.12914884E 00
10.7	0.0	0.0	0.11962458E-01	0.13017845E 00
10.8	0.0	0.0	0.12395676E-01	0.13120443E 00
10.9	0.0	0.0	0.12835465E-01	0.13222748E 00
11.0	0.0	0.0	0.13281722E-01	0.13324761E 00
11.1	0.0	0.0	0.13734348E-01	0.13426489E 00
11.2	0.0	0.0	0.14193233E-01	0.13527864E 00
11.3	0.0	0.0	0.14658272E-01	0.13628900E 00
11.4	0.0	0.0	0.15129350E-01	0.13729656E 00
11.5	0.0	0.0	0.15606429E-01	0.13830030E 00
11.6	0.0	0.0	0.16089395E-01	0.13930130E 00
11.7	0.0	0.0	0.16578183E-01	0.14029956E 00
11.8	0.0	0.0	0.17072663E-01	0.14129400E 00
11.9	0.0	0.0	0.17572764E-01	0.14228570E 00
12.0	0.0	0.0	0.18078417E-01	0.14327443E 00

```
      COMPLEX KK2,PVN,PVD,PHN,PHD,CSQRT,CSQ,CMPLX
      DIMENSION FREQ(3),H(7),SIGMA(3),PSID(18)
      DATA PI/3.141592653589793/,A/6378166./,D/
     $35803001./,FREQ/2.E9,4.E8,137.E6/,H/6096.,15240.,30480.,160934.4,
     $321868.8,643737.6,1287475.2/,SIGMA/.15,1.5,15./,PSID/0.,2.,4.,
     $6.,8.,10.,12.,14.,16.,18.,20.,30.,40.,50.,60.,70.,80.,90./
      HALFPI=PI/2.
      FOURPI=4.*PI
      DO 900 IFREQ=1,3
      KK2=CMPLX(80.,-7.2E10/FREQ(IFREQ))
      WAVE=2.9979250E8/FREQ(IFREQ)
      DO 800 ISIG=1,3
      CON=(FOURPI*SIGMA(ISIG)/WAVE)**2
      DO 700 IH=1,7
      WRITE(6,1)FREQ(IFREQ),SIGMA(ISIG),H(IH)
1     FORMAT('1FREQUENCY = ',-6PF7.1,' MHZ'/' SIGMA = ',0PF6.2,
     $' METERS'/' PLATFORM ALTITUDE = ',-3PF10.4,' KM'/' PSI',
     $T30,'SPECULAR',T70,'DIFFUSE'/1X,'(DEGREES)',T20,'VERTICAL',T40,
     $'HORIZONTAL',T60,'VERTICAL',T80,'HORIZONTAL')
      DO 600 IPSI = 1,18
      PSIR=PI*PSID(IPSI)/180.
      CP2P=COS(HALFPI+PSIR)
      BNEG=A*CP2P
      BSQ=BNEG*BNEG
      R1=BNEG+SQRT(BSQ+H(IH)**2+2.*A*H(IH))
      R2=BNEG+SQRT(BSQ+D*D+2.*A*D)
      SP2P=SIN(HALFPI+PSIR)
      ALFA1=ARSIN(A*SP2P/(A+H(IH)))
      ALFA2=ARSIN(A*SP2P/(A+D))
      PHI=PI-PSIR-PSIR-ALFA1-ALFA2
      BIGD=A*(R1+R2)*SQRT(SIN(PSIR)*COS(PSIR))/SQRT(((A+D)*R1*COS(ALFA2
     $)+(A+H(IH))*R2*COS(ALFA1))*(A+H(IH))*(A+D)*SIN(PHI))
      CSQ=CSQRT(KK2-COS(PSIR)**2)
      SINPSI=SIN(PSIR)
      PVN=KK2*SINPSI-CSQ
      PVD=KK2*SINPSI+CSQ
      PV=CABS(PVN/PVD)
      PHN=SINPSI-CSQ
      PHD=SINPSI+CSQ
      PH=CABS(PHN/PHD)
      PS2=EXP(-CON*SINPSI*SINPSI)
      PDV=BIGD*BIGD*PV*PV
      PDH=BIGD*BIGD*PH*PH
      PSV=PS2*PDV
      PSH=PS2*PDH
      WRITE(6,2)PSID(IPSI),PSV,PSH,PDV,PDH
2     FORMAT(1X,F5.1,T20,E15.8,T40,E15.8,T60,E15.8,T80,E15.8)
600   CONTINUE
700   CONTINUE
800   CONTINUE
900   CONTINUE
      STOP
      END
```

APPENDIX B

DETAILED SCHEMATICS OF PSEUDONOISE MODEM

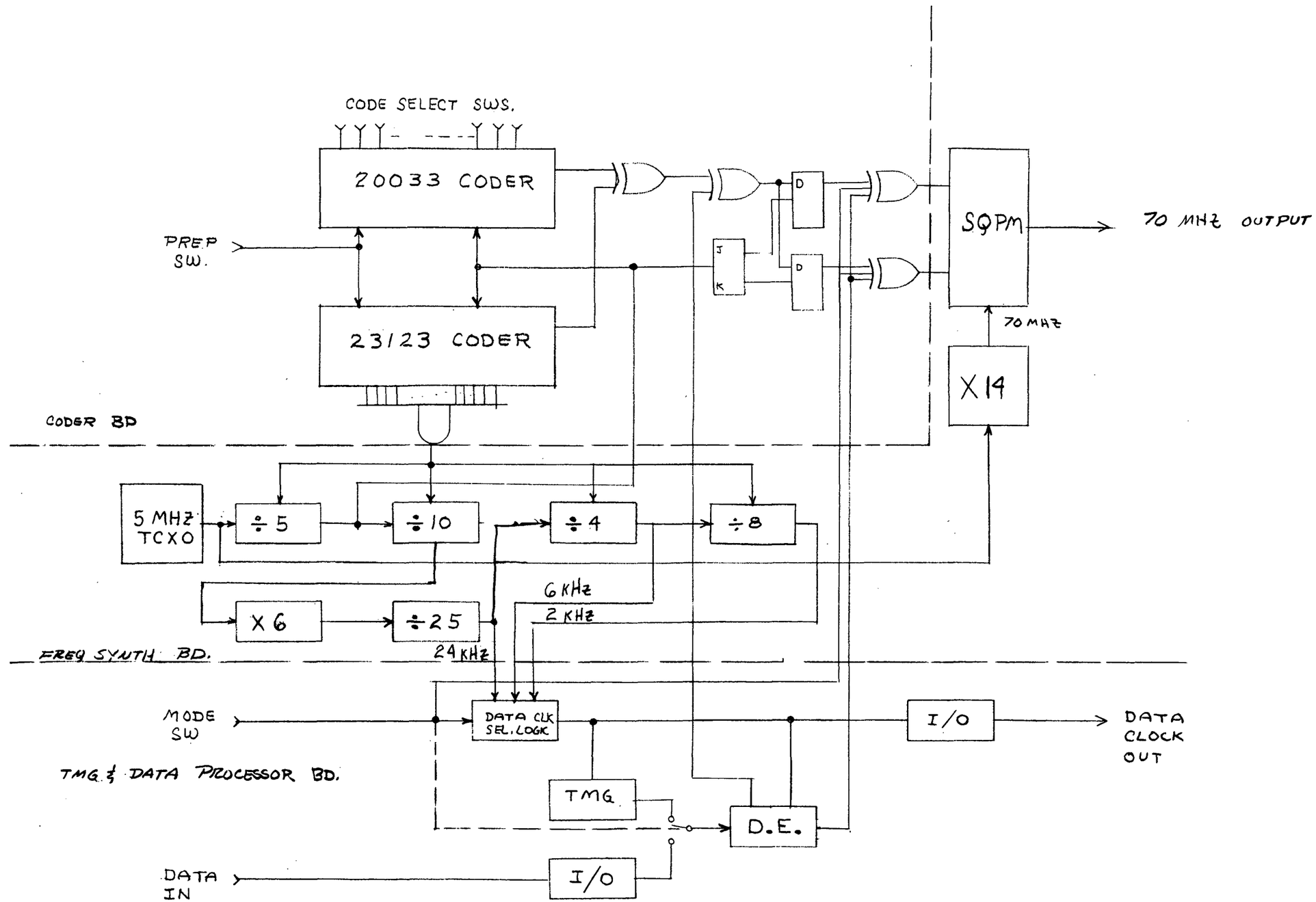

TX MX32X Block Diagram

B-3/B-4 Blank

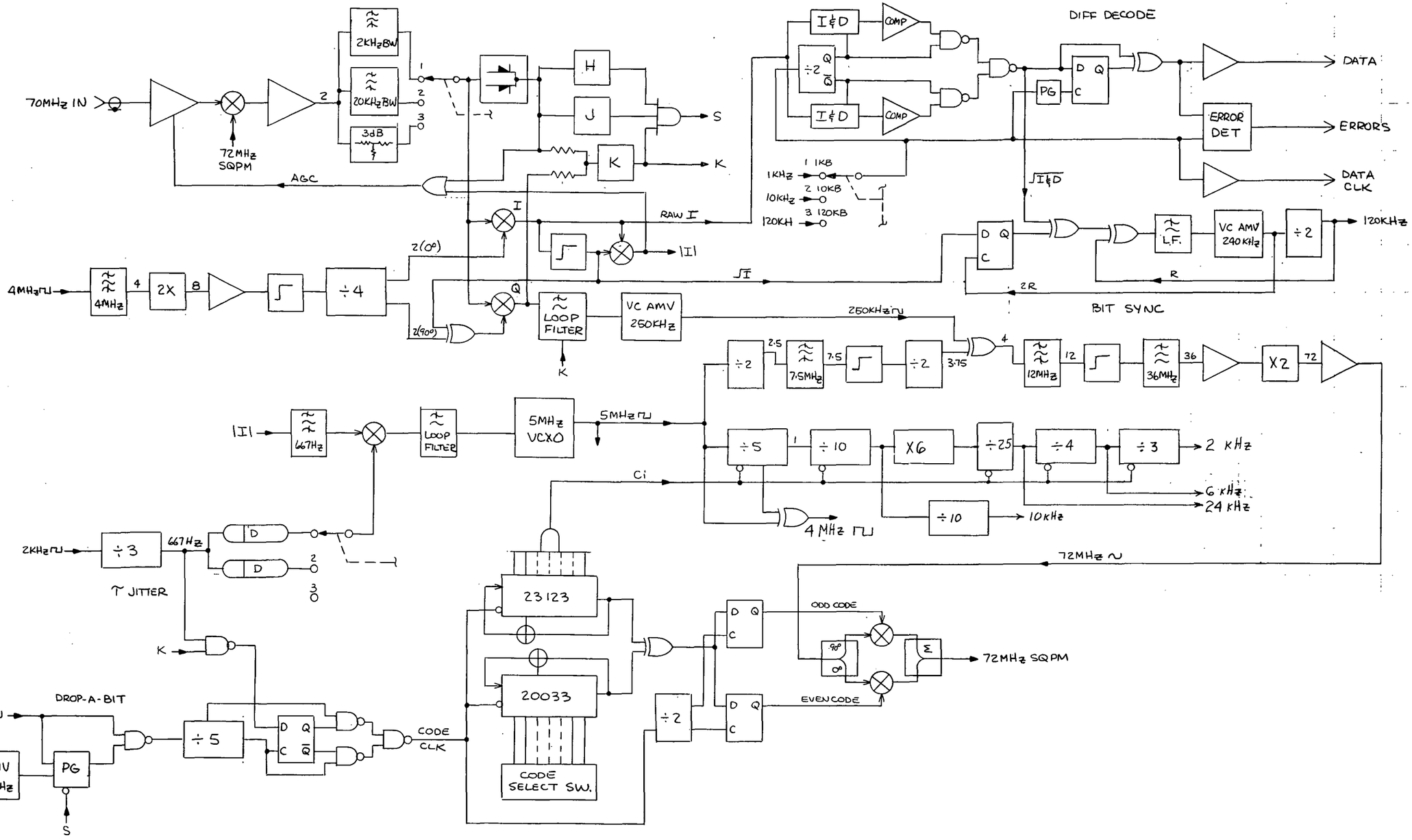

MX 32Y RX Block Diagram

B-5/B-6 Blank

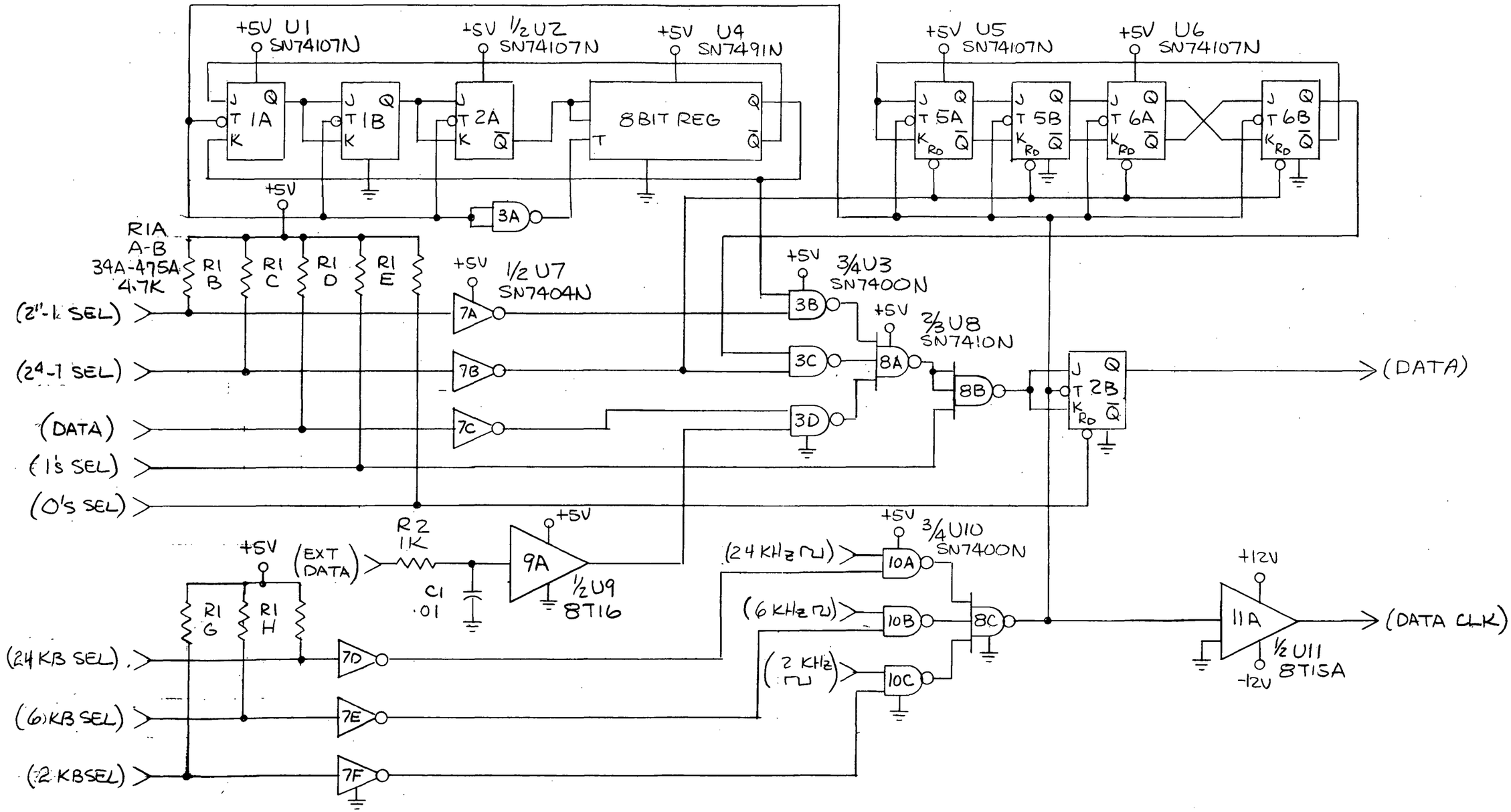

Data Processor and TMG 1A1
MX32X - Schematic Diagram

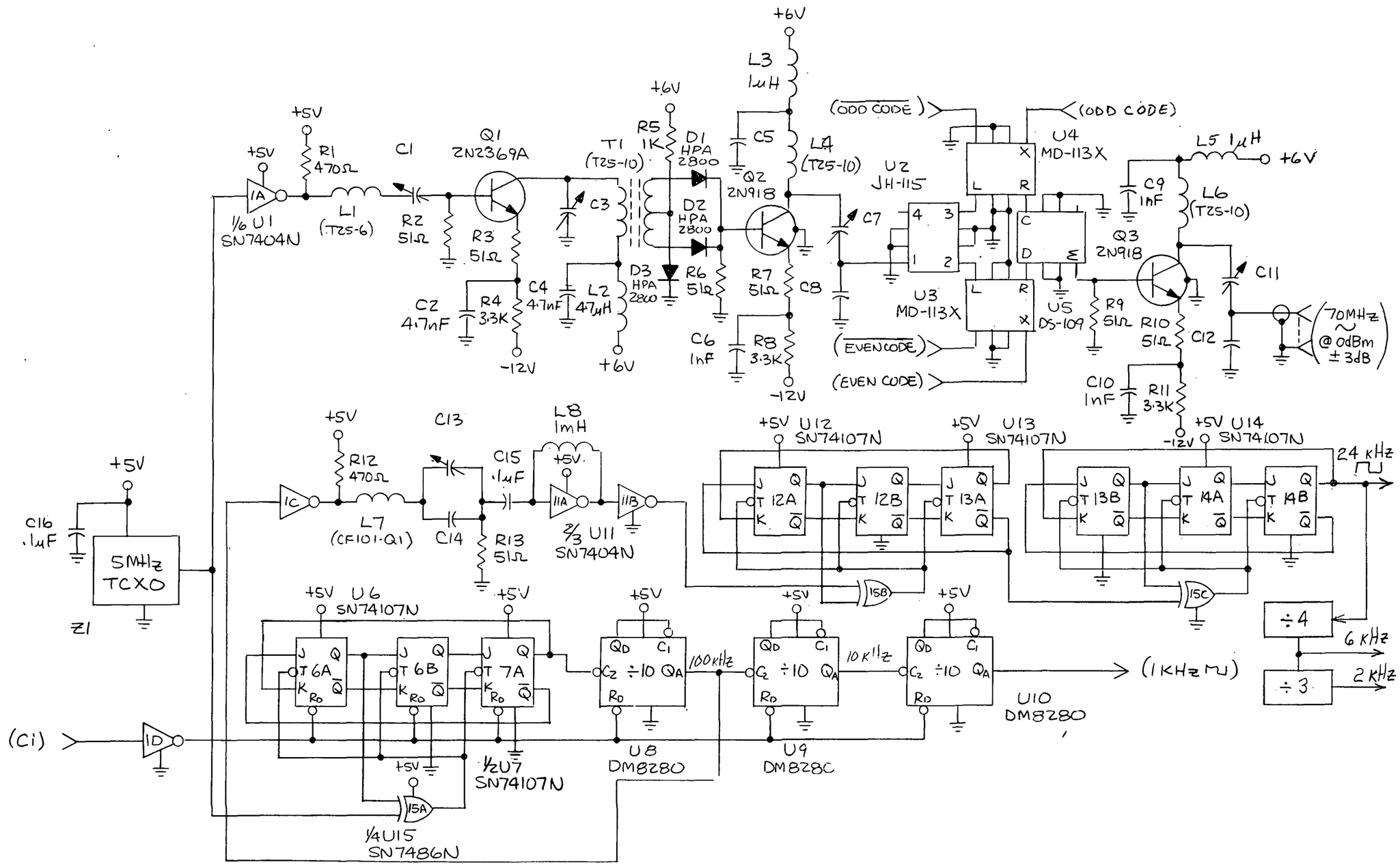

TX Frequency Synthesizer 1A2
MX32X - Schematic Diagram

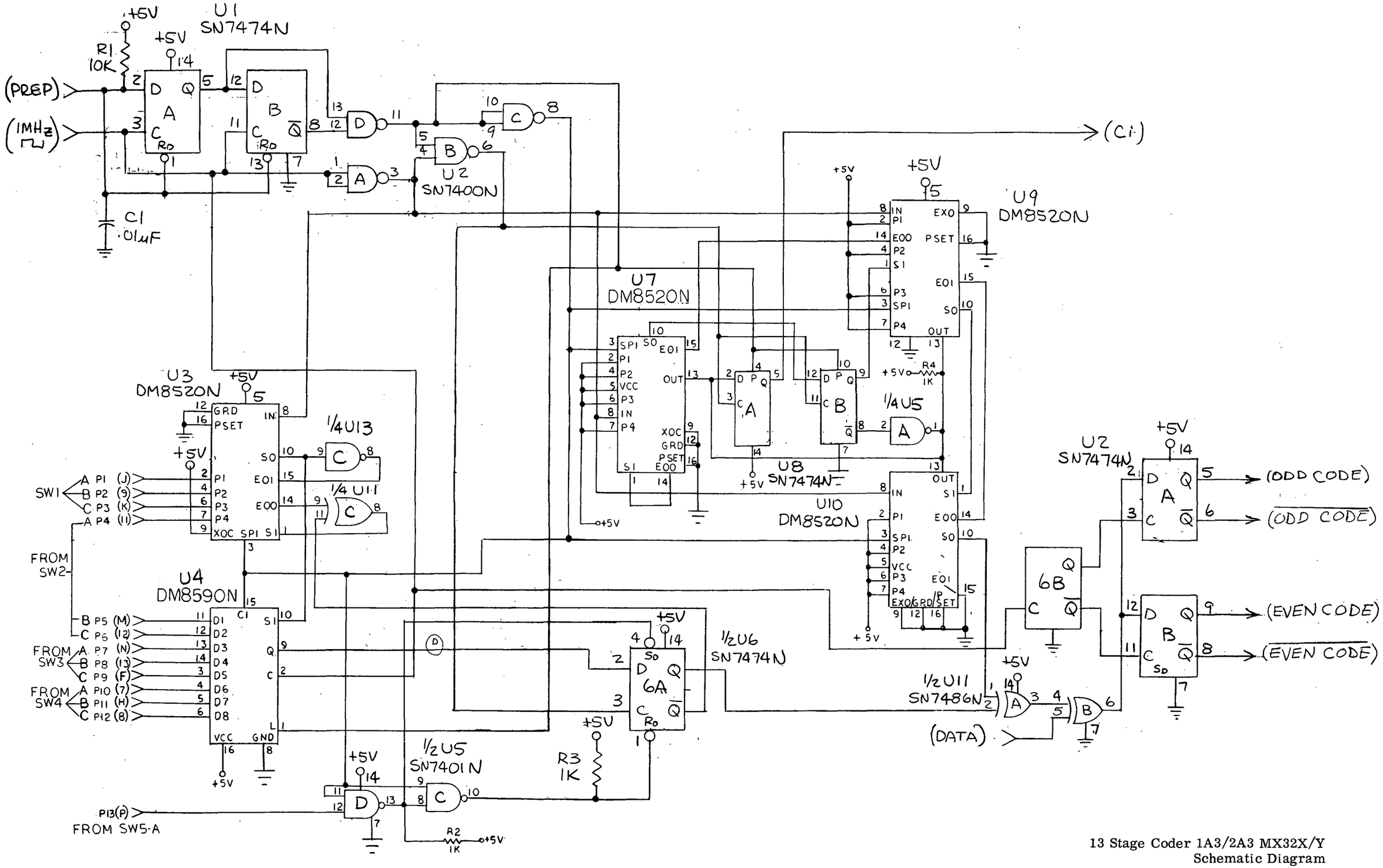

13 Stage Coder 1A3/2A3 MX32X/Y
Schematic Diagram

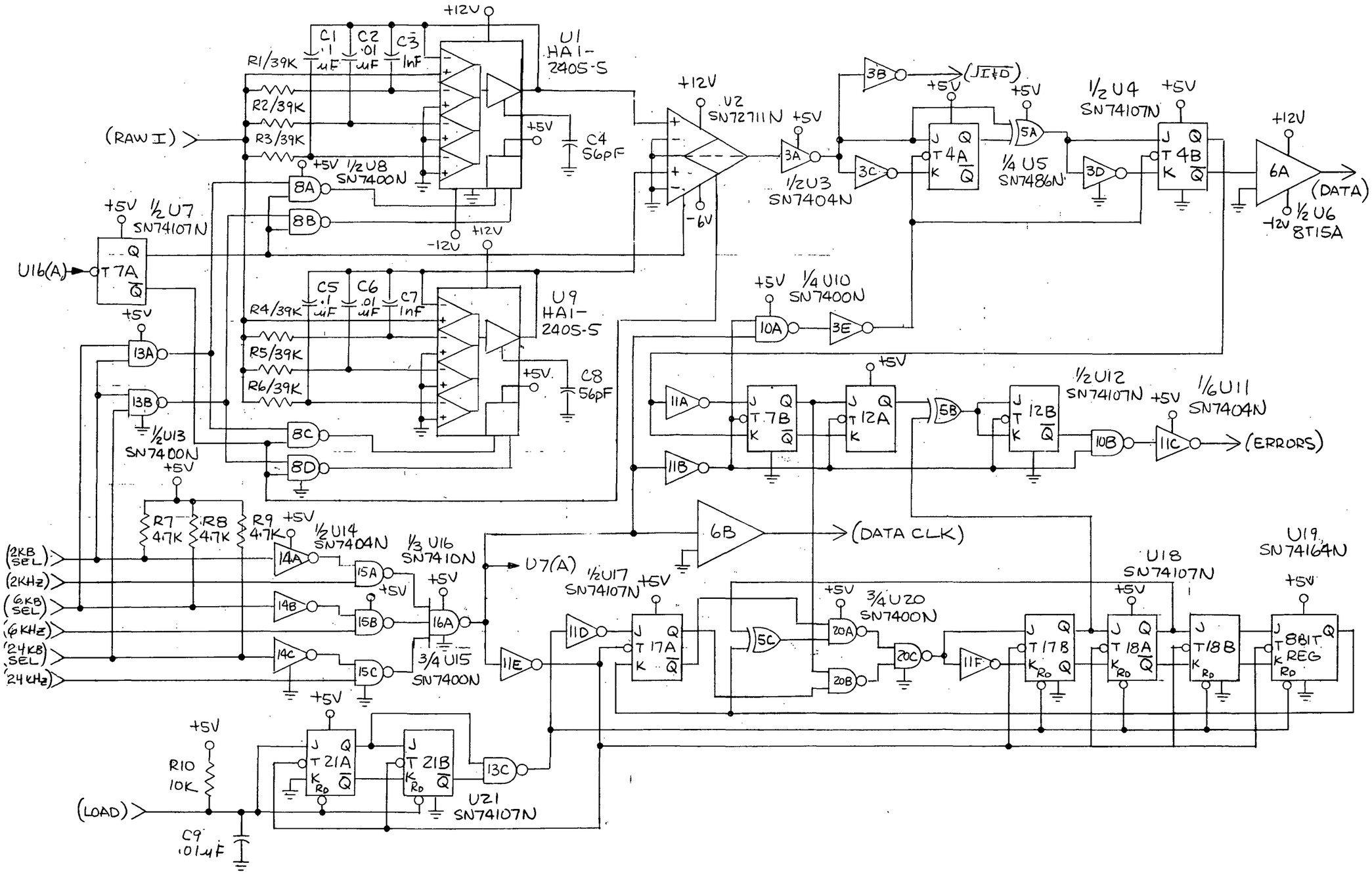

Data Processor and Error Detector
MX 32Y 2A1 - Schematic Diagram

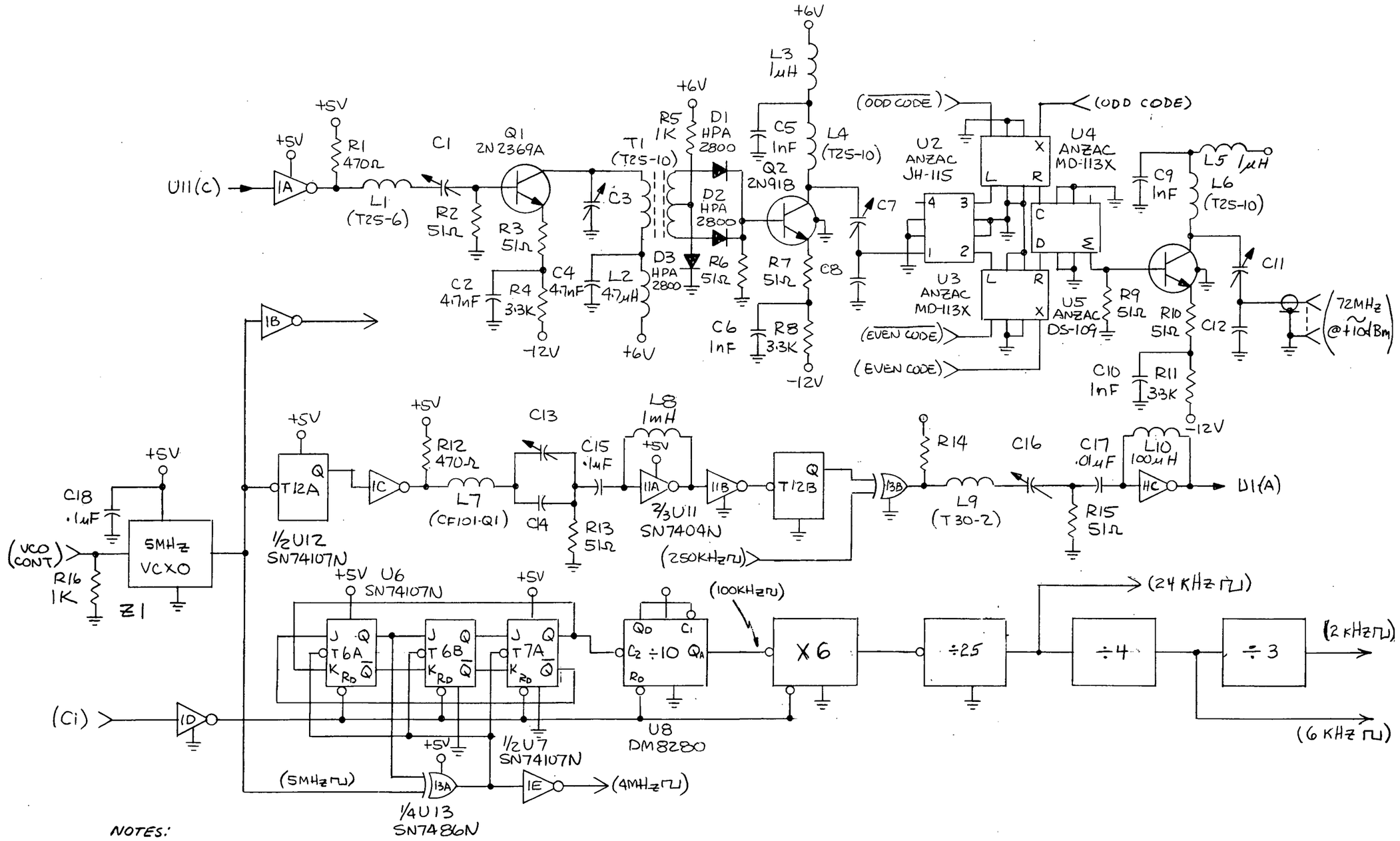

NOTES:

1.- FOR POWER SUPPLY DISTRIBUTION SEE DWG _____

RX Frequency Synthesizer MX 32Y
2A2 - Schematic Diagram

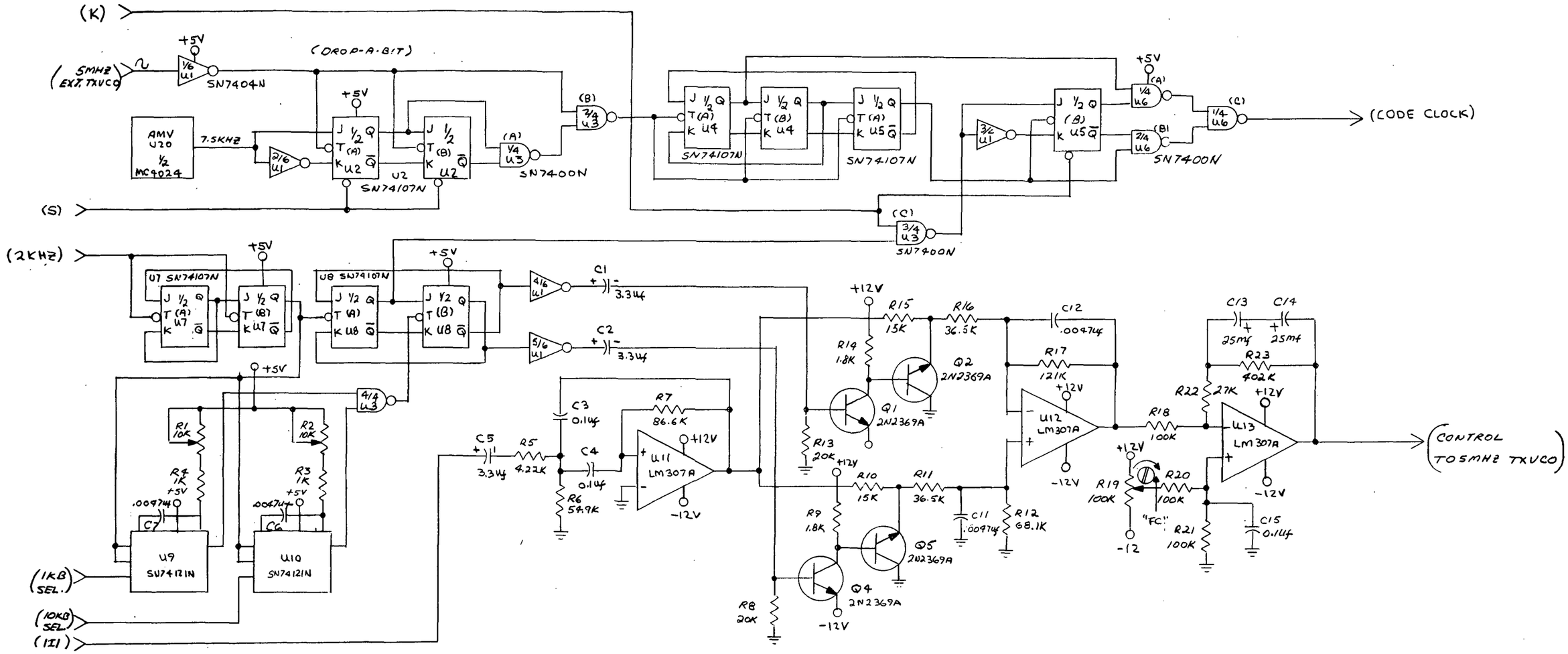

Code Clk Synth MX32Y
Schematic Diagram

B-17/B-18 Blank

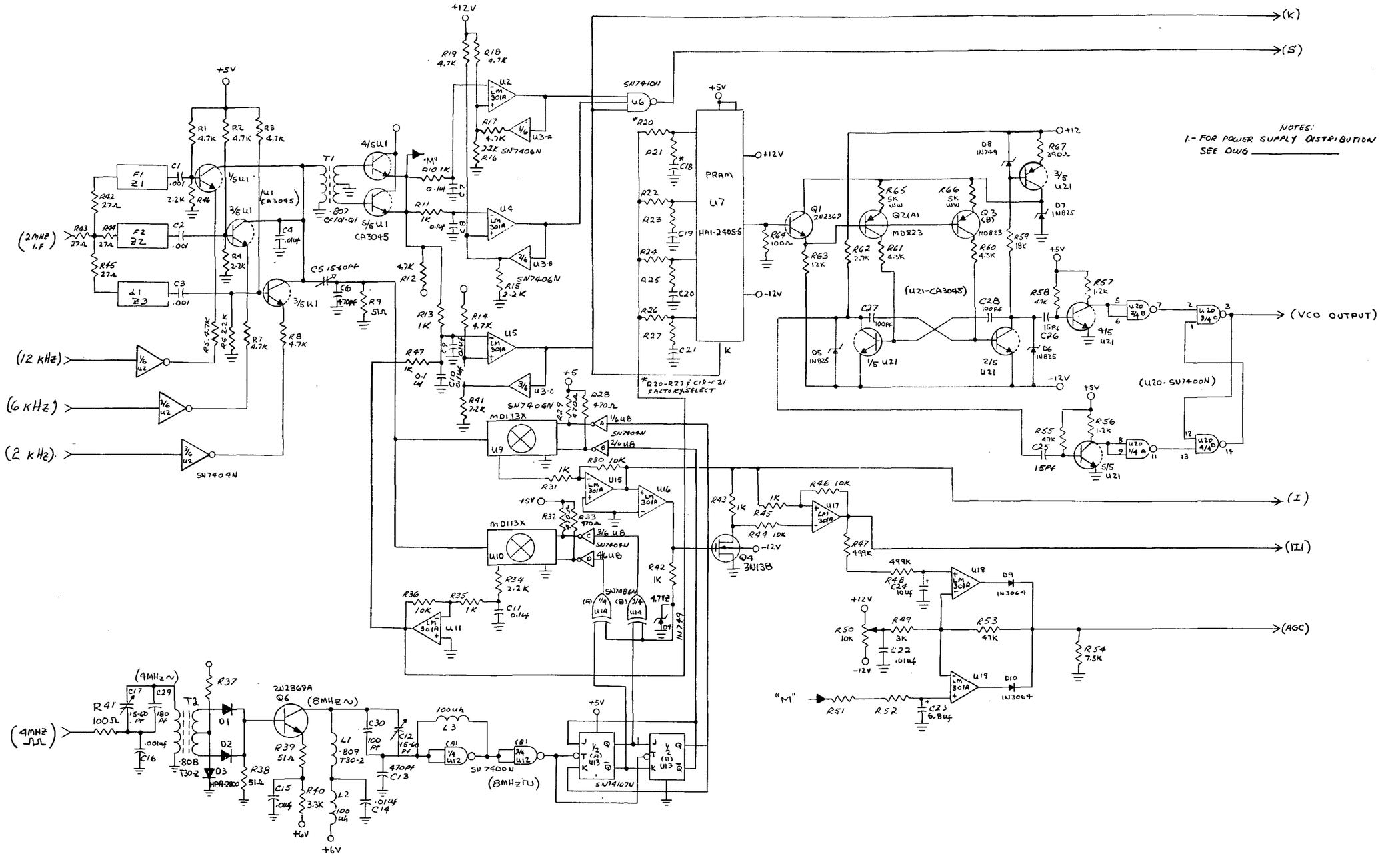

Costa Loop and Synth Decision
MX32Y - Schematic Diagram

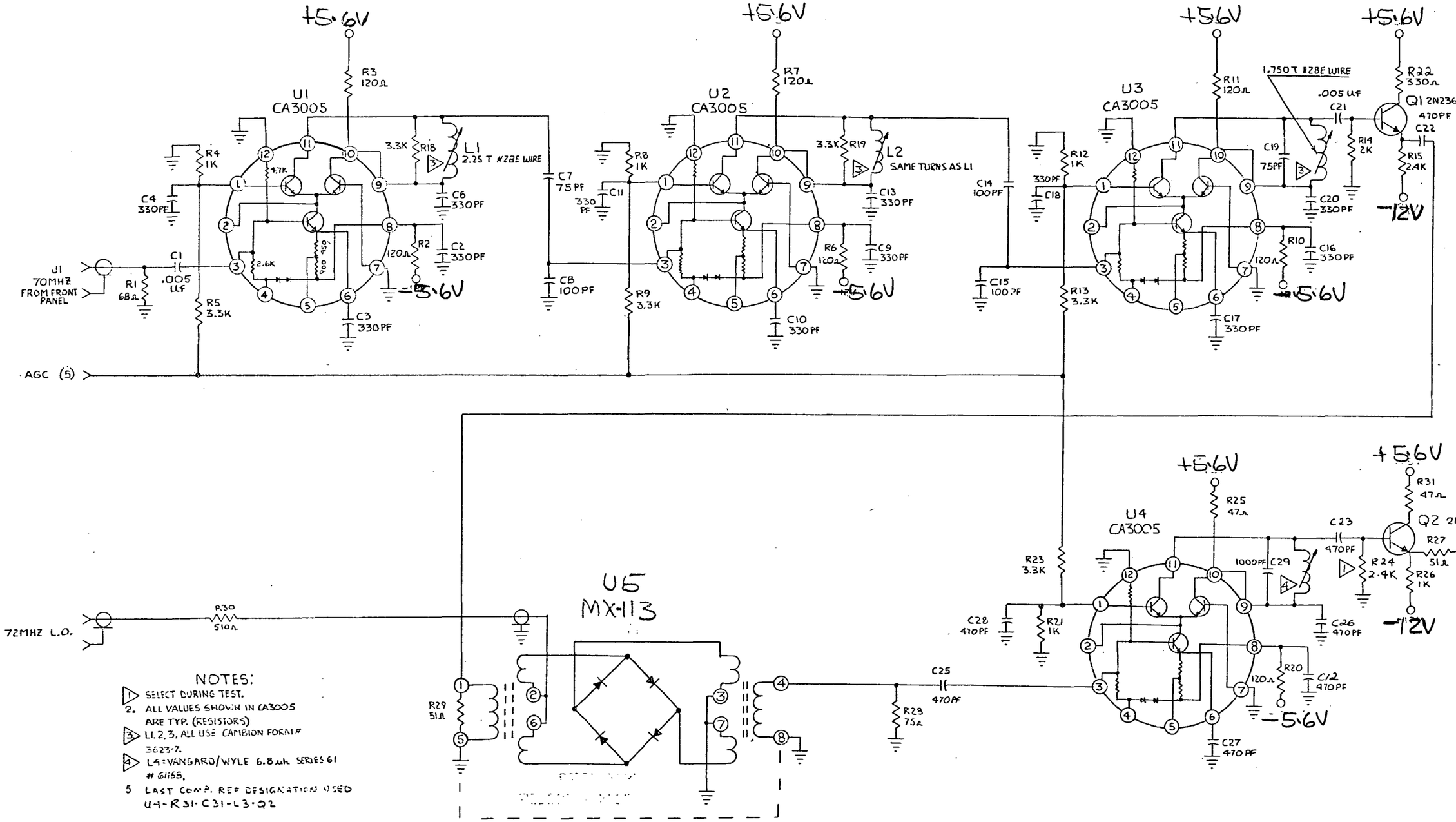

NOTES:

1. SELECT DURING TEST.
2. ALL VALUES SHOWN IN CA3005 ARE TYP. (RESISTORS)
3. L1, 2, 3, ALL USE CAMBION FORM # 3623-7.
4. L4=VANGARD/WYLE 6.8 uh SERIES 61 # 61155.
5. LAST COMP. REF DESIGNATIONS USED U4-R31-C31-L3-Q2

70 MHz Amp 2A6 MX 32Y
Schematic Diagram

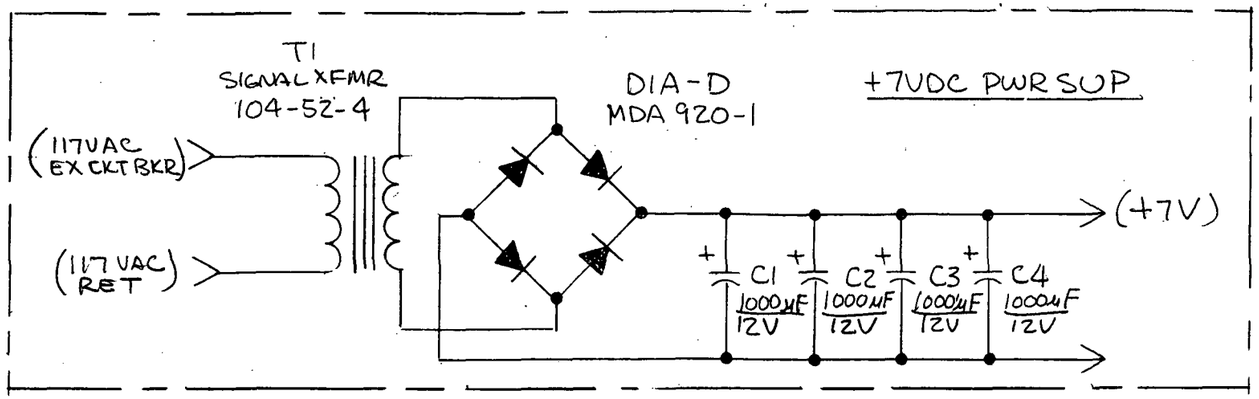

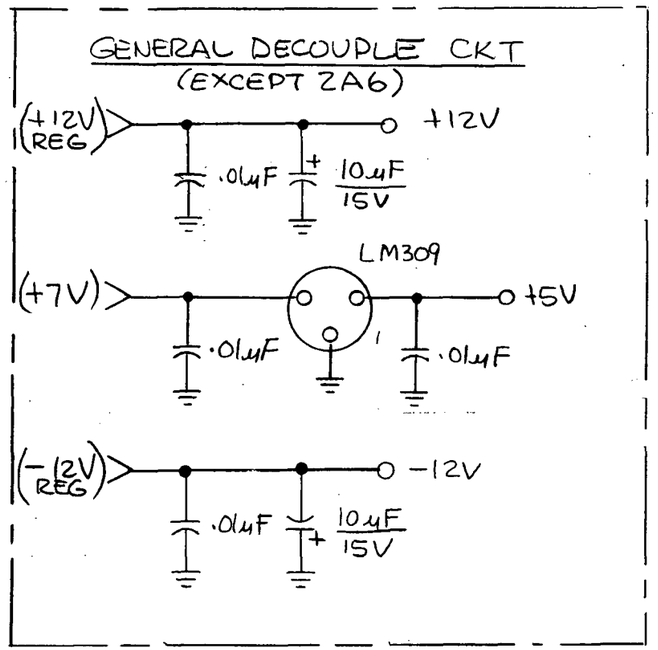

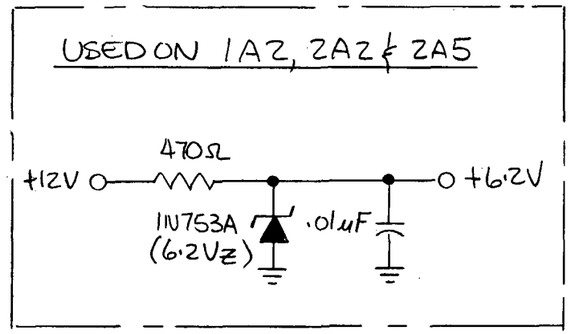

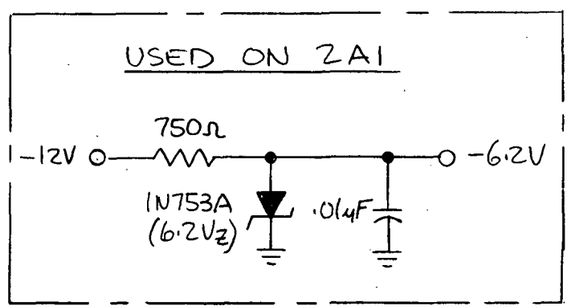

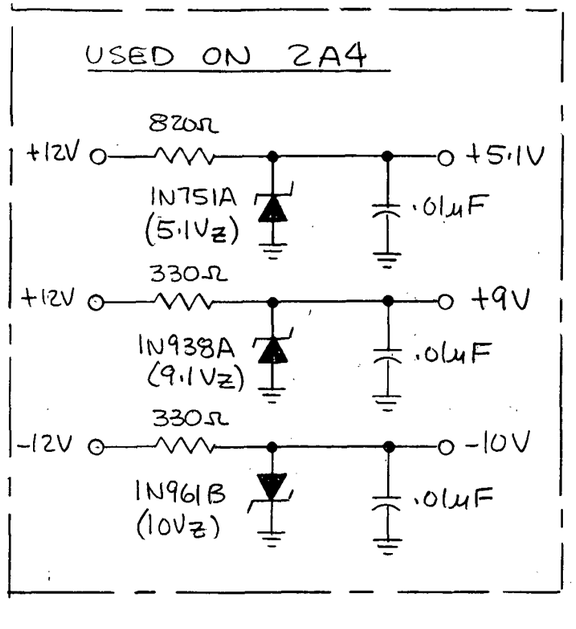

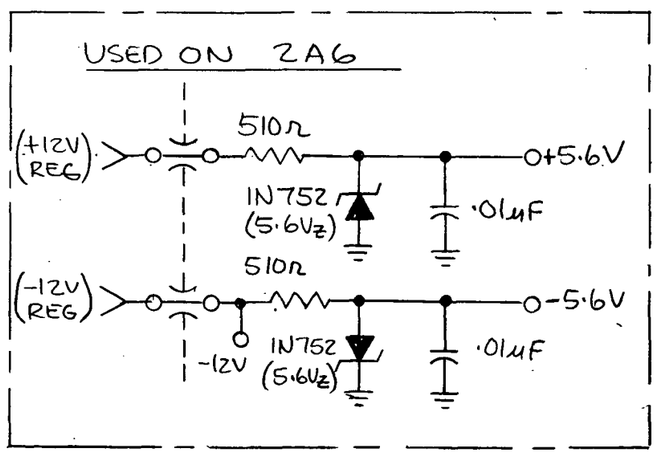

Power Distribution MX32X/32Y
Schematic Diagram

BIBLIOGRAPHIC DATA

1. Report No.	2. Government Accession No.	3. Recipient's Catalog No.

4. Title and Subtitle
DEFINITION OF MULTIPATH/RFI EXPERIMENTS FOR ORBITAL TESTING WITH A SMALL APPLICATIONS TECHNOLOGY SATELLITE

5. Report Date
December 1, 1972

6. Performing Organization Code

7. Author(s)
J. N. Birch, R. H. French

8. Performing Organization Report No.
ASAO-PR20041-8

9. Performing Organization Name and Address
THE MAGNAVOX COMPANY
Advanced Systems Analysis Office
8720 Georgia Avenue
Silver Spring, Maryland 20910

10. Work Unit No.

11. Contract or Grant No.
NAS9-12705

12. Sponsoring Agency Name and Address
National Aeronautics and Space Administration
Manned Spacecraft Center
Houston, Texas 77058
Technical Monitor: Mr. S. W. Novosad

13. Type of Report and Period Covered
Final Report
May 1 - Dec. 1, 1972

14. Sponsoring Agency Code

15. Supplementary Notes
DRL unnumbered Line Item 4. DRD No. MA-129T

16. Abstract

An investigation was made to define experiments for collection of RFI and multipath data for application to a synchronous relay satellite/low orbiting satellite configuration. A survey of analytical models of the multipath signal was conducted. Data has been gathered concerning the existing RFI and other noise sources in various bands at VHF and UHF.

Additionally, designs are presented for equipments to combat the effects of RFI and multipath: an adaptive delta mod voice system, a forward error control coder/decoder, a PN transmission system, and a wideband FM system. The performance of these systems was then evaluated.

Also, the report discusses techniques for measuring multipath and RFI. Finally, recommended data collection experiments are presented.

The report contains as an Appendix an extensive tabulation of theoretical predictions of the amount of signal reflected from a rough, spherical earth.

17. Key Words (Selected by Author(s))	18. Distribution Statement
.Communications Systems .SATS .Radio Frequency Interference .RFI .Multipath .Convolutional Coding .PN Systems .PSK .Satellites .Scientific Satellites .TDRS	

19. Security Classif. (of this report)	20. Security Classif. (of this page)	21. No. of Pages	22. Price*
UNCLASSIFIED	UNCLASSIFIED		

*For sale by the Clearinghouse for Federal Scientific and Technical Information, Springfield, Virginia 22151.